Ingvar Lindgren

Relativistic Many-Body Theory

A New Field-Theoretical Approach



Springer Series on Atomic, Optical, and Plasma Physics

Volume 63

Series Editors

W.E. Baylis Uwe Becker Philip George Burke Robert N. Compton M.R. Flannery Charles J. Joachain Brian R. Judd Kate Kirby Peter Lambropoulos Gerd Leuchs Pierre Meystre

For further volumes: http://www.springer.com/series/411

Ingvar Lindgren

Relativistic Many-Body Theory

A New Field-Theoretical Approach

With 97 Figures



Ingvar Lindgren
Department of Physics
University of Gothenburg
SE-412 96 Göteborg
Sweden
ingvar.lindgren@physics.gu.se

ISSN 1615-5653 ISBN 978-1-4419-8308-4 e-ISBN 978-1-4419-8309-1 DOI 10.1007/978-1-4419-8309-1 Springer New York Dordrecht Heidelberg London

Library of Congress Control Number: 2011921721

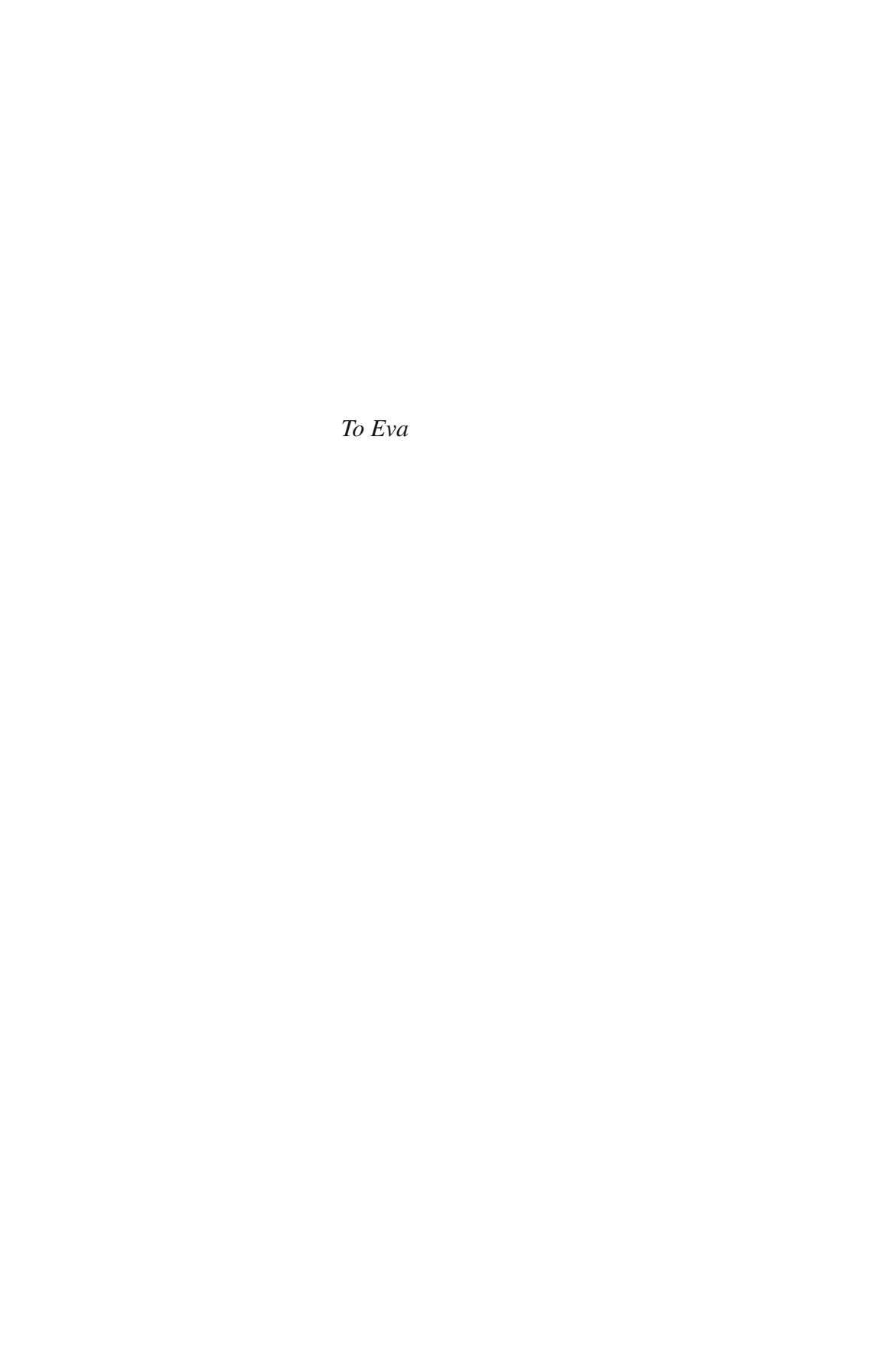
© Springer Science+Business Media, LLC 2011

All rights reserved. This work may not be translated or copied in whole or in part without the written permission of the publisher (Springer Science+Business Media, LLC, 233 Spring Street, New York, NY 10013, USA), except for brief excerpts in connection with reviews or scholarly analysis. Use in connection with any form of information storage and retrieval, electronic adaptation, computer software, or by similar or dissimilar methodology now known or hereafter developed is forbidden.

The use in this publication of trade names, trademarks, service marks, and similar terms, even if they are not identified as such, is not to be taken as an expression of opinion as to whether or not they are subject to proprietary rights.

Printed on acid-free paper

Springer is part of Springer Science+Business Media (www.springer.com)



Preface

It is now almost 30 years since the first edition of my book together with John Morrison, *Atomic Many-Body Theory* [6], appeared, and the second edition appeared some years later. It has been out of print for quite some time, but fortunately has recently been made available again through a reprint by Springer Verlag.

During the time that has followed, there has been a tremendous development in the treatment of many-body systems, conceptually as well as computationally. Particularly the relativistic treatment has expanded considerably, a treatment that has been extensively reviewed recently by Ian Grant in the book *Relativistic Quantum Theory of Atoms and Molecules* [2].

Also, the treatment of quantum-electrodynamical (QED) effects in atomic systems has developed considerably in the last few decades, and several review articles have appeared in the field [7, 11, 13] besides the book by Labzowsky et al., *Relativistic Effects in Spectra of Atomic Systems* [5].

An impressive development has taken place in the field of many-electron systems by means of various coupled-cluster approaches, with applications particularly on molecular systems. The development during the last 50 years has been summarized in the book *Recent Progress in Coupled Cluster Methods*, edited by Čársky, Paldus, and Pittner [14].

The present book is aimed at combining atomic many-body theory with quantumelectrodynamics, which is a long-sought goal in quantum physics. The main problem in this effort has been that the methods for QED calculations, such as the S-matrix formulation, and the methods for many-body perturbation theory (MBPT) have completely different structures. With the development of the new method for QED calculations, the *covariant evolution operator formalism* by the Gothenburg atomic theory group [7], the situation has changed, and quite new possibilities appeared to formulate a unified theory.

The new formalism is based on field theory, and in its full extent the unification process represents a formidable problem, and we can in this book describe only how some steps toward this goal can be taken. This book is largely based upon the previous book on *Atomic Many Body Theory* [6], and it is assumed that the reader has absorbed most of that book, particularly Part II. In addition, the reader is expected to have basic knowledge in quantum field theory that is explained in

viii Preface

books such as *Quantum Theory of Many-Particle Systems* by Fetter and Walecka [1] (mainly parts I and II), *An introduction to Quantum Field Theory* by Peskin and Schroeder [12], and *Quantum Field Theory* by Mandl and Shaw [10].

The material of this book is largely based upon lecture notes and recent publications by the Gothenburg Atomic-Theory Group [3, 4, 7–9], and I want to express my sincere gratitude particularly to my previous coauthor John Morrison and to my present coworkers, Sten Salomonson and Daniel Hedendahl, as well as to the previous collaborators Ann-Marie Pendrill, Jean-Louis Heully, Eva Lindroth, Björn Åsén, Hans Persson, Per Sunnergren, Martin Gustavsson, and Håkan Warston for valuable collaboration.

In addition, I want to thank the late pioneers of the field, Per-Olov Löwdin, who taught me the foundations of perturbation theory some 40 years ago, and Hugh Kelly, who introduced the diagrammatic representation into atomic physics – two corner stones of the later developments. Furthermore, I have benefitted greatly from communications with many other national and international colleagues and friends (in alphabetic order), Rod Bartlett, Erkki Brändas, Gordon Drake, Ephraim Eliav, Stephen Fritzsche, Gerald Gabrielse, Walter Greiner, Paul Indelicato, Karol Jankowski, Jürgen Kluge, Leonti Labzowsky, Peter Mohr, Debashis Mukherjee, Marcel Nooijen, Joe Paldus, Vladimir Shabaev, Thomas Stöhlker, Gerhard Soff †, Joe Sucher, Peter Surjan, and many others.

The outline of the book is the following. The main text is divided into three parts. Part I gives some basic formalism and the basic many-body theory that will serve as a foundation for the following. In Part II, three numerical procedures for calculation of QED effects on bound electronic states are described, the S-matrix formulation, the Green's-function, and the covariant-evolution-operator methods. A procedure toward combining QED with MBPT is developed in Part III. Part IV contains a number of Appendices, where basic concepts are summarized. Certain sections of the text that can be omitted at first reading are marked with an asterisk (*).

References

- Fetter, A.L., Walecka, J.D.: The Quantum Mechanics of Many-Body Systems. McGraw-Hill, N.Y. (1971)
- 2. Grant, I.P.: Relativistic Quantum Theory of Atoms and Molecules. Springer, Heidelberg (2007)
- 3. Hedendahl, D.: *Towards a Relativistic Covariant Many-Body Perturbation Theory*. Ph.D. thesis, University of Gothenburg, Gothenburg, Sweden (2010)
- 4. Hedendahl, D., Salomonson, S., Lindgren, I.: . Phys. Rev. p. (to be published) (2011)
- Labzowski, L.N., Klimchitskaya, G., Dmitriev, Y.: Relativistic Effects in Spactra of Atomic Systems. IOP Publ., Bristol (1993)
- 6. Lindgren, I., Morrison, J.: *Atomic Many-Body Theory*. Second edition, Springer-Verlag, Berlin (1986, reprinted 2009)
- Lindgren, I., Salomonson, S., Åsén, B.: The covariant-evolution-operator method in boundstate QED. Physics Reports 389, 161–261 (2004)
- Lindgren, I., Salomonson, S., Hedendahl, D.: Many-body-QED perturbation theory: Connection to the two-electron Bethe-Salpeter equation. Einstein centennial review paper. Can. J. Phys. 83, 183–218 (2005)

Preface

9. Lindgren, I., Salomonson, S., Hedendahl, D.: Many-body procedure for energy-dependent perturbation: Merging many-body perturbation theory with QED. Phys. Rev. A 73, 062,502 (2006)

- 10. Mandl, F., Shaw, G.: Quantum Field Theory. John Wiley and Sons, New York (1986)
- Mohr, P.J., Plunien, G., Soff, G.: QED corrections in heavy atoms. Physics Reports 293, 227–372 (1998)
- 12. Peskin, M.E., Schroeder, D.V.: An introduction to Quantun Field Theory. Addison-Wesley Publ. Co., Reading, Mass. (1995)
- 13. Shabaev, V.M.: Two-times Green's function method in quantum electrodynamics of high-Z few-electron atoms. Physics Reports 356, 119–228 (2002)
- 14. Čársky, P., Paldus, J., Pittner, J. (eds.): Recent Progress in Coupled Cluster Methods: Theory and Applications. Springer (2009)

Gothenburg, Sweden

Ingvar Lindgren

Contents

1	Intro	duction		I
	1.1	Standa	rd Many-Body Perturbation Theory	1
	1.2	Quantı	ım-Electrodynamics	2
	1.3	Bethe-	-Salpeter Equation	3
	1.4	Heliun	n Atom: Analytical Approach	4
	1.5		Theoretical Approach to Many-Body Perturbation Theory	
	Refe	rences		7
Pa	rt I B	Basics: St	tandard Many-Body Perturbation Theory	
2	Time	e-Indepe	ndent Formalism	13
	2.1	First Q	uantization	13
		2.1.1	De Broglie's Relations	13
		2.1.2	The Schrödinger Equation	14
	2.2	Second	l Quantization	16
		2.2.1	Schrödinger Equation in Second Quantization	16
		2.2.2	Particle-Hole Formalism: Normal Order and	
			Contraction	18
		2.2.3	Wick's Theorem	19
	2.3	Time-I	ndependent Many-Body Perturbation Theory	20
		2.3.1	Bloch Equation	20
		2.3.2	Partitioning of the Hamiltonian	21
	2.4	Graphi	cal Representation	25
		2.4.1	Goldstone Diagrams	25
		2.4.2	Linked-Diagram Expansion	28
	2.5	All-Or	der Methods: Coupled-Cluster Approach	30
		2.5.1	Pair Correlation	30
		2.5.2	Exponential Ansatz	33
		2.5.3	Various Models for Coupled-Cluster	
			Calculations: Intruder-State Problem	36
	2.6	Relativ	ristic MBPT: No-Virtual-Pair Approximation	37
		2.6.1	QED Effects	39

xii Contents

	2.7		Numerical Results of Standard MBPT and CC	
			ations, Applied to Atoms	
	Ref	erences		43
3	Tim	e-Depend	lent Formalism	47
	3.1	•	ion Operator	
	3.2		atic Damping: Gell-Mann–Low Theorem	
		3.2.1	Gell-Mann-Low Theorem	
	3.3	Extend	ed Model Space: The Generalized	
			Iann–Low Relation	52
	Refe			
Par	t II	Ouantur	n-Electrodynamics: One-Photon	
			o-Photon Exchange	
4	C N	[atniv		59
4	4.1		ion of the S-Matrix: Feynman Diagrams	
	4.1		on Propagator	
	4.2		1 6	
	4.3	4.3.1	Propagator Feynman Gauge	
		4.3.1	Coulomb Gauge	
	4.4		e de la companya de	
	4.4	4.4.1	Photon Exchange	
		4.4.1	Covariant Gauge	
		4.4.2		
	4.5		Single-Particle Potential	
	4.3	4.5.1	hoton Exchange	
		4.5.1	Two-Photon Cross	
	4.6		Corrections	
	4.0	4.6.1	Bound-Electron Self-Energy	
		4.6.2	Vertex Correction	
		4.6.3	Vacuum Polarization	
		4.6.4	Photon Self-Energy	
	4.7		an Diagrams for the S-Matrix: Feynman Amplitude	
	4.7	4.7.1	Feynman Diagrams	
		4.7.1	Feynman Amplitude	
	Refe		Teynnan Amphidae	
5	C	onla Eve	ctions	91
5	5.1			
	5.1		al Green's Function	
	3.2	5.2.1		
			Definition of the Field-Theoretical Green's Function	
		5.2.2	Single-Photon Exchange Fourier Transform of the Green's Function	
		5.2.3	Fourier Transform of the Green's Function	90

Contents xiii

	5.3	Graphi	ical Representation of the Green's Function	100
		5.3.1	Single-Particle Green's Function	100
		5.3.2	Many-Particle Green's Function	105
		5.3.3	Self-Energy: Dyson Equation	108
		5.3.4	Numerical Illustration	110
	5.4	Field-7	Theoretical Green's Function: Open-Shell Case	110
		5.4.1	Definition of the Open-Shell Green's Function	
		5.4.2	Two-Times Green's Function of Shabaev	
		5.4.3	Single-Photon Exchange	
	Refe	rences		
6	Cova	ariant Ev	volution Operator and Green's Operator	119
	6.1		tion of the Covariant Evolution Operator	
	6.2		-Photon Exchange in the	
			ant-Evolution-Operator Formalism	122
		6.2.1	Single-Photon Ladder	
	6.3	Multip	hoton Exchange	
		6.3.1	General	
		6.3.2	Irreducible Two-Photon Exchange	
		6.3.3	Potential with Radiative Parts	
	6.4	Relativ	vistic Form of the Gell-Mann–Low Theorem	
	6.5		Гheoretical Many-Body Hamiltonian	
	6.6		's Operator	
		6.6.1	Definition	
		6.6.2	Relation Between the Green's Operator	
			and Many-Body Perturbation Procedures	136
	6.7	Model-	-Space Contribution	
		6.7.1	Lowest Orders	139
		6.7.2	All Orders	
	6.8	Bloch	Equation for Green's Operator	
	6.9		Dependence of the Green's Operator. Connection	
			Bethe–Salpeter Equation	151
		6.9.1	Single-Reference Model Space	
		6.9.2	Multireference Model Space	
	Refe	rences		
7	Num	erical II	lustrations to Part II	157
		S-Matr		
	,	7.1.1	Electron Self-Energy of Hydrogen-Like Ions	
		7.1.2	Lamb Shift of Hydrogen-Like Uranium	
		7.1.2	Lamb Shift of Lithium-Like Uranium	
		7.1.3	Two-Photon Nonradiative Exchange	
		7.1.1	in Helium-Like Ions	160
		7.1.5	Electron Correlation and QED Calculations	
		,.1.5	on Ground States of Helium-Like Ions	163

xiv Contents

		7.1.6 g-Factor of Hydrogen-Like Ions:	
		Mass of the Free Electron	
	7.2	Green's-Function and Covariant-Evolution-Operate	or Methods165
		7.2.1 Fine-Structure of Helium-Like Ions	165
		7.2.2 Energy Calculations of 1 <i>s</i> 2 <i>s</i> Levels	
		of Helium-Like Ions	167
	Refe	erences	168
_			
Par	t III	Quantum-Electrodynamics Beyond Two-Photon	
		Field-Theoretical Approach to Many-Body Pertu	irpation
		Theory	
0	Com	namicus Englution Combined with Electron Comple	4°an 172
8	8.1	variant Evolution Combined with Electron Correla	
	0.1	General Single-Photon Exchange	
	8.2		
	0.2	General QED Potential	
		8.2.1 Single Photon with Crossed Coulomb Inte	
		8.2.2 Electron Self-Energy and Vertex Correction8.2.3 Vertex Correction with Further Coulomb I	
	0.2	8.2.4 General Two-Body Potential	193
	8.3	Unification of the MBPT and QED Procedures:	102
		Connection to Bethe–Salpeter Equation	
	8.4	8.3.1 MBPT-QED Procedure	
		Coupled-Cluster-QED Expansionerences	
	Refe	erences	198
9	The	Bethe-Salpeter Equation	199
	9.1	The Original Derivations by the Bethe–Salpeter Eq	
		9.1.1 Derivation by Salpeter and Bethe	199
		9.1.2 Derivation by Gell-Mann and Low	202
		9.1.3 Analysis of the Derivations of the	
		Bethe–Salpeter Equation	203
	9.2	Quasi-Potential and Effective-Potential	
		Approximations: Single-Reference Case	205
	9.3	Bethe–Salpeter–Bloch Equation: Multireference Ca	ase206
	9.4	Problems with the Bethe–Salpeter Equation	208
	Refe	erences	209
4.0		A A A A A A A A A A A A A A A A A A A	
10		plementation of the MBPT-QED Procedure Numerical Results	211
	10.1		
	10.1	*	
	10.2		
	10.3	10.3.1 Illustration	
		10.J.1 IIIuSu auoii	

Contents xv

		10.3.2	Full Treatment	
		10.3.3	Higher Orders	
	10.4		cal Results	
		10.4.1	Two-Photon Exchange	
		10.4.2	Beyond Two Photons	
		10.4.3	Outlook	
	Refer	ences		224
11	Anal		eatment of the Bethe–Salpeter Equation	
	11.1		Fine Structure	
	11.2		proach of Sucher	
	11.3		ation Expansion of the BS Equation	
	11.4		mmatic Representation	
	11.5		rison with the Numerical Approach	
	Refer	ences		235
12	Regu		n and Renormalization	
	12.1		ee-Electron QED	
		12.1.1	The Free-Electron Propagator	
		12.1.2	The Free-Electron Self-Energy	239
		12.1.3	The Free-Electron Vertex Correction	
	12.2	Renorm	nalization Process	
		12.2.1	Mass Renormalization	242
		12.2.2	Charge Renormalization	
	12.3	Bound-	State Renormalization: Cutoff Procedures	
		12.3.1	Mass Renormalization	
		12.3.2	Evaluation of the Mass Term	249
		12.3.3	Bethe's Nonrelativistic Treatment	251
		12.3.4	Brown–Langer–Schaefer Regularization	252
		12.3.5	Partial-Wave Regularization	255
	12.4	Dimens	sional Regularization in Feynman Gauge	257
		12.4.1	Evaluation of the Renormalized Free-Electron	
			Self-Energy in Feynman Gauge	258
		12.4.2	Free-Electron Vertex Correction in Feynman Gauge	
	12.5	Dimens	sional Regularization in Coulomb Gauge	263
		12.5.1	Free-Electron Self-Energy in the Coulomb Gauge	263
	12.6	Direct 1	Numerical Regularization of the Bound-State	
			ergy	267
		12.6.1	Feynman Gauge	
		12.6.2	Coulomb Gauge	
	Refer	ences		
13	Sumi	nary and	d Conclusions	271

xvi Contents

Appendices

A	Nota	tions and	d Definitions	273
	A.1	Four-Co	omponent Vector Notations	273
	A.2	Vector	Spaces	275
		A.2.1	Notations	275
		A.2.2	Basic Definitions	275
		A.2.3	Special Spaces	277
	A.3	Special	Functions	277
		A.3.1	Dirac Delta Function	277
		A.3.2	Integrals over Δ Functions	279
		A.3.3	The Heaviside Step Function	282
	Refe	rences		282
В	Seco	nd Quan	tization	283
	B.1	Definiti	ions	283
	B.2	Heisenl	berg and Interaction Pictures	286
	Refe	rences		287
C	Repr	esentatio	ons of States and Operators	289
	C.1		Representation of States	
	C.2		Representation of Operators	
	C.3		nate Representations	
		C.3.1	Representation of Vectors	
		C.3.2	Closure Property	292
		C.3.3	Representation of Operators	293
D	Dira	c Equatio	on and the Momentum Representation	295
	D.1		Equation	
		D.1.1	Free Particles	295
		D.1.2	Dirac Equation in an Electromagnetic Field	300
	D.2	Momen	ntum Representation	300
		D.2.1	Representation of States	300
		D.2.2	Representation of Operators	301
		D.2.3	Closure Property for Momentum Functions	302
	D.3	Relation	ns for the Alpha and Gamma Matrices	302
	Refe	rence		303
E	Lagr	angian F	Field Theory	305
	E.1		al Mechanics	
		E.1.1	Electron in External Field	307
	E.2	Classic	al Field Theory	308
	E.3		Equation in Lagrangian Formalism	
	Refe	ences		310

Contents xvii

F	Semi	iclassical	Theory of Radiation	311
	F.1	Classic	al Electrodynamics	311
		F.1.1	Maxwell's Equations in Covariant Form	311
		F.1.2	Coulomb Gauge	315
	F.2	Quantiz	zed Radiation Field	317
		F.2.1	Transverse Radiation Field	317
		F.2.2	Breit Interaction	318
		F.2.3	Transverse Photon Propagator	321
		F.2.4	Comparison with the Covariant Treatment	322
	Refe	rences		324
G	Cova	ariant Th	neory of Quantum ElectroDynamics	325
	G .1	Covaria	ant Quantization: Gupta–Bleuler Formalism	325
	G.2	Gauge '	Transformation	327
		G.2.1	General	327
		G.2.2	Covariant Gauges	328
		G.2.3	Noncovariant Gauge	329
	G.3	Gamma	a Function	
		G.3.1	$z = -1 - \epsilon$	333
		G.3.2	$z = -2 - \epsilon$	333
	Refe	rences		334
Н	Feyn	man Dia	grams and Feynman Amplitude	335
	H.1		an Diagrams	
		H.1.1	S-Matrix	335
		H.1.2	Green's Function	336
		H.1.3	Covariant Evolution Operator	336
	H.2	Feynma	an Amplitude	337
I	Eval	uation R	ules for Time-Ordered Diagrams	341
	I.1		Photon Exchange	
	I.2	Two-Pł	noton Exchange	343
		I.2.1	No Virtual Pair	344
		I.2.2	Single Hole	345
		I.2.3	Double Holes	346
	I.3	Genera	l Evaluation Rules	347
	Refe	rences		348
J	Som	e Integra	ıls	349
	J.1			
	J.2	Evaluat	an Integrals	351
	J.3	Evaluat	tion of the Integral $\int \frac{d^3k}{(2\pi)^3} \left(\alpha_1 \cdot \hat{k}\right) \left(\alpha_2 \cdot \hat{k}\right) \frac{e^{ik \cdot r_{12}}}{q^2 - k^2 + i\eta}$	352
	Refe	rences	() () () 4 K + M	354

xviii Contents

K Unit	Systems and Dimensional Analysis	355
	Unit Systems	
	K.1.1 SI System	355
	K.1.2 Relativistic or "Natural" Unit System	
	K.1.3 Hartree Atomic Unit System	356
	K.1.4 cgs Unit Systems	357
K.2	Dimensional Analysis	
Abbrevia	tions	361
Index		363

Chapter 1 Introduction

1.1 Standard Many-Body Perturbation Theory

The quantum-mechanical treatment of many-electron systems, based on the Schrödinger equation and the Coulomb interaction between the electrons, was developed shortly after the advent of quantum mechanics, particularly by John Slater in the late 1920s and early 1930s [58]. Self-consistent-field (SCF) schemes were early developed by Slater, Hartree, Fock, and others. Perturbative schemes for quantum-mechanical system, based on the Rayleigh-Schrödinger and Brillouin-Wigner schemes, were developed in the 1930s and 1940s, leading to the important linked-diagram expansion, introduced by Brueckner [13] and Goldstone [28] in the 1950s, primarily for nuclear applications. That scheme was in the 1960s and 1970s also applied to electronic systems [31] and extended to degenerate and quasi-degenerate energy levels [10, 35]. The next step in this development was the introduction of "all-order methods" of coupled-cluster type, where certain effects are taken to all orders of the perturbation expansion. This represents the last and probably final – major step of the development of a nonrelativistic many-body perturbation theory (MBPT).² The first step toward a relativistic treatment of manyelectron systems was taken in the early 1930s by Breit [11], extending works made somewhat earlier by Gaunt [25]. Physically, the Gaunt interaction represents the magnetic interaction between the electrons, which is a purely relativistic effect. Breit augmented this treatment by including the leading retardation effect, due to the fact that the Coulomb interaction is not instantaneous, which is an effect of the same order.

A proper relativistic theory should be *Lorentz covariant*, like the Dirac single-electron theory.³ The Dirac equation for the individual electrons together with the

¹ For a review of the SCF methods, the reader is referred to the book by Froese-Fischer [24].

² By MBPT, we understand here perturbative methods based upon the Rayleigh–Schrödinger perturbation scheme and the linked-diagram expansion. To that group, we also include nonperturbative schemes, such as the coupled-cluster approach (CCA), which are based upon the same formalism.

³ A physical quantity (scalar, vector, tensor) is said to be Lorentz covariant, if it transforms according to a representation of the Lorentz group. (Only a scalar is invariant under that transformation.)

2 1 Introduction

instantaneous Coulomb and Breit interactions between the electrons represents for a many-electron system all effects up to order α^2 H(artree atomic units) or α^4 m_ec^2 . This procedure, however, is NOT Lorentz covariant, and the Breit interaction can only be treated to first order in perturbation theory, unless projection operators are introduced to prevent the intermediate states from falling into the "Dirac sea" of negative-energy states, as discussed early by Brown and Ravenhall [12] and later by Sucher [62]. The latter approach has been successfully employed for a long time in relativistic many-body calculations and is known as the *no-virtual-pair approximation* (NVPA).

A fully covariant relativistic many-body theory requires a field-theoretical approach, i.e., the use of *quantum-electrodynamics* (QED). In principle, there is no sharp distinction between relativity and QED, but conventionally we shall refer to effects beyond the NVPA as QED effects. This includes effects of *retardation*, *virtual pairs*, *and radiative effects* (self-energy, vacuum polarization, vertex correction). The systematic treatment of these effects requires a covariant approach, where the QED effects are included in the wave function. The main purpose of this book is to formulate the foundations of such a procedure.

1.2 Quantum-Electrodynamics

Already in the 1930s deviations were observed between the results of precision spectroscopy and the Dirac theory for simple atomic systems, primarily the hydrogen atom. Originally, this deviation was expected to be due to *vacuum polarization*, i.e., spontaneous creation of electron–positron pairs in the vacuum, but this effect turned out to be too small and even of the wrong sign. An alternative explanation was the *electron self-energy*, i.e., the emission and absorption of a virtual photon on the same electron – another effect that is not included in the Dirac theory. Early attempts to calculate this effect, however, were unsuccessful, due to singularities (infinities) in the mathematical expressions.

The first experimental observation of a clear-cut deviation from the Dirac theory was the detection in 1947 by Lamb and Retherford of the so-called *Lamb shift* [34], namely the shift between the 2s and $2p_{1/2}$ levels in atomic hydrogen, levels that are exactly degenerate in the Dirac theory [17, 18]. In the same year, Bethe was able to explain the shift by a nonrelativistic calculation, eliminating the singularity of the self-energy by means of a *renormalization process* [5]. At the same time, Kusch and Foley observed that the magnetic g-factor of the free electron deviates slightly but significantly from the Dirac value -2 [32, 33]. These observations led

An equation or a theory, like the theory of relativity or Maxwell's theory of electromagnetism, is said to be Lorentz covariant, if it can be expressed entirely in terms of covariant quantities (see, for instance, the books of Bjorken and Drell [7,8]).

 $^{^4}$ α is the fine-structure constant ≈1/137 and m_ec^2 is the electron rest energy (see Appendix K).

to the development of the modern form of the quantum-electrodynamic theory by Feynman, Schwinger, Dyson, Tomanaga, and others by which the deviations from the Dirac theory could be explained with good accuracy [20, 22, 23, 56, 64].⁵

The original theory of QED was applied to free electrons. During the last four decades, several methods have been developed for numerical calculation of QED effects in *bound* electronic states. The scattering-matrix or *S-matrix formulation*, originally developed for dealing with the scattering of free particles, was made applicable also to bound states by Sucher [60], and the numerical procedure was refined in the 1970s particularly by Mohr [38]. During the last two decades, the method has been extensively used in studies of highly charged ions to test the QED theory under extreme conditions, works that have been pioneered by Mohr and Soff (for a review, see [39]).

The *Green's function* is one of the most important tools in mathematical physics with applications in essentially all branches of physics.⁶ In 1990s, the method was adopted to bound-state QED problems by Shabaev et al. [57]. This procedure is referred to as the *Two-times Green's function* and has recently been extensively applied to highly charged ions by the St Petersburg group.

During the first decade of this century, another procedure for numerical QED calculations was developed by the Gothenburg atomic theory group, termed the *Covariant-evolution-operator* (CEO) method [36], which has been applied to the fine structure and other energy-level separations of helium-like ions.

1.3 Bethe-Salpeter Equation

The first completely covariant treatment of a bound-state problem was presented in 1951 by Salpeter and Bethe [6, 52] and by Gell-Mann and Low [26]. The Bethe–Salpeter (BS) equation contains in principle the complete relativistic and interelectronic interaction, i.e., all kinds of electron correlation and QED effects.

The BS equation is associated with several fundamental problems, which were discussed in the early days, particularly by Dyson [21], Goldstein [27], Wick [65], and Cutkosky [16]. Dyson found that the question of relativistic quantum mechanics is "full of obscurities and unsolved problems" and that "the physical meaning of the four-dimensional wave function is quite unclear." It seems that some of these problems still remain.

The BS equation is based upon field theory, and there is no direct connection to the Hamiltonian approach of relativistic quantum mechanics. The solution of the field-theoretical BS equation leads to a four-dimensional wave function with individual times for the two particles. This is not in accordance with the standard

⁵ For the history of the development of the QED theory, the reader is referred to the authoritative review by Schweber [55].

⁶ For a comprehensive account of the applications, particularly in condensed-matter physics, the reader is referred to the book by Mahan [37].

4 1 Introduction

quantum-mechanical picture, which has a single time variable also for many-particle systems. The additional time variable leads sometimes to "abnormal solutions" with no counterparts in nonrelativistic quantum mechanics, as discussed particularly by Nakanishi [40] and Namyslowski [41].

Much efforts have been devoted to simplifying the BS equation by reducing it to a three-dimensional equation, in analogy with the standard quantum-mechanical equations (for reviews, see [9, 15]). Salpeter [51] derived early an "instantaneous" approximation, neglecting retardation, which led to a relativistically exact threedimensional equation, similar to – but not exactly equal to – the Breit equation. More sophisticated is the so-called quasi-potential approximation, introduced by Todorov [63], frequently used in scattering problems. Here, a three-dimensional Schrödinger-type equation is derived with an energy-dependent potential, deduced from scattering theory. Sazdjian [53, 54] was able to separate the BS equation into a three-dimensional equation of Schrödinger type and one equation for the relative time of the two particles, serving as a perturbation - an approach that is claimed to be exactly equivalent to the original BS equation. This approach establishes a definitive link between the Hamiltonian relativistic quantum mechanics and field theory. Connell [15] further developed the quasi-potential approximation of Todorov by introducing series of corrections, a procedure that also is claimed to be formally equivalent to the original BS equation.

Caswell and Lepage [14] applied the quasi-potential method to evaluate the hyperfine structure of muonium and positronium to the order $\alpha^6 m_e c^2$ by combining analytical and perturbative approaches. Grotch and Yennie [9, 30] have applied the method to evaluate higher-order nuclear corrections to the energy levels of the hydrogen atom, and Adkins and Fell [1, 2] have applied it to positronium.

The procedure we shall develop in the following is to combine the covariant-evolution-operator method with electron correlation, which will constitute a step toward a fully covariant treatment of many-electron systems. This will form another approximation of the full Bethe–Salpeter equation that seems feasible for electronic systems.

A vast literature on the Bethe–Salpeter equation, its fundamental problems and its applications, has been gathered over the years since the original equation appeared. Most applications are performed in the strong-coupling case (QCD), where the fundamental problems of the equation are more pronounced. The interested reader is here referred to some reviews of the field, where numerous references to original works can be found [29, 40–42, 54].

1.4 Helium Atom: Analytical Approach

An approach to solve the BS equation, known as the *external-potential approach*, was first developed by Sucher [59, 61] to evaluate the lowest-order QED contributions to the ground-state energy of the helium atom, and equivalent results were at the same time also derived by Araki [3]. The electrons are here assumed to move

in the field of the (infinitely heavy) atomic nucleus. The relative time of the two electrons is eliminated by integrating over the corresponding energy of the Fourier transform, which leads to a Schrödinger-like equation, as in the quasi-potential method. The solution of this equation is expanded in terms of a Brillouin–Wigner perturbation series. This work has been further developed and applied by Douglas and Kroll [19] and by Zhang and Drake [69, 70] by considering higher-order terms in the α and $Z\alpha$ expansions. This approach, which is reviewed in Chap. 11, can be used for light systems, such as light helium-like ions, where the power expansions are sufficiently convergent. The QED effects are here evaluated by means of highly correlated wave functions of Hylleraas type, which implies that QED and electron-correlation effects are highly mixed. A related technique, referred to as the *effective Hamiltonian approach*, has been developed and applied to helium-like systems by Pachucki and Sapirstein [43–45].

A problem that has been controversial for quite some time is the fine structure of the lowest P state of the neutral helium atom. The very accurate analytical results of Drake et al. and by Pachucki et al. give results close to the experimental results obtained by Gabrielse and others [68], but there have for quite some time been significant deviations – well outside the estimated limits of error. Very recently, Pachucki and Yerokhin have by means of improved calculations shown that the controversy has been resolved [46, 47, 66, 67].

1.5 Field-Theoretical Approach to Many-Body Perturbation Theory

The methods previously mentioned for numerical QED calculations can for computational reasons be applied only to one- and two-photon exchange, which implies that the electron correlation is treated at most to second order. This might be sufficiently accurate for highly charged systems, where the QED effects dominate over the electron correlation, but is usually quite insufficient for lighter systems, where the situation is reversed. To remedy the situation to some extent, higher-order many-body contributions can be added to the two-photon energy, a technique applied by the Gothenburg and St Petersburg groups [4,48].

In the numerical procedures for standard (relativistic) MBPT, the electron correlation can be evaluated effectively to essentially all orders by technique of coupled-cluster type. QED effects can here be included only as first-order energy corrections, a technique applied particularly by the Notre-Dame group [49]. To treat electron correlation, relativity and QED in a unified manner would require a field-theoretical approach.

The above-mentioned methods for QED calculations are all based upon field-theory. Of these methods, the covariant-evolution method has the advantage that it has a structure that is quite akin to that of standard MBPT, which has the consequence that it can serve as a basis for a unified field-theoretical many-body approach. The QED effects can here be included in the wave function, which will

6 1 Introduction

make it possible to treat the QED and correlation effects in a more unified way. To solve this problem completely is a formidable task, but it will be a main theme of this book to describe how some steps can be taken in this direction, along the line that is presently being pursued by the Gothenburg atomic theory group. The covariant evolution operator, which describes the time evolution of the *relativistic* state vector, is the key tool in this treatment. This operator is closely related to the field-theoretical Green's function. It should be mentioned that a related idea was proposed by Leonard Rosenberg already 20 years ago [50], namely of including Coulomb interactions in the QED Hamiltonian, and this is essentially the procedure we are pursuing in this book.

The covariant evolution operator is singular, as is the standard evolution operator of nonrelativistic quantum mechanics, but the singularities can be eliminated in a similar way as the corresponding singularities of the Green's function. The regular part of the covariant evolution operator is referred to as the *Green's operator*, which can be regarded as an extension of the Green's-function concept and shown to serve as a link between field theory and standard many-body perturbation theory. The perturbation used in this procedure represents the interaction between the electromagnetic field and the individual electrons. This implies that the equations operate in an extended *photonic Fock space* with variable number of photons.

The strategy in dealing with the combined QED and correlation problem is first to construct a field-theoretical "QED potential" with a single retarded photon, containing all first-order QED effects (retardation, virtual pairs, radiative effects), which – after proper regularization and renormalization – can be included in a perturbative expansion of MBPT or coupled-cluster type. In this way, the QED effects can – for the first time – be built into the wave function and treated together with the electron correlation in a coherent manner. For practical reasons, only a single retarded photon (together with arbitrary number of Coulomb interactions) can be included in this procedure at present time, but due to the fact that these effects are included in the wave function, this corresponds to higher-order effects in the energy. When extended to interactions of multiphoton type, this leads for two-particle systems to the Bethe–Salpeter equation, and in the multireference case to an extension of this equation, referred to as the Bethe–Salpeter–Bloch equation.

In combining QED with electron correlation, it is necessary to work in the *Coulomb gauge*, in order to take advantage of the development in standard MBPT. Although this gauge is *noncovariant* in contrast to, for instance, the simpler Feynman gauge, it can be argued that the deviation from a fully covariant treatment will have negligible effect in practical applications when handled properly. This makes it possible to mix a larger number of Coulomb interactions with the retarded-photon interactions, which is expected to lead to the same ultimate result as a fully covariant approach but with faster convergence rate due to the dominating role of the Coulomb interaction.

The procedure can also be extended to systems with more than two electrons, and due to the complete compatibility between the standard and the extended procedures, the QED effects need only be included where they are expected to be most significant.

References 7

In principle, also the procedure outlined here leads to *individual times* for the particles involved, consistent with the full Bethe–Salpeter equation but not with the standard quantum-mechanical picture. We shall mainly work in the *equal-time approximation* here, and we shall not analyze effects beyond this approximation in any detail. It is expected that – if existing – any such effect would be extremely small for electronic systems.

References

- Adkins, G.S., Fell, R.N.: Bound-state formalism for positronium. Phys. Rev. A 60, 4461–75 (1999)
- 2. Adkins, G.S., Fell, R.N., Mitrikov, P.M.: Calculation of the positronium hyperfine interval using the Bethe-Salpeter formalism. Phys. Rev. A 65, 042,103 (2002)
- 3. Araki, H.: Quantum-Electrodynamical Corrections to Energy-levels of Helium. Prog. Theor. Phys. (Japan) 17, 619–42 (1957)
- 4. Artemyev, A.N., Shabaev, V.M., Yerokhin, V.A., Plunien, G., Soff, G.: *QED calculations of the n = 1 and n = 2 energy levels in He-like ions*. Phys. Rev. A **71**, 062,104 (2005)
- 5. Bethe, H.A.: The Electromagnetic Shift of Energy Levels. Phys. Rev. 72, 339–41 (1947)
- 6. Bethe, H.A., Salpeter, E.E.: An Introduction to Relativistic Quantum Field Theory. Quantum Mechanics of Two-Electron Atoms. Springer, Berlin (1957)
- 7. Bjorken, J.D., Drell, S.D.: Relativistic Quantum Fields. Mc-Graw-Hill Pbl. Co, N.Y. (196)
- 8. Bjorken, J.D., Drell, S.D.: *Relativistic Quantum Mechanics*. Mc-Graw-Hill Pbl. Co, N.Y. (1964)
- 9. Boldwin, G.T., Yennie, D.R., Gregorio, M.A.: Recoil effects in the hyperfine structure of QED bound states. Rev. Mod. Phys. 57, 723–82 (1985)
- Brandow, B.H.: Linked-Cluster Expansions for the Nuclear Many-Body Problem. Rev. Mod. Phys. 39, 771–828 (1967)
- 11. Breit, G.: Dirac's equation and the spin-spin interaction of two electrons. Phys. Rev. 39, 616–24 (1932)
- Brown, G.E., Ravenhall, D.G.: On the Interaction of Two electrons. Proc. R. Soc. London, Ser. A 208, 552–59 (1951)
- 13. Brueckner, K.A.: Many-Body Problems for Strongly Interacting Particles. II. Linked Cluster Expansion. Phys. Rev. 100, 36–45 (1955)
- 14. Caswell, W.E., Lepage, G.P.: Reduction of the Bethe-Salpeter equation to an equivalent Schrödinger equation, with applications. Phys. Rev. A 18, 810–19 (1978)
- 15. Connell, J.H.: *QED test of a Bethe-Salpeter solution method*. Phys. Rev. D **43**, 1393–1402 (1991)
- 16. Cutkosky, R.E.: Solutions of the Bethe-Salpeter equation. Phys. Rev. 96, 1135–41 (1954)
- 17. Dirac, P.A.M.: Roy. Soc. (London) 117, 610 (1928)
- Dirac, P.A.M.: The Principles of Quantum Mechanics. Oxford Univ. Press, Oxford (1930, 1933, 1947, 1958)
- Douglas, M.H., Kroll, N.M.: Quantum Electrodynamical Corrections to the Fine Structure of Helium. Ann. Phys. (N.Y.) 82, 89–155 (1974)
- Dyson, F.J.: The radiation Theories of Tomonaga, Schwinger, and Feynman. Phys. Rev. 75, 486–502 (1949)
- 21. Dyson, F.J.: The Wave Function of a Relativistic System. Phys. Rev. 91, 1543–50 (1953)
- 22. Feynman, R.P.: Space-Time Approach to Quantum Electrodynamics. Phys. Rev. **76**, 769–88 (1949)
- 23. Feynman, R.P.: *The Theory of Positrons*. Phys. Rev. **76**, 749–59 (1949)
- 24. Froese-Fischer, C.: *The Hartree-Fock method for atoms*. John Wiley and Sons, New York, London, Sidney, Toronto (1977)

8 1 Introduction

- 25. Gaunt, J.A.: The Triplets of Helium. Proc. R. Soc. London, Ser. A 122, 513–32 (1929)
- 26. Gell-Mann, M., Low, F.: Bound States in Quantum Field Theory. Phys. Rev. 84, 350-54 (1951)
- Goldstein, J.S.: Properties of the Salpeter-Bethe Two-Nucleon Equation. Phys. Rev. 91, 1516–24 (1953)
- Goldstone, J.: Derivation of the Brueckner many-body theory. Proc. R. Soc. London, Ser. A 239, 267–279 (1957)
- 29. Grotch, H., Owen, D.A.: Bound states in Quantum Electrodynamics: Theory and Applications. Fundamentals of Physics **32**, 1419–57 (2002)
- 30. Grotch, H., Yennie, D.R.: Effective Potential Model for Calculating Nuclear Corrections to the Eenergy Levels of Hydrogen. Rev. Mod. Phys. 41, 350–74 (1969)
- 31. Kelly, H.P.: Application of many-body diagram techniques in atomic physics. Adv. Chem. Phys. 14, 129–190 (1969)
- 32. Kusch, P., Foley, H.M.: Precision Measurement of the Ratio of the Atomic 'g Values' in the ${}^{2}P_{3/2}$ and ${}^{2}P_{1/2}$ States of Gallium. Phys. Rev. **72**, 1256–57 (1947)
- 33. Kusch, P., Foley, H.M.: On the Intrinsic Moment of the Electron. Phys. Rev. 73, 412 (1948)
- 34. Lamb, W.W., Retherford, R.C.: Fine structure of the hydrogen atom by microwave method. Phys. Rev. 72, 241–43 (1947)
- 35. Lindgren, I.: The Rayleigh-Schrödinger perturbation and the linked-diagram theorem for a multi-configurational model space. J. Phys. B 7, 2441–70 (1974)
- 36. Lindgren, I., Salomonson, S., Åsén, B.: *The covariant-evolution-operator method in bound-state QED*. Physics Reports **389**, 161–261 (2004)
- 37. Mahan, G.D.: Many-particle Physics, second edition. Springer Verlag, Heidelberg (1990)
- 38. Mohr, P.J.: Numerical Evaluation of the 1s_{1/2}-State Radiative Level Shift. Ann. Phys. (N.Y.) **88**, 52–87 (1974)
- Mohr, P.J., Plunien, G., Soff, G.: QED corrections in heavy atoms. Physics Reports 293, 227–372 (1998)
- Nakanishi, N.: Normalization condition and normal and abnormal solutions of Bethe-Salpeter equation. Phys. Rev. 138, B1182 (1965)
- 41. Namyslowski, J.M.: *The Relativistic Bound State Wave Function*. in *Light-Front Quantization and Non-Perturbative QCD*, J.P. Vary and F. Wolz, eds. (International Institute of Theoretical and Applied Physics, Ames) (1997)
- 42. Onida, G., Reining, L., Rubio, A.: *Electronic excitations: density-functional versus many-body Green's-function approaches.* Rev. Mod. Phys. **74**, 601–59 (2002)
- 43. Pachucki, K.: Quantum electrodynamics effects on helium fine structure. J. Phys. B 32, 137–52 (1999)
- 44. Pachucki, K.: Improved Theory of Helium Fine Structure. Phys. Rev. Lett. 97, 013,002 (2006)
- 45. Pachucki, K., Sapirstein, J.: Contributions to helium fine structure of order $m\alpha^7$. J. Phys. B 33, 5297–5305 (2000)
- Pachucky, K., Yerokhin, V.A.: Reexamination of the helium fine structure (vol 79, 062516, 2009). Phys. Rev. Lett. 80, 19,902 (2009)
- Pachucky, K., Yerokhin, V.A.: Reexamination of the helium fine structure (vol 79, 062516, 2009). Phys. Rev. A 81, 39,903 (2010)
- 48. Persson, H., Salomonson, S., Sunnergren, P., Lindgren, I.: Two-electron Lamb-Shift Calculations on Heliumlike Ions. Phys. Rev. Lett. 76, 204–07 (1996)
- 49. Plante, D.R., Johnson, W.R., Sapirstein, J.: Relativistic all-order many-body calculations of the n = 1 and n = 2 states of heliumlike ions. Phys. Rev. A 49, 3519–30 (1994)
- 50. Rosenberg, L.: Virtual-pair effects in atomic structure theory. Phys. Rev. A 39, 4377–86 (1989)
- Salpeter, E.E.: Mass Correction to the Fine Structure of Hydrogen-like Atoms. Phys. Rev. 87, 328–43 (1952)
- 52. Salpeter, E.E., Bethe, H.A.: A Relativistic Equation for Bound-State Problems. Phys. Rev. 84, 1232–42 (1951)
- 53. Sazdjian, H.: Relativistiv wave equations for the dynamics of two interacting particles. Phys. Rev. D 33, 3401–24 (1987)

References 9

54. Sazdjian, H.: The connection of two-particle relativistic quantum mechanics with the Bethe-Salpeter equation. J. Math. Phys. 28, 2618–38 (1987)

- 55. Schweber, S.S.: *The men who madt it: Dyson, Feynman, Schwinger and Tomonaga*. Princeton University Press, Princeton (1994)
- 56. Schwinger, J.: Quantum electrodynamics I. A covariant formulation. Phys. Rev. 74, 1439 (1948)
- 57. Shabaev, V.M.: Two-times Green's function method in quantum electrodynamics of high-Z few-electron atoms. Physics Reports 356, 119–228 (2002)
- 58. Slater, J.: Quantum Theory of Atomic Spectra. McGraw-Hill, N.Y. (1960)
- Sucher, J.: Energy Levels of the Two-Electron Atom to Order α³ Ry; Ionization Energy of Helium. Phys. Rev. 109, 1010–11 (1957)
- 60. Sucher, J.: S-Matrix Formalism for Level-Shift Calculations. Phys. Rev. 107, 1448–54 (1957)
- Sucher, J.: Ph.D. thesis, Columbia University (1958). Univ. Microfilm Internat., Ann Arbor, Michigan
- Sucher, J.: Foundations of the Relativistic Theory of Many Electron Atoms. Phys. Rev. A 22, 348–62 (1980)
- 63. Todorov, I.T.: Quasipotential Equation Corresponding to the relativistic Eikonal Approximation. Phys. Rev. D 3, 2351–56 (1971)
- 64. Tomanaga, S.: On Infinite Field Reactions in Quantum Field Theory. Phys. Rev. 74, 224–25 (1948)
- 65. Wick, G.C.: Properties of Bethe-Salpeter Wave Functions. Phys. Rev. 96, 1124–34 (1954)
- 66. Yerokhin, K.P.V.A.: Reexamination of the helium fine structure. Phys. Rev. Lett. **79**, 62,616 (2009)
- 67. Yerokhin, K.P.V.A.: Fine Structure of Heliumlike Ions and Determination of the Fine Structure Constant. Phys. Rev. Lett. **104**, 70,403 (2010)
- 68. Zelevinsky, T., Farkas, D., Gabrielse, G.: Precision Measurement of the Three 2³ P_J Helium Fine Structure Intervals. Phys. Rev. Lett. **95**, 203,001 (2005)
- 69. Zhang, T.: Corrections to $O(\alpha^7(\ln \alpha)mc^2)$ fine-structure splittings and $O(\alpha^6(\ln \alpha)mc^2)$ energy levels in helium. Phys. Rev. A **54**, 1252–1312 (1996)
- 70. Zhang, T., Drake, G.W.F.: Corrections to $O(\alpha^7 mc^2)$ fine-structure splitting in helium. Phys. Rev. A **54**, 4882–4922 (1996)

Part I Basics: Standard Many-Body Perturbation Theory

Chapter 2

Time-Independent Formalism

In this first part of the book, we shall review some basics of quantum mechanics and the many-body theory for bound electronic systems that will form the foundations for the following treatment. This material can also be found in several standard text books. The time-independent formalism is summarized in the present chapter¹ and the time-dependent formalism in the following one.

2.1 First Quantization

First quantization is the term for the elementary treatment of quantized systems, where the particles of the system are treated quantum-mechanically, for instance, in terms of Schrödinger wave functions, while the surrounding fields are treated classically.

2.1.1 De Broglie's Relations

As an introduction to the quantum mechanics, we shall derive the Schrödinger equation from the classical relations of de Broglie.

According to Planck–Einstein's quantum theory, the electromagnetic radiation is associated with particle-like *photons* with the energy (E) and momentum (p) given by the relations

$$\begin{cases} E = h\nu = \omega\hbar \\ p = h/\lambda = \hbar k \end{cases}$$
 (2.1)

¹ This chapter is essentially a short summary of the second part of the book *Atomic Many-Body Theory* by Lindgren and Morrison, and the reader who is not well familiar with the subject is recommended to consult that book.

where $\hbar = h/2\pi$, h being Planck's constant (see further Appendix K), ν the cyclic frequency of the radiation (cycles/s) and $\omega = 2\pi\nu$ the angular frequency (radians/s). $\lambda = c/\nu$ (c being the velocity of light in vacuum) is the wavelength of the radiation and $k = 2\pi/\lambda$ the wave number.

De Broglie assumed that the relations (2.1) for photons would hold also for material particles, like electrons. Nonrelativistically, we have for a free electron in one dimension

$$E = \frac{p^2}{2m_e} \qquad \text{or} \qquad \hbar\omega = \frac{\hbar^2 k^2}{2m_e},\tag{2.2}$$

where m_e is the mass of the electron.

De Broglie assumed that a particle could be represented by a wave packet

$$\chi(t,x) = \int dk \, a(k) \, e^{i(kx - \omega t)}. \tag{2.3}$$

The relation (2.2) then leads to the one-dimensional wave equation for a free electron

$$i\hbar \frac{\partial \chi(t,x)}{\partial t} = -\frac{\hbar^2}{2m_e} \frac{\partial^2 \chi(t,x)}{\partial x^2},$$
 (2.4)

which is the Schrödinger equation for a free particle. This can be obtained from the first of the relations (2.2) by means of the substitutions

$$E \to i\hbar \frac{\partial}{\partial t} \qquad p \to -i\hbar \frac{\partial}{\partial x}.$$
 (2.5)

2.1.2 The Schrödinger Equation

We can generalize the treatment above to an electron in three dimensions in an external field, $v_{\text{ext}}(x)$, for which the energy Hamiltonian is

$$E = H = \frac{\mathbf{p}^2}{2m_e} + v_{\text{ext}}(\mathbf{x}). \tag{2.6}$$

Generalizing the substitutions above to²

$$\mathbf{p} \to \hat{\mathbf{p}} = -i\hbar \nabla$$
 and $x \to \hat{x} = x$, (2.7)

where ∇ is the vector gradient operator (see Appendix A.1) leads to the *Hamilton* operator

$$\hat{H} = \frac{\hat{\mathbf{p}}^2}{2m_a} + v_{\text{ext}}(\mathbf{x}) = -\frac{\hbar^2}{2m_a} \nabla^2 + v_{\text{ext}}(\mathbf{x})$$
 (2.8)

² Initially, we shall use the 'hat' symbol to indicate an *operator*, but later we shall use this symbol only when the operator character needs to be emphasized.

and to the Schrödinger equation for a single electron

$$i\hbar \frac{\partial}{\partial t} \chi(t, \mathbf{x}) = \hat{H} \chi(t, \mathbf{x}) = \left(-\frac{\hbar^2}{2m_e} \nabla^2 + v_{\text{ext}}(\mathbf{x}) \right) \chi(t, \mathbf{x}).$$
 (2.9)

For an N-electron system, the Schrödinger equation becomes correspondingly³

$$i\hbar \frac{\partial}{\partial t} \chi(t; \boldsymbol{x}_1, \boldsymbol{x}_2, \cdots \boldsymbol{x}_N) = \hat{H} \chi(t; \boldsymbol{x}_1, \boldsymbol{x}_2, \cdots \boldsymbol{x}_N), \tag{2.10}$$

where we assume the Hamiltonian to be of the form $\hat{H} = \hat{H}_1 + \hat{H}_2$ [see Appendix (B.19)]⁴

$$\hat{H}_{1} = \sum_{n=1}^{N} \left(-\frac{\hbar^{2}}{2m_{e}} \nabla_{n}^{2} + v_{\text{ext}}(\boldsymbol{x}_{n}) \right) =: \sum_{n=1}^{N} \hat{h}_{1}(n),$$

$$\hat{H}_{2} = \sum_{m < n}^{N} \frac{e^{2}}{4\pi \epsilon_{0} r_{mn}} =: \sum_{m < n}^{N} \hat{h}_{2}(m, n).$$
(2.11)

Here, r_{mn} is the interelectronic distance, $r_{mn} = |x_m - x_n|$ and v_{ext} represents the external (essentially nuclear) energy potential.

Generally, the quantum-mechanical operators \hat{A} , \hat{B} that represent the corresponding classical quantities A, B in the Hamilton formulation (see Appendix E) should satisfy the *quantization condition*

$$[\hat{A}, \hat{B}] = \hat{A}\hat{B} - \hat{B}\hat{A} = i\hbar\{A, B\},$$
 (2.12)

where the square bracket (with a comma) represents the *commutator* and the curly bracket the *Poisson bracket* (E.10). For *conjugate momenta*, like the coordinate vector \mathbf{x} and the momentum vector \mathbf{p} , the Poisson bracket equals unity, and the quantization conditions for the corresponding operators become

$$[\hat{x}, \hat{p_x}] = [\hat{y}, \hat{p_y}] = [\hat{z}, \hat{p_z}] = i\hbar,$$
 (2.13)

which is consistent with the substitutions (2.7).

We shall be mainly concerned with *stationary*, *bound states of electronic systems*, for which the wave function can be separated into a time function and a space function

$$\gamma(t; x_1, \dots, x_N) = F(t) \Psi(x_1, x_2, \dots, x_N).$$

³ Note that according to the quantum-mechanical picture the wave function has a *single time* also for a many-electron system. This question will be discussed further below.

⁴ The symbol "=:" indicates that this is a definition.

As shown in standard text books, this leads to a separation into two equations, one for the time part and one for the space part. The time equation becomes

$$i\hbar \frac{\partial}{\partial t} F(t) = E F(t),$$

with the solution

$$F(t) \propto e^{-iEt/\hbar}$$

and the space part is the standard time-independent Schrödinger equation

$$\hat{H}\Psi(x_1,\cdots x_N) = E\,\Psi(x_1,\cdots x_N). \tag{2.14}$$

Thus, for stationary states the time-dependent wave function is of the form

$$\chi(t; \mathbf{x}_1, \dots \mathbf{x}_N) = e^{-iEt/\hbar} \Psi(\mathbf{x}_1, \dots \mathbf{x}_N). \tag{2.15}$$

The separation constant E is interpreted as the energy of the state.

2.2 Second Quantization

2.2.1 Schrödinger Equation in Second Quantization*

In the following, we shall consistently base our treatment upon *second quantization*, which implies that also the particles and fields are quantized and expressed in terms of (creation and absorption) field operators (see Appendices B and C). Here, we shall first derive the second-quantized form of the time-dependent Schrödinger equation (SE) (2.9), which reads

$$i\hbar \frac{\partial}{\partial t} |\chi(t)\rangle = H|\chi(t)\rangle.$$
 (2.16)

With the partitioning (2.11), the operator becomes in second quantization (B.12)

$$\hat{H} = c_i^{\dagger} \langle i|h_1|j\rangle c_j + \frac{1}{2}c_i^{\dagger}c_j^{\dagger} \langle ij|h_2|kl\rangle c_l c_k$$
 (2.17)

and the state is expressed as a vector (C.4). The equation (2.16) is by no means obvious, and we shall here indicate the proof. (The proof follows largely that given by Fetter and Walecka [19, Chap. 1].)

For the sake of concretization, we consider a two-electron system. With the coordinate representation (C.19) of the state vector

$$\chi(x_1, x_2) = \langle x_1, x_2 | \chi(t) \rangle, \qquad (2.18)$$

the SE (2.16) becomes

$$i\hbar \frac{\partial}{\partial t} \langle x_1, x_2 | \chi(t) \rangle = \langle x, x_2 | H | \chi(t) \rangle. \tag{2.19}$$

We consider first the effect of the one-body part of the Hamiltonian (2.17) operating on the wave function (2.18), and we shall show that this is equivalent to operating with the second-quantized form of the operator (B.19)

$$\hat{H} = c_i^{\dagger} \langle i | h_1 | j \rangle c_j \tag{2.20}$$

on the state vector $| \chi(t) \rangle$.

We start by expanding the state vector in terms of straight products of singleelectron state vectors $(t_1 = t_2 = t)$

$$|\chi(t)\rangle = a_{kl}(t)|k\rangle|l\rangle,$$
 (2.21)

 $(a_{kl} = -a_{lk})$. The coordinate representation of this relation is

$$\chi(x_1, x_2) = \langle x_1, x_2 | \chi(t) \rangle = a_{kl}(t) \langle x_1 | k \rangle \langle x_2 | l \rangle. \tag{2.22}$$

We now operate with the single-particle operator (2.20) on the state vector expansion (2.21)

$$\hat{H}_1|\chi(t)\rangle = c_i^{\dagger} \langle i|h_1|j\rangle c_i a_{kl}(t)|k\rangle|l\rangle. \tag{2.23}$$

For j = k, the electron in position 1 is annihilated in the state k and replaced by an electron in the state i, yielding

$$\langle i | h_1 | k \rangle \ a_{kl}(t) | i \rangle | l \rangle$$
.

The coordinate representation of this relation becomes

$$\langle x_1|i\rangle\langle i|h_1|k\rangle \ a_{kl}(t)\langle x_2|l\rangle = \langle x_1|h_1|k\rangle \ a_{kl}(t)\langle x_2|l\rangle$$

using the resolution of the identity (C.12). The right-hand side of (2.23) can also be expressed

$$h_1(x_1)\phi_k(x_1)\phi_l(x_2) a_{kl}(t) = h_1(x_1)\chi(x_1, x_2).$$

Together with the case j = l this leads to

$$\langle x_1, x_2 | H_1 | \chi(t) \rangle = (h_1(x_1) + h_1(x_2)) \chi(x_1, x_2) = H_1 \chi(x_1, x_2).$$

Thus, we have shown the important relation

$$\langle x_1, x_2 | H_1 | \chi(t) \rangle = H_1 \chi(x_1, x_2).$$
 (2.24)

A similar relation can be derived for the two-body part of the Hamiltonian, which implies that

$$\langle \mathbf{x}_1, \mathbf{x}_2 | H | \chi(t) \rangle = H \chi(x_1, x_2) \tag{2.25}$$

and from the relation (2.19)

$$i\hbar \frac{\partial}{\partial t} \langle \mathbf{x}_1, \mathbf{x}_2 | \chi(t) \rangle = \langle \mathbf{x}_1, \mathbf{x}_2 | H | \chi(t) \rangle. \tag{2.26}$$

This is the coordinate representation of the Schrödinger equation (2.16), which is thus verified. It should be observed that (2.16) does not contain any space coordinates. The treatment is here performed for the two-electron case, but it can easily be extended to the general case.

2.2.2 Particle-Hole Formalism: Normal Order and Contraction

In the *particle–hole formalism*, we separate the single-particle states into *particle and hole states*, a division that is to some extent arbitrary. Normally, core states (closed-shell states) are treated as hole states and virtual and valence states as particle states, but sometimes it might be advantageous to treat some closed-shell states as valence states or some valence states as hole states.

If time increases from right to left, the creation/annihilation operators are said to be *time ordered*. Time ordering can be achieved by using the *Wick time-ordering operator*, which for fermions reads

$$T[A(t_1)B(t_2)] = \begin{cases} A(t_1)B(t_2) & (t_1 > t_2) \\ -B(t_2)A(t_1) & (t_1 < t_2) \end{cases}$$
 (2.27)

The case $t_1 = t_2$ will be discussed later.

The creation/annihilation operators are said to be in <u>normal order</u>, if the particle-creation and hole-annihilation operators appear to the left of the particle-annihilation and hole-creation operators

$$c_{\rm p}^{\dagger}c_{\rm p}c_{\rm h}c_{\rm h}^{\dagger}, \qquad (2.28)$$

where p,h stand for particle/hole states.

• A <u>contraction</u> of two operators is defined as the <u>difference between the time-ordered and the normal-ordered products</u>,

$$\boxed{x \ y = T[xy] - N[xy]}.$$
 (2.29)

In the following, we shall use *curly brackets to denote the normal product* [38]

$$N[xy] \equiv \{x \ y\}. \tag{2.30}$$

From these definitions, it follows that the nonvanishing contractions of the *electron-field operators* (B.28) are

$$\hat{\psi}_{+}(x_{1})\hat{\psi}_{+}^{\dagger}(x_{2}) = -\hat{\psi}_{+}^{\dagger}(x_{2})\hat{\psi}_{+}(x_{1}) = \begin{cases}
\phi_{p}(x_{1})\phi_{p}^{*}(x_{2}) e^{-i\varepsilon_{p}(t_{1}-t_{2})/\hbar} & t_{1} > t_{2} \\
0 & t_{1} < t_{2}
\end{cases},$$

$$\hat{\psi}_{-}(x_{1})\hat{\psi}_{-}^{\dagger}(x_{2}) = -\hat{\psi}_{-}^{\dagger}(x_{2})\hat{\psi}_{-}(x_{1}) = \begin{cases}
0 & t_{1} > t_{2} \\
\phi_{h}(x_{1})\phi_{h}^{*}(x_{2}) e^{-i\varepsilon_{h}(t_{1}-t_{2})/\hbar} & t_{1} < t_{2}
\end{cases}.$$

$$(2.31)$$

Here, $\hat{\psi}_{\pm}$ represents the positive-/negative-energy part of the spectrum, respectively, and ϕ_p and ϕ_h denote particle (positive-energy) and hole (negative-energy) states, respectively.

The results can be summarized as

$$\hat{\psi}(x_1)\hat{\psi}^{\dagger}(x_2) = -\hat{\psi}^{\dagger}(x_2)\hat{\psi}(x_1) = \phi_j(x_1)\phi_j^*(x_2) e^{-i\varepsilon_j(t_1 - t_2)/\hbar}, \qquad (2.32)$$

if $t_1 > t_2$ for particles and $t_1 < t_2$ for holes with all other contractions vanishing.

2.2.3 Wick's Theorem

The handling of operators in second quantization is greatly simplified by *Wick's theorem* [80] (for an introduction, see, for instance, Fetter and Walecka [19, Sect. 8] or Lindgren and Morrison [40, Chap. 11]), which states that a product of creation and annihilation operators \hat{A} can be written as the normal product plus all single, double ... contractions with the uncontracted operators in normal form, or symbolically

$$\hat{A} = \{\hat{A}\} + \{\hat{A}\}. \tag{2.33}$$

A particularly useful form of Wick's theorem is the following. If \hat{A} and \hat{B} are operators in normal form, then the product is equal to the normal product plus all normal-ordered contractions between \hat{A} and \hat{B} , or formally

$$\hat{A}\,\hat{B} = \{\hat{A}\,\hat{B}\} + \{\hat{A}\,\hat{B}\}. \tag{2.34}$$

With this formulation, there are no further contractions within the operators to be multiplied. This forms the basic rule for the graphical representation of the operators and operator relations to be discussed below.

2.3 Time-Independent Many-Body Perturbation Theory

2.3.1 Bloch Equation

Here, we shall summarize the most important concepts of standard time-independent many-body perturbation theory (MBPT) as a background for the further treatment. (For more details, the reader is referred to designated books, such as Lindgren–Morrison, *Atomic Many-Body Theory* [40].)

We are considering a number of stationary electronic states, $|\Psi^{\alpha}\rangle$ ($\alpha=1\cdots d$), termed *target states*, that satisfy the Schrödinger equation

$$H|\Psi^{\alpha}\rangle = E^{\alpha}|\Psi^{\alpha}\rangle \quad (\alpha = 1 \cdots d).$$
 (2.35)

For each target state, there exists an "approximate" or $\underline{model\ state}$, $|\Psi_0^{\alpha}\rangle$ ($\alpha=1\cdots d$), which is more easily accessible and which forms the starting point for the perturbative treatment. We assume that the model states are linearly independent and that they span a $\underline{model\ space}$. The $\underline{projection\ operator}$ for the model space is denoted P and that for the complementary or $\underline{orthogonal\ space}$ by Q, which together form the $\underline{identity\ operator}$

$$P + Q = I. (2.36)$$

A <u>wave operator</u> is introduced – also known as the Møller operator [53] – which transforms the model states back to the exact states,

$$|\Psi^{\alpha}\rangle = \Omega |\Psi_0^{\alpha}\rangle \quad (\alpha = 1 \cdots d)$$
 (2.37)

and this operator is the same for all states under consideration.

We define an <u>effective Hamiltonian</u> with the property that operating on a model function it generates the corresponding <u>exact</u> energy

$$H_{\text{eff}}|\Psi_0^{\alpha}\rangle = E^{\alpha}|\Psi_0^{\alpha}\rangle \quad (\alpha = 1 \cdots d),$$
 (2.38)

with the eigenvectors representing the model states. Operating on this equation with Ω from the left, using the definition (2.37), yields

$$\Omega H_{\text{eff}} |\Psi_0^{\alpha}\rangle = E^{\alpha} |\Psi^{\alpha}\rangle, \qquad (2.39)$$

which we compare with the Schrödinger equation (2.35)

$$H\Omega|\Psi_0^{\alpha}\rangle = E^{\alpha}|\Psi^{\alpha}\rangle.$$
 (2.40)

Since this relation holds for each state of the model space, we have the important operator relation

$$\Omega H_{\text{eff}} P = H \Omega P, \qquad (2.41)$$

which as known as the generalized Bloch equation.

The form above of the Bloch equation is valid independently on the choice of normalization. In the following, we shall mainly work with the <u>intermediate</u> normalization (IN), which implies

$$\langle \Psi_0^{\alpha} | \Psi^{\alpha} \rangle = 1, \tag{2.42a}$$

$$|\Psi_0^{\alpha}\rangle = P|\Psi^{\alpha}\rangle \quad (\alpha = 1 \cdots d).$$
 (2.42b)

Then we have after projecting the Schrödinger equation onto the model space

$$PH\Omega|\Psi_0^{\alpha}\rangle = E^{\alpha}|\Psi_0^{\alpha}\rangle \tag{2.43}$$

and we find that the effective Hamiltonian (2.38) becomes in IN

$$H_{\text{eff}} = PH\Omega P. \tag{2.44}$$

Normally, the multidimensional or multireference model space is applied in connection with *valence universality*, implying that the same operators are used for different stages of ionization (see further Sect. 2.5).

2.3.2 Partitioning of the Hamiltonian

For electrons moving in an external (nuclear) potential, v_{ext} , the single-electron (Schrödinger) Hamiltonian (2.8) is

$$h_{\rm S} = -\frac{\hbar^2}{2m_{\rm e}} \, \nabla^2 + v_{\rm ext}.$$
 (2.45)

The corresponding Schrödinger equation

$$h_{S} \phi_{i}(\mathbf{x}) = \varepsilon_{i} \phi_{i}(\mathbf{x}) \tag{2.46}$$

generates a complete spectrum of functions, which can form the basis for numerical calculations. This is known to as the *Furry picture*. These single-electron functions are normally referred to as (single-electron) *orbitals* – or *spin-orbitals*, if a spin eigenfunction is adhered. Degenerate orbitals (with the same eigenvalue) form an *electron shell*.

The Hamiltonian for a many-electron system (2.11) is

$$H = \sum_{n}^{N} \left(-\frac{\hbar^2}{2m_e} \nabla^2 + v_{\text{ext}} \right)_n + \sum_{n < m}^{N} \frac{e^2}{4\pi\epsilon_0 \, r_{nm}},\tag{2.47}$$

where the last term represents the interelectronic interaction. For the perturbation treatment, we separate the many-electron Hamiltonian into

$$H = H_0 + V, (2.48)$$

where H_0 a model Hamiltonian that is a sum of single-electron Hamiltonians

$$H_0 = \sum_{n=0}^{N} \left(-\frac{\hbar^2}{2m_e} \nabla^2 + v_{\text{ext}} + u \right)_n =: \sum_{n=0}^{N} h_0(n)$$
 (2.49)

and V is a perturbation

$$V = -\sum_{n=0}^{N} u_n + \sum_{n \le m}^{N} \frac{e^2}{4\pi\epsilon_0 \, r_{nm}}.$$
 (2.50)

The potential u is optional and used primarily to improve the convergence properties of the perturbation expansion.

The *antisymmetrized* N-electron eigenfunctions of H_0 can be expressed as determinantal products of single-electron orbitals (see Appendix B)

$$H_0 \Phi_A(x_1, x_2 \cdots x_N) = E_0^A \Phi_A(x_1, x_2 \cdots x_N),$$

$$\Phi_A(x_1, x_2 \cdots x_N) = 1/\sqrt{N!} \mathcal{A}\{\phi_1(x_1)\phi_2(x_2) \cdots \phi_N(x_N)\}, \quad (2.51)$$

where A is an antisymmetrizing operator. The determinants are referred to as *Slater determinants* and constitute our basis functions. The eigenvalues are given by

$$E_0 = \sum_{n=1}^{N} \varepsilon_n \tag{2.52}$$

summed over the spin-orbitals of the determinant.

Degenerate determinants form a *configuration*. The model space is supposed to be formed by one or several configurations that can have different energies. We distinguish between three kinds of orbitals

- Core orbitals, present in all determinants of the model space
- Valence orbitals, present in some determinants of the model space
- Virtual orbitals, not present in any determinants of the model space

The model space is said to be <u>complete</u>, if it contains all configurations that can be formed by distributing the <u>valence</u> electrons among the valence orbitals in all <u>possible ways</u>. In the following, we shall normally assume this to be the case.

With the partitioning (2.48), the Bloch equation above can be expressed

$$\boxed{(\Omega H_{\text{eff}} - H_0 \Omega) P = V \Omega P.}$$
(2.53)

With H_0 of the form (2.49), it commutes with the projection operator P. Then, we find that

$$H_{\rm eff} = PH_0P + PV\Omega P \tag{2.54}$$

and we shall refer to the second term as the effective interaction

$$V_{\text{eff}} = P V \Omega P. \tag{2.55}$$

• The partitioning leads to the commonly used form of the *generalized Bloch equation* [36, 37, 40]

$$[\Omega, H_0] P = Q (V\Omega - \Omega V_{\text{eff}}) P, \qquad (2.56)$$

which is frequently used as the basis for many-body perturbation theory (MBPT). The last term appears only for open-shell systems with unfilled valence shell(s) and is graphically represented by so-called *folded* or *backwards* diagrams, first introduced by Brandow in nuclear physics [7], (see further below).

If the model space is completely degenerate with a single energy E_0 , the general Bloch equation reduces to its original form, derived in the late 1950s by Claude Bloch [4,5],

$$(E_0 - H_0) \Omega P = V \Omega P - \Omega V_{\text{eff}}. \tag{2.57}$$

This equation can be used to generate the standard *Rayleigh–Schrödinger* perturbation expansion, found in many text books.

The generalized Bloch equation (2.56) is valid for a general model space, which can contain different zeroth-order energy levels. Using such an *extended model space* represents usually a convenient way of treating very closely spaced or *quasi-degenerate* unperturbed energy levels, a phenomenon that otherwise can lead to serious convergence problems. This can be illustrated by the relativistic calculation of the fine structure of helium-like ions, where a one-dimensional model space leads to convergence problems for light elements, a problem that can normally be remedied in a straightforward way by means of the extended model space [50, 62]. But the extended model space can also lead to problems, due to so-called *intruder states*, as will be further discussed below.

With an extended model space, we can separate the projection operator into the corresponding energy components⁵

$$P = \sum_{\mathcal{E}} P_{\mathcal{E}}; \qquad H_0 P_{\mathcal{E}} = \mathcal{E} P_{\mathcal{E}}. \tag{2.58}$$

 $^{^5}$ In the case of an extended model space, we shall normally use the symbol ${\cal E}$ for the different energies of the model space.

Operating with the general Bloch equation (2.56) on a particular component, then yields

$$(\mathcal{E} - H_0) \Omega P_{\mathcal{E}} = Q (V\Omega - \Omega V_{\text{eff}}) P_{\mathcal{E}}. \tag{2.59}$$

Expanding the wave operator order-by-order

$$\Omega = 1 + \Omega^{(1)} + \Omega^{(2)} + \cdots \tag{2.60}$$

leads to the recursive formula

$$(\mathcal{E} - H_0) \Omega^{(n)} P_{\mathcal{E}} = Q \left(V \Omega^{(n-1)} - (\Omega V_{\text{eff}})^{(n)} \right) P_{\mathcal{E}}$$
 (2.61)

or

$$\Omega^{(n)} P_{\mathcal{E}} = \Gamma_{\mathcal{Q}}(\mathcal{E}) \left(V \Omega^{(n-1)} - (\Omega V_{\text{eff}})^{(n)} \right) P_{\mathcal{E}}, \tag{2.62}$$

where

$$V_{\text{eff}}^{(k)} = P V \Omega^{(k-1)} P. \tag{2.63}$$

Here,

$$\Gamma(\mathcal{E}) = \frac{1}{\mathcal{E} - H_0} \tag{2.64}$$

and

$$\Gamma_O(\mathcal{E}) = Q\Gamma(\mathcal{E}) \tag{2.65}$$

are known as the resolvent and the reduced resolvent, respectively [45].

The recursive formula (2.62) can generate a *generalized form of the Rayleigh–Schrödinger perturbation expansion* (see [40, Chap. 9]), valid also for a *quasi-degenerate model space*. We see from the form of the resolvent that in each new order of the perturbation expansion there is a denominator equal to the energy difference between the initial and final states. This leads to the *Goldstone rules* in the evaluation of the time-ordered diagrams to be considered in the following section.

Even if the perturbation is energy independent, we see that the wave operator and effective interaction will still generally be energy dependent, due to the energy dependence of the resolvent. In first order, we have

$$\Omega^{(1)}P_{\mathcal{E}} = \Gamma_Q(\mathcal{E})VP_{\mathcal{E}} \tag{2.66}$$

and in second order

$$\Omega^{(2)}(\mathcal{E})P_{\mathcal{E}} = \Gamma_{\mathcal{Q}}(\mathcal{E})\left(V\Omega^{(1)}(\mathcal{E}) - \Omega^{(1)}(\mathcal{E}')P_{\mathcal{E}'}V_{\text{eff}}^{(1)}\right)P_{\mathcal{E}},\tag{2.67}$$

where $V_{\rm eff}^{(1)} = PVP$. Note that the wave operator in the last term operates on the projection operator $P_{\mathcal{E}'}$ and therefore depends on the corresponding energy \mathcal{E}' . We now have

$$\frac{\delta\Omega^{(1)}(\mathcal{E})}{\delta\mathcal{E}} = \frac{\delta\Gamma_{\mathcal{Q}}(\mathcal{E})}{\delta\mathcal{E}}V = \frac{\Gamma_{\mathcal{Q}}(\mathcal{E}') - \Gamma_{\mathcal{Q}}(\mathcal{E})}{\mathcal{E}' - \mathcal{E}}V = -\Gamma_{\mathcal{Q}}(\mathcal{E})\Gamma_{\mathcal{Q}}(\mathcal{E}')V$$

$$= -\Gamma_{\mathcal{Q}}(\mathcal{E})\Omega^{(1)}(\mathcal{E}') \tag{2.68}$$

and we note that the last folded term in (2.67) has a *double denominator*. We can express the second-order Bloch equation as

$$\Omega^{(2)}(\mathcal{E})P_{\mathcal{E}} = \Gamma_{\mathcal{Q}}(\mathcal{E})V\Omega^{(1)}(\mathcal{E})P_{\mathcal{E}} + \frac{\delta\Omega^{(1)}(\mathcal{E})}{\delta\mathcal{E}}V_{\text{eff}}^{(1)}(\mathcal{E})P_{\mathcal{E}}.$$
(2.69)

In the limit of complete degeneracy space, the difference ratio, of course, goes over into the partial derivative. We shall show in later chapters that the second-order expression above holds also when the perturbation is energy dependent (6.77).

2.4 Graphical Representation

In this section, we shall briefly describe a way of representing the perturbation expansion graphically. (For further details, the reader is referred to the book by Lindgren and Morrison [40].)

2.4.1 Goldstone Diagrams

The Rayleigh–Schrödinger perturbation expansion can be conveniently represented in terms of diagrams by means of second quantization (see above and Appendix B). The perturbation (2.50) becomes in second quantization

$$\hat{V} = c_i^{\dagger} c_j \langle i|f|j \rangle + \frac{1}{2} c_i^{\dagger} c_j^{\dagger} c_l c_k \langle ij|g|kl \rangle, \qquad (2.70)$$

where f is the negative potential f = -u and g is the Coulomb interaction between the electrons. When some of the states above are hole states, the expression (2.70) is not in normal order. By normal ordering the expression, zero-, one-, and two-body operators will appear [40, Eq. 11.39]

$$V = V_0 + V_1 + V_2, (2.71)$$

where

$$V_{0} = \sum_{i}^{\text{hole}} \langle i | f | i \rangle + \frac{1}{2} \sum_{ij}^{\text{hole}} \left[\langle ij | g | kl \rangle - \langle ji | g | kl \rangle \right],$$

$$V_{1} = \{ c_{i}^{\dagger} c_{j} \} \langle i | v_{\text{eff}} | j \rangle,$$

$$V_{2} = \frac{1}{2} \{ c_{i}^{\dagger} c_{j}^{\dagger} c_{l} c_{k} \} \langle ij | g | kl \rangle.$$
(2.72)

In the one- and two-body parts, the summation is performed over all orbitals. Here.

$$\langle i|v_{\text{eff}}|j\rangle = \langle i|f|j\rangle + \sum_{k}^{\text{hole}} [\langle ik|g|jk\rangle - \langle ki|g|jk\rangle]$$
 (2.73)

is known as the *effective potential interaction* and can be represented graphically as shown in Fig. 2.3. The summation term represents the *Hartree–Fock potential*

$$\langle i | v_{\text{HF}} | j \rangle = \sum_{k}^{\text{hole}} \left[\langle i k | g | j k \rangle - \langle k i | g | j k \rangle \right],$$
 (2.74)

where the first term is a "direct" integral and the second term an "exchange" integral. In the Hartree–Fock model, we have $u = v_{HF}$, and the effective potential vanishes [40].

We can now represent the perturbation (2.72) by the <u>normal-ordered diagrams</u> in Fig. 2.1. The zero- and one-body parts are shown in more detail in Figs. 2.2 and 2.3. In our diagrams, the dotted line with the cross represents the potential interaction, f = -u, and the dotted line between the electrons the Coulomb interaction, $g = e^2/4\pi\epsilon_0 r_{12}$. We use here a simplified version of Goldstone diagrams. Each free vertical line at the top (bottom) represents an electron creation (absorption) operator but normally we do not distinguish between the different kinds of orbitals (core, valence, and virtual) as done traditionally. There is a summation of internal lines over all orbitals of the same category. We use here **heavy lines** to indicate

$$V = V_0 + \bigcup_{i=0}^{j} \frac{1}{-u} \otimes U_i + \bigcup_{i=0}^{j} \frac{1}{u} \otimes U_i + \bigcup_{i=0}^{j} \frac{1}{$$

Fig. 2.1 Graphical representation the effective-potential interaction (2.72). The *heavy lines* represent the orbitals in the Furry picture. The *dotted line* with the *cross* represents the potential -u and the *dotted, horizontal lines* the Coulomb interaction. The zero-body and one-body parts of the interaction are depicted in Figs. 2.2 and 2.3, respectively

$$V_0 = \bigodot^{i} \xrightarrow{-u} \times + \bigodot^{k} \xrightarrow{1} + \bigodot^{k}$$

Fig. 2.2 Graphical representation of the zero-body part of the effective-potential interaction (2.72). The orbitals are summed over all core/hole states

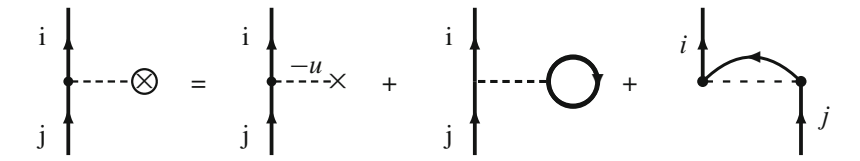


Fig. 2.3 Graphical representation of the effective-potential interaction (2.73). For the closed orbital lines (with no free end), there is a summation over the core/hole states. The last two diagrams represent the "Hartree–Fock" potential, and the entire effective-potential interaction vanishes when HF orbitals are used

that the orbitals are generated in an external (nuclear) potential, i.e., the *bound-state* representation or *Furry picture*.

By means of Wick's theorem, we can now normal order the right-hand side (r.h.s.) of the perturbation expansion of the Bloch equation (2.62), and

• Each resulting normal-ordered term will be represented by a diagram.

The first-order wave operator (2.66)

$$\Omega^{(1)}P_{\mathcal{E}} = \Gamma_{\mathcal{Q}}(\mathcal{E}) V P_{\mathcal{E}} = \Gamma_{\mathcal{Q}}(\mathcal{E}) (V_1 + V_2) P_{\mathcal{E}}$$
(2.75)

becomes in second quantization (2.72)

$$\Omega^{(1)}P_{\mathcal{E}} = Q\left[\left\{c_i^{\dagger} c_j\right\} \frac{\langle i | v_{\text{eff}} | j \rangle}{\varepsilon_j - \varepsilon_i} + \frac{1}{2} \left\{c_i^{\dagger} c_j^{\dagger} c_l c_k\right\} \frac{\langle ij | g | kl \rangle}{\varepsilon_k + \varepsilon_l - \varepsilon_i - \varepsilon_j}\right] P_{\mathcal{E}}.$$
(2.76)

This can be represented in the same way as the open part $(V_1 + V_2)$ of the perturbation (2.70) (Fig. 2.1), if we include the extra energy denominator according to the Goldstone rules, summarized below.

In second order, we have from (2.67), using Wick's theorem (2.34),

$$\Omega^{(2)}P_{\mathcal{E}} = \Gamma_{\mathcal{Q}}(\mathcal{E})\left(\left\{V\Omega_{\mathcal{E}}^{(1)}\right\} + \left\{V\Omega_{\mathcal{E}}^{(1)}\right\} - \left\{\Omega_{\mathcal{E}}^{(1)}P_{\mathcal{E}'}V_{\text{eff}}^{(1)}\right\} - \left\{\Omega_{\mathcal{E}'}^{(1)}P_{\mathcal{E}'}V_{\text{eff}}^{(1)}\right\}\right)P_{\mathcal{E}},\tag{2.77}$$

where the hook represents a contraction. The first uncontracted term is represented by combinations of the diagrams in Fig. 2.1, such as



considered as a single diagram. This diagram can be of two types.

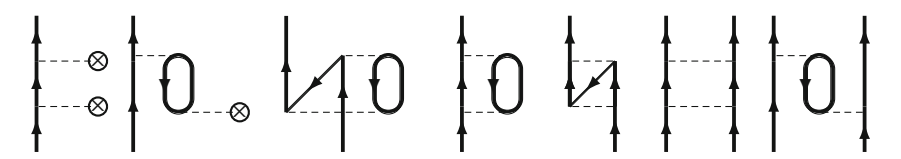


Fig. 2.4 Examples of second-order wave-operator diagrams, excluding folded diagrams

• If, on the one hand, both disconnected parts are open, the diagram is referred to as <u>linked</u>. If, on the other hand, at least one of them is <u>closed</u>, the diagram is referred to as <u>unlinked</u>.

In the unlinked part of the second term in (2.77), the closed part represents $V_{\rm eff}^{(1)}$, and since the order of the operators in the normal product is immaterial, this unlinked diagram appears also in the third term and is therefore eliminated. The last contracted term survives and represents the "folded" term. Here, the wave operator depends on the energy (\mathcal{E}') of the intermediate state, which might differ from the energy of the initial state (\mathcal{E}). We can then express the second-order wave operator by

$$\Omega^{(2)} P_{\mathcal{E}} = \Gamma_{\mathcal{Q}}(\mathcal{E}) \left(V \Omega_{\mathcal{E}}^{(1)} - \Omega_{\mathcal{E}'}^{(1)} P_{\mathcal{E}'} V_{\text{eff}}^{(1)} \right)_{\text{linked}} P_{\mathcal{E}}, \tag{2.79}$$

where only linked diagrams are maintained (see Fig. 2.4).

The diagrams in Fig. 2.4 are second-order *time-ordered Goldstone diagrams*. In these diagrams, time is supposed to run from the bottom (although the formalism is here time independent). The diagrams are evaluated by the *standard Goldstone rules* with a denominator after each interaction equal to the energy difference between the (model-space) state at the bottom and that directly after the interaction (see Appendix I and [40, Sect. 12.4]). (In later chapters, we shall mainly use *Feynman diagrams*, which contain all possible time orderings between the interactions.)

2.4.2 Linked-Diagram Expansion

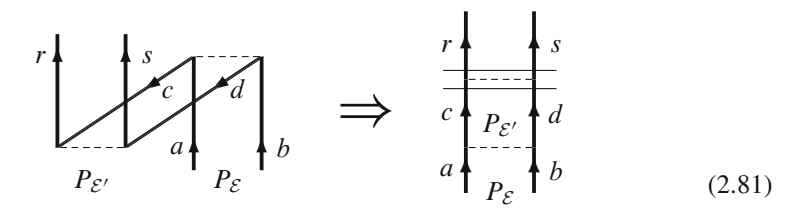
2.4.2.1 Complete Model Space

Written more explicitly, the second-order wave operator (2.79) becomes

$$\Omega^{(2)} P_{\mathcal{E}} = \left(\Gamma_{Q}(\mathcal{E}) V \Gamma_{Q}(\mathcal{E}) V - \Gamma_{Q}(\mathcal{E}) \Gamma_{Q}(\mathcal{E}') V P_{\mathcal{E}'} V \right)_{\text{linked}} P_{\mathcal{E}}. \tag{2.80}$$

⁶ A <u>closed</u> diagram has the initial as well as the final state in the model space. Such a diagram can – in the case of complete model space – have no other free lines than valence lines. A diagram that is not <u>closed</u> is said to be *open*.

Here, the second term has a *double resolvent* (double denominator, which might contain different model-space energies), and it is traditionally drawn in a "folded" way, as shown in the left diagram below (see, for instance, [40, Sect. 13.3])



The reason for drawing the diagram folded in this way is that the two pieces – before and after the fold – should be evaluated with their denominators independently. In the general case, by considering all possible time-orderings between the two pieces, together with the Goldstone evaluation rules, it can be shown that the denominators do *factorize*. In a relativistic treatment, which we shall employ for the rest of this book, the treatment is most conveniently based upon Feynman diagrams, which automatically contain all possible time-orderings, and then it is more natural to draw the diagram straight, as shown in the second diagram above. Factorization then follows directly. The double bar indicates that the diagram is "folded." In such a diagram, the upper part has double denominators – one denominator with the energy of the initial state and one with that of the intermediate model-space state. The second-order wave operator can then be illustrated as shown in Fig. 2.5. Note that there is a minus sign associated with the folded diagram.

The general ladder diagram (Fig. 2.5) may contain a (quasi)singularity, when the intermediate state lies in the model space and is (quasi)degenerate with the initial state. This singularity is automatically eliminated in the Bloch equation and leads to the folded term. Later, in Sect. 6.6 we shall discuss this kind of singularity in more detail in connection with energy-dependent interactions, and then we shall refer to the finite remainder as the *model-space contribution* (MSC).

We have seen that the so-called unlinked diagrams are eliminated in the secondorder wave operator (2.79). When the model space is "complete" (see definition above), it can be shown that unlinked diagrams disappear in all orders of perturbation theory. This is the *linked-cluster or linked-diagram theorem* (LDE), first

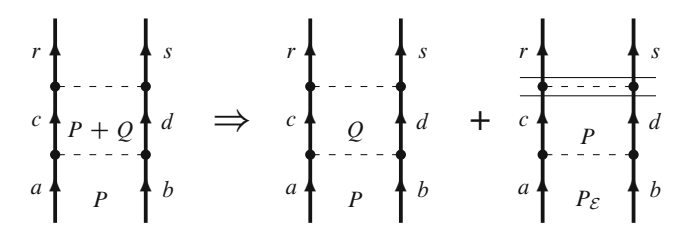


Fig. 2.5 Removing the singularity from a ladder diagram leads to finite remainder, represented by a "folded" diagram (*last*). The *double bar* represents a double denominator (with a factor of -1)

demonstrated in 1950s by Brueckner [9] and Goldstone [21] for a degenerate model space. It holds also for a complete quasi-degenerate model space, as was first shown by Brandow [7], using a double perturbation expansion. This was demonstrated more directly by Lindgren [37] by means of the generalized Bloch equation (2.56), and the result can then be formulated⁷

$$[\Omega, H_0] P = (V\Omega P - \Omega V_{\text{eff}})_{\text{linked}} P.$$
 (2.82)

This equation is a convenient basis for many-body perturbation theory, as developed, for instance, in [40]. It will also constitute a fundament of the theory developed in this book.

2.4.2.2 Incomplete Model Spaces

When the model space is *incomplete*, i.e., does not contain all configurations that can be formed by the valence orbitals, the expansion is not necessarily completely linked. As first shown by Mukherjee [41, 56], the linked-diagram theorem can still be shown to hold, if the normalization condition (2.42a) is abandoned. As will be discussed later, a complete model space often has the disadvantage of so-called *intruder states*, which destroy the convergence. Then also other means of circumventing this problem will be briefly discussed.

2.5 All-Order Methods: Coupled-Cluster Approach

2.5.1 Pair Correlation

Instead of solving the Bloch equation order-by-order, it is often more efficient to solve it iteratively. By separating the second-quantized wave operator into normal-ordered zero-, one-, two-,... body parts

$$\Omega = \Omega_0 + \Omega_1 + \Omega_2 + \cdots \tag{2.83}$$

⁷ The Rayleigh–Schrödinger and the linked-diagram expansions have the advantage compared to, for instance, the Brillouin–Wigner expansion, that they are *size-extensive*, which implies that the energy of a system increases linearly with the size of the system. This idea was actually behind the discovery of the linked-diagram theorem by Brueckner [9], who found that the so-called unlinked diagrams have a nonphysical nonlinear energy dependence and therefore must be eliminated in the complete expansion. The concept of size extensivity should not be confused with the term *size consistency*, introduced by Pople [64, 65], which implies that the *wave function* separates correctly when a molecule dissociates. The Rayleigh–Schrödinger or linked-diagram expansions are generally *not* size consistent. The coupled-cluster approach (to be discussed below) does have this property in addition to the property of size extensivity.

with

$$\begin{cases}
\Omega_1 = \left\{ c_i^{\dagger} c_j \right\} x_j^i \\
\Omega_2 = \frac{1}{2} \left\{ c_i^{\dagger} c_j^{\dagger} c_l c_k \right\} x_{kl}^{ij}, \\
\text{etc.}
\end{cases} (2.84)$$

the Bloch equation can be separated into the following coupled n-particle equations

$$[\Omega_1, H_0] P = (V\Omega - \Omega W)_{\text{linked}, 1} P,$$

$$[\Omega_2, H_0] P = (V\Omega - \Omega W)_{\text{linked}, 2} P,$$
(2.85)

etc., where

$$W = V_{\text{eff}} = P V \Omega P \tag{2.86}$$

is the effective interaction.

Usually, the two-body operator dominates heavily, since it contains the important pair correlation between the electrons. Therefore, a good approximation for many cases is

$$\Omega \approx 1 + \Omega_1 + \Omega_2,\tag{2.87}$$

which yields

$$[\Omega_1, H_0] P = (V_1 + V\Omega_1 + V\Omega_2 - \Omega_1 W_1)_{\text{linked}, 1} P,$$

$$[\Omega_2, H_0] P = (V_2 + V\Omega_1 + V\Omega_2 - \Omega_1 W_2 - \Omega_2 W_1 - \Omega_2 W_2)_{\text{linked}, 2} P, \quad (2.88)$$

where

$$W_1 = (V_1 + V_1 \Omega_1)_{\text{closed}, 1},$$

$$W_2 = (V_2 + V \Omega_1 + V \Omega_2)_{\text{closed}, 2}.$$
(2.89)

We see here that the equations are coupled, so that Ω_1 appears in the equation of Ω_2 and *vice versa*. This approach is known as the *pair-correlation approach*. Solving these coupled equations self-consistently is equivalent to a perturbation expansion – including one- and two-body effects – to essentially all orders. It should be noted, though, that each iteration does not correspond to a certain order of the perturbative expansion.

As a simple illustration, we consider the simplified pair-correlation approach

$$\Omega = \Omega_2 \tag{2.90}$$

omitting single excitations. (This would be exact for a two-electron system using hydrogenic basis functions, in which case there are no core orbitals, but is a good approximation also in other cases.) The equation for Ω_2 is

$$[\Omega_2, H_0] P = (V + V\Omega_2 - \Omega_2 W_2)_{\text{linked, 2}} P.$$
 (2.91)

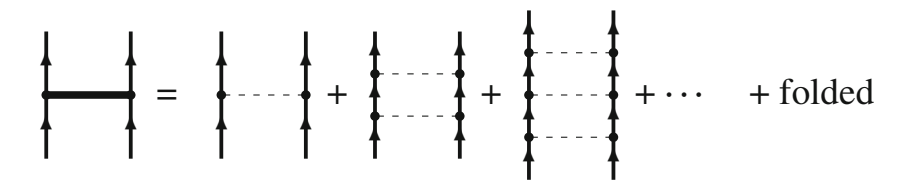


Fig. 2.6 Graphical representation of the pair function (2.96)

Operating on an initial two-electron state of energy \mathcal{E} , the solution can be expressed

$$\Omega_2 P_{\mathcal{E}} = \Gamma_Q(\mathcal{E}) (V + V \Omega_2 - \Omega_2 W_2)_{\text{linked}} P_{\mathcal{E}}. \tag{2.92}$$

Solving this iteratively leads to

$$\Omega_{2}^{(1)}P_{\mathcal{E}} = \Gamma_{\mathcal{Q}}(\mathcal{E})VP_{\mathcal{E}}, \tag{2.93}$$

$$\Omega_{2}^{(2)}P_{\mathcal{E}} = \Gamma_{\mathcal{Q}}(\mathcal{E})\left(V\Omega_{2}^{(1)} - \Omega_{2}^{(1)}P_{\mathcal{E}'}W_{2}^{(1)}\right)P_{\mathcal{E}}$$

$$= \Gamma_{\mathcal{Q}}(\mathcal{E})V\Gamma_{\mathcal{Q}}(\mathcal{E})VP_{\mathcal{E}} - \Gamma_{\mathcal{Q}}(\mathcal{E})\Gamma_{\mathcal{Q}}(\mathcal{E}')VP_{\mathcal{E}'}VP_{\mathcal{E}},$$
etc., (2.94)

where all terms are assumed to be linked. This leads to the "ladder sequence," illustrated in Fig. 2.6. Note that in the expression above, all energies of the first term depend on the initial state, while in the folded term the wave operator depends on the energy of the intermediate state (\mathcal{E}') (c.f., the "dot product," introduced in Sect. 6.6).

Operating with Ω_2 in (2.84) on the initial state $|ab\rangle$ leads to the pair function

$$\Omega_2|ab\rangle = x_{ab}^{rs}|rs\rangle = \rho_{ab}(x_1, x_2), \tag{2.95}$$

which inserted in (2.88) leads to the pair equation

$$(\varepsilon_a + \varepsilon_b - h_0(1) - h_0(2)) \ \rho_{ab}(x_1, x_2) = (|rs\rangle \langle rs|V|ab\rangle + |rs\rangle \langle rs|V|\rho_{ab}\rangle - |\rho_{cd}\rangle \langle cd|W_2|ab\rangle)_{\text{linked}}. \tag{2.96}$$

(For simplicity, we work with straight product functions – not antisymmetrized – in which case we sum over all combinations of r, s (without the factor of 1/2) with $x_{ab}^{rs} = -x_{ab}^{sr}$.)

We can also express the pair function as

$$|\rho_{ab}\rangle = \Gamma_Q(\mathcal{E}) I^{\text{Pair}} |ab\rangle,$$
 (2.97)

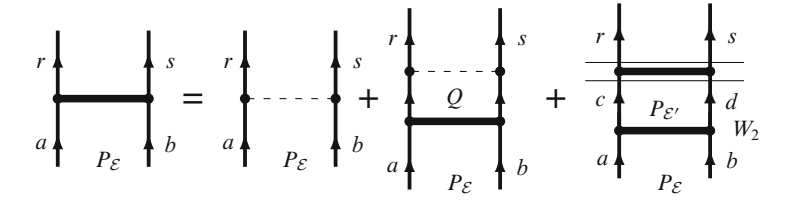


Fig. 2.7 Graphical representation of the self-consistent pair equation (2.99). The *last diagram* represents the "folded" term $-\Omega_2 W_2$. The *double line* represents the double denominator (double resolvent)

where $\Gamma_{\mathcal{Q}}(\mathcal{E})$ is the reduced resolvent (2.65) and \mathcal{E} is the energy of the initial state $|ab\rangle$. I^{Pair} represents the ladder sequence of Coulomb interactions (including folded terms), corresponding to the heavy line in Fig. 2.6, and including the resolvent (final denominator) leads to the pair function $|\rho_{ab}\rangle$. The effective interaction W_2 can be expressed as

$$W_2 = P_{\mathcal{E}'} I^{\text{Pair}} P_{\mathcal{E}}, \tag{2.98}$$

which can be represented by the same diagrams as in Fig. 2.6 (with no final denominator) if the final state (with energy \mathcal{E}') lies in the model space. The pair function (2.92) can now be expressed

$$\Gamma_{Q}(\mathcal{E})I^{\text{Pair}}P_{\mathcal{E}} = \Gamma_{Q}(\mathcal{E})\left(V + V\Gamma_{Q}(\mathcal{E})I^{\text{Pair}} - \Gamma_{Q}(\mathcal{E}')I^{\text{Pair}}P_{\mathcal{E}'}I^{\text{Pair}}P_{\mathcal{E}}\right)P_{\mathcal{E}}. \quad (2.99)$$

This relation can be represented graphically as shown in Fig. 2.7.

2.5.2 Exponential Ansatz

A particulary effective form of the all-order approach is the *Exponential Ansatz* or *Coupled-Cluster Approach* (CCA), first developed in nuclear physics by Hubbard, Coster, and Kümmel [12, 13, 23, 33, 34]. It was introduced into quantum chemistry by Čižek [11] and has been extensively used during the last decades for more details. (The reader is referred to a recent book "*Recent Progress in Coupled Cluster Methods*" [79], which reviews the development of the methods since the start.) The CCA is a nonlinear approach, and the linear all-order approach (2.85), discussed above, is sometimes inadvertently referred to as "*linear CCA*"(!) – a term we shall not use here. In the exponential Ansatz, the wave operator is expressed in the form of an exponential

$$\Omega = e^S = 1 + S + \frac{1}{2}S^2 + \frac{1}{3!}S^3 + \cdots,$$
 (2.100)

S is the *cluster operator* (in chemical literature normally denoted by T). It can then be shown that for a degenerate model space the cluster operator is represented by *connected* diagrams only.⁸ This implies that the linked but disconnected diagrams of the wave operator are here represented by the higher powers in the expansion of the exponential.

For *open-shell systems* (with unfilled valence shell), it is convenient to represent the Ansatz in the *normal-ordered form*, introduced by Lindgren [38, 40],

$$\Omega = \left\{ e^{S} \right\} = 1 + S + \frac{1}{2} \left\{ S^{2} \right\} + \frac{1}{3!} \left\{ S^{3} \right\} + \cdots. \tag{2.101}$$

This form has the advantage that unwanted contractions between the cluster operators are avoided. The cluster operator is completely connected also in this case, if the model space is complete [41], which can be formulated by means of the Bloch equation

$$[S, H_0] P = Q (V\Omega P - \Omega V_{\text{eff}})_{\text{conn}}.$$
 (2.102)

Expanding the cluster operator in analogy with the wave-operator expansion (2.83) in terms on one-, two-,... body operators,

$$S = S_1 + S_2 + S_3 + \cdots \tag{2.103}$$

yields

$$\Omega = \left\{ e^{S} \right\} = 1 + S_1 + S_2 + \frac{1}{2} \left\{ S_1^2 \right\} + \left\{ S_1 S_2 \right\} + \frac{1}{2} \left\{ S_2^2 \right\} + \frac{1}{2} \left\{ S_1^2 S_2 \right\} + \frac{1}{3!} \left\{ S_1^3 \right\} + \cdots$$
(2.104)

With the approximation

$$S = S_1 + S_2, \tag{2.105}$$

the cluster operators satisfy the coupled Bloch equations

$$[S_1, H_0] P = (V\Omega - \Omega W)_{\text{conn}, 1} P$$

$$[S_2, H_0] P = (V\Omega - \Omega W)_{\text{conn}, 2} P$$
(2.106)

illustrated in analogy with Fig. 2.7 in Fig. 2.8. These equations lead to one- and two-particle equations, analogous to the pair equation given above (2.96). Also these equations have to be solved *iteratively*, and we observe that they are *coupled*, as are the corresponding equations (2.88) for the full wave operator.

⁸ The distinction between *linked* and *connected* diagrams should be noted. A linked diagram can be disconnected, if all parts are *open*, as defined in Sect. 2.4.

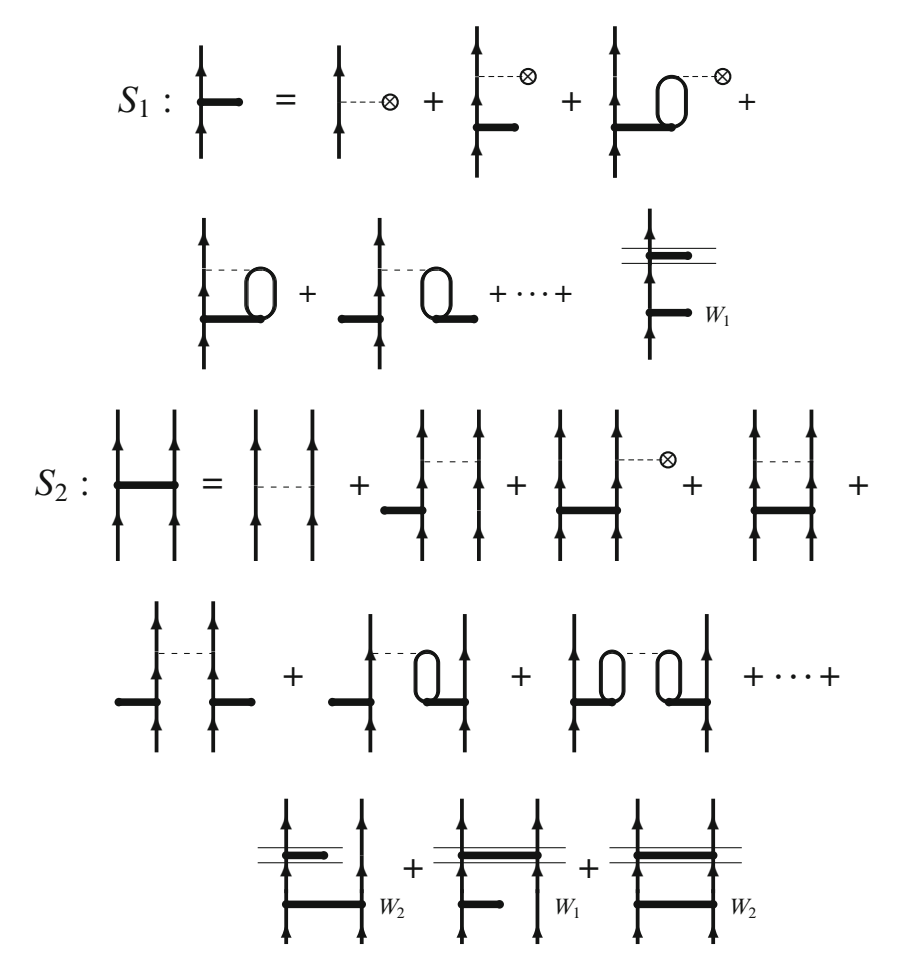


Fig. 2.8 Diagrammatic representation of the equations for the cluster operators S_1 and S_2 (2.106). The circle with a cross represents the "effective potential" in Fig. 2.3. The second diagram in the second row and the diagrams in the fourth row are examples of coupled-cluster diagrams. The last diagram in the second row and the three diagrams in the last row represent folded terms (c.f. Fig. 2.7)

The normal-ordered scheme is usually combined with a *complete model space* – or complete active space (CAS) – and the *valence universality*. This might lead to problems due to *intruder states* to be discussed further below.

For atomic systems with essentially *spherical symmetry*, on the one hand, the cluster equations can be separated into angular and radial parts, where the former can be treated analytically and only the radial part has to have solved numerically

(see, for instance, [40, Chap. 15]). For molecular systems, on the other hand, analytical basis-set functions of Slater or Gaussian types are normally used to solve the coupled-cluster equations, as described in numerous articles in the field.

As mentioned, the advantage of the normal ordering of the exponential Ansatz is that a number of unwanted contractions between open-shell operators is avoided. More recently, Mukherjee has shown that certain valence-shell contractions are actually desired, particularly when valence holes and strong relaxation are involved [26]. He then introduced a modified normal ordering

$$\Omega = \{ \{ \exp(S) \} \}, \tag{2.107}$$

where contractions involving passive (spectator) valence lines are reintroduced compared to the original normal ordering.

2.5.3 Various Models for Coupled-Cluster Calculations: Intruder-State Problem

The early forms of coupled-cluster models were of *single-reference* type (SRCC) with a one-dimensional (closed-shell) model space. In the last few decades, various versions of *multireference* (MRCC) models with multidimensional model space have appeared (for reviews, see e.g., [2, 41, 58]). These are essentially two major types, known as *valence-universal* multireference (VU-MRCC) [38, 57] and *state-universal* multireference (SU-MRCC) [27, 28] methods, respectively. In the valence-universal methods, the same cluster operators are being used for different ionization states and therefore particularly useful for calculating ionization energies and affinities. In the state-universal methods, specific operators are used for a particular ionization stage and particularly used when different states of the same ionization are considered or in the molecular case for studying potential energy surfaces (PES).

A serious problem that can appear in MBPT with a multireference model space is what is known as the "intruder-state-problem." This appears when a state outside the model space – of the same symmetry as the state under consideration – has a perturbed energy between those of the same symmetry originating from the model space. This will destroy the convergence of the perturbation expansion. This problem was first observed in nuclear physics [74], but it was early observed also in atomic physics for the beryllium atom [69]. Here, the ground state is $1s^22s^2 1S$, and the excited state $1s^2 2p^2 1S$ has a low unperturbed energy, while the true state lies close to the 2s ionization limit. This implies that when the perturbation is gradually turned on, a large number of "outside" states, $1s^2 2s ns$, will cross the energy of the $1s^22p^2 1S$ state, and there will be no convergence beyond the crossing point.

The convergence problem due to intruders is particularly serious in perturbation theory, when the states are expanded order-by-order from the unperturbed ones. In the coupled-cluster approach, which in principle is *nonperturbative*, it might be

possible to find a self-consistent solution of the coupled equations without reference to any perturbative expansion. It was first shown by Jankowski and Malinowski [24, 25, 48] that it was in fact possible to find a solution to the beryllium problem with a complete model space. Lindroth and Mårtensson [44] solved the same problem by means of *complex rotation*.

Several other methods have been developed to reduce the intruder-state problem. One way is to reduce the model space and make it *incomplete*. It was shown by Mukherjee [56] that by abandoning the intermediate normalization (2.42a), the linked character of the diagram expansion could still be maintained. The criteria for the connectivity of the coupled-cluster expansion have been analyzed by Lindgren and Mukherjee [41].

Another approach to avoid or reduce the intruder-state problem is to apply an *intermediate-effective Hamiltonian*, a procedure developed by the Toulouse group (Malrieu, Durand et al.) in the mid 1980s [15]. Here, only a limited number of roots of the secular equation are being looked for. A modified approach of the method has been developed by Meissner and Malinowski [51] and applied to the abovementioned beryllium case.

A third approach to the problem is the *state-specific multireference* (SS-MRCC) approach, where a multireference is used but only a single state is considered [47]. This approach can be regarded as an extreme of the intermediate-Hamiltonian approach and is frequently used particularly for studying potential-energy surfaces.

All the coupled-cluster approaches can also be applied in the relativistic formalism, although applications are here still quite limited. We shall return briefly to this problem in Chap. 8.

2.6 Relativistic MBPT: No-Virtual-Pair Approximation

In setting up a Hamiltonian for relativistic quantum mechanics, it may be tempting to replace the single-electron Schrödinger Hamiltonian in the many-body Hamiltonian (2.11) by the Dirac Hamiltonian (see Appendix D)

$$h_{\rm D} = c\boldsymbol{\alpha} \cdot \hat{\mathbf{p}} + \beta mc^2 + v_{\rm ext}, \tag{2.108}$$

which with the Coulomb interaction between the electrons

$$V_{\rm C} = \sum_{i < j}^{N} \frac{e^2}{4\pi\epsilon_0 \, r_{ij}} \tag{2.109}$$

yields the Dirac-Coulomb Hamiltonian

$$H_{\rm DC} = \sum_{i=1}^{N} h_{\rm D}(i) + V_{\rm C}.$$
 (2.110)

This Hamiltonian, however, has several serious shortcomings. First, it is not bound from below, because nothing prevents the electrons from falling into the "Dirac sea" of negative-energy electron states. A many-electron state with a mixture of negative-energy and positive-energy electron states can then be accidentally degenerate with a state with only positive-energy states – a phenomenon known as the *Brown–Ravenhall disease* [8]. In Chap. 6, we shall derive a field-theoretical many-body Hamiltonian that will be used in the further development. In this model, there is no "Dirac sea," but the negative-energy states correspond to the creation of *positron states*, which are highly excited. Then there can be no Brown–Ravenhall effect.

Within the conventional many-body treatment, the Brown–Ravenhall effect can be circumvented by means of projection operators [78], which exclude negative-energy states, leading to the *projected Dirac–Coulomb Hamiltonian*

$$H_{\text{DCproj}} = \Lambda_{+} \left[\sum_{i=1}^{N} h_{\text{D}}(i) + V_{\text{C}} \right] \Lambda_{+}.$$
 (2.111)

Including also the *instantaneous Breit interaction* (see Appendix F)

$$V_{\rm B} = -\frac{e^2}{8\pi\epsilon_0} \sum_{i<1} \left[\frac{\alpha_i \cdot \alpha_j}{r_{ij}} + \frac{(\alpha_i \cdot r_{ij})(\alpha_j \cdot r_{ij})}{r_{ij}^2} \right], \tag{2.112}$$

where α_i is the Dirac alpha matrix vector for particle *i* (see Appendix D), leads to the *projected Dirac–Coulomb–Breit Hamiltonian*

$$H_{\text{NVPA}} = \Lambda_{+} \left[\sum_{i=1}^{N} h_{\text{D}}(i) + V_{\text{C}} + V_{\text{B}} \right] \Lambda_{+},$$
 (2.113)

which is known as the <u>No-Virtual-Pair Approximation</u> (NVPA). With the partitioning (2.48)

$$H = H_0 + V, (2.114)$$

we choose the model Hamiltonian to be

$$H_0 = \sum_{i}^{N} (h_D + u)_i =: \sum_{i}^{N} h_0(i)$$
 (2.115)

and the perturbation

$$V = -\sum_{i}^{N} u(i) + V_{\rm C} + V_{\rm B}.$$
 (2.116)

The Dirac-Coulomb and Dirac-Coulomb-Breit Hamiltonians, which are valid only in the *Coulomb gauge* (see Appendix G.2), have been extensively used in

relativistic MBPT calculations and particularly in self-consistent-field calculations of *Dirac–Fock* type. In the latter type of calculations, the projection operators can often be left out, since the boundary conditions usually excludes negative-energy solutions (see the book by I.P. Grant for a modern review [22]).

NVPA is a good approximation for many purposes, and it includes all effects to order α^2 H, but it is *not Lorentz covariant* (see definition in the Introduction). In later chapters, we shall consider a more rigorous many-body Hamiltonian, based upon field theory.

2.6.1 QED Effects

As mentioned, we shall refer to effects beyond the NVPA as *QED effects*, although this separation is to some extent arbitrary. These effects are of two kinds

- *Nonradiative effects*, representing effects due to negative-energy states and to retardation of the Breit interaction, shown in the upper line of Fig. 2.9. These effects are also referred to as the *Araki–Sucher* effects [1, 76, 77].
- Radiative effects, represented by the lower line of Fig. 2.9, which are "true" quantum-electrodynamical effects due to the electron self-energy (first diagram), vacuum polarization (next two diagrams), or vertex correction (last diagram) (see further Chap. 4).

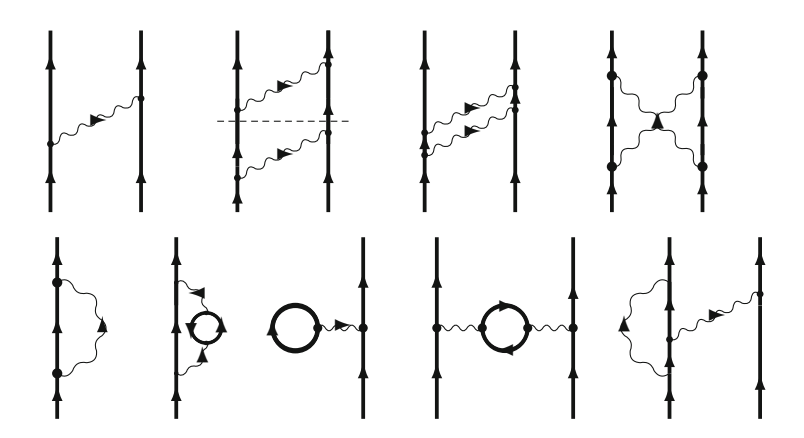


Fig. 2.9 Nonradiative (*upper line*) and radiative (*lower line*) "QED effects." These diagrams are *Feynman diagrams*, where the orbital lines can represent particle as well as hole or antiparticle states (see further Chap. 4). The *second diagram* in the *first row* is reducible (there is an intermediate time with no photon), while the remaining ones are irreducible

The QED effects can also be separated into *reducible* and *irreducible* effects, where a reducible effect is represented by a diagram that can be separated into two legitimate diagrams by a horizontal cut, such as the second nonradiative diagram in Fig. 2.9. Remaining diagrams are irreducible.

2.7 Some Numerical Results of Standard MBPT and CC Calculations, Applied to Atoms

In the book *Atomic Many-Body Theory* [18, Sect. 15.5] a brief summary is given of the situation in the late 1970s concerning the numerical application of many-body perturbation theories. Most effective at that time to handle the electron-correlation problem were various pair-correlation approaches, based on works of Kelly [32], Meyer [52], Sinanŏglu [75], Nesbet [59], Kutzelnigg [35], and others. Coupled-cluster methods were available at that time but still relatively undeveloped. Also methods of treating open shells and the quasi-degenerate problem, using the extended model space [37] (2.56), were available but not particularly well known.

In the three decades that have followed, a dramatic development regarding numerical implementations has taken place. All-order methods, in particular, coupled-cluster methods, have been developed to a stage of "almost perfection." Also, the open-shell techniques have been further developed and are now routinely used. Here, two main lines have emerged, based upon *multireference* or *single-reference states*. The latter technique has been developed mainly to circumvent the *intruder problem*, although there are methods of dealing with this problem also in the multireference case, as was briefly mentioned above. We shall in no way try to review this immense field here but limit ourselves to some comments concerning developments that are most relevant for the theme of this book. (We refer to the previously mentioned book, edited by Čársky et al. [79], for more details.) We also call attention to a comprehensive review of all-order relativistic atomic calculations that has recently been published by Safronova and Johnson [67].

The coupled-cluster approach was early applied to various molecular systems, particularly by Čižek, Paldus, and coworkers in the Waterloo group [60, 61]. Extensions of the method and extensive calculations have been performed by Bartlett and his collaborators at Gainesville [3, 66]. The paper by Purvis and Bartlett [66], together with the simultaneous publication by Pople et al. [63], represent the first applications of CCA with both single and double excitations (CCSDs). Bartlett et al. have later extended the technique to include part of triples, CCSD(T), and quadruples, CCSD(TQ), techniques that are now widely spread.

⁹ Unfortunately, different definitions of reducible and irreducible diagrams occur in the literature. We use in this book the original interpretation of the concepts, due to the pioneers Feynman, Dyson, Bethe, Salpeter, and others [16, 73].

In molecular calculations, functional basis sets of Slater or Gaussian-type are normally used. For atomic systems, it is normally preferable to use numerical integration of the radial coordinates. Such techniques have been developed and applied particularly by the groups at Notre Dame, Gothenburg, and Tel Aviv.

The Notre-Dame group has for a long time performed relativistic many-body calculations on atomic systems by applying and further developed the *spline technique* with piece-wise polynomial fitting [29]. This was first used for calculations to second order (third order in energy) of the helium atom, and the sodium isoelectronic sequence [30]. The method was then extended by Blundell et al. [6] to an all-order technique (linear with singles and doubles) and applied to the Li atom and the Be⁺ ion and by Plante et al. [62] to a sequence of helium-like ions. In Table 2.1, we reproduce from the latter work the contributions to the ground-state ionization energies due to (a) all-order Coulomb interactions, (b) same with one instantaneous Breit interaction, (c) same with TWO instantaneous Breit interactions, (d) first-order QED contribution (from [14]), (e) total ionization energy. Later, the Notre–Dame group, partly together with Safronova, has extended the technique to full relativistic CCSD, including also some triples, CCSD(T), and applied it extensively to various atomic and ionic systems [46, 67] (see Tables 2.2 and 2.3).

The Gothenburg group developed numerical nonrelativistic all-order and coupled-cluster approaches in the late 1970s and early 1980s. Mårtensson (Pendrill) [49] developed an all-order pair program (LD) – linear with doubles without coupled clusters – based upon the first-order pair program developed by Morrison [20, 54], and first applied it to the helium atom. This technique was later

Table 2.1	Contributions to the ground-state ionization energies of helium-
like ions. I	From [62] (in Hartrees)

Z	Coulomb	Breit	Double Breit	QED	Total
10	43.962	0.010708	0.000048	-0.004610	43.946
20	188.636	0.096696	0.000433	-0.054905	168.485
40	792.126	0.83482	0.00409	-0.57860	790.717
60	1,855.119	2.97236	0.01528	-2.22984	1,849.832
80	3,472.330	7.51789	0.03914	-5.89519	3,458.965
100	5,841.499	16.0999	0.0836	-12.9704	5,812.513

Table 2.2 Binding energies of the two lowest states of the lithium atom (in μ H)

	Lithium atom			
	2^2S	$2^{2}P$	References	
Expt'l	198 159	130 246		
Hartree-Fock	196 304	128 637		
Difference	1 854	1 609		
LSD	1 855	1 582	Blundell et al. [6]	
CCSD	1 850	1 584	Lindgren [39]	
CCSD	1 835	1 534	Eliav et al. [17]	

atom (in µm) (nom [ooj)					
	Sodium atom				
	3^2S	$3^{2}P_{1/2}$	$3^{2}P_{3/2}$	4^2S	References
Expt'l	6 825	2121	2110	1415	
LSD	6 835	2118	2108	1418	Safronova et al. [68]
CCSD	6 458				Salomonson-Ynnerman [72]
CCSD	6 385				Eliav et al. [17]
CCSD(T)	6 840				Salomonson-Ynnerman [72]

Table 2.3 Correlation energy of some low-lying states of the sodium atom (in μH) (from [68])

Table 2.4 Correlation energy of the ground state of the beryllium atom and the negative lithium ion (in μ H) (from [10])

	Beryllium atom and negative lithium ion			
	Be	Li ⁻	References	
CCD	-92.960	-71.148	Bukowski et al. [10]	
CCD	-92.961	71.266	Salomonson-öster [70]	
CCSD	-93.665	72.015	Bukowski et al. [10]	
CCSD	-93.667	72.142	Salomonson-öster [70]	

converted into a coupled-cluster program with doubles (CCD) by Salomonson [42] and applied to various atomic systems. It was also applied to open-shell systems [55, 69] – in the second paper (concerning the beryllium atom) the famous *intruder problem*, mentioned above, was probably observed for the first time in an atomic system. The procedure of the Gothenburg group was extended to the full CCSD procedure and applied by Lindgren [39] (see Table 2.2) and Salomonson et al. [70, 72] (see Tables 2.3 and 2.4).

A *relativistic* version of the linear all-order pair program (LD) was developed by Eva Lindroth [43], and applied to the helium atom. This was extended to a relativistic coupled-cluster program by Salomonson and öster, who also developed a new numerical, highly accurate technique, referred to as the *discretization technique* [71]. This technique was early applied relativistically as well as nonrelativistically to a number of atomic systems [70,72] and is used also in all later works of the group.

In Tables 2.2–2.4, we have compared some all-order calculations for the lithium, sodium, and beryllium atoms as well as for the Li⁻ ion. The calculations on Be and Li⁻ demonstrate clearly the importance of single excitations in this case. The results for sodium show the importance of triple excitations in this case. (The results by Safronova et al. are probably fortuitous, indicating that effects of nonlinear coupled-cluster terms and triples accidentally cancel.) The accurate results from numerical integrations by Salomonson et al. are sometimes used as benchmarks for testing calculations with finite basis sets [10].

References 43

The Tel-Aviv group has applied the relativistic coupled-cluster technique with singles and doubles (CCSD) particularly to very heavy atoms and simple molecules (see, for instance, the review article by Kaldor and Eliav [31], as well as Tables 2.2 and 2.3).

References

- Araki, H.: Quantum-Electrodynamical Corrections to Energy-levels of Helium. Prog. Theor. Phys. (Japan) 17, 619–42 (1957)
- 2. Bartlett, R.J.: Coupled-cluster approach to molecular structure and spectra: A step toward predictive quantum chemistry. J. Phys. Chem. 93, 1697–1708 (1989)
- 3. Bartlett, R.J., Purvis, G.D.: Many-Body Perturbation Theory, Coupled-Pair Many-Electron Theory, and the Importance of Quadruple Excitations for the Correlation Problem. Int. J. Quantum Chem. 14, 561–81 (1978)
- 4. Bloch, C.: Sur la détermination de l'etat fondamental d'un système de particules. Nucl. Phys. 7, 451–58 (1958)
- 5. Bloch, C.: Sur la théorie des perurbations des etats liés. Nucl. Phys. 6, 329-47 (1958)
- 6. Blundell, S.A., Johnson, W.R., Liu, Z.W., Sapirstein, J.: Relativistic all-order calculations of energies and matrix elements for Li and Be⁺. Phys. Rev. A 40, 2233–46 (1989)
- Brandow, B.H.: Linked-Cluster Expansions for the Nuclear Many-Body Problem. Rev. Mod. Phys. 39, 771–828 (1967)
- 8. Brown, G.E., Ravenhall, D.G.: On the Interaction of Two electrons. Proc. R. Soc. London, Ser. A 208, 552–59 (1951)
- 9. Brueckner, K.A.: Many-Body Problems for Strongly Interacting Particles. II. Linked Cluster Expansion. Phys. Rev. 100, 36–45 (1955)
- 10. Bukowski, R., Jeziorski, B., Szalewicz, K.: Gaussian geminals in explicitly correlated coupled cluster theory including single and double excitations. J. Chem. Phys. 110, 4165–83 (1999)
- 11. Čižek, J.: On the Correlation Problem in Atomic and Molecular Systems. Calculations of Wavefunction Components in the Ursell-Type Expansion Using Quantum-Field Theoretical Methods. J. Chem. Phys. **45**, 4256–66 (1966)
- 12. Coster, F.: Bound states of a many-particle system. Nucl. Phys. 7, 421–24 (1958)
- Coster, F., Kümmel, H.: Short-range correlations in nuclear wave functions. Nucl. Phys. 17, 477–85 (1960)
- 14. Drake, G.W.F.: Theoretical energies for the n=1 and 2 states of the helium isoelectronic sequence up to Z=100. Can. J. Phys. **66**, 586–611 (1988)
- 15. Durand, P., Malrieu, J.P.: Multiconfiguration Dirac-Fock studies of two-electron ions: II. Radiative corrections and comparison with experiment. Adv. Chem. Phys. 67, 321 (1987)
- Dyson, F.J.: The radiation Theories of Tomonaga, Schwinger, and Feynman. Phys. Rev. 75, 486–502 (1949)
- 17. Eliav, E., Kaldor, U., Ishikawa, Y.: *Ionization potentials and excitation energies of the alkalimetal atoms by the relativistic coupled-cluster method.* Phys. Rev. A **50**, 1121–28 (1994)
- 18. E.Lindroth, Mårtensson-Pendrill, A.M.: Isotope Shifts and Energies of the 1s2p States in Helium. Z. Phys. A 316, 265–273 (1984)
- Fetter, A.L., Walecka, J.D.: The Quantum Mechanics of Many-Body Systems. McGraw-Hill, N.Y. (1971)
- 20. Garpman, S., Lindgren, I., Lindgren, J., Morrison, J.: Calculation of the hyperfine interaction using an effective-operator form of many-body theory. Phys. Rev. A 11, 758–81 (1975)
- Goldstone, J.: Derivation of the Brueckner many-body theory. Proc. R. Soc. London, Ser. A 239, 267–279 (1957)
- 22. Grant, I.P.: Relativistic Quantum Theory of Atoms and Molecules. Springer, Heidelberg (2007)

- 23. Hubbard, J.: The description of collective motions in terms of many-body perturbation theory.

 3. The extension of the theory to non-uniform gas. Proc. R. Soc. London, Ser. A 243, 336–52 (1958)
- 24. Jankowski, K., Malinowski, P.: A valence-universal coupled-cluster single- and double-excitations method for atoms: II. Application to Be. J. Phys. B 27, 829–42 (1994)
- Jankowski, K., Malinowski, P.: A valence-universal coupled-cluster single- and doubleexcitations method for atoms: III. Solvability problems in the presence of intruder states. J. Phys. B 27, 1287–98 (1994)
- Jena, D., Datta, D., Mukherjee, D.: A novel VU-MRCC formalism for the simultaneous treatment of strong relaxation and correlation effects with applications to electron affinity of neutral radicals. Chem. Phys. 329, 290–306 (2006)
- 27. Jeziorski, B., Monkhorst, H.J.: ACoupled-cluster method for multideterminantal reference states. Phys. Rev. A 24, 1668–81 (1981)
- Jeziorski, B., Paldus, J.: Spin-adapted multireference coupled-cluster approach: Linear approximation for two closed-shell-type reference configuration. J. Chem. Phys. 88, 5673–87 (1988)
- 29. Johnson, W.R., Blundell, S.A., Sapirstein, J.: Finite basis sets for the Dirac equation constructed from B splines. Phys. Rev. A 37, 307–15 (1988)
- 30. Johnson, W.R., Blundell, S.A., Sapirstein, J.: Many-body perturbation-theory calculations of energy-levels along the sodium isoelectronic sequence. Phys. Rev. A 38, 2699–2706 (1988)
- 31. Kaldor, U., Eliav, E.: *High-Accuracy Calculations for Heavy and Super-Heavy Elements*. Adv. Quantum Chem. **31**, 313–36 (1999)
- 32. Kelly, H.P.: Application of many-body diagram techniques in atomic physics. Adv. Chem. Phys. 14, 129–190 (1969)
- 33. Kümmel, H.: In: E.R. Caianiello (ed.) Lecture Notes on Many-Body Problems. Academic Press, N.Y. (1962)
- 34. Kümmel, H., Lührman, K.H., Zabolitsky, J.G.: Many-fermion theory in exp S (or coupled cluster) form. Phys. Rep. 36, 1–135 (1978)
- 35. Kutzelnigg, W.: Methods in Electronic Structure Theory. Plenum, New York (1977)
- Kvasnička, V.: Construction of Model Hamiltonians in framework of Rayleigh- Schrodinger perturbation-theory. Czech. J. Phys. B 24, 605 (1974)
- 37. Lindgren, I.: The Rayleigh-Schrödinger perturbation and the linked-diagram theorem for a multi-configurational model space. J. Phys. B 7, 2441–70 (1974)
- 38. Lindgren, I.: A Coupled-Cluster Approach to the Many-Body Perturbation Theory for Open-Shell Systems. Int. J. Quantum Chem. **S12**, 33–58 (1978)
- 39. Lindgren, I.: Accurate many-body calculations on the lowest ²S and ²P states of the lithium atom. Phys. Rev. A **31**, 1273–86 (1985)
- 40. Lindgren, I., Morrison, J.: *Atomic Many-Body Theory*. Second edition, Springer-Verlag, Berlin (1986, reprinted 2009)
- 41. Lindgren, I., Mukherjee, D.: On the connectivity criteria in the open-shell coupled-cluster theory for the general model spaces. Phys. Rep. 151, 93–127 (1987)
- Lindgren, I., Salomonson, S.: A Numerical Coupled-Cluster Procedure Applied to the Closed-Shell Atoms Be and Ne. Presented at the Nobel Symposium on Many-Body Effects in Atoms and Solids, Lerum, 1979. Physica Scripta 21, 335–42 (1980)
- 43. Lindroth, E.: *Numerical soultion of the relativistic pair equation.* Phys. Rev. A **37**, 316–28 (1988)
- 44. Lindroth, E., Mårtensson-Pendrill, A.M.: $2p^{2}$ S state of Beryllium. Phys. Rev. A **53**, 3151–56 (1996)
- 45. Löwdin, P.O.: Studies in Perturbation Theory. X. Lower Bounds to Eigenvalues in Perturbation-Theory Ground State. Phys. Rev. 139, A357–72 (1965)
- M. S. Safronova, W.R.J., Derevianko, A.: Relativistic many-body calculations of energy levels, hyperfine constants, electric-dipole matrix elements, and static polarizabilities for alkalimetal atoms. Phys. Rev. A 560, 4476–87 (1999)

References 45

 Mahapatra, U.S., Datta, B., Mukherjee, D.: Size-consistent state-specific multireference couloed cluster theory: Formal developments and molecular applications. J. Chem. Phys. 110, 6171–88 (1999)

- 48. Malinowski, P., Jankowski, K.: A valence-universal coupled-cluster single- and double-excitation method for atoms. I. Theory and application to the C²⁺ ion. J. Phys. B **26**, 3035–56 (1993)
- 49. Mårtensson, A.M.: An Iterative, Numerical Procedure to obtain Pair Functions Applied to Two-electron Systems. J. Phys. B 12, 3995–4012 (1980)
- 50. Mårtensson-Pendrill, A.M., Lindgren, I., Lindroth, E., Salomonson, S., Staudte, D.S.: *Convergence of relativistic perturbation theory for the* 1*s*2*p states in low-Z heliumlike systems*. Phys. Rev. A **51**, 3630–35 (1995)
- 51. Meissner, L., Malinowski, P.: Intermediate Hamiltonian formulation of the valence-universal coupled-cluster method for atoms. Phys. Rev. A 61, 062,510 (2000)
- 52. Meyer, W.: PNO-CI studies of electron correlation effects. 1. Configuration expansion by means of nonorthogonal orbitals, and application to ground-state and ionized states of methane. J. Chem. Phys. 58, 1017–35 (1973)
- 53. Møller, C., Plesset, M.S.: *Note on an Approximation Treatment for Many-Electron Systems*. Phys. Rev. **46**, 618–22 (1934)
- 54. Morrison, J.: Many-Body calculations for the heavy atoms. III. Pair correlations. J. Phys. B 6, 2205–12 (1973)
- Morrison, J., Salomonson, S.: Many-Body Perturbation Theory of the Effective Electron-Electron Interaction for Open-shell Atoms. Presented at the Nobel Symposium.., Lerum, 1979. Physica Scripta 21, 343–50 (1980)
- Mukherjee, D.: Linked-Cluster Theorem in the Open-Shell Coupled-Cluster Theory for Incomplete Model Spaces. Chem. Phys. Lett. 125, 207–12 (1986)
- Mukherjee, D., Moitra, R.K., Mukhopadhyay, A.: Application of non-perturbative many-body formalism to open-shell atomic and molecular problems calculation of ground and lowest π π* singlet and triplet energies and first ionization potential of trans-butadine. Mol. Phys 33, 955–969 (1977)
- 58. Mukherjee, D., Pal, J.: Adv. Chem. Phys. 20, 292 (1989)
- 59. Nesbet, R.K.: Electronic correlation in atoms and molecules. Adv. Chem. Phys. 14, 1 (1969)
- 60. Paldus, J., Čižek, J.: Time-Independent Diagrammatic Approach to Perturbation Theory of Fermion Systems. Adv. Quantum Chem. 9, 105–197 (1975)
- 61. Paldus, J., Čižek, J., Saute, M., Laforge, A.: Correlation problems in atomic and molecular systems. IV. Coupled-cluster approach to open shells. Phys. Rev. A 17, 805–15 (1978)
- 62. Plante, D.R., Johnson, W.R., Sapirstein, J.: *Relativistic all-order many-body calculations of the n=1 and n=2 states of heliumlike ions*. Phys. Rev. A **49**, 3519–30 (1994)
- 63. Pople, J.A., Krishnan, R., Schlegel, H.B., Binkley, J.S.: *Electron Correlation Theories and Their Application to the Study of Simple Reaction Potential Surfaces*. Int. J. Quantum Chem. **14**, 545–60 (1978)
- 64. Pople, J.A., Santry, D.P., Segal, G.A.: *Approximate self-consistent molecular orbital theory.I. Invariant procedures.* J. Chem. Phys. **43**, S129 (1965)
- 65. Pople, J.A., Segal, G.A.: Approximate self-consistent molecular orbital theory. 3. CNDO results for AB2 and AB3 systems. J. Chem. Phys. 44, 3289 (1966)
- 66. Purvis, G.D., Bartlett, R.J.: A full coupled-cluster singles and doubles model: The inclusion of disconnected triples. J. Chem. Phys. 76, 1910–18 (1982)
- 67. Safronova, M.S., Johnson, W.R.: All-Order Methods for Relativistic Atomic Structure Calculations, Advances in Atomic Molecular and Optical Physics series, vol. 55 (2007)
- 68. Safronova, M.S., Sapirstein, J., Johnson, W.R.: Relativistic many-body calculations of energy levels, hypeerfine constants, and transition rates for sodiumlike ions. Phys. Rev. A 58, 1016–28 (1998)
- Salomonson, S., Lindgren, I., Mårtensson, A.M.: Numerical Many-Body Perturbation Calculations on Be-like Systems Using a Multi-Configurational Model Space. Presented at the Nobel Symposium on Many-Body Effects in Atoms and Solids, Lerum, 1979. Physica Scripta 21, 335–42 (1980)

- 70. Salomonson, S., Öster, P.: Numerical solution of the coupled-cluster single- and double-excitation equations with application to Be and Li⁻. Phys. Rev. A **41**, 4670–81 (1989)
- 71. Salomonson, S., Öster, P.: Relativistic all-order pair functions from a discretized single-particle Dirac Hamiltonian. Phys. Rev. A 40, 5548, 5559 (1989)
- 72. Salomonson, S., Ynnerman, A.: Coupled-cluster calculations of matrix elements and ionization energies of low-lying states of sodium. Phys. Rev. A 43, 88–94 (1991)
- 73. Salpeter, E.E., Bethe, H.A.: A Relativistic Equation for Bound-State Problems. Phys. Rev. 84, 1232–42 (1951)
- 74. Schäfer, L., Weidenmüller, H.A.: Self-consistency in application of Brueckner's method to doubly-closed-shell nuclei. Nucl. Phys. A 174, 1 (1971)
- 75. Sinanŏglu, O.: *Electronic correlation in atoms and molecules*. Adv. Chem. Phys. **14**, 237–81 (1969)
- 76. Sucher, J.: Energy Levels of the Two-Electron Atom to Order α³ Ry; Ionization Energy of Helium. Phys. Rev. **109**, 1010–11 (1957)
- 77. Sucher, J.: Ph.D. thesis, Columbia University (1958). Univ. Microfilm Internat., Ann Arbor, Michigan
- 78. Sucher, J.: Foundations of the Relativistic Theory of Many Electron Atoms. Phys. Rev. A 22, 348–62 (1980)
- 79. Čársky, P., Paldus, J., Pittner, J. (eds.): Recent Progress in Coupled Cluster Methods: Theory and Applications. Springer (2009)
- 80. Wick, C.G.: The Evaluation of the Collision Matrix. Phys. Rev. 80, 268–272 (1950)

Chapter 3

Time-Dependent Formalism

In this chapter, we shall summarize the fundamentals of time-dependent perturbation theory. Although we shall be only concerned with stationary problems in this book, it will be advantageous to apply time-dependent methods. We restrict ourselves in this chapter to the *nonrelativistic formalism* and return to the relativistic one in later chapters.

3.1 Evolution Operator

It follows from the second-quantized Schrödinger equation (2.16) that the state vector evolves in time according to

$$|\chi_{\mathcal{S}}(t)\rangle = e^{-iH(t-t_0)/\hbar} |\chi_{\mathcal{S}}(t_0)\rangle. \tag{3.1}$$

This is known as the *Schrödinger picture* (SP), indicated by the subscript "S." In another representation, known as the *interaction picture* (IP) [see Appendix B, (B.23)], the Hamiltonian is partitioned according to (2.48), $H = H_0 + V$, and the state vectors and the operators are transformed according to

$$|\chi_{\rm I}(t)\rangle = \mathrm{e}^{\mathrm{i}H_0t/\hbar} |\chi_{\rm S}(t)\rangle; \qquad \mathcal{O}_{\rm I}(t) = \mathrm{e}^{\mathrm{i}H_0t/\hbar} \mathcal{O}_{\rm S} \,\mathrm{e}^{-\mathrm{i}H_0t/\hbar}.$$
 (3.2)

This implies that the state vectors are normally much more slowly varying with time, and most of the time dependence is instead transferred to the operators that are normally time independent in SP.

The Schrödinger equation is in IP transformed to

$$\left| i\hbar \frac{\partial}{\partial t} |\chi_{\rm I}(t)\rangle = V_{\rm I}(t) |\chi_{\rm I}(t)\rangle, \right|$$
 (3.3)

with the solution

$$|\chi_{\mathrm{I}}(t)\rangle = |\chi_{\mathrm{I}}(t_0)\rangle - \frac{\mathrm{i}}{\hbar} \int_{t_0}^t \mathrm{d}t_1 \ V_{\mathrm{I}}(t_1) \left| \chi_{\mathrm{I}}(t_1) \right\rangle. \tag{3.4}$$

 $V_{\rm I}(t)$ is the perturbation in the interaction picture, which is assumed to be *time* independent in the Schrödinger picture.

For a *stationary state* of energy E, the time dependence (2.15) is $e^{-iEt/\hbar}$. It then follows that the state in the IP is of the form

$$|\chi_{\rm I}(t)\rangle = e^{-it(E - H_0)/\hbar} |\chi_{\rm I}(t=0)\rangle. \tag{3.5}$$

The time-evolution operator in IP, $U_{\rm I}(t,t_0)$, is defined by the relation

$$|\chi_{\rm I}(t)\rangle = U_{\rm I}(t, t_0) |\chi_{\rm I}(t_0)\rangle \qquad (t > t_0).$$
(3.6)

Evidently, we then have

$$U_{\rm I}(t,t) = 1, \tag{3.7}$$

$$U_{\rm I}(t,t_1)\,U_{\rm I}(t_1,t_2) = U_{\rm I}(t,t_2). \tag{3.8}$$

From the relation (3.1), it follows that the corresponding evolution operator in SP is

$$U_{\rm S}(t,t_0) = e^{-iH(t-t_0)/\hbar}$$
 (3.9)

Transforming (3.2) to IP then yields¹

$$U_{\rm I}(t,t_0) = e^{iH_0t/\hbar} e^{-iH(t-t_0)/\hbar} e^{-iH_0t_0/\hbar}.$$
 (3.10)

This evolution operator satisfies the differential equation

$$\left| i\hbar \frac{\partial}{\partial t} U_{\rm I}(t, t_0) = V_{\rm I}(t) U_{\rm I}(t, t_0), \right|$$
 (3.11)

which leads to the expansion2

$$U(t,t_0) = 1 - \frac{\mathrm{i}}{\hbar} \int_{t_0}^t \mathrm{d}t_1 \, V(t_1) \, U(t_1,t_0)$$

$$= 1 - \frac{\mathrm{i}}{\hbar} \int_{t_0}^t \mathrm{d}t_1 \, V(t_1) + \left(\frac{-\mathrm{i}}{\hbar}\right)^2 \int_{t_0}^t \mathrm{d}t_1 \, V(t_1) \int_{t_0}^{t_1} \mathrm{d}t_2 \, V(t_2) \, U(t_2,t_0),$$
(3.12)

¹ It should be noted that generally $e^{iH_0t/\hbar}e^{-iHt/\hbar} \neq e^{-iVt/\hbar}$, since the operators do not necessarily commute.

² Unless specified otherwise, we shall in the following assume that the evolution operators always are expressed in IP and leave out the subscript _I.

etc. By extending the second integration from t_0 to t, this can be expressed [2, Fig. 6.1]

$$U(t,t_0) = 1 - \frac{\mathrm{i}}{\hbar} \int_{t_0}^t \mathrm{d}t_1 \ V(t_1) + \frac{1}{2} \left(\frac{-\mathrm{i}}{\hbar}\right)^2 \int_{t_0}^t \mathrm{d}t_1 \int_{t_0}^t \mathrm{d}t_2 \ T[V(t_1)V(t_2)] \ U(t_2,t_0),$$
(3.13)

where *T* is the *time-ordering operator*, which orders the operators after decreasing time (without any sign change). This leads to the expansion

$$U_{1}(t, t_{0}) = -\frac{i}{\hbar} \int_{t_{0}}^{t} dt_{1} V(t_{1}),$$

$$U_{2}(t, t_{0}) = \frac{1}{2} \left(\frac{-i}{\hbar}\right)^{2} \int_{t_{0}}^{t} dt_{1} \int_{t_{0}}^{t} dt_{2} T[V(t_{1}) V(t_{2})], \qquad (3.14)$$

etc., which can be generalized to [2, Eq. 6.23], [4, Eq. 4-56]

$$U(t,t_0) = \sum_{n=0}^{\infty} \frac{1}{n!} \left(\frac{-i}{\hbar}\right)^n \int_{t_0}^t dt_1 \dots \int_{t_0}^t dt_n \, T[V(t_1) \dots V(t_n)]. \tag{3.15}$$

(We have here included the term n = 0 to replace the unity.)

We introduce the *Hamiltonian density* $\mathcal{H}(x)$ by

$$V(t) = \int d^3x \, \mathcal{H}(t, \mathbf{x}). \tag{3.16}$$

We do not have to specify the perturbation at this point, but we shall later assume that it is given by the interaction between the electrons (of charge -e) and the electromagnetic radiation field (see Appendix E.3)

$$\mathcal{H}(x) = -\hat{\psi}^{\dagger}(x)ec\alpha^{\mu}A_{\mu}(x)\hat{\psi}(x). \tag{3.17}$$

Here, α^{μ} is the Dirac operator (see Appendix D) and A_{μ} is the covariant radiation field [Appendix (G.2)]

$$A_{\mu}(x) = \sqrt{\frac{\hbar}{2\epsilon_0 \omega V}} \sum_{kr} \varepsilon_{\mu r} \left[a_{kr}^{\dagger} e^{ikx} + a_{kr} e^{-ikx} \right]. \tag{3.18}$$

The evolution operator (3.15) can now be expressed

$$U(t,t_0) = \sum_{n=0}^{\infty} \frac{1}{n!} \left(\frac{-i}{c\hbar}\right)^n \int_{t_0}^t dx_1^4 \dots \int_{t_0}^t dx_n^4 T \left[\mathcal{H}(x_1) \dots \mathcal{H}(x_n)\right].$$
(3.19)

The factor of c in the denominator is due to the fact that we now use the integration variable $x_0 = ct$. The integrations are performed over all space and over time as indicated. Alternatively, this can be expressed

$$U(t, t_0) = T \left[\exp\left(\frac{-i}{c\hbar} \int_{t_0}^t d^4x \,\mathcal{H}(x)\right) \right]. \tag{3.20}$$

The evolution operator can be represented graphically be means of Goldstone diagrams in the same way as the wave operator, discussed previously. As a simple example, we consider the first-order interaction with a time-independent potential interaction v(x). In second quantization, the evolution operator becomes

$$U^{(1)}(t,t_0) = -\frac{i}{\hbar} \int_{t_0}^t dt \ c_r^{\dagger} \langle r | v(\mathbf{x}_1) | a \rangle \ c_a$$
 (3.21)

or after summing over the states

$$U^{(1)}(t,t_0) = -\frac{\mathrm{i}}{\hbar} \int_{t_0}^t \mathrm{d}t_1 \int \mathrm{d}^3 x_1 \, \hat{\psi}^{\dagger}(x_1) \, \nu(x_1) \, \hat{\psi}(x_1), \tag{3.22}$$

which is illustrated in Fig. 3.1 (left).

The two-body interaction can be given by a *contraction* of *two* perturbations (3.17), corresponding to the exchange of one virtual photon, $v(x_1, x_2)$, as will be further discussed in Chap. 4. The corresponding, second-order evolution operator then becomes (Fig. 3.1, right)

$$U^{(2)}(t,t_0) = \frac{1}{2} \left(\frac{-i}{\hbar}\right)^2 \iint_{t_0}^t dt_1 dt_2$$

$$\times \iint d^3 x_1 d^3 x_2 \, \hat{\psi}^{\dagger}(x_1) \, \hat{\psi}^{\dagger}(x_2) \, \nu(x_1,x_2) \, \hat{\psi}(x_2) \, \hat{\psi}(x_1). \quad (3.23)$$

In higher orders, the operator can have connected as well as disconnected parts and can be separated into zero-, one-, two-,... body parts. The connected one- and

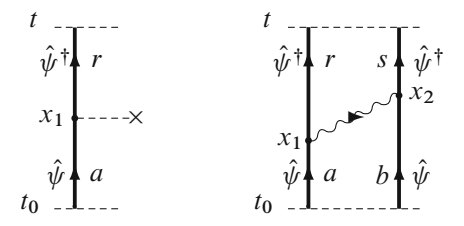


Fig. 3.1 Graphical representation of the evolution operator for first-order potential interaction and single-photon exchange

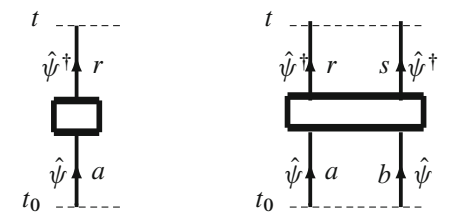


Fig. 3.2 Schematic graphical representation of the connected one- and two-body parts of the evolution operator

two-body pieces are schematically illustrated in Fig. 3.2. Expressions with uncontracted photons fall in an *extended photonic Fock space*, as will be further discussed in later chapters.

3.2 Adiabatic Damping: Gell-Mann-Low Theorem

For the mathematical treatment, we shall find it convenient to apply an "adiabatic damping factor" to the perturbation,

$$V(t) \to V(t) e^{-\gamma |t|}, \tag{3.24}$$

where γ is a small, positive number, which implies that

$$H \to H_0 \quad \text{as} \quad t \to -\infty.$$
 (3.25)

The expansion (3.19) then becomes

$$U_{\gamma}(t,t_{0}) = \sum_{n=0}^{\infty} \frac{1}{n!} \left(\frac{-i}{c\hbar}\right)^{n} \times \int_{t_{0}}^{t} dx_{1}^{4} \dots \int_{t_{0}}^{t} dx_{n}^{4} T[\mathcal{H}(x_{1}) \dots \mathcal{H}(x_{n})] e^{-\gamma(|t_{1}|+|t_{2}|\dots+|t_{n}|)}.$$
(3.26)

The damping is adiabatically 'switched off' at the end of the calculation. The evolution operator satisfies now the equation (3.11)

$$i\hbar \frac{\partial}{\partial t} U_{\gamma}(t, t_0) = (V(t) \mp i\gamma) U_{\gamma}(t, t_0),$$
 (3.27)

where the upper sign is valid for t > 0.

3.2.1 Gell-Mann-Low Theorem

The damped perturbation (3.24) vanishes, when $\gamma t \to \pm \infty$, and the perturbed (target) state vector approaches in these limits an eigenstate of H_0 ,

$$\left|\chi_{\mathrm{I}\gamma}(t)\right\rangle \Rightarrow \left|\Phi\right\rangle,\tag{3.28}$$

which we call the *parent state*. Gell-Mann and Low have shown that for t = 0 and in the limit $\gamma \to 0$, the state vector

$$\lim_{\gamma \to 0} |\chi_{I\gamma}(0)\rangle = \lim_{\gamma \to 0} \frac{U_{\gamma}(0, -\infty)|\Phi\rangle}{\langle \Phi|U_{\gamma}(0, -\infty)|\Phi\rangle} =: |\Psi\rangle$$
 (3.29)

is a solution of the time-independent Schrödinger equation

$$(H_0 + V)|\Psi\rangle = E|\Psi\rangle, \qquad (3.30)$$

where H_0 is the model Hamiltonian (2.49) without the interaction. Here,

$$E = E_0 + i\hbar\gamma\lambda \frac{\langle \Phi | \frac{\partial}{\partial\lambda} U_{\gamma}(0, -\infty) | \Phi \rangle}{\langle \Phi | U_{\gamma}(0, -\infty) | \Phi \rangle}.$$
 (3.31)

This is the famous <u>Gell-Mann-Low theorem</u> (GML) [3], [2, p. 61], [10, p. 336], which represents one of the fundamentals of the theory presented here. The perturbation, V, must in the limit $\gamma \to 0$ be <u>time independent in the Schrödinger picture</u>, which is the case with the interaction (3.17).

3.3 Extended Model Space: The Generalized Gell-Mann–Low Relation

The original Gell-Mann–Low theorem (3.29) is valid only in the single-reference case (one-dimensional model space). The time-dependent MBPT was in 1960s and 1970s further developed by several groups [1,5,6,8,9,11], mainly in connection with nuclear calculations. We shall extend this treatment here and prove a generalization of the Gell-Mann–Low theorem for an arbitrary model space. This treatment follows mainly that performed in [7] (see also [2, Sect. 6]).

We choose the parent states to be the (normalized) limits of the target states for finite γ as $t \to -\infty$, as introduced by Tolmachev [11],

$$|\Phi^{\alpha}\rangle = C^{\alpha} \lim_{t \to -\infty} |\chi^{\alpha}\rangle_{\gamma} \qquad (\alpha = 1, 2 \cdots d),$$
 (3.32)

where C^{α} is a normalization constant. The parent functions are then eigenfunctions of H_0 ,

$$H_0 \left| \Phi^{\alpha} \right\rangle = E_0^{\alpha} \left| \Phi^{\alpha} \right\rangle, \tag{3.33}$$

but generally we do not know which eigenvalue a specific target state will converge to.

In analogy with the single-reference case (3.29), we construct the state

$$\left|\Psi_{\gamma}^{\alpha}\right\rangle = \frac{U_{\gamma}(0, -\infty)\left|\Phi^{\alpha}\right\rangle}{\left\langle\Psi_{0}^{\alpha}\left|U_{\gamma}(0, -\infty)\right|\Phi^{\alpha}\right\rangle},\tag{3.34}$$

which is normalized in the intermediate normalization, $\langle \Psi_0^{\alpha} \mid \Phi^{\alpha} \rangle$.

We shall now demonstrate that this state is in the limit $\gamma \to 0$ an eigenstate of the time-independent Hamiltonian of the system for all values of α ,

$$(H_0 + V)|\Psi^{\alpha}\rangle = E^{\alpha}|\Psi^{\alpha}\rangle \qquad (\alpha = 1, 2, \dots d). \tag{3.35}$$

• This is a generalization of the original Gell-Mann–Low relation (3.29), and it holds also for a quasi-degenerate model space with several energy levels [7].

In order to prove the theorem, we consider one term in the expansion (3.26)

$$U_{\gamma}^{(n)}(t, -\infty) = \frac{1}{n!} \left(\frac{-\mathrm{i}}{\hbar}\right)^n \int_{-\infty}^t \mathrm{d}t_n$$

$$\times \int_{-\infty}^t \mathrm{d}t_{n-1} \cdots T[V(t_n)V(t_{n-1})\cdots] e^{\gamma(t_1 + t_2 \dots + t_n)}. \tag{3.36}$$

(As long as t does not approach $+\infty$, we can leave out the absolute signs in the damping factor.) Using the identity

$$[H_0, ABC \cdots] = [H_0, A]BC \cdots + A[H_0, B]C \cdots + \cdots,$$

we obtain, noting that in IP $V_{\rm I}(t)={\rm e}^{{\rm i}tH_0/\hbar}V_{\rm S}\,{\rm e}^{-{\rm i}tH_0/\hbar}$ and that V is assumed to be time independent in the SP,

$$\frac{\partial V_{12}(t)}{\partial t} = i [H_0, V_{12}(t)]$$
 (3.37)

and

$$\left[H_0, V(t_n)V(t_{n-1})\cdots\right] = -i\hbar \left(\frac{\partial}{\partial t_n} + \frac{\partial}{\partial t_{n-1}} + \cdots\right)V(t_n)V(t_{n-1})\cdots. \tag{3.38}$$

This gives

$$[H_0, U_{\gamma}^{(n)}(t, -\infty)] = -\frac{1}{n!} \left(\frac{-i}{\hbar}\right)^{(n-1)} \int_{-\infty}^{t} dt_n \int_{-\infty}^{t} dt_{n-1} \cdots \times T \left[\left(\frac{\partial}{\partial t_n} + \frac{\partial}{\partial t_{n-1}} + \cdots\right) V(t_n) V(t_{n-1}) \cdots \right] \times e^{\gamma(t_1 + t_2 \dots + t_n)}.$$

When integrating by parts, each term gives the same contribution, yielding

$$[H_0, U_{\gamma}^{(n)}(t, -\infty)] = -V(t) U_{\gamma}^{(n-1)}(t, -\infty) + i\hbar \, n\gamma \, U_{\gamma}^{(n)}(t, -\infty), \qquad (3.39)$$

where the last term originates from derivating the damping term. Introducing an order parameter, λ ,

$$H = H_0 + \lambda V(t), \tag{3.40}$$

the result can be expressed

$$[H_0, U_{\gamma}(t, -\infty)] = -V(t) U_{\gamma}(t, -\infty) + i\hbar\gamma\lambda \frac{\partial}{\partial\lambda} U_{\gamma}(t, -\infty). \tag{3.41}$$

By operating with the commutator on the parent function (3.32), utilizing the fact that the parent state Φ^{α} is an eigenstate of H_0 , we obtain for t=0

$$\left(H_0 - E_0^{\alpha} + V\right) U_{\gamma}(0, -\infty) \left| \Phi^{\alpha} \right\rangle = i\hbar\gamma\lambda \frac{\partial}{\partial\lambda} U_{\gamma}(0, -\infty) \left| \Phi^{\alpha} \right\rangle, \tag{3.42}$$

where V = V(0) or with the state (3.34)

$$(H_0 + V - E_0^{\alpha}) |\Psi_{\gamma}^{\alpha}\rangle = i\hbar\gamma\lambda \frac{\frac{\partial}{\partial\lambda} U_{\gamma}(0, -\infty) |\Phi^{\alpha}\rangle}{(\Psi_0^{\alpha}) U_{\gamma}(0, -\infty) |\Phi^{\alpha}\rangle}.$$
 (3.43)

(Note that at t = 0 the Schrödinger and interaction pictures are identical.) We note from the relation (3.34), that

$$\frac{\partial}{\partial \lambda} |\Psi_{\gamma}^{\alpha}\rangle = \frac{\partial}{\partial \lambda} \frac{U_{\gamma}(0, -\infty) |\Phi^{\alpha}\rangle}{\langle \Psi_{0}^{\alpha} | U_{\gamma}(0, -\infty) | \Phi^{\alpha}\rangle} = \frac{\frac{\partial}{\partial \lambda} U_{\gamma}(0, -\infty) |\Phi^{\alpha}\rangle}{\langle \Psi_{0}^{\alpha} | U_{\gamma}(0, -\infty) | \Phi^{\alpha}\rangle} - \frac{\langle \Psi_{0}^{\alpha} | \frac{\partial}{\partial \lambda} U_{\gamma}(0, -\infty) | \Phi^{\alpha}\rangle}{\langle \Psi_{0}^{\alpha} | U_{\gamma}(0, -\infty) | \Phi^{\alpha}\rangle} \frac{U_{\gamma}(0, -\infty) |\Psi_{0}^{\alpha}\rangle}{\langle \Psi_{0}^{\alpha} | U_{\gamma}(0, -\infty) | \Phi^{\alpha}\rangle}.$$
(3.44)

Therefore, the r.h.s. of (3.43) can be expressed

$$\mathrm{i}\hbar\gamma\lambda\,\frac{\frac{\partial}{\partial\lambda}U_{\gamma}(0,-\infty)|\varPhi^{\alpha}\rangle}{\left|\varPsi_{0}^{\alpha}\left|U_{\gamma}(0,-\infty)\right|\varPhi^{\alpha}\right\rangle}=\Delta E_{\gamma}^{\alpha}\left|\varPsi_{\gamma}^{\alpha}\right\rangle+\mathrm{i}\gamma\lambda\,\frac{\partial}{\partial\lambda}\left|\varPsi_{\gamma}^{\alpha}\right\rangle,$$

where

$$\Delta E_{\gamma}^{\alpha} = i\hbar\gamma\lambda \frac{\left\langle \Psi_{0}^{\alpha} \left| \frac{\partial}{\partial\lambda} U_{\gamma}(0, -\infty) \right| \Phi^{\alpha} \right\rangle}{\left\langle \Psi_{0}^{\alpha} \left| U_{\gamma}(0, -\infty) \right| \Phi^{\alpha} \right\rangle}$$

and this yields

$$(H_0 + V - E_0^{\alpha} - \Delta E_{\gamma}^{\alpha}) |\Psi_{\gamma}^{\alpha}\rangle = i\hbar\gamma\lambda \frac{\partial}{\partial\lambda} |\Psi_{\gamma}^{\alpha}\rangle. \tag{3.45}$$

Provided that the perturbation expansion of $|\Psi_{\gamma}^{\alpha}\rangle$ converges, the r.h.s. will vanish as $\gamma \to 0$. Then

• The generalized Gell-Mann-Low (GML) relation reads

$$\left| \Psi^{\alpha} \right\rangle = \lim_{\gamma \to 0} \left| \Psi^{\alpha}_{\gamma} \right\rangle = \lim_{\gamma \to 0} \frac{U_{\gamma}(0, -\infty) \left| \Phi^{\alpha} \right\rangle}{\left\langle \Psi^{\alpha}_{0} \left| U_{\gamma}(0, -\infty) \right| \Phi^{\alpha} \right\rangle}.$$
(3.46)

This state vector will satisfy the time-independent Schrödinger equation

$$\overline{\left(H_0 + V(0)\right) \left| \Psi^{\alpha} \right\rangle} = E^{\alpha} \left| \Psi^{\alpha} \right\rangle,$$
(3.47)

where H_0 is the model or independent-particle Hamiltonian 2.49 and V is the perturbation (3.16).

This relation is derived in the interaction picture with t = 0, which implies that it holds also in the Schrödinger picture (SP). The perturbation must be time-independent in SP, apart from possible damping, as is the case with the perturbation (3.17).

The energy eigenvalue corresponding the Gell-Mann–Low state (3.46) becomes

$$E^{\alpha} = \lim_{\gamma \to 0} \left[E_0^{\alpha} + i\hbar\gamma\lambda \frac{\left\langle \Psi_0^{\alpha} \middle| \frac{\partial}{\partial\lambda} U_{\gamma}(0, -\infty) \middle| \Phi^{\alpha} \right\rangle}{\left\langle \Psi_0^{\alpha} \middle| U_{\gamma}(0, -\infty) \middle| \Phi^{\alpha} \right\rangle} \right]. \tag{3.48}$$

This expression is not very useful for evaluating the energy, since the eigenvalue E_0^{α} of the parent state is generally not known. The procedure is here used mainly to demonstrate that the functions satisfy the Schrödinger equation. Instead, we shall derive an expression for the effective Hamiltonian (2.54), which is the natural tool for a multilevel model space.³

In the one-dimensional model space, singularities appear in U for unlinked terms. In the general multidimensional case, singularities can appear also for

³ It should be noted that a necessary condition for the proof of the theorem given here is that the parent state (3.33) is an eigenstate of the model Hamiltonian H_0 [see (3.42)]. This is in conflict with the statement of Kuo et al. [6], who claim that it is sufficient that this state has a nonzero overlap with the corresponding target state.

linked diagrams that have an *intermediate state in the model space*. The remaining diagrams are regular. In addition, so-called *quasi-singularities* can appear – i.e., very large, but finite, contributions – when an intermediate state is *quasi-degeneracy* with the initial state. All singularities and quasi-singularities are eliminated in the ratio (3.46) – in analogy with the original Gell-Mann–Low theorem, although in the general case there is a *finite remainder*, so-called *model-space contribution* (MSC). The elimination of these quasi-singularities represents the major advantage of the procedure using an extended model space. We shall see how this procedure can also be applied in quantum-electrodynamical calculations in the following sections.

References

- Brown, G.E., Kuo, T.T.S.: Structure of finite nuclei and the nucleon-nucleon interaction. Nucl. Phys. A 92, 481–94 (1967)
- Fetter, A.L., Walecka, J.D.: The Quantum Mechanics of Many-Body Systems. McGraw-Hill, N.Y. (1971)
- Gell-Mann, M., Low, F.: Bound States in Quantum Field Theory. Phys. Rev. 84, 350–54 (1951)
- 4. Itzykson, C., Zuber, J.B.: Quantum Field Theory. McGraw-Hill (1980)
- Jones, R.W., Mohling, F.: Perturbation theory of a many-fermion system. Nucl. Phys. A 151, 420–48 (1970)
- 6. Kuo, T.T.S., Lee, S.Y., Ratcliff, K.F.: A folded-diagram expansion of the model-space effective Hamiltonian. Nucl. Phys. A 176, 65–88 (1971)
- Lindgren, I., Salomonson, S., Åsén, B.: The covariant-evolution-operator method in boundstate QED. Physics Reports 389, 161–261 (2004)
- 8. Morita, T.: Perturbation Theory for Degenerate Problems of Many-Fermion Systems. Progr. Phys. (Japan) 29, 351–69 (1963)
- 9. Oberlechner, G., Owono-N'-Guema, F., Richert, J.: Perturbation Theory for the Degenerate Case in the Many-Body Problem. Nouvo Cimento B 68, 23–43 (1970)
- Schweber, S.S.: An Introduction to Relativistic Quantum Field Theory. Harper and Row, N.Y. (1961)
- 11. Tolmachev, V.V.: The field-theoretic form of the perturbation theory for many-electron atoms. I. Abstract theory. Adv. Chem. Phys. 14, 421, 471 (1969)

Part II Quantum-Electrodynamics: One-Photon and Two-Photon Exchange

Chapter 4 S-Matrix

In Part I, we have considered methods for treating atomic many-body systems within the standard relativistic MBPT and coupled-cluster schemes, in what is known as the *no-virtual-pair approximation* (NVPA). In the second part, we shall include effects beyond this approximation, which we shall refer to as *quantum-electrodynamical* (*QED*) *effects*. We shall describe three methods for numerical calculations of QED effects on bound states, developed in the last few decades, which are all based upon field theory.¹

In this chapter, we present the most frequently applied scheme for bound-state QED calculations, namely the *S-matrix formulation*. In this chapter, we also come into contact with the important question of the choice of gauge. The Maxwell equations are invariant under a certain class of gauge transformations, as shown in Appendix G. So far, practically all QED calculations have been performed using what is known as *covariant gauges*, particularly the Feynman gauge, where the expressions involved are particularly simple. However, for bound-state problems, where the Coulomb interaction often dominates, it would be more advantageous to use the Coulomb gauge. It has been demonstrated by several authors [1,14] that it is perfectly legitimate to use the Coulomb gauge also in QED calculations and that this leads to results that are renormalizable and completely equivalent to those obtained using covariant gauges.

In the next chapter, we consider the *Green's-function method*, which is frequently used in various fields of physics. In Chap. 6, we shall present the recently introduced *covariant-evolution operator method*, which will form the basis for the unified approach we are developing in the following chapters.

¹ From now on we shall for simplicity set $\hbar=1$ but maintain the remaining fundamental constants. In this way, our results will be valid in the relativistic or natural unit system as well as in the Hartree atomic unit system. They will also be valid in the cgs unit system, as long as we stay consistently to either the electrostatic or the magnetic version, but they will NOT be valid in the Gaussian system that is a mixture of the two. With our choice, it will still be possible to perform a meaningful dimensional analysis (see further Appendix K).

4.1 Definition of the S-Matrix: Feynman Diagrams

The *scattering matrix* or *S-matrix* was introduced by Wheeler [18] and Werner Heisenberg in 1930s, particularly for studying the scattering processes between elementary particles. The formalism is not particularly suited for bound-state problems but has in the last few decades been applied also to such problems in connection with QED calculations (see, for instance, the review article by Mohr, Plunien, and Soff [11] for a modern update).

The S-matrix relates the initial state of a particle or system of particles, $\Phi_i = \Phi(t = -\infty)$, before the interaction has taken place, to the final state after the interaction is completed, $\Phi_f = \Phi(t = +\infty)$,

$$\Phi(t = +\infty) = S \,\Phi(t = -\infty). \tag{4.1}$$

We know that the time evolution of the state vector in the interaction picture is governed by the evolution operator (3.6), which leads to the connection

$$S = U(\infty, -\infty). \tag{4.2}$$

This is assumed to hold also relativistically (see, for instance, Bjorken and Drell [2]). With the expansion (3.26), this becomes

$$S = \sum_{n=0}^{\infty} \frac{1}{n!} \left(\frac{-i}{c}\right)^n \int dx_1^4 \dots \int dx_n^4 T \left[\mathcal{H}(x_1) \dots \mathcal{H}(x_n)\right] e^{-\gamma(|t_1|+|t_2|\dots|t_n|)}.$$
(4.3)

Here, x is the four-dimensional coordinate vector x = (ct, x), which explains the factor of c in the denominator. The S-matrix is – in contrast to the evolution operator for finite times – *Lorentz covariant* (see footnote in the Introduction), which is manifestly demonstrated by its form given here. We shall normally assume that the perturbation density is given by the interaction between the electrons and the electromagnetic radiation field (3.17)

$$\mathcal{H}(x) = -\hat{\psi}^{\dagger}(x)ec\alpha^{\mu}A_{\mu}(x)\hat{\psi}(x). \tag{4.4}$$

The S-matrix can conveniently be represented by so-called *Feynman diagrams*. Feynman has in his famous papers from 1949 [5, 6] developed a set of rules for evaluating the S-matrix for various elementary processes (see Appendix H), and this has formed the basis for much of the developments that followed in quantum-electrodynamics and field theory in general (see, for instance, the books by Mandl and Shaw [10, Chap. 7] and Peskin and Schroeder [13]). This has also formed the basis for the diagrammatic representation of many-body perturbation theory (MBPT), discussed earlier [8].

In order to represent the S-matrix by means of Feynman diagrams, this has to be transformed into *normal order*, which can be performed by means of Wick's theorem (see Sect. 2.2). This leads to all possible (zero, single, double ...) contractions between the perturbations \mathcal{H} and to diagrams of the type shown in Fig. 2.9. (Details of this process are found in standard text books, e.g., Fetter and Walecka [4] or Lindgren-Morrison [8].) Below we shall illustrate this by a few simple examples.

Even if the S-matrix formulation was initially set up for scattering problems, we shall here be mainly concerned with applications to bound-state problems. Since the final time of the scattering process is $t=+\infty$, we cannot directly apply the Gell-Mann–Low theorem [(3.31) and (3.46)]. Sucher [16] has, however, modified the Gell-Mann–Low energy formula so that it can be applied also to the S-matrix. With the S-matrix expanded in a perturbation series

$$S = \sum_{n} S^{(n)},\tag{4.5}$$

the energy shift can be expressed

$$\Delta E = \lim_{\gamma \to 0} \frac{i\gamma}{2} \frac{\sum n \langle \Phi | S^{(n)} | \Phi \rangle}{\langle \Phi | S | \Phi \rangle}.$$
 (4.6)

This energy formula can also be applied to a *degenerate* multistate model space – but *not* in the case of *quasi-degeneracy*, when there are several distinct energy levels within the model space. Furthermore, in the S-matrix formulation no information can be derived for the corresponding change of the state vector or wave function. For these reasons, the S-matrix formulation is not suited as a basis for a unification with many-body perturbation theory that is our main concern in this book. We shall return to this problem in later chapters.

Before we consider some physical processes, we shall define two very important concepts, namely the *Feynman electron* and *photon propagators* that will be frequently used in the following.

4.2 Electron Propagator

The *contraction* between two electron-field operators is defined as *the difference* between the time and normal orderings (see Sect. 2.2)

$$\hat{\psi}(x_1)\hat{\psi}^{\dagger}(x_2) = T \left[\hat{\psi}(x_1)\hat{\psi}^{\dagger}(x_2)\right] - N \left[\hat{\psi}(x_1)\hat{\psi}^{\dagger}(x_2)\right]. \tag{4.7}$$

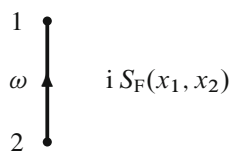


Fig. 4.1 Graphical representation of the (bound-state) electron propagator. As before, we shall let *thick vertical lines* represent electron propagators in the bound-state representation (Furry picture) and *thin lines* in the free-electron representation

Since the vacuum expectation value vanishes for every normal-ordered product, it follows that the contraction is equal to the vacuum expectation of the time-ordered product²

$$\hat{\psi}(x_1)\hat{\psi}^{\dagger}(x_2) = \langle 0|T[\hat{\psi}(x_1)\hat{\psi}^{\dagger}(x_2)]|0\rangle
= \langle 0|\Theta(t_1 - t_2)\hat{\psi}(x_1)\hat{\psi}^{\dagger}(x_2) - \Theta(t_2 - t_1)\hat{\psi}^{\dagger}(x_2)\hat{\psi}(x_1)|0\rangle$$
(4.8)

considering that the electron fields operators are fermions that anticommute. Θ is the Heaviside step function [Appendix A, (A.29)].

• The Feynman electron propagator is defined (see Fig. 4.1)³

$$\widehat{\hat{\psi}}(x_1)\widehat{\psi}^{\dagger}(x_2) = \langle 0|T[\widehat{\psi}(x_1)\widehat{\psi}^{\dagger}(x_2)]|0\rangle =: i S_F(x_1, x_2).$$
(4.9)

Separating the field operators into particle (p) and hole (h) parts, $\hat{\psi} = \hat{\psi}_+ + \hat{\psi}_-$, above and below the Fermi surface, respectively, it follows that the expression (4.8) is identical to

$$\begin{aligned} & \langle 0 \big| \Theta(t_1 - t_2) \, \hat{\psi}_+(x_1) \hat{\psi}_+^{\dagger}(x_2) - \Theta(t_2 - t_1) \, \hat{\psi}_-^{\dagger}(x_2) \hat{\psi}_-(x_1) \big| 0 \rangle \\ &= \Theta(t_1 - t_2) \, \phi_p(\mathbf{x}_1) \phi_p^{\dagger}(\mathbf{x}_2) \, \mathrm{e}^{-\varepsilon_p(t_1 - t_2)} - \Theta(t_2 - t_1) \, \phi_h^{\dagger}(\mathbf{x}_2) \phi_h(\mathbf{x}_1) \, \mathrm{e}^{-\varepsilon_h(t_1 - t_2)} \end{aligned}$$

² In field theory, the vacuum state is normally the "true" vacuum with no (positive-energy) particles or photons present. In the Dirac picture, this implies that the negative-energy states or "hole" states of the "Dirac sea" are filled. In many-body applications without reference to field theory, the "vacuum" is normally a closed-shell state related to the system (finite or infinite) under study, obtained for instance by removing the valence or open-shell single-electron states. Single-electron states present in this vacuum state are referred to as hole states and those not present as virtual or particle states. In our unified approach, we shall let hole states include negative-energy (antiparticle) states as well as core states.

³ Note that we define here the electron propagator, using $\hat{\psi}^{\dagger}$ rather than $\bar{\hat{\psi}} = \hat{\psi}^{\dagger}\beta$, which is more frequently used. We find the present definition more convenient in working with the combination of QED and MBPT.

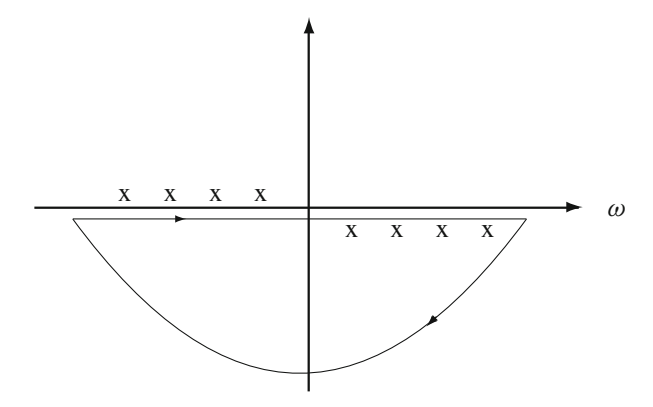


Fig. 4.2 Complex integration of the electron propagator (4.10)

using the time dependence of the field operators in IP in Appendix B (B.28). As will be demonstrated below,

• The electron propagator can be expressed as a complex integral

$$S_{F}(x_{1}, x_{2}) = \int \frac{d\omega}{2\pi} \frac{\phi_{j}(x_{1}) \phi_{j}^{\dagger}(x_{2})}{\omega - \varepsilon_{j} + i\eta \operatorname{sgn}(\varepsilon_{j})} e^{-i\omega(t_{1} - t_{2})}, \qquad (4.10)$$

where η is a small, positive number.

In order to verify the integral formula (4.10), we first consider the case $t_1 > t_2$. Here, the integrand vanishes exponentially as $\omega \to -\mathrm{i} \infty$, and we then integrate over the *negative* half-plane, as illustrated in Fig. 4.2. Here, the poles appear at $\omega = \varepsilon_j$ when this is positive. The contribution to the integral from this pole is $-2\pi\mathrm{i}$ times the pole value – with the minus sign due to the negative (clockwise) integration – or $-\mathrm{i}\phi_j(x_1)\,\phi_j^\dagger(x_2)\,\mathrm{e}^{-\mathrm{i}\varepsilon_j(t_1-t_2)}$. Similarly, when $t_1 < t_2$, we integrate over the *positive* half plane with the result $+\mathrm{i}\phi_j(x_1)\,\phi_j^\dagger(x_2)\,\mathrm{e}^{-\mathrm{i}\varepsilon_j(t_1-t_2)}$, when ε_j is negative. It then follows that i S_F , as defined by the integral, is identical to the time-ordered vacuum expectation (4.8).

• The Fourier transform of the electron propagator with respect to time is

$$S_{F}(\omega; \mathbf{x}_{1}, \mathbf{x}_{2}) = \frac{\phi_{j}(\mathbf{x}_{1}) \, \phi_{j}^{*}(\mathbf{x}_{2})}{\omega - \varepsilon_{j} + i \eta \, \text{sgn}(\varepsilon_{j})}, \tag{4.11}$$

which can be regarded as the *coordinate representation* (see Appendix C)

$$S_{F}(\omega; \mathbf{x}_{1}, \mathbf{x}_{2}) = \langle \mathbf{x}_{1} | \hat{S}_{F}(\omega) | \mathbf{x}_{2} \rangle = \frac{\langle \mathbf{x}_{1} | j \rangle \langle j | \mathbf{x}_{2} \rangle}{\omega - \varepsilon_{j} + i \eta \operatorname{sgn}(\varepsilon_{j})}$$
(4.12)

of the operator⁴

$$\hat{S}_{F}(\omega) = \frac{|j\rangle \langle j|}{\omega - \varepsilon_{i} (1 - i\eta)}.$$
(4.13)

Using the relation in Appendix (D.49), this can also be expressed

$$\hat{S}_{F}(\omega) = \frac{1}{\omega - \hat{h}_{D} (1 - i\eta)}, \tag{4.14}$$

where \hat{h}_D is the Dirac hamiltonian *operator* (see Appendix D).

The contraction has so far been defined only for $t_1 \neq t_2$. For the bound-state problem, it is necessary to consider also *equal-time contractions*. We then define the time-ordering for equal time as

$$T[\psi(x_1)\psi^{\dagger}(x_2)] = \frac{1}{2} [\psi(x_1)\psi^{\dagger}(x_2) - \psi^{\dagger}(x_2)\psi(x_1)] \qquad (t_1 = t_2). \quad (4.15)$$

In this case we have

$$\begin{split} \psi(x_1)\psi^{\dagger}(x_2) &= \langle 0| \ T\big[\psi(x_1)\psi^{\dagger}(x_2)\big] \ |0\rangle \\ &= \frac{1}{2} \ \langle 0| \ \psi(x_1)\psi^{\dagger}(x_2) - \psi^{\dagger}(x_2)\psi(x_1) \ |0\rangle \\ &= \frac{1}{2} \sum_{\mathbf{p}} \phi_{\mathbf{p}}(x_1) \ \phi_{\mathbf{p}}^{\dagger}(x_2) - \frac{1}{2} \sum_{\mathbf{h}} \phi_{\mathbf{h}}(x_1) \ \phi_{\mathbf{h}}^{\dagger}(x_2) \\ &= \frac{1}{2} \sum_{i} \operatorname{sgn}(\varepsilon_i) \ \phi_{i}(x_2) \ \phi_{j}^{\dagger}(x_1), \end{split}$$

where j as before runs over particles and holes. This can still be expressed by the integral above, as can be seen from the relation

$$\frac{1}{\varepsilon_{j} - z - i\eta \operatorname{sgn}(\varepsilon_{j})} = \frac{\varepsilon_{j} - z}{(\varepsilon_{j} - z)^{2} + \eta^{2}} + \frac{i\eta \operatorname{sgn}(\varepsilon_{j})}{(\varepsilon_{j} - z)^{2} + \eta^{2}}$$

$$= P \frac{1}{\varepsilon_{j} - z} + i\pi \operatorname{sgn}(\varepsilon_{j}) \delta(\varepsilon_{j} - z), \tag{4.16}$$

P stands for the *principal-value integration*, which does not contribute here. Therefore, *the electron-propagator expression* (4.10) *is valid also for equal times*.

⁴ As stated before, we use the 'hat' symbol to emphasize that the quantity is an *operator*. In cases where this is obvious, the hat will normally be omitted.

4.3 Photon Propagator

The exchange of a single photon between the electrons corresponds to a *contraction* (2.29) of two photon-field operators (3.18), defined as in the electron-field case (4.7),

$$\begin{aligned}
A_{\mu}(x_{1})A_{\nu}(x_{2}) &= \langle 0|T[A_{\mu}(x_{1})A_{\nu}(x_{2})]|0\rangle \\
&= \langle 0|\Theta(t_{1} - t_{2})A_{\mu}(x_{1})A_{\nu}(x_{2}) + \Theta(t_{2} - t_{1})A_{\nu}(x_{2})A_{\mu}(x_{1})|0\rangle, \\
(4.17)
\end{aligned}$$

(the photon-field operators commute in contrast to the electron-field operators), and in analogy with the electron propagator we have

• The Feynman photon propagator is defined (see Fig. 4.3)

$$\overline{ A_{\mu}(x_1) A_{\nu}(x_2) = \langle 0 | T [A_{\mu}(x_1) A_{\nu}(x_2)] | 0 \rangle =: i D_{F\mu\nu}(x_1, x_2). }$$
 (4.18)

We shall also sometimes for convenience use the short-hand notation

$$D_{\rm F}(x_1, x_2) = \alpha^{\mu} \alpha^{\nu} D_{\rm F}(x_1, x_2) \tag{4.19}$$

using the summation convention.

With $A_{\mu} = A_{\mu}^{+} + A_{\mu}^{-}$ we see that (4.17) is identical to

$$\langle 0 | \Theta(t_1 - t_2) [A_{\mu}^+(x_1), A_{\nu}^-(x_2)] + \Theta(t_2 - t_1) [A_{\nu}^+(x_2), A_{\mu}^-(x_1)] | 0 \rangle$$

where the square bracket with a comma between the operators represents the commutator (2.12) and noting that the photon-field operators do commute.

Before evaluating the photon propagator, we have to make a choice of gauge (see Appendix G.2). In so-called *covariant gauges*, the field components are related by a Lorentz transformation. Most commonly used of the covariant gauges is the *Feynman gauge*, because of its simplicity. In our work with combined QED and electron correlation, however, it will be necessary to use the *noncovariant Coulomb gauge* in order to take advantage of the development in standard many-body perturbation theory. We shall demonstrate that this is quite feasible, although not always straightforward.

$$1, \mu \bullet \sim \nu, 2$$
 i $D_{F\nu\mu}(x_2, x_1)$

Fig. 4.3 Graphical representation of the photon propagator

4.3.1 Feynman Gauge

In the Feynman gauge we have, using the commutation rule in Appendix G (G.11),

$$[A_{\mu}^{+}(x_{1}), A_{\nu}^{-}(x_{2})] = \frac{1}{2\epsilon_{0}\omega V} \epsilon_{\mu r} \epsilon_{\nu r'} [a_{kr}, a_{k'r'}^{\dagger}] e^{-i(kx_{1} - k'x_{2})}$$
$$= -\frac{1}{2\epsilon_{0}\omega V} g_{\mu\nu} \delta_{k,k'} \delta_{r,r'} e^{-ik(x_{1} - x_{2})}.$$

With $kx_1 = k_0x_{10} - k \cdot x_1$ and $k'x_2 = k'_0x_{20} - k' \cdot x_2$ ($x_0 = ct$, $\omega = ck_0$), this yields for the vacuum expectation in (4.18)

$$\langle 0|T[A_{\mu}(x_{1})A_{\nu}(x_{2})]|0\rangle$$

$$= -\frac{1}{2\epsilon_{0}ck_{0}V}g_{\mu\nu}\Big[\Theta(t_{1}-t_{2})e^{-ik(x_{1}-x_{2})} + \Theta(t_{2}-t_{1})e^{ik(x_{1}-x_{2})}\Big]$$

$$= -g_{\mu\nu}\sum_{k}\frac{1}{2\epsilon_{0}ck_{0}V}e^{ik\cdot\mathbf{r}_{12}}\Big[\Theta(t_{1}-t_{2})e^{-ik_{0}(x_{10}-x_{20})} + \Theta(t_{2}-t_{1})e^{ik_{0}(x_{10}-x_{20})}\Big], \tag{4.20}$$

with $r_{12} = x_1 - x_2$. The sign of the exponent $k \cdot r_{12}$ is immaterial.

The expression in the square brackets of (4.20) can as in analogy with (4.10) be written as a complex integral

$$\Theta(t_1 - t_2)e^{-ik_0(x_{10} - x_{20})} + \Theta(t_2 - t_1)e^{ik_0(x_{10} - x_{20})} = 2ik_0 \int_{-\infty}^{\infty} \frac{dq}{2\pi} \frac{e^{-iq(x_{10} - x_{20})}}{q^2 - k_0^2 + i\eta}.$$
(4.21)

Thus (see Appendix, Sect. D.2),

$$\langle 0|T[A_{\mu}(x_{1})A_{\nu}(x_{2})]|0\rangle = -ig_{\mu\nu}\frac{1}{\epsilon_{0}cV}\sum_{\mathbf{k}}e^{i\mathbf{k}\cdot\mathbf{r}_{12}}\int_{-\infty}^{\infty}\frac{dq}{2\pi}\frac{e^{-iq(x_{10}-x_{20})}}{q^{2}-\mathbf{k}^{2}+i\eta}$$

$$\rightarrow -ig_{\mu\nu}\frac{1}{c\epsilon_{0}}\int\frac{d^{3}\mathbf{k}}{(2\pi)^{3}}e^{i\mathbf{k}\cdot\mathbf{r}_{12}}\int_{-\infty}^{\infty}\frac{dq}{2\pi}\frac{e^{-iq(x_{10}-x_{20})}}{q^{2}-\mathbf{k}^{2}+i\eta},$$
(4.22)

with $k_0 = |\mathbf{k}|$, and the photon propagator (4.18) becomes in the *Feynman gauge* [c.f Appendix (F.62)]

$$D_{F\mu\nu}^{F}(x_{1}, x_{2}) = -\frac{g_{\mu\nu}}{c\epsilon_{0}} \int \frac{d^{3}\mathbf{k}}{(2\pi)^{3}} e^{i\mathbf{k}\cdot\mathbf{r}_{12}} \int_{-\infty}^{\infty} \frac{dq}{2\pi} \frac{e^{-iq(x_{10}-x_{20})}}{q^{2} - \mathbf{k}^{2} + i\eta}$$
$$= -\frac{g_{\mu\nu}}{\epsilon_{0}} \int \frac{d^{3}\mathbf{k}}{(2\pi)^{3}} e^{i\mathbf{k}\cdot\mathbf{r}_{12}} \int_{-\infty}^{\infty} \frac{dz}{2\pi} \frac{e^{-iz(t_{1}-t_{2})}}{z^{2} - c^{2}\mathbf{k}^{2} + i\eta}, \quad (4.23)$$

where z = cq is the energy parameter. It then follows that

• The Fourier transform of the photon propagator with respect to $x_0 = ct$ becomes in Feynman gauge

$$D_{F\mu\nu}^{F}(q; \mathbf{x}_{1}, \mathbf{x}_{2}) = -\frac{g_{\mu\nu}}{\epsilon_{0}} \int \frac{d^{3}\mathbf{k}}{(2\pi)^{3}} \frac{e^{i\mathbf{k}\cdot\mathbf{r}_{12}}}{q^{2} - \mathbf{k}^{2} + i\eta}$$
(4.24)

and the inverse transformation becomes

$$D_{F\mu\nu}^{F}(x_{1}, x_{2}) = \int \frac{dq}{2\pi} D_{F\mu\nu}^{F}(q; \mathbf{x}_{1}, \mathbf{x}_{2}) e^{-iq(x_{10} - x_{20})}.$$
(4.25)

After integration over the angular part (see Appendix J), this becomes

$$D_{F\mu\nu}^{F}(q; \mathbf{x}_{1}, \mathbf{x}_{2}) = -\frac{g_{\mu\nu}}{4\pi^{2}c\epsilon_{0}r_{12}} \int_{0}^{\infty} \frac{2\kappa \,\mathrm{d}\kappa \,\sin\kappa r_{12}}{q^{2} - \kappa^{2} + \mathrm{i}\eta},$$
(4.26)

where $\kappa = |\mathbf{k}|$, and $q = k_0$ is now decoupled from $|\mathbf{k}|$.⁵ Fourier transforming (4.25) with respect to space yields

$$D_{\mathrm{F}\mu\nu}^{\mathrm{F}}(q;\mathbf{k}) = -\frac{g_{\mu\nu}}{c\epsilon_0} \frac{1}{q^2 - \kappa^2 + \mathrm{i}\eta}$$
(4.27)

or in covariant notation

$$D_{F\mu\nu}^{F}(k) = -\frac{g_{\mu\nu}}{c\epsilon_{0}} \frac{1}{k^{2} + i\eta},$$
(4.28)

where k is the four-dimensional momentum vector, $k^2 = k_0^2 - k^2$. The Fourier transforms with respect to time are similarly

$$D_{F\mu\nu}^{F}(z; \mathbf{x}_{1}, \mathbf{x}_{2}) = -\frac{g_{\mu\nu}}{\epsilon_{0}} \int \frac{d^{3}\mathbf{k}}{(2\pi)^{3}} \frac{e^{i\mathbf{k}\cdot\mathbf{r}_{12}}}{q^{2} - \mathbf{k}^{2} + i\eta}$$
$$= -\frac{g_{\mu\nu}}{4\pi^{2}\epsilon_{0}r_{12}} \int_{0}^{\infty} \frac{2\kappa \, d\kappa \, \sin\kappa r_{12}}{z^{2} - c^{2}\kappa^{2} + i\eta}, \tag{4.29}$$

$$D_{F\mu\nu}^{F}(z; \mathbf{k}) = -\frac{g_{\mu\nu}}{\epsilon_0} \frac{1}{z^2 - c^2\kappa^2 + i\eta},$$
 (4.30)

⁵ In some literature $|\mathbf{k}|$ is denoted by k, but here we introduce a new notation (κ) , reserving k for the four-dimensional vector, in order to avoid confusion.

which differ from the previous transforms with respect to momentum (4.26) and (4.27) by a factor of c (see Appendix K.2). z = cq is the energy parameter. The inverse transformation is here

$$D_{F\mu\nu}^{F}(x_1, x_2) = \int \frac{dz}{2\pi} D_{F\mu\nu}^{F}(z; \boldsymbol{x}_1, \boldsymbol{x}_2) e^{-iz(t_1 - t_2)}.$$
 (4.31)

4.3.2 Coulomb Gauge

Above we have found an expression for the photon propagator in the Feynman gauge, and by means of the formulas for gauge transformation in Appendix G.2, we can derive the corresponding expressions in other gauges.

In the *Coulomb gauge* (G.19), the scalar part ($\mu\nu=00$) of the photon propagator is

$$D_{\text{F00}}^{\text{C}}(k) = \frac{1}{c\epsilon_0 k^2}.$$
 (4.32)

Transforming back to four-dimensional space yields according to (4.23)

$$D_{\text{F00}}^{\text{C}}(x_1, x_2) = \frac{1}{c\epsilon_0} \int \frac{\mathrm{d}^3 \mathbf{k}}{(2\pi)^3} \frac{\mathrm{e}^{\mathrm{i}\mathbf{k}\cdot\mathbf{r}_{12}}}{\mathbf{k}^2} \int \frac{\mathrm{d}k_0}{2\pi} \, \mathrm{e}^{-\mathrm{i}k_0(x_{01} - x_{02})}$$
$$= \frac{1}{4\pi^2 c\epsilon_0 r_{12}} \int_0^\infty \frac{2\kappa \, \mathrm{d}\kappa \, \sin\kappa r_{12}}{\kappa^2} \int \frac{\mathrm{d}k_0}{2\pi} \, \mathrm{e}^{-\mathrm{i}k_0(x_{01} - x_{02})}$$

using the relation (J.17). With $x_0 = ct$ and $z = ck_0$, this can be expressed

$$D_{\text{F00}}^{\text{C}}(x_1, x_2) = \frac{V_{\text{C}}}{e^2 c^2} \int \frac{\mathrm{d}z}{2\pi} e^{-iz(t_1 - t_2)},$$
(4.33)

where $V_{\rm C}$ is the Coulomb interaction (2.109). With the damping factor, the integral tends to a delta function (A.15)

$$D_{\text{F00}}^{\text{C}}(x_1, x_2) \Rightarrow \frac{V_{\text{C}}}{e^2 c^2} \delta(t_1 - t_2),$$
 (4.34)

but we shall normally use the more explicit expression (4.33).

From the relation (4.33), we find that the Fourier transform with respect to time becomes

$$D_{\text{F00}}^{\text{C}}(z; \mathbf{x}_1, \mathbf{x}_2) = \frac{1}{4\pi^2 c^2 \epsilon_0 r_{12}} \int_0^\infty \frac{2\kappa \, d\kappa \, \sin \kappa r_{12}}{\kappa^2} = \frac{V_{\text{C}}}{e^2 c^2}.$$
 (4.35)

The vector part of the propagator is according to (G.19) $(q = k_0)$

$$D_{Fij}^{C}(k) = -\frac{1}{c\epsilon_0(k^2 + i\eta)} \left(g_{ij} + \frac{k_i k_j}{k^2} \right)$$
(4.36)

and transforming back to three-dimensional space yields

$$D_{\text{Fij}}^{C}(q; \mathbf{x}_{1}, \mathbf{x}_{2}) = -\frac{1}{c\epsilon_{0}} \int \frac{d^{3}\mathbf{k}}{(2\pi)^{3}} \frac{e^{i\mathbf{k}\cdot\mathbf{r}_{12}}}{q^{2} - \mathbf{k}^{2} + i\eta} \left(g_{ij} + \frac{k_{i}k_{j}}{\mathbf{k}^{2}}\right)$$

$$= -\frac{1}{c\epsilon_{0}} \int_{0}^{\infty} \frac{2\kappa \, d\kappa \, \sin\kappa \, r_{12}}{q^{2} - \kappa^{2} + i\eta} \left(g_{ij} + \frac{k_{i}k_{j}}{\mathbf{k}^{2}}\right)$$

$$= cD_{\text{Fij}}^{C}(z; \mathbf{x}_{1}, \mathbf{x}_{2}) \qquad (z = cq). \tag{4.37}$$

4.4 Single-Photon Exchange

We consider now the exchange of a single photon between the electrons, represented by the Feynman diagram in Fig. 4.4 (left). We start with a general covariant gauge, such as the Feynman gauge, and consider then the noncovariant Coulomb gauge.

4.4.1 Covariant Gauge

The second-order S-matrix (4.3) is given by

$$S^{(2)} = \frac{1}{2} \left(\frac{-i}{c} \right)^2 \iint d^4 x_2 d^4 x_1 T \left[\mathcal{H}(x_2) \mathcal{H}(x_1) \right] e^{-\gamma(|t_1| + |t_2|)}. \tag{4.38}$$

With the interaction density (4.4), this becomes

$$S^{(2)} = \frac{(ie)^2}{2} \iint d^4x_2 d^4x_1 T \Big[(\psi^{\dagger}(x)\alpha^{\nu}A_{\nu}(x)\psi(x))_2 (\psi^{\dagger}(x)\alpha^{\mu}A_{\mu}(x)\psi(x))_1 \Big] \times e^{-\gamma(|t_1|+|t_2|)}, \tag{4.39}$$

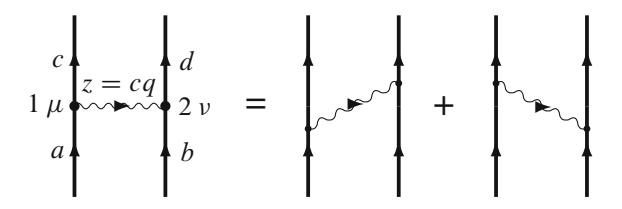


Fig. 4.4 The Feynman representation of the exchange of a single, virtual photon between two electrons. This contains two time-orderings

where the contraction between the radiation-field operators yields the photon propagator, $iD_{F\mu\nu}$ (4.18), or with the short-hand notation (4.19),

$$S^{(2)} = \frac{(ie)^2}{2} \iint d^4x_2 d^4x_1 \ \psi^{\dagger}(x_1) \psi^{\dagger}(x_2)$$

$$\times iD_F(x_2, x_1) \ \psi(x_2) \psi(x_1) e^{-\gamma(|t_1| + |t_2|)}.$$
(4.40)

Identification with the second-quantized form (see Appendix B)

$$S^{(2)} = \frac{1}{2} c_c^{\dagger} c_d^{\dagger} \left\langle cd \left| S^{(2)} \right| ab \right\rangle c_b c_a \tag{4.41}$$

yields a particular matrix element of the $S^{(2)}$ matrix

$$\langle cd | S^{(2)} | ab \rangle = - \iint d^{4}x_{2} d^{4}x_{1} \phi_{c}^{\dagger}(x_{1}) \phi_{d}^{\dagger}(x_{2}) ie^{2} D_{F}(x_{2}, x_{1})$$

$$\times \phi_{b}(x_{2}) \phi_{a}(x_{1}) e^{-\gamma(|t_{1}| + |t_{2}|)}$$

$$= \int \frac{dz}{2\pi} \langle cd | -ie^{2} D_{F}(z, \mathbf{x}_{2}, \mathbf{x}_{1}) | ab \rangle$$

$$\times \iint c^{2} dt_{1} dt_{2} e^{-it_{1}(\varepsilon_{a} - \varepsilon_{c} - z)} e^{-it_{2}(\varepsilon_{b} - \varepsilon_{d} + z)} e^{-\gamma(|t_{1}| + |t_{2}|)}$$
(4.42)

using the Fourier transform (4.31). After performing the time integrations (A.14)

$$\langle cd | S^{(2)} | ab \rangle = \int \frac{\mathrm{d}z}{2\pi} \langle cd | -ie^2 c^2 D_{\mathrm{F}}(z, \mathbf{x}_2, \mathbf{x}_1) | ab \rangle$$

$$\times 2\pi \Delta_{\gamma}(\varepsilon_a - z - \varepsilon_c) 2\pi \Delta_{\gamma}(\varepsilon_b + z - \varepsilon_d). \tag{4.43}$$

• We introduce the single-photon interaction

$$I(x_1, x_2) = V_{\rm sp}(x_1, x_2) = e^2 c^2 \alpha_1^{\mu} \alpha_2^{\nu} D_{\rm F}_{\mu\nu}(x_1, x_2) = e^2 c^2 D_{\rm F}(x_1, x_2)$$
(4.44)

with the Fourier transform with respect to time

$$I(z; \mathbf{x}_1, \mathbf{x}_2) = e^2 c^2 \alpha_1^{\mu} \alpha_2^{\nu} D_{F\mu\nu}(z; \mathbf{x}_1, \mathbf{x}_2) = e^2 c^2 D_F(z; \mathbf{x}_1, \mathbf{x}_2),$$
 (4.45)

which has the form of an energy potential. We shall generally express the Fourier transform of the interaction with respect to time as

$$I(z; \mathbf{x}_1, \mathbf{x}_2) = e^2 c^2 \alpha_1^{\mu} \alpha_2^{\nu} D_{F\mu\nu}(z; \mathbf{x}_1, \mathbf{x}_2) = \int \frac{2c^2 \kappa \, d\kappa \, f(\kappa, \mathbf{x}_1, \mathbf{x}_2)}{z^2 - c^2 \kappa^2 + i\eta},$$
(4.46)

where $f(\kappa, x_1, x_2)$ is a gauge-dependent function. This transform, as well as the function $f(\kappa, x_1, x_2)$, has the dimension of energy (or s^{-1} with our convention with $\hbar = 1$).⁶

With the notation above the S-matrix element (4.43) becomes

$$\langle cd | S^{(2)} | ab \rangle = \int dz \langle cd | -iI(z) | ab \rangle 2\pi \Delta_{\gamma} (\varepsilon_a - z - \varepsilon_c) 2\pi \Delta_{\gamma} (\varepsilon_b + z - \varepsilon_d).$$
(4.47)

In Appendix A.3.2, it is shown that

$$\int \frac{dz}{2\pi} 2\pi \Delta_{\gamma}(a-z) 2\pi \Delta_{\gamma}(b-z) \frac{1}{z^2 - c^2 \kappa^2 + i\eta}$$

$$= 2\pi \Delta_{2\gamma}(a-b) \frac{1}{z^2 - c^2 \kappa^2 + i\gamma},$$
(4.48)

where we observe that the infinitesimally small quantity η , appearing in the propagators to indicate the position of the poles, is replaced by the adiabatic damping parameter, γ , which is a finite quantity (that eventually tends to zero). This gives

$$\langle cd | S^{(2)} | ab \rangle = 2\pi \Delta_{2\gamma} (\varepsilon_a + \varepsilon_b - \varepsilon_c - \varepsilon_d) \langle cd | -iI(z) | ab \rangle$$
 (4.49)

with $z = cq = \varepsilon_a - \varepsilon_c$. This can also be expressed

$$\langle cd | S^{(2)} | ab \rangle \Rightarrow 2\pi \Delta_{2\gamma} (E_{\text{in}} - E_{\text{out}}) \langle cd | -iI(z) | ab \rangle,$$
 (4.50)

where $E_{\rm in}$ and $E_{\rm out}$ are the incoming and outgoing energies, respectively. Using the Sucher energy formula (4.6) and the relation (A.17)

$$\lim_{\gamma \to 0} 2\pi \gamma \Delta_{2\gamma}(x) = \delta_{x,0},\tag{4.51}$$

the corresponding energy shift becomes

$$\Delta E^{(1)} = \delta_{E_{\text{in}}, E_{\text{out}}} \langle cd | I(z) | ab \rangle. \tag{4.52}$$

Assuming that $\Phi_{\text{out}} = \Phi_{\text{in}} = \Phi$ is the antisymmetrized state

$$|\Phi\rangle = |\{ab\}\rangle = \frac{1}{\sqrt{2}} [|ab\rangle - |ba\rangle],$$

the first-order energy shift becomes

$$\Delta E = \langle \Phi | I(z) | \Phi \rangle = \langle ab | I(z) | ab \rangle - \langle ba | I(z) | ab \rangle, \tag{4.53}$$

⁶ The constants of the expressions can be conveniently checked by dimensional analysis (see Appendix K.2).

which is consistent with the interpretation of the interaction I(z) as an equivalent energy-dependent perturbing potential.

We have seen here that the time integration – in the limit $\gamma \to 0$ – leads to

• Energy conservation at each vertex with the propagator energy parameters treated as energies.

Due to the energy conservation of the scattering process, only diagonal ("onthe-energy-shell") matrix elements are obtained from the analysis of the S-matrix. Therefore, the technique cannot be used for studying quasi-degenerate states by means of the extended-model-space technique (see Sect. 2.3). *Off-diagonal elements* needed for this approach can be evaluated using the covariant-evolution operator technique, demonstrated in Chap. 6.

4.4.1.1 Feynman Gauge

With the expression (4.29) of the photon propagator in Feynman gauge, the corresponding interaction (4.45) becomes (z = cq)

$$I^{F}(z; \mathbf{x}_{1}, \mathbf{x}_{2}) = -\frac{e^{2}}{4\pi^{2}\epsilon_{0}r_{12}}\alpha_{1}^{\mu}\alpha_{2\mu}\int \frac{2\kappa\,\mathrm{d}\kappa\,\sin\kappa r_{12}}{q^{2}-\kappa^{2}+\mathrm{i}\eta}.$$
 (4.54)

The corresponding f function in (4.46) then becomes

$$f^{F}(\kappa, \mathbf{x}_{1}, \mathbf{x}_{2}) = -\frac{e^{2}}{4\pi^{2}\epsilon_{0}} \alpha_{1}^{\mu} \alpha_{2\mu} \frac{\sin \kappa r_{12}}{r_{12}} = -\frac{e^{2}}{4\pi^{2}\epsilon_{0}} (1 - \alpha_{1} \cdot \alpha_{2}) \frac{\sin \kappa r_{12}}{r_{12}}.$$
(4.55)

Evaluating the integral in (4.54), using the result in Appendix J, we obtain

$$I^{F}(z; \mathbf{x}_{1}, \mathbf{x}_{2}) = \frac{e^{2}}{4\pi\epsilon_{0}r_{12}} (1 - \boldsymbol{\alpha}_{1} \cdot \boldsymbol{\alpha}_{2}) e^{i|z|r_{12}/c}, \qquad (4.56)$$

which agrees with the semiclassical potential (Appendix F.73).

4.4.2 Noncovariant Coulomb Gauge

In the Coulomb gauge, we separate the interaction into the *instantaneous Coulomb* part and the *time-dependent transverse (Breit) part*,

$$I^{C} = I_{C}^{C} + I_{T}^{C}. (4.57)$$

The transverse part of the interaction can be treated in analogy with the covariant gauges. According to (4.44) we have

$$I_{\rm T}^{\rm C}(x_1, x_2) = e^2 c^2 \alpha_1^i \alpha_2^j D_{\rm Fij}^{\rm C}(x_1, x_2), \tag{4.58}$$

which with (4.37) yields

$$I_{\mathrm{T}}^{\mathrm{C}}(z; \mathbf{x}_{1}, \mathbf{x}_{2}) = \frac{e^{2}}{\epsilon_{0}} \int \frac{\mathrm{d}^{3} \mathbf{k}}{(2\pi)^{3}} \left(\boldsymbol{\alpha}_{1} \cdot \boldsymbol{\alpha}_{2} - \frac{(\boldsymbol{\alpha}_{1} \cdot \mathbf{k}) (\boldsymbol{\alpha}_{2} \cdot \mathbf{k})}{\mathbf{k}^{2}} \right) \frac{\mathrm{e}^{\mathrm{i}\mathbf{k} \cdot \mathbf{r}_{12}}}{q^{2} - \mathbf{k}^{2} + \mathrm{i}\eta}$$

$$= \frac{e^{2}}{\epsilon_{0}} \int \frac{\mathrm{d}^{3} \mathbf{k}}{(2\pi)^{3}} \left(\boldsymbol{\alpha}_{1} \cdot \boldsymbol{\alpha}_{2} - \frac{(\boldsymbol{\alpha}_{1} \cdot \nabla_{1}) (\boldsymbol{\alpha}_{2} \cdot \nabla_{2})}{\mathbf{k}^{2}} \right) \frac{\mathrm{e}^{\mathrm{i}\mathbf{k} \cdot \mathbf{r}_{12}}}{q^{2} - \mathbf{k}^{2} + \mathrm{i}\eta}$$

$$= \frac{e^{2}}{4\pi^{2} \epsilon_{0} r_{12}} \int \frac{2\kappa \, \mathrm{d}\kappa \, \sin \kappa r_{12}}{q^{2} - \kappa^{2} + \mathrm{i}\eta} \left(\boldsymbol{\alpha}_{1} \cdot \boldsymbol{\alpha}_{2} - \frac{(\boldsymbol{\alpha}_{1} \cdot \nabla_{1}) (\boldsymbol{\alpha}_{2} \cdot \nabla_{2})}{\kappa^{2}} \right)$$

$$(4.59)$$

and the corresponding f function becomes (4.46)

$$f_{\mathrm{T}}^{\mathrm{C}}(\kappa, \mathbf{x}_{1}, \mathbf{x}_{2}) = \frac{e^{2}}{4\pi^{2}\epsilon_{0}} \frac{\sin(\kappa r_{12})}{r_{12}} \left[\boldsymbol{\alpha}_{1} \cdot \boldsymbol{\alpha}_{2} - \frac{(\boldsymbol{\alpha}_{1} \cdot \nabla_{1})(\boldsymbol{\alpha}_{2} \cdot \nabla_{2})}{\kappa^{2}} \right]. \tag{4.60}$$

Performing the κ integration in (4.59), using the integrals in Appendix J, yields for the transverse (Breit) part

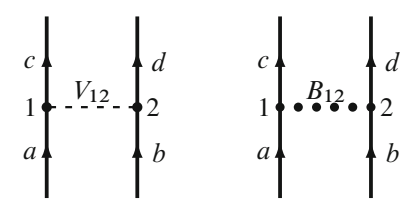
$$I_{\rm T}^{\rm C}(z;x_1,x_2) = -\frac{e^2}{4\pi\epsilon_0} \left[\alpha_1 \cdot \alpha_2 \, \frac{{\rm e}^{{\rm i}|q|r_{12}}}{r_{12}} - (\alpha_1 \cdot \nabla_1)(\alpha_2 \cdot \nabla_2) \, \frac{{\rm e}^{{\rm i}|q|r_{12}} - 1}{q^2 \, r_{12}} \right]. \tag{4.61}$$

This agrees with the semiclassical result obtained in Appendix F.2 (F.54). The instantaneous *Breit interaction* is obtained by letting $q \Rightarrow 0$, (Fig. 4.5)

$$I^{\text{Breit}} = B_{12}^{\text{Inst}} = -\frac{e^2}{4\pi\epsilon_0 r_{12}} \left[\frac{1}{2} \alpha_1 \cdot \alpha_2 + \frac{(\alpha_1 \cdot r_{12})(\alpha_1 \cdot r_{12})}{2r_{12}} \right], \quad (4.62)$$

which is the interaction in the Dirac-Coulomb-Breit approximation (NVPA) (2.112) and agrees with the expression derived in Appendix F (F.55).

Fig. 4.5 Instantaneous Coulomb and Breit interactions between the electrons



The (instantaneous) Coulomb part of the interaction becomes, using the relations (4.33) and (4.35),

$$I_{C}^{C}(x_{1}, x_{2}) = \frac{e^{2}}{4\pi^{2}\epsilon_{0}r_{12}} \int \frac{2\kappa \, d\kappa \, \sin\kappa r_{12}}{\kappa^{2}} \int \frac{dz}{2\pi} \, e^{-iz(t_{1}-t_{2})}$$
$$= V_{C} \int \frac{dz}{2\pi} \, e^{-iz(t_{1}-t_{2})}, \tag{4.63a}$$

$$I_{\rm C}^{\rm C}(z; \mathbf{x}_1, \mathbf{x}_2) = \frac{e^2}{4\pi^2 \epsilon_0 r_{12}} \int \frac{2\kappa \, \mathrm{d}\kappa \, \sin \kappa r_{12}}{\kappa^2} = V_{\rm C}.$$
 (4.63b)

This leads to, using (4.43),

$$\langle cd | S^{(2)} | ab \rangle = \int \frac{\mathrm{d}z}{2\pi} \langle cd | -iV_{\mathrm{C}} | ab \rangle 2\pi \Delta_{\gamma} (\varepsilon_a - z - \varepsilon_c) 2\pi \Delta_{\gamma} (\varepsilon_b + z - \varepsilon_d)$$

and in analogy with (4.49)

$$\langle cd | S^{(2)} | ab \rangle = \langle cd | -iV_{C} | ab \rangle \Delta_{2\gamma} (\varepsilon_{a} + \varepsilon_{b} - \varepsilon_{c} - \varepsilon_{d}).$$

The Sucher energy formula (4.6) then gives the expected result for the first-order energy shift

$$\Delta E^{(1)} = \delta_{E_{\text{in}}, E_{\text{out}}} \langle cd | V_{\text{C}} | ab \rangle, \qquad (4.64)$$

where, as before, $E_{\rm in} = \varepsilon_a + \varepsilon_b$ is the initial and $E_{\rm out} = \varepsilon_c + \varepsilon_d$ is the final energy. Again this demonstrates that the interaction (4.45) represents an equivalent interaction potential and that the energy is conserved for the S-matrix.

4.4.3 Single-Particle Potential

Finally, we consider in this subsection the simple case of an interaction between a single electron and a time-independent external field, $A_{\mu}(x)$ (Fig. 4.6). Here, the scattering amplitude becomes from (4.3) with the interaction density (4.4)

$$S^{(1)} = ie \int d^4x \, \hat{\psi}^{\dagger}(x) \, \alpha^{\mu} A_{\mu}(x) \, \hat{\psi}(x) \, e^{-\gamma |t|}$$
 (4.65)

with $A_{\mu} = (\phi/c, -A)$ according to (F.6) in Appendix F. In analogy with the previous cases, this yields $(dx_0 = c dt)$

$$\langle b|S^{(1)}|a\rangle = iec \langle b|\alpha^{\mu}A_{\mu}|a\rangle 2\pi \Delta_{\gamma}(\varepsilon_a - \varepsilon_b).$$
 (4.66)

We consider a scalar *energy* potential, $V(x) = -e\phi(x)$ and $A_0 = -V/ec$, which with is given by and the S-matrix element then becomes

$$\langle b|S^{(1)}|a\rangle = 2\pi\Delta_{\nu}(\varepsilon_a - \varepsilon_b) \langle b| - iV|a\rangle. \tag{4.67}$$

The Sucher energy formula (4.6) then yields the expected result

$$\Delta E^{(1)} = \delta_{\varepsilon_a, \varepsilon_b} \langle b|V|a\rangle. \tag{4.68}$$

4.5 Two-Photon Exchange

4.5.1 Two-Photon Ladder

We consider next the exchange of two uncrossed photons in a covariant gauge, such as the Feynman gauge, illustrated in Fig. 4.7 (left). Again, this is a *Feynman diagram*, which contains all relative time orderings of the times involved, still with the photons uncrossed.

As before, we consider first this problem using a general *covariant gauge*, such as the Feynman gauge, and then we shall consider the Coulomb gauge, in particular. In analogy with the single-photon exchange, the S-matrix becomes

$$S^{(4)} = \frac{(ie)^4}{4!} \iiint d^4x_1 d^4x_2 d^4x_3 d^4x_4 \,\hat{\psi}^{\dagger}(x_3) \hat{\psi}^{\dagger}(x_4) i D_F(x_4, x_3) \times i S_F(x_3, x_1) i S_F(x_4, x_2) i D_F(x_2, x_1) \hat{\psi}(x_2) \hat{\psi}(x_1) e^{-\gamma(|t_1| + |t_2| + |t_3| + |t_4|)},$$
(4.69)

where $D_{\rm F}$ is defined in (4.19).

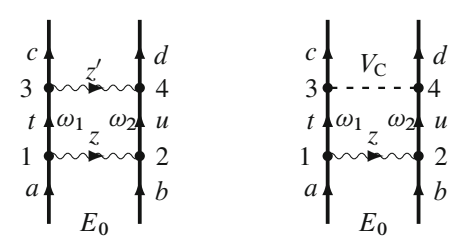


Fig. 4.7 The Feynman representation of the two-photon exchange. The *left diagram* represents a Coulomb and a transverse photon interaction in Coulomb gauge

The vertices can here be permuted in 4! ways, and this leads to pairwise identical diagrams, related only by a reflection in a vertical plane. The 12 pairs represent equivalent but distinct terms in the expansion, and by considering only one of them, we have

$$S^{(4)} = \frac{(ie)^4}{2} \iiint d^4x_1 d^4x_2 d^4x_3 d^4x_4 \,\hat{\psi}^{\dagger}(x_3) \hat{\psi}^{\dagger}(x_4) i D_F(x_4, x_3) \times i S_F(x_3, x_1) i S_F(x_4, x_2) i D_F(x_2, x_1) \hat{\psi}(x_2) \hat{\psi}(x_1) e^{-\gamma(|t_1| + |t_2| + |t_3| + |t_4|)}.$$
(4.70)

Identifying with the second-quantized expression and performing the time integrations as in the single-photon case (4.43), using the interaction (4.44), the matrix elements becomes⁷

$$\langle cd|S^{(4)}|ab\rangle = \iint \frac{\mathrm{d}z}{2\pi} \frac{\mathrm{d}z'}{2\pi} \iint \frac{\mathrm{d}\omega_{1}}{2\pi} \frac{\mathrm{d}\omega_{2}}{2\pi} \langle cd|(-\mathrm{i})I(z'; \mathbf{x}_{4}, \mathbf{x}_{3}) \,\mathrm{i}S_{F}(\omega_{1}; \mathbf{x}_{3}, \mathbf{x}_{1})$$

$$\times \,\mathrm{i}S_{F}(\omega_{2}; \mathbf{x}_{4}, \mathbf{x}_{2}) \,(-\mathrm{i})I(z; \mathbf{x}_{2}, \mathbf{x}_{1})|ab\rangle \,2\pi \,\Delta_{\gamma}(\varepsilon_{a} - z - \omega_{1})$$

$$\times \,2\pi \,\Delta_{\gamma}(\varepsilon_{b} + z - \omega_{2})2\pi \,\Delta_{\gamma}(\omega_{1} - z' - \varepsilon_{c})2\pi \,\Delta_{\gamma}(\omega_{2} + z' - \varepsilon_{d}).$$

Integrations over ω_1 , ω_2 then yield

$$\langle cd | S^{(4)} | ab \rangle = \iint \frac{\mathrm{d}z}{2\pi} \frac{\mathrm{d}z'}{2\pi} \langle cd | (-\mathrm{i})I(z'; \mathbf{x}_4, \mathbf{x}_3) \, \mathrm{i}S_{\mathrm{F}}(\varepsilon_a - z; \mathbf{x}_3, \mathbf{x}_1)$$

$$\times \mathrm{i}S_{\mathrm{F}}(\varepsilon_b + z; \mathbf{x}_4, \mathbf{x}_2) \, (-\mathrm{i})I(z; \mathbf{x}_2, \mathbf{x}_1) | ab \rangle$$

$$\times 2\pi \Delta_{2\nu}(\varepsilon_a - \varepsilon_c - z - z') \, 2\pi \Delta_{2\nu}(\varepsilon_b - \varepsilon_d + z + z').$$
 (4.71)

(As shown before, the η parameter in the electron propagators should here be replaced by the adiabatic damping parameter γ .) After integration over z', we have

$$\langle cd | S^{(4)} | ab \rangle = \int \frac{\mathrm{d}z}{2\pi} \left\langle cd \left| (-\mathrm{i})I(\varepsilon_a - \varepsilon_c - z; \boldsymbol{x}_3, \boldsymbol{x}_4) \mathrm{i} S_{\mathrm{F}}(\varepsilon_a - z; \boldsymbol{x}_3, \boldsymbol{x}_1) \right. \right. \\ \left. \times \mathrm{i} S_{\mathrm{F}}(\varepsilon_b + z; \boldsymbol{x}_4, \boldsymbol{x}_2) (-\mathrm{i})I(z; \boldsymbol{x}_2, \boldsymbol{x}_1) \middle| ab \right\rangle \\ \left. \times 2\pi \Delta_{4\gamma}(\varepsilon_a + \varepsilon_b - \varepsilon_c - \varepsilon_d). \right.$$

$$(4.72)$$

To evaluate this integral is straightforward but rather tedious, and we shall not perform this here (see, for instance, [9]).

Next, we shall consider the special case, where we have *one instantaneous* Coulomb interaction and one transverse-photon interaction (Fig. 4.7, right), using the Coulomb gauge.

⁷ We have here an illustration of the general rules for setting up the S-matrix, given in Appendix H, that there is (1) factor iS_F for each electron propagator, (2) a factor -iI for each single-photon exchange and (3) a Δ factor for each vertex.

Separating the interaction according to (4.57), we now have

$$\langle cd|S^{(4)}|ab\rangle = \int \frac{\mathrm{d}z}{2\pi} \left\langle cd \left| (-\mathrm{i})I_{\mathrm{C}}^{\mathrm{C}}(z; \boldsymbol{x}_{4}, \boldsymbol{x}_{3}) \, \mathrm{i}S_{\mathrm{F}}(\varepsilon_{a} - z; \boldsymbol{x}_{3}, \boldsymbol{x}_{1}) \right. \right. \\ \left. \times \mathrm{i}S_{\mathrm{F}}(\varepsilon_{b} + z; \boldsymbol{x}_{4}, \boldsymbol{x}_{2}) \, (-\mathrm{i})I_{\mathrm{T}}^{\mathrm{C}}(z; \boldsymbol{x}_{2}, \boldsymbol{x}_{1}) \middle| ab \right\rangle \\ \left. \times 2\pi\Delta_{2\gamma}(\varepsilon_{a} - \varepsilon_{c} - z) \, 2\pi\Delta_{4\gamma}(\varepsilon_{a} + \varepsilon_{b} - \varepsilon_{c} - \varepsilon_{d}). \right.$$
(4.73)

Inserting the expressions for the electron propagators (4.10) and the interaction (4.46), this yields

$$\langle cd | S^{(4)} | ab \rangle = \langle cd | V_{C} \int \frac{dz}{2\pi} \frac{|t\rangle \langle t|}{\varepsilon_{a} - z - \varepsilon_{t} + i\gamma_{t}} \frac{|u\rangle \langle u|}{\varepsilon_{b} + z - \varepsilon_{u} + i\gamma_{u}} \times \int \frac{2\kappa c^{2} d\kappa f_{T}^{C}(\kappa)}{z^{2} - c^{2}\kappa^{2} + i\eta} |ab\rangle 2\pi \Delta_{4\gamma}(\varepsilon_{a} + \varepsilon_{b} - \varepsilon_{c} - \varepsilon_{d}), \quad (4.74)$$

where $V_{\rm C}$ is the Coulomb interaction $f_{\rm T}^{\rm C}$ (4.63b) and $f_{\rm T}^{\rm C}$ is given by (4.60). The products of the propagators can be expressed

$$\frac{1}{\varepsilon_{a} - z - \varepsilon_{t} + i\gamma_{t}} \frac{1}{\varepsilon_{b} + z - \varepsilon_{u} + i\gamma_{u}}$$

$$= \frac{1}{E_{0} - \varepsilon_{t} - \varepsilon_{u}} \left[\frac{1}{\varepsilon_{a} - z - \varepsilon_{t} + i\gamma_{t}} + \frac{1}{\varepsilon_{b} + z - \varepsilon_{u} + i\gamma_{u}} \right]$$
(4.75)

with $E_0 = \varepsilon_a + \varepsilon_b$. The poles are here at $z = \varepsilon_a - \varepsilon_t + i\gamma_t$, $z = \varepsilon_u - \varepsilon_b - i\gamma_u$ and $z = \pm (c\kappa - i\eta)$. Integrating the first term over the negative half plane $(z = c\kappa - i\eta)$ and the second term over the positive half plane $(z = -c\kappa + i\eta)$, yields⁸

$$\langle cd|S^{(4)}|ab\rangle = -\mathrm{i}\langle cd|V_{\mathrm{C}}\frac{|tu\rangle\langle tu|}{E_{0} - \varepsilon_{t} - \varepsilon_{u}}V_{\mathrm{T}}|ab\rangle 2\pi\Delta_{4\gamma}(E_{0} - E_{\mathrm{out}}),$$
 (4.76)

where

$$\langle tu|V_{\rm T}|ab\rangle = \left\langle tu \middle| \int c \, \mathrm{d}\kappa \, f_{\rm T}^{\rm C}(\kappa) \right.$$

$$\times \left[\frac{1}{\varepsilon_a - \varepsilon_t - (c\kappa - \mathrm{i}\gamma)_t} + \frac{1}{\varepsilon_b - \varepsilon_u - (c\kappa - \mathrm{i}\gamma)_u} \right] \left| ab \right\rangle \quad (4.77)$$

is the *transverse-photon potential*. The corresponding energy shift becomes in analogy with the single-photon case (4.53)

$$\Delta E = \left\langle \Phi \middle| V_{C} \frac{|tu\rangle\langle tu|}{E_{0} - \varepsilon_{t} - \varepsilon_{u}} V_{T} \middle| \Phi \right\rangle. \tag{4.78}$$

This holds when particle as well as hole states are involved.

 $^{^8}$ This is an illustration of the rule given in Appendix H that there is a factor of -i for each "non-trivial" integration, not involving a Δ factor.

In principle, the adiabatic damping has to be switched off *simultaneously* at all vertices. If the intermediate state is not degenerate with the initial state, the damping can be switched off at each vertex independently, which leads to energy conservation at each vertex, using the orbital energies of the free lines and the energy parameters of the propagators. The degenerate case, which leads to what is referred to as the *reference-state contribution*, is more complicated to handle [3, 9], and we shall not consider that further here. This kind of contribution is easier to evaluate in the covariant-evolution-operator formalism that we shall consider in Chap. 6.

4.5.2 Two-Photon Cross

For two crossed photons (Fig. 4.8), the S-matrix becomes

$$\langle cd|S^{(4)}|ab\rangle = \iint \frac{\mathrm{d}z}{2\pi} \frac{\mathrm{d}z'}{2\pi} \iint \frac{\mathrm{d}\omega_1}{2\pi} \frac{\mathrm{d}\omega_2}{2\pi} \langle cd|(-\mathrm{i})I(z'; x_4, x_3)\mathrm{i}S_F(\omega_1; x_4, x_1)$$

$$\times \mathrm{i}S_F(\omega_2; x_2, x_3) (-\mathrm{i})I(z; x_2, x_1)|ab\rangle 2\pi\Delta_{\gamma}(\varepsilon_a - z - \omega_1)$$

$$\times 2\pi\Delta_{\gamma}(\varepsilon_b - z' - \omega_2)2\pi\Delta_{\gamma}(\omega_1 + z' - \varepsilon_c)2\pi\Delta_{\gamma}(\omega_2 + z - \varepsilon_d).$$

Integrations over ω_1 , ω_2 yield

$$\langle cd|S^{(4)}|ab\rangle = \iint \frac{\mathrm{d}z}{2\pi} \frac{\mathrm{d}z'}{2\pi} \langle cd|(-\mathrm{i})I(z'; x_4, x_3) \,\mathrm{i}S_{\mathrm{F}}(\varepsilon_a - z; x_4, x_1) \times \mathrm{i}S_{\mathrm{F}}(\varepsilon_b - z'; x_2, x_3) \,(-\mathrm{i})I(z; x_2, x_1)|ab\rangle \times 2\pi \Delta_{2\gamma}(\varepsilon_a - \varepsilon_c - z + z') \,2\pi \Delta_{2\gamma}(\varepsilon_b - \varepsilon_d + z - z').$$
(4.79)

Again, we consider the simpler case with *one Coulomb and one transverse interaction* (Fig. 4.8, right), using the Coulomb gauge. Then the diagonal element becomes

$$\langle ab|S^{(4)}|ab\rangle = \langle ab | V_{C} \int \frac{dz}{2\pi} \frac{|t\rangle \langle t|}{\varepsilon_{a} - z - \varepsilon_{t} + i\gamma_{t}} \frac{|u\rangle \langle u|}{\varepsilon_{d} - z - \varepsilon_{u} + i\gamma_{u}}$$

$$\times \int \frac{2c^{2}\kappa \, d\kappa \, f_{T}^{C}(\kappa)}{z^{2} - c^{2}\kappa^{2} + i\eta} |ab\rangle \, 2\pi \Delta_{4\gamma}(0)$$
(4.80)

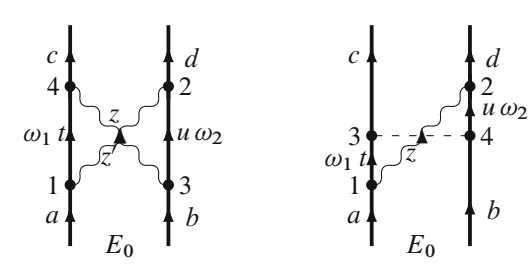


Fig. 4.8 The Feynman representation of the two-photon cross

4.6 QED Corrections 79

using the fact that $\varepsilon_a + \varepsilon_b = \varepsilon_c + \varepsilon_d$. Integration over z leads in analogy with (4.77) to

$$\langle ab|S^{(4)}|ab\rangle = -\mathrm{i}\langle ab \mid V_{\mathrm{C}} \frac{|tu\rangle\langle tu|}{\varepsilon_{a} - \varepsilon_{d} - \varepsilon_{t} + \varepsilon_{u}} V_{\mathrm{T}}^{X} \mid ab \rangle 2\pi \Delta_{4\gamma}(0),$$
 (4.81)

where $V_{\rm T}^{X}$ is the potential

$$\langle tu|V_{\rm T}^{X}|ab\rangle = \left\langle tu \middle| \int c \, \mathrm{d}\kappa \, f_{\rm T}^{\rm C}(\kappa) \right.$$

$$\times \left[\frac{1}{\varepsilon_{d} - \varepsilon_{t} - (c\kappa - \mathrm{i}\gamma)_{t}} - \frac{1}{\varepsilon_{d} - \varepsilon_{u} - (c\kappa - \mathrm{i}\gamma)_{u}} \right] \middle| ab \right\rangle. \quad (4.82)$$

If ε_t and ε_u have the same sign, the denominators in the expression (4.81) can be expressed

$$\frac{1}{\varepsilon_a - \varepsilon_t - (c\kappa - i\gamma)_t} \frac{1}{\varepsilon_d - \varepsilon_u - (c\kappa - i\gamma)_u},$$

which is in agreement with the evaluation rules for time-ordered diagrams, derived in Appendix I.

The two-photon ladder and the two-photon cross have been studied in great detail by means of the S-matrix technique for the ground-state of helium-like systems by Blundell et al. [3] and by Lindgren et al. [9]. Some numerical results are given in Chap. 7.

4.6 QED Corrections

In this section, we shall consider how various first-order QED corrections – beyond the no-virtual-pair approximation (see Sect. 2.6) – can be evaluated using the S-matrix formulation. With this formulation, only corrections to the energy can be evaluated. In Chap. 6, we shall demonstrate a way of including these effects directly into the wave functions, which makes it possible to incorporate them into the many-body procedure in a more systematic way. Some QED effects contain singularities (divergences), which can be handled by means of *regularization* and *renormalization*, as will be discussed in Chap. 12.

4.6.1 Bound-Electron Self-Energy

When the photon is emitted from and absorbed on the same electron, we have an effect of the *electron self-energy*, illustrated in Fig. 4.9. This forms the major part of the *Lamb shift*, discovered experimentally by Lamb and Retherford in 1947 [7].

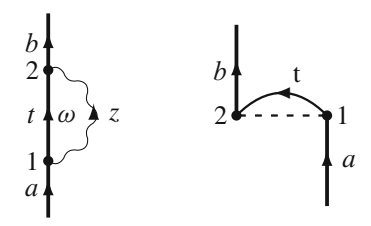


Fig. 4.9 Diagram representing the first-order bound-electron self-energy. The *second diagram* represents the Coulomb part of the self-energy in Coulomb gauge

This was the starting point for the development of modern QED (see the book by Schweber [15]). The second most important part of the Lamb shift is the *vacuum polarization*, to be treated below.

We treat first the self-energy and start with a covariant gauge and then consider the noncovariant Coulomb gauge.

4.6.1.1 Covariant Gauge

For the electron self-energy (Fig. 4.9), we can set up the expression for the S-matrix in analogy with the single-photon exchange (4.40),

$$S_{\text{SE}} = \frac{(ie)^2}{2} \iint d^4x_2 d^4x_1 \ \psi^{\dagger}(x_2) iS_F(x_2, x_1) iD_F(x_2, x_1) \psi(x_1) e^{-\gamma(|t_1| + |t_2|)}.$$
(4.83)

Considering the equivalent case with $1 \leftrightarrow 2$, the matrix element becomes

$$\langle b|S_{\text{SE}}|a\rangle = \iint \frac{\mathrm{d}z}{2\pi} \frac{\mathrm{d}\omega}{2\pi} \left\langle b \middle| iS_{\text{F}}(\omega; \mathbf{x}_{2}, \mathbf{x}_{1}) \left(-i\right) I(z; \mathbf{x}_{2}, \mathbf{x}_{1}) \middle| a \right\rangle$$

$$\times 2\pi \Delta_{\mathbf{y}} (\varepsilon_{a} - z - \omega) 2\pi \Delta_{\mathbf{y}} (\omega + z - \varepsilon_{b})$$
(4.84)

and after integration over ω

$$\langle b|S_{\rm SE}|a\rangle = 2\pi\Delta_{2\gamma}(\varepsilon_a-\varepsilon_b)\,\langle b| -\mathrm{i}\varSigma(\varepsilon_a)|a\rangle$$

with

$$\Sigma(\varepsilon_a) = i \int \frac{dz}{2\pi} S_F(\varepsilon_a - z; \boldsymbol{x}_2, \boldsymbol{x}_1) I(z; \boldsymbol{x}_2, \boldsymbol{x}_1)$$
 (4.85)

being the *self-energy function*.

The Sucher energy formula (4.6) yields the corresponding energy shift

$$\Delta E_{\rm SE} = \lim_{\gamma \to 0} i\gamma \langle b | S_{\rm SE} | a \rangle = \delta_{\varepsilon_a, \varepsilon_b} \langle b | \Sigma(\varepsilon_a) | a \rangle \tag{4.86}$$

4.6 QED Corrections 81

using the relation between the Dirac delta function and the Kroenecker delta factor in Appendix (A.17).

With the expressions for the electron propagator (4.10), the bound-state self-energy becomes

$$\langle a|\Sigma(\varepsilon_{a})|a\rangle = i\left\langle at \right| \int \frac{\mathrm{d}z}{2\pi} \frac{1}{\varepsilon_{a} - \varepsilon_{t} - z + i\eta_{t}} I(z; \mathbf{x}_{2}, \mathbf{x}_{1}) \left| ta \right\rangle$$

$$= i\left\langle at \right| \int \frac{\mathrm{d}z}{2\pi} \frac{1}{\varepsilon_{a} - \varepsilon_{t} - z + i\eta_{t}} \int \frac{2c^{2}\kappa}{z^{2} - c^{2}\kappa^{2} + i\eta} \left| ta \right\rangle$$
(4.87)

using the f function defined in (4.46).

In the Feynman gauge, we have

$$\langle a|\Sigma(\varepsilon_a)|a\rangle = i \left\langle at \right| \int \frac{dz}{2\pi} \frac{1}{\varepsilon_a - \varepsilon_t - z + i\eta_t} \int \frac{2c^2\kappa \, d\kappa \, f^F(\kappa)}{z^2 - c^2\kappa^2 + i\eta} \, \left| ta \right\rangle, \tag{4.88}$$

where $f^{\rm F}$ is given by (4.55). Performing the z integration yields

$$\langle a|\Sigma(\varepsilon_a)|a\rangle = \left\langle at \right| \int \frac{c \, \mathrm{d}\kappa f^{\mathrm{F}}(\kappa)}{\varepsilon_a - \varepsilon_t - (c\kappa - \mathrm{i}\eta)_t} \, \left| ta \right\rangle \tag{4.89}$$

and

$$\left\langle a|\Sigma(\varepsilon_a)|a\rangle = -\frac{e^2}{4\pi^2\epsilon_0} \left\langle at \left| \frac{\alpha_1^{\mu}\alpha_{2\mu}}{r_{12}} \int \frac{c \, \mathrm{d}\kappa \, \sin\kappa r_{12}}{\varepsilon_a - \varepsilon_t - (c\kappa - \mathrm{i}\eta)_t} \right| ta \right\rangle. \right.$$
(4.90)

4.6.1.2 Coulomb Gauge

In the *Coulomb gauge*, the *transverse part* can be treated in analogy with the covariant gauge (4.89)

$$\langle a|\Sigma(\varepsilon_a)|a\rangle_{\text{Trans}} = \langle at \Big| \int \frac{c \, d\kappa f_{\text{T}}^{\text{C}}(\kappa)}{\varepsilon_a - \varepsilon_t - (c\kappa - i\eta)_t} \Big| ta \rangle$$
 (4.91)

or with (4.60)

$$\langle a|\Sigma(\varepsilon_{a})|a\rangle_{\text{Trans}} = \frac{e^{2}}{4\pi^{2}\epsilon_{0}} \left\langle at \left| \frac{1}{r_{12}} \int \frac{c \, d\kappa \, \sin\kappa r_{12}}{\varepsilon_{a} - \varepsilon_{t} - (c\kappa - i\eta)_{t}} \right. \right. \\ \left. \times \left[\alpha_{1} \cdot \alpha_{2} - \frac{(\alpha_{1} \cdot \nabla_{1}) (\alpha_{2} \cdot \nabla_{2})}{\kappa^{2}} \right] \left| ta \right\rangle.$$
 (4.92)

For the *Coulomb part*, we insert the expression for $I_{\rm C}^{\rm C}$ in (4.63b) into (4.85), yielding

$$\Sigma(\varepsilon_{a})_{\text{Coul}} = \frac{\mathrm{i}e^{2}}{4\pi^{2}\epsilon_{0}r_{12}} \int \frac{\mathrm{d}z}{2\pi} S_{F}(\varepsilon_{a} - z; \boldsymbol{x}_{2}, \boldsymbol{x}_{1}) \int \frac{2\kappa \,\mathrm{d}\kappa \,\sin\kappa r_{12}}{\kappa^{2}}$$
$$= \mathrm{i} \int \frac{\mathrm{d}z}{2\pi} S_{F}(\varepsilon_{a} - z; \boldsymbol{x}_{2}, \boldsymbol{x}_{1}) V_{C}$$
(4.93)

and

$$\langle a|\Sigma(\varepsilon_a)|a\rangle_{\text{Coul}} = i\langle at \Big| \int \frac{\mathrm{d}z}{2\pi} \frac{1}{\varepsilon_a - z - \varepsilon_t + i\eta_t} V_{\mathrm{C}} \Big| ta \rangle.$$
 (4.94)

The integral can be evaluated as a principal integral (which vanishes) and *half* a pole, yielding the result $-i \operatorname{sgn}(\varepsilon_t)/2$. The self-energy then becomes

$$\langle a|\Sigma(\varepsilon_a)|a\rangle_{\text{Coul}} = \frac{1}{2}\operatorname{sgn}(\varepsilon_t)\langle at|V_C|ta\rangle.$$
 (4.95)

The electron self-energy is *divergent* and has to be renormalized, as will be discussed in Chap. 12. Some numerical results, using the Feynman gauge, are given in Chap. 7.

4.6.2 Vertex Correction

The vertex correction, shown in Fig. 4.10, is a correction to the single-potential interaction in Fig. 4.6, and the S-matrix becomes in analogy with the self-energy

$$\langle b|S_{VC}|a\rangle = \iint \frac{\mathrm{d}z}{2\pi} \frac{\mathrm{d}\omega}{2\pi}$$

$$\times \langle bu | iS_{F}(\omega; \mathbf{x}_{2}, \mathbf{x}_{3}) iec \, \alpha_{\sigma} A^{\sigma}(\mathbf{x}_{3})$$

$$iS_{F}(\omega; \mathbf{x}_{3}, \mathbf{x}_{1}) (-i)I(z; \mathbf{x}_{2}, \mathbf{x}_{1}) | ta \rangle$$

$$\times 2\pi \Delta_{\gamma} (\varepsilon_{a} - z - \omega) 2\pi \Delta_{\gamma} (\omega + z - \varepsilon_{b})$$

$$(4.96)$$

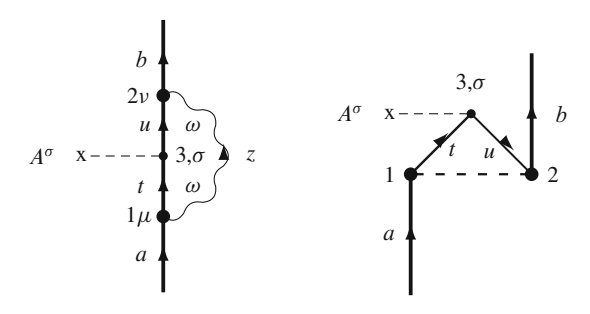


Fig. 4.10 Diagram representing the first-order vertex correction

4.6 QED Corrections 83

and after integration over ω

$$\langle bu|S_{VC}|ta\rangle = 2\pi \Delta_{2\gamma}(\varepsilon_a - \varepsilon_b) \langle bu| - iec \Lambda_{\sigma}(\varepsilon_a, \varepsilon_a) A^{\sigma}(x_3) |ta\rangle, \qquad (4.97)$$

where

$$\Lambda_{\sigma}(\varepsilon_{a}, \varepsilon_{a}) = -i \alpha_{\sigma} \int \frac{\mathrm{d}z}{2\pi} S_{F}(\varepsilon_{a} - z; \boldsymbol{x}_{2}, \boldsymbol{x}_{3}) S_{F}(\varepsilon_{a} - z; \boldsymbol{x}_{3}, \boldsymbol{x}_{1}) I(z; \boldsymbol{x}_{2}, \boldsymbol{x}_{1})$$

$$(4.98)$$

is the first-order vertex-correction function.

4.6.2.1 Covariant Gauge

With the expression for the electron and the photon propagators in a covariant gauge, we have

$$\Lambda_{\sigma}(\varepsilon_{a}, \varepsilon_{a}) = -i\alpha_{\sigma} \int \frac{dz}{2\pi} \frac{1}{\varepsilon_{a} - \varepsilon_{u} - z + i\eta_{u}} \frac{1}{\varepsilon_{a} - \varepsilon_{t} - z + i\eta_{t}} \int \frac{2c^{2}\kappa \, d\kappa \, f(\kappa)}{z^{2} - c^{2}\kappa^{2} + i\eta}$$
$$= -\alpha_{\sigma} \int \frac{c \, d\kappa \, f(\kappa)}{(\varepsilon_{a} - \varepsilon_{u} - c\kappa + i\eta)(\varepsilon_{a} - \varepsilon_{t} - c\kappa + i\eta)}$$
(4.99)

assuming *positive* intermediate states. The corresponding expressions of the particular gauge is obtained by inserting the expression for f(k) in that gauge.

Comparing with the self-energy above, we find for the diagonal part, t = u, what is known as

• The Ward identity (see also Chap. 12).

$$\frac{\partial}{\partial \varepsilon_a} \Sigma(\varepsilon_a) = \Lambda_0(\varepsilon_a, \varepsilon_a). \tag{4.100}$$

Also, the vertex correction is singular and has to renormalized, as will be discussed in Chap. 12.

4.6.2.2 Coulomb Gauge

The transverse part in Coulomb gauge is analogous the expression in the covariant gauge, using the corresponding f function. For the Coulomb part, we insert the Coulomb interaction (4.63b) in expression (4.98), yielding

$$\Lambda_{\sigma}(\varepsilon_{a}, \varepsilon_{a}) = -i \left\langle u \middle| \alpha_{\sigma} \int \frac{\mathrm{d}z}{2\pi} \frac{1}{\varepsilon_{a} - \varepsilon_{u} - z + i\eta_{u}} \frac{1}{\varepsilon_{a} - \varepsilon_{t} - z + i\eta_{t}} V_{C} \middle| t \right\rangle$$

$$= - \left\langle u \middle| \operatorname{sgn}(\varepsilon_{t}) \alpha_{\sigma} \frac{V_{C}}{\varepsilon_{t} - \varepsilon_{u}} \middle| t \right\rangle$$
(4.101)

provided ε_t and ε_u have different sign. If $\varepsilon_t = \varepsilon_u$ this vanishes, which is consistent with the Ward identity, since the corresponding self-energy contribution is energy independent.

4.6.3 Vacuum Polarization

The field near the atomic nucleus can give rise to a "polarization effect" in the form of the creation of electron–positron pairs, an effect referred to as the *vacuum polarization*. The first-order effect, illustrated in Fig. 4.11, forms together with the first-order self-energy (Fig. 4.9) the leading contributions to the *Lamb shift*.

In order to set up the S-matrix for the leading vacuum polarization (first diagram in Fig. 4.11), we go back to the relation (4.39) for single-photon exchange

$$-\iint_{\mathcal{X}} d^4x_2 d^4x_1 T \left[(\psi^{\dagger}(x)e\alpha^{\nu} A_{\nu}(x)\psi(x))_2 (\psi^{\dagger}(x)e\alpha^{\mu} A_{\mu}(x)\psi(x))_1 \right]$$

leaving out the factor of 1/2, since we can interchange 1 and 2, and inserting the contraction between the creation and absorption electron-field operators at vertex 2 to represent the closed orbital loop. Explicitly writing out the spinor components, we have at this vertex

$$\psi_{\sigma}^{\dagger}(x_2)e\alpha_{\sigma\tau}^{\nu}A_{\nu}(x_2)\psi_{\tau}(x_2) = \operatorname{Tr}\left[\psi^{\dagger}(x_2)e\alpha^{\nu}A_{\nu}(x_2)\psi(x_2)\right],$$

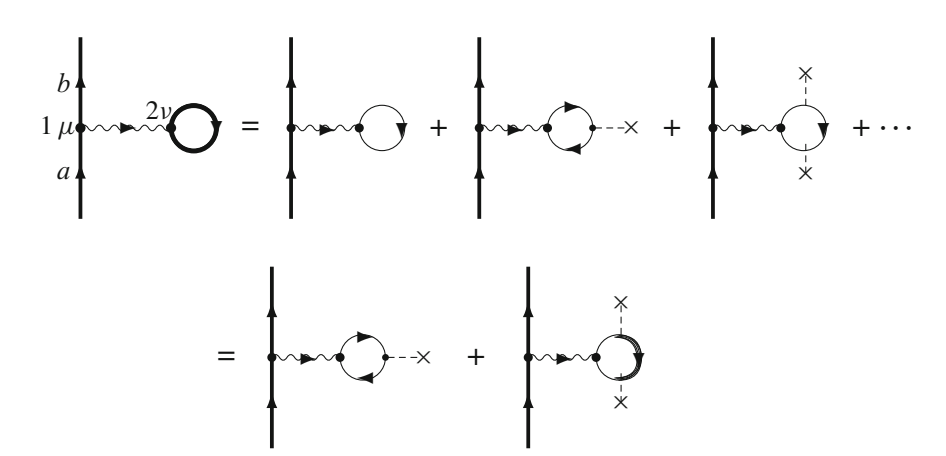


Fig. 4.11 Diagram representing the first-order vacuum polarization according to (4.107). The closed loop contains summation over *all* orbitals (particles and holes). The *first and third diagrams* on the r.h.s. of the *first row* vanish due to Furry's theorem (see text). The *first diagram* in the *second row* represents the Uehling part and the *final diagrams* the Wickmann–Kroll part. The *heavy lines* represent the *bound-state* propagator and the *thin lines* the *free-electron* propagator

4.6 QED Corrections 85

where "Tr" stands for the *trace* of the matrix, i.e., the sum of the diagonal elements. The contraction leads here to $-iS_F(x_2, x_2)$, according to the definition (4.9). We then have the S-matrix element

$$-e^2 \iint d^4x_2 d^4x_1 i\alpha_1^{\mu} D_{F\nu\mu}(x_2, x_1) \operatorname{Tr} \left[\alpha_2^{\nu}(-i) S_F(x_2, x_2)\right] e^{-\gamma(|t_1|+|t_2|)}.$$

With the Fourier transforms $S_F(\omega; x_2, x_2)$ and $D_{F\nu\mu}(z; x_2, x_1)$, the time dependence is

$$e^{-it_1(\varepsilon_b-\varepsilon_a-z)-\gamma|t_1|}e^{-it_2(\omega-\omega+z)-\gamma|t_2|}$$

and this leads after time integrations to the S-matrix element

$$\langle b|S_{\rm SE}^{(2)}|a\rangle = -2\pi\Delta_{\gamma}(\varepsilon_{a} - \varepsilon_{b} - z) 2\pi\Delta_{\gamma}(\omega - \omega + z) \times e^{2} \iint \frac{\mathrm{d}\omega}{2\pi} \frac{\mathrm{d}z}{2\pi} \left\langle b \middle| \alpha_{1}^{\mu} D_{\mathrm{F}\nu\mu}(z; \boldsymbol{x}_{2}, \boldsymbol{x}_{1}) \operatorname{Tr} \left[\alpha_{2}^{\nu} S_{\mathrm{F}}(\omega; \boldsymbol{x}_{2}, \boldsymbol{x}_{2})\right] \middle| a \right\rangle,$$

$$(4.102)$$

and in the limit $\gamma \to 0$, using the relation (A.28) in Appendix A,

$$\langle b|S_{\rm SE}^{(2)}|a\rangle = -2\pi \,\Delta_{2\gamma}(\varepsilon_a - \varepsilon_b)$$

$$\times e^2 \int \frac{\mathrm{d}\omega}{2\pi} \, \langle b \, | \, \alpha_1^{\mu} D_{\mathrm{F}\nu\mu}(0; \boldsymbol{x}_2, \boldsymbol{x}_1) \, \mathrm{Tr} \big[\alpha_2^{\nu} S_{\mathrm{F}}(\omega; \boldsymbol{x}_2, \boldsymbol{x}_2) \big] \, \Big| a \rangle.$$

$$(4.103)$$

According to Sucher's energy formula (4.6), we have in second order

$$\Delta E = \lim_{\gamma \to 0} i\gamma \langle \Phi | S^{(2)} | \Phi \rangle \tag{4.104}$$

and using the relation (A.17)

$$\Delta E = -\mathrm{i}\delta(\varepsilon_a, \varepsilon_b)$$

$$\times e^2 \int \frac{\mathrm{d}\omega}{2\pi} \left\langle b \middle| \alpha_1^{\mu} D_{\mathrm{F}\nu\mu}(0; \mathbf{x}_2, \mathbf{x}_1) \operatorname{Tr} \left[\alpha_2^{\nu} S_{\mathrm{F}}(\omega; \mathbf{x}_2, \mathbf{x}_2)\right] \middle| a \right\rangle. \tag{4.105}$$

It can furthermore be shown that only $\nu=0$, i.e., $\alpha^{\nu}=1$ will contribute here [12]. The vacuum polarization contribution is divergent and has to renormalized, which in this case turns out to be not too difficult (see below).

The bound-state electron propagator, $S_{\rm F}(\omega)$, is in operator form (4.14)

$$\hat{S}_{F}(\omega) = \frac{1}{\omega - \hat{h}_{\text{bau}} (1 - i\eta)}.$$
(4.106)

Expressing the Dirac Hamiltonian for an electron in an external (nuclear) potential $v_{\rm ext}$ as $\hat{h}_{\rm bau} = \hat{h}_{\rm free} + v_{\rm ext}$, where $\hat{h}_{\rm free}$ is the free-electron Hamiltonian, the propagator (4.102) can be expanded as

$$\begin{split} \frac{1}{z - \hat{h}_{\text{bau}}(1 - \mathrm{i}\eta)} &= \frac{1}{z - \hat{h}_{\text{free}}(1 - \mathrm{i}\eta)} + \frac{1}{z - \hat{h}_{\text{free}}(1 - \mathrm{i}\eta)} V \frac{1}{z - \hat{h}_{\text{free}}(1 - \mathrm{i}\eta)} \\ &+ \frac{1}{z - \hat{h}_{\text{free}}(1 - \mathrm{i}\eta)} V \frac{1}{z - \hat{h}_{\text{free}}(1 - \mathrm{i}\eta)} V \times \frac{1}{z - \hat{h}_{\text{free}}(1 - \mathrm{i}\eta)} + \cdots \\ &= \frac{1}{z - \hat{h}_{\text{free}}(1 - \mathrm{i}\eta)} + \frac{1}{z - \hat{h}_{\text{free}}(1 - \mathrm{i}\eta)} V \frac{1}{z - \hat{h}_{\text{free}}(1 - \mathrm{i}\eta)} \\ &+ \frac{1}{z - \hat{h}_{\text{free}}(1 - \mathrm{i}\eta)} V \frac{1}{z - \hat{h}_{\text{bau}}(1 - \mathrm{i}\eta)} V \frac{1}{z - \hat{h}_{\text{free}}(1 - \mathrm{i}\eta)}, \end{split}$$

$$(4.107)$$

which leads to the expansion is illustrated in Fig. 4.11.

The first and third diagrams on the r.h.s. in the first row in Fig. 4.11 vanish due to "Furry's theorem". According to this theorem, a diagram will vanish if it contains a free-electron loop with an *odd number of vertices* [10, Sect. 9.1]. The first diagram in the second row represents the *Uehling part* [17], and the second part is the so-called *Wickmann–Kroll* [19] part. The Uehling part is *divergent*, but Uehling was already in 1934 able to handle this divergence and derive an analytic expression for the renormalized potential. The Wickmann–Kroll part is finite and has to be evaluated numerically.

Both the Uehling and the Wickmann–Kroll effects can be expressed in terms of single-particle potentials that can be added to the external potential, used to generate the single particle spectrum, and in this way the effects can be automatically included in the calculations to arbitrary order (see, for instance, Persson et al. [12]). In Table 4.1, we show the result of some accurate vacuum-polarization calculations. The diagrams above for the vacuum-polarization and the self-energy can be compared with the corresponding many-body diagrams, discussed in Sect. 2.4 (Fig. 2.3). In the MBPT case, the internal lines represent core orbitals only, while in the present case they can *represent all orbitals – particle as well as hole states*.

Table 4.1 Vacuum-polarization effects in the ground state of some hydrogen-like systems (in eV) (from Persson et al. [12])

₃₆ Kr	Uehling	-1.35682
	Wickmann-Kroll	0.01550
₅₄ Xe	Uehling	-7.3250
	Wickmann-Kroll	0.1695
₇₀ Yb	Uehling	-23.4016
	Wickmann-Kroll	0.8283
₉₂ U	Uehling	-93.5868
	Wickmann-Kroll	4.9863



Fig. 4.12 Diagram representing the first-order photon self-energy

4.6.4 Photon Self-Energy

The interaction between the photon and the electron–positron fields can give rise to another form of *vacuum polarization*, illustrated in Fig. 4.12. The S-matrix for this process can be obtained from that of single-photon exchange (4.40) by replacing $-ie^2\alpha_1^{\mu}D_{F\nu\mu}(x_1,x_2)\alpha_2^{\nu}$ by

$$\iint d^4x_3 d^4x_4 (-ie^2) \alpha_1^{\mu} D_{F\mu\sigma}(x_1, x_3) i \Pi^{\sigma\tau}(x_3, x_4) (-ie^2) \alpha_2^{\nu} D_{F\tau\nu}(x_4, x_2),$$
(4.108)

where

$$i\Pi^{\sigma\tau}(x_{3}, x_{4}) = \alpha_{3}^{\sigma} \hat{\psi}^{\dagger}(x_{3}) \hat{\psi}^{\dagger}(x_{4}) \hat{\psi}^{\dagger}(x_{4}) \hat{\psi}^{\iota}(x_{4}) \alpha_{4}^{\nu}$$

$$= \alpha_{3}^{\sigma} \hat{\psi}(x_{3}) \hat{\psi}^{\dagger}(x_{4}) \hat{\psi}^{\dagger}(x_{3}) \hat{\psi}(x_{4}) \alpha_{4}^{\nu}$$

$$= -\text{Tr}[\alpha_{3}^{\sigma} iS_{F}(x_{3}, x_{4}) iS_{F}(x_{4}, x_{3}) \alpha_{4}^{\nu}] \qquad (4.109)$$

is the *first-order polarization tensor* [10, Eqs. (7.22) and (9.5)]. The contractions lead here to the *trace* as in the previous case, and there is also here a minus sign due to the closed loop.

The photon self-energy is (charge) divergent and requires a *renormalization*, as is discussed further in Chap. 12, and after the renormalization there is a *finite remainder*.

4.7 Feynman Diagrams for the S-Matrix: Feynman Amplitude

4.7.1 Feynman Diagrams

We have in this chapter constructed S-matrix expressions for a number of Feynman diagrams, and we summarize here the rules that can be deduced for this construction. We also introduce the so-called *Feynman amplitude*, introduced by Richard Feynman in his original works on quantum-field theory, which we shall

find convenient to use also in other procedures to be discussed later. These rules are also summarized in Appendix H.

The S-matrix is given by (3.26) and (4.3)

$$S = \sum_{n=0}^{\infty} \left(\frac{-i}{c}\right)^n \frac{1}{n!} \int dx_1^4 \dots \int dx_n^4 T \left[\mathcal{H}(x_1) \dots \mathcal{H}(x_n)\right] e^{-\gamma(|t_1|+|t_2|\dots|t_n|)}$$

with the interaction density (4.4)

$$\mathcal{H}(x) = -\hat{\psi}^{\dagger}(x)ec\alpha^{\mu}A_{\mu}(x)\hat{\psi}(x).$$

This leads to the following rules: There is

- An electron-field creation/absorption operator, $\hat{\psi}^{\dagger}/\hat{\psi}$, for each outgoing/incoming electron orbital.
- An *electron propagator* (4.10) (times imaginary unit) for each internal orbital line

$$\hat{\psi}(x_1)\hat{\psi}^{\dagger}(x_2) = i S_F(x_1, x_2) = i \int \frac{d\omega}{2\pi} S_F(\omega; x_1, x_2) e^{-i\omega(t_1 - t_2)}.$$

• A *single-photon interaction* [(4.44) and (4.45)] (times negative imaginary unit) for each single internal photon line

$$I(x_1, x_2) = \int \frac{dz}{2\pi} (-i) I(z; \boldsymbol{x}_1, \boldsymbol{x}_2) e^{-iz(t_1 - t_2)},$$

where the interaction is given by (4.46)

$$I(z; x_1, x_2) = \int \frac{2c^2\kappa \, d\kappa \, f(\kappa, x_1, x_2)}{z^2 - c^2\kappa^2 + in} = \int \frac{2\kappa \, d\kappa \, f(\kappa, x_1, x_2)}{a^2 - \kappa^2 + in}$$

$$(\kappa = |\mathbf{k}|, z = ck_0 = cq).$$

- At each vertex a space integration and a time integral $2\pi\Delta_{\gamma}(arg)$, where the argument is equal to incoming minus outgoing energy parameters.
- A factor of -1 and a *trace symbol* for each closed orbital loop.

4.7.2 Feynman Amplitude

The Feynman amplitude, \mathcal{M} , is

For the S-matrix defined by the relation

$$\langle cd|S|ab\rangle = 2\pi\delta(E_{\rm in} - E_{\rm out})\langle cd|\mathcal{M}|ab\rangle,$$
 (4.110)

where $E_{\rm in}$, $E_{\rm out}$ are the incoming and outgoing energies, respectively.

References 89

• The first-order energy shift is given by

$$\Delta E = \delta_{E_{\rm in}, E_{\rm out}} \langle cd | i\mathcal{M} | ab \rangle.$$
 (4.111)

References

- Adkins, G.: One-loop renormalization of Coulomb-gauge QED. Phys. Rev. D 27, 1814–20 (1983)
- 2. Bjorken, J.D., Drell, S.D.: *Relativistic Quantum Mechanics*. Mc-Graw-Hill Pbl. Co, N.Y. (1964)
- 3. Blundell, S., Mohr, P.J., Johnson, W.R., Sapirstein, J.: Evaluation of two-photon exchange graphs for highly charged heliumlike ions. Phys. Rev. A 48, 2615–26 (1993)
- Fetter, A.L., Walecka, J.D.: The Quantum Mechanics of Many-Body Systems. McGraw-Hill, N.Y. (1971)
- Feynman, R.P.: Space-Time Approach to Quantum Electrodynamics. Phys. Rev. 76, 769–88 (1949)
- 6. Feynman, R.P.: *The Theory of Positrons*. Phys. Rev. **76**, 749–59 (1949)
- 7. Lamb, W.W., Retherford, R.C.: Fine structure of the hydrogen atom by microwave method. Phys. Rev. **72**, 241–43 (1947)
- 8. Lindgren, I., Morrison, J.: *Atomic Many-Body Theory*. Second edition, Springer-Verlag, Berlin (1986, reprinted 2009)
- 9. Lindgren, I., Persson, H., Salomonson, S., Labzowsky, L.: Full QED calculations of two-photon exchange for heliumlike systems: Analysis in the Coulomb and Feynman gauges. Phys. Rev. A 51, 1167–1195 (1995)
- 10. Mandl, F., Shaw, G.: Quantum Field Theory. John Wiley and Sons, New York (1986)
- 11. Mohr, P.J., Plunien, G., Soff, G.: *QED corrections in heavy atoms*. Physics Reports **293**, 227–372 (1998)
- 12. Persson, H., Lindgren, I., Salomonson, S., Sunnergren, P.: Accurate vacuum-polarization calculations. Phys. Rev. A 48, 2772–78 (1993)
- 13. Peskin, M.E., Schroeder, D.V.: *An introduction to Quantun Field Theory*. Addison-Wesley Publ. Co., Reading, Mass. (1995)
- Rosenberg, L.: Virtual-pair effects in atomic structure theory. Phys. Rev. A 39, 4377–86 (1989)
- 15. Schweber, S.S.: *The men who madt it: Dyson, Feynman, Schwinger and Tomonaga*. Princeton University Press, Princeton (1994)
- 16. Sucher, J.: S-Matrix Formalism for Level-Shift Calculations. Phys. Rev. 107, 1448–54 (1957)
- 17. Uehling, E.A.: Polarization Effects in the Positron Theory. Phys. Rev. 48, 55–63 (1935)
- 18. Wheeler, J.A.: On the Mathematical Description of Light Nuclei by the Method of Resonating Group Structure. Phys. Rev. **52**, 1107–22 (1937)
- Wichmann, E.H., Kroll, N.M.: Vacuum Polarization in a Strong Coulomb Field. Phys. Rev. 101, 843–59 (1956)

Chapter 5 Green's Functions

The *Green's function* is an important tool with applications in classical as well as quantum physics (for an introduction, see particularly the book by Fetter and Walecka [5, Chap. 3], see also the book by Mahan [8]). More recently, it has been applied also to quantum-electrodynamics by Shabaev et al. [12]. As a background, we shall first consider the classical Green's function.

5.1 Classical Green's Function

The classical *Green's function*, $G(x, x_0)$, can be defined so that it describes the propagation of a wave from one space-time point $x_0 = (t_0, x_0)$ to another spacetime point x = (t, x), known as the Huygens' principle (see, for instance, the book by Bjorken and Dell [4, Sect. 6.2])

$$\chi(x) = \int d^3 x_0 G(x, x_0) \chi(x_0). \tag{5.1}$$

The *retarded* Green's function is defined as the part of the functions $G(x, x_0)$ for which $t > t_0$

$$G_{+}(x, x_{0}) = \Theta(t - t_{0}) G(x, x_{0}), \tag{5.2}$$

where $\Theta(t)$ is the Heaviside step function (Appendix A.29), which implies

$$\Theta(t - t_0) \chi(x) = \int d^3 x_0 G_+(x, x_0) \chi(x_0). \tag{5.3}$$

We assume now that the function $\chi(x)$ satisfies a differential equation of Schrödinger type

$$\left(i\frac{\partial}{\partial t} - H(x)\right)\chi(x) = 0. \tag{5.4}$$

92 5 Green's Functions

Operating with the bracket on (5.3) yields

$$i\delta(t - t_0) \chi(x) = \int d^3x_0 \left(i\frac{\partial}{\partial t} - H(x) \right) G_+(x, x_0) \chi(x_0)$$

using the relation (A.31), which implies that

• the retarded Green's function satisfies the differential equation

$$\left[\left(i\frac{\partial}{\partial t} - H(x)\right)G_{+}(x, x_{0}) = i\delta^{4}(x - x_{0}).\right]$$
(5.5)

- A relation often taken as the definition of the (mathematical) Green's function.

The Green's function can be used for solving inhomogeneous differential equations. If we have

$$\left(i\frac{\partial}{\partial t} - H(x)\right)\Psi(x) = f(x),\tag{5.6}$$

then the solution can be expressed

$$\Psi(x) = \int dx' G_{+}(x', x) f(x'). \tag{5.7}$$

5.2 Field-Theoretical Green's Function: Closed-Shell Case

5.2.1 Definition of the Field-Theoretical Green's Function

• In the **closed-shell case**, the field-theoretical single-particle Green's function can be defined [5]¹

$$G(x, x_0) = \frac{\left\langle 0_{\rm H} \left| T \left[\hat{\psi}_{\rm H}(x) \hat{\psi}_{\rm H}^{\dagger}(x_0) \right] \right| 0_{\rm H} \right\rangle}{\left\langle 0_{\rm H} \right| 0_{\rm H} \right\rangle},\tag{5.8}$$

where T is the *Wick time-ordering* operator (2.27) and $\hat{\psi}_H$, $\hat{\psi}_H^{\dagger}$ are the electron-field operators in the Heisenberg representation (HP) (B.27). The state $|0_H\rangle$ is the "vacuum in the Heisenberg representation," i.e., the state in the Heisenberg representation with no particles or holes. In a "closed-shell state," the single reference or model state is identical to the vacuum state (see Sect. 2.3).

¹ Different definitions of the field-theoretical Green's function are used in the literature. The definition used here agrees with that of Itzykson and Zuber [7], while that of Fetter and Walecka [5] differs by a factor of i.

The Heisenberg vacuum is time independent and equal to the corresponding vacuum state in the interaction picture at t = 0, i.e.,

$$|0_{\rm H}\rangle = U(0, -\infty)|0\rangle, \tag{5.9}$$

where $U(t, t_0)$ is the evolution operator (3.6) and $|0\rangle$ is the unperturbed vacuum or the IP vacuum as $t \to -\infty$ [c.f. (3.28)].

Using the relation between the electron-field operators in HP and IP (B.25)

$$\hat{\psi}_{H}(x) = U(0, t) \,\hat{\psi}(x) \, U(t, 0), \tag{5.10}$$

we can transform the Green's function (5.8) to the interaction picture

$$G(x,x_0) = \frac{\left\langle 0 \left| U(\infty,0)T \left[U(0,t)\hat{\psi}(x)U(t,0)U(0,t_0)\hat{\psi}^{\dagger}(x_0)U(t_0,0) \right] U(0,-\infty) \right| 0 \right\rangle}{\left\langle 0 | U(\infty,-\infty)| 0 \right\rangle}.$$
(5.11)

For $t > t_0$, the numerator becomes

$$\left\langle 0 \left| U(\infty, t) \,\hat{\psi}(x) U(t, t_0) \hat{\psi}^{\dagger}(x_0) U(t_0, -\infty) \right| 0 \right\rangle \tag{5.12a}$$

and for $t < t_0$

$$\left\langle 0 \left| U(\infty, t_0) \,\hat{\psi}^{\dagger}(x_0) U(t_0, t) \hat{\psi}(x) U(t, -\infty) \right| 0 \right\rangle$$
 (5.12b)

using the relation (3.8). From the expansion (3.15), we obtain the identity

$$U(t,t_{0}) = \sum_{\nu=0}^{\infty} \frac{(-i)^{\nu}}{\nu!} \int_{t_{0}}^{t} dt_{1} \dots \int_{t_{0}}^{t} dt_{\nu} T[V(t_{1}) \dots V(t_{\nu})] e^{-\gamma(|t_{1}|+|t_{2}|\dots)}$$

$$= \sum_{n=0}^{\infty} \frac{(-i)^{n}}{n!} \int_{t_{1}}^{t} dt_{1} \dots \int_{t_{1}}^{t} dt_{n} T[V(t_{1}) \dots V(t_{n})] e^{-\gamma(|t_{1}|+|t_{2}|\dots)}$$

$$\times \sum_{m=0}^{\infty} \frac{(-i)^{m}}{m!} \int_{t_{0}}^{t_{1}} dt_{1} \dots \int_{t_{0}}^{t_{1}} dt_{m} T[V(t_{1}) \dots V(t_{m}) e^{-\gamma(|t_{1}|+|t_{2}|\dots)}],$$
(5.13)

where we have included the unity as the zeroth-order term in the summation. If we concentrate on the ν :th term of the first sum, we have the identity (leaving out the damping factor)

$$\frac{1}{\nu!} \int_{t_0}^t dt_1 \dots \int_{t_0}^t dt_{\nu} T[V(t_1) \dots V(t_{\nu})]$$

$$= \sum_{m+n=\nu} \frac{1}{m! \, n!} \int_{t_1}^t dt_1 \dots \int_{t_1}^t dt_n T[\dots] \int_{t_0}^{t_1} dt_1 \dots \int_{t_0}^{t_1} dt_m T[\dots]. \quad (5.14)$$

We can now apply this identity to the first part of the numerator (5.12a), $U(\infty,t) \hat{\psi}(x) U(t,t_0)$. The interaction times of $U(\infty,t)$, $\hat{\psi}(x)$ and $U(t,t_0)$ are time ordered, and hence the result can be expressed

$$\frac{1}{\nu!} \int_{t_0}^{\infty} \mathrm{d}t_1 \dots \int_{t_0}^{\infty} \mathrm{d}t_{\nu} \, T \left[V(t_1) \dots V(t_{\nu}) \, \hat{\psi}(x) \right]. \tag{5.15}$$

The same procedure can be applied to the rest of the expression (5.12a) as well as to the other time ordering (5.12b). With the perturbation (3.16), the numerator of the single-particle Green's function (5.11) then becomes [5, Eq. 8.9]

$$\left\langle 0_{\mathrm{H}} \left| T \left[\hat{\psi}_{\mathrm{H}}(x) \hat{\psi}_{\mathrm{H}}^{\dagger}(x_{0}) \right] \right| 0_{\mathrm{H}} \right\rangle = \sum_{n=0}^{\infty} \frac{1}{n!} \left(\frac{-\mathrm{i}}{c} \right)^{n} \int d^{4}x_{1} \cdots \int d^{4}x_{n}$$

$$\times \left\langle 0 \left| T \left[\hat{\psi}(x) \mathcal{H}(x_{1}) \cdots \mathcal{H}(x_{n}) \hat{\psi}^{\dagger}(x_{0}) \right] \right| 0 \right\rangle e^{-\gamma(|t_{1}| + |t_{2}| \cdots)}$$
(5.16)

with integrations over all *internal* times. In transforming the time-ordering to normal ordering by means of Wick's theorem, only *fully connected* terms remain, since the vacuum expectation of any normal-ordered expression vanishes (see Sect. 4.41).

The denominator in (5.8) becomes, using the relation (5.9),

$$\langle 0_{\rm H} | 0_{\rm H} \rangle = \langle 0 | U(\infty, -\infty) | 0 \rangle = \langle 0 | S | 0 \rangle,$$

where S is the S-matrix (4.2). Then

• the Green's function can be expressed

$$G(x, x_0) = \frac{\left\langle 0_{\rm H} \left| T \left[\hat{\psi}_{\rm H}(x) \hat{\psi}_{\rm H}^{\dagger}(x_0) \right] \right| 0_{\rm H} \right\rangle}{\left\langle 0 | S | 0 \right\rangle}.$$
 (5.17)

We see that this expansion is very similar to that of the S-matrix (4.3), the main difference being the two additional electron-field operators. Therefore,

• the Green's function can also be expressed as

$$G(x, x_0) = \frac{\left\langle 0 \left| T \left[\hat{\psi}(x) U(\infty, -\infty) \hat{\psi}^{\dagger}(x_0) \right] \right| 0 \right\rangle}{\left\langle 0 | S | 0 \right\rangle}, \tag{5.18}$$

where the time-ordered product is connected to form a one-body operator. This leads to

$$G(x, x_0) = \frac{1}{\langle 0|S|0\rangle} \sum_{n=0}^{\infty} \frac{1}{n!} \left(\frac{-\mathrm{i}}{c}\right)^n \int \mathrm{d}^4 x_1 \cdots \int \mathrm{d}^4 x_n$$

$$\times \left\langle 0 \left| T \left[\hat{\psi}(x) \mathcal{H}(x_1) \cdots \mathcal{H}(x_n) \hat{\psi}^{\dagger}(x_0) \right] \right| 0 \right\rangle e^{-\gamma(|t_1| + |t_2| \cdots)}. \quad (5.19)$$

The Green's function is like the S-matrix Lorentz covariant.

The two-particle Green's function is defined in an analogous way

$$G(x, x'; x_0, x_0') = \frac{\langle 0|T \left[\hat{\psi}_{H}(x) \,\hat{\psi}_{H}(x') \,\hat{\psi}_{H}^{\dagger}(x_0') \,\hat{\psi}_{H}^{\dagger}(x_0)\right]|0\rangle}{\langle 0|S|0\rangle}$$
(5.20)

and transforming to the interaction picture leads similarly to

$$G(x, x'; x_0, x'_0) = \frac{1}{\langle 0|S|0\rangle} \sum_{n=0}^{\infty} \frac{1}{n!} \left(\frac{-i}{c}\right)^n \int d^4x_1 \cdots \int d^4x_n \\ \times \langle 0|T[\hat{\psi}(x)\hat{\psi}(x')\mathcal{H}(x_1)\cdots\mathcal{H}(x_n)\hat{\psi}^{\dagger}(x'_0)\hat{\psi}^{\dagger}(x_0)]|0\rangle e^{-\gamma(|t_1|+|t_2|\cdots)}$$
(5.21)

and analogously in the general many-particle case. Note that the coordinates are here four-dimensional space-time coordinates, which implies that the particles have *individual initial and final times*. This is in contrast to the quantum-mechanical wave function or state vector, which has the same time for all particles. We shall discuss this question further below.

We can transform the time-ordered products above to normal-ordered ones by means of Wick's theorem (see Sect. 2.2.3). Since normal-ordered products do not contribute to the vacuum expectation value, it follows that only fully contracted contribute to the Green's function. The contractions between the electron-field operators and the interaction operators lead to *electron propagators* (S_F) (4.9) on the in- and outgoing lines as well as all internal lines (see Fig. 5.1).² This allows time to run in both directions, and *both particle and hole states can be involved*.

5.2.2 Single-Photon Exchange

The Green's function for single-photon exchange in Fig. 5.2 can be constructed in close analogy to that of the corresponding S-matrix in Sect. 4.4,

$$G(x, x', x_0, x'_0) = \iint d^4x_2 d^4x_1 iS_F(x, x_1) iS_F(x', x_2)$$

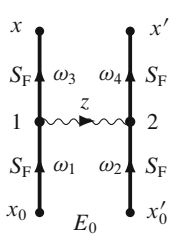
$$\times (-i)e^2 D_F(x_2, x_1) iS_F(x_1, x_0) iS_F(x_2, x'_0) e^{-\gamma(|t_1| + |t_2|)}. (5.22)$$

$$x = \sum_{S_F} \sum_{S_F$$

Fig. 5.1 Graphical representation of the one- and two-particle Green's function. The orbital lines between *dots* represent electron propagators

² In our notations, an orbital line between heavy dots always represents an electron propagator.

Fig. 5.2 Green's function for single-photon exchange



With the transforms (4.10) and (4.31), this becomes after integrating over the internal limes [using the relation (A.17)]

$$G(x, x', x_{0}, x'_{0}) = e^{-it\omega_{3}} e^{-it'\omega_{4}} e^{it_{0}\omega_{1}} e^{it'_{0}\omega_{2}} \iint d^{3}x_{1} d^{3}x_{2} \iint \frac{d\omega_{3}}{2\pi} \frac{d\omega_{4}}{2\pi}$$

$$\times \iint \frac{d\omega_{1}}{2\pi} \frac{d\omega_{2}}{2\pi} \int \frac{dz}{2\pi} iS_{F}(\omega_{3}; x, x_{1})$$

$$\times iS_{F}(\omega_{4}; x', x_{2}) (-i)e^{2}D_{F}(z; x_{2}, x_{1}) iS_{F}(\omega_{1}; x_{1}, x_{0})$$

$$\times iS_{F}(\omega_{2}; x_{2}, x'_{0})2\pi \Delta_{\gamma}(\omega_{1} - z - \omega_{3}) 2\pi \Delta_{\gamma}(\omega_{2} + z - \omega_{4}).$$
(5.23)

In the *equal-time approximation*, where the particles have the same initial and final times (t=t') and $t_0=t'_0$, the external time dependence becomes $e^{-it(\omega_3+\omega_4)}e^{it_0(\omega_1+\omega_2)}$. In the limit $\gamma\to 0$, we have after z-integration $\omega_1+\omega_2=\omega_3+\omega_4$, and if we consider the diagram as a part of a ladder, this is equal to the initial energy E_0 .

We define the Feynman amplitude for the Green's function as the function with the external time dependence removed. This gives

$$G(x, x', x_0, x'_0) = \mathcal{M}_{sp}(x, x'; x_0, x'_0) e^{-i(t-t_0)E_0}$$
(5.24)

and

$$\mathcal{M}_{sp}(x, x'; x_0, x'_0) = \iint d^3x_1 d^3x_2 \iint \frac{d\omega_3}{2\pi} \frac{d\omega_4}{2\pi} \iint \frac{d\omega_1}{2\pi} \frac{d\omega_2}{2\pi} \times iS_F(\omega_4; x', x_2)(-i)I(\omega_1 - \omega_3; x_2, x_1) iS_F(\omega_1; x_1, x_0) \times iS_F(\omega_2; x_2, x'_0)2\pi \Delta_{2\gamma}(\omega_1 + \omega_2 - \omega_3 - \omega_4)$$
(5.25)

using the definition (4.44).

5.2.3 Fourier Transform of the Green's Function

5.2.3.1 Single-Particle Green's Function

Assuming the Heisenberg vacuum state $|0_H\rangle$ to be normalized, the single-particle Green's function (5.8) becomes

$$G(x, x_{0}) = \langle 0_{H} | T [\hat{\psi}_{H}(x) \hat{\psi}_{H}^{\dagger}(x_{0})] | 0_{H} \rangle$$

$$= \Theta(t - t_{0}) \langle 0_{H} | \hat{\psi}_{H}(x) \hat{\psi}_{H}^{\dagger}(x_{0}) | 0_{H} \rangle - \Theta(t_{0} - t) \langle 0_{H} | \hat{\psi}_{H}^{\dagger}(x_{0}) \hat{\psi}_{H}(x) | 0_{H} \rangle.$$
(5.26)

The retarded part (5.2) is then, using the relation (B.27) in Appendix B,

$$G_{+}(x, x_{0}) = \langle 0_{H} | \hat{\psi}_{H}(x) \, \hat{\psi}_{H}^{\dagger}(x_{0}) | 0_{H} \rangle$$

$$= \langle 0_{H} | (e^{iHt} \hat{\psi}_{S}(x) e^{-iHt}) \, (e^{iHt_{0}} \hat{\psi}_{S}^{\dagger}(x_{0}) e^{-iHt_{0}}) | 0_{H} \rangle. \tag{5.27}$$

Inserting between the field operators a complete set of positive-energy eigenstates of the second-quantized Hamiltonian H (2.17), corresponding to the (N+1)-particle system

$$H|n\rangle = E_n|n\rangle \tag{5.28}$$

yields the Lehmann representation

$$G_{+}(x,x_{0}) = \sum_{n} \langle 0_{H} | e^{iHt} \hat{\psi}_{S}(x) | n \rangle e^{-iE_{n}(t-t_{0})} \langle n | \hat{\psi}_{S}^{\dagger}(x_{0}) e^{-iHt} | 0_{H} \rangle$$
 (5.29)

summed over the intermediate states of the (N + 1) system. The ground state as well as the inserted intermediate states are eigenstates of the Hamiltonian H, and setting the energy of the former to zero, this yields

$$G_{+}(x,x_{0}) = \sum_{n} \langle 0_{H} | \hat{\psi}_{S}(x) | n \rangle e^{-iE_{n}(t-t_{0})} \langle n | \hat{\psi}_{S}^{\dagger}(x_{0}) | 0_{H} \rangle.$$
 (5.30)

Performing a Fourier transform of the Green's function, including the *adiabatic* damping $e^{-\gamma\tau}$ (see Sect. 3.2), yields $(\tau = t - t_0 > 0)$

$$G_{+}(E; \boldsymbol{x}, \boldsymbol{x}_{0}) = \int_{0}^{\infty} d\tau \, e^{iE\tau} \, G_{+}(\tau, \boldsymbol{x}, \boldsymbol{x}_{0}) = i \frac{\langle 0_{H} | \hat{\psi}_{S}(\boldsymbol{x}) | n \rangle \, \langle n | \hat{\psi}_{S}^{\dagger}(\boldsymbol{x}_{0}) | 0_{H} \rangle}{E - E_{n} + i\gamma}$$
(5.31)

using

$$\int_0^\infty dt \, e^{i\alpha t} \, e^{-\gamma t} = \frac{i}{\alpha + i\gamma}.$$
 (5.32)

Analogous results are obtained for the *advanced* part $(t < t_0)$ of the Green's function, corresponding to a *hole* in the initial system.

The expression $\langle n | \hat{\psi}_S^{\dagger}(x) | 0_{\rm H} \rangle$ represents a state $\Psi_n(x)$ of the (N+1) system in the Schrödinger picture, and an equivalent expression of

• the Fourier transform of the Green's function becomes

$$G_{+}(E; x, x_{0}) = i \sum_{n} \frac{\Psi_{n}(x)\Psi_{n}^{*}(x_{0})}{E - E_{n} + i\gamma}.$$
 (5.33)

This implies that

• the poles of the retarded/advanced single-particle Green's function represent the true energies of the vacuum plus/minus one particle, relative to the vacuum state.

In order to show that the definition (5.8) of the Green's function is compatible with the classical definition [(5.1) and (5.5)], we form the reverse transformation

$$G_{+}(x,x_{0}) = G_{+}(\tau,x,x_{0}) = \int \frac{dE}{2\pi} e^{-iE\tau} i \sum_{n} \frac{\Psi_{n}(x)\Psi_{n}^{*}(x_{0})}{E - E_{n} + i\gamma}.$$
 (5.34)

We then find that

$$\left(i\frac{\partial}{\partial t} - H(x)\right)G_{+}(x, x_0) = \int \frac{\mathrm{d}E}{2\pi} \,\mathrm{e}^{-\mathrm{i}E\tau} \,\mathrm{i} \sum_{n} \frac{E - E_n}{E - E_n + \mathrm{i}\gamma} \,\Psi_n(x) \,\Psi_n^*(x_0). \tag{5.35}$$

Letting $\gamma \to 0$ and using the closure property (C.27)

$$\sum_{n} \Psi_{n}(x) \, \Psi_{n}^{*}(x_{0}) = \delta^{3}(x - x_{0})$$

and the integral

$$\int \frac{\mathrm{d}E}{2\pi} \,\mathrm{e}^{-\mathrm{i}E\tau} = \delta(\tau) = \delta(t - t_0),$$

we confirm that the retarded part of the Green's function (5.8) satisfies the relation (5.5)

$$\left(i\frac{\partial}{\partial t} - H(x)\right)G_{+}(x, x_0) = i\delta^4(x - x_0). \tag{5.36}$$

5.2.3.2 Electron Propagator

We consider now the zeroth-order single-particle Green's function (5.19)

$$G_0(x, x_0) = \left\langle 0 \left| T[\hat{\psi}(x)\hat{\psi}^{\dagger}(x_0)] \right| 0 \right\rangle, \tag{5.37}$$

where the vacuum and the field operators are expressed in the interaction picture. Then we find that

• the single-particle Green's function is identical to the Feynman electron propagator (4.9) times the imaginary unit i

$$G_0(x, x_0) \equiv iS_F(x, x_0).$$
 (5.38)

The retarded operator can be transformed in analogy with the Lehmann representation above

$$G_{0+}(x,x_0) = \sum_{n} \left\langle 0_{\rm H} \left| \hat{\psi}_{\rm S}(x) \right| n^0 \, \mathrm{e}^{-\mathrm{i}E_n^0(t-t_0)} n^0 \, \left| \hat{\psi}_{\rm S}^{\dagger}(x_0) \right| 0_{\rm H} \right\rangle, \tag{5.39}$$

where $|n^0\rangle$ are eigenstates of the zeroth-order Hamiltonian for the (N+1)-particle system (B.22)

$$H_0|n^0\rangle = E_n^0|n^0\rangle$$

and E_n^0 are the energies relative the vacuum. Performing the time integration yields the Fourier transform

$$G_{0+}(x, x_0, E) = i \sum_{n} \frac{\langle x | n^0 \rangle \langle n^0 | x_0 \rangle}{E - E_n^0 + i \gamma}.$$
 (5.40)

The corresponding advanced function becomes

$$G_{0-}(x,x_0,E) = -i\sum_{n} \frac{\langle x|n^0\rangle\langle n^0|x_0\rangle}{E - E_n^0 - i\gamma}.$$
(5.41)

Both of these results can be expressed by means of a complex integral

$$G_0(x, x_0) = iS_F(x, x_0) = i \int \frac{dE}{2\pi} \frac{\langle x | n^0 \rangle \langle n^0 | x_0 \rangle}{E - E_n^0 + i \gamma_n} e^{-iE(t - t_0)},$$
 (5.42)

where γ_n has the same sign as E_n^0 , i.e., positive for particle states and negative for hole or antiparticle states.

The zeroth-order Green's function or electron propagator can also be expressed in operator form as

$$\hat{G}_0(E) = i\hat{S}_F(E) = \frac{i}{E - H_0 \pm i\gamma}.$$
 (5.43)

5.2.3.3 Two-Particle Green's Function in the Equal-Time Approximation

Setting the initial and final times equal for the two particles, t = t' and $t_0 = t'_0$, the retarded two-particle Green's function (5.20) becomes

$$G_{+}(x, x'; x_{0}, x'_{0}) = \langle 0_{H} | \hat{\psi}_{H}(x) \hat{\psi}_{H}(x') \hat{\psi}_{H}^{\dagger}(x'_{0}) \hat{\psi}_{H}^{\dagger}(x_{0}) | 0_{H} \rangle$$

$$= \langle 0_{H} | (e^{iHt} \hat{\psi}_{S}(x) \hat{\psi}_{S}(x') e^{-iHt})$$

$$\times (e^{iHt_{0}} \hat{\psi}_{S}^{\dagger}(x'_{0}) \hat{\psi}_{S}^{\dagger}(x_{0}) e^{-iHt_{0}}) | 0_{H} \rangle.$$
(5.44)

We introduce a complete set of two-particle states (5.28), which leads to the Lehmann representation

$$G_{+}(x, x'; x_{0}, x'_{0}) = \sum_{n} \left\langle 0_{H} \left| \hat{\psi}_{S}(x) \hat{\psi}_{S}(x') \right| n \right\rangle e^{-iE_{n}(t-t_{0})} \left\langle n \left| \hat{\psi}_{S}^{\dagger}(x'_{0}) \hat{\psi}_{S}^{\dagger}(x_{0}) \right| 0_{H} \right\rangle$$

$$(5.45)$$

with the Fourier transform

$$G_{+}(E; \boldsymbol{x}, \boldsymbol{x}'; \boldsymbol{x}_{0}, \boldsymbol{x}'_{0}) = \sum_{n} \frac{\langle 0_{H} | \hat{\psi}_{S}(\boldsymbol{x}) \, \hat{\psi}_{S}(\boldsymbol{x}') | n \rangle \, \langle n | \hat{\psi}_{S}^{\dagger}(\boldsymbol{x}'_{0}, \hat{\psi}_{S}^{\dagger}(\boldsymbol{x}_{0})) | 0_{H} \rangle}{E - E_{n} \pm i \gamma}$$
(5.46)

with the upper (lower) sign for the retarded (advanced) function. Here, $\langle n | \hat{\psi}_S^{\dagger}(x_0) \rangle$ $\hat{\psi}_S^{\dagger}(x_0') | 0_H \rangle$ represents a two-particle state $\Psi_n(x,x')$ in the Schrödinger picture, which yields the Fourier transform

$$G_{+}(E; x, x'; x_{0}, x'_{0}) = i \sum_{n} \frac{\Psi_{n}(x, x') \, \Psi_{n}^{*}(x_{0}, x'_{0})}{E - E_{n} \pm i \gamma}.$$
 (5.47)

This implies that also in this case the poles of the Green's function represent the exact eigenvalues of the system, relative to the vacuum. Note that this holds in the many-particle case only in the *equal-time approximation*, where there is only a single time coordinate $\tau = t - t_0$.

5.3 Graphical Representation of the Green's Function *

We shall now demonstrate how the expansions of the Green's-functions [(5.19) and (5.21)] can be conveniently represented by means of *Feynman diagrams* [6], discussed in the previous chapter, and we start with the single-particle case.

5.3.1 Single-Particle Green's Function

The zeroth-order Green's function is (with our definition) identical to the Feynman electron propagator times the imaginary unit (5.38) or equal to the contraction (4.9)

$$G_0(x, x_0) = \left\langle 0 \left| T \left[\hat{\psi}(x) \hat{\psi}^{\dagger}(x_0) \right] \right| 0 \right\rangle = \hat{\psi}(x) \hat{\psi}^{\dagger}(x_0), \tag{5.48}$$

which we represent graphically as in Fig. 4.1.

$$G_0(x, x_0) = \int_{x_0}^{x} f(x, x_0) dx$$
 (5.49)

This contains both time orderings, i.e., *j* represents *both particle and hole/ antiparticle states*.

In next order, the numerator of the Green's function (5.16) has the form

$$-\frac{1}{2c^2} \left\langle 0 \right| \iint d^4 x_1 d^4 x_2 T \left[\hat{\psi}(x) \mathcal{H}(x_1) \mathcal{H}(x_2) \hat{\psi}^{\dagger}(x_0) \right] \left| 0 \right\rangle. \tag{5.50}$$

The photon fields have to be contracted, which leads to a two-particle interaction, in analogy with the single-photon interaction $V_{\rm sp}$ (4.44),

$$\mathcal{H}(x_1)\mathcal{H}(x_2) = \nu(x_1, x_2) \tag{5.51}$$

with the Fourier transform with respect to time $v(z; x_1, x_2)$, which we represent graphically as

The vacuum expectation (5.50) can then be illustrated by the following picture

where the vertical lines represent the electron-field operators. The procedure is now to transform the time ordering to normal ordering (see Sect. 2.2), which we can do by means of Wick's theorem (2.34). This leads to a normal-ordered totally uncontracted and all possible normal-ordered single, doubly, ... contracted terms. In the vacuum expectation only fully contracted terms will survive.

We can here distinguish between two cases: <u>either</u> the electron-field operators are connected to each other and disconnected from the interaction <u>or</u> all parts are connected to a single piece. The former case leads to the diagrams

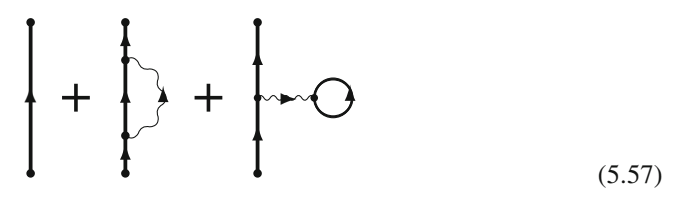
where the disconnected, closed parts represent the closed first-order S-matrix diagrams

The diagrams in (5.54) can then be expressed $G_0S_{cl}^{(1)}$. Connecting all parts of the expression (5.53) leads to the diagrams

(5.56)

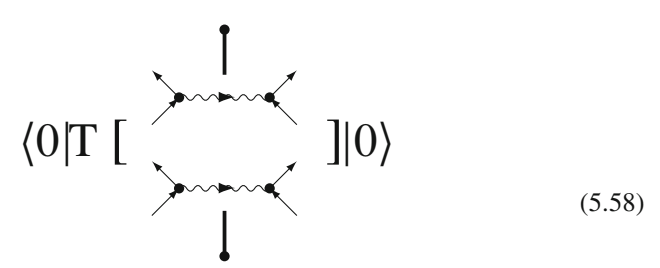
These diagrams are quite analogous to the S-matrix diagrams for vacuum polarization and self-energy, discussed in Sect. 4.6, the only difference being that the Green's-function diagrams contain in- and outgoing electron propagators. We note that all internal lines do represent *electron propagators*, containing particle as well as hole states.

We can now see that the disconnected parts of the diagrams (5.54) are eliminated by the denominator in the definition of the Green's function (5.8). Therefore, we can then represent the Green's function up to first order by connected diagrams only (Fig. 5.57).



We shall now indicate that this holds also in higher orders.

Next, we consider a Green's-function term with two two-particle interactions.



We can here distinguish different cases.

We consider first the case where both interactions are disconnected from the electron-field operators. Leaving out the latter, we then have

This corresponds to the vacuum expectation of the second-order S-matrix and leads to connected diagrams

and to the disconnected diagrams

We denote these diagrams by $S_{\rm cl}^{(2)}=\langle 0|S^{(2)}|0\rangle$. In addition, we have the free electron-field operators, which combine to the zeroth-order Green's function G_0 . Therefore, we can express the corresponding GF diagrams as $G_0S_{\rm cl}^{(2)}$.

Next, we consider the case where one of the interactions in (5.59) is closed by itself, while the remaining part is connected. This leads to disconnected diagrams, where the disconnected part is the closed first order (5.55) and the connected part is identical to the connected first-order diagrams in Fig. 5.56, which we can express the disconnected diagram as $G_{\rm C}^{(1)}S_{\rm cl}^{(1)}$.

Finally, we have the case where all diagram parts are completely connected, shown in Fig. 5.3, which we denote by $G_{\rm C}^{(2)}$.

Going to third order, we find similarly that we can have $G_0 = G^{(0)}$ combined with the closed diagrams $S_{\rm cl}^{(3)}$, $G_{\rm C}^{(1)}$ combined with $S_{\rm cl}^{(2)}$, $G_{\rm C}^{(2)}$ combined with $S_{\rm cl}^{(1)}$ and finally completely connected $G_{\rm C}^{(3)}$ diagrams. This leads to the sequence

$$\begin{cases} G^{(0)} \\ G_{\rm C}^{(1)} + G^{(0)} S_{\rm cl}^{(1)} \\ G_{\rm C}^{(2)} + G_{\rm C}^{(0)} S_{\rm cl}^{(1)} + G^{(0)} S_{\rm cl}^{(2)} \\ G_{\rm C}^{(3)} + G_{\rm C}^{(2)} S_{\rm cl}^{(1)} + G_{\rm C}^{(1)} S_{\rm cl}^{(2)} + G^{(0)} S_{\rm cl}^{(3)} \\ \text{etc..} \end{cases},$$

which summarizes to

$$(G^{(0)} + G_{\rm C}^{(1)} + G_{\rm C}^{(2)} + \cdots)(1 + S_{\rm cl}^{(1)} + S_{\rm cl}^{(2)} + \cdots) = (G_0 + G_{\rm C})(1 + S_{\rm cl}), (5.62)$$

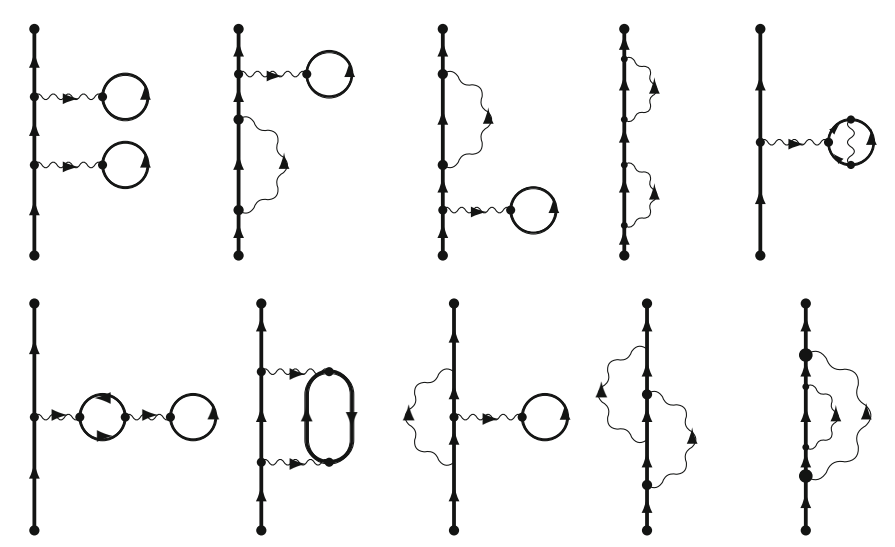


Fig. 5.3 Second-order connected diagrams of the one-body Green's function, assuming a two-body interaction

where $G_{\rm C}$ represents all connected diagrams of the numerator of the GF expression (5.21) and $S_{\rm cl}$ represents all closed S diagrams. But the last factor is the vacuum expectation of the S matrix to all orders

$$\langle 0|S|0\rangle = 1 + S_{cl},\tag{5.63}$$

which implies that this is canceled by the denominator in the definition (5.8). Hence,

• the single-particle Green's function can in the close-shell case be represented by completely connected diagrams

$$iG(x,x_0) = \left[\sum_{n=0}^{\infty} \frac{1}{n!} \left(\frac{-1}{c^2} \right)^n \int \cdots \int d^4 x_1 \cdots d^4 x_{2n} \right.$$

$$\times \left\langle 0T \left[\hat{\psi}(x) \mathcal{H}(x_1, x_2) \cdots \mathcal{H}(x_{2n-1}, x_{2n}) \hat{\psi}^{\dagger}(x_0) \right] 0 \right\rangle \right]_{\text{conn}}.$$
(5.64)

This can also be expressed

$$G(x, x_0) = \langle 0_{\mathrm{H}} | T[\hat{\psi}_{\mathrm{H}}(x)\hat{\psi}_{\mathrm{H}}^{\dagger}(x_0)] | 0_{\mathrm{H}} \rangle_{\mathrm{conn}}.$$
 (5.65)

The connectedness of the Green's function can also be shown in a somewhat different way. If we remove the two electron-fields operators and the denominator from the Green's function expansion (5.19), then we retrieve the vacuum expectation of

the S-matrix (4.3) $\langle 0|S|0\rangle$. Therefore, if the field operators are connected to each other and the interactions among themselves, the result (after including the denominator) is simply the zeroth-order Green's function $iG^{(0)}$. If the field operators are connected to one of the interactions, they form the connected first-order Green's function $iG^{(1)}_{\text{conn}}$ and the remaining interactions again form $\langle 0|S|0\rangle$. Continuing the process leads to

$$G = G^{(0)} + G_{\text{conn}}^{(1)} + G_{\text{conn}}^{(2)} + \cdots,$$
 (5.66)

which proves that the single-particle Green's function is entirely connected.

5.3.1.1 One-Body Interaction

We shall now consider the case when we, in addition to the two-body interaction, have a one-body interaction of potential type

$$\bullet \sim \sim \times \tag{5.67}$$

The graphical representation can then be constructed in the same way as before, and we then find in first order the additional diagrams

The first diagram is unconnected, and the closed part is a part of $\langle 0|S|0\rangle$ and hence this diagram is eliminated by the denominator of (5.19), as before. It is not difficult to show that the single-particle Green's function is represented by connected diagrams only, when we have a mixture of one- and two-body interactions. The additional connected diagrams in second order are shown in Fig. 5.4.

5.3.2 Many-Particle Green's Function

We now turn to the two-particle Green's function (5.21). The zeroth-order Green's function is in analogy with the one-particle function (5.49) represented by

$$G_0(x, x'; x_0, x'_0) = \begin{cases} x \\ x_0 \end{cases} = iS_F(x, x_0) iS_F(x', x'_0)$$

$$x'_0$$
(5.69)

or a product of two Feynman electron propagators.

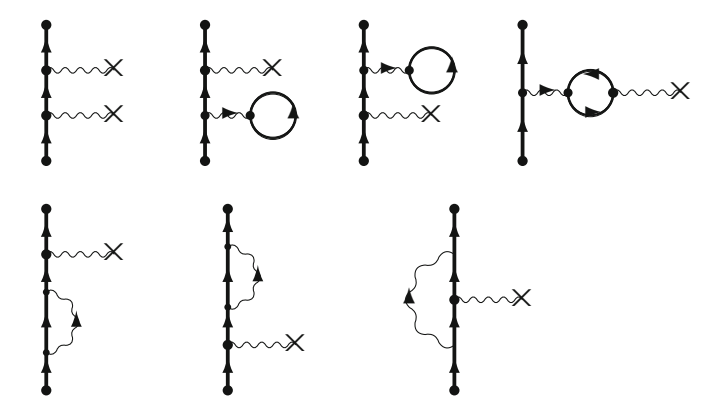
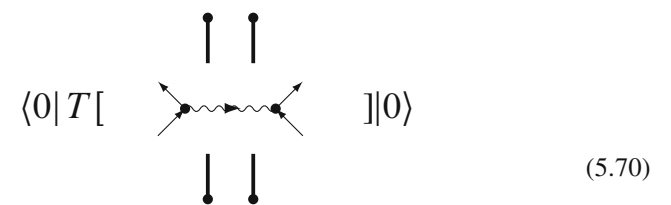


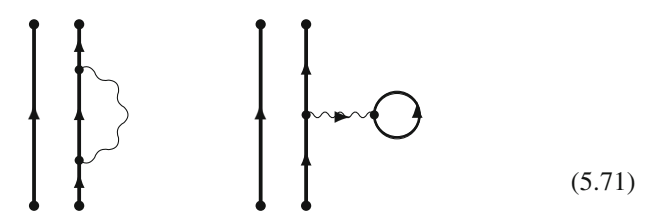
Fig. 5.4 Additional second-order diagrams of the single-particle Green's function – in addition to those in Fig. 5.3 – with a combination of one- and two-body interactions

As mentioned earlier, the (initial and final) times of the two particles in principle can be different, although we shall in most applications assume that they are equal, as will be further discussed in the following.

In first order, we have in analogy with the single-particle case (5.53)



This can lead to disconnected diagrams, composed of the zeroth-order function (5.69) and the closed first-order diagrams (5.55). Another type of disconnected diagrams is the combination of zeroth-order single-particle GF and the connected first-order GF



It should be noted that both parts are here consider as *open* (not closed).³ Finally, we can have an open two-particle diagram

³ Generally, a diagram is considered closed if it has no free lines/propagators, like the diagrams in (5.60) and (5.61), while an open diagram has at least one pair of free lines, like those in Fig. 5.3. An operator or a function represented by a closed/open diagram is said to be closed/open.



In second order, we can have the zeroth-order two-particle Green's function, combined with second-order closed diagrams, $S_{\rm cl}^{(2)}$, and connected first-order diagrams combined with first-order closed diagrams, $S_{\rm cl}^{(1)}$. In addition, we can have disconnected diagrams with two open first-order single-particle diagrams (5.56).

Continuing this process leads formally to the same result as in the single-particle case (5.62) – the diagrams with a disconnected closed part are eliminated by the denominator. Formally, the diagrams can still be disconnected, like (5.71), since there is a disconnected zeroth-order Green's function part. We shall refer to such diagrams as *linked* in analogy with the situation in MBPT (Sect. 2.4). The result is then expressed

$$G(x, x'; x_0, x'_0) = \left[\sum_{n=0}^{\infty} \frac{1}{n!} \left(\frac{-1}{c^2} \right)^n \int d^4 x_1 \cdots \int d^4 x_{2n} \left\langle 0 \left| T \left[\hat{\psi}(x) \hat{\psi}(x') \right. \right. \right. \right. \\ \left. \times v(x_1, x_2) \cdots v(x_{2n-1}, x_{2n}) \, \hat{\psi}^{\dagger}(x'_0) \hat{\psi}^{\dagger}(x_0) \right] 0 \right| \right\rangle \right]_{\text{linked}}, (5.73)$$

a result that can easily be extended to the general many-particle case.

The two-body interactions used here correspond to two contracted interactions of the type (4.4). Uncontracted interactions of this kind cannot contribute to the Green's function, since this is a vacuum expectation. Therefore, the results above can in the single-particle case also be expressed

$$G(x, x_0) = \sum_{n=0}^{\infty} \frac{1}{n!} \left(\frac{-i}{c}\right)^n \int d^4 x_1 \cdots \int d^4 x_n$$

$$\times \left\langle 0 \left| T \left[\hat{\psi}(x) \mathcal{H}(x_1) \cdots \mathcal{H}(x_n) \hat{\psi}^{\dagger}(x_0) \right] \right| 0_{\text{conn}} \right\rangle$$
(5.74)

including even- as well as odd order terms, and similarly in the many-particle case. This can also be expressed

$$G(x, x_0) = \langle 0_{\rm H} | T[\hat{\psi}_{\rm H}(x)\hat{\psi}_{\rm H}^{\dagger}(x_0)] | 0_{\rm H} \rangle_{\rm conn}$$

$$(5.75)$$

and in the two-particle case

$$G(x, x'; x_0, x'_0) = \langle 0_H | T[\hat{\psi}_H(x)\hat{\psi}_H^{\dagger}(x')\hat{\psi}_H(x'_0)\hat{\psi}_H^{\dagger}(x_0)] | 0_H \rangle_{linked}.$$
 (5.76)

The linked character of the Green's function can also in the two-particle case be shown as we did at the end on the single-particle section. If all interactions of the expansion (5.21) are connected among themselves, they form the vacuum expectation value of the S-matrix, canceling the denominator, and the electron-field operators form the two-body zeroth-order Green's function $G_2^{(0)}$. If one pair of field operators are internally connected, then the remaining part is identical to the single-particle Green's function G_1 , which has been shown to be connected. The result $G_1^{(0)}G_1$ is disconnected but since both parts are open, this is linked with the convention we use. If one pair of field operators are connected to some of the interactions and the other pair to the remaining ones, the result is G_1G_1 , which is also disconnected but linked. Finally, all field operators can be connected to the interactions, which leads to the connected two-particle Green's function $G_{2,\text{conn}}$. The remaining interactions form $\langle 0|S|0\rangle$, canceling the denominator, and the result becomes $G_{2,\text{conn}}$. In summary, the two-particle Green's function becomes

$$G_2 = G_2^{(0)} + G_{1,\text{conn}} G_{1,\text{conn}} + G_{2,\text{conn}},$$
 (5.77)

which can be disconnected but linked. This argument can easily be generalized, implying that

• the many-particle Green's function in the closed-shell case is linked.

5.3.3 Self-Energy: Dyson Equation

All diagrams of the one-particle Green's function can be expressed in the form

$$G(x, x_0) = G(x, x_0) + \iint d^4 dx_1 d^4 dx_2 G_0(x, x_1) (-i) \Sigma(x_1, x_2) G_0(x_2, x_0),$$
(5.78)

where $\Sigma(x_2, x_1)$ represents the self-energy. This can be represented as shown in Fig. 5.5, i.e., as the zeroth-order Green's function plus all self-energy diagrams.

Some of the second-order self-energy diagrams in Figs. 5.3 and 5.4 have the form of two first-order diagrams, connected by a zeroth-order GF. All diagrams of that kind can be represented as a sequence of *proper self-energy diagrams*, Σ^* , which have the property that they cannot be separated into lower-order diagrams by cutting a single line. This leads to the expansion of the total self-energy shown in Fig. 5.6, where the crossed box represents the proper self-energy. The single-particle Green's function can then be represented as shown in Fig. 5.7, which corresponds to the *Dyson equation for the single-particle Green's function*.

$$G(x, x_0) = G_0(x, x_0) + \iint d^4x_1 d^4x_2 G_0(x, x_2) (-i) \Sigma^*(x_2, x_1) G(x_1, x_0).$$
(5.79)

Fig. 5.5 The single-particle Green's function expressed in terms of the self-energy

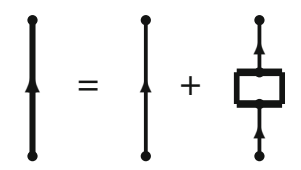


Fig. 5.6 Expansion of the total self-energy in terms of proper self-energies. The *crossed box* represents the proper self-energy Σ^*

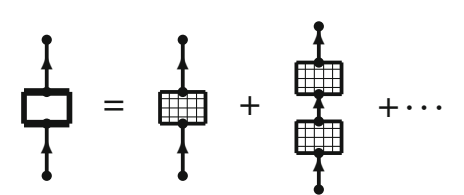
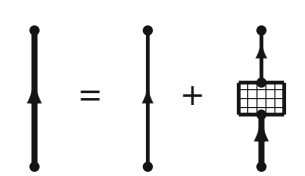


Fig. 5.7 Graphical representation of the Dyson equation for the single-particle Green's function (5.79), using the proper self-energy Σ^*



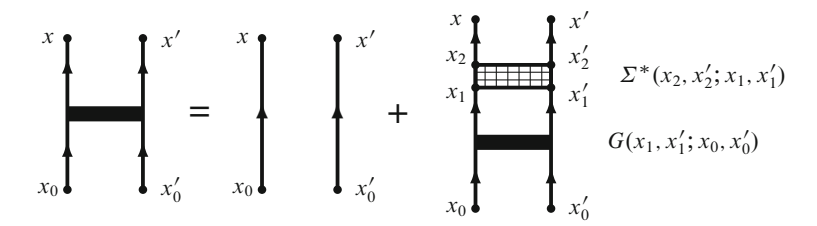


Fig. 5.8 Graphical representation of the Dyson equation for the two-particle Green's function (5.80). The *crossed box* represents the proper two-particle self-energy

Similarly, the Dyson equation for two-particle Green's function becomes

$$G(x, x'; x_0, x'_0) = G_0(x, x'; x_0, x'_0) + \iiint d^4 x_1 d^4 x_2 d^4 x'_1 d^4 x'_2$$

$$\times G_0(x, x'; x_2, x'_2) (-i) \Sigma^*(x_2, x'_2; x_1, x'_1)$$

$$\times G(x_1, x'_1; x_0, x'_0). \tag{5.80}$$

This equation is illustrated in Fig. 5.8, where the crossed box represents the proper two-particle self-energy.

	$4p_{1/2}$	$4p_{3/2}$	Reference
Theory	19	-13	Salomonson [11]
Theory	22	-18	Avgoustoglou [3]
Theory	49	-18	Dzuba [3]
Expt'l	24.55	-19.73	Petrunin [10]
Expt'l	18.4		Walter [13]
Expt'l	17.5		Nadeau [9]

Table 5.1 Electron affinity of Ca atom (in meV)

5.3.4 Numerical Illustration

Here, we shall illustrate the application of the Green's-function technique for manybody calculation by the electron affinity of the calcium atom (Table 5.1). The negative calcium ion is a very delicate system, with a very feeble binding energy, and it has been quite difficult to determine this quantity experimentally as well as theoretically. It is only recently that it has been possible to obtain reasonable agreement.

The calculation of Salomonson et al. is performed by means of the Green's-function method, that of Dzuba et al. by many-body perturbation theory and that of Avgoustoglou by all-order pair-correlation method.

5.4 Field-Theoretical Green's Function: Open-Shell Case *

In this section, we indicate how the Green's-function concept could be extended to the open-shell case, when the model states are separated from the vacuum state. It is recommended that Chap. 6 is first studied, where the treatment is more akin to the normal situation in MBPT, discussed in Sect. 2.3. We leave out most details here and refer to the treatment of the covariant evolution operator and the Green's operator, which is quite equivalent. In this section, we +in particular look into the special approach due to Shabaev [12].

5.4.1 Definition of the Open-Shell Green's Function

In the general open-shell case, singularities of the Green's function can appear also for connected diagrams, as in the covariant-evolution operator (see below). If we consider a sequence of ladder diagrams of single-photon exchange, V, as discussed in the next chapter (Fig. 6.3), considering only particle states (no-pair), the Feynman amplitude for the Green's function is the same as for the covariant evolution operator (6.20) with no model-space states,

$$\mathcal{M} = 1 + \Gamma_O(E_0) V(E_0) + \Gamma_O(E_0) V(E_0) \Gamma_O(E_0) V(E_0) + \cdots, \quad (5.81)$$

where

$$\Gamma_{Q}(E_{0}) = \frac{Q}{E_{0} - H_{0} + i\gamma} = \frac{|rs\rangle \langle rs|}{E_{0} - \varepsilon_{r} - \varepsilon_{s} + i\gamma}$$

is the reduced resolvent (2.65) and E_0 is the energy parameter (of the Fourier transform) of the Green's function. The GF becomes singular, when there is an intermediate state $|rs\rangle$ of energy E_0 . Including the residuals after removing the singularities (model-space contributions) leads as shown below (6.117) to a shift of the energy parameter, $E_0 \rightarrow E = E_0 + \Delta E$,

$$\mathcal{M} = 1 + \Gamma_{O}(E) V(E) + \Gamma_{O}(E) V(E) \Gamma_{O}(E) V(E) + \cdots$$
 (5.82)

This is a Brillouin-Wigner perturbation expansion, and it can be summed to

$$\mathcal{M} = \frac{1}{E - H + i\gamma} = \frac{|n\rangle \langle n|}{E - E_n + i\gamma}$$
 (5.83)

with $H = H_0 + V(E)$ and $|n\rangle$ represents the exact eigenstates of the system with the energy E_n . This agrees with the Fourier transform of the GF derived above (5.47), demonstrating that the transform has poles at the exact energies. Consequently, this holds also in the open-shell case.

The Green's-function technique yields information only about the energy of the system. This is in contrast to the *Green's-operator formalism*, to be treated in the next chapter, which can give information also about the wave function or state vector of the system under study.

5.4.2 Two-Times Green's Function of Shabaev

The use of the Green's-function technique for atomic calculations has been further developed by Shabaev et al. [12] under the name of the "Two-times Green's function" (which is equivalent to the equal-time approximation, discussed above). This technique is also applicable to degenerate and quasi-degenerate energy states, and we shall outline its principles here.

We return to the *extended-model* concept, discussed in Sect. 2.3. Given are a number of eigenstates (target states) of the many-body Hamiltonian

$$H|\Psi^{\alpha}\rangle = E^{\alpha}|\Psi^{\alpha}\rangle \quad (\alpha = 1 \cdots d).$$
 (5.84)

The corresponding model states are in intermediate normalization the projections on the model space

$$|\Psi_0^{\alpha}\rangle = P|\Psi^{\alpha}\rangle \quad (\alpha = 1 \cdots d).$$
 (5.85)

The model states are generally *nonorthogonal*, and following Shabaev we introduce a "dual set" $\{|\widetilde{\Psi}_0^{\beta}\}\$, defined by

$$\left|\widetilde{\Psi}_{0}^{\beta}\right\rangle\langle\Psi_{0}^{\alpha}| = \left|\Psi_{0}^{\beta}\right\rangle\left\langle\widetilde{\Psi}_{0}^{\alpha}\right| = \delta_{\alpha,\beta}.\tag{5.86}$$

Then the standard projection operator becomes

$$P = \sum_{\beta \in D} \left| \widetilde{\Psi}_0^{\beta} \right\rangle \left\langle \Psi_0^{\beta} \right| = \sum_{\beta \in D} \left| \Psi_0^{\beta} \right\rangle \left\langle \widetilde{\Psi}_0^{\beta} \right| \tag{5.87}$$

with the summation performed over the model space D. We also define an alternative projection operator as

$$\mathcal{P} = \sum_{\beta \in D} \left| \Psi_0^{\beta} \right\rangle \left\langle \Psi_0^{\beta} \right| \qquad \mathcal{P}^{-1} = \sum_{\beta} \left| \widetilde{\Psi}_0^{\beta} \right\rangle \left\langle \widetilde{\Psi}_0^{\beta} \right|. \tag{5.88}$$

Then

$$\mathcal{P}\left|\widetilde{\Psi}_{0}^{\alpha}\right\rangle = \left|\Psi_{0}^{\alpha}\right\rangle \quad \text{and} \quad \mathcal{P}^{-1}\left|\Psi_{0}^{\alpha}\right\rangle = \left|\widetilde{\Psi}_{0}^{\alpha}\right\rangle.$$
 (5.89)

The Fourier transform of the retarded Green's function is generally (5.33)

$$G_{+}(E; x, x_{0}) = i \sum_{n} \frac{\langle x | \Psi_{n} \rangle \langle \Psi_{n} | x_{0} \rangle}{E - E_{n} + i \gamma}, \tag{5.90}$$

where we let x, x_0 represent the space coordinates of all outgoing/incoming particles. It then follows that

$$\oint_{\Gamma_n} dE G_+(E; \mathbf{x}, \mathbf{x}_0) = -2\pi \langle \mathbf{x} | \Psi_n \rangle \langle \Psi_n | \mathbf{x}_0 \rangle$$
 (5.91)

and

$$\oint_{\Gamma_n} E \, \mathrm{d}E \, G_+(E; \mathbf{x}, \mathbf{x}_0) = -2\pi \, \langle \mathbf{x} | \Psi_n \rangle \, E_n \, \langle \Psi_n | \mathbf{x}_0 \rangle, \tag{5.92}$$

where Γ_n is a closed contour, encircled in the positive direction and containing the single target energy E_n and no other pole. (This holds if all poles are distinct. In the case of degeneracy, we can assume that an artificial interaction is introduced that lifts the degeneracy, an interaction that finally is adiabatically switched off.) This yields the relation [12, Eq. (44)]

$$E_n = \frac{\oint_{\Gamma_n} E \, dE \, G_+(E; \mathbf{x}, \mathbf{x}_0)}{\oint_{\Gamma_n} dE \, G_+(E; \mathbf{x}, \mathbf{x}_0)}.$$
 (5.93)

Following Shabaev, we also introduce a "projected" Green's function by

$$g_{+}(E; \boldsymbol{x}, \boldsymbol{x}_{0}) = i \sum_{\beta \in D} \frac{\left\langle \boldsymbol{x} \middle| \Psi_{0}^{\beta} \middle| \left\langle \Psi_{0}^{\beta} \middle| \boldsymbol{x}_{0} \right\rangle}{E - E^{\beta} + i \gamma}, \tag{5.94}$$

which is the coordinate representation (see Appendix C.3) of the corresponding operator

$$\hat{g}_{+}(E) = i \sum_{\beta \in D} \frac{\left| \Psi_{0}^{\beta} \right\rangle \left\langle \Psi_{0}^{\beta} \right|}{E - E^{\beta} + i\gamma} = i \sum_{\beta \in D} \frac{P \left| \Psi^{\beta} \right\rangle \left\langle \Psi^{\beta} \right| P}{E - E^{\beta} + i\gamma}$$
(5.95)

operating only within the model space.

The effective Hamiltonian (2.54) is defined by

$$H_{\rm eff}|\Psi_0^{\alpha}\rangle = E^{\alpha}|\Psi_0^{\alpha}\rangle$$

and we can then express this operator as

$$H_{\text{eff}} = \sum_{\beta \in D} \left| \Psi_0^{\beta} \right\rangle E^{\beta} \left\langle \widetilde{\Psi}_0^{\beta} \right| = \mathcal{H}_{\text{eff}} \mathcal{P}^{-1}, \tag{5.96}$$

where

$$\mathcal{H}_{\text{eff}} = \sum_{\beta \in \mathcal{D}} = \left| \Psi_0^{\beta} \right\rangle E^{\beta} \left\langle \Psi_0^{\beta} \right|. \tag{5.97}$$

From the definition (5.94), it follows that

$$\mathcal{H}_{\text{eff}} = -\frac{1}{2\pi} \oint E \, dE \, g(E), \tag{5.98}$$

where the integration contour contains the energies all target states. As before, we assume that the poles are distinct.

Expanding the effective Hamiltonian (5.96) order-by-order leads to

$$H_{\text{eff}} = \mathcal{H}_{\text{eff}}^{(0)} + \mathcal{H}_{\text{eff}}^{(1)} - \mathcal{H}_{\text{eff}}^{(0)} \mathcal{P}^{(1)} + \cdots$$
 (5.99)

The first-order operator \mathcal{H}_{eff} becomes

$$\mathcal{H}_{\text{eff}}^{(1)} = -\frac{1}{2\pi} \oint E \, dE \, g_+^{(0)}(E), \tag{5.100}$$

where

$$g_{+}^{(0)}(E; \boldsymbol{x}, \boldsymbol{x}_{0}) = i \sum_{\beta \in D} \frac{\left\langle \boldsymbol{x} \middle| \Psi_{0}^{\beta} \middle\rangle \left\langle \Psi_{0}^{\beta} \middle| \boldsymbol{x}_{0} \middle\rangle}{E - E^{\beta} + i \gamma}.$$
 (5.101)

The effective Hamiltonian above is *nonhermitian*, as in the MBPT treatment in Sect. 2.3. It can also be given a hermitian form [12], but we shall maintain the nonhermitian form here, since it makes the formalism simpler and the analogy with the later treatments more transparent.

5.4.3 Single-Photon Exchange

We shall now apply the two-times Greens function above to the case of single-photon exchange between the electrons, discussed above (Fig. 5.2). We shall evaluate the contribution to the effective Hamiltonian in the general quasi-degenerate case. In the equal-time approximation, the (first-order) Green's function (5.25) is given by

$$G^{(1)}(x, x', x_0, x'_0) = \mathcal{M}_{sp}^{(1)}(x, x'; x_0, x'_0) e^{-it(\omega_3 + \omega_4)} e^{it_0(\omega_1 + \omega_2)}$$
(5.102)

and the first-order Feynman amplitude is given by (5.23)

$$\mathcal{M}_{\rm sp}^{(1)}(\mathbf{x}, \mathbf{x}'; \mathbf{x}_0, \mathbf{x}'_0) = -i \iint \frac{\mathrm{d}\omega_3}{2\pi} \frac{\mathrm{d}\omega_4}{2\pi} \iint \frac{\mathrm{d}\omega_1}{2\pi} \frac{\mathrm{d}\omega_2}{2\pi} S_{\rm F}(\omega_3; \mathbf{x}, \mathbf{x}_1)$$

$$\times S_{\rm F}(\omega_4; \mathbf{x}', \mathbf{x}_2) I(\omega_1 - \omega_3; \mathbf{x}_2, \mathbf{x}_1) S_{\rm F}(\omega_1; \mathbf{x}_1, \mathbf{x}_0)$$

$$\times S_{\rm F}(\omega_2; \mathbf{x}_2, \mathbf{x}'_0) 2\pi \Delta_{2\gamma}(\omega_1 + \omega_2 - \omega_3 - \omega_4), \quad (5.103)$$

after integrations over z.

The Fourier transform of the Green's function with respect to t and t_0 is

$$G^{(1)}(E',E) = \iint \frac{\mathrm{d}t}{2\pi} \, \frac{\mathrm{d}t_0}{2\pi} \, \mathrm{e}^{\mathrm{i}E't} \, \mathrm{e}^{\mathrm{i}Et_0} \, G^{(1)}(x,x',x_0,x'_0)$$

= $\Delta_{\gamma}(E'-\omega_3-\omega_4) \, \Delta_{\gamma}(E-\omega_1-\omega_2) \, \mathcal{M}_{\mathrm{sp}}^{(1)}(x,x';x_0,x'_0)$ (5.104)

or

$$G^{(1)}(E',E) = -i \iint \frac{d\omega_3}{2\pi} \frac{d\omega_1}{2\pi} S_F(\omega_3; \mathbf{x}, \mathbf{x}_1) S_F(E' - \omega_3; \mathbf{x}', \mathbf{x}_2) \times I(\omega_1 - \omega_3; \mathbf{x}_2, \mathbf{x}_1) S_F(\omega_1; \mathbf{x}_1, \mathbf{x}_0) S_F(E - \omega_1; \mathbf{x}_2, \mathbf{x}'_0) \times 2\pi \Delta_{2\nu}(E' - E),$$
(5.105)

after integrations over ω_2 , ω_4 . With the expression for the electron propagator (4.12), the matrix element of the Green's function becomes

$$\langle rs|G^{(1)}(E',E)|tu\rangle = \left\langle rs \left| \iint \frac{\mathrm{d}\omega_3}{2\pi} \frac{\mathrm{d}\omega_1}{2\pi} \frac{1}{\omega_3 - \varepsilon_r + \mathrm{i}\gamma_u} \frac{1}{E' - \omega_3 - \varepsilon_s + \mathrm{i}\gamma_s} \right. \right.$$

$$\times \left. I(\omega_1 - \omega_3) \frac{1}{\omega_1 - \varepsilon_t + \mathrm{i}\gamma_t} \frac{1}{E - \omega_1 - \varepsilon_u + \mathrm{i}\gamma_u} \right| tu\rangle$$

$$\times \left. 2\pi\Delta_{2\nu}(E' - E). \tag{5.106}$$

With $|rs\rangle$ and $|tu\rangle$ in the model space, this is the same as the matrix element of the projected Green's function (5.94), considering only poles corresponding to the relevant target states. We define the single-energy Fourier transform by

$$G(E) = \int \frac{dE'}{2\pi} G(E', E),$$
 (5.107)

which yields

$$\langle rs|G^{(1)}(E)|tu\rangle = -i \left\langle rs \left| \iint \frac{d\omega_3}{2\pi} \frac{d\omega_1}{2\pi} I(\omega_1 - \omega_3) \right| \right. \\ \left. \times \frac{1}{E - \varepsilon_r - \varepsilon_s} \left[\frac{1}{\omega_3 - \varepsilon_r + i\gamma_r} + \frac{1}{E - \omega_3 - \varepsilon_s + i\gamma_s} \right] \right. \\ \left. \times \frac{1}{E - \varepsilon_t - \varepsilon_u} \left[\frac{1}{\omega_1 - \varepsilon_t + i\gamma_t} + \frac{1}{E - \omega_1 - \varepsilon_u + i\gamma_u} \right] \right| tu \right\rangle.$$

$$(5.108)$$

We assume here that the initial and final states lie in the model space with all single-particle states involved being particle states. The relevant poles are here

$$E = \varepsilon_t + \varepsilon_u = E_{\text{in}}$$
 and $E = \varepsilon_r + \varepsilon_s = E_{\text{out}}$.

The contribution of the first pole is

$$\frac{-\mathrm{i}}{2\pi\mathrm{i}} \left\langle rs \left| \iint \frac{\mathrm{d}\omega_{3}}{2\pi} \frac{\mathrm{d}\omega_{1}}{2\pi} I(\omega_{1} - \omega_{3}) \right. \right. \\
\times \frac{E_{\mathrm{in}}}{E_{\mathrm{in}} - E_{\mathrm{out}}} \left[\frac{1}{\omega_{3} - \varepsilon_{r} + \mathrm{i}\gamma} + \frac{1}{E_{\mathrm{in}} - \omega_{3} - \varepsilon_{s} + \mathrm{i}\gamma} \right] \\
\times \left[\frac{1}{\omega_{1} - \varepsilon_{t} + \mathrm{i}\gamma} + \frac{1}{E_{\mathrm{in}} - \omega_{1} - \varepsilon_{u} + \mathrm{i}\gamma} \right] \left| tu \right\rangle. \tag{5.109}$$

The last bracket yields $-2\pi i \Delta_{\gamma}(\omega_1 - \varepsilon_t)$, and integration over ω_1 yields

$$i \left\langle rs \left| \int \omega_3 \ I(\varepsilon_t - \omega_3) \frac{E_{\rm in}}{E_{\rm in} - E_{\rm out}} \left[\frac{1}{\omega_3 - \varepsilon_r + i\gamma} + \frac{1}{E_{\rm in} - \omega_3 - \varepsilon_s + i\gamma} \right] \right| tu \right\rangle. \tag{5.110}$$

Similarly, the other pole yields

$$i \left\langle rs \left| \int \frac{d\omega_{1}}{2\pi} I(\omega_{1} - \varepsilon_{r}) \right. \right. \\ \left. \times \frac{E_{\text{out}}}{E_{\text{in}} - E_{\text{out}}} \left[\frac{1}{\omega_{1} - \varepsilon_{t} + i\gamma} + \frac{1}{E_{\text{out}} - \omega_{1} - \varepsilon_{u} + i\gamma} \right] \left| tu \right\rangle. \quad (5.111)$$

The matrix element of $\mathcal{P}^{(1)}$ is similar with $E_{\rm in}$ and $E_{\rm out}$ in the numerator removed. The matrix element of $\mathcal{H}^{(0)}_{\rm eff}\mathcal{P}^{(1)}$ is obtained by multiplying by $E_{\rm out}$, and the first-order contribution then becomes

$$\left\langle rs \left| H_{\text{eff}}^{(1)} \right| tu \right\rangle = i \left\langle rs \left| \int \frac{d\omega_3}{2\pi} I(\varepsilon_t - \omega_3) \right| \times \left[\frac{1}{\omega_3 - \varepsilon_r + i\gamma} + \frac{1}{E_{\text{in}} - \omega_3 - \varepsilon_s + i\gamma} \right] \right| tu \right\rangle. \tag{5.112}$$

The photon interaction is in the Feynman gauge given by (4.46)

$$I(q; \mathbf{x}_1, \mathbf{x}_2) = \int \frac{2c^2 \kappa \, d\kappa \, f^F(\kappa; \mathbf{x}_1, \mathbf{x}_2)}{q^2 - c^2 \kappa^2 + i\eta}$$
 (5.113)

with f^F given by (4.55). This gives

$$I(\varepsilon_t - \omega_3) = \int \frac{2c^2\kappa \,\mathrm{d}\kappa \,f^F(\kappa; x_1, x_2)}{(\varepsilon_t - \omega_3)^2 - c^2\kappa^2 + \mathrm{i}\eta}$$
 (5.114)

with the poles at $\omega_3 = \varepsilon_t \pm (-i\eta)$. Integrating the relation (5.112) over ω_3 then yields

$$\langle rs|H_{\text{eff}}^{(1)}|tu\rangle = \left\langle rs\left|\int c\,\mathrm{d}\kappa\ f^F\left[\frac{1}{\varepsilon_t - \varepsilon_r - (\kappa - \mathrm{i}\eta)} + \frac{1}{\varepsilon_u - \varepsilon_s - (\kappa - \mathrm{i}\eta)}\right]\right|tu\right\rangle. \tag{5.115}$$

This agrees with the result obtained with the covariant evolution operator (CEO) method in the next chapter (6.16). The CEO result is more general, since it is valid also when the initial and/or final states lie in the complementary \mathcal{Q} space, in which case the result contributes to the wave function or wave operator.

In contrast to the S-matrix formulation, the Green's-function method is applicable also when the initial and final states have different energies, which makes it possible to evaluate the effective Hamiltonian in the case of an extended model space and to handle the quasi-degenerate case.

The two-times Green's function has in recent years been successfully applied to numerous highly charged ionic systems by Shabaev, Artemyev et al. of the St. Petersburg group for calculating two-photon radiative effects, fine structure separations, and g-factors of hydrogenic systems [1,2,14,15]. Some numerical results are given in Chap. 7.

References 117

References

Artemyev, A.N., Beier, T., Plunien, G., Shabaev, V.M., Soff, G., Yerokhin, V.A.: Vacuum-polarization screening corrections to the energy levels of heliumlike ions. Phys. Rev. A 62, 022,116.1–8 (2000)

- 2. Artemyev, A.N., Shabaev, V.M., Yerokhin, V.A., Plunien, G., Soff, G.: *QED calculations of the n=1 and n=2 energy levels in He-like ions*. Phys. Rev. A **71**, 062,104 (2005)
- 3. Avgoustoglou, E.N., Beck, D.R.: *All-order relativistic many-body calculations for the electron affinities of Ca*⁻, *Sr*⁻, *Ba*⁻, *and Yb*⁻ *negative ions*. Phys. Rev. A **55**, 4143–49 (1997)
- 4. Bjorken, J.D., Drell, S.D.: *Relativistic Quantum Mechanics*. Mc-Graw-Hill Pbl. Co, N.Y. (1964)
- Fetter, A.L., Walecka, J.D.: The Quantum Mechanics of Many-Body Systems. McGraw-Hill, N.Y. (1971)
- 6. Feynman, R.P.: *The Theory of Positrons*. Phys. Rev. **76**, 749–59 (1949)
- 7. Itzykson, C., Zuber, J.B.: Quantum Field Theory. McGraw-Hill (1980)
- 8. Mahan, G.D.: Many-particle Physics, second edition. Springer Verlag, Heidelberg (1990)
- 9. Nadeau, M.J., Zhao, X.L., Garvin, M.A., Litherland, A.E.: Ca negative-ion binding energy. Phys. Rev. A 46, R3588–90 (1992)
- Petrunin, V.V., Andersen, H.H., Balling, P., Andersen, T.: Structural Properties of the Negative Calcium Ion: Binding Energies and Fine-Structure Splitting. Phys. Rev. Lett. 76, 744 (1996)
- 11. Salomonson, S., Warston, H., Lindgren, I.: Many-Body Calculations of the Electron Affinity for Ca and Sr. Phys. Rev. Lett. 76, 3092–95 (1996)
- 12. Shabaev, V.M.: Two-times Green's function method in quantum electrodynamics of high-Z few-electron atoms. Physics Reports 356, 119–228 (2002)
- 13. Walter, C., Peterson, J.: Shape resonance in Ca⁻ photodetachment and the electron affinity of Ca(¹S). Phys. Rev. Lett. **68**, 2281–84 (1992)
- 14. Yerokhin, V.A., Artemyev, A.N., Beier, T., Plunien, G., Shabaev, V.M., Soff, G.: Two-electron self-energy corrections to the $2p_{1/2}-2s$ transition energy in Li-like ions. Phys. Rev. A **60**, 3522–40 (1999)
- Yerokhin, V.A., Artemyev, A.N., Shabaev, V.M., Sysak, M.M., Zherebtsov, O.M., Soff, G.: Evaluation of the two-photon exchange graphs for the 2p_{1/2} - 2s transition in Li-like Ions. Phys. Rev. A 64, 032,109.1-15 (2001)

Chapter 6 Covariant Evolution Operator and Green's Operator

The third method we shall consider for numerical QED calculation on bound states is the *covariant-evolution-operator* (*CEO*) *method*, developed during the last decade by the Gothenburg group [9]. This procedure is based upon the nonrelativistic time-evolution operator, discussed in Chap. 3, but it is made covariant in order to be applicable in relativistic calculations. Later, we shall demonstrate that this procedure forms a convenient basis for a *covariant relativistic many-body perturbation procedure*, including QED as well as correlational effects, which for two-electron systems is fully compatible with the *Bethe–Salpeter equation*. This question will be the main topic of the rest of the book.

6.1 Definition of the Covariant Evolution Operator

In the standard time-evolution operator (3.6), $U(t,t_0)$, time is assumed to evolve only *forwards* in the positive direction, which implies that $t \ge t_0$. Internally, time may run also *backwards* in the negative direction, which in the Feynman/Stückelberg interpretation [6, 15] represents the propagation of *hole or antiparticle states* with negative energy. However, all internal times (t_i) are limited to the interval $t_i \in [t,t_0]$.

In the S-matrix (4.2), the initial and final times are $t_0 = -\infty$ and $t = +\infty$, respectively, which implies that the internal integrations do run over <u>all times</u>, making the concept *Lorentz covariant*.¹

In order to make the time-evolution operator covariant also for *finite* times, it has to be modified. This leads to what is referred to as the *covariant evolution operator* (CEO), introduced by Lindgren, Salomonson, and coworkers in early 2000s [7–11].

The CEO is, as well as the S-matrix and the Green's function, *field-theoretical concepts*, and the perturbative expansions of these objects are quite similar. The integrations are performed over all times, and therefore, these objects are normally represented by *Feynman diagrams* instead of time-ordered *Goldstone diagrams*, discussed earlier (Sect. 2.4).

¹ See footnote in the Introduction.

The evolution operator contains generally (quasi)singularities, when it is unlinked or when an intermediate state lies in the model space. Later in this chapter, we see how these singularities can be removed for the CEO, leading to what we refer to as the *Green's operator*, since it is quite analogous to the Green's *function*, which is also free of singularities.

As mentioned earlier, the covariant perturbation expansion we shall formulate here leads for two-particle systems ultimately to the full Bethe-Salpeter (BS) equation [10]. In principle, the BS equation has separate time variables for the individual particles, which makes it manifestly covariant. This is also the case for the CEO as well as for the Green's function. In most applications, however, times are equalized, so that the objects depend only on a single time, which is known as the equal-time approximation. This makes the procedure in line with the standard quantum-mechanical picture, where the wave function has a single time variable, $\Psi(t, x_1, x_2 \cdots)$, but the covariance is then partly lost. Here, we shall mainly work with this approximation in order to be able to combine the procedure with the standard many-body perturbation theory.

As a first illustration, we consider the single-photon exchange with the standard evolution operator (Fig. 6.1, left), the Green's function (middle), and the CEO (right). In the standard evolution operator only *particle states* (positive-energy states) are involved in the lines in and out. Therefore, this operator is NOT Lorentz covariant. In the Green's function, there are electron propagators on the free lines, involving *particle as well as hole states* (positive- and negative-energy states), and the internal times can flow in both directions between $-\infty$ and $+\infty$, which makes the concept covariant. In the CEO electron propagators are inserted on the free lines of the standard evolution operator with integration over the space coordinates, making it covariant. This implies that we attach a *density operator* [3] to the free lines

$$\hat{\rho}(x) = \hat{\psi}^{\dagger}(x)\hat{\psi}(x) \tag{6.1}$$

with integration over the space coordinates. We can also see the CEO as the Green's function, with electron-field operators attached to the free ends.

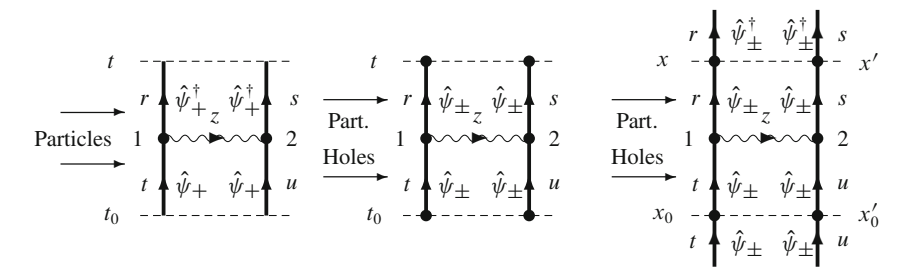
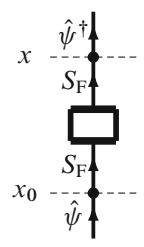


Fig. 6.1 Comparison between the standard evolution operator, the Green's function, and the covariant evolution operator for single-photon exchange in the equal-time approximation

• We generally define the *Covariant Evolution Operator* (CEO) in the single-particle case by the one-body operator²

$$U_{\text{Cov}}^{1}(t,t_{0}) = \iint d^{3}x d^{3}x_{0} \hat{\psi}^{\dagger}(x) \langle 0_{H} | T[\hat{\psi}_{H}(x)\hat{\psi}_{H}^{\dagger}(x_{0})] | 0_{H} \rangle \hat{\psi}(x_{0}).$$
 (6.2)

We use here the same vacuum expectation in the Heisenberg representation as in the definition of the Green's function (5.8) with two additional electron-field operators, $\hat{\psi}^{\dagger}(x)$ and $\hat{\psi}(x_0)$, with space integrations over x, x_0 . In contrast to the Green's function, we shall assume here that the number of photons does not need to be conserved. When this number <u>is</u> conserved, the vacuum expectation is a number and represents the corresponding Green's function. The space integration makes the electron-field operators attached to this function, as illustrated in the figure below (c.f. Fig. 5.1, left).



• In analogy with the expression (5.18) for the Green's function, we can also express the covariant evolution operator as

$$U_{\text{Cov}}^{1}(t, t_{0}) = \iint d^{3}x \, d^{3}x_{0} \, \hat{\rho}(x) \, U^{1}(\infty, -\infty) \, \hat{\rho}(x_{0}),$$
(6.3)

where the density operators are connected to the standard (one-body) evolution operator or S-matrix.

• In expanding the S-matrix [see (5.16)], we obtain

$$U_{\text{Cov}}^{1}(t,t_{0}) = \sum_{n=0}^{\infty} \frac{1}{n!} \iint d^{3}x \, d^{3}x_{0} \left(\frac{-\mathrm{i}}{c}\right)^{n} \int d^{4}x_{1} \cdots \int d^{4}x_{n}$$
$$\times T \left[\hat{\rho}(x) \mathcal{H}(x_{1}) \cdots \mathcal{H}(x_{n}) \, \hat{\rho}(x_{0})\right]_{1} e^{-\gamma(|t_{1}|+|t_{2}|\cdots)}, \tag{6.4}$$

where the operators are connected to form a one-body operator.

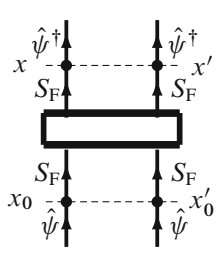
² An "*n-body operator*" is an operator with *n* pairs of creation/absorption operators (for particles), while an "*m-particle*" function or operator is an object of *m* particles outside our vacuum. In principle, *n* can take any value $n \le m$, although we shall normally assume that n = m.

• Similarly, the two-particle CEO becomes – in analogy with the corresponding Green's function (5.21) and Fig. 5.1 (right)

$$U_{\text{Cov}}^{2}(t, t'; t_{0}, t'_{0}) = \sum_{n=0}^{\infty} \frac{1}{n!} \iiint d^{3}x \, d^{3}x' d^{3}x_{0} \, d^{3}x'_{0} \left(\frac{-i}{c}\right)^{n}$$

$$\times \int d^{4}x_{1} \cdots \int d^{4}x_{n} \, T \left[\hat{\rho}(x)\hat{\rho}(x') \, \mathcal{H}(x_{1}) \cdots \mathcal{H}(x_{n})\right]$$

$$\times \hat{\rho}(x'_{0})\hat{\rho}(x_{0}) \Big|_{2} e^{-\gamma(|t_{1}| + |t_{2}| \cdots)}. \tag{6.5}$$



6.2 Single-Photon Exchange in the Covariant-Evolution-Operator Formalism

We shall now consider the exchange of a single photon between the electrons in the covariant-evolution-operator formalism. We consider here a general *covariant gauge* (see Sect. 4.3), such as the Feynman gauge, and we shall later consider the noncovariant Coulomb gauge.

We assume here that *the initial state is unperturbed* and return to the more general situation in Chap. 8.

The CEO for the exchange of a single photon (Fig. 6.1, rightmost) is in the general case given by

$$U_{\rm sp}(t,t';t_0,t_0') = \iint d^3x \, d^3x' \, \iint d^3x_0 \, d^3x_0' \, \hat{\psi}^{\dagger}(x) \hat{\psi}^{\dagger}(x') \left\{ \frac{1}{2} \iint d^4x_1 \, d^4x_2 \right.$$

$$\times iS_{\rm F}(x,x_1) \, iS_{\rm F}(x',x_2) \, (-i) \, e^2 D_{\rm F}(x_2,x_1) \, iS_{\rm F}(x_1,x_0)$$

$$\times iS_{\rm F}(x_2,x_0') \, e^{-\gamma(|t_1|+|t_2|)} \right\} \, \hat{\psi}(x_0') \hat{\psi}(x_0) \tag{6.6}$$

[with $D_{\rm F}$ defined in (4.19)] in analogy with the corresponding S-matrix and Green's-function expressions. The expression in the curly brackets is the corresponding Green's function (5.22) (the denominator does not contribute in first order). The CEO contains additional electron creation/annihilation operators and integration over the space coordinates at the initial and final times. This makes the CEO into an *operator*, while the Green's function is a *function*.

When the initial state is unperturbed, it implies with the adiabatic damping that the initial time (t_0, t'_0, \ldots) is $-\infty$. From the definition of the electron propagator (4.8), it can be shown that, as $t_0 \to -\infty$,

$$\int d^3 \mathbf{x}_0 i S_F(x, x_0) \,\hat{\psi}(x_0) \Rightarrow \hat{\psi}(x), \tag{6.7}$$

when the incoming state is a particle state. Therefore, we can leave out the propagators on the incoming lines, as illustrated in the first diagram of Fig. 6.2, corresponding to the expression

$$U_{\rm sp}(t,t';-\infty) = \iint d^3x \, d^3x' \, \hat{\psi}^{\dagger}(x) \hat{\psi}^{\dagger}(x') \left\{ \frac{1}{2} \iint d^4x_1 \, d^4x_2 \, i \, S_{\rm F}(x,x_1) \right.$$
$$\left. \times i \, S_{\rm F}(x',x_2) \, (-i) e^2 D_{\rm F}(x_2,x_1) \, e^{-\gamma(|t_1|+|t_2|)} \right\} \, \hat{\psi}(x_2) \hat{\psi}(x_1). \tag{6.8}$$

Identification with the expression for the second quantization (Appendix B) leads to the matrix element

$$\langle rs|U_{\rm sp}(t,t';-\infty)|ab\rangle = e^{\mathrm{i}(t\varepsilon_r + t'\varepsilon_s)} \iint \mathrm{d}t_1 \mathrm{d}t_2 \langle rs|\mathbf{x},\mathbf{x}'\rangle \langle \mathbf{x},\mathbf{x}'|\mathrm{i}S_{\rm F}(\mathbf{x},\mathbf{x}_1)$$

$$\times \mathrm{i}S_{\rm F}(\mathbf{x}',\mathbf{x}_2) (-\mathrm{i})e^2 D_{\rm F}(\mathbf{x}_2,\mathbf{x}_1)|\mathbf{x}_1,\mathbf{x}_2\rangle \langle \mathbf{x}_1,\mathbf{x}_2||ab\rangle$$

$$\times e^{-\mathrm{i}(t_1\varepsilon_a + t_2\varepsilon_b)} e^{-\gamma(|t_1| + |t_2|)}$$

where we for clarity have indicated the integration variables (see Appendix C.3).

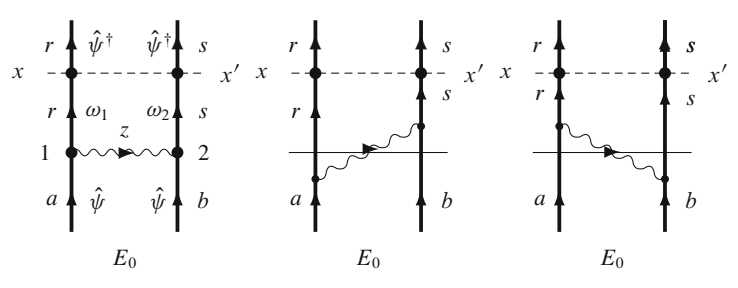


Fig. 6.2 The evolution-operator diagram for single-photon exchange

The external-time dependence is here $e^{-it(\omega_1-\varepsilon_r)}e^{-it'(\omega_2-\varepsilon_r)}$, which in the equal-time approximation (t=t') becomes $e^{-it(\omega_1+\omega_2-\varepsilon_r-\varepsilon_s)}$. Since in the limit $\gamma \to 0$ $\omega_1 + \omega_2 = \varepsilon_a + \varepsilon_b = E_0$ is the *initial* energy and $\varepsilon_r + \varepsilon_s$ is the *final* energy, we have in this limit

$$\langle rs|U_{\rm sp}(t,-\infty)|ab\rangle = e^{-it(E_0 - \varepsilon_r - \varepsilon_s)} \langle rs|\mathcal{M}_{\rm sp}|ab\rangle$$
 (6.9)

or

$$U_{\rm sp}(t, -\infty)|ab\rangle = e^{-it(E_0 - H_0)}|rs\rangle\langle rs|\mathcal{M}_{\rm sp}|ab\rangle,$$
 (6.10)

where \mathcal{M}_{sp} represents the *Feynman amplitude*. This is defined as the *operator without the external time dependence*, in analogy with the Green's function (5.23) (see also Appendix H.2). This yields

$$\langle rs | \mathcal{M}_{sp} | ab \rangle = \left\langle rs \left| \iint \frac{d\omega_1}{2\pi} \frac{d\omega_2}{2\pi} \int \frac{dz}{2\pi} iS_F(\omega_1; \boldsymbol{x}, \boldsymbol{x}_1) iS_F(\omega_2; \boldsymbol{x}', \boldsymbol{x}_2) \right. \right. \\ \left. \times (-i) I(z; \boldsymbol{x}_2, \boldsymbol{x}_1) 2\pi \Delta_{\gamma} (\varepsilon_a - z - \omega_1) \right. \\ \left. \times 2\pi \Delta_{\gamma} (\varepsilon_b + z - \omega_2) \left| ab \right\rangle \right.$$
(6.11)

and after integration over ω_1, ω_2 in the limit $\gamma \to 0$

$$\langle rs|\mathcal{M}_{\rm sp}|ab\rangle = \left\langle rs \middle| \int \frac{\mathrm{d}z}{2\pi} iS_{\rm F}(\varepsilon_a - z; \boldsymbol{x}, \boldsymbol{x}_1) iS_{\rm F}(\varepsilon_b + z; \boldsymbol{x}', \boldsymbol{x}_2) \right.$$

$$\times (-i)I(z; \boldsymbol{x}_2, \boldsymbol{x}_1) 2\pi \Delta_{2\gamma}(\varepsilon_b + \varepsilon_b - \omega_1 - \omega_2) \left| ab \right\rangle. \quad (6.12)$$

Inserting the expressions for the propagator (4.10) and the interaction (4.46) then yields

$$\langle rs|\mathcal{M}_{sp}|ab\rangle = \left\langle rs \left| i \int \frac{\mathrm{d}z}{2\pi} \frac{1}{\varepsilon_a - z - \varepsilon_r + i\gamma_r} \frac{1}{\varepsilon_b + z - \varepsilon_s + i\gamma_s} \right. \right.$$

$$\times \int \frac{2c^2\kappa \,\mathrm{d}\kappa \, f(\kappa)}{z^2 - c^2\kappa^2 + i\eta} \left| ab \right\rangle. \tag{6.13}$$

With the identity (4.75), this can be expressed

$$\langle rs|\mathcal{M}_{\rm sp}|ab\rangle = \frac{1}{E_0 - \varepsilon_r - \varepsilon_s} \langle rs|V_{\rm sp}|ab\rangle$$
 (6.14)

or

$$\mathcal{M}_{\rm sp}(\mathbf{x}, \mathbf{x}')|ab\rangle = \frac{1}{E_0 - H_0} V_{\rm sp}|ab\rangle, \qquad (6.15)$$

where $V_{\rm sp}$ is the potential for single-photon exchange (4.77),

$$\langle rs|V_{\rm sp}|ab\rangle = \left\langle rs \middle| \int_0^\infty c \, d\kappa \, f(\kappa) \right\rangle \times \left[\frac{1}{\varepsilon_a - \varepsilon_r - (c\kappa - i\gamma)_r} + \frac{1}{\varepsilon_b - \varepsilon_s - (c\kappa - i\gamma)_s} \right] \middle| ab \rangle. \tag{6.16}$$

The evolution operator (6.10) then becomes

$$\left| U_{\rm sp}(t, -\infty) \middle| ab \right\rangle = \frac{\mathrm{e}^{-\mathrm{i}t(E_0 - H_0)}}{E_0 - H_0} V_{\rm sp} |ab\rangle.$$
 (6.17)

The results above hold in any covariant gauge, like the Feynman gauge. They do hold also for the <u>transverse part</u> in the Coulomb gauge by using the transverse part of the f function (4.60).

The result (6.16) is identical to the Green's-function result (5.115), when the final state, $|rs\rangle$, lies in the model space. In the CEO case, the final state can also lie in the complementary Q space, in which case the evolution operator contributes to the wave function/operator.

The CEO result can be represented by means of two time-ordered Feynman diagrams, as shown in Fig. 6.2. We then see that the denominators are given essentially by the *Goldstone rules* of standard many-body perturbation theory [5, Sect. 12.4], i.e., the unperturbed energy minus the energies of the orbital lines cut by a horizontal line, in the present case including also -k for cutting the photon line.³

When the initial and final states have the same energy, the potential (6.16) above becomes

$$\langle cd | V_{\rm sp} | ab \rangle = \left\langle cd \left| \int_0^\infty \frac{2\kappa \, d\kappa \, f(\kappa)}{q^2 - \kappa^2 + i\gamma} \right| ab \right\rangle, \tag{6.18}$$

where $cq = \varepsilon_a - \varepsilon_c = \varepsilon_d - \varepsilon_b$, which is the energy-conservative S-matrix result (4.46) and (4.52).

We have seen here that the covariant evolution operator for single-photon exchange has the time dependence $e^{-it(E_0-H_0)}$, which differs from that of the nonrelativistic evolution operator (3.11). We shall return to this question at the end of this chapter.

³ It should be observed that a Goldstone diagram is generally distinct from a "time-ordered Feynman diagram," as is further analyzed in Appendix I.

6.2.1 Single-Photon Ladder

We can now construct the covariant evolution operator for some ladder-type interactions provided *no hole states are appearing in the intermediate states* (see Chap. 8). The diagram in Fig. 6.3 represents two *reducible* single-photon interactions with an intermediate time (t') that separates the interactions. The Feynman amplitude is then obtained by combining two single-photon interactions (6.16) with corresponding resolvents,

$$\mathcal{M}P_{\mathcal{E}} = \Gamma(\mathcal{E}) V_{\rm sp}(\mathcal{E}) \Gamma(\mathcal{E}) V_{\rm sp}(\mathcal{E}) P_{\mathcal{E}}.$$
 (6.19)

where (see 8.11)

$$\langle rs | V_{\rm sp}(\mathcal{E}) | tu \rangle = \langle rs | \int_0^\infty c \, d\kappa \, f(\kappa) \left[\frac{1}{\mathcal{E} - \varepsilon_t - \varepsilon_s - c\kappa} + \frac{1}{\mathcal{E} - \varepsilon_r - \varepsilon_u - c\kappa} \right] | tu \rangle$$

 $P_{\mathcal{E}}$ is the projection operator of the part of the model space with energy \mathcal{E} , and $\Gamma(\mathcal{E})$ is the resolvent (2.64).

This procedure can be repeated to a general single-photon ladder

$$\mathcal{M}_{Ladd}P_{\mathcal{E}} = \Gamma(\mathcal{E}) V_{sp}(\mathcal{E}) \Gamma(\mathcal{E}) V_{sp}(\mathcal{E}) \cdots \Gamma(\mathcal{E}) V_{sp}(\mathcal{E}) P_{\mathcal{E}}. \tag{6.20}$$

The corresponding part of the evolution operator is according to (6.10)

$$U_0(t, -\infty)_{\text{Ladd}} P_{\mathcal{E}} = e^{-it(\mathcal{E} - H_0)} \mathcal{M}_{\text{Ladd}} P_{\mathcal{E}}, \tag{6.21}$$

where subscript "0" is used to indicate that there are no intermediate model-space states (see further below). This evolution operator can be singular due to intermediate <u>and/or</u> final model-space states, which can be eliminated by means of counterterms, leading to "folds" (model-space contributions, MSC), as we shall demonstrate below.

It should be observed that

• In the equal-time approximation the interactions and the resolvents as well as the time factor of the ladder without folds all depend on the energy of the initial, unperturbed state.

The folds will affect the time dependence, as will be discussed in Sect. 6.9. In Part III, we shall treat the ladder in the presence of virtual pairs and higher-order interactions and see how the procedure can be fitted into a many-body procedure.

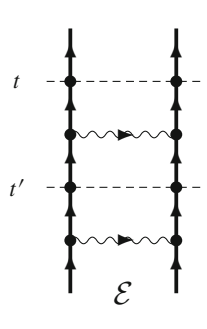


Fig. 6.3 Feynman diagram representing second-order ladder diagram (6.19)

6.3 Multiphoton Exchange

6.3.1 General

We shall now briefly consider the general case of multiphoton exchange. We can describe this by means of a general many-body potential, which we can separate into one-, two-, ... body parts,

$$\mathcal{V} = V_1 + V_2 + V_3 + \cdots \tag{6.22}$$

and which contains all *irreducible* interactions.⁴ By iterating such a potential, all *reducible* interactions will be generated. In Figs. 6.4 and 6.6, we illustrate the one- and two-body parts of this potential, including radiative effects – vacuum polarization, self-energy, vertex correction (see Sect. 2.6) – which, of course, have to be properly renormalized (see Chap. 12).

The one-body potential contains an effective-potential interaction (Fig. 6.5) in analogy to that in ordinary MBPT (2.73). In the effective potential here, however, the internal lines can be hole lines as well as particle lines. This implies that the second diagram on the r.h.s. in Fig. 6.5 contains the direct Hartree–Fock potential as well as the radiative effect of vacuum polarization and the last diagram the exchange

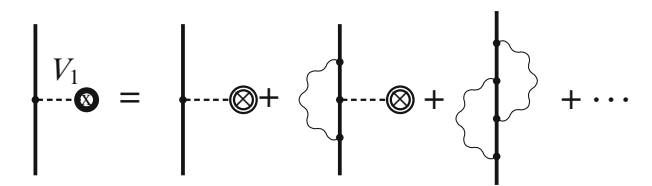


Fig. 6.4 Graphical representation of the one-body part of the effective potential (6.22), containing the one-body potential in Fig. 6.5 as well as irreducible one-body potential diagrams, including radiative effects

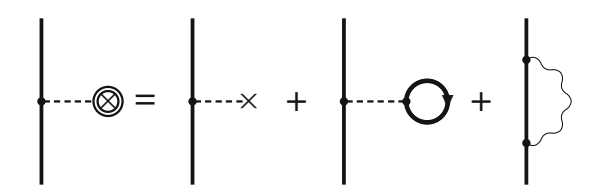


Fig. 6.5 Graphical representation of the "extended" effective potential interaction. This is analogous to the effective potential in Fig. 2.3, but the internal lines represent here *all* orbitals (particles as well as holes). This implies that the last two diagrams include the (renormalized) vacuum polarization and self-energy

⁴ Concerning the definition of the concepts "reducible" and "irreducible," see Sect. 2.6.

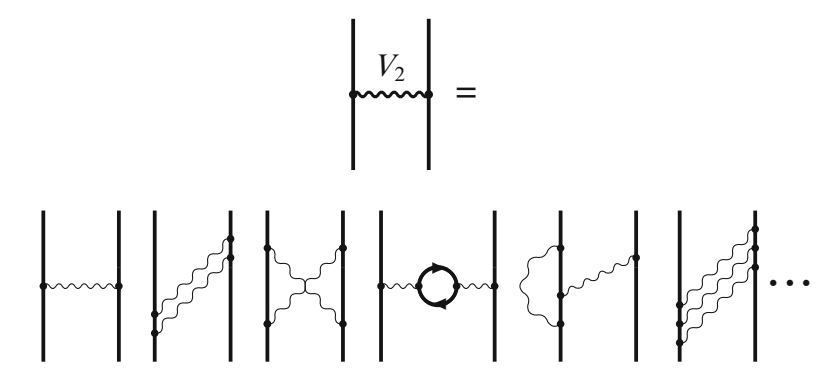


Fig. 6.6 The two-body part of the effective potential (6.22) contains all irreducible two-body potential diagrams

part of the HF potential as well as the and electron self-energy (both radiative effects properly renormalized). All heavy lines here represent orbitals in the external (nuclear) potential, which implies that the vacuum polarization contains the Uehling potential [16] (see Sect. 4.6) as well as the Wickmann–Kroll [17] correction, discussed earlier in Sect. 4.6.

6.3.2 Irreducible Two-Photon Exchange*

We consider next the general two-photon exchange, illustrated in Fig. 6.7, still assuming the equal-time approximation and unperturbed initial state.

6.3.2.1 Uncrossing Photons

Generalizing the result for single-photon exchange (6.6), we find that the *kernel* of the first (ladder)diagram becomes

$$iS_F(x, x_3) iS_F(x', x_4) (-i)e^2 D_F(x_4, x_3) iS_F(x_3, x_1)$$

 $\times iS_F(x_4, x_2) (-i)e^2 D_F(x_2, x_1).$ (6.23)

This leads to the Feynman amplitude in analogy with (6.11)

$$\begin{split} \mathcal{M}_{\rm sp}(x,x';x_0,x_0') &= \iiint \int \frac{{\rm d}\omega_1}{2\pi} \, \frac{{\rm d}\omega_2}{2\pi} \, \frac{{\rm d}\omega_3}{2\pi} \, \frac{{\rm d}\omega_4}{2\pi} \iint \frac{{\rm d}z}{2\pi} \, \frac{{\rm d}z'}{2\pi} \, {\rm i}S_{\rm F}(\omega_3;x,x_3) \\ & \times {\rm i}S_{\rm F}(\omega_4;x',x_4) \, (-{\rm i})I(z';x_4,x_3) \, {\rm i}S_{\rm F}(\omega_1;x_3,x_1) \\ & \times {\rm i}S_{\rm F}(\omega_2;x_4,x_2) \, (-{\rm i})I(z;x_2,x_1) \, 2\pi \Delta_{\gamma}(\varepsilon_a-\omega_1-z) \end{split}$$

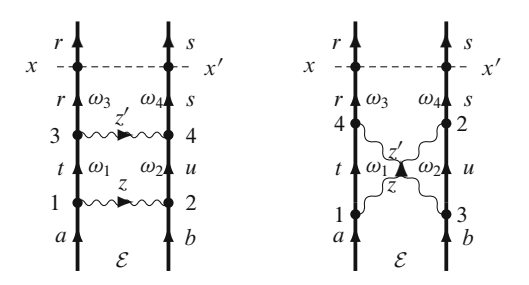


Fig. 6.7 Covariant-evolution-operator diagrams for two-photon ladder and "cross"

$$\times 2\pi \Delta_{\gamma}(\varepsilon_b - \omega_2 + z) 2\pi \Delta_{\gamma}(\omega_1 - z' - \omega_3)$$

$$\times 2\pi \Delta_{\gamma}(\omega_2 + z' - \omega_4).$$
(6.24)

Integration over ω_1 , ω_2 leads to

$$\mathcal{M}_{sp}(x, x') = \iint \frac{d\omega_{3}}{2\pi} \frac{d\omega_{4}}{2\pi} \iint \frac{dz}{2\pi} \frac{dz'}{2\pi} iS_{F}(\omega_{3}; x, x_{3}) iS_{F}(\omega_{4}; x', x_{4})$$

$$\times (-i)I(z'; x_{4}, x_{3}) iS_{F}(\varepsilon_{a} - z; x_{3}, x_{1}) iS_{F}(\varepsilon_{b} + z; x_{4}, x_{2})$$

$$\times (-i)I(z; x_{2}, x_{1}) 2\pi \Delta_{2\gamma}(\varepsilon_{a} - z - z' - \omega_{3})$$

$$\times 2\pi \Delta_{2\gamma}(\varepsilon_{b} + z + z' - \omega_{4})$$
(6.25)

and over ω_3 , ω_4

$$\mathcal{M}_{sp}(x, x') = \iint \frac{dz}{2\pi} \frac{dz'}{2\pi} i S_{F}(\varepsilon_{a} - z - z'; x, x_{3}) i S_{F}(\varepsilon_{b} + z + z'; x', x_{4})$$

$$\times (-i) I(z'; x_{4}, x_{3}) i S_{F}(\varepsilon_{a} - z; x_{3}, x_{1})$$

$$\times i S_{F}(\varepsilon_{b} + z; x_{4}, x_{2}) (-i) I(z; x_{2}, x_{1}). \tag{6.26}$$

Integration over z' leads to the denominators

$$\frac{1}{\mathcal{E} - \varepsilon_r - \varepsilon_s} \left[\frac{1}{\varepsilon_a - \varepsilon_r - z - (c\kappa' - i\gamma)_r} + \frac{1}{\varepsilon_b - \varepsilon_s + z - (c\kappa' - i\gamma)_s} \right]$$

and the remaining part of the integrand is

$$\frac{1}{\mathcal{E} - \varepsilon_t - \varepsilon_u} \left[\frac{1}{\varepsilon_a - \varepsilon_t - z + i\gamma_t} + \frac{1}{\varepsilon_b + z + i\gamma_u} \right] \frac{1}{z^2 - c^2\kappa^2 + i\eta}.$$

6.3.2.2 Crossing Photons

For the crossed-photon exchange in Fig. 6.7 (right), the corresponding result is

$$\mathcal{M}_{sp}(x, x'; x_{0}, x'_{0}) = \iiint \frac{d\omega_{1}}{2\pi} \frac{d\omega_{2}}{2\pi} \frac{d\omega_{3}}{2\pi} \frac{d\omega_{4}}{2\pi} \iint \frac{dz}{2\pi} \frac{dz'}{2\pi} iS_{F}(\omega_{3}; x, x_{4})$$

$$\times iS_{F}(\omega_{4}; x', x_{2}) (-i)I(z'; x_{4}, x_{3}) iS_{F}(\omega_{1}; x_{4}, x_{1})$$

$$\times iS_{F}(\omega_{2}; x_{2}, x_{3}) (-i)I(z; x_{2}, x_{1}) 2\pi \Delta_{\gamma}(\varepsilon_{a} - \omega_{1} - z)$$

$$\times 2\pi \Delta_{\gamma}(\varepsilon_{b} - \omega_{2} - z') 2\pi \Delta_{\gamma}(\omega_{1} - z' - \omega_{3})$$

$$\times 2\pi \Delta_{\gamma}(\omega_{2} + z - \omega_{4}). \tag{6.27}$$

Integration over the omegas yields

$$\mathcal{M}_{sp}(x, x') = \iint \frac{dz}{2\pi} \frac{dz'}{2\pi} i S_{F}(\varepsilon_{a} + z' - z; x, x_{4}) i S_{F}(\varepsilon_{b} + z - z'; x', x_{2})$$

$$\times (-i) I(z'; x_{4}, x_{3}) i S_{F}(\varepsilon_{a} - z; x_{4}, x_{1})$$

$$\times i S_{F}(\varepsilon_{b} - z; x_{2}, x_{3}) (-i) I(z; x_{2}, x_{1}). \tag{6.28}$$

Integration over z' leads to the denominators

$$\frac{1}{\mathcal{E} - \varepsilon_r - \varepsilon_s} \left[\frac{1}{\varepsilon_a - \varepsilon_r - z - (c\kappa' - i\gamma)_r} + \frac{1}{\varepsilon_b - \varepsilon_s + z - (c\kappa' - i\gamma)_s} \right]$$

and the remaining part of the integrand is

$$\frac{1}{\varepsilon_a - \varepsilon_t - z + i\gamma_t} \frac{1}{\varepsilon_b - \varepsilon_u - z + i\gamma_u} \frac{1}{z^2 - c^2\kappa^2 + i\eta}.$$

To evaluate the integrals above is quite complicated, but they are considered in detail in [9, Appendix B] and in the thesis of Björn Åsén [2]. The two-photon effects have been evaluated for helium-like ions, and some results are shown in the following chapter.

6.3.3 Potential with Radiative Parts

Two-photon potentials with self-energy and vacuum-polarization insertions can also be evaluated in the covariant-evolution-operator formalism, as discussed in [9]. We shall not consider this any further here, but return to these effects in connection with the MBPT–QED procedure in Chap. 8.

6.4 Relativistic Form of the Gell-Mann-Low Theorem

We have in Chap. 3 considered the nonrelativistic form of the Gell-Mann–Low theorem, and we shall now extend this to the relativistic formalism. This theorem plays a fundamental role in the formalism we shall develop here.

We shall start with

• a conjecture that the time evolution of the relativistic state vector is governed by the CEO in the equal-time approximation (in the interaction picture), in analogy with the situation in the nonrelativistic case (3.6) (c.f. [4, Sect. 6.4]),

$$\left| \chi_{\text{Rel}}^{\alpha}(t) \right\rangle = U_{\text{Cov}}(t, t_0) \left| \chi_{\text{Rel}}^{\alpha}(t_0) \right\rangle.$$
 (6.29)

We shall later demonstrate that this conjecture is consistent with the standard quantum-mechanical picture (6.120) [see also (9.13)]. It should be noted that the evolution operator does not generally preserve the (intermediate) normalization.

It can now be shown as in the nonrelativistic case in Sect. 3.3 that the conjecture above leads to a

relativistic form of the Gell-Mann-Low theorem for a general quasi-degenerate model space

$$\left| \chi_{\text{Rel}}^{\alpha}(0) \rangle = \left| \Psi_{\text{Rel}}^{\alpha} \right\rangle = \lim_{\gamma \to 0} \frac{U_{\text{Cov}}(0, -\infty) \left| \Phi_{\text{Rel}}^{\alpha} \right\rangle}{\left| \Psi_{0_{\text{Rel}}}^{\alpha} \right| U_{\text{Cov}}(0, -\infty) \left| \Phi_{\text{Rel}}^{\alpha} \right\rangle},$$
(6.30)

which is quite analogous to the nonrelativistic theorem (3.46). Here, $|\Phi_{Rel}^{\alpha}\rangle$ is, as before, the *parent state* (3.32), i.e., the limit of the corresponding target state, as the perturbation is adiabatically turned off,

$$\left|\Phi_{\text{Rel}}^{\alpha}\right\rangle = C^{\alpha} \lim_{t \to -\infty} \left|\chi_{\text{Rel}}^{\alpha}(t)\right\rangle,$$
 (6.31)

 $(C^{\alpha}$ is a normalization constant) and $|\Psi_{0}^{\alpha}_{\mathrm{Rel}}\rangle=P|\Psi^{\alpha}_{\mathrm{Rel}}\rangle$ is the (normalized) model state.

• The state vector $|\Psi^{\alpha}_{Rel}\rangle$ satisfies a *relativistic eigenvalue equation*, analogous to the nonrelativistic (Schrödinger-like) *Gell-Mann–Low equation* (3.35),

$$(6.32)$$

$$(H_0 + V_F)|\Psi^{\alpha}_{Rel}\rangle = E^{\alpha}|\Psi^{\alpha}_{Rel}\rangle,$$

where $V_{\rm F}$ is the perturbation, used in generating the evolution operator (6.5).

In proving the relativistic form of the GML theorem, we observe that the covariant evolution operator differs from the corresponding nonrelativistic operator particularly by the replacement of the electron-field operators by the corresponding density operators (6.1). It then follows that the commutator of H_0 with the covariant operator is the same as with the nonrelativistic operator, which implies that the proof in Sect. 3.3 can be used also in the covariant case.

A condition for the GML theorem to hold is as in the nonrelativistic case that *the perturbation is time-independent in the Schrödinger picture* (apart from damping), which is the case for the perturbation we shall use here (see further below).

6.5 Field-Theoretical Many-Body Hamiltonian

In the unified MBPT–QED procedure, we shall apply the Coulomb gauge in order to be able to utilize the developments of the MBPT procedure. In this gauge, we separate the interaction between the electrons in the *instantaneous Coulomb interaction* and the *transverse interaction*, with the Coulomb part being (2.109)

$$V_{\rm C} = \sum_{i < j}^{N} \frac{e^2}{4\pi\epsilon_0 \, r_{ij}}.\tag{6.33}$$

The exchange of a virtual transverse photon is represented by TWO perturbations of the one-body perturbation

$$v_{\mathrm{T}}(t) = \int \mathrm{d}^3 x \, \mathcal{H}(t, x), \tag{6.34}$$

where the perturbation density given by (4.4)

$$\mathcal{H}(x) = \mathcal{H}(t, \mathbf{x}) = -\hat{\psi}^{\dagger}(x) e c \alpha^{\mu} A_{\mu}(x) \hat{\psi}(x)$$
 (6.35)

with A_μ being the quantized, transverse radiation field (see Appendix F.2). The total perturbation is then

$$V_{\rm F} = V_{\rm C} + v_{\rm T}.$$
 (6.36)

The perturbation (6.35) represents the emission/absorption of a photon. Therefore, with this perturbation the GML equation works in a *photonic Fock space*,⁵ where the number of photons is not preserved. (The perturbation above is not time independent in the Schrödinger picture as required by the GML relation, but it can be transformed into equivalent, time-independent interactions, as will be demonstrated in Sect. 10.1).

The model many-body Hamiltonian we shall apply is primarily a sum of Dirac single-electron Hamiltonians in an external (nuclear) field (Furry picture) (2.108)

$$h_{\rm D} = c\boldsymbol{\alpha} \cdot \hat{\mathbf{p}} + \beta mc^2 + v_{\rm ext}. \tag{6.37}$$

⁵ Also, the Fock space is a form of Hilbert space, and therefore we shall refer to the Hilbert space with a constant number of photons as the *restricted (Hilbert) space* and the space with a variable number of photons as the (extended) *photonic Fock space* (see Appendix A.2).

[As before, we may include an optional potential, u, in the model Hamiltonian (2.49) – and subtract the same quantity in the perturbation – in order to improve the convergence rate for many-electron systems.]

However, since the number of photons is no longer constant in the space we work in, we have to include in the model Hamiltonian also the radiation field, H_{Rad} [see Appendix (G.12) and (B.20)], yielding

$$H_0 = \sum h_{\rm D} + H_{\rm Rad}.$$
 (6.38)

The full field-theoretical many-body Hamiltonian will then be

$$H = H_0 + V_F = H_0 + V_C + v_T$$
 (6.39)

sometimes also referred to as the *many-body Dirac Hamiltonian*. This leads with the GML relation (6.32) to the corresponding *Fock-space many-body equation*⁶

$$\boxed{H\Psi = E\Psi.} \tag{6.40}$$

In comparing our many-body Dirac Hamiltonian with the Coulomb–Dirac–Breit Hamiltonian of standard MBPT (2.113), we see that we have included the radiation field, $H_{\rm Rad}$, and replaced the instantaneous Breit interaction with the transverse field interaction, $v_{\rm T}$, in addition to removing the projection operators.

Using second quantization (see Appendices B and E),

• the field-theoretical many-body Hamiltonian (6.39) becomes

$$H = \int d^{3}x \,\hat{\psi}^{\dagger}(x) \Big(c \,\alpha \cdot \hat{p} + \beta mc^{2} + v_{\text{ext}}(x) - ec\alpha^{\mu} A_{\mu}(x) \Big) \hat{\psi}(x)$$

$$+ H_{\text{Rad}} + \frac{1}{2} \iint d^{3}x_{1} \,d^{3}x_{2} \,\hat{\psi}^{\dagger}(x_{1}) \,\hat{\psi}^{\dagger}(x_{2}) \frac{e^{2}}{4\pi\epsilon_{0}r_{12}} \,\hat{\psi}(x_{2}) \,\hat{\psi}(x_{1}),$$
(6.4)

(6.41)

where $v_{\rm ext}(x)$ is the external (nuclear) field of the electrons (Furry picture). We have here assumed that the Coulomb gauge is employed, and therefore the operator $A_{\mu}(x)$ represents only the *transverse* part of the radiation field. (As mentioned previously, it is quite possible to use the Coulomb gauge in QED calculation, as demonstrated by Adkins [1], Rosenberg [13], and others.)

⁶ This equation is not completely covariant, because it has a single time, in accordance with the established quantum-mechanical picture. This is the *equal-time approximation*, mentioned above and further discussed later. In addition, a complete covariant treatment would require that also the interaction between the electrons and the nucleus is treated in a covariant way by means of the exchange of virtual photons (see, for instance, [14]).

• By treating the Coulomb and the transverse photon interactions separately, a formal departure is made from a fully covariant treatment. However, this procedure is, when performed properly, in practice equivalent to the use of a covariant gauge.

We define the wave-operator in analogy with the nonrelativistic case $(2.37)^7$

$$|\Psi^{\alpha}\rangle = \Omega |\Psi_0^{\alpha}\rangle \quad (\alpha = 1 \cdots d)$$
 (6.42)

but now acting in the extended photonic Fock space.

The effective Hamiltonian has the same definition as before (2.38), which leads to

$$H_{\rm eff} = PH\Omega P \tag{6.43}$$

and the effective interaction is defined by

$$V_{\text{eff}} = H_{\text{eff}} - PH_0P = P(H - H_0)\Omega P \tag{6.44}$$

or using the Hamiltonian (6.39)

$$V_{\text{eff}} = P V_{\text{F}} \Omega P = P (V_{\text{C}} + v_{\text{T}}) \Omega P.$$
 (6.45)

This is a *Fock-space relation*, and the corresponding relation in the restricted space without uncontracted photons is given by (6.123).

By solving the many-body equation (6.40) iteratively, all possible perturbations will be produced. This is the basic principle of the covariant relativistic many-body perturbation procedure we shall develop in this book. How this can be accomplished will be discussed in the following. First, we shall treat the simple case of single-photon exchange.

6.6 Green's Operator

6.6.1 Definition

The vacuum expectation used to define the Green's function (5.8) contains singularities in the form of unlinked diagrams, where the disconnected parts represent the vacuum expectation of the S-matrix. This is a *number*, and it then follows that the singularities could be eliminated by dividing by this number. For the covariant

⁷ In the following, we shall leave out the subscript "Rel."

6.6 Green's Operator 135

evolution operator (CEO) (6.2), the situation is more complex, since this in an *operator*, and the disconnected parts will also in general be operators. Therefore, we shall here proceed in a somewhat different manner.

As mentioned.

• we shall refer to the *regular part of the CEO* as the *Green's operator* – in the single-particle case denoted $\mathcal{G}(t, t_0)$ – due to its great similarity with the Green's function. We define the single-particle Green's operator by the relation⁸

$$U(t,t_0)P = \mathcal{G}(t,t_0) \cdot PU(0,t_0)P,$$
(6.46)

where P is the projection operator for the model space, and analogously in the many-particle case. Below we shall demonstrate that *the Green's operator is regular*.

The definition of the Green's operator contains the important concept of a *heavy dot*, which is defined in the following way.

If the operators are *disconnected*, there is no difference between the dot product and an ordinary (normal-ordered) product. If the operators are *connected* to a diagram of ladder type in Fig. 6.3 (6.20), then we have seen that all interactions in an ordinary product depend on the energy of the *initial* state. We now introduce the convention that *in a dot product the operators do not operate beyond the heavy dot.*⁹

The definitions above imply that the interactions and the resolvents to the left of the dot depend on the energy of the unperturbed state at the position of the dot. If we operate to the right on the part of the model space $P_{\mathcal{E}}$ of energy \mathcal{E} and the intermediate model-space state lies in the part $P_{\mathcal{E}'}$ of energy \mathcal{E}' , we can express the two kinds of products as

$$\begin{cases}
AP_{\mathcal{E}'}BP_{\mathcal{E}} = A(\mathcal{E}) \ P_{\mathcal{E}'}B(\mathcal{E})P_{\mathcal{E}} \\
A \cdot P_{\mathcal{E}'}BP_{\mathcal{E}} = A(\mathcal{E}') \ P_{\mathcal{E}'}B(\mathcal{E})P_{\mathcal{E}}
\end{cases} (6.47)$$

with the energy parameter of A equal to \mathcal{E} in the first case and to \mathcal{E}' in the second case. By the hooks we indicate that the operators must be connected by at least one contraction. We shall soon see the implication of this definition.

⁸ The Green's operator is closely related – but not quite identical – to the *reduced covariant evolution operator*, previously introduced by the Gothenburg group [9].

⁹ This can be compared with the situation in the MBPT Bloch equation (2.56), where – using the heavy dot – the folded term could be expressed $\Omega \cdot PV_{\rm eff}P$, indicating that the energy parameters of the wave operator depend on the intermediate model-space state.

6.6.2 Relation Between the Green's Operator and Many-Body Perturbation Procedures

From the conjecture (6.29) and the definition (6.46), we have in the limit of vanishing damping

$$|\chi^{\alpha}(t)\rangle = N_{\alpha}U(t, -\infty)|\Phi^{\alpha}\rangle = N_{\alpha}\mathcal{G}(t, -\infty) \cdot PU(0, -\infty)P|\Phi^{\alpha}\rangle, \quad (6.48)$$

where N_{α} is the normalization constant

$$N_{\alpha} = \frac{1}{\langle \Psi_0^{\alpha} | U(0, -\infty | \Phi^{\alpha} \rangle)}$$
 (6.49)

making the state vector intermediately normalized for t=0. Here, $|\Phi^{\alpha}\rangle$ is the parent state (6.31), and $|\Psi^{\alpha}\rangle = N_{\alpha}U(0,-\infty)|\Phi^{\alpha}\rangle$ is the target state (for t=0). The model state is

$$|\Psi_0^{\alpha}\rangle = P|\Psi^{\alpha}\rangle = N_{\alpha}PU(0, -\infty)|\Phi^{\alpha}\rangle.$$

This leads directly to

• the relation

$$\left| \left| \chi^{\alpha}(t) \right\rangle = \mathcal{G}(t, -\infty) \left| \Psi_0^{\alpha} \right\rangle, \right|$$
 (6.50)

which implies that the time dependence of the relativistic state vector is governed by the Green's operator.

- Therefore, the Green's operator can be regarded as a time-dependent wave operator but it is NOT an evolution operator in the sense, discussed in Sect. 3.1.
- For the time t = 0, we have the *covariant analogue of the standard wave operator of MBPT* (2.37)

$$|\chi^{\alpha}(0)\rangle = |\Psi^{\alpha}\rangle = \Omega_{\text{Cov}}|\Psi^{\alpha}\rangle$$
 (6.51)

with

$$\Omega_{\text{Cov}} = \mathcal{G}(0, -\infty). \tag{6.52}$$

It follows directly from the definition (6.46) that

$$P\mathcal{G}(0, -\infty)P = P \tag{6.53}$$

and the relation above can also be expressed

$$\Omega_{\text{Cov}} = 1 + Q\mathcal{G}(0, -\infty). \tag{6.54}$$

6.6 Green's Operator 137

We note here that it is important that the Green's operator is defined with the dot product (6.46). The definition of the wave operator (2.37) can be expressed

$$|\Psi^{\alpha}\rangle = \Omega_{\text{Cov}} \cdot P|\Psi^{\alpha}\rangle = \Omega_{\text{Cov}} \cdot PU(0, -\infty)|\Phi^{\alpha}\rangle$$
 (6.55)

indicating that the energy parameter of the wave operator depends on the intermediate model-space state.

We shall also define a *covariant effective interaction*, analogous to the operator of MBPT (2.55). The time dependence of the relativistic state vector is formally the same as that of the nonrelativistic one (2.15) [which is verified below (6.120)], i.e., in interaction picture

$$\left|\chi^{\alpha}(t)\right\rangle = e^{-it(E^{\alpha} - H_0)} \left|\chi^{\alpha}(0)\right\rangle = e^{-it(E^{\alpha} - H_0)} \left|\Psi^{\alpha}\right\rangle \tag{6.56}$$

or

$$i\frac{\partial}{\partial t}|\chi^{\alpha}(t)\rangle = (E^{\alpha} - H_0)|\chi^{\alpha}(t)\rangle.$$
 (6.57)

With the relation (6.50), this yields for the time t = 0

$$i\left(\frac{\partial}{\partial t}\left|\chi^{\alpha}(t)\right\rangle\right)_{t=0}\left|\Psi^{\alpha}\right\rangle = i\left(\frac{\partial}{\partial t}\mathcal{G}(t,-\infty)\right)_{t=0}\left|\Psi^{\alpha}_{0}\right\rangle = (E^{\alpha} - H_{0})\left|\Psi^{\alpha}\right\rangle. \quad (6.58)$$

Here, the r.h.s. becomes, using the GML relation (6.32) and the wave-operator relation (6.51),

$$(H - H_0)|\Psi^{\alpha}\rangle = V_F|\Psi^{\alpha}\rangle = V_F \Omega_{Cov}|\Psi_0^{\alpha}\rangle.$$
 (6.59)

These relations hold for all model states, which leads us to the important operator relation for the entire model space

$$i\left(\frac{\partial}{\partial t}\mathcal{G}(t,-\infty)\right)_{t=0}P = V_{F}\Omega_{Cov}P,$$
(6.60)

which we refer to as the *reaction operator*. Projecting this onto the model space, yields according to the definition (6.44) to

• the covariant relativistic effective interaction

$$V_{\text{eff}}^{\text{Cov}} = P V_{\text{F}} \Omega_{\text{Cov}} P = P \left(i \frac{\partial}{\partial t} \mathcal{G}(t, -\infty) \right)_{t=0} P.$$
 (6.61)

This is a relation in the *photonic Fock space*, closely analogous to the corresponding relation of standard MBPT (2.55) [c.f. the relation (6.123)].

Our procedure here is based upon quantum-field theory, and the Green's operator can be regarded as a *field-theoretical extension of the traditional wave-operator concept* of MBPT, and it serves as a *connection between field theory and MBPT*.

6.7 Model-Space Contribution

We shall now demonstrate how the singularities of the covariant evolution operator can be eliminated in the general multireference case. We assume that the initial time is $t_0 = -\infty$. We also work in the *equal-time approximation*, where all final times are the same.

We work in the *restricted Hilbert space* with **no uncontracted photons** and consider a *ladder of complete single-photon interactions* (6.21), transverse and Coulomb parts (see Fig. 6.3). (We shall later expand this to more general, irreducible interactions.)

We start by expanding the relation (6.46) order-by-order, using the fact that $U^{(0)}(0)P = P$,

$$U^{(0)}(t)P = \mathcal{G}^{(0)}(t) \cdot PU^{(0)}(0)P = \mathcal{G}^{(0)}(t)P$$

$$U^{(1)}(t)P = \mathcal{G}^{(1)}(t)P + \mathcal{G}^{(0)}(t) \cdot PU^{(1)}(0)P$$

$$U^{(2)}(t)P = \mathcal{G}^{(2)}(t)P + \mathcal{G}^{(1)}(t) \cdot PU^{(1)}(0)P + \mathcal{G}^{(0)}(t) \cdot PU^{(2)}(0)P$$

$$U^{(3)}(t)P = \mathcal{G}^{(3)}(t)P + \mathcal{G}^{(2)}(t) \cdot PU^{(1)}(0)P + \mathcal{G}^{(1)}(t) \cdot PU^{(2)}(0)P$$

$$+ \mathcal{G}^{(0)}(t) \cdot PU^{(3)}(0)P, \tag{6.62}$$

etc.

It follows from (6.21) that the time dependence of the ladder is given by $e^{-it(E_{in}-E_{out})}$, where E_{in} and E_{out} represent the incoming and outgoing energies. When operating on the part of the model space of energy \mathcal{E} , the operator can be expressed as

$$U(t)P_{\mathcal{E}} = e^{-it(\mathcal{E} - H_0)} U(0)P_{\mathcal{E}}.$$
(6.63)

Solving the equations (6.62) for the Green's operator, we then have

$$\mathcal{G}^{(0)}(t)P = U^{(0)}(t)P
\mathcal{G}^{(1)}(t)P = U^{(1)}(t)P - \mathcal{G}^{(0)}(t) \cdot PU^{(1)}(0)P
\mathcal{G}^{(2)}(t)P = U^{(2)}(t)P - \mathcal{G}^{(0)}(t) \cdot PU^{(2)}(0)P - \mathcal{G}^{(1)}(t) \cdot PU^{(1)}(0)P
\mathcal{G}^{(3)}(t)P = U^{(3)}(t)P - \mathcal{G}^{(0)}(t) \cdot PU^{(3)}(0)P - \mathcal{G}^{(1)}(t) \cdot PU^{(2)}(0)P
- \mathcal{G}^{(2)}(t) \cdot PU^{(1)}(0)P,$$
(6.64)

etc. We shall demonstrate that the negative terms above, referred to as *counterterms*, will remove the singularities of the evolution operator.

It follows directly from the definition of the dot product above that the singularities due to *disconnected* parts are exactly eliminated by the counterterms. Therefore, we need only consider the *connected* (ladder) part, and we consider a fully contracted two-body diagram as an illustration (Fig. 6.3). It is sufficient for our present purpose to consider only positive intermediate states, as in (6.20).

6.7.1 Lowest Orders

From the above, it follows that the zeroth-order Green's operator is

$$\mathcal{G}^{(0)}(t,\mathcal{E})P_{\mathcal{E}} = U^{(0)}(t,\mathcal{E})P_{\mathcal{E}} = e^{-it(\mathcal{E}-H_0)}P_{\mathcal{E}} = P_{\mathcal{E}}.$$
 (6.65)

(For clarity, we insert the energy parameter in the operator symbol.) In *first order*, we have from (6.64)

$$\mathcal{G}^{(1)}(t,\mathcal{E})P_{\mathcal{E}} = U^{(1)}(t,\mathcal{E})P_{\mathcal{E}} - \mathcal{G}^{(0)}(t,\mathcal{E}')P_{\mathcal{E}'}U^{(1)}(0,\mathcal{E})P_{\mathcal{E}}, \tag{6.66}$$

where we observe that the Green's operator in the counterterm has the energy parameter \mathcal{E}' , due to the heavy dot in the expression (6.64). The first term is (quasi)-singular, when the final state lies in the model space, and we shall show that this singularity is eliminated by the counterterm.

From (6.63), we have

$$P_{\mathcal{E}'}U^{(1)}(t,\mathcal{E})P_{\mathcal{E}} = P_{\mathcal{E}'}\mathcal{G}^{(0)}(t,\mathcal{E})U^{(1)}(0,\mathcal{E})P_{\mathcal{E}}$$

(with the energy parameter \mathcal{E} in the Green's operator) and hence the corresponding part of the Green's operator (6.66) becomes

$$P_{\mathcal{E}'}\mathcal{G}^{(1)}(t,\mathcal{E})P_{\mathcal{E}} = \left(\mathcal{G}^{(0)}(t,\mathcal{E}) - \mathcal{G}^{(0)}(t,\mathcal{E}')\right)P_{\mathcal{E}'}U^{(1)}(0,\mathcal{E})P_{\mathcal{E}}$$
(6.67)

(P commutes with H_0). According to (6.20)

$$P_{\mathcal{E}'}U^{(1)}(0,\mathcal{E})P_{\mathcal{E}} = P_{\mathcal{E}'}\Gamma(\mathcal{E}) V_{\text{sp}}(\mathcal{E})P_{\mathcal{E}} = P_{\mathcal{E}'}\frac{1}{\mathcal{E} - H_0} V_{\text{sp}}(\mathcal{E})P_{\mathcal{E}} = P_{\mathcal{E}'}\frac{V_{\text{sp}}(\mathcal{E})}{\mathcal{E} - \mathcal{E}'} P_{\mathcal{E}}$$
(6.68)

and hence we can express the first-order Green's operator (6.66) as

$$\mathcal{G}^{(1)}(t,\mathcal{E})P_{\mathcal{E}} = QU^{(1)}(t,\mathcal{E})P_{\mathcal{E}} + \frac{\delta\mathcal{G}^{(0)}(t,\mathcal{E}',\mathcal{E})}{\delta\mathcal{E}}P_{\mathcal{E}'}V_{\rm sp}P_{\mathcal{E}},\tag{6.69}$$

where $QU^{(1)}(t,\mathcal{E}) = \mathcal{G}^{(0)}(t,\mathcal{E})\Gamma_Q(\mathcal{E})V(\mathcal{E})P_{\mathcal{E}}$. We assume here that there is a summation over \mathcal{E}' , so that the entire intermediate model-space is covered. The *difference ratio* above is defined

$$\frac{\delta \mathcal{G}^{(0)}(t, \mathcal{E}', \mathcal{E})}{\delta \mathcal{E}} = \frac{\mathcal{G}^{(0)}(t, \mathcal{E}) - \mathcal{G}^{(0)}(t, \mathcal{E}')}{\mathcal{E} - \mathcal{E}'} \Rightarrow \frac{\partial \mathcal{G}^{(0)}(t, \mathcal{E})}{\partial \mathcal{E}}, \tag{6.70}$$

which turns into a derivative at complete degeneracy. Furthermore,

$$P_{\mathcal{E}'}V_{\rm sp}P_{\mathcal{E}} = P_{\mathcal{E}'}V_{\rm eff}^{(1)}P_{\mathcal{E}} \tag{6.71}$$

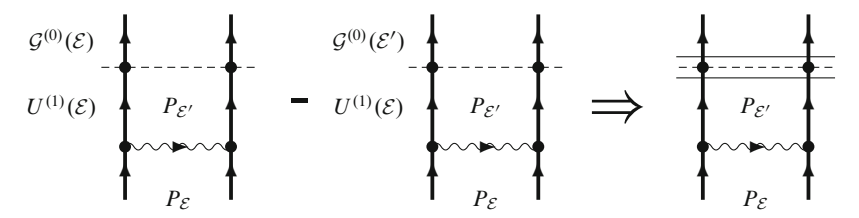


Fig. 6.8 Illustration of the elimination of singularity of the first-order evolution operator, due to a final model-space state. The *double bar* represents the difference ratio/derivative of the zeroth-order Green's operator (c.f. Fig. 6.9)

is the first-order effective interaction, which is in accordance with the Fock-space expression (6.45) [see also (6.123)].

The first-order elimination process is illustrated in Fig. 6.8.

In second order, we have from (6.21)

$$U_0^{(2)}(t,\mathcal{E})_{\text{Ladd}} P_{\mathcal{E}} = U_0^{(1)}(t,\mathcal{E}) U_0^{(1)}(0,\mathcal{E}) P_{\mathcal{E}}.$$
(6.72)

This can be (quasi)singular, if the final \underline{or} intermediate state lies in the model space. If there is a model-space state only at the final state, the counterterm will lead – in complete analogy with the previous case (6.69) – to the contribution

$$\frac{\delta \mathcal{G}^{(0)}(t, \mathcal{E}'', \mathcal{E})}{\delta \mathcal{E}} P_{\mathcal{E}''} W_0^{(2)} P_{\mathcal{E}'}, \tag{6.73}$$

where

$$P_{\mathcal{E}''}W_0^{(2)}P_{\mathcal{E}'} = P_{\mathcal{E}''}V_{\rm sp}(\mathcal{E})\Gamma_{\mathcal{Q}}(\mathcal{E})V_{\rm sp}(\mathcal{E})P_{\mathcal{E}}$$
(6.74)

is the second-order *effective interaction without any intermediate model-space state*. If there is an intermediate model-space state in the second-order evolution operator (6.72), we have

$$U_0^{(1)}(t,\mathcal{E})P_{\mathcal{E}'}U_0^{(1)}(0,\mathcal{E})P_{\mathcal{E}} = U_0(t,\mathcal{E})\frac{P_{\mathcal{E}'}}{\mathcal{E}-\mathcal{E}'}V_{\rm sp}(\mathcal{E})P_{\mathcal{E}}.$$
 (6.75)

The singularity will here be eliminated in a similar way by the corresponding counterterm (6.64). If also the final state lies in the model space, there is an additional singularity, which is eliminated by replacing $U_0^{(1)}(t,\mathcal{E})$ by the corresponding Green's operator (6.69), yielding for the entire second-order Green's operator

$$\mathcal{G}^{(2)}(t,\mathcal{E})P_{\mathcal{E}} = \mathcal{G}^{(0)}(t,\mathcal{E})\Gamma_{Q}(\mathcal{E})V\mathcal{E})\Gamma_{Q}(\mathcal{E})V\mathcal{E})P_{\mathcal{E}} + \frac{\delta\mathcal{G}^{(0)}(t,\mathcal{E}'',\mathcal{E})}{\delta\mathcal{E}}P_{\mathcal{E}''}W_{0}^{(2)}P_{\mathcal{E}} + \frac{\delta\mathcal{G}^{(1)}(t,\mathcal{E}',\mathcal{E})}{\delta\mathcal{E}}P_{\mathcal{E}'}V_{sp}P_{\mathcal{E}}.$$
(6.76)

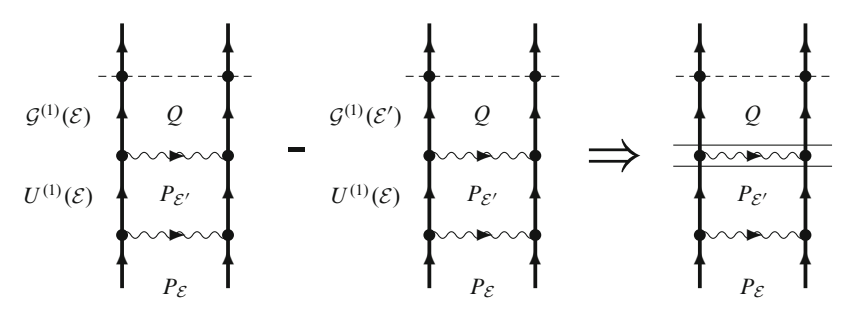


Fig. 6.9 Elimination of singularity of the second-order evolution operator, due to an intermediate model-space state. This leads to a residual contribution that corresponds to the folded diagram in standard many-body perturbation theory (Fig. 2.5). In addition, there can be a singularity at the final state, as in first order (see Fig. 6.8)

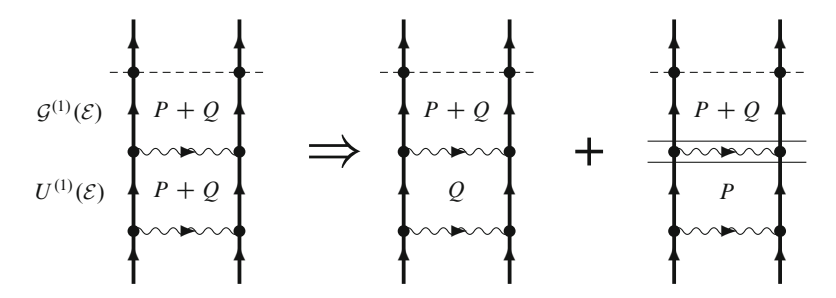


Fig. 6.10 Elimination of the singularity of the second-order evolution operator due to an intermediate model-space state

The second-order elimination process, due to intermediate model-space state, is illustrated in Fig. 6.9, and the corresponding part of the Green's operator is illustrated in Fig. 6.10. This process is quite analogous to the appearance of *folded diagram*, discussed in connection with standard MBPT (2.81). Since we are here dealing with Feynman diagrams, it is more logical to draw the "folded" part straight, indicating the position of the "fold" by a double bar from which the denominators of the upper part are to be evaluated. (The elimination process in first order has no analogy in standard MBPT, since there final model-space states do not appear in the wave function.)

For t = 0, we have from (6.76)

$$Q\mathcal{G}^{(2)}(0,\mathcal{E})P_{\mathcal{E}} = \Gamma_{\mathcal{Q}}(\mathcal{E})V_{\rm sp}(\mathcal{E})\Gamma_{\mathcal{Q}}(\mathcal{E})V_{\rm sp}(\mathcal{E})P_{\mathcal{E}} + Q\frac{\delta\mathcal{G}^{(1)}(t,\mathcal{E}',\mathcal{E})}{\delta\mathcal{E}}P_{\mathcal{E}'}V_{\rm eff}^{(1)}P_{\mathcal{E}},$$
(6.77)

which is quite analogous to the corresponding second-order wave operator in ordinary time-independent perturbation theory (2.69). The only difference is here that

the derivative of the first-order Green's operator leads in addition to the standard folded term to a term with the energy-derivative of the interaction. The latter term is sometimes referred to as the *reference-state contribution* [12], but here we shall refer to both terms as the *model-space contribution* (MSC), which is more appropriate in the general multireference case.

We have assumed so far that in the ladder the interactions are identical. If the interactions are different, some precaution is required. We see in the second-order expression that the differential/derivative in the last term should refer to the SEC-OND interaction, while if we treat this in an order-by-order fashion, we would get the differential of the FIRST interaction. If the interactions are in order V_1 and V_2 , then last term above becomes

$$\frac{\delta(\Gamma_Q V_2)}{\delta \mathcal{E}} P_{\mathcal{E}'} V_1 P_{\mathcal{E}} \tag{6.78}$$

(leaving out the arguments). This issue will be further discussed below.

6.7.2 All Orders*

The procedure performed above can be generalized to all orders of perturbation theory. We still consider a two-particle system in the ladder approximation. The treatment here follows mainly those of [10, 11] but is more general.

We consider an evolution operator in the form of a ladder (6.21) with a general interaction, $V(\mathcal{E})$, and with all <u>intermediate</u> model-space states removed, including also the zeroth-order term,

$$U_0(t,\mathcal{E})P_{\mathcal{E}} = \mathcal{G}^{(0)}(t,\mathcal{E})\left(1 + \Gamma(\mathcal{E})V(\mathcal{E}) + \Gamma(\mathcal{E})V(\mathcal{E})\Gamma_{\mathcal{Q}}(\mathcal{E})V(\mathcal{E}) + \cdots\right)P_{\mathcal{E}},$$
(6.79)

which may have a $\underline{\text{final}}$ model-space state. The corresponding Green's operator is according to (6.64)

$$U_0(t,\mathcal{E})P_{\mathcal{E}} - \mathcal{G}^{(0)}(t,\mathcal{E}) \cdot P_{\mathcal{E}'} \left(U_0(0,\mathcal{E}) - 1 \right) P_{\mathcal{E}}, \tag{6.80}$$

which can be expressed

$$QU_0(t,\mathcal{E})P_{\mathcal{E}} + \delta\mathcal{G}^{(0)}(t,\mathcal{E}',\mathcal{E}) \cdot P_{\mathcal{E}'} \left(U_0(0,\mathcal{E}) - 1 \right) P_{\mathcal{E}}. \tag{6.81}$$

But in analogy with (6.68), we have

$$P_{\mathcal{E}'}\left(U_0(0,\mathcal{E}) - 1\right)P_{\mathcal{E}} = \frac{P_{\mathcal{E}'}W_0(\mathcal{E})P_{\mathcal{E}}}{\mathcal{E} - \mathcal{E}'},\tag{6.82}$$

where W_0 is the effective interaction without intermediate model-space states or folds, in analogy with (6.74),

$$W_0(\mathcal{E})P_{\mathcal{E}} = (V(\mathcal{E}) + V(\mathcal{E})\Gamma_O(\mathcal{E})V(\mathcal{E}) + \cdots)P_{\mathcal{E}}.$$
(6.83)

Then the relation (6.81) becomes

$$QU_0(t,\mathcal{E})P_{\mathcal{E}} + \frac{\delta \mathcal{G}^{(0)}(t,\mathcal{E}',\mathcal{E})}{\delta \mathcal{E}} P_{\mathcal{E}'}W_0P_{\mathcal{E}}.$$
 (6.84)

The second term eliminates the singularity due to the <u>final</u> model-space state, and we shall refer also to this as a *folded contribution*, in analogy with those eliminating intermediate model-space singularities.

The Green's operator with no folds (intermediate or final) is

$$\mathcal{G}_{0}(t,\mathcal{E})P_{\mathcal{E}} = \mathcal{G}^{(0)}(t,\mathcal{E})P_{\mathcal{E}} + QU_{0}(t,\mathcal{E})P_{\mathcal{E}}$$

$$= \mathcal{G}^{(0)}(t,\mathcal{E})\left(1 + \Gamma_{\mathcal{Q}}(\mathcal{E})V(\mathcal{E}) + \Gamma_{\mathcal{Q}}(\mathcal{E})V(\mathcal{E})\Gamma_{\mathcal{Q}}(\mathcal{E})V(\mathcal{E}) + \cdots\right)P_{\mathcal{E}}.$$
(6.85)

The evolution operator with exactly one <u>intermediate</u> model-space state can be expressed $(\mathcal{G}^{(0)}(0)=1)$

$$QU_0(t,\mathcal{E})P_{\mathcal{E}'}(U_0(0,\mathcal{E})-1)P_{\mathcal{E}}$$
(6.86)

and the folded part of (6.84) provides a final fold, yielding the Green's operator with one intermediate or final fold,

$$\mathcal{G}_1(t,\mathcal{E}) = \frac{\delta \mathcal{G}_0(t,\mathcal{E},\mathcal{E}')}{\delta \mathcal{E}} P_{\mathcal{E}'} W_0 P_{\mathcal{E}}. \tag{6.87}$$

The evolution operator with two intermediate folds can be expressed in analogy with (6.86)

$$U_2(t,\mathcal{E})P_{\mathcal{E}} = QU_0(t,\mathcal{E})P_{\mathcal{E}'}(U_0(0,\mathcal{E}) - 1)P_{\mathcal{E}'}(U_0(0,\mathcal{E}) - 1)P_{\mathcal{E}}.$$
 (6.88)

The two leftmost factors represent the Green's operator (6.86) with one intermediate fold, and including also a final fold we can replace this by the operator (6.87)

$$\mathcal{G}_1(t,\mathcal{E}')P_{\mathcal{E}''}(U_0(0,\mathcal{E})-1)P_{\mathcal{E}}.$$

This represents the operator with exactly two intermediate <u>or</u> final model-space state with the singularity due to the leftmost one being eliminated. Eliminating also the second fold leads to the Green's operator with two folds

$$\mathcal{G}_2(t,\mathcal{E})P_{\mathcal{E}} = \frac{\delta \mathcal{G}_1(t,\mathcal{E}',\mathcal{E})}{\delta \mathcal{E}} P_{\mathcal{E}'}W_0(\mathcal{E})P_{\mathcal{E}}. \tag{6.89}$$

Continuing this process leads to (with somewhat simplified notations)

$$\mathcal{G}(t,\mathcal{E})P_{\mathcal{E}} = \left(\mathcal{G}_{0}(t,\mathcal{E}) + \mathcal{G}_{1}(t,\mathcal{E}) + \mathcal{G}_{2}(t,\mathcal{E}) + \cdots\right)P_{\mathcal{E}}$$

$$= \left[\mathcal{G}_{0}(t,\mathcal{E}) + \left(\frac{\delta\mathcal{G}_{0}(t,\mathcal{E})}{\delta\mathcal{E}} + \frac{\delta\mathcal{G}_{1}(t,\mathcal{E})}{\delta\mathcal{E}} + \cdots\right)W_{0}\right]P_{\mathcal{E}}.$$

This yields

$$\mathcal{G}(t,\mathcal{E})P_{\mathcal{E}} = \mathcal{G}_0(t,\mathcal{E})P_{\mathcal{E}} + \frac{\delta \mathcal{G}(t,\mathcal{E})}{\delta \mathcal{E}} W_0 P_{\mathcal{E}}.$$
(6.90)

Here, the second term represents all intermediate/final folds (model-space contributions). This relation is *valid for the entire model space* and it is consistent with [11, Eq. (6.54)] but more general. The expressions given here are *valid for all times* and for the final state in P as well as Q spaces. The corresponding wave-operator relation is obtained by setting t = 0.

We can find an alternative expression for the folded term in (6.90) by considering

$$\mathcal{G} = \mathcal{G}_0 + \mathcal{G}_1 + \mathcal{G}_2 + \cdots.$$

From the expressions above, we find

$$\mathcal{G}_{1} = \frac{\delta \mathcal{G}_{0}}{\delta \mathcal{E}} W_{0}
\mathcal{G}_{2} = \frac{\delta \mathcal{G}_{1}}{\delta \mathcal{E}} W_{0} = \frac{\delta}{\delta \mathcal{E}} \left(\frac{\delta \mathcal{G}_{0}}{\delta \mathcal{E}} W_{0} \right) W_{0} = \frac{\delta^{2} \mathcal{G}_{0}}{\delta \mathcal{E}^{2}} W_{0}^{2} + \frac{\delta \mathcal{G}_{0}}{\delta \mathcal{E}} \frac{\delta W_{0}}{\delta \mathcal{E}} W_{0}
= \frac{\delta^{2} \mathcal{G}_{0}}{\delta \mathcal{E}^{2}} W_{0}^{2} + \frac{\delta \mathcal{G}_{0}}{\delta \mathcal{E}} W_{1}$$
(6.91)

with

10

$$W_n = \frac{\delta W_{n-1}}{\delta \mathcal{E}} W_0 \tag{6.92}$$

being the effective interaction with exactly n folds. Similarly, 10

$$\begin{split} \frac{\delta \mathcal{G}}{\delta \mathcal{E}} &= \frac{\mathcal{G}_{\mathcal{E}} - \mathcal{G}_{\mathcal{E}'}}{\mathcal{E} - \mathcal{E}'}; \quad \frac{\delta}{\delta \mathcal{E}} \left(\frac{\delta \mathcal{G}}{\delta \mathcal{E}} V \right) = \frac{\left(\frac{\delta \mathcal{G}}{\delta \mathcal{E}} \right)_{\mathcal{E}} V_{\mathcal{E}} - \left(\frac{\delta \mathcal{G}}{\delta \mathcal{E}} \right)_{\mathcal{E}'} V_{\mathcal{E}'}}{\mathcal{E} - \mathcal{E}'} \\ &= \frac{\left(\frac{\delta \mathcal{G}}{\delta \mathcal{E}} \right)_{\mathcal{E}} V_{\mathcal{E}} - \left(\frac{\delta \mathcal{G}}{\delta \mathcal{E}} \right)_{\mathcal{E}'} V_{\mathcal{E}} + \left(\frac{\delta \mathcal{G}}{\delta \mathcal{E}} \right)_{\mathcal{E}'} V_{\mathcal{E}} - \left(\frac{\delta \mathcal{G}}{\delta \mathcal{E}} \right)_{\mathcal{E}'} V_{\mathcal{E}'}}{\mathcal{E} - \mathcal{E}'} = \frac{\delta^2 \mathcal{G}}{\delta \mathcal{E}} V + \frac{\delta \mathcal{G}}{\delta \mathcal{E}} \frac{\delta V}{\delta \mathcal{E}} \\ &\frac{\delta}{\delta \mathcal{E}} V^2 = \frac{\delta}{\delta \mathcal{E}} V_{\mathcal{E}''} V_{\mathcal{E}} = V_{\mathcal{E}''} \frac{V_{\mathcal{E}} - V_{\mathcal{E}'}}{\mathcal{E} - \mathcal{E}'} = V \frac{\delta V}{\delta \mathcal{E}}. \end{split}$$

This can be generalized to

$$\frac{\delta^n(AB)}{\delta \mathcal{E}^n} = \sum_{m=0}^n \frac{\delta^m A}{\delta \mathcal{E}^m} \frac{\delta^{n-m} B}{\delta \mathcal{E}^{n-m}}$$

(see further [11, Appendix B]).

$$\mathcal{G}_{3} = \frac{\delta \mathcal{G}_{2}}{\delta \mathcal{E}} W_{0}$$

$$= \frac{\delta^{3} \mathcal{G}_{0}}{\delta \mathcal{E}^{3}} W_{0}^{3} + \frac{\delta^{2} \mathcal{G}_{0}}{\delta \mathcal{E}^{2}} \frac{\delta W_{0}}{\delta \mathcal{E}} W_{0}^{2} + \frac{\delta^{2} \mathcal{G}_{0}}{\delta \mathcal{E}^{2}} W_{1} W_{0} + \frac{\delta \mathcal{G}_{0}}{\delta \mathcal{E}} \frac{\delta W_{1}}{\delta \mathcal{E}} W_{0}$$

or

$$\mathcal{G}_3 = \frac{\delta^3 \mathcal{G}_0}{\delta \mathcal{E}^3} W_0^3 + \frac{\delta^2 \mathcal{G}_0}{\delta \mathcal{E}^2} 2W_1 W_0 + \frac{\delta \mathcal{G}_0}{\delta \mathcal{E}} W_2.$$

Summing this sequence leads to

$$\mathcal{G} = \mathcal{G}_0 + \frac{\delta \mathcal{G}_0}{\delta \mathcal{E}} \left(W_0 + W_1 + W_2 + \cdots \right)$$

+
$$\frac{\delta^2 \mathcal{G}_0}{\delta \mathcal{E}^2} \left(W_0^2 + 2W_0 W_1 + \cdots \right) + \frac{\delta^3 \mathcal{G}_0}{\delta \mathcal{E}^3} \left(W_0^3 + \cdots \right) + \cdots .$$
 (6.93)

It can be shown by induction [10] that this leads to

$$\mathcal{G} = \mathcal{G}_0 + \sum_{n=1}^{\infty} \frac{\delta^n \mathcal{G}_0}{\delta \mathcal{E}^n} \left(W_0 + W_1 + W_2 + \cdots \right)^n. \tag{6.94}$$

Here,

$$V_{\text{eff}} = W_0 + W_1 + W_2 + \cdots \tag{6.95}$$

is the total effective interaction, which leads to

$$\mathcal{G}(t,\mathcal{E})P_{\mathcal{E}} = \mathcal{G}_0(t,\mathcal{E})P_{\mathcal{E}} + \sum_{n=1}^{\infty} \frac{\delta^n \mathcal{G}_0(t,\mathcal{E})}{\delta \mathcal{E}^n} \left(V_{\text{eff}}\right)^n P_{\mathcal{E}}.$$
 (6.96)

This relation is consistent with the results in [10, Eq. (100)] and [11, Eq. (61)], where more details of the derivations are given. As the previous relation (6.90), it is *valid for all times* and with the final state in Q as well as P space. In case the interactions are different, *the derivatives should be taken of the latest interactions*.

We can generalize the treatment here and replace the single-photon potential by the two-body part of the complete irreducible multiphoton exchange potential (6.22) in Fig. 6.6, $V \Rightarrow V_2 = V$.

It follows from the treatment here that the counterterms eliminate all singularities so that *the Green's operator is completely regular at all times*.

6.7.2.1 Linkedness of the Green's Operator

All parts of the expansions above are linked, so this demonstrates that

- The Green's operator is completely linked also in the multireference case.
- The *linkedness of the single-particle Green's operator* can be expressed, using (6.4),

$$\mathcal{G}^{1}(t,t_{0}) = \left[\sum_{n=0}^{\infty} \frac{1}{n!} \iint d^{3}x \, d^{3}x_{0} \, \left(\frac{-i}{c} \right)^{n} \int d^{4}x_{1} \cdots \int d^{4}x_{n} \right]$$

$$\times \langle 0 | T \left[\hat{\rho}(x) \, \mathcal{H}(x_{1}) \cdots \mathcal{H}(x_{n}) \, \hat{\rho}(x_{0}) \right] | 0 \rangle \, e^{-\gamma(|t_{1}| + |t_{2}| \cdots)} \right]_{\text{linked+folded}}$$
(6.97)

and similarly in the many-particle case.

• This represents a field-theoretical extension of the linked-diagram theorem of standard many-body perturbation theory (2.82).

6.8 Bloch Equation for Green's Operator*

We now want to transform the general expression above for the Green's operator into a general Bloch-type of equation (2.56) that, in principle, can be solved iteratively (self-consistently). Iterations can be performed, only if the in- and outgoing states contain only particle states of positive energy (no holes). Therefore, we assume this to be the case. If we have an interaction with hole states in or out, we can apply a Coulomb interaction, so that all in- and outgoing states are particle states, as will be discussed further in later chapters.

We still work in the *restricted Hilbert space* with complete single-photon (or multiphoton) interactions.

We want to have an equation of the form

$$\left[\mathcal{G}^{(n)}, H_0\right] P = V \mathcal{G}^{(n-1)} P + \text{folded}$$
(6.98)

or

$$\mathcal{G}^{(n)}P_{\mathcal{E}} = \mathcal{G}^{(0)}P_{\mathcal{E}} + \Gamma_{\mathcal{Q}}\left(V\mathcal{G}^{(n-1)} + \text{folded}\right)P_{\mathcal{E}},\tag{6.99}$$

where *V* is the *last* interaction.

We start from the relation (6.90),

$$\mathcal{G} = \mathcal{G}_0 + \frac{\delta \mathcal{G}}{\delta \mathcal{E}} W_0, \tag{6.100}$$

where

$$G = G_0 + G_1 + G_2 + \cdots$$

and \mathcal{G}_m is the operator with exactly m intermediate/final folds,

$$\mathcal{G}_m = \frac{\delta \mathcal{G}_{m-1}}{\delta \mathcal{E}} W_0.$$

Furthermore, the total effective interaction is (6.95)

$$V_{\text{eff}} = W_0 + W_1 + W_2 + \cdots$$
 (6.101)

where W_m is the effective interaction (6.92) with m folds and

$$W_m = \frac{\delta W_{m-1}}{\delta \mathcal{E}} W_0. \tag{6.102}$$

The folded contribution of order n > 0 is according to (6.99)

$$\mathcal{G}^{(n)} - \Gamma_Q V \mathcal{G}^{(n-1)} - \mathcal{G}^{(0)} = \mathcal{G}_0^{(n)} - \Gamma_Q V \mathcal{G}_0^{(n-1)} - \mathcal{G}^{(0)} + \mathcal{G}_1^{(n)} - \Gamma_Q V \mathcal{G}_1^{(n-1)} + \mathcal{G}_2^{(n)} - \Gamma_Q V \mathcal{G}_2^{(n-1)} + \cdots$$

We then see that in the case of no folds we have (6.85)

$$\mathcal{G}_0^{(n)} - \Gamma_Q V \mathcal{G}_0^{(n-1)} - \mathcal{G}^{(0)} = 0. \tag{6.103}$$

In the case of a single fold, we have

$$\Delta_1 = \mathcal{G}_1^{(n)} - \Gamma_Q V \mathcal{G}_1^{(n-1)} = \left(\frac{\delta \mathcal{G}_0}{\delta \mathcal{E}} W_0\right)^{(n)} - \Gamma_Q V \left(\frac{\delta \mathcal{G}_0}{\delta \mathcal{E}} W_0\right)^{(n-1)}.$$

Here, all terms cancel except those where the last factor of $\Gamma_Q V$ is being differentiated in the first part of Δ_1 and, in addition, terms with a fold in the final state. Obviously, those terms do not appear in the second part of the difference. This yields¹¹

$$\Delta_1 = \left(\frac{\delta^* \mathcal{G}_0}{\delta \mathcal{E}} W_0\right)^{(n)},\tag{6.104}$$

$$\begin{split} \mathcal{G}_{0} &= \mathcal{G}^{(0)} \big(1 + \varGamma_{\mathcal{Q}} V_{1} + \varGamma_{\mathcal{Q}} V_{1} \varGamma_{\mathcal{Q}} V_{2} + \cdots \big) \\ \Delta_{1} &= \Big[\frac{\delta \mathcal{G}_{0}}{\delta \mathcal{E}} - \varGamma_{\mathcal{Q}} V_{1} \frac{\delta \mathcal{G}_{0}}{\delta \mathcal{E}} \Big] W_{0} = \Big[\frac{\delta \mathcal{G}^{(0)}}{\delta \mathcal{E}} + \mathcal{G}_{0} \frac{\delta (\varGamma_{\mathcal{Q}} V_{1})}{\delta \mathcal{E}} \left(1 + \varGamma_{\mathcal{Q}} V_{2} + \cdots \right) \Big] W_{0} \\ &= : \frac{\delta^{*} \mathcal{G}_{1}}{\delta \mathcal{E}} \Big[\frac{\delta^{2} \mathcal{G}_{0}}{\delta \mathcal{E}^{2}} - \varGamma_{\mathcal{Q}} V_{1} \frac{\delta^{2} \mathcal{G}_{0}}{\delta \mathcal{E}^{2}} \Big] W_{0} \\ &= \Big[\frac{\delta^{2} \mathcal{G}^{(0)}}{\delta \mathcal{E}^{2}} + \frac{\delta \mathcal{G}^{(0)}}{\delta \mathcal{E}} \frac{\delta (\varGamma_{\mathcal{Q}} V_{1})}{\delta \mathcal{E}} \left(1 + \varGamma_{\mathcal{Q}} V_{2} + \cdots \right) + \mathcal{G}^{(0)} \frac{\delta^{2} (\varGamma_{\mathcal{Q}} V_{1})}{\delta \mathcal{E}^{2}} \left(1 + \varGamma_{\mathcal{Q}} V_{2} + \cdots \right) \\ &+ \mathcal{G}^{(0)} \frac{\delta (\varGamma_{\mathcal{Q}} V_{1})}{\delta \mathcal{E}} \frac{\delta (\varGamma_{\mathcal{Q}} V_{2})}{\delta \mathcal{E}} \left(1 + \varGamma_{\mathcal{Q}} V_{3} + \cdots \right) + \cdots \Bigg] W_{0} = : \frac{\delta^{*} \mathcal{G}_{1}}{\delta \mathcal{E}}. \end{split}$$

¹¹ Distinguishing the various interactions, we can write

where we have introduced the notation δ^* , with the asterisk indicating that the differentiation applies only to the last interaction, including the associated resolvent, $\Gamma_Q V$,

$$\frac{\delta^*(\Gamma_Q V_a \Gamma_Q V_b \cdots)}{\delta \mathcal{E}} = \frac{\delta(\Gamma_Q V_a)}{\delta \mathcal{E}} \, \Gamma_Q V_b \cdots \tag{6.105}$$

and, in addition, differentiation of $\mathcal{G}^{(0)}$ in case there is no $\Gamma_Q V$ factor. In the case of two folds, we have

$$\begin{split} \Delta_2 &= \mathcal{G}_2^{(n)} - \varGamma_{\mathcal{Q}} V \mathcal{G}_2^{(n-1)} = \left(\frac{\delta \mathcal{G}_1}{\delta \mathcal{E}} \, W_0\right)^{(n)} - \varGamma_{\mathcal{Q}} V \left(\frac{\delta \mathcal{G}_1}{\delta \mathcal{E}} \, W_0\right)^{(n-1)} \\ &= \left[\frac{\delta}{\delta \mathcal{E}} \left(\frac{\delta \mathcal{G}_0}{\delta \mathcal{E}} \, W_0\right) \, W_0\right]^{(n)} \\ &- \varGamma_{\mathcal{Q}} V \left[\frac{\delta}{\delta \mathcal{E}} \left(\frac{\delta \mathcal{G}_0}{\delta \mathcal{E}} \, W_0\right) \, W_0\right]^{(n-1)} \\ &= \left[\frac{\delta^2 \mathcal{G}_0}{\delta \mathcal{E}^2} \, (W_0)^2\right]^{(n)} - \varGamma_{\mathcal{Q}} V \left[\frac{\delta^2 \mathcal{G}_0}{\delta \mathcal{E}^2} \, (W_0)^2\right]^{(n-1)} \\ &+ \left[\frac{\delta \mathcal{G}_0}{\delta \mathcal{E}} \, W_1\right]^{(n)} - \varGamma_{\mathcal{Q}} V \left[\frac{\delta \mathcal{G}_0}{\delta \mathcal{E}} \, W_1\right]^{(n-1)} \,. \end{split}$$

With the convention above, we can express the folds

$$\Delta_2 = \left(\frac{\delta^* \mathcal{G}_0}{\delta \mathcal{E}} W_1\right)^{(n)} + \left(\frac{\delta^* \mathcal{G}_1}{\delta \mathcal{E}} W_0\right)^{(n)}.$$

Continuing this process leads to the total folded contribution

$$\left(\frac{\delta^* \mathcal{G}_0}{\delta \mathcal{E}} + \frac{\delta^* \mathcal{G}_1}{\delta \mathcal{E}} + \dots + \dots\right) (W_0 + W_1 + \dots) = \frac{\delta^* \mathcal{G}}{\delta \mathcal{E}} V_{\text{eff}}$$

with differentiation with respect to the last factor of $\Gamma_Q V$ and to $\mathcal{G}^{(0)}$, when no factor of $\Gamma_Q V$ appears.

• We then have *the generalized Bloch equation* for an *arbitrary energy-dependent interaction* (V)

$$\mathcal{G} = \mathcal{G}^{(0)} + \Gamma_Q V \mathcal{G} + \frac{\delta^* \mathcal{G}}{\delta \mathcal{E}} V_{\text{eff}},$$
(6.106)

where $v_{\rm eff}$ is given by (6.101).

• This equation is *valid also when the interactions are different*, and then it can be expressed more explicitly as (n > 0)

$$\mathcal{G}^{(n)} = \Gamma_Q V_n \mathcal{G}^{(n-1)} + \sum_{m=0}^{n-1} \frac{\delta^* \mathcal{G}^{(m)}}{\delta \mathcal{E}} \left(V_{\text{eff}} \right)^{(n-m)}, \tag{6.107}$$

where V_n is the last interaction and the operator $\mathcal{G}^{(m)}$ is formed by the m last interactions.

We can check the formula (6.106) by considering the first few orders,

$$\mathcal{G}^{(0)} = e^{-it(\mathcal{E} - H_0)}
\mathcal{G}^{(1)} = \Gamma_Q V \mathcal{G}^{(0)} + \frac{\delta \mathcal{G}^{(0)}}{\delta \mathcal{E}} W_0^{(1)}
\mathcal{G}^{(2)} = \Gamma_Q V \mathcal{G}^{(1)} + \frac{\delta \mathcal{G}^{(0)}}{\delta \mathcal{E}} V_{\text{eff}}^{(2)} + \frac{\delta^* \mathcal{G}^{(1)}}{\delta \mathcal{E}} W_0^{(1)},$$
(6.108)

where the last term becomes

$$\frac{\delta^* \mathcal{G}^{(1)}}{\delta \mathcal{E}} W_0^{(1)} = \frac{\delta(\Gamma_Q V)}{\delta \mathcal{E}} \mathcal{G}^{(0)} W_0^{(1)} + \frac{\delta^2 \mathcal{G}^{(0)}}{\delta \mathcal{E}^2} (W_0^{(1)})^2.$$
 (6.109)

This can easily be shown to reproduce the expansions (6.90) and (6.96).

We can also illustrate the validity of the generalized Bloch equation (6.106) by considering the third-order case with *different interactions*, V_1, V_2, V_3 , (see Fig. 6.11). For simplicity, we assume t=0 and therefore make the replacement $\mathcal{G} \to \Omega$.

If there is no model-space state directly after the first interaction (Fig. 6.11a), the contribution becomes

$$\Omega^{(2)} \Gamma_Q V_1 P = \left(\Gamma_Q V_3 \Gamma_Q V_2 + \frac{\delta(\Gamma_Q V_3)}{\delta \mathcal{E}} P V_2 \right) \Gamma_Q V_1 P$$

using the second-order expression (6.78) with the last two interactions (V_2, V_3) .

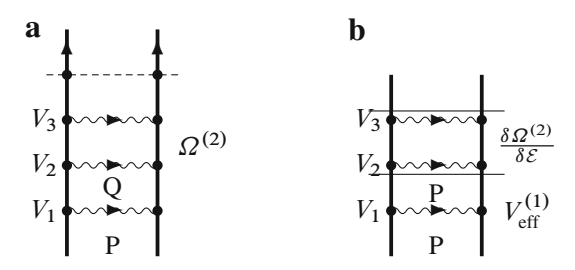


Fig. 6.11 Third-order Green's operator with different interactions

With a model-space state directly after the first interaction (Fig. 6.11b), the contribution is

$$\begin{split} \frac{\delta \Omega^{(2)}}{\delta \mathcal{E}} \, V_{\text{eff}}^{(1)} &= \frac{\delta}{\delta \mathcal{E}} \left(\varGamma_{\mathcal{Q}} V_3 \varGamma_{\mathcal{Q}} V_2 + \frac{\delta (\varGamma_{\mathcal{Q}} V_3)}{\delta \mathcal{E}} \, P \, V_2 \right) P \, V_1 P \\ &= \left(\frac{\delta \varGamma_{\mathcal{Q}} V_3}{\delta \mathcal{E}} \, \varGamma_{\mathcal{Q}} V_2 + \varGamma_{\mathcal{Q}} V_3 \, \frac{\delta \varGamma_{\mathcal{Q}} V_2}{\delta \mathcal{E}} + \frac{\delta^2 \varGamma_{\mathcal{Q}} V_3}{\delta \mathcal{E}^2} \, P \, V_2 \right. \\ &\quad \left. + \frac{\delta \varGamma_{\mathcal{Q}} V_3}{\delta \mathcal{E}} \, P \, \frac{\delta V_2}{\delta \mathcal{E}} \, P \right) P \, V_1 P. \end{split}$$

We can now identify the terms above with the Bloch equation (6.106), where the differentiation should apply to the last interaction. Then we have

$$\Gamma_{Q} V_{3} \Omega^{(2)} = \Gamma_{Q} V_{3} \Gamma_{Q} V_{2} \Gamma_{Q} V_{1} P + \Gamma_{Q} V_{3} \frac{\delta(\Gamma_{Q} V_{2})}{\delta \mathcal{E}} P V_{1} P
\frac{\delta^{*} \Omega^{(2)}}{\delta \mathcal{E}} V_{\text{eff}}^{(1)} = \frac{\delta \Gamma_{Q} V_{3}}{\delta \mathcal{E}} \Gamma_{Q} V_{2} P V_{1} P + \frac{\delta^{2} \Gamma_{Q} V_{3}}{\delta \mathcal{E}^{2}} P V_{2} P V_{1} P
\frac{\delta^{*} \Omega^{(1)}}{\delta \mathcal{E}} V_{\text{eff}}^{(2)} = \frac{\delta \Gamma_{Q} V_{3}}{\delta \mathcal{E}} \left(W_{0}^{(2)} + W_{1}^{(2)} \right)
= \frac{\delta \Gamma_{Q} V_{3}}{\delta \mathcal{E}} \left(P V_{2} \Gamma_{Q} V_{1} P + P \frac{\delta V_{2}}{\delta \mathcal{E}} P V_{1} P \right),$$

the sum of which is identical to the sum of the two previous expressions.

In most applications, we want to have an expression for the wave operator in the form of a Bloch equation, where we start from a wave operator $\Omega_{\rm I}$ and then add an interaction V that might be different from those involved in $\Omega_{\rm I}$. The Bloch equation is then of the form

$$\Omega P = (\Omega_{\rm I} + \Gamma_{\mathcal{Q}}(\mathcal{E})V\Omega_{\rm I} + \text{folded})P,$$

where we want to find the form of the folded part. We then make the replacement $\Omega_0 \Rightarrow \Gamma_Q V \Omega_{I0}$ in the expression (6.96), where Ω_{I0} is the wave operator without folds, yielding

$$\Omega = \sum_{n=0}^{\infty} \frac{\delta^n (\Gamma_Q V \Omega_{10})}{\delta \mathcal{E}^n} (V_{\text{eff}})^n.$$
 (6.110)

The sum can be reformulated as, noting the modified differentiating rules given above,

$$\Omega = \sum_{n=0}^{\infty} \frac{\delta^{n} (\Gamma_{Q} V \Omega_{10})}{\delta \mathcal{E}^{n}} (V_{\text{eff}})^{n} = \sum_{n=0}^{\infty} \sum_{m=0}^{\infty} \frac{\delta^{m} \Gamma_{Q} V}{\delta \mathcal{E}^{m}} (V_{\text{eff}})^{m} \frac{\delta^{n-m} \Omega_{10}}{\delta \mathcal{E}^{n-m}} (V_{\text{eff}})^{n-m}$$

$$= \sum_{m=0}^{\infty} \frac{\delta^{m} \Gamma_{Q} V}{\delta \mathcal{E}^{m}} (V_{\text{eff}})^{m} \sum_{n=m}^{\infty} \frac{\delta^{n-m} \Omega_{10}}{\delta \mathcal{E}^{n-m}} (V_{\text{eff}})^{n-m} = \sum_{m=0}^{\infty} \frac{\delta^{m} \Gamma_{Q} V}{\delta \mathcal{E}^{m}} \Omega_{1} (V_{\text{eff}})^{m}, \tag{6.111}$$

and this leads to the relation

$$\Omega = \Gamma_Q V \Omega_{\rm I} + \sum_{n=1}^{\infty} \frac{\delta^n (\Gamma_Q V)}{\delta \mathcal{E}^n} \Omega_{\rm I} (V_{\rm eff})^n.$$
 (6.112)

Since the full wave operator appears only on the left-hand side, this equation does not have to be solved self-consistently.

We can understand the appearance of the sequence of difference ratios above in the following way. Each model-space contribution (MSC) should contain a differentiation of all the following interactions. In $\Omega_{\rm I}$, the last interaction, $\mathcal V$, is not involved, and therefore a differentiation of $\Gamma_O V$ for each interaction in $\Omega_{\rm I}$ is required.

We can illustrate the formula above with the third-order case considered previously (Fig. 6.11), now assuming that we have two Coulomb interactions (V_C), followed by an energy-dependent potential (V). Then, we have instead

$$\Omega^{(3)}P = \Gamma_{Q}V\Gamma_{Q}V_{C}\Gamma_{Q}V_{C}P + \frac{\delta\Gamma_{Q}V}{\delta\mathcal{E}}PV_{C}\Gamma_{Q}V_{C}P + \frac{\delta^{2}\Gamma_{Q}V}{\delta\mathcal{E}}PV_{C}PV_{C}P - \Gamma_{Q}V\Gamma_{Q}^{2}V_{C}PV_{C}P + \frac{\delta^{2}\Gamma_{Q}V}{\delta\mathcal{E}^{2}}PV_{C}PV_{C}P,$$

which can be expressed

$$\begin{split} \varOmega^{(3)}P &= \varGamma_{Q} V \varOmega_{\mathrm{I}}^{(2)} P + \frac{\delta \varGamma_{Q} V}{\delta \mathcal{E}} \Big(\varOmega_{\mathrm{I}}^{(1)} V_{\mathrm{eff}}^{(1)} + \varOmega_{\mathrm{I}}^{(0)} V_{\mathrm{eff}}^{(2)} \Big) \\ &+ \frac{\delta^{2} \varGamma_{Q} V}{\delta \mathcal{E}^{2}} \, \varOmega_{\mathrm{I}}^{(0)} \Big(V_{\mathrm{eff}}^{(1)} \Big)^{2}, \end{split}$$

where

$$\Omega_{\rm I}^{(1)} = \Gamma_{Q} V_{\rm C} \qquad V_{\rm eff}^{(1)} = P V_{\rm C} P
\Omega_{\rm I}^{(2)} = \Gamma_{Q} V_{\rm C} \Gamma_{Q} V_{\rm C} - \Gamma_{Q}^{2} V_{\rm C} P V_{\rm C} P \qquad V_{\rm eff}^{(2)} = P V_{\rm C} \Gamma_{Q} V_{\rm C} P.$$

This is in agreement with the general formula (6.112).

6.9 Time Dependence of the Green's Operator. Connection to the Bethe-Salpeter Equation*

6.9.1 Single-Reference Model Space

Operating with the relation (6.96) on a model function, Ψ_0 , of energy E_0 , yields

$$\mathcal{G}(t, E_0) | \Psi_0 \rangle = \left[\mathcal{G}_0(t, \mathcal{E}) + \sum_{n=1}^{\infty} \frac{\delta^n \mathcal{G}_0(t, \mathcal{E})}{\delta \mathcal{E}^n} \left(\Delta E \right)^n \right]_{\mathcal{E} = E_0} | \Psi_0 \rangle. \tag{6.113}$$

We have here used the fact (6.44) that

$$V_{\text{eff}}|\Psi_0\rangle = (E - E_0)|\Psi_0\rangle = \Delta E|\Psi_0\rangle. \tag{6.114}$$

The expansion (6.113) is a Taylor series, and the result can be expressed

$$\boxed{\mathcal{G}(t, E_0)|\Psi_0\rangle = \mathcal{G}_0(t, E)|\Psi_0\rangle,}$$
(6.115)

where \mathcal{G}_0 is the Green's operator without model-space states (6.85). This implies that the sum in (6.113), representing

• the model-space contributions (MSC) to all orders, has the effect of shifting the energy parameter from the model energy E_0 to the target energy E.

From the relations (6.21) and (6.64), we have the Green's operator for the ladder *without MSC* in the present case, including also the zeroth order and the time factor,

$$\mathcal{G}_{0}(t, E_{0})|\Psi_{0}\rangle = e^{-it(E_{0}-H_{0})} \Big[1 + \Gamma_{Q}(E_{0}) V(E_{0}) + \Gamma_{Q}(E_{0}) V(E_{0}) V(E_{0}) + \cdots \Big] |\Psi_{0}\rangle.$$
 (6.116)

The result (6.115) then implies that the Green's operator <u>with</u> model-space contributions (MSC) becomes

$$\mathcal{G}(t, E_0)|\Psi_0\rangle = \mathcal{G}_0(t, E)|\Psi_0\rangle = e^{-it(E - H_0)} \times \left[1 + \Gamma_Q(E) V(E) + \Gamma_Q(E) V(E) \Gamma_Q(E) V(E) + \cdots\right] |\Psi_0\rangle.$$
(6.117)

• shifting also the energy parameter of the time dependence. 12

From this, it follows that

$$i\frac{\partial}{\partial t} \mathcal{G}(t, E_0) |\Psi_0\rangle = (E - H_0) \mathcal{G}(t, E_0) |\Psi_0\rangle$$
(6.118)

and, using (6.52),

$$\left(i\frac{\partial}{\partial t} \mathcal{G}(t, E_0)\right)_{t=0} |\Psi_0\rangle = (E - H_0) \Omega |\Psi_0\rangle. \tag{6.119}$$

¹² We observe here that also the zeroth-order term has changed its time dependence, which is a consequence of the fact that the zeroth-order Green's operator, $\mathcal{G}^{(0)}$, is being modified by the expansion (6.96).

According to (6.50), the Green's operator has the same time-dependence as the state vector, in the interaction picture

$$|\chi(t)\rangle = e^{-it(E - H_0)} |\Psi\rangle \tag{6.120}$$

(with $|\Psi\rangle = |\chi(0)\rangle$), which implies that the result above – which is a consequence of the initial conjecture (6.29) – is *in accordance with the elementary quantum-mechanical result* (2.15) and (3.2).

Setting the time t=0 yields with the identity (6.52), $\Omega |\Psi_0\rangle = \mathcal{G}(0, E_0)|\Psi_0\rangle$, the corresponding relation for the wave operator

$$|\Psi\rangle = \Omega|\Psi_0\rangle = \left[1 + \Gamma_Q(E)V(E) + \Gamma_Q(E)V(E)\Gamma_Q(E)V(E) + \cdots\right]|\Psi_0\rangle,$$
(6.121)

which is the Brillouin-Wigner expansion of the wave function.

From the relation (6.83), we have that the effective interaction without folds is

$$W_0(E_0)|\Psi_0\rangle = P\left(V(E_0) + V(E_0)\Gamma_Q(E_0)V(E_0) + \cdots\right)|\Psi_0\rangle.$$
 (6.122)

It can be shown in the same way as for the wave function that inclusion of the folds (MSC) leads to the replacement $E_0 \to E$ (see [10]) and to the expression for the full effective interaction (6.95)

$$V_{\text{eff}}|\Psi_0\rangle = W_0(E)|\Psi_0\rangle = P\left(V(E) + V(E)\Gamma_Q(E_0)V(E) + \cdots\right)|\Psi_0\rangle.$$

But according to the definition (6.44), $V_{\text{eff}} = P(H - H_0)\Omega P$, which gives

$$V_{\text{eff}} | \Psi_0 \rangle = P(H - H_0) \Omega P = P V(E) \Omega | \Psi_0 \rangle.$$
 (6.123)

This is an expression for the effective interaction in the restricted Hilbert space with no uncontracted photons, equivalent to the photonic-Fock-space relation (6.45). This is analogous to the MBPT result (2.55), but now the perturbation is *energy dependent*.

We can generalize this treatment by replacing the single-photon potential V by the *irreducible multiphoton potential* in Fig. 6.6, $V \Rightarrow V_2 = V$. Then we have from (6.117)

$$\mathcal{G}(t, E_0)|\Psi_0\rangle = \mathcal{G}_0(t, E)|\Psi_0\rangle = e^{-it(E - H_0)}
\times \left[1 + \Gamma_Q(E) \mathcal{V}(E) + \Gamma_Q(E) \mathcal{V}(E) \Gamma_Q(E) \mathcal{V}(E) + \cdots\right] |\Psi_0\rangle
(6.124)$$

and

$$|V_{\text{eff}}|\Psi_0\rangle = P(E - H_0)\Omega|\Psi_0\rangle = PV(E)\Omega|\Psi_0\rangle.$$
 (6.125)

From the relation, (6.118) we have

$$Q\left(i\frac{\partial}{\partial t} \mathcal{G}(t, E_0)\right)_{t=0} |\Psi_0\rangle = Q(E - H_0) \Omega |\Psi_0\rangle$$

$$= Q\left[\mathcal{V}(E) + \mathcal{V}(E)\Gamma_Q(E_0) \mathcal{V}(E) + \cdots\right] |\Psi_0\rangle$$

$$= Q\mathcal{V}(E) \Omega |\Psi_0\rangle.$$

Combining this with (6.125) leads to the Schrödinger-like equation in the restricted space

$$(H_0 + \mathcal{V}(E))|\Psi\rangle = E|\Psi\rangle$$
(6.126)

and an energy-dependent Hamilton operator

$$H = H_0 + \mathcal{V}(E). \tag{6.127}$$

These relation can be compared with the corresponding GML relations (6.32) and (6.39) in the photonic Fock space. The equation (6.126) is identical to the effective-potential form of the *Bethe–Salpeter equation* (9.20).

6.9.2 Multireference Model Space

We shall now investigate the time dependence of the Green's operator in a general, quasi-degenerate model space. We can express the relation (6.96), using the general perturbation, as

$$\mathcal{G}(t,\mathcal{E})P_{\mathcal{E}} = \mathcal{G}_0(t,\mathcal{E})P_{\mathcal{E}} + \sum_{n=1}^{\infty} \frac{\delta^n \mathcal{G}_0(t,\mathcal{E})}{\delta \mathcal{E}^n} \left(\mathcal{V}_{\text{eff}} \right)^n P_{\mathcal{E}}, \tag{6.128}$$

valid in the general multireference (quasi-degenerate) case, where $P_{\mathcal{E}}$ is the part of the model space with energy \mathcal{E} and \mathcal{V}_{eff} is given by (6.138). This can be formally expressed as an *operator relation*

$$\mathcal{G}(t, H_0^*)P = \mathcal{G}_0(t, H_0^*)P + \sum_{n=1}^{\infty} \frac{\delta^n \mathcal{G}_0(t, H_0^*)}{\delta(H_0^*)^n} \left(\mathcal{V}_{\text{eff}}^*\right)^n P, \tag{6.129}$$

valid in the entire model space. We have here introduced the symbol A^* , which implies that the operator A operates directly on the model-space state to the right. Thus, $H_0^*BP_{\mathcal{E}} = \mathcal{E}BP_{\mathcal{E}} = BH_0^*P_{\mathcal{E}}$. Similarly, $H_{\text{eff}}^*B|\Psi_0^{\alpha}\rangle = E^{\alpha}B|\Psi_0^{\alpha}\rangle = BH_{\text{eff}}^*|\Psi_0^{\alpha}\rangle$.

In analogy with (6.45), we have

$$V_{\text{eff}}|\Psi_0^{\alpha}\rangle = P(E^{\alpha} - H_0)\Omega|\Psi_0^{\alpha}\rangle = PV(E^{\alpha})\Omega|\Psi_0^{\alpha}\rangle \tag{6.130}$$

or in operator form

$$\mathcal{V}_{\text{eff}}^* P = P(H_{\text{eff}}^* - H_0) \Omega P = P \mathcal{V}(H_{\text{eff}}^*) \Omega P. \tag{6.131}$$

The relation (6.129) is a Taylor expansion in analogy with (6.115), yielding

$$\boxed{\mathcal{G}(t, H_0^*) P = \mathcal{G}_0(t, H_{\text{eff}}^*) P}$$
(6.132)

using the fact (6.44) that

$$H_{\text{eff}}^* = PH_0^*P + V_{\text{eff}}^*. \tag{6.133}$$

From (6.116), it follows

$$\mathcal{G}_{0}(t,\mathcal{E})P_{\mathcal{E}} = e^{-it(\mathcal{E}-H_{0})} \left[1 + \Gamma_{Q}(\mathcal{E}) \mathcal{V}(\mathcal{E}) + \Gamma_{Q}(\mathcal{E}) \mathcal{V}(\mathcal{E}) \Gamma_{Q}(\mathcal{E}) \mathcal{V}(\mathcal{E}) + \cdots \right] P_{\mathcal{E}}$$
(6.134)

or in operator form

$$\mathcal{G}_{0}(t, H_{0}^{*})P = e^{-it(H_{0}^{*} - H_{0})} \left[1 + \Gamma_{Q}(H_{0}^{*}) \mathcal{V}(H_{0}^{*}) + \Gamma_{Q}(H_{0}^{*}) \mathcal{V}(H_{0}^{*}) \mathcal{V}(H_{0}^{*}) \mathcal{V}(H_{0}^{*}) + \cdots \right] P.$$
(6.135)

This leads in analogy with (6.117), using the relation (6.115), to

$$\mathcal{G}(t, H_0^*)P = \mathcal{G}_0(t, H_{\text{eff}}^*)P = e^{-it(H_{\text{eff}}^* - H_0)} \left[1 + \Gamma_Q(H_{\text{eff}}^*) \mathcal{V}(H_{\text{eff}}^*) + \Gamma_Q(H_{\text{eff}}^*) \mathcal{V}(H_{\text{eff}}^*) \mathcal{V}(H_{\text{eff}}^*) \mathcal{V}(H_{\text{eff}}^*) + \cdots \right] P.$$
 (6.136)

From this, we conclude that

• the general time dependence of the Green's operator is given by

$$i\frac{\partial}{\partial t}\mathcal{G}(t, H_0^*)P = (H_{\text{eff}}^* - H_0)\mathcal{G}(t, H_0^*)P.$$
(6.137)

This gives with (6.133)

$$P\left(i\frac{\partial}{\partial t}\mathcal{G}(t, H_0^*)\right)_{t=0}P = \mathcal{V}_{\text{eff}}^*P,\tag{6.138}$$

which is the expected result.

In analogy with the single-reference case, the effective interaction becomes

$$V_{\text{eff}} = PV(H_{\text{eff}}^*)\Omega P \tag{6.139}$$

and the Schrödinger-like equation [10, Eq. (113)]

$$(6.140)$$

$$(H_0 + \mathcal{V}(E^{\alpha}))|\Psi^{\alpha}\rangle = E^{\alpha})|\Psi^{\alpha}\rangle.$$

This agrees with the equation derived in [10, Eq. (133)] and it is equivalent to the *Bethe-Salpeter-Bloch equation*, discussed in Chap. 9 (9.30).

References

- Adkins, G.: One-loop renormalization of Coulomb-gauge QED. Phys. Rev. D 27, 1814–20 (1983)
- Åsén, B.: QED effects in excited states of helium-like ions. Ph.D. thesis, Department of Physics, Chalmers University of Technology and University of Gothenburg, Gothenburg, Sweden (2002)
- 3. Bjorken, J.D., Drell, S.D.: Relativistic Quantum Fields. Mc-Graw-Hill Pbl. Co, N.Y. (196)
- 4. Bjorken, J.D., Drell, S.D.: *Relativistic Quantum Mechanics*. Mc-Graw-Hill Pbl. Co, N.Y. (1964)
- 5. E.Lindroth, Mårtensson-Pendrill, A.M.: Isotope Shifts and Energies of the 1s2p States in Helium. Z. Phys. A 316, 265–273 (1984)
- 6. Feynman, R.P.: *The Theory of Positrons*. Phys. Rev. **76**, 749–59 (1949)
- Lindgren, I.: Can MBPT and QED be merged in a systematic way? Mol. Phys. 98, 1159–1174 (2000)
- 8. Lindgren, I., Åsén, B., Salomonson, S., Mårtensson-Pendrill, A.M.: *QED procedure applied to the quasidegenerate fine-structure levels of He-like ions*. Phys. Rev. A **64**, 062,505 (2001)
- Lindgren, I., Salomonson, S., Åsén, B.: The covariant-evolution-operator method in boundstate QED. Physics Reports 389, 161–261 (2004)
- Lindgren, I., Salomonson, S., Hedendahl, D.: Many-body-QED perturbation theory: Connection to the two-electron Bethe-Salpeter equation. Einstein centennial review paper. Can. J. Phys. 83, 183–218 (2005)
- 11. Lindgren, I., Salomonson, S., Hedendahl, D.: Many-body procedure for energy-dependent perturbation: Merging many-body perturbation theory with QED. Phys. Rev. A 73, 062,502 (2006)
- 12. Mohr, P.J., Plunien, G., Soff, G.: *QED corrections in heavy atoms*. Physics Reports 293, 227–372 (1998)
- 13. Rosenberg, L.: Virtual-pair effects in atomic structure theory. Phys. Rev. A 39, 4377–86 (1989)
- Shabaev, V.M., Artemyev, A.N., Beier, T., Plunien, G., Yerokhin, V.A., Soff, G.: Recoil correction to the ground-state energy of hydrogenlike atoms. Phys. Rev. A 57, 4235–39 (1998)
- 15. Stuckelberg, E.C.G.: . Helv.Phys.Acta 15, 23 (1942)
- 16. Uehling, E.A.: Polarization Effects in the Positron Theory. Phys. Rev. 48, 55–63 (1935)
- 17. Wichmann, E.H., Kroll, N.M.: *Vacuum Polarization in a Strong Coulomb Field.* Phys. Rev. **101**, 843–59 (1956)

Chapter 7

Numerical Illustrations to Part II

In this chapter, we shall give some numerical illustrations of the three QED methods described in Part II, the S-matrix, the two-times Green's function, and the covariant-evolution-operator methods.

7.1 S-Matrix

7.1.1 Electron Self-Energy of Hydrogen-Like Ions

In the early days of quantum-electrodynamics, the effects were calculated analytically, applying a double expansion in α and $Z\alpha$. For high nuclear charge, Z, such an expansion does not work well, and it is preferable to perform the evaluation numerically to all orders of $Z\alpha$. The first numerical evaluations of the electron self-energy on heavy, many-electron atoms were performed by Brown et al. in late 1950s [14] and by Desiderio and Johnson in 1971 [18], applying a scheme devised by Brown, Langer, and Schaefer [13] (see Sect. 12.3).

An improved method for self-energy calculations, applicable also for lighter systems, was developed and successfully applied to hydrogen-like ions by Mohr [34, 39–42]. The energy shift due to the first-order electron self-energy is conventionally expressed as:

$$\Delta E = \frac{\alpha}{\pi} \frac{(Z\alpha)^4}{n^3} F(Z\alpha) mc^2$$
 (7.1)

where n is the main quantum number. The function $F(Z\alpha)$ is evaluated numerically, and some results are given in Table 7.1.

Performing accurate self-energy calculations for low Z is complicated due to slow convergence. Mohr has estimated the first-order Lamb shift (self-energy + vacuum polarization) by means of elaborate extrapolation from heavier elements and obtained the value 1057.864(14) MHz for the $2s - 2p_{1/2}$ shift in neutral hydrogen [40], in excellent agreement with the best experimental value at the time, 1057.893(20) MHz. More recently, Jentschura et al. [26] have extended the method

Table 7.1 The $F(Z\alpha)$ function for the ground state of hydrogen-like mercury

Table 7.2 Ground-state Lamb shift of hydrogen-like uranium (in eV, mainly from [43])

Reference	$F(Z\alpha)$
Desiderio and Johnson [18]	1.48
Mohr [38]	1.5032(6)
Blundell and Snyderman [9]	1.5031(3)
Mohr [34]	1.5027775(4)

Correction	Value	Reference
Nuclear size	198.82	
First-order self-energy	355.05	[34, 45]
Vacuum polarization	-88.59	[49]
Second-order effects	-1.57	
Nuclear recoil	0.46	
Nuclear polarization	-0.20	
Total theory	463.95	
Experimental	460.2(4.6	5)

of Mohr to calculate directly the self-energy of light elements down to hydrogen with extremely high accuracy. Accurate calculations have also been performed for highly excited states [27].

The original method of Mohr was limited to point-like nuclei but was extended to finite nuclei in a work with Gerhard Soff [45]. An alternative method also applicable to finite nuclei has been devised by Blundell and Snyderman [9, 10].

7.1.2 Lamb Shift of Hydrogen-Like Uranium

In high-energy accelerators, like that at GSI in Darmstadt, Germany, highly charged ions up to hydrogen-like uranium can be produced. For such systems the QED effects are quite large, and accurate comparison between experimental and theoretical results can here serve as an important test of the QED theory in extremely strong electromagnetic fields – a test that has never been performed before.

The first experimental determination of the Lamb-shift in hydrogen-like uranium was made by the GSI group (Stöhlker, Mokler et al.) in 1993 [56]. The result was 429(23) eV, a result that has gradually been improved by the group, and the most recent value is 460.2(4.6) eV [55]. The shift is here defined as the experimental binding energy compared to the Dirac theory for a *point nucleus*, implying that it includes also the effect of the finite nuclear size. In Table 7.2, we show the various contributions to the theoretical value. The self-energy contribution was evaluated by Mohr [34] and the finite-nuclear-size effect by Mohr and Soff [45]. The vacuum polarization, including the Wickmann–Kroll correction (see Sect. 4.6.3), was evaluated by Persson et al. [49]. The second-order QED effects, represented by the diagrams in Fig. 7.1, have also been evaluated. Most of the reducible part was evaluated by Persson et al. [48]. The last two irreducible too-loop diagrams are much more elaborate to calculate and have only recently been fully evaluated by Yerokhin et al. [60].

¹ See Sect. 2.6.

7.1 S-Matrix 159

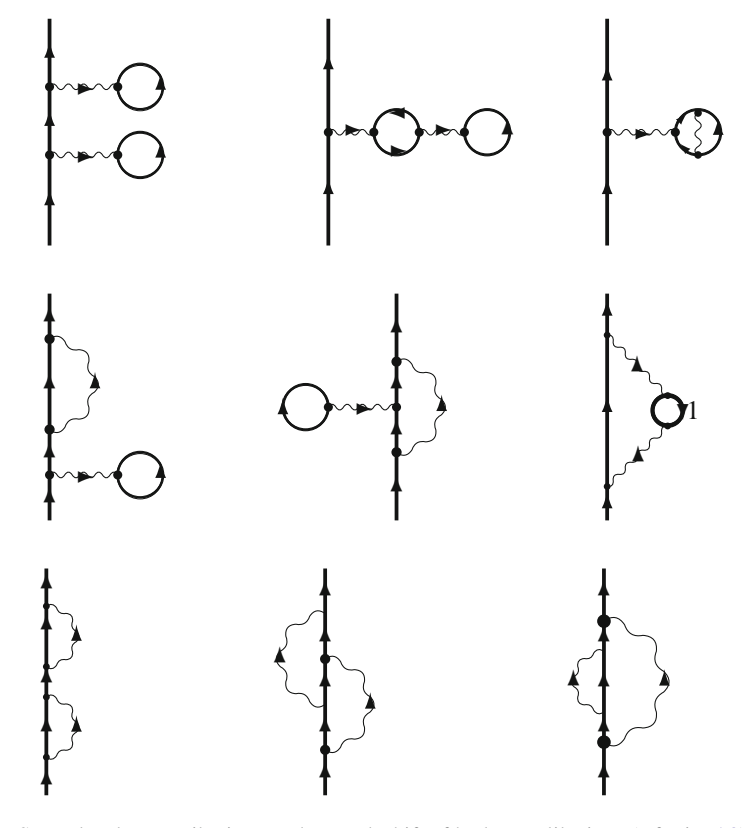


Fig. 7.1 Second-order contributions to the Lamb shift of hydrogen-like ions (c.f. Fig. 5.3)

The main uncertainty of the theoretical calculation on hydrogen-like uranium stems from the finite-nuclear-size effect, which represents almost half of the entire shift from the Dirac point-nuclear value. Even if the experimental accuracy would be significantly improved, it will hardly be possible to test with any reasonable accuracy the second-order QED effects, which are only about 1% of the nuclear-size effect. For that reason, other systems, like lithium-like ions, seem more promising for testing such effects.

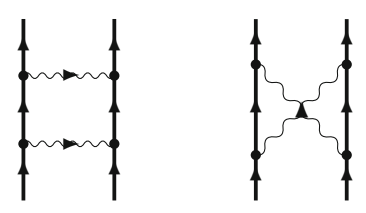
7.1.3 Lamb Shift of Lithium-Like Uranium

The $2s - 2p_{1/2}$ Lamb shift of lithium-like uranium was measured at the Berkeley HILAC accelerator by Schweppe et al. in 1991 [54]. The first theoretical evaluations of the self-energy was performed by Cheng et al. [15] and the complete first-order shift, including vacuum polarization, by Blundell [7], Lindgren et al. [31],

Correction	Ref. [7]	Ref. [48]	Ref. [58]
Relativistic MBPT	322.41	322.32	322.10
First-order self-energy	-53.94	-54.32	
First-order vacuum polarization	(12.56)	12.56	
First-order self-energy $+$ vac. pol.	-41.38	-41.76	-41.77
Second-order self-energy $+$ vac. pol.		0.03	0.17
Nuclear recoil	(0.10)	(-0.08)	-0.07
Nuclear polarization	(0.10)	(0.03)	-0.07
Total theory	280.83(10)	280.54(15)	280.48(20)
Experimental	280.59(9)		

Table 7.3 $2s - 2p_{1/2}$ Lamb shift of lithium-like uranium (in eV)

Fig. 7.2 Feynman diagrams representing the two-photon exchange (*ladder and cross*) for helium-like ions



and Persson et al. [48], the latter calculation including also some reducible second-order QED effects. Later, more complete calculations were performed by Yerokhin et al. [58]. The results are summarized in Table 7.3.

In lithium-like systems, the nuclear-size effect is considerably smaller than in the corresponding hydrogen-like system and can be more easily accounted for. The second-order QED effects in Li-like uranium are of the same order as the present uncertainties in theory and experiment, and with some improvement these effects can be tested. Therefore, systems of this kind seem to have the potential for the most accurate test of high-field QED at the moment.

7.1.4 Two-Photon Nonradiative Exchange in Helium-Like Ions

Accurate S-matrix calculations of the *nonradiative* two-photon exchange for helium-like ions (ladder and cross), corresponding to the Feynman diagrams in Fig. 7.2, have been performed by Blundell et al. [8] and Lindgren et al. [30]. The results are illustrated in Fig. 7.3 (taken from [30]). In the figure, the contributions are displayed *versus* the nuclear charge, relative to the zeroth-order nonrelativistic ionization energy, $Z^2/2$ (in atomic Hartree units). The vertical scale is logarithmic, so that -1 corresponds to α , -2 to α^2 , etc.

As comparison, we show in the top picture of Fig. 7.3 the energy contribution due to *first-order* Coulomb and Breit interactions as well as the first-order Lamb shift, corresponding to Feynman diagrams shown in the top line of Fig. 7.4.

For low Z, the first-order Coulomb interaction is proportional to Z, the first-order Breit interaction to $Z^3\alpha^2$, and the first-order Lamb shift to $Z^4\alpha^3$. For high

7.1 S-Matrix 161

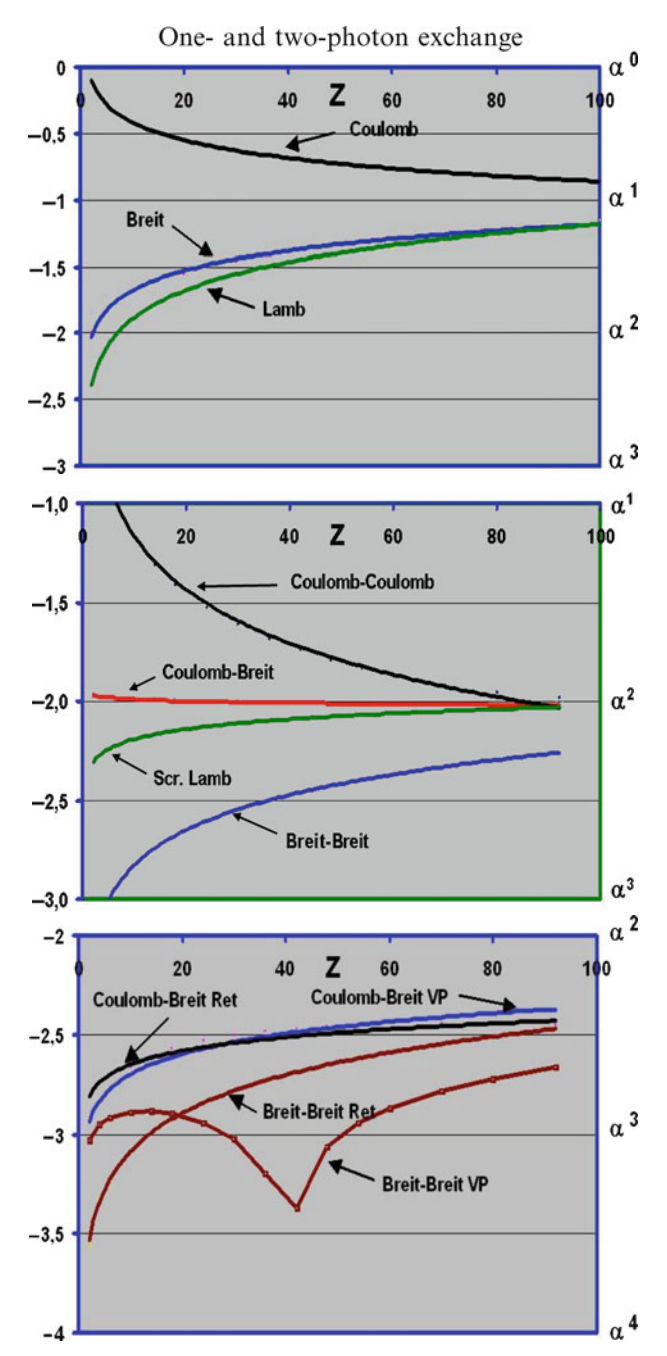


Fig. 7.3 Various contributions to the ground-state energy of He-like ions. The *top picture* represents the first-order contributions, the *middle picture* the second-order contributions in the NVPA as well as the screened Lamb shift, and the *bottom picture* contributions due to retardation and virtual pairs (see Fig. 7.4). The values are normalized to the nonrelativistic ionization energy, and the scale is logarithmic (powers of the fine-structure constant α)

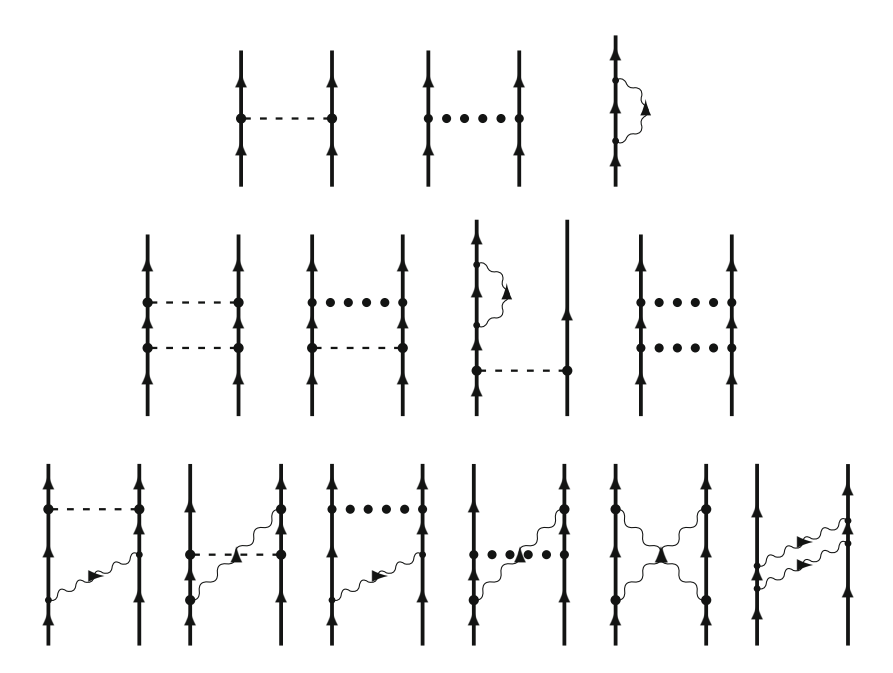


Fig. 7.4 Feynman diagrams representing the one- and two-photon exchange, separated into Coulomb, instantaneous Breit and retarded Breit interactions

Z, we can replace $Z\alpha$ by unity, and then after dividing by Z^2 , all first-order effects tend to α as Z increases, as is clearly seen in the top picture of Fig. 7.3 (see also Fig. 10.9 and Table 10.1).

An additional Coulomb interaction reduces the effect for small Z by a factor of Z. Therefore, the Coulomb–Coulomb interaction, i.e., the leading electron correlation, is in first order independent of Z and the Coulomb–Breit interaction proportional to $Z^2\alpha^2$. The screened Lamb shift is proportional to $Z^3\alpha^3$ and the second-order Breit interaction (in the no-pair approximation) to $Z^4\alpha^4$. After division with Z^2 , we see (second picture of Fig. 7.3) that all second-order effects tend to α^2 . The corresponding Feynman diagrams are shown in the second row of Fig. 7.4.

The third picture in Fig. 7.3 shows the effect of the retarded Coulomb–Breit and Breit–Breit interactions without and with virtual pairs, corresponding to diagrams in the bottom row of Fig. 7.4. For low Z, these effects are one order of α smaller than the corresponding unretarded interactions with no virtual pairs, while for high Z they tend – rather slowly – to the same α^2 limit. It is notable that for the Coulomb–Breit interactions the retardation and virtual pairs have nearly the same effect but with opposite sign. For the Breit–Breit interactions, the effects of single and double pairs have opposite sign and the total effect changes its sign around Z=40.

7.1 S-Matrix 163

Table 7.4 Two-photon effects on some excited states of helium-like ions (in μ.Hartree, from [44])

Z		$2^{3}S_{1}$	$2^{3}P_{0}$	$2^{3}P_{2}$
30	MBPT	-49 541	-88 752	- 75 352
	QED	-8.7	145	77.6
50	MBPT	-53762	$-123\ 159$	-79949
	QED	64	1340	767
80	MBPT	-66954	-251982	-93
	QED	966	9586	5482

Table 7.5 Two-electron effects on the ground-state energy of helium-like ions (in eV, from [50])

Z	Plante et al.	Indelicato et al.	Drake	Persson et al.	Expt'l
32	652.0	562.1	562.1	562.0	562.5±1.5
54	1,028.4	1,028.2	1,028.8	1,028.2	$1,027.2\pm3.5$
66	1,372.2	1,336.5	1,338.2	1,336.6	$1,341.6\pm4.3$
74	1,574.8	1,573.6	1,576.6	1,573.9	$1,568\pm15$
83		1,880.8	1,886.3	1,881.5	$1,876\pm14$

More recently, Mohr and Sapirstein have performed S-matrix calculations also on the excited states of helium-like ions and compared with second-order MBPT calculations to determine the effect of nonradiative QED, retardation, and virtual pairs [44], and some results are shown in Table 7.4.

7.1.5 Electron Correlation and QED Calculations on Ground States of Helium-Like Ions

The two-electron effect on the ground-state energy of some helium-like ions has been measured by Marrs et al. at Livermore Nat. Lab. by comparing the ionization energies of the corresponding helium-like and hydrogen-like ions [33]. (The larger effect due to single-electron Lamb shift is eliminated in this type of experiment.) Persson et al. [50] have calculated the two-electron contribution by adding to the all-order MBPT result the effect of two-photon QED, using dimensional regularization (see Chap. 12). The results are compared with the experimental results as well as with other theoretical estimates in Table 7.5. The results of Drake were obtained by expanding relativistic and QED effects in powers of α and $Z\alpha$, using Hylleraas type of wave functions [20]. The calculations of Plante et al. were made by means of relativistic MBPT and adding first-order QED corrections taken from the work of Drake [52], and the calculations of Indelicato et al. were made by means of multiconfigurational Dirac-Fock with an estimate of the Lamb shift [25]. The agreement between experiments and theory is quite good, although the experimental accuracy is not good enough to test the QED parts, which lie in the range 1-5 eV. The agreement between the various theoretical results is very good – only the results of Drake are somewhat off for the heaviest elements, which is due to the shortcoming of the power expansion.

7.1.6 g-Factor of Hydrogen-Like Ions: Mass of the Free Electron

The Zeeman splitting of hydrogen-like ions in a magnetic field is another good test of QED effects in highly charged ions. The lowest-order contributions to this effect are represented by the Feynman diagrams in Fig. 7.5.

The bound-electron g-factor can be expanded as [51]:

$$g_J = -2 \left\{ \frac{1}{3} \left[1 + 2\sqrt{1 - (Z\alpha)^2} \right] + \frac{\alpha}{\pi} \left(\frac{1}{2} + \frac{(Z\alpha)^2}{12} + \cdots \right) \right\},$$
 (7.2)

where Z is the nuclear charge. The first term represents the relativistic value with a correction from the Dirac value of order α^2 . The second term, proportional to α , is the leading QED correction, known as the *Schwinger correction*, and the following term, proportional to α^3 , is the next-order QED correction, first evaluated by Grotsch [23].

Numerical calculations to all orders in $Z\alpha$ have been performed by Blundell et al. [11] [only self-energy part, (b,c) in Fig. 7.5] and by the Gothenburg group [6,51] [incl. the vacuum polarization (d,e)]. The results are displayed in Fig. 7.6, showing the comparison between the Grotsch term (the leading QED correction beyond the Schwinger correction) and the numerical result. (The common factor of $2\alpha/\pi$ has been left out.) More accurate calculations have later been performed by the St Petersburg group, including also two-loop corrections and the nuclear recoil [59,61].

The g-factors of hydrogen-like ions have been measured with high accuracy by the Mainz group, using an ion trap of Penning type [4, 24]. The accuracy of the experimental and theoretical determinations is so high that the main uncertainty is due to the experimental mass of the electron. Some accurate dates for H-like carbon are shown in Table 7.6. By fitting the theoretical and experimental values, a value of the electron mass (in atomic mass units) $m_{\rm e} = 0.0005485799093(3)$ is deduced from the carbon experiment and the value $m_{\rm e} = 0.0005485799092(5)$ from a similar experiment on oxygen [4]. These results are four times more accurate than the previously accepted value, $m_{\rm e} = 0.0005485799110(12)$ [37]. The new value is now included in the latest adjustments of the fundamental constants [35, 36].

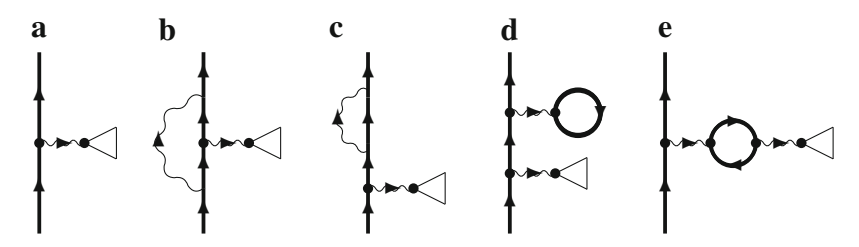


Fig. 7.5 Feynman diagrams representing the lowest-order contributions to the Zeeman effect of hydrogen-like ions. Diagrams (b) and (c) represent the leading self-energy correction to the first-order effect (a,d) and (c) the leading vacuum-polarization correction

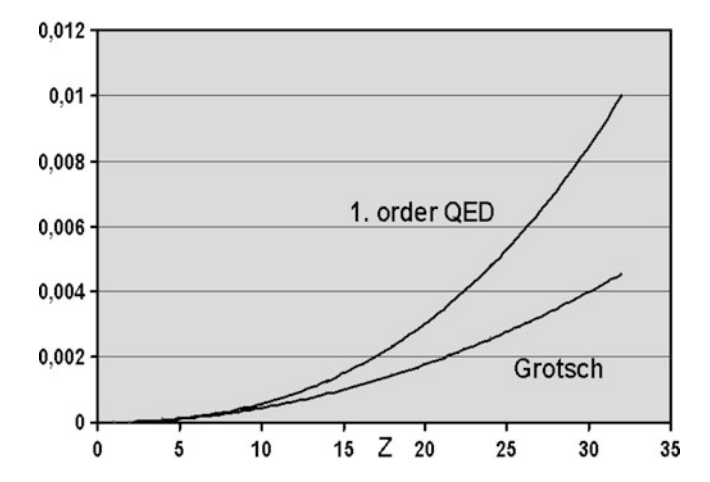


Fig. 7.6 The first-order, numerically evaluated, QED correction to the g_j value of hydrogen-like ions, compared with the leading analytical (Grotsch) term (7.2). Both results are first-order in α but the numerical result is all order in $Z\alpha$, while the Grotsch result contains only the leading term (from [51]). A common factor $2\alpha/\pi$ is left out

Table 7.6 Theoretical contributions to the g-factor of hydrogen-like carbon (mainly from [5])

Correction	Value
Dirac theory	1.998 721 3544
Finite nuclear-size corr.	+0.000 000 0004
Nuclear recoil	+0.000 000 0876
Free-electron QED, first order	+0.002 322 8195
Free-electron QED, higher orders	+0.000 003 5151
Bound-electron QED, first order	$+0.000\ 000\ 8442$
Bound-electron QED, higher orders	-0.000 000 0011
Total theory	2.001 041 5899

7.2 Green's-Function and Covariant-Evolution-Operator Methods

7.2.1 Fine-Structure of Helium-Like Ions

The two-times Green's function and the covariant-evolution-operator methods have the important advantage over the S-matrix formulation that they can be applied also to *quasi-degenerate* energy levels. As an illustration, we consider here the evaluation of some fine-structure separations of the lowest P state of helium-like ions (see Table 7.7). The calculations of Plante et al. [52] are relativistic many-body calculations in the NVPA scheme (see Sect. 2.6) with first-order QED-energy corrections, taken from the work of Drake [20]. The calculations by Åsén et al. [2, 29],

Table 7.7 The $1s2p^3P$ fine structure of He-like ions. (Values for Z=2,3 given in MHz and the remaining ones in μ Hartree)

<u>Z_</u>	$^{3}P_{1} - ^{3}P_{0}$	$^{3}P_{2} - ^{3}P_{0}$	$^{3}P_{2}-^{3}P_{1}$	Ref. Expt'l	Ref. Theory
2	29616.95166(70) 29616.9527(10) 29616.9509(9)		2291.17759(51)	Gabrielse et al. [62] Giusfredi et al. [22] Hessels et al. [21]	
	29616.9523(17)		2291.17753(35) 2291.1789(17)	Hessels et al. [12]	Pachucki et al. [57]
3	155704.27(66)		-62678.41(65) -62678.46(98)	Riis et al. [53] Clarke et al. [16]	
	155703.4(1,5)		-62679.4(5)		Drake et al. [20]
9	701(10) 680 681 690	5064(8) 5050 5045 5050	4364.517(6) 4362(5) 4364 4364	Myers et al. [46]	Drake et al. [20] Plante et al. [52] Åsén et al. [2, 32]
10	1371(7) 1361(6) 1370 1370	8458(2) 8455(6) 8469 8460	7087(8) 7094(8) 7099 7090	Curdt et al. [17]	Drake et al. [20] Plante et al. [52] Åsén et al. [29]
12	3789(26) 3796(7) 3778(10) 3796	20069(9) 20046(10) 20072	16280(27) 16268(13) 16276	Curdt et al. [17] Myers et al. [47]	Drake et al. [20] Plante et al. [52]
14	3800,1 8108(23) 8094	20071 40707(9) 40708(23) 40707 40712	32601(33) 32613	Curdt et al. [17]	Artemyev et al. [1] Drake et al. [20] Plante et al. [52] Artemyev et al. [1]
18	23692 23790	124960(30) 124810(60) 124942 124940 124945(3)	101250 101150	Kukla et al. [28]	Drake et al. [20] Plante et al. [52] Åsén et al. [29] Artemyev et al. [1]

using the recently developed covariant-evolution-operator method, was the first numerical evaluation of QED effects (nonradiative) on quasi-degenerate energy levels. It can be noted that the energy of the $1s2p^3P_1$ state, which a linear combination of the closely spaced states $1s2p_{1/2}$ and $1s2p_{1/3}$, could not be evaluated by the S-matrix formulation (see, for instance, the above-mentioned work of Mohr and Sapirstein [44]). Later, calculations have also been performed on these systems by the St Petersburg group, using the two-times-Green's-function method [1], where also the radiative parts are evaluated numerically.

The accuracy of the experimental and theoretical fine-structure results is not sufficient to distinguish between the first-order energy QED corrections and the

Table 7.8	The transition
$1s2s {}^{1}S_{0} -$	$-1s2p^{3}P_{1}$ for
He-like Si	(in cm^{-1})

		Reference
Expt'l	7230.585(6)	Myers et al. [19]
Theory	7231.1	Plante et al. [52]
	7229(2)	Artemyev et al. [1]

Table 7.9 Two-photon calculations on the $1s2s^{-1}S$, ${}^{3}S$ states of helium-like ions (in μ Hartree, first two columns from Åsén et al. [3], last column from Mohr and Sapirstein [44])

Z		$2^{3}S_{0}$	$2^{3}S_{1}$	$2^{3}S_{1}$
10	MBPT	-116 005	-47 638	
	QED	6.2	-1.2	
18	MBPT	-119381	$-48\ 158$	
	QED	3.8	4.6	
30	MBPT	-128349	-49542	-49541
	QED	93	6.9	8.7
60	MBPT	-177732	-57025	-57023
	QED	2358	216	224

numerical evaluation of Åsen and Artemyev. On the other hand, the experimental accuracy of the separation of Fluorine (Z=9) seems to be sufficient to test even higher-order QED effects. Here, present theory cannot match the experimental accuracy, but this might be a good testing case for the new combined QED-correlation procedure, discussed in the following.

As a second illustration, we consider the transition $1s2s^{1}S_{0} - 1s2p^{3}P_{1}$ for He-like silicon, which has recently been very accurately measured by Myers et al. [19] (see Table 7.8). Corresponding calculations have been performed by Plante et al. [52], using relativistic MBPT with first-order QED correction, and by Artemyev et al. [1], using the two-times Green's function. Here, it can be seen that the experiment is at least two orders of magnitude more accurate than the theoretical estimates. Also here the combined MBPT-QED corrections are expected to be significant.

7.2.2 Energy Calculations of 1s2s Levels of Helium-Like Ions

The covariant-evolution-operator method has also been applied by Åén et al. [2, 3] to evaluate the two-photon diagrams in Fig. 7.2 for the first excited *S* states of some helium-like ions. The results are compared with relativistic MBPT results, to determine the nonradiative QED effects, as in Table 7.4 above. The results are shown in Table 7.9, where comparison is also made with some results of Mohr and Sapirstein [44].

References

- 1. Artemyev, A.N., Shabaev, V.M., Yerokhin, V.A., Plunien, G., Soff, G.: *QED calculations of the n=1 and n=2 energy levels in He-like ions*. Phys. Rev. A **71**, 062,104 (2005)
- Åsén, B.: QED effects in excited states of helium-like ions. Ph.D. thesis, Department of Physics, Chalmers University of Technology and University of Gothenburg, Gothenburg, Sweden (2002)
- 3. Åsén, B., Salomonson, S., Lindgren, I.: *Two-photon exchange QED effects in the* 1s2s ¹S and ³S states of heliumlike ions. Phys. Rev. A **65**, 032,516 (2002)
- Beier, T., Djekic, S., Häffner, H., Indelicato, P., Kluge, H.J., Quint, W., Shabaev, V.S., Verdu, J., Valenzuela, T., Werth, G., Yerokhin, V.A.: *Determination of electron's mass from g-factor experiments on* ¹²C+⁵ and ¹⁶O+⁷. Nucl. Instrum. Methods **205**, 15–19 (2003)
- 5. Beier, T., Häffner, H., Hermanspahn, N., Karshenboim, S.G., Kluge, H.J.: New Determination of the Electron's Mass. Phys. Rev. Lett. 88, 011,603.1–4 (2002)
- 6. Beier, T., Lindgren, I., Persson, H., Salomonson, S., Sunnergren, P., Häffner, H., Hermanspahn, N.: g_j factor of an electron bound in a hydrogenlike ion. Phys. Rev. A **62**, 032,510 (2000)
- 7. Blundell, S.: Calculations of the screened self-energy and vacuum polarization in Li-like, Nalike, and Cu-like ions. Phys. Rev. A 47, 1790–1803 (1993)
- 8. Blundell, S., Mohr, P.J., Johnson, W.R., Sapirstein, J.: Evaluation of two-photon exchange graphs for highly charged heliumlike ions. Phys. Rev. A 48, 2615–26 (1993)
- 9. Blundell, S., Snyderman, N.J.: Basis-set approach to calculating the radiative self-energy in highly ionized atoms. Phys. Rev. A 44, R1427–30 (1991)
- Blundell, S.A.: Accurate screened QED calculations in high-Z many-electron ions. Phys. Rev. A 46, 3762–75 (1992)
- 11. Blundell, S.A., Cheng, K.T., Sapirstein, J.: Radiative corrections in atomic physics in the presence of perturbing potentials. Phys. Rev. A 55, 1857–65 (1997)
- Borbely, J.S., George, M.C., Lombardi, L.D., Weel, M., Fitzakerley, D.W., Hessels, E.A.: . Phys. Rev. A 79, 060,503 (2009)
- 13. Brown, G.E., Langer, J.S., Schaeffer, G.W.: Lamb shift of a tightly bound electron. I. Method. Proc. R. Soc. London, Ser. A 251, 92–104 (1959)
- 14. Brown, G.E., Mayers, D.F.: Lamb shift of a tightly bound electron. II. Calculation for the K-electron in Hg. Proc. R. Soc. London, Ser. A 251, 105–109 (1959)
- 15. Cheng, T.K., Johnson, W.R., Sapirstein, J.: Screend Lamb-shift calculations for Lithiumlike Uranium, Sodiumlike Platimun, and Copperlike Gold. Phys. Rev. Lett. 23, 2960–63 (1991)
- 16. Clarke, J.J., van Wijngaaren, W.A.: . Phys. Rev. A 67, 12,506 (2003)
- 17. Curdt, W., Landi, E., Wilhelm, K., Feldman, U.: Wavelength measurements of heliumlike 1s2s ${}^3S_1 1s2p \, {}^2P_{0,2}$ transitions in Ne^{8+} , Na^{9+} , Mg^{10+} , and Si^{12+} emitted by solar flare plasmas. Phys. Rev. A **62**, 022,502.1–7 (2000)
- 18. Desiderio, A.M., Johnson, W.R.: Lamb Shift and Binding Energies of K Electrons in Heavy Atoms. Phys. Rev. A 3, 1267–75 (1971)
- DeVore, T.R., Crosby, D.N., Myers, E.G.: Improved Measurement of the 1s2s 1S0 1s2p 3P1 Interval in Heliumlike Silicon. Phys. Rev. Lett. 100, 243,001 (2008)
- 20. Drake, G.W.F.: Theoretical energies for the n=1 and 2 states of the helium isoelectronic sequence up to Z=100. Can. J. Phys. **66**, 586–611 (1988)
- 21. George, M.C., Lombardi, L.D., Hessels, E.A.: *Precision Microwave Measurement of the* $2^3P_1 2^3P_0$ *Interval in Atomic Helium: A determination of the Fine-Structure Constant.* Phys. Rev. Lett. **87**, 173,002 (2001)
- Giusfredi, G., Pastor, P.C., Natale, P.D., Mazzotti, D., deMauro, C., Fallani, L., Hagel, G., Krachmalnicoff, V., Ingusio, M.: Present status of the fine structure of the 2 ³ P helium level. Can. J. Phys. 83, 301–10 (2005)
- 23. Grotsch, H.: . Phys. Rev. Lett. 24, 39 (1970)
- Häffner, H., Beier, T., Hermanspahn, N., Kluge, H.J., Quint, W., Stahl, S., Verdú, J., Werth, G.: High-Acuuracy Measurements of the Magnetic Anomaly of the Electron Bound in Hydrogenlike Carbon. Phys. Rev. Lett. 85, 5308–11 (2000)

References 169

 Indelicato, P., Gorciex, O., Desclaux, J.P.: Multiconfiguration Dirac-Fock studies of twoelectron ions: II. Radiative corrections and comparison with experiment. J. Phys. B 20, 651–63 (1987)

- Jentschura, U.D., Mohr, P.J., Soff, G.: Calculation of the Electron Self-Energy for Low Nuclear Charge. Phys. Rev. Lett. 61, 53–56 (1999)
- 27. Jentschura, U.D., Mohr, P.J., Tan, J.N., Wundt, B.J.: Fundamental Constants and Tests of Theory in Rydberg States of Hydrogenlike Ions. Phys. Rev. Lett. 100, 160,404 (2008)
- 28. Kukla, K.W., Livingston, A.E., Suleiman, J., Berry, H.G., Dunford, R.W., Gemmel, D.S., Kantor, E.P., Cheng, S., Curtis, L.J.: *Fine-structure energies for the* 1s2s ³S 1s2p ³P transition in heliumlike Ar⁺. Phys. Rev. A **51**, 1905–17 (1995)
- 29. Lindgren, I., Åsén, B., Salomonson, S., Mårtensson-Pendrill, A.M.: *QED procedure applied to the quasidegenerate fine-structure levels of He-like ions*. Phys. Rev. A **64**, 062,505 (2001)
- Lindgren, I., Persson, H., Salomonson, S., Labzowsky, L.: Full QED calculations of twophoton exchange for heliumlike systems: Analysis in the Coulomb and Feynman gauges. Phys. Rev. A 51, 1167–1195 (1995)
- 31. Lindgren, I., Persson, H., Salomonson, S., Ynnerman, A.: *Bound-state self-energy calculation using partial-wave renormalization*. Phys. Rev. A 47, R4555–58 (1993)
- 32. Lindgren, I., Salomonson, S., Åsén, B.: *The covariant-evolution-operator method in bound-state QED*. Physics Reports **389**, 161–261 (2004)
- 33. Marrs, R.E., Elliott, S.R., Stöhkler, T.: Measurement of two-electron contributions to the ground-state energy of heliumlike ions. Phys. Rev. A 52, 3577–85 (1995)
- 34. Mohr, P.: Self-energy correction to one-electron energy levels in a strong Coulomb field. Phys. Rev. A **46**, 4421–24 (1992)
- 35. Mohr, P., Taylor, B.: *CODATA recommended values of the fundamental constants 2002*. Rev. Mod. Phys. **77**, 1–107 (2005)
- 36. Mohr, P., Taylor, B.: CODATA recommended values of the fundamental constants 2002. Rev. Mod. Phys. (2008)
- 37. Mohr, P., Taylor, B.N.: *CODATA recommended values of the fundamental physical constants:* 1998. Rev. Mod. Phys. **72**, 351–495 (2000)
- 38. Mohr, P.J.: Numerical Evaluation of the $1s_{1/2}$ -State Radiative Level Shift. Ann. Phys. (N.Y.) **88**, 52–87 (1974)
- 39. Mohr, P.J.: Self-Energy Radiative Corrections. Ann. Phys. (N.Y.) 88, 26,52 (1974)
- 40. Mohr, P.J.: Lamb Shift in a Strong Coulomb Field. Phys. Rev. Lett. 34, 1050-52 (1975)
- 41. Mohr, P.J.: Self-energy of the n=2 states in a strong Coulomb field. Phys. Rev. A **26**, 2338–54 (1982)
- 42. Mohr, P.J.: Quantum electrodynamics of high-Z few-electron atoms. Phys. Rev. A 32, 1949–57 (1985)
- 43. Mohr, P.J., Plunien, G., Soff, G.: *QED corrections in heavy atoms*. Physics Reports 293, 227–372 (1998)
- 44. Mohr, P.J., Sapirstein, J.: Evaluation of two-photon exchange graphs for excited states of highly charged heliumlike ions. Phys. Rev. A 62, 052,501.1–12 (2000)
- 45. Mohr, P.J., Soff, G.: *Nuclear Size Correction to the Electron Self Energy*. Phys. Rev. Lett. **70**, 158–161 (1993)
- 46. Myers, E.G., Margolis, H.S., Thompson, J.K., Farmer, M.A., Silver, J.D., Tarbutt, M.R.: *Precision Measurement of the* 1s2p³P₂ ³P₁ *Fine Structure Interval in Heliumlike Fluorine*. Phys. Rev. Lett. **82**, 4200–03 (1999)
- 47. Myers, E.G., Tarbutt, M.R.: Measurement of the $1s2p^3P_0$ $-^3$ P_1 fine structure interval in heliumlike magnesium. Phys. Rev. A **61**, 010,501R (1999)
- 48. Persson, H., Labzowsky, I.L.L.N., Plunien, G., Beier, T., Soff, G.: Second-order self-energy-vacuum-polarization contributions to the Lamb shift in highly charged few-electron ions. Phys. Rev. A 54, 2805–13 (1996)
- Persson, H., Lindgren, I., Salomonson, S., Sunnergren, P.: Accurate vacuum-polarization calculations. Phys. Rev. A 48, 2772–78 (1993)
- 50. Persson, H., Salomonson, S., Sunnergren, P., Lindgren, I.: Two-electron Lamb-Shift Calculations on Heliumlike Ions. Phys. Rev. Lett. 76, 204–07 (1996)

- 51. Persson, H., Salomonson, S., Sunnergren, P., Lindgren, I.: *Radiative corrections to the electron g-factor in H-like ions*. Phys. Rev. A **56**, R2499–2502 (1997)
- 52. Plante, D.R., Johnson, W.R., Sapirstein, J.: *Relativistic all-order many-body calculations of* the n = 1 and n = 2 states of heliumlike ions. Phys. Rev. A **49**, 3519–30 (1994)
- 53. Riis, E., Sinclair, A.G., Poulsen, O., Drake, G.W.F., Rowley, W.R.C., Levick, A.P.: *Lamb shifts and hyperfine structure in* $^{6}Li^{+}$ *and* $^{7}Li^{+}$: *Theory and experiment*. Phys. Rev. A **49**, 207–20 (1994)
- Schweppe, J., Belkacem, A., Blumenfield, L., Clayton, N., Feinberg, B., Gould, H., Kostroun, V.E., Levy, L., Misawa, S., Mowat, J.R., Prior, M.H.: Measurement of the Lamb Shift in Lithiumlike Uranium (U⁺⁸⁹). Phys. Rev. Lett. 66, 1434–37 (1991)
- 55. Sthöhlker, T., Beyer, H.F., Gumberidze, A., Kumar, A., Liesen, D., Reuschl, R., Spillmann, U., Trassinelli, M.: *Ground state Lamb-shift of heavy hydrogen-like ions: status and prspectives*. Hyperfine Interactions 172, 135–40 (2006)
- 56. Stöhlker, T., Mokler, P.H., et al., K.B.: Ground-state Lamb Shift for Hydrogenlike Uranium Measured at the ESR Storage Ring. Phys. Rev. Lett. 14, 2184–87 (1993)
- 57. Yerokhin, K.P.V.A.: Fine Structure of Heliumlike Ions and Determination of the Fine Structure Constant. Phys. Rev. Lett. **104**, 70,403 (2010)
- 58. Yerokhin, V.A., Artemyev, A.N., Shabaev, V.M., Sysak, M.M., Zherebtsov, O.M., Soff, G.: Evaluation of the two-photon exchange graphs for the $2p_{1/2} 2s$ transition in Li-like Ions. Phys. Rev. A **64**, 032,109.1–15 (2001)
- 59. Yerokhin, V.A., Indelicato, P., Shabaev, V.M.: Self-energy Corrections to the Bound-Electron g Factor in H-like Ions. Phys. Rev. Lett. 89, 134,001 (2002)
- Yerokhin, V.A., Indelicato, P., Shabaev, V.M.: Two-Loop Self-Energy Correction in High-Z Hydrogenlike Ions. Phys. Rev. Lett. 91, 073,001 (2003)
- 61. Yerokhin, V.A., Indelicato, P., Shabaev, V.M.: Evaluation of the self-energy correction to the g Factor of S states in H-like Ions. Phys. Rev. A 69, 052,203 (2004)
- 62. Zelevinsky, T., Farkas, D., Gabrielse, G.: Precision Measurement of the Three 2³ P_J Helium Fine Structure Intervals. Phys. Rev. Lett. **95**, 203,001 (2005)

Part III
Quantum-Electrodynamics Beyond
Two-Photon Exchange: Field-Theoretical
Approach to Many-Body Perturbation
Theory

Chapter 8 Covariant Evolution Combined with Electron Correlation

In Part I, we have considered some standard methods for many-body calculations on atomic systems. These methods are well developed and can treat certain electron-correlation effects to essentially all orders of perturbation theory. In Part II, we have considered three different methods for numerical QED calculations on bound systems, which have been successfully applied to various problems. All these methods are, however, in practice limited to *one- and two-photon exchange*, implying that electron correlation can only be treated in quite a restricted way. For many systems the electron correlation is of great importance, and to evaluate the QED effects accurately, it may be necessary to take into account also the *combination* of *QED and correlational effects*, which has not been done previously.

In Part III, we demonstrate that one of the methods presented in the previous part, *the covariant-evolution-operator method*, forms a suitable basis for a combined QED–MBPT procedure. This leads to a perturbative procedure that is ultimately equivalent to an *extension of the relativistically covariant Bethe–Salpeter equation*, valid also in the multireference case and referred to as as the *Bethe–Salpeter–Bloch equation*. In this work, we normally use the *Coulomb gauge*, and we shall apply the *equal-time approximation*, discussed in Chap. 6. In Chap. 10, we illustrate how this procedure can be implemented and give some numerical results.

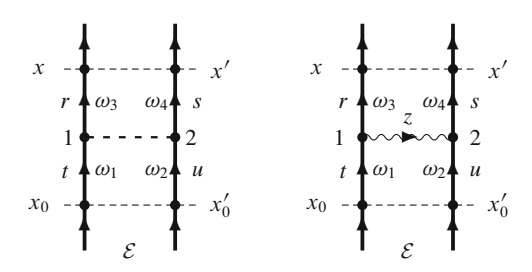
8.1 General Single-Photon Exchange

In the treatment of single-photon exchange in Chap. 6, the incoming state was assumed to be unperturbed. We shall now generalize this treatment and allow the incoming state to be perturbed, involving *particle as well as hole states*. As mentioned, we shall deal particularly with the Coulomb gauge, where the total interaction is according to (4.57) separated into a *Coulomb and a transverse part* (see Fig. 8.1).

$$I^{\rm C} = I_{\rm C}^{\rm C} + I_{\rm T}^{\rm C}.$$
 (8.1)

¹ The treatment in Part III is largely based on [3,6,7] and the thesis of Daniel Hedendahl [2].

Fig. 8.1 In the Coulomb gauge, the single-photon exchange is separated into a Coulomb and a transverse (Breit) part



The corresponding single-photon potential is similarly separated into:

$$V_{\rm sp} = V_{\rm C} + V_{\rm T}. \tag{8.2}$$

We start with the transverse part and consider the Coulomb part later.

8.1.1 Transverse Part

The kernel of the transverse part of the single-photon exchange in Coulomb gauge according to (6.6) is given by:

i
$$S_{F}(x, x_{1})$$
 i $S_{F}(x', x_{2})$ (-i) $I_{T}^{C}(x_{2}, x_{1})$ i $S_{F}(x_{1}, x_{0})$ i $S_{F}(x_{2}, x'_{0})$ $e^{-\gamma(|t_{1}| + |t_{2}|)}$. (8.3)

The external time dependence is (with the notations in Figs. 8.1 and 8.2) in the *equal-time approximation* in analogy with the previous case (6.9):

$$e^{-it(\omega_3+\omega_4-\varepsilon_r-\varepsilon_s)}e^{it_0(\omega_1+\omega_2-\varepsilon_t-\varepsilon_u)}$$
.

As before, we can argue that in the limit $\gamma \to 0$ $\omega_1 + \omega_2 = \omega_3 + \omega_4 = \mathcal{E}$, i.e., equal to the initial energy, and the dependence becomes:

$$e^{-it(\mathcal{E}-\varepsilon_r-\varepsilon_s)} e^{it_0(\mathcal{E}-\varepsilon_t-\varepsilon_u)}$$
.

We then have the relation:

$$U_{\rm T}(t, t_0) = e^{-it(\mathcal{E} - H_0)} \mathcal{M}_{\rm T} e^{it_0(\mathcal{E} - H_0)},$$
 (8.4)

where \mathcal{M}_T is the corresponding *Feynman amplitude*, defined as before (6.11). This yields:

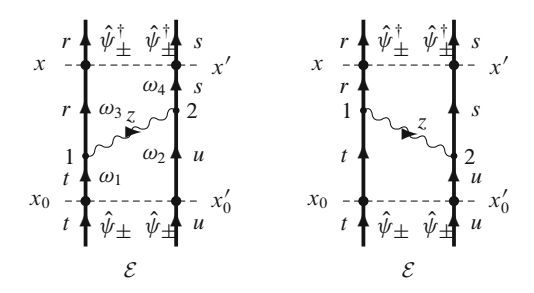
$$\mathcal{M}_{T}(x, x'; x_{0}, x'_{0}) = \frac{1}{2} \iiint \int \frac{d\omega_{1}}{2\pi} \frac{d\omega_{2}}{2\pi} \frac{d\omega_{3}}{2\pi} \frac{d\omega_{4}}{2\pi} \int \frac{dz}{2\pi} iS_{F}(\omega_{3}; x, x_{1})$$

$$\times iS_{F}(\omega_{4}; x', x_{2}) (-i) I_{T}^{C}(z; x_{2}, x_{1}) iS_{F}(\omega_{1}; x_{1}, x_{0})$$

$$\times iS_{F}(\omega_{2}; x_{2}, x'_{0}) 2\pi \Delta_{\gamma}(\omega_{1} - z - \omega_{3}) 2\pi \Delta_{\gamma}(\omega_{2} + z - \omega_{4})$$

$$(8.5)$$

Fig. 8.2 Time-ordered evolution-operator diagrams for single-photon exchange, transverse part



leaving out the internal space integrations. (The factor of 1/2 is, as before, eliminated when a specific matrix element is considered.)

After integrations over ω_2 , ω_3 , ω_4 , the amplitude becomes:

$$\mathcal{M}_{T}(x, x', x_{0}, x'_{0}) = \frac{1}{2} \iint \frac{d\omega_{1}}{2\pi} \frac{dz}{2\pi} iS_{F}(\omega_{1} - z; x, x_{1}) iS_{F}(\mathcal{E} - \omega_{1} - z; x', x_{2}) \times (-i)I_{T}^{C}(z; x_{2}, x_{1}) iS_{F}(\omega_{1}; x_{1}, x_{0}) iS_{F}(\mathcal{E} - \omega_{1}; x_{2}, x'_{0}).$$
(8.6)

Inserting the expressions for the electron propagator (4.10) and the interaction (4.46), a specific matrix element becomes:

$$\langle rs|\mathcal{M}_{T}|ab\rangle = \left\langle rs \middle| -i \int \frac{d\omega_{1}}{2\pi} \int \frac{dz}{2\pi} \frac{1}{\omega_{1} - z - \varepsilon_{r} + i\gamma_{r}} \frac{1}{\mathcal{E} - \omega_{1} + z - \varepsilon_{s} + i\gamma_{s}} \right.$$

$$\times \frac{1}{\omega_{1} - \varepsilon_{t} + i\gamma_{t}} \frac{1}{\mathcal{E} - \omega_{1} - \varepsilon_{u} + i\gamma_{u}} \int \frac{2c^{2}\kappa \, d\kappa \, f_{T}^{C}(\kappa)}{z^{2} - c^{2}\kappa^{2} + i\eta} \middle| ab \right\rangle, \tag{8.7}$$

where $f_{\rm T}^{\rm C}$ is the transverse part of the f function in Coulomb gauge (4.60). Integration over z now yields – in analogy with the treatment in Chap. 6

$$\mathcal{M}_{\mathrm{T}} = (-\mathrm{i})^2 \int c \, \mathrm{d}\kappa \, f_{\mathrm{T}}^{\mathrm{C}}(\kappa)$$

times the propagator expressions

$$\frac{1}{\mathcal{E} - \varepsilon_r - \varepsilon_s} \left[\frac{1}{\omega_1 - \varepsilon_r - (c\kappa - i\gamma)_r} + \frac{1}{\mathcal{E} - \omega_1 - \varepsilon_s - (c\kappa - i\gamma)_s} \right]$$

and

$$\frac{1}{\mathcal{E} - \varepsilon_t - \varepsilon_u} \left[\frac{1}{\omega_1 - \varepsilon_t + i\gamma_t} + \frac{1}{\mathcal{E} - \omega_1 - \varepsilon_u + i\gamma_u} \right].$$

We have now *four combinations* that contribute depending on the sign of the orbital energies (after integration over ω_1):

$$sgn(\varepsilon_r) \neq sgn(\varepsilon_t) : \frac{sgn(\varepsilon_t)}{\varepsilon_t - \varepsilon_r - (c\kappa - i\gamma)_r}$$

$$sgn(\varepsilon_s) = sgn(\varepsilon_t) : \frac{sgn(\varepsilon_t)}{\mathcal{E} - \varepsilon_t - \varepsilon_s - (c\kappa - i\gamma)_s}$$

$$sgn(\varepsilon_u) = sgn(\varepsilon_r) : \frac{sgn(\varepsilon_u)}{\mathcal{E} - \varepsilon_r - \varepsilon_u - (c\kappa - i\gamma)_r}$$

$$sgn(\varepsilon_u) \neq sgn(\varepsilon_s) : \frac{sgn(\varepsilon_u)}{\varepsilon_u - \varepsilon_s - (c\kappa - i\gamma)_s}$$
(8.8)

times (-i).

The Feynman amplitude for the transverse part of the single-photon exchange now becomes:

$$\mathcal{M}_{T} = \Gamma(\mathcal{E}) i V_{T}(\mathcal{E}) \Gamma(\mathcal{E}), \tag{8.9}$$

where $\Gamma(\mathcal{E})$ is the resolvent (2.64). This yields for the present process:

$$\left| \langle rs \big| \mathcal{M}_{T}(\mathcal{E}) \big| tu \rangle = \frac{i}{\mathcal{E} - \varepsilon_{r} - \varepsilon_{s}} \left| \langle rs \big| V_{T}(\mathcal{E}) \big| tu \rangle \left| \frac{1}{\mathcal{E} - \varepsilon_{t} - \varepsilon_{u}} \right| \right|$$
(8.10)

where $V_T(\mathcal{E})$ is now the generalized transverse-photon potential:

$$\langle rs | V_{T}(\mathcal{E}) | tu \rangle = \langle rs | \int c \, d\kappa \, f_{T}^{C}(\kappa) \left[\pm \frac{t_{\pm} r_{\mp}}{\varepsilon_{t} - \varepsilon_{r} \pm c\kappa} \right.$$

$$\pm \frac{t_{\pm} s_{\pm}}{\mathcal{E} - \varepsilon_{t} - \varepsilon_{s} \mp c\kappa} \pm \frac{u_{\pm} r_{\pm}}{\mathcal{E} - \varepsilon_{r} - \varepsilon_{u} \mp c\kappa} \pm \frac{u_{\pm} s_{\mp}}{\varepsilon_{u} - \varepsilon_{s} \pm c\kappa} \right] | tu \rangle.$$

$$(8.11)$$

Here, t_{\pm} etc. represent *projection operators* for particle/hole states. The upper or lower sign should be used consistently in each term, inclusive of the sign in the front, but all combinations of upper and lower signs in the four term should be used, corresponding to the 16 time-ordered combinations, shown in Fig. 8.3.

It should be noted that the expression above is valid also for the entire interaction in any covariant gauge, using the appropriate f function.

We shall now illustrate the potential (8.11) by giving explicit expressions in a few cases.

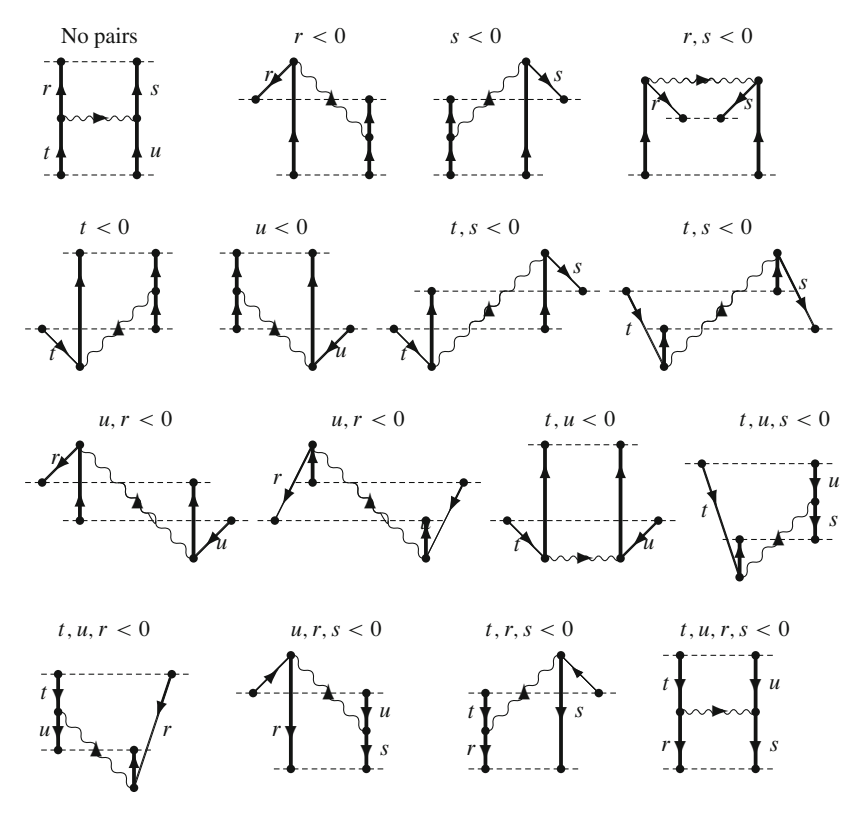


Fig. 8.3 All 16 time-ordered diagrams corresponding to the transverse single-photon exchange given by (8.11)

No virtual pairs



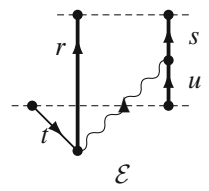
The potential becomes here:

$$\langle rs | V_{T}(\mathcal{E}) | tu \rangle = \left\langle rs \left| \int c \, d\kappa \, f_{T}^{C}(\kappa) \right| \right.$$

$$\times \left[\left. \frac{1}{\mathcal{E} - \varepsilon_{r} - \varepsilon_{u} - c\kappa} + \frac{1}{\mathcal{E} - \varepsilon_{t} - \varepsilon_{s} - c\kappa} \right] \right| tu \rangle \quad (8.12)$$

and the Feynman amplitude agrees with the previous result (6.16). This agrees with the result of the evaluation of the corresponding time-ordered diagram according to the rules of Appendix I.

Single hole in (t)



The potential becomes here:

$$\langle rs | V_{\rm T}(\mathcal{E}) | tu \rangle = \langle rs \left| \int c \, \mathrm{d}\kappa \, f_{\rm T}^{\rm C}(\kappa) \left[\frac{-1}{\varepsilon_t - \varepsilon_r - c\kappa} + \frac{1}{\mathcal{E} - \varepsilon_r - \varepsilon_u - c\kappa} \right] \right| tu \rangle, \tag{8.13}$$

which can also be expressed

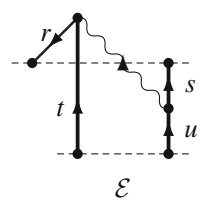
$$\langle rs | V_{T}(\mathcal{E}) | tu \rangle = -(\mathcal{E} - \varepsilon_{t} - \varepsilon_{u}) \left\langle rs \left| \int c \, d\kappa \, f_{T}^{C}(\kappa) \right| \right\rangle \times \frac{1}{\varepsilon_{t} - \varepsilon_{r} - c\kappa} \frac{1}{\mathcal{E} - \varepsilon_{r} - \varepsilon_{u} - c\kappa} \left| tu \right\rangle$$
(8.14)

and the denominators of the Feynman amplitude become:

$$-\frac{1}{\mathcal{E} - \varepsilon_r - \varepsilon_s} \frac{1}{\varepsilon_t - \varepsilon_r - c\kappa} \frac{1}{\mathcal{E} - \varepsilon_r - \varepsilon_u - c\kappa}.$$
 (8.15)

This agrees with the evaluation rules of Appendix I. We see here that one of the resolvents in (8.9) can be singular ("Brown–Ravenhall effect"), which is eliminated by the potential.

Single hole out (r)



The potential (8.11) becomes:

$$\langle rs|V_{T}(\mathcal{E})|tu\rangle = \left\langle rs \left| \int c \, d\kappa \, f_{T}^{C}(\kappa) \right| \times \left[\frac{1}{\varepsilon_{t} - \varepsilon_{r} + ck} + \frac{1}{\mathcal{E} - \varepsilon_{t} - \varepsilon_{s} - c\kappa} \right] \right| tu \right\rangle. \quad (8.16)$$

The denominators can here be expressed as:

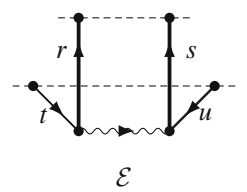
$$(\mathcal{E} - \varepsilon_r - \varepsilon_s) \frac{1}{\varepsilon_t - \varepsilon_r + c\kappa} \frac{1}{\mathcal{E} - \varepsilon_t - \varepsilon_s - c\kappa}$$
(8.17)

and the denominators of the Feynman amplitude becomes:

$$\frac{1}{\varepsilon_t - \varepsilon_r + c\kappa} \frac{1}{\mathcal{E} - \varepsilon_t - \varepsilon_s - c\kappa} \frac{1}{\mathcal{E} - \varepsilon_t - \varepsilon_u - c\kappa},$$
(8.18)

which agrees with the evaluation rules of Appendix I.

Double hole in t,u



The potential (8.11) is here:

$$\langle rs | V_{\rm T}(\mathcal{E}) | tu \rangle = \langle rs | \int c \, \mathrm{d}\kappa \, f_{\rm T}^{\rm C}(\kappa) \left[\frac{-1}{\varepsilon_t - \varepsilon_r - c\kappa} + \frac{-1}{\varepsilon_u - \varepsilon_s - c\kappa} \right] | tu \rangle \quad (8.19)$$

and the denominators of the Feynman amplitude become:

$$\frac{-1}{\mathcal{E} - \varepsilon_r - \varepsilon_s} \left[\frac{1}{\varepsilon_t - \varepsilon_r - c\kappa} + \frac{1}{\varepsilon_u - \varepsilon_s - c\kappa} \right] \frac{1}{\mathcal{E} - \varepsilon_t - \varepsilon_u}.$$
 (8.20)

We shall demonstrate explicitly here that this agrees with the evaluation rules of Appendix I. With one time-ordering $t_{34} > t_2 > t > -\infty$ and $\infty > t_{34} > t_2$, the time integrations yield:

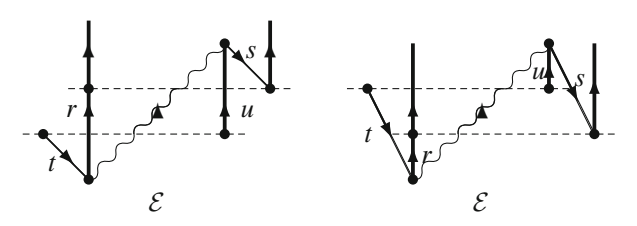
$$(-i)^{3} \int_{t_{34}}^{-\infty} dt_{2} e^{-id_{2}t_{2}} \int_{t_{2}}^{\infty} dt_{34} e^{-id_{34}t_{34}} \int_{t_{2}}^{-\infty} dt_{1} e^{-id_{1}t_{1}}.$$
 (8.21)

Together with the alternative time ordering $1 \leftrightarrow 2$, this becomes:

$$\frac{-1}{d_{1234}d_{34}} \left[\frac{1}{d_1} + \frac{1}{d_2} \right] \tag{8.22}$$

with the notations of Appendix I, which is identical to the result (8.20). Note that this is NOT in agreement with the standard Goldstone rules of MBPT [4].

Single hole in and out (t,s)



The potential (8.11) yields:

$$\langle rs|V_{T}(\mathcal{E})|tu\rangle = \langle rs \left| \int c \, d\kappa \, f_{T}^{C}(\kappa) \left[\frac{-1}{\varepsilon_{t} - \varepsilon_{r} - c\kappa} + \frac{-1}{\mathcal{E} - \varepsilon_{t} - \varepsilon_{s} + c\kappa} + \frac{1}{\varepsilon_{u} - \varepsilon_{s} + c\kappa} \right] \right| tu\rangle.$$

$$\left. + \frac{1}{\mathcal{E} - \varepsilon_{u} - \varepsilon_{r} - c\kappa} + \frac{1}{\varepsilon_{u} - \varepsilon_{s} + c\kappa} \right] \right| tu\rangle.$$
(8.23)

Using the notations of Appendix I:

$$d_1 = \varepsilon_t - \varepsilon_r - c\kappa; \quad d_2 = \varepsilon_u - \varepsilon_s + c\kappa; \quad d_3 = \varepsilon_a - \varepsilon_t - c\kappa;$$

$$d_4 = \varepsilon_b - \varepsilon_u + c\kappa; \quad d_{34} = \mathcal{E} - \varepsilon_t - \varepsilon_u;$$

$$d_{134} = \mathcal{E} - \varepsilon_r - \varepsilon_u - c\kappa; \quad d_{234} = \mathcal{E} - \varepsilon_t - \varepsilon_s + c\kappa; \quad d_{1234} = \mathcal{E} - \varepsilon_r - \varepsilon_s,$$

the bracket above becomes:

$$-\frac{1}{d_1} - \frac{1}{d_{234}} + \frac{1}{d_2} + \frac{1}{d_{134}} = \frac{d_{1234}d_{34}}{d_{134}d_{234}} \left[\frac{1}{d_2} - \frac{1}{d_1} \right]$$
(8.24)

and the denominators of the Feynman amplitude (8.10):

$$\frac{1}{d_{134}d_{234}} \left[\frac{1}{d_2} - \frac{1}{d_1} \right] = \frac{1}{d_1d_2} \left[\frac{1}{d_{134}} - \frac{1}{d_{234}} \right], \tag{8.25}$$

which agrees with the rules of Appendix I.

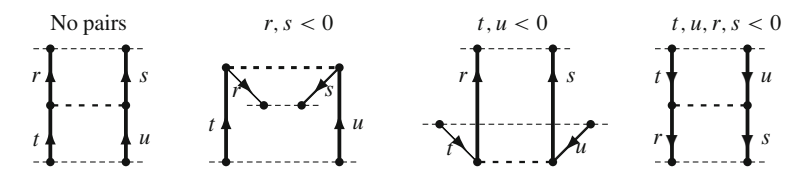


Fig. 8.4 Same as Fig. 8.3 for the Coulomb interaction

8.1.2 Coulomb Interaction

The Coulomb part of the interaction is obtained in a similar way (see Fig. 8.4). In analogy with (8.5), we now have:

$$\mathcal{M}_{C} = \frac{1}{2} \iint \frac{d\omega_{1}}{2\pi} \frac{d\omega_{3}}{2\pi} \int \frac{dz}{2\pi} iS_{F}(\omega_{1}) iS_{F}(E_{0} - \omega_{1})$$
$$\times (-i)I_{C}^{C} iS_{F}(\omega_{3}) iS_{F}(E_{0} - \omega_{3})$$

leaving out the space coordinates. After z integration, using (4.63b), and with the explicit form of the propagators this leads to:

$$\langle rs|\mathcal{M}_{C}|ab\rangle = \left\langle rs \left| -i \iint \frac{d\omega_{1}}{2\pi} \frac{d\omega_{3}}{2\pi} \frac{1}{\omega_{1} - \varepsilon_{r} + i\gamma_{r}} \frac{1}{E_{0} - \omega_{1} - \varepsilon_{s} + i\gamma_{s}} \right.\right.$$

$$\times V_{C} \frac{1}{\omega_{3} - \varepsilon_{t} + i\gamma_{t}} \frac{1}{E_{0} - \omega_{3} - \varepsilon_{u} + i\gamma_{u}} \left| ab \right\rangle$$

$$= \left\langle rs \left| \pm \frac{i}{E_{0} - \varepsilon_{r} - \varepsilon_{s}} V_{C} \frac{1}{E_{0} - \varepsilon_{t} - \varepsilon_{u}} \right| ab \right\rangle, \tag{8.26}$$

where $V_{\rm C}$ is the Coulomb interaction (2.109). Here, the plus sign is used if $sgn(\varepsilon_t) = sgn(\varepsilon_u) = sgn(\varepsilon_r) = sgn(\varepsilon_s)$ and the minus sign if $sgn(\varepsilon_t) = sgn(\varepsilon_u) \neq sgn(\varepsilon_r) = sgn(\varepsilon_s)$.

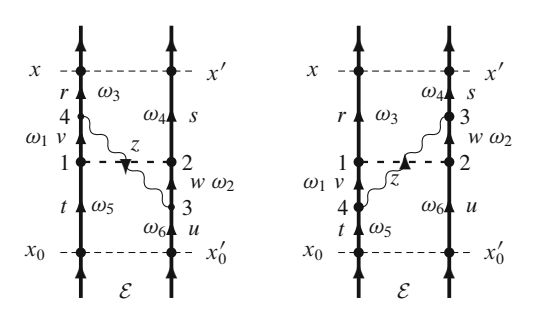
8.2 General QED Potential

We shall now see how the potential above can be extended to include also crossing Coulomb interactions as well as various radiative effects.

8.2.1 Single Photon with Crossed Coulomb Interaction*

We start by considering a transverse photon with a crossing Coulomb interaction (Fig. 8.5), using the Coulomb gauge.

Fig. 8.5 Feynman diagram representing the exchange of a retarded covariant photon with crossing Coulomb interaction



The Feynman amplitude becomes for the left diagram:

$$M(x, x'; x_{0}, x'_{0}) = \frac{1}{2} \iint \frac{d\omega_{1}}{2\pi} \frac{d\omega_{2}}{2\pi} \iint \frac{d\omega_{3}}{2\pi} \frac{d\omega_{4}}{2\pi} \iint \frac{d\omega_{5}}{2\pi} \frac{d\omega_{6}}{2\pi} \int \frac{dz}{2\pi}$$

$$\times iS_{F}(\omega_{3}; x, x_{4}) iS_{F}(\omega_{4}; x', x_{2}) iS_{F}(\omega_{1}; x_{4}, x_{1})$$

$$\times iS_{F}(\omega_{2}; x_{2}, x_{3}) iS_{F}(\omega_{5}; x_{1}, x_{0}) iS_{F}(\omega_{6}; x_{3}, x'_{0})$$

$$\times (-i)I_{T}^{C}(z; x_{4}, x_{3}) (-i)V_{C}(x_{2}, x_{1})$$

$$\times 2\pi \Delta_{\gamma}(\omega_{1} - z - \omega_{3}) 2\pi \Delta_{\gamma}(\omega_{6} + z - \omega_{2})$$

$$\times 2\pi \Delta_{\gamma}(\mathcal{E} - \omega_{5} - \omega_{6}) 2\pi \Delta_{\gamma}(\omega_{1} + \omega_{4} - \omega_{5} - \omega_{2}). \quad (8.27)$$

Integrations over ω_3 , ω_4 , ω_5 , ω_6 lead in the adiabatic limit to

$$\omega_3 = \omega_1 - z$$
, $\omega_4 = \mathcal{E} - \omega_1 + z$, $\omega_5 = \mathcal{E} - \omega_2 + z$, $\omega_6 = \omega_2 - z$

and to

$$M(x, x'; x_0, x'_0) = \frac{1}{2} \iint \frac{d\omega_1}{2\pi} \frac{dz}{2\pi} iS_F(\omega_1 - z; x, x_4) iS_F(\mathcal{E} - \omega_1 + z; x', x_2)$$

$$\times iS_F(\omega_1; x_4, x_1) iS_F(\omega_2; x_2, x_3) iS_F(\mathcal{E} - \omega_2 + z; x_1, x_0)$$

$$\times iS_F(\omega_2 - z; x_2, x'_0) (-i) I_T^C(z; x_2, x_3) (-i) V_C(x_4, x_3).$$
(8.28)

More explicitly the electron propagators become:

$$\frac{1}{(\omega_{1} - \varepsilon_{v} + i\eta_{v})} \frac{1}{(\mathcal{E} - \varepsilon_{r} - \varepsilon_{s})} \left[\frac{1}{(\omega_{1} - z - \varepsilon_{r} + i\gamma_{r})} + \frac{1}{(\mathcal{E} - \omega_{1} + z - \varepsilon_{s} + i\gamma_{s})} \right] \times \frac{1}{(\omega_{2} - w + i\eta_{w})} \frac{1}{(\mathcal{E} - \varepsilon_{t} - \varepsilon_{u})} \left[\frac{1}{(\mathcal{E} - \omega_{2} + z - \varepsilon_{t} + i\gamma_{t})} + \frac{1}{(\omega_{2} - z - \varepsilon_{u} + i\gamma_{u})} \right].$$
(8.29)

The integrations over ω_1 , ω_2 lead in analogy with (8.8) to

$$sgn(\varepsilon_{\nu}) \neq sgn(\varepsilon_{r}) : \quad \pm \frac{\nu_{\pm}r_{\mp}}{\varepsilon_{\nu} - z - \varepsilon_{r} \mp i\gamma} \quad =: \pm \frac{\nu_{\pm}r_{\mp}}{a_{\mp}}$$

$$sgn(\varepsilon_{\nu}) = sgn(\varepsilon_{s}) : \quad \pm \frac{\nu_{\pm}s_{\pm}}{\mathcal{E} - \varepsilon_{\nu} + z - \varepsilon_{s} \pm i\gamma} =: \pm \frac{\nu_{\pm}s_{\pm}}{b_{\pm}}$$

$$sgn(\varepsilon_w) = sgn(\varepsilon_w): \quad \pm \frac{w_{\pm}t_{\pm}}{\mathcal{E} - \varepsilon_w + z - \varepsilon_t \pm i\gamma} =: \pm \frac{w_{\pm}t_{\pm}}{c_{\pm}}$$

$$sgn(\varepsilon_w) \neq sgn(\varepsilon_u): \quad \pm \frac{w_{\pm}u_{\mp}}{\varepsilon_w - z - \varepsilon_u \mp i\gamma} =: \pm \frac{w_{\pm}u_{\mp}}{d_{\mp}} \quad (8.30)$$

times $(-i)^2$. Here, the first two terms should be combined with the last two, and the propagators (8.28) reduce to:

$$\frac{1}{\mathcal{E} - \varepsilon_r - \varepsilon_r} \frac{1}{\mathcal{E} - \varepsilon_t - \varepsilon_u} \times \left[\pm \frac{v_{\pm} r_{\mp}}{a_{\mp}} \pm \frac{v_{\pm} s_{\pm}}{b_{\pm}} \right] \\
\left[\pm \frac{w_{\pm} t_{\pm}}{c_{\pm}} \mp \frac{w_{\mp} t_{\mp}}{c_{\mp}} \pm \frac{w_{\pm} u_{\mp}}{d_{\mp}} \mp \frac{w_{\mp} u_{\pm}}{d_{\pm}} \right].$$
(8.31)

Upper or lower sign should be used consistently in all four operators in each product. We use here the notations:

$$\begin{cases}
A_{\pm} = \varepsilon_{v} - \varepsilon_{r} \mp c\kappa \\
B_{\pm} = \mathcal{E} - \varepsilon_{v} - \varepsilon_{s} \mp c\kappa \\
C_{\pm} = \mathcal{E} - \varepsilon_{w} - \varepsilon_{t} \mp c\kappa \\
D_{\pm} = \varepsilon_{w} - \varepsilon_{u} \mp c\kappa
\end{cases}$$

$$\begin{cases}
a_{\pm} = \varepsilon_{v} - z - \varepsilon_{r} \pm i\gamma \\
b_{\pm} = \mathcal{E} - \varepsilon_{v} + z - \varepsilon_{s} \pm i\gamma \\
c_{\pm} = \mathcal{E} - \varepsilon_{w} + z - \varepsilon_{u} \pm i\gamma \\
d_{\pm} = \varepsilon_{w} - z - \varepsilon_{u} \pm i\gamma.
\end{cases}$$

$$(8.32)$$

The photon interaction has one pole in each half-plane, and for the combinations where the electron propagator poles are in the same half-plane the z integration leads directly to the replacement $a_{\pm} \to A_{\pm}$ etc. This part then becomes $1/(\mathcal{E} - \varepsilon_r - \varepsilon_r)$ $1/(\mathcal{E} - \varepsilon_t - \varepsilon_u)$ times

$$V_{C1} = \left[\frac{v_{\pm}r_{\mp}}{A_{\mp}} + \frac{v_{\pm}s_{\pm}}{B_{+}} \right] \left[\frac{w_{\pm}t_{\pm}}{C_{+}} + \frac{w_{\pm}u_{\mp}}{D_{\mp}} \right]. \tag{8.33}$$

Again, upper or lower sign should be used consistently in all four operators in each product. Expressing the Feynman amplitude in analogy with (8.10),

$$\langle rs | \mathcal{M}(\mathcal{E}) | tu \rangle = \frac{i}{\mathcal{E} - H_0} \langle rs | V_{TC}(\mathcal{E}) | tu \rangle \frac{1}{\mathcal{E} - H_0},$$
 (8.34)

the corresponding part of the potential becomes:

$$\langle rs|V_{\rm TC}\rangle_1|tu\rangle = \int c \,\mathrm{d}\kappa \,f_{\rm T}^{\rm C}(\kappa) \,\langle vs|V_{\rm C}|tw\rangle \,\langle rw|V_{\rm C1}|vu\rangle \,. \tag{8.35}$$

When the electron propagators have one pole in each half-plane, we have to separate the propagators as before. For instance, the product

$$-\frac{v_{\pm}r_{\mp}}{a_{\mp}} \frac{w_{\mp}u_{\mp}}{c_{\mp}} = -\frac{v_{\pm}r_{\mp}}{\varepsilon_{\nu} - z - \varepsilon_{r} \mp i\gamma} \frac{w_{\mp}t_{\mp}}{\mathcal{E} - \varepsilon_{w} + z - \varepsilon_{t} \mp i\gamma}$$

is rewritten as

$$-\frac{v_{\pm}r_{\mp}w_{\mp}t_{\mp}}{a+c}\left[\frac{1}{a_{\mp}}+\frac{1}{c_{\mp}}\right] \Rightarrow -\frac{v_{\pm}r_{\mp}w_{\mp}t_{\mp}}{a+c}\left[\frac{1}{A_{\mp}}+\frac{1}{C_{\mp}}\right],$$

after z integration, or

$$-\frac{v_{\pm}r_{\mp}w_{\mp}t_{\mp}}{\mathcal{E}-\varepsilon_{w}-\varepsilon_{t}+\varepsilon_{v}-\varepsilon_{r}}\left[\frac{1}{\varepsilon_{v}-\varepsilon_{r}\pm c\kappa}+\frac{1}{\mathcal{E}-\varepsilon_{w}-\varepsilon_{t}\pm c\kappa}\right].$$

Similarly,

$$-\frac{v_{\pm}r_{\mp}}{a_{\mp}} \frac{w_{\mp}u_{\pm}}{d_{\pm}} = -\frac{v_{\pm}r_{\mp}}{\varepsilon_{v} - z - \varepsilon_{r} \mp i\gamma} \frac{w_{\mp}u_{\pm}}{\varepsilon_{w} - z - \varepsilon_{u} \pm i\gamma}$$

is rewritten as

$$\frac{v_{\pm}r_{\mp}w_{\mp}u_{\pm}}{a-d}\left[\frac{1}{a_{\mp}} - \frac{1}{d_{\pm}}\right] \Rightarrow \frac{v_{\pm}r_{\mp}w_{\mp}u_{\pm}}{a-d}\left[\frac{1}{A_{\mp}} - \frac{1}{D_{\pm}}\right].$$

But $A_{\mp} - D_{\pm} = a - d$; so this can also be written as:

$$-\frac{v_{\pm}r_{\mp}w_{\mp}u_{\pm}}{A_{\mp}D_{+}}.$$

All similar combinations lead to

$$V_{C2} = -\frac{v_{\pm}r_{\mp}w_{\mp}t_{\mp}}{a+c} \left[\frac{1}{A_{\mp}} + \frac{1}{C_{\mp}} \right] - \frac{v_{\pm}r_{\mp}w_{\mp}u_{\pm}}{A_{\mp}D_{\pm}} - \frac{v_{\pm}s_{\pm}w_{\mp}t_{\mp}}{B_{\pm}C_{\mp}} - \frac{v_{\pm}s_{\pm}w_{\mp}u_{\pm}}{b+d} \left[\frac{1}{B_{+}} + \frac{1}{D_{+}} \right], \tag{8.36}$$

where upper and lower sings are used consistently in all four operators in each term. The notations are defined in (8.32). This complete expression is quite complicated, particularly due to the denominator a+c.

Equations (8.33) and (8.36) represent the complete potential for all 64 time-ordered diagrams, corresponding to the Feynman diagram in Fig. 8.5:

$$\langle rs|V_{\rm TC}|tu\rangle = \int c \, \mathrm{d}\kappa \, f_{\rm T}^{\rm C}(\kappa) \, \langle vs|V_{\rm C}|tw\rangle \, \langle rw|V_{\rm C1} + V_{\rm C2}|vu\rangle \,. \tag{8.37}$$

We can simplify the results above by assuming that the incoming orbitals t, u are particle states. Then (8.33) reduces to

$$\left[\frac{v_{+}r_{-}}{A_{-}} + \frac{v_{+}s_{+}}{B_{+}}\right] \frac{w_{+}t_{+}}{C_{+}} + \left[\frac{v_{-}r_{+}}{A_{+}} + \frac{v_{-}s_{-}}{B_{-}}\right] \frac{w_{-}u_{+}}{D_{+}}$$
(8.38)

and (8.36) to

$$-\frac{v_{-}r_{+}w_{+}t_{+}}{a+c}\left[\frac{1}{A_{+}}+\frac{1}{C_{+}}\right]-\frac{v_{+}s_{+}w_{-}u_{+}}{b+d}\left[\frac{1}{B_{+}}+\frac{1}{D_{+}}\right].$$
 (8.39)

With *no pairs*, we then have:

$$\frac{v_{+}s_{+}}{B_{+}} \frac{w_{+}t_{+}}{C_{+}} = \frac{v_{+}s_{+}w_{+}t_{+}}{(\mathcal{E} - \varepsilon_{v} - \varepsilon_{s} - c\kappa)(\mathcal{E} - \varepsilon_{w} - \varepsilon_{t} - c\kappa)}$$

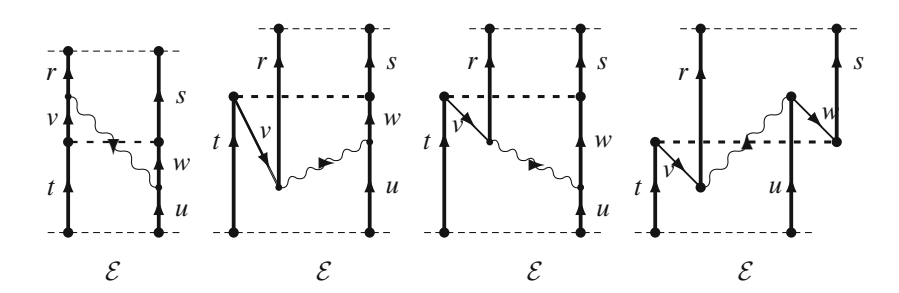
with *single pair* (v)

$$\begin{split} -\frac{v_{-}r_{+}w_{+}t_{+}}{a+c} \left[\frac{1}{A_{+}} + \frac{1}{C_{+}} \right] &= -\frac{v_{-}r_{+}w_{+}t_{+}}{\mathcal{E} - \varepsilon_{w} - \varepsilon_{t} + \varepsilon_{v} - \varepsilon_{r}} \\ &\times \left[\frac{1}{\varepsilon_{v} - \varepsilon_{r} - c\kappa} + \frac{1}{\mathcal{E} - \varepsilon_{w} - \varepsilon_{t} - c\kappa} \right] \end{split}$$

and *double pairs* (v, w)

$$\frac{v_-r_+}{A_+} \frac{w_-u_+}{D_+} = \frac{v_-r_+w_-u_+}{(\varepsilon_v - \varepsilon_r - c\kappa)(\varepsilon_w - \varepsilon_u - c\kappa)}.$$

This corresponds to the time-ordered diagrams shown below, and the results are in agreement with the evaluation rules for time-ordered diagrams. Also here some diagrams are complicated to evaluate, due to the denominator a+c.



Another, probably more reasonable approximation is to assume that the intermediate states v, w are *particle* states. Then only the simpler term (8.33) survives, yielding

$$V_{C1+} = \left[\frac{v_{+}r_{-}}{A_{-}} + \frac{v_{+}s_{+}}{B_{+}} \right] \left[\frac{w_{+}t_{+}}{C_{+}} + \frac{w_{+}u_{-}}{D_{-}} \right]$$
(8.40)

and the potential

$$\langle rs|V_{\text{TC}}^{+}|tu\rangle = \int c \,d\kappa \,f_{\text{T}}^{\text{C}}(\kappa) \,\langle vs|V_{\text{C}}|tw\rangle \,\langle rw|V_{\text{C}1+}|vu\rangle. \tag{8.41}$$

This part of the potential can be generated by iterating the pair equation, as discussed in Chap. 10. This is true also for repeated Coulomb crossings.

8.2.2 Electron Self-Energy and Vertex Correction

Next, we shall see how some *radiative effects*, previously treated in the S-matrix formalism (see Sect. 4.6), can be included in the QED potential. Since we are using the Coulomb gauge, we have to treat the Coulomb and transverse parts separately as in Sect. 4.6.

We start with the *transverse* part, illustrated in Fig. 8.6 (left). The kernel is here (c.f. 4.84):

$$i S_F(x, x_2) i S_F(x_2, x_1) (-i) I_T^C(x_2, x_1),$$
 (8.42)

where $I_{\rm T}^{\rm C}$ is the transverse part of the interaction (4.59). The *Feynman amplitude* becomes in analogy with previous cases (8.4)

$$M_{SE}(\mathbf{x}) = \iint \frac{d\omega_1}{2\pi} \frac{d\omega_2}{2\pi} \frac{dz}{2\pi} iS_F(\omega_2; \mathbf{x}, \mathbf{x}_2) iS_F(\omega_1; \mathbf{x}_2, \mathbf{x}_1) (-i) I_T^C(z; \mathbf{x}_2, \mathbf{x}_1) \times 2\pi \Delta_{\gamma}(\varepsilon_a - \omega_1 - z) 2\pi \Delta_{\gamma}(\omega_1 - \omega_2 + z)$$
(8.43)

integrated over the internal space coordinates and with the energy parameters given in the figure. After integration over the omegas, this becomes:

$$M_{\rm SE}(x) \int \frac{\mathrm{d}z}{2\pi} i S_{\rm F}(\varepsilon_a; x, x_2) i S_{\rm F}(\varepsilon_a - z; x_2, x_1) (-i) I_{\rm T}^{\rm C}(z; x_2, x_1).$$
 (8.44)

The matrix element of the evolution operator is:

$$\langle r|U_{\rm SE}(t)|a\rangle = e^{-it(\varepsilon_a - \varepsilon_r)} \langle rt|M_{\rm SE}(x)|ta\rangle,$$
 (8.45)

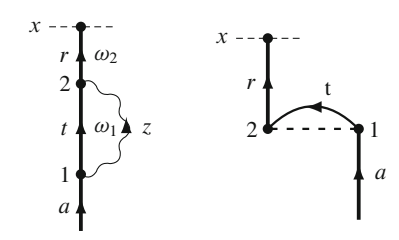
which we can express

$$\langle r | U_{\text{SE}}(t) | a \rangle = \frac{e^{-it(\varepsilon_a - \varepsilon_r)}}{\varepsilon_a - \varepsilon_r} \langle r | -i\Sigma(\varepsilon_a) | a \rangle,$$
 (8.46)

where $\Sigma(\varepsilon_a)$ is the *self-energy operator* (4.85)

$$\langle r|\Sigma(\varepsilon_a)|a\rangle = \left\langle rt \left| \int \frac{\mathrm{d}z}{2\pi} \,\mathrm{i} S_{\mathrm{F}}(\varepsilon_a - z; \boldsymbol{x}_2, \boldsymbol{x}_1) \, I_{\mathrm{T}}^{\mathrm{C}}(z; \boldsymbol{x}_2, \boldsymbol{x}_1) \right| ta \right\rangle. \tag{8.47}$$

Fig. 8.6 Diagram representing the transverse and Coulomb parts of the first-order self-energy of a bound electron in the covariant-evolution-operator formalism (c.f. Fig. 4.9)



Inserting the explicit expressions for the propagators, yields

$$\langle r|\Sigma(\varepsilon_a)|a\rangle_{\text{Trans}} = \left\langle rt \left| \int \frac{c \, d\kappa \, f_{\text{T}}^{\text{C}}(\kappa)}{\varepsilon_a - \varepsilon_t - (c\kappa - i\eta)_t} \right| ta \right\rangle$$
 (8.48)

consistent with the diagonal S-matrix (4.89).

It should be noted that the self-energy is diagonal in energy in the S-matrix formulation, due to the energy conservation, while also nondiagonal parts will appear in the covariant-evolution formulation. As we shall see, *only the diagonal part is divergent* and has to be renormalized, as will be discussed in Chap. 12.

The Coulomb part of the self-energy (Fig. 8.6 right) becomes in analogy with the S-matrix result (4.95)

$$\langle r | \Sigma(\varepsilon_a) | a \rangle_{\text{Coul}} = \frac{1}{2} \left\langle rt \left| \frac{e^2}{4\pi^2 \epsilon_0 r_{12}} \int \frac{2\kappa \, d\kappa \, \sin \kappa r_{12}}{\kappa^2} \right| ta \right\rangle$$

$$= \frac{1}{2} \operatorname{sgn}(\varepsilon_t) \, \langle rt | V_C | ta \rangle$$
(8.49)

with summation over positive- as well as negative-energy states.

8.2.2.1 General Two-Electron Self-Energy

We consider now a general self-energy operator (transverse part) in analogy with the general single-photon exchange in Sect. 8.1, illustrated in Fig. 8.7. (The Coulomb part can be treated similarly.) The kernel is now

i
$$S_{\rm F}(x,x_2)$$
 i $S_{\rm F}(x_2,x_1)$ (-i) $I_{\rm T}^{\rm C}(x_2,x_1)$ i $S_{\rm F}(x_1,x_0)$ i $S_{\rm F}(x',x'_0)$ ${\rm e}^{-\gamma(|t_1|+|t_2|)}$ (8.50)

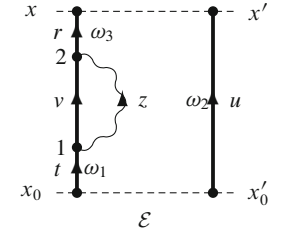


Fig. 8.7 General two-electron self-energy with incoming and outgoing electron propagators

and the Feynman amplitude

$$\mathcal{M}_{SE}(\mathbf{x}, \mathbf{x}'; \mathbf{x}_{0}, \mathbf{x}'_{0}) = \iiint \frac{d\omega_{1}}{2\pi} \frac{d\omega_{2}}{2\pi} \frac{d\omega_{3}}{2\pi} \frac{d\omega_{4}}{2\pi} \int \frac{dz}{2\pi} iS_{F}(\omega_{3}; \mathbf{x}, \mathbf{x}_{2})$$

$$\times iS_{F}(\omega_{4}; \mathbf{x}_{2}, \mathbf{x}_{1}) iS_{F}(\omega_{1}; \mathbf{x}_{1}, \mathbf{x}_{0}) iS_{F}(\omega_{2}; \mathbf{x}', \mathbf{x}'_{0})$$

$$\times (-i)I_{T}^{C}(z; \mathbf{x}_{2}, \mathbf{x}_{1}) 2\pi \Delta_{\gamma}(\omega_{1} - z - \omega_{4})$$

$$\times 2\pi \Delta_{\gamma}(\omega_{4} + z - \omega_{3}) 2\pi \Delta_{\gamma}(\mathcal{E} - \omega_{1} - \omega_{2}). \quad (8.51)$$

After integrations over ω_2 , ω_3 , ω_4 , this becomes

$$\mathcal{M}_{SE}(x, x', x_0, x'_0) = \iint \frac{d\omega_1}{2\pi} \frac{dz}{2\pi} iS_F(\omega_1; x, x_2) iS_F(\omega_1 - z; x_2, x_1) \times (-i)I_T^C(z; x_2, x_1) iS_F(\omega_1; x_1, x_0) iS_F(\mathcal{E} - \omega_1; x', x'_0)$$
(8.52)

as before, leaving out the internal integrations. Integration over z now yields

$$\mathcal{M}_{SE} = (-i)^2 \int c \, d\kappa \, f_T^{C}(\kappa)$$

times the propagator expressions

$$\frac{1}{\varepsilon_r - \varepsilon_v - (-\mathrm{i}\gamma)_v} \left[\frac{1}{\omega_1 - \varepsilon_r + \mathrm{i}\gamma_r} - \frac{1}{\omega_1 - \varepsilon_v - (c\kappa - \mathrm{i}\gamma)_v} \right]$$

and

$$\frac{1}{\mathcal{E} - \varepsilon_t - \varepsilon_u} \left[\frac{1}{\omega_1 - \varepsilon_t + i\gamma_t} + \frac{1}{\mathcal{E} - \omega_1 - \varepsilon_u + i\gamma_u} \right]. \tag{8.53}$$

The integration over ω_1 yields another factor of -i, and this leads in analogy with (8.10) to:

$$\langle ru|\mathcal{M}_{SE}(\mathcal{E})|tu\rangle = \frac{\mathrm{i}}{\varepsilon_r - \varepsilon_v - (c\kappa - \mathrm{i}\gamma)_v} \langle ru|V_{SE}(\mathcal{E})|tu\rangle \frac{1}{\mathcal{E} - \varepsilon_t - \varepsilon_u},$$
 (8.54)

where $V_{\rm SE}(\mathcal{E})$ is the potential

$$\langle rs | V_{SE}(\mathcal{E}) | tu \rangle = \left\langle rs \left| \int c \, d\kappa \, f_{T}^{C}(\kappa) \left[\pm \frac{t_{\pm} r_{\mp}}{\varepsilon_{t} - \varepsilon_{r}} \pm \frac{r_{\pm} u_{\pm}}{\mathcal{E} - \varepsilon_{r} - \varepsilon_{u}} \right] \right.$$

$$\left. \mp \frac{t_{\pm} v_{\mp}}{\varepsilon_{t} - \varepsilon_{v} \pm c\kappa} \mp \frac{v_{\pm} u_{\pm}}{\mathcal{E} - \varepsilon_{u} - \varepsilon_{v} \mp c\kappa} \right] \right| tu \rangle.$$
 (8.55)

If all states are particle states, we find that the bracket above becomes:

$$\frac{1}{\mathcal{E} - \varepsilon_r - \varepsilon_u} - \frac{1}{\mathcal{E} - \varepsilon_u - \varepsilon_v - c\kappa} = \frac{\varepsilon_r - \varepsilon_v - c\kappa}{(\mathcal{E} - \varepsilon_r - \varepsilon_u)(\mathcal{E} - \varepsilon_u - \varepsilon_v - c\kappa)}$$

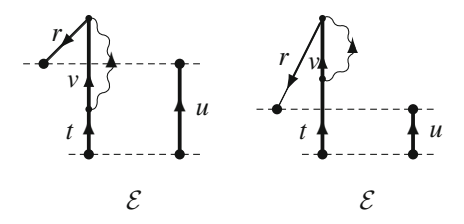
and the Feynman amplitude

$$\frac{i}{(\mathcal{E} - \varepsilon_r - \varepsilon_u)(\mathcal{E} - \varepsilon_u - \varepsilon_v - c\kappa)} \frac{1}{\mathcal{E} - \varepsilon_t - \varepsilon_u},$$
(8.56)

in agreement with the evaluation rules for time-ordered diagrams, derived in Appendix I.

Next, we consider some specific cases with virtual holes, and, as before, we apply the potential to a Coulomb interaction.

Hole out (r) (remaining ones particle states)

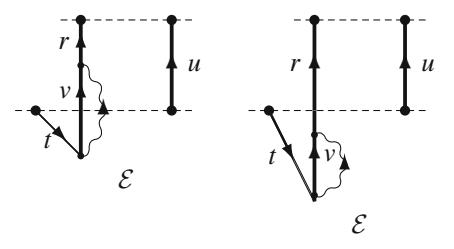


The Feynman amplitude (8.54) becomes:

$$\frac{\mathrm{i}}{\varepsilon_r - \varepsilon_v - c\kappa} \left[\frac{1}{\varepsilon_t - \varepsilon_r} - \frac{1}{\mathcal{E} - \varepsilon_u - \varepsilon_v - ck} \right] \frac{1}{\mathcal{E} - \varepsilon_t - \varepsilon_u}. \tag{8.57}$$

This corresponds to the two time-ordered diagrams in the marginal.

Hole in (t)



The Feynman amplitude becomes:

$$\frac{\mathrm{i}}{\varepsilon_{r} - \varepsilon_{v} - c\kappa} \left[-\frac{1}{\varepsilon_{t} - \varepsilon_{r}} + \frac{1}{\varepsilon - \varepsilon_{r} - \varepsilon_{u}} + \frac{1}{\varepsilon_{t} - \varepsilon_{v} - c\kappa} - \frac{1}{\varepsilon_{t} - \varepsilon_{u} - \varepsilon_{v} - ck} \right] \frac{1}{\varepsilon - \varepsilon_{t} - \varepsilon_{u}},$$
(8.58)

which can also be expressed as

$$i\left[\frac{-1}{(\varepsilon_r - \varepsilon_t)(\varepsilon_t - \varepsilon_v - c\kappa)} + \frac{1}{(\mathcal{E} - \varepsilon_r - \varepsilon_u)(\mathcal{E} - \varepsilon_u - \varepsilon_v - c\kappa)}\right] \times \frac{1}{\mathcal{E} - \varepsilon_t - \varepsilon_u}.$$
(8.59)

After some additional algebra, this can be shown to be identical to

$$\frac{-\mathrm{i}}{(\varepsilon_t - \varepsilon_v - c\kappa)(\mathcal{E} - \varepsilon_r - \varepsilon_u)} \left[\frac{1}{\mathcal{E} - \varepsilon_u - \varepsilon_v - c\kappa} + \frac{1}{\varepsilon_t - \varepsilon_r} \right] \tag{8.60}$$

corresponding to the time-ordered diagrams in the marginal.

8.2.2.2 General Vertex Correction

The general vertex correction (transverse part), illustrated in Fig. 8.8, leads to

$$\mathcal{M}_{Vx}(x, x', x_0, x'_0) = \iint \frac{d\omega_1}{2\pi} \frac{d\omega_1}{2\pi} \int \frac{dz}{2\pi} iS_F(\omega_3; x, x_2) iS_F(\omega_3 - z; x_2, x_3)$$

$$\times iS_F(\mathcal{E} - \omega_3; x', x_4)(-i)I_T^C(z; x_2, x_1)$$

$$\times (-i)V_C(x_4, x_3) iS_F(\omega_1 - z; x_3, x_1)$$

$$\times iS_F(\omega_1; x_1, x_0) iS_F(\mathcal{E} - \omega_1; x_4, x'_0). \tag{8.61}$$

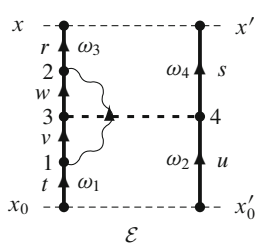


Fig. 8.8 General vertex correction with incoming and outgoing electron propagators

More explicitly, the electron propagators become:

$$\frac{1}{\mathcal{E} - \varepsilon_r - \varepsilon_s} \frac{1}{\omega_3 - \varepsilon_w - z - i\gamma_w} \left[\frac{1}{\omega_3 - \varepsilon_r + i\gamma_r} + \frac{1}{\mathcal{E} - \omega_3 - \varepsilon_s + i\gamma_s} \right]$$

times

$$\frac{1}{\mathcal{E} - \varepsilon_t - \varepsilon_u} \frac{1}{\omega_1 - \varepsilon_v - z - i\gamma_v} \left[\frac{1}{\omega_1 - \varepsilon_t + i\gamma_t} + \frac{1}{\mathcal{E} - \omega_1 - \varepsilon_u + i\gamma_u} \right]. \quad (8.62)$$

If the energies of the orbitals v and w have the same sign, then the integration over z leads to:

$$\mathcal{M}_{\mathrm{Vx}} = -\mathrm{i} \int c \, \mathrm{d}\kappa \, f_{\mathrm{T}}^{\mathrm{C}}(\kappa)$$

times

$$\frac{1}{\mathcal{E} - \varepsilon_r - \varepsilon_s} \frac{1}{\omega_3 - \varepsilon_w - (c\kappa - i\gamma)_w} \left[\frac{1}{\omega_3 - \varepsilon_r + i\gamma_r} + \frac{1}{\mathcal{E} - \omega_3 - \varepsilon_s + i\gamma_s} \right]$$

and

$$\frac{1}{\mathcal{E} - \varepsilon_t - \varepsilon_u} \frac{1}{\omega_1 - \varepsilon_v - (c\kappa - i\gamma)_v} \left[\frac{1}{\omega_1 - \varepsilon_t + i\gamma_t} + \frac{1}{\mathcal{E} - \omega_1 - \varepsilon_u + i\gamma_u} \right]$$
(8.63)

and to the Feynman amplitude, in analogy with (8.54):

$$\langle rs | \mathcal{M}_{Vx}(\mathcal{E}) | tu \rangle = \frac{i}{\mathcal{E} - \varepsilon_x - \varepsilon_s} \langle rs | V_{Vx}(\mathcal{E}) | tu \rangle \frac{1}{\mathcal{E} - \varepsilon_t - \varepsilon_u},$$
 (8.64)

where $V_{\text{Vx}}(\mathcal{E})$ is the potential

$$\langle rs | V_{Vx}(\mathcal{E}) | tu \rangle = \langle ws | V_{C} | vu \rangle \langle rv | \int c \, d\kappa \, f_{T}^{C}(\kappa)$$

$$\times \left[\pm \frac{r_{\pm}w_{\mp}}{\varepsilon_{r} - \varepsilon_{w} \pm ck} \pm \frac{s_{\pm}w_{\pm}}{\mathcal{E} - \varepsilon_{s} - \varepsilon_{w} \mp c\kappa} \right]$$

$$\times \left[\pm \frac{t_{\pm}v_{\mp}}{\varepsilon_{t} - \varepsilon_{v} \pm c\kappa} \pm \frac{v_{\pm}u_{\pm}}{\mathcal{E} - \varepsilon_{u} - \varepsilon_{v} \mp c\kappa} \right] | wt \rangle. \quad (8.65)$$

If the orbitals *v* and *w* are of *different* kind (particle or hole), the evaluation becomes more complicated. This case is expected to be less important.

If all states are particle states, we find that the brackets above become:

$$\frac{1}{\mathcal{E} - \varepsilon_{s} - \varepsilon_{w} - c\kappa} \frac{1}{\mathcal{E} - \varepsilon_{u} - \varepsilon_{v} - c\kappa},$$

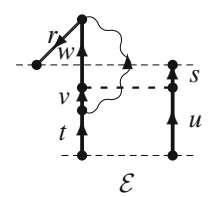
in agreement with the evaluation rules for time-ordered diagrams. If r is a hole state and the others particle states, we have instead

$$\begin{split} & \left[-\frac{1}{\varepsilon_r - \varepsilon_w - c\kappa} + \frac{1}{\mathcal{E} - \varepsilon_s - \varepsilon_w - c\kappa} \right] \times \frac{1}{\mathcal{E} - \varepsilon_u - \varepsilon_v - c\kappa} \\ & = -\frac{\mathcal{E} - \varepsilon_r - \varepsilon_s}{(\varepsilon_r - \varepsilon_w - c\kappa)(\mathcal{E} - \varepsilon_s - \varepsilon_w - c\kappa)} \times \frac{1}{\mathcal{E} - \varepsilon_u - \varepsilon_v - c\kappa}. \end{split}$$

This leads to the denominators of the Feynman amplitude (8.64)

$$-\frac{1}{(\varepsilon_r - \varepsilon_w - c\kappa)(\mathcal{E} - \varepsilon_s - \varepsilon_w - c\kappa)(\mathcal{E} - \varepsilon_u - \varepsilon_v - c\kappa)(\mathcal{E} - \varepsilon_t - \varepsilon_u)}$$

and corresponds to the time-ordered diagram.



8.2.3 Vertex Correction with Further Coulomb Iterations

The Coulomb interactions of the vertex correction can be iterated before the photon interaction is closed, in the same way as for the retarded photon with crossed Coulomb, treated above, leading to diagrams of the type shown in Fig. 8.9. Assuming that the intermediate states v, w, as well as the states between the Coulomb interactions are particle states, the corresponding analytical expression is obtained from (8.64) by replacing the matrix element $\langle ws|V_C|vu\rangle$ by:

$$\langle ws|V_{\rm C}\frac{|xy\rangle\langle xy|}{\mathcal{E}-\varepsilon_x-\varepsilon_y-c\kappa}V_{\rm C}|vu\rangle$$
.

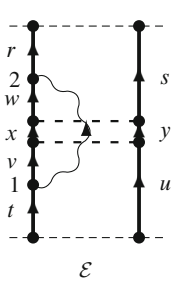


Fig. 8.9 Vertex correction with double Coulomb interactions

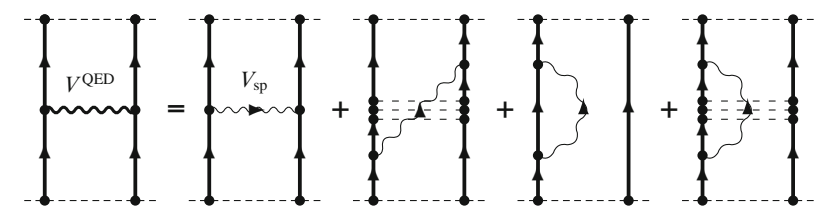


Fig. 8.10 Feynman diagram representing the "QED potential," $V^{\rm QED}$, in (8.66). The first diagram on the r.h.s. includes the Coulomb potential

8.2.4 General Two-Body Potential

We can now form a general "two-body QED potential" by adding the contributions derived above:

$$V^{\text{QED}} = V_{\text{sp}} + V_{\text{TC}} + V_{\text{SE}} + V_{\text{Vx}},$$
 (8.66)

where $V_{\rm sp}$, as before, represents the <u>combined</u> Coulomb and transverse-photon exchange (8.2). This is illustrated in Fig. 8.10. Here, particle as well as holes are allowed in and out.

8.3 Unification of the MBPT and QED Procedures: Connection to Bethe–Salpeter Equation

We shall now see how the general QED potentials, derived above by means of the field-theoretical Green's operator, can be combined with the standard MBPT procedure, leading to a unified MBPT–QED procedure. The procedure is valid for an arbitrary (quasi-degenerate) model space and equivalent to an *extension of the standard Bethe–Salpeter equation*, referred to as the *Bethe–Salpeter–Bloch equation*, briefly mentioned in Sect. 6.9 and further discussed in the next chapter (see also [5]). The procedure is also applicable to systems with more than two electrons, as will be briefly discussed at the end of this chapter.

8.3.1 MBPT-QED Procedure

The general potentials derived above – with possible hole states on the in- and outgoing lines – cannot be used iteratively in the way discussed in Chap. 6. Therefore, it cannot be used directly in a Bloch equation, like that in (6.106). For that purpose, we shall insert one extra Coulomb interaction, when holes are present, leading to the replacements

$$V^{\text{QED}} \Rightarrow V^{\text{QED}} + V^{\text{QED}} \Gamma_{\mathcal{Q}}(\mathcal{E}) V_{\text{C}} + V_{\text{C}} \Gamma_{\mathcal{Q}}(\mathcal{E}) V^{\text{QED}} + V_{\text{C}} \Gamma_{\mathcal{Q}}(\mathcal{E}) V^{\text{QED}} \Gamma_{\mathcal{Q}}(\mathcal{E}) V_{\text{C}}$$
(8.67)

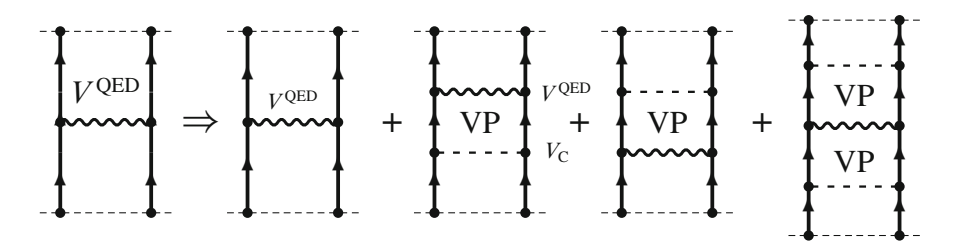


Fig. 8.11 Illustration of the modified potential (8.67), which can be iterated. It has only positive-energy states in and out and is free from the Brown–Ravenhall effect

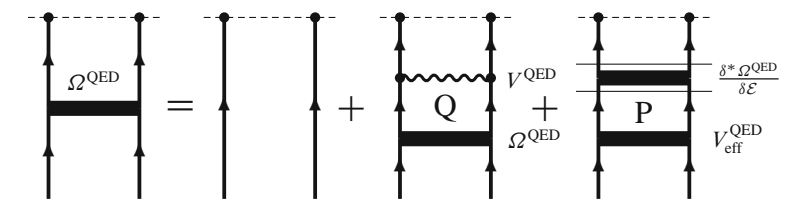


Fig. 8.12 Graphical representation of the single-photon Bloch equation (8.68). The *last diagram* represents the "folded" term, i.e., the last term of the equation. This equation can be compared with the Bethe–Salpeter equation in Fig. 9.4, valid only in the single-reference case, where there is no folded contribution. The order-by-order expansion of this equation is illustrated in Fig. 8.13

illustrated in Fig. 8.11. This potential has only particle states (positive energy) in and out, and can therefore be used iteratively in a Bloch equation.

When we have a single negative-energy state in the output, we can have a vanishing denominator of the final resolvent, which leads to a singularity of the Brown–Ravenhall type [1]. As demonstrated, though, at the beginning of this chapter, such singularities cancel when combined with the general potential. But then it is of vital importance that the potential and resolvent appear in "*matching pairs*." This will always be the case when the modified potential (8.67) is applied.

Inserting the modified potential (8.67) into the Bloch equation (6.106) leads to

$$\Omega^{\text{QED}} = 1 + \Gamma_Q V^{\text{QED}} \Omega^{\text{QED}} + \frac{\delta^* \Omega^{\text{QED}}}{\delta \mathcal{E}} V_{\text{eff}}^{\text{QED}},$$
(8.68)

where $V_{\rm eff}^{\rm QED} = PV^{\rm QED}(H_{\rm eff}^*)\Omega^{\rm QED}P$ is the corresponding effective interaction (6.139). In the last folded term only the last interaction, with the corresponding resolvent, is differentiated [see (6.105)]. The modified potential (8.67) is here regarded as a *single unit*. This equation is illustrated graphically by the Dyson type of equation in Fig. 8.12. The iterative expansion of the equation is displayed in Fig. 8.13. Solving the equation iteratively is equivalent to solving the corresponding version of the $Bethe-Salpeter-Bloch\ equation\ [see\ (6.140)\ and\ (9.30)]$.

The potential discussed above represents the dominating part of the QED effects. In order to get further, also *irreducible* combinations of transverse interactions

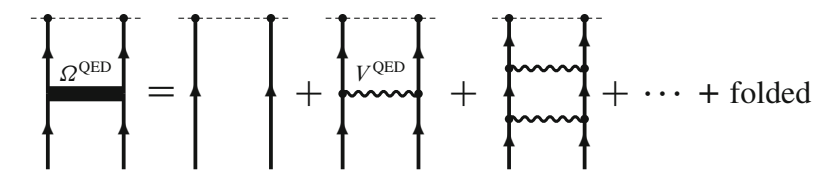


Fig. 8.13 Graphical representation of the order-by-order expansion of the Bloch equation in Fig. 8.12

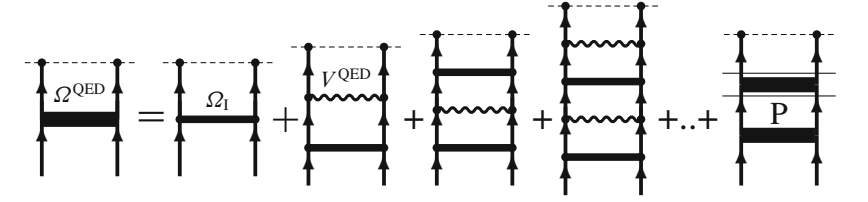


Fig. 8.14 Graphical representation of the Bloch equation (8.70), where a standard pair function (Ω_I) is combined with a QED potential

should be included (see Fig. 6.6). Formally, we can express the corresponding Bloch equation:

$$\Omega^{\text{QED}} = 1 + \Gamma_{\mathcal{Q}} \mathcal{V}^{\text{QED}} \Omega^{\text{QED}} + \frac{\delta^* \Omega^{\text{QED}}}{\delta \mathcal{E}} \mathcal{V}_{\text{eff}}^{\text{QED}},$$
(8.69)

where \mathcal{V}^{QED} is the QED potential, based on the generalized multiphoton potential, used previously (Fig. 6.6), and $\mathcal{V}^{\text{QED}}_{\text{eff}}$ is the corresponding effective interaction (6.139). This corresponds to the full Bethe–Salpeter–Bloch equation (without singles). For the time being, though, it does not seem feasible to go beyond a single transverse photon. However, the two-photon exchange can be approximated by including one retarded and one instantaneous transverse (Breit) interaction.

The potential (8.67) can also be combined with standard pair functions without virtual pairs (Fig. 2.6). This leads to the Bloch equation

$$\Omega^{\text{QED}} = \Omega_{\text{I}} + \Gamma_{Q} V^{\text{QED}} \Omega^{\text{QED}} + \frac{\delta^{*} \Omega^{\text{QED}}}{\delta \mathcal{E}} V_{\text{eff}}^{\text{QED}}$$
(8.70)

illustrated in Fig. 8.14 (and analogously in the generalized case). This implies that the Coulomb interaction is iterated to much higher order than the transverse interaction. But since the Coulomb interaction normally dominated heavily over the transverse interaction, this procedure usually represents a much faster way of generating a perturbative scheme than that represented by (8.68) and Fig. 8.12.

In the next section, we shall describe how the QED potential (8.67) can be used in a *coupled-cluster expansion*, in analogy with the standard procedure of MBPT, described in Sect. 2.5. Then also single-particle effects can be included in a systematic way, and the procedure would, in principle, be *fully equivalent to the complete*

Bethe–Salpeter–Bloch equation with singles, applicable also to open-shell systems. This approach will also make it possible to apply the procedure to more than two electrons.

In the next chapter, we analyze the Bethe–Salpeter and the Bethe–Salpeter–Bloch equations further. In Chap. 10, we discuss how the iterative procedure discussed here with a single transverse photon can be implemented and give some in numerical illustrations. The renormalization procedure is discussed in Chap. 12.

8.4 Coupled-Cluster-QED Expansion

With the interactions derived above, we can construct an effective *QED-Coupled-Cluster procedure* in analogy with that used in standard MBPT, described in Sect. 2.5 (see [7]). Considering the singles-and-doubles approximation (2.105)

$$S = S_1 + S_2, (8.71)$$

the MBPT/CC equations are illustrated in Fig. 2.8. In order to obtain the corresponding equations with the covariant potential (6.6), we make the replacements illustrated in Fig. 8.15, which leads to the equations illustrated in Fig. 8.16.

The CC-QED procedure can also be applied to systems with more than two electrons. For instance, if we consider the simple approximation (2.101)

$$\Omega = 1 + S_2 + \frac{1}{2} \{ S_2^2 \},$$

then we will have in addition to the pair function also the coupled-cluster term, illustrated in Fig. 8.17 (left). Here, one or both of the pair functions can be replaced by the QED pair function in Fig. 8.12 (right) to insert QED effects on this level. In addition, of course, single-particle clusters can be included, as in the two-particle case discussed above (Fig. 8.15).

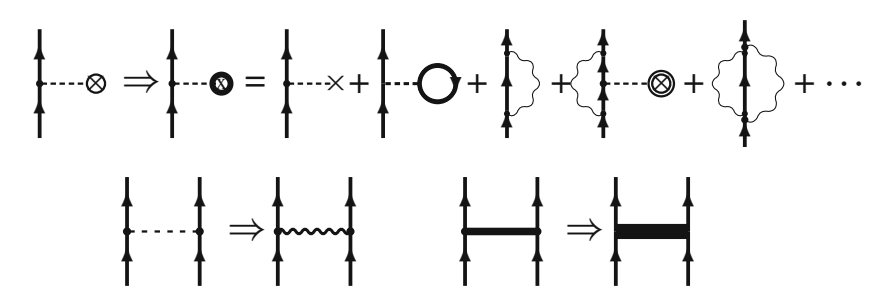


Fig. 8.15 Replacements to be made in the CC equations in Fig. 2.8 to generate the corresponding CC-QED equations (c.f. Figs. 6.4 and 6.5). The *wavy line* in the *second row* represents the modified potential (8.67) with only particle states in and out

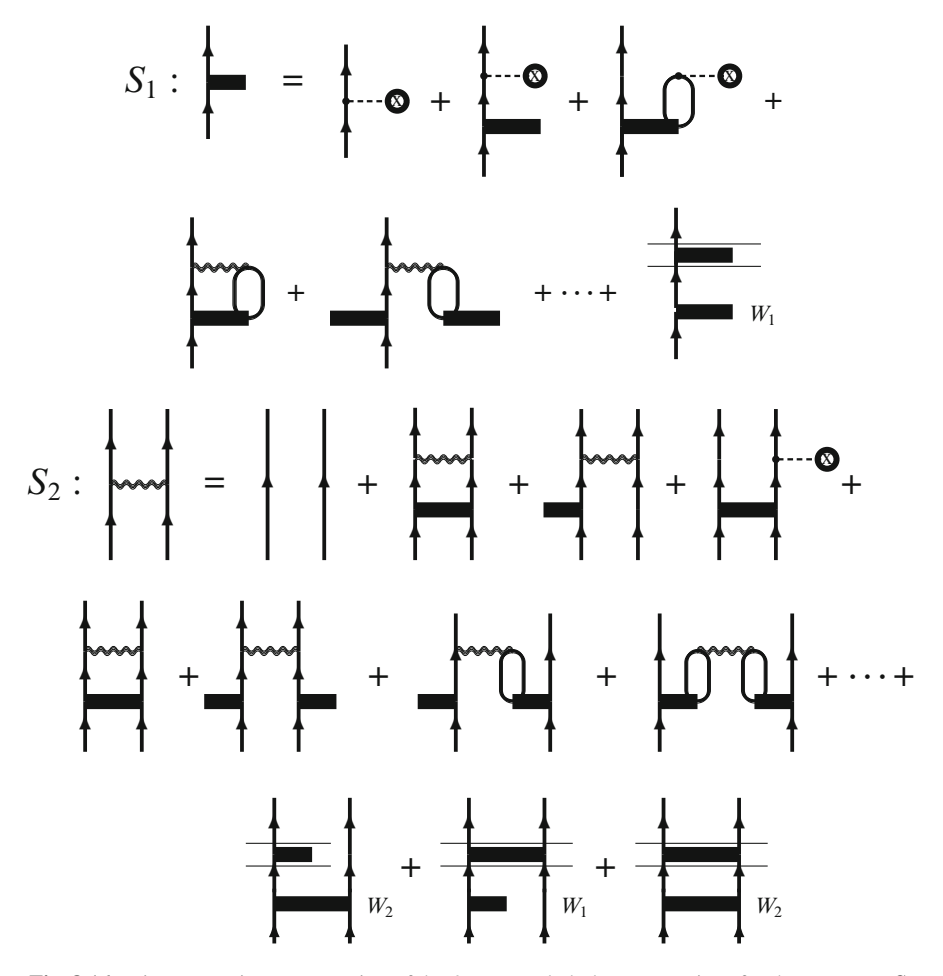


Fig. 8.16 Diagrammatic representation of the QED-coupled-cluster equations for the operators S_1 and S_2 . The *second diagram* in the *second row* and the *diagrams* in the *fourth row* are examples of coupled-cluster diagrams. The *last diagram* in the *second row* and the three *diagrams* in the *last row* represent folded terms (c.f. the corresponding standard CC equations in Fig. 2.8)

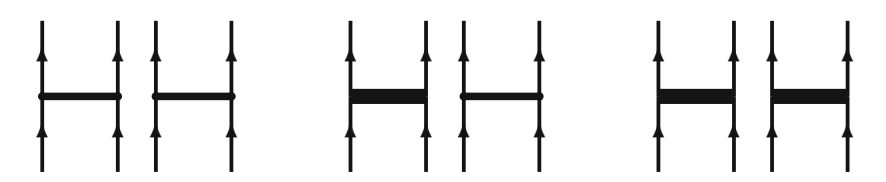


Fig. 8.17 Diagrammatic representation of the QED-coupled-cluster term $\frac{1}{2}S_2^2$ with standard pair functions (*left*) and one and two inserted QED pair function, defined in Fig. 8.12, (*right*)

We can summarize the results obtained here in the following way:

- When all one- and two-particle effects are included, the MBPT-QED procedure is fully compatible with the two-particle Bethe-Salpeter(-Bloch) equation including singles.
- The advantage of the MBPT-QED procedure is thanks to the complete compatibility with the standard MBPT procedure that the QED potentials need to be included only in cases where the effect is expected to be sufficiently important.

The procedure described here is based on the use of the Coulomb gauge (6.41), and therefore not strictly covariant. As mentioned, however, in practice, it is equivalent to a fully covariant procedure, and, furthermore, it seems to be the only feasible way for the time being to treat effects beyond two-photon exchange in a systematic fashion.

References

- Brown, G.E., Ravenhall, D.G.: On the Interaction of Two electrons. Proc. R. Soc. London, Ser. A 208, 552–59 (1951)
- 2. Hedendahl, D.: Towards a Relativistic Covariant Many-Body Perturbation Theory. Ph.D. thesis, University of Gothenburg, Gothenburg, Sweden (2010)
- 3. Hedendahl, D., Salomonson, S., Lindgren, I.: . Phys. Rev. p. (to be published) (2011)
- 4. Lindgren, I., Morrison, J.: *Atomic Many-Body Theory*. Second edition, Springer-Verlag, Berlin (1986, reprinted 2009)
- Lindgren, I., Salomonson, S., Hedendahl, D.: Many-body-QED perturbation theory: Connection to the two-electron Bethe-Salpeter equation. Einstein centennial review paper. Can. J. Phys. 83, 183–218 (2005)
- Lindgren, I., Salomonson, S., Hedendahl, D.: Many-body procedure for energy-dependent perturbation: Merging many-body perturbation theory with QED. Phys. Rev. A 73, 062,502 (2006)
- Lindgren, I., Salomonson, S., Hedendahl, D.: Coupled clusters and quantum electrodynamics. In: P. Čársky, J. Paldus, J. Pittner (eds.) Recent Progress in Coupled Cluster Methods: Theory and Applications, pp. 357–374. Springer Verlag (2010)

Chapter 9 The Bethe–Salpeter Equation

In this chapter, we discuss the *Bethe–Salpeter equation* and its relation to the procedure we have developed so far. We start by summarizing the original derivations of the equation by Bethe and Salpeter and by Gell-Mann and Low, which represented the first rigorous covariant treatments of the *bound-state* problem. We demonstrate that this field-theoretical treatment is completely compatible with the presentation made here. The treatments of Bethe and Salpeter and of Gell-Mann and Low concern the single-reference situation, while our procedure is more general. We, later in this chapter, extend the Bethe–Salpeter equation to the multireference case, which will lead to what we refer to as the *Bethe–Salpeter–Bloch equation* in analogy with corresponding equation in MBPT.

9.1 The Original Derivations by the Bethe-Salpeter Equation

The original derivations of the Bethe–Salpeter equation by Salpeter and Bethe [15] and by Gell-Mann and Low [9] were based on procedures developed in late 1940s for the relativistic treatment of the scattering of two or more particles by Feynman [7, 8], Schwinger [18, 19], Tomanaga [23] and others, and we here summarize their derivations.

9.1.1 Derivation by Salpeter and Bethe

Salpeter and Bethe [15] start their derivation from the Feynman formalism of the scattering problem [7, 8], illustrated in terms of Feynman graphs. A Feynman diagram represents in Feynman's terminology the "amplitude function" or "kernel" for the scattering process, which in the case of two-particle scattering, denoted K(3, 4; 1, 2), is the probability amplitude for one particle propagating from one space-time point x_1 to another x_3 and the other particle from space-time x_2 to x_4 . For the process involving one irreducible graph $G^{(n)}$, i.e., a graph that cannot be

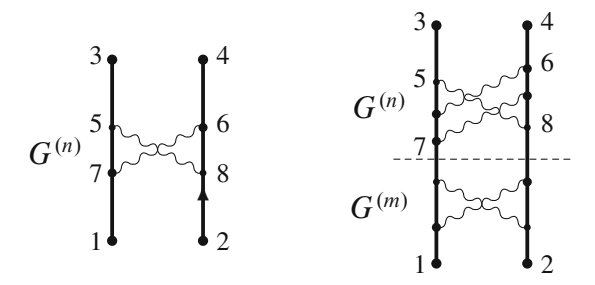


Fig. 9.1 Examples of Feynman graphs representing scattering amplitudes in Eqs. (9.1) and (9.2) of the Salpeter–Bethe paper [15]. The *first diagram* is irreducible, while the *second* is reducible, since it can be separated into two allowed diagrams by a horizontal cut

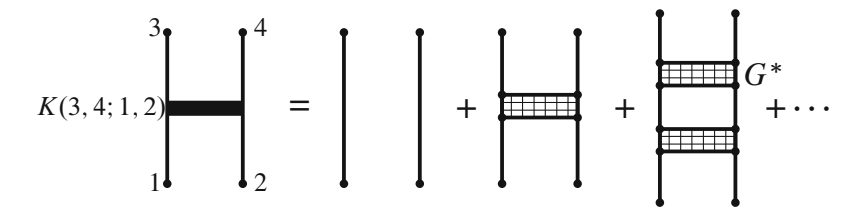


Fig. 9.2 Graphical representation of the expansion of the Feynman kernel in terms of irreducible graphs

separated into two simpler graphs, as illustrated in Fig. 9.1 (left part), the kernel is given by (in Feynman's notations)

$$K^{(n)}(3,4;1,2) = -i \iiint d\tau_5 \cdots d\tau_8 K_{+a}(3,5) K_{+b}(4,6)$$

$$\times G^{(n)}(5,6;7,8) K_{+a}(7,1) K_{+b}(8,2), \tag{9.1}$$

where K_{+a} , K_{+b} represent free-particle propagators (positive-energy part). For a process involving *two* irreducible graphs, the kernel illustrated in the right part of the figure becomes:

$$K^{(n,m)}(3,4;1,2) = -i \iiint d\tau_5 \cdots d\tau_8 K_{+a}(3,5) K_{+b}(4,6)$$

$$\times G^{(n)}(5,6;7,8) K^{(m)}(7,8;1,2). \tag{9.2}$$

This leads to the sequence illustrated in Fig. 9.2, where G^* represents the sum of *all irreducible two-particle self-energy graphs*. From this, Salpeter and Bethe arrived at an integral equation for the total kernel

$$K(3,4;1,2) = K_{+a}(3,1)K_{+b}(4,2) - i \iiint d\tau_5 \cdots d\tau_8 K_{+a}(3,5)K_{+b}(4,6)$$
$$\times G^*(5,6;7,8) K(7,8;1,2). \tag{9.3}$$

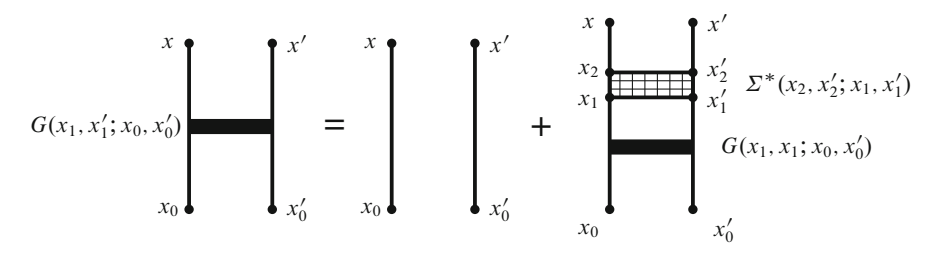


Fig. 9.3 Graphical representation of the integral equation (9.3) for the Feynman kernel of Salpeter and Bethe – identical to the Dyson equation for the two-particle Green's function (Fig. 5.8)

This is the equation for the two-particle Greens function (5.80) in the form of a *Dyson equation*, in our notations written as:

$$G(x, x'; x_0, x'_0) = G_0(x, x'; x_0, x'_0) + \iiint d^4x_1 d^4x_2 d^4x'_1 d^4x'_2 \times G_0(x, x'; x_2, x'_2) (-i) \Sigma^*(x_2, x'_2; x_1, x'_1) G(x_1, x'_1; x_0, x'_0)$$

$$(9.4)$$

and depicted in Fig. 9.3 (see also Fig. 5.8). Note that the two-particle kernel K in the terminology of Feynman and Salpeter–Bethe corresponds to our Green's function G, and the irreducible interaction G^* corresponds to our proper self-energy Σ^* . The proper (or irreducible) self-energy is identical to the irreducible two-particle potential in Fig. 6.6. Furthermore, the electron propagators are in the Feynman–Salpeter–Bethe treatment free-particle propagators. Note that the intermediate lines in Fig. 9.3 represent a Green's function, where the singularities are eliminated.

Salpeter and Bethe then argued that a similar equation could be set up for the *bound-state wave function*. Since the free lines of the diagrams in the Feynman formulation represent free particles, they concluded that the first (inhomogeneous) term on the right-hand side could not contribute, as the bound-state wave function cannot contain any free-particle component. This leads in their notations to the *homogeneous* equation:

$$\Psi(3,4) = -i \iiint d\tau_5 \cdots d\tau_8 K_{+a}(3,5) K_{+b}(4,6) G^*(5,6;7,8) \Psi(7,8).$$
(9.5)

This is the famous *Bethe–Salpeter equation*. In the *Furry picture* we use here, where the basis single-electron states are generated in an external (nuclear) potential, the inhomogeneous term does survive, and the equation becomes in our notations

$$\Psi(x, x') = \Phi(x, x') + \iiint d^4x_1 d^4x_2 d^4x'_1 d^4x'_2 \times G_0(x, x'; x_2, x'_2) (-i) \Sigma^*(x_2, x'_2; x_1, x'_1) \Psi(x_1, x'_1).$$
(9.6)

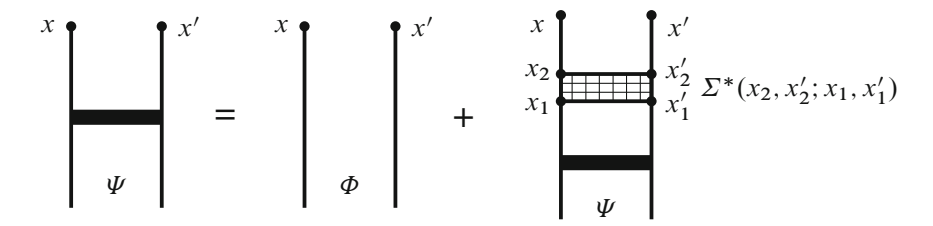


Fig. 9.4 Graphical representation of the *inhomogeneous* Bethe–Salpeter equation (9.6). Σ^* represents the proper self-energy, which contains all irreducible interaction graphs and is identical to the irreducible two-particle potential in Fig. 6.6. This equation can be compared with that represented in Fig. 8.12, valid also in the multireference case

This is the *inhomogeneous Bethe–Salpeter equation* we shall use, and it is graphically depicted in Fig. 9.4.

9.1.2 Derivation by Gell-Mann and Low

The derivation of Gell-Mann and Low [9] starts from the "Feynman two-body kernel," used in the definition of the Green's function (5.20) (in their slightly modified notations):

$$K(x_1, x_2; x_3, x_4) = \langle \Psi_0 | T[\hat{\psi}_H(x_1)\hat{\psi}_H(x_2)\hat{\psi}_H^{\dagger}(x_4)\hat{\psi}_H^{\dagger}(x_3)] | \Psi_0 \rangle. \tag{9.7}$$

T is the time-ordering operator (2.27) and $\hat{\psi}_{\rm H}$, $\hat{\psi}_{\rm H}^{\dagger}$ are the particle-field operators in the Heisenberg representation. Ψ_0 is the vacuum (ground state) of the interacting system in the *Heisenberg picture*, $|0_{\rm H}\rangle$.

In an Appendix of the same paper, Gell-Mann and Low derive a relation between the interacting (Ψ_0) and the noninteracting (Φ_0) vacuum states (both in the interaction picture):

$$c\Psi_0 = \frac{U(0, -\infty)\Phi_0}{\langle \Phi_0 | U(0, -\infty) | \Phi_0 \rangle},\tag{9.8}$$

which is the famous Gell-Mann-Low theorem (3.29), discussed previously. Here, c is a normalization constant (equal to unity in the intermediate normalization that we use). This can be eliminated by considering

$$1 = \langle \Psi_0 | \Psi_0 \rangle = \frac{\langle \Phi_0 | U(\infty, -\infty) | \Phi_0 \rangle}{c^2 \langle \Phi_0 | U(\infty, 0) | \Phi_0 \rangle \langle \Phi_0 | U(0, -\infty) | \Phi_0 \rangle}.$$
 (9.9)

Inserting the expression (9.8) into the kernel (9.7), using the relation (9.9), yields:

$$K(x_1, x_2; x_3, x_4) = \frac{\langle \Phi_0 | U(\infty, 0) T[\hat{\psi}_{H}(x_1) \hat{\psi}_{H}(x_2) \hat{\psi}_{H}^{\dagger}(x_4) \hat{\psi}_{H}^{\dagger}(x_3)] U(0, -\infty) | \Phi_0 \rangle}{\langle \Phi_0 | U(\infty, -\infty) | \Phi_0 \rangle},$$
(9.10)

which is equivalent to the field-theoretical definition of the Green's function $G(x_1, x_2; x_3, x_4)$ in (5.20).

Gell-Mann and Low then conclude that expanding the expression above in a perturbation series leads to the two-body kernel of Feynman in terms of Feynman diagrams, as we have performed in Chap. 5. This is identical to the expansion given by Salpeter and Bethe, and hence leads also to the integral equation (9.3). Gell-Mann and Low then use the same arguments as Salpeter and Bethe to set up the Bethe–Salpeter equation (9.5) for the wave function. In addition, they argue that *single-particle self-energy parts* can easily be included by modifying the single-particle propagators.

The derivation of Gell-Mann and Low, which starts from the field-theoretical definition of the Green's function, has a firm field-theoretical basis. This is true, in principle, also of the derivation of Salpeter and Bethe, which is based on Feynman diagrams for scattering of field-theoretical origin.

In Sect. 9.1.3, we shall see how the Bethe–Salpeter equation can be motivated from the graphical form of the Dyson equation in Fig. 9.3.

9.1.3 Analysis of the Derivations of the Bethe-Salpeter Equation

We can understand the Bethe–Salpeter equation graphically, if we let the Dyson equation in Fig. 9.3 act on the zeroth-order state, $\Phi(x_0, x_0')$, which we represent by two vertical lines without interaction. (The treatment can easily be extended to the situation, where the model function is a linear combination of straight products.) From the relation (6.7), we see that the electron propagator acting on an electron-field operator (with space integration) shifts the coordinates of the operator. Therefore, acting with the zeroth-order Green's function on the model function shifts the coordinates of the function according to:

$$\Phi(x, x') = \iint d^3 \mathbf{x}_0 d^3 \mathbf{x}'_0 G_0(x, x'; x_0, x'_0) \Phi(x_0, x'_0). \tag{9.11}$$

This is illustrated in Fig. 9.5 (left) and corresponds to the first diagram on the right-hand side of Fig. 9.4. Similarly, operating with the *full* Green's function in Fig. 9.5 on the model function leads to

$$\Psi(x, x') = \iint d^3 \mathbf{x}_0 d^3 \mathbf{x}'_0 G(x, x'; x_0, x'_0) \Phi(x_0, x'_0)$$
(9.12)

illustrated in Fig. 9.5 (right). Then the entire equation (9.6), illustrated in Fig. 9.4, is reproduced.

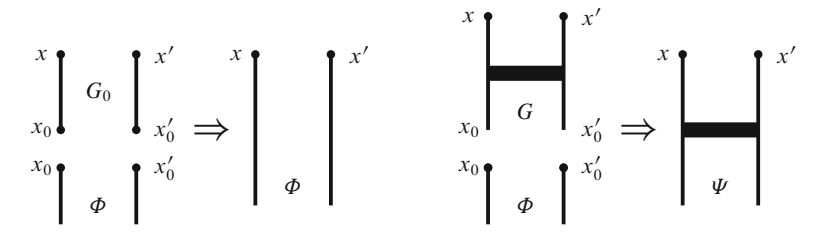


Fig. 9.5 Graphical illustration of Eqs. (9.11) and (9.12)

The equation (9.12) is consistent with the definition of the classical Green's function (5.1), which propagates a wave function from one space-time point to another – in our case from one *pair* of space-time point to another. This equation can also be expressed as an *operator equation*

$$|\Psi(t,t')\rangle = \mathcal{G}(t,t';t_0,t_0')|\Psi(t_0,t_0')\rangle,$$
 (9.13)

where \mathcal{G} is the *Green's operator*, introduced in Sect. 6.6. The coordinate representation of this equation

$$\langle x, x' | \Psi(t, t') \rangle = \langle x, x' | \mathcal{G}(t, t'; t_0, t'_0) | x_0, x'_0 \rangle \langle x_0, x'_0 | \Psi(t_0, t'_0) \rangle$$
(9.14)

is identical to (9.12).

This implies that:

- The Green's function is the coordinate representation of the Green's operator.
- The four-times Green's operator represents the time propagation of the two-particle Bethe-Salpeter state vector.

In the equal-time approximation, this is consistent with our previous result (6.50) and with our conjecture (6.29).

It is of interest to compare the Bethe–Salpeter equation (9.6), depicted in Fig. 9.4, with the Dyson equation for the combined QED-electron correlation effects in Fig. 8.12. If in the latter more and more effects are included in the QED potential, then the Coulomb interactions, represented by the standard pair function, become insignificant. Then, this equation is identical to the Bethe–Salpeter equation. Solving the original BS equation iteratively, however, is extremely tedious and often very slowly converging, due to the dominating Coulomb interaction. As mentioned in the previous chapter, the QED-correlation equation is expected to be a faster road to reach the same goal. One- and two-photon exchange in the QED potential will very likely yield extremely good results, while such effects in the BS equation will often be quite insufficient (c.f. the discussion about the QED methods in Part II).

9.2 Quasi-Potential and Effective-Potential Approximations: Single-Reference Case

In the equal-time approximation, where we equalize the times of the two particles in the Bethe–Salpeter equation (9.6), we can make a Fourier transformation of it with a single energy parameter as in the treatment of the single-particle Green's function in Sect. 5.2.3. The Q part, falling outside the model space, then leads to:

$$Q \Psi(E) = Q G_0(E) (-i) \Sigma^*(E) \Psi(E)$$
(9.15)

leaving out the space coordinates and integrations.

Replacing the zeroth-order Green's function with the resolvent (5.43)

$$G_0(E) = \frac{i}{E - H_0},\tag{9.16}$$

we obtain

$$O(E - H_0)\Psi(E) = O\Sigma^*(E)\Psi(E).$$
 (9.17)

If we identify the proper self-energy with the generalized potential (8.11)

$$\mathcal{V}(E) = \Sigma^*(E),\tag{9.18}$$

the equation above leads together with the relation (6.125)

$$P(H - H_0)\Omega\Psi(E) = PV(E)\Psi(E) \tag{9.19}$$

to

• The effective-potential form of the Bethe-Salpeter equation

$$(E - H_0)|\Psi\rangle = \mathcal{V}(E)|\Psi\rangle$$
(9.20)

frequently used in various applications. This equation was also derived above, using the Green's operator only (6.126).

The equation (9.20) can also be expressed

$$|\Psi\rangle = |\Psi_0\rangle + \frac{Q}{E - H_0} \mathcal{V}(E)|\Psi\rangle,$$
 (9.21)

where Ψ_0 is the model state $\Psi_0 = P\Psi$. This is equivalent to the **Lippmann-Schwinger equation** [12], frequently used in scattering theory. Formally, the equation (9.20) can also be expressed in the form of the time-independent Schrödinger equation

$$H\Psi = E\Psi, \tag{9.22}$$

where H is the energy-dependent Hamiltonian

$$H(E) = H_0 + \mathcal{V}(E).$$
 (9.23)

Equation (9.20) operates entirely in the restricted Hilbert space with constant number of photons. This can be related to the equivalent equation (6.32), derived by means of the Gell-Mann–Low theorem, which operates in the *photonic Fock space*. We can then regard the equation above as the *projection of the Fock-space equation onto the restricted space*.

9.3 Bethe-Salpeter-Bloch Equation: Multireference Case

We can extend the treatment above to the general multireference case. From the expression (6.117), using the fact that the Green's operator at time t=0 is identical to the wave operator (6.52), we have in the *single-reference case* (one-dimensional) model space

$$|\Psi\rangle = \Omega|\Psi_0\rangle = \left[1 + \Gamma_Q(E)\,\mathcal{V}(E) + \Gamma_Q(E)\,\mathcal{V}(E)\Gamma_Q(E)\,V(E) + \cdots\right] |\Psi_0\rangle,\tag{9.24}$$

where $|\Psi_0\rangle$ is the model state, $|\Psi_0\rangle = P|\Psi\rangle$, and

$$\Gamma_Q(E) = \frac{Q}{E - H_0}$$

is the reduced resolvent (2.65).

Operating on (9.24) from the left with $Q(E - H_0)$ now yields

$$Q(E - H_0)|\Psi\rangle = QV(E)|\Psi\rangle, \qquad (9.25)$$

which is identical to the equation (9.17) with the identification (9.18).

For a general multidimensional (quasi-degenerate) model space, we have similarly

$$Q(E^{\alpha} - H_0)|\Psi^{\alpha}\rangle = Q\mathcal{V}(E^{\alpha})|\Psi^{\alpha}\rangle \tag{9.26}$$

and

$$P(E^{\alpha} - H_0)|\Psi^{\alpha}\rangle = P\mathcal{V}(E^{\alpha})|\Psi^{\alpha}\rangle. \tag{9.27}$$

This leads to

$$(E^{\alpha} - H_0)|\Psi^{\alpha}\rangle = \mathcal{V}(E^{\alpha})|\Psi^{\alpha}\rangle \tag{9.28}$$

or in operator form

$$(H_{\text{eff}}^* - H_0)\Omega P = \mathcal{V}(H_{\text{eff}}^*)\Omega P \tag{9.29}$$

using the notations introduced in Sect. 6.9. But

$$H_{\text{eff}}^* \Omega P = \Omega H_{\text{eff}} P = \Omega H_0 P + \Omega V_{\text{eff}} P$$

which yields the commutator relation

$$[\Omega, H_0] P = \mathcal{V}(H_{\text{eff}}^*) \Omega P - \Omega P \mathcal{V}_{\text{eff}} P,$$
 (9.30)

where according to (6.139) $\mathcal{V}_{\mathrm{eff}}P = P\mathcal{V}(H_{\mathrm{eff}}^*)\Omega P$. Here, the energy parameter of $\mathcal{V}(H_{\mathrm{eff}}^*)$ is given by the model-space state to the far right, while the energy parameter of Ω of the folded term depends on the intermediate model-space state (see footnote in Sect. 6.6). This equation is valid in the general *multireference* (*quasi-degenerate*) *situation* and represents an extension of the effective-potential form (9.20) of the Bethe–Salpeter equation. Due to its close resemblance with the standard Bloch equation of MBPT (2.56), we refer to it as the *Bethe–Salpeter–Bloch equation*. This is equivalent to the generalized Bethe–Salpeter equation, derived in Chap. 6 (6.140).

In analogy with the MBPT treatment in Sect. 2.5, we can separate the BS-Bloch equation into

$$[\Omega_{1}, H_{0}]P = (\mathcal{V}(H_{\text{eff}}^{*})\Omega P - \Omega P \mathcal{V}_{\text{eff}}(H_{0}^{*})P)_{\text{linked},1},$$

$$[\Omega_{2}, H_{0}]P = (\mathcal{V}(H_{\text{eff}}^{*})\Omega P - \Omega P \mathcal{V}_{\text{eff}}(H_{0}^{*})P)_{\text{linked},2},$$
(9.31)

etc. It should be noted that the potential operator $\mathcal{V}(H_{\text{eff}}^*)$ is an operator or matrix where each element is an operator/matrix. In the first iteration, we set $H_{\text{eff}} = H_0$ and in the next iteration $H_{\text{eff}} = H_0 + V_{\text{eff}}^{(1)}$ etc. Continued iterations correspond to the sum term in the expression (6.96), representing the model-space contributions. The two-particle BS-Bloch equation above is an extension of the ordinary pair equation, discussed in Sect. 2.5 (Fig. 2.6).

The Bethe–Salpeter–Bloch equation leads to a perturbation expansion of Rayleigh–Schrödinger or linked-diagram type, analogous to that of standard MBPT expansions. It differs from the standard Bloch equation by the fact that the Coulomb interaction is replaced by all irreducible multiphoton interactions.

Solving the BS-Bloch equation (9.30) is NOT equivalent to solving the single-state equation for a number of states. The Bloch equation (9.30) leads to a Rayleigh/Schrödinger/linked-diagram expansion with folded terms that *is size extensive*. The single-state equation (9.20), on the other hand, leads to a Brillouin–Wigner expansion (see footnote in Sect. 2.4), that is *not* size extensive.

Due to the very complicate form of the potential of the Bethe–Salpeter–Bloch equation, it is very difficult to handle this equation in its full extent. In the previous chapters, we have considered a simpler way of achieving essentially the same goal.

9.4 Problems with the Bethe–Salpeter Equation

There are several fundamental problems with the Bethe–Salpeter equation and with relativistic quantum mechanics in general, as briefly mentioned in the Introduction. Dyson says in his 1953 paper [6] that this is a subject "full of obscurities and unsolved problems." The question concerns the relation between the three-dimensional and the four-dimensional wave functions. In standard quantum mechanics, the three-dimensional wave function describes the system at a particular time, while the four-dimensional two-particle wave function describes the probability amplitude for finding particle one at a certain position at a certain time and particle two at another position at another time, etc. The latter view is that of the Bethe-Salpeter equation, and Dyson establishes a connection between the two views. The main problem is here the individual times associated with the particles involved, the physical meaning of which is not completely understood. This problem was further analyzed by Wick [24] and Cutkoski [4] and others. The relative time of the particles leads to a number of anomalous or spurious states – states that do not have nonrelativistic counterparts. This problem was analyzed in detail in 1965 by Nakanishi [13], and the situation was summarized in 1997 in a comprehensive paper by Namyslowski [14].

The Bethe–Salpeter equation was originally set up for the bound-state problem involving nucleons, such as the ground state of the deuteron. The equation has lately been extensively used for scattering problems in quantum chromodynamics, quark–quark/antiquark scattering. The equation has also been used for a long time in high-accuracy works on simple atomic systems, such as positronium, muonium, hydrogen, and helium-like ions. The problems with the BS equation, associated with the relative time, are most pronounced at strong coupling and assumed to be negligible in atomic physics, due to the very weak coupling. One important question is, of course, whether this is true also in the very high accuracy that is achieved in recent time.

To attack the BS equation directly is very complicated, and for that reason various approximations and alternative schemes have been developed. The most obvious approximation is to eliminate the relative time of the particles, the *equal-time approximation* or *external-potential approach*. The first application of this technique seems to be have been made in the thesis of Sucher in the late 1950s [20, 21] for the evaluation of the leading QED corrections to the energy levels of the helium atom. This work has been extended by Douglas and Kroll [5] and by Drake, Zhang, and coworkers [25, 26], as will be further discussed in the Chap. 11. Another early application of an effective-potential approach was that of Grotch and Yennie [11] to obtain high-order effects of the nuclear recoil on the energy levels of atomic hydrogen. They derived an "*effective potential*" from scattering theory and applied that in a Schrödinger-like equation. A similar approach was applied to strongly interacting nucleons in the same year by Gross [10], assuming that one of the particles was "on the mass shell." Related techniques have been applied to bound-state QED problems among others by Caswell and Lepage [2] and by Bodwin et al. [1]. A more

References 209

formal derivation of a "quasipotential" method for scattering as well as bound-state problems was made by Todorov [22], starting from the Lippmann–Schwinger scattering theory [12].

Several attempts have been made to correct for the equal-time approximation. Sazdjian [16, 17] has converted the BSE into *two* equations, one for the relative time and one eigenvalue equation of Schrödinger type. Connell [3] has developed a series of approximations, which ultimately are claimed to lead to the exact BSE. The approaches were primarily intended for strong interactions, but Connell tested the method on QED problems.

References

- Boldwin, G.T., Yennie, D.R., Gregorio, M.A.: Recoil effects in the hyperfine structure of QED bound states. Rev. Mod. Phys. 57, 723–82 (1985)
- 2. Caswell, W.E., Lepage, G.P.: Reduction of the Bethe-Salpeter equation to an equivalent Schrödinger equation, with applications. Phys. Rev. A 18, 810–19 (1978)
- Connell, J.H.: QED test of a Bethe-Salpeter solution method. Phys. Rev. D 43, 1393–1402 (1991)
- 4. Cutkosky, R.E.: Solutions of the Bethe-Salpeter equation. Phys. Rev. 96, 1135–41 (1954)
- Douglas, M.H., Kroll, N.M.: Quantum Electrodynamical Corrections to the Fine Structure of Helium. Ann. Phys. (N.Y.) 82, 89–155 (1974)
- 6. Dyson, F.J.: The Wave Function of a Relativistic System. Phys. Rev. 91, 1543–50 (1953)
- 7. Feynman, R.P.: Space-Time Approach to Quantum Electrodynamics. Phys. Rev. **76**, 769–88 (1949)
- 8. Feynman, R.P.: *The Theory of Positrons*. Phys. Rev. **76**, 749–59 (1949)
- 9. Gell-Mann, M., Low, F.: Bound States in Quantum Field Theory. Phys. Rev. 84, 350-54 (1951)
- 10. Gross, F.: *Three-dimensionsl Covariant Integral Equations for Low-Energy Systems*. Phys. Rev. **186**, 1448–62 (1969)
- 11. Grotch, H., Yennie, D.R.: Effective Potential Model for Calculating Nuclear Corrections to the Eenergy Levels of Hydrogen. Rev. Mod. Phys. 41, 350–74 (1969)
- 12. Lippmann, B.A., Schwinger, J.: Variational Principles for Scattering Processes. I. Phys. Rev. 79, 469–80 (1950)
- 13. Nakanishi, N.: Normalization condition and normal and abnormal solutions of Bethe-Salpeter equation. Phys. Rev. 138, B1182 (1965)
- Namyslowski, J.M.: The Relativistic Bound State Wave Function. in Light-Front Quantization and Non-Perturbative QCD, J.P. Vary and F. Wolz, eds. (International Institute of Theoretical and Applied Physics, Ames) (1997)
- Salpeter, E.E., Bethe, H.A.: A Relativistic Equation for Bound-State Problems. Phys. Rev. 84, 1232–42 (1951)
- Sazdjian, H.: Relativistiv wave equations for the dynamics of two interacting particles. Phys. Rev. D 33, 3401–24 (1987)
- 17. Sazdjian, H.: The connection of two-particle relativistic quantum mechanics with the Bethe-Salpeter equation. J. Math. Phys. 28, 2618–38 (1987)
- 18. Schwinger, J.: On quantum electrodynamics and the magnetic moment of the electron. Phys. Rev. 73, 416 (1948)
- 19. Schwinger, J.: Quantum electrodynamics I. A covariant formulation. Phys. Rev. 74, 1439 (1948)
- 20. Sucher, J.: Energy Levels of the Two-Electron Atom to Order α³ Ry; Ionization Energy of Helium. Phys. Rev. **109**, 1010–11 (1957)

- Sucher, J.: Ph.D. thesis, Columbia University (1958). Univ. Microfilm Internat., Ann Arbor, Michigan
- 22. Todorov, I.T.: Quasipotential Equation Corresponding to the relativistic Eikonal Approximation. Phys. Rev. D 3, 2351–56 (1971)
- 23. Tomanaga, S.: On Infinite Field Reactions in Quantum Field Theory. Phys. Rev. 74, 224–25 (1948)
- 24. Wick, G.C.: Properties of Bethe-Salpeter Wave Functions. Phys. Rev. 96, 1124–34 (1954)
- 25. Zhang, T.: Corrections to $O(\alpha^7(\ln \alpha)mc^2)$ fine-structure splittings and $O(\alpha^6(\ln \alpha)mc^2)$ energy levels in helium. Phys. Rev. A **54**, 1252–1312 (1996)
- 26. Zhang, T., Drake, G.W.F.: A rigorous treatment of O(α⁶ mc²) QED corrections to the fine structure splitting of helium. J. Phys. B **27**, L311–16 (1994)

Chapter 10

Implementation of the MBPT-QED Procedure with Numerical Results

In this chapter, we shall see how the combined covariant-evolution-QED approach developed in the previous chapters can be implemented numerically. In principle, this is equivalent to solving the complete Bethe–Salpeter equation *perturbatively*, but in practice, of course, approximations have to be made. We shall consistently work in the Coulomb gauge.¹

We shall restrict ourselves here to the exchange of a *single transverse photon* together with a number of Coulomb interactions. We shall first apply the procedure in the no-pair case, and later a different procedure in the presence of virtual pairs will be applied. We work in the photonic Fock space, and initially we shall derive some relations for that space.

10.1 The Fock-Space Bloch Equation

We have seen earlier that with the perturbation (6.35)

$$\mathcal{H}(x) = \mathcal{H}(t, \mathbf{x}) = -\hat{\psi}^{\dagger}(x) e c \alpha^{\mu} A_{\mu}(x) \hat{\psi}(x), \tag{10.1}$$

the wave function partly lies in an *extended photonic Fock space*, where the number of photons is no longer constant. According to the Gell-Mann–Low theorem, we have a Schrödinger-like equation (6.32) in that space

$$(H_0 + V_F)|\Psi^{\alpha}\rangle = E^{\alpha}|\Psi^{\alpha}\rangle, \qquad (10.2)$$

where $V_{\rm F}$ is the perturbation (6.36) with the Coulomb and the transverse parts, $V_{\rm F} = V_{\rm C} + v_{\rm T}$. We shall demonstrate below that, for single-photon exchange, this leads to a perturbation that is *time-independent* in the Schrödinger picture, which is a requirement for the GML theorem. Furthermore, in working in the extended space

¹ This chapter is mainly based on [3,5] and, in particular, on the thesis of Daniel Hedendahl [1].

with uncontracted perturbations, it is necessary to include in the model Hamiltonian (H_0) also the energy operator of the photon field (6.38)

$$H_0 = H_0 + c\kappa \, a_i^{\dagger}(\mathbf{k}) \, a_i(\mathbf{k}),$$
 (10.3)

where $\kappa = |\mathbf{k}|$.

The wave operator is, as before, given by the Green's operator at t = 0 (6.52), which may now contain uncontracted photon terms

$$|\Psi^{\alpha}\rangle = \Omega|\Psi_0^{\alpha}\rangle. \tag{10.4}$$

 $|\Psi_0^{\alpha}\rangle=P|\Psi^{\alpha}\rangle$ is the corresponding model state, which lies entirely within the restricted space with no uncontracted photons.

From the GML equation (10.2), it can be shown in the same way as for the restricted space that the standard Bloch equation (2.56) is still valid also in the extended space

$$\boxed{\left[\Omega, H_0\right] P = \left(V_F \Omega - \Omega V_{\text{eff}}\right) P.}$$
(10.5)

The effective interaction is here given by $V_{\rm eff} = P V_{\rm F} \Omega P$ (6.61). The equation is formally the same as in the standard MBPT (2.56), but the operators involved now have somewhat different interpretation.

The expressions for single transverse-photon exchange are given by (8.11). In the Coulomb gauge, these expressions involve the functions f_T^C , given by (4.60)

$$f_{\mathrm{T}}^{\mathrm{C}}(\kappa) = \frac{e^2}{4\pi^2 \epsilon_0} \left[\alpha_1 \cdot \alpha_2 \frac{\sin(\kappa r_{12})}{r_{12}} - (\alpha_1 \cdot \nabla_1) (\alpha_2 \cdot \nabla_2) \frac{\sin(\kappa r_{12})}{\kappa^2 r_{12}} \right]. \quad (10.6)$$

By means of the expansion theorem

$$\frac{\sin \kappa r_{12}}{\kappa r_{12}} = \sum_{l=0}^{\infty} (2l+1) j_l(\kappa r_1) j_l(\kappa r_2) \mathbf{C}^l(1) \cdot \mathbf{C}^l(2), \tag{10.7}$$

where $j_l(\kappa r)$ are radial Bessel functions and C^l vector spherical harmonics [4], we can express the function f_T^C as a sum of products of single-electron operators [5, Appendix B]

$$f_{\mathrm{T}}^{\mathrm{C}}(\kappa) = \sum_{l=0}^{\infty} \left[V_{\mathrm{G}}^{l}(\kappa r_{1}) \cdot V_{\mathrm{G}}^{l}(\kappa r_{2}) + V_{\mathrm{sr}}^{l}(\kappa r_{1}) \cdot V_{\mathrm{sr}}^{l}(\kappa r_{2}) \right], \tag{10.8}$$

where

$$V_{\rm G}^l(\kappa r) = \frac{e}{2\pi\sqrt{\epsilon_0}}\sqrt{\kappa(2l+1)} \ j_l(\kappa r) \alpha C^l, \tag{10.9a}$$

$$V_{\rm sr}^{l}(\kappa r) = \frac{e}{2\pi\sqrt{\epsilon_0}}\sqrt{\frac{\kappa}{2l+1}} \left[\sqrt{(l+1)(2l+3)} \, j_{l+1}(\kappa r) \{\alpha C^{l+1}\}^{l} + \sqrt{l(2l-1)} \, j_{l-1}(\kappa r) \{\alpha C^{l-1}\}^{l} \right]. \quad (10.9b)$$

In (10.6), the first term represents the *Gaunt interaction* and the second term the *scalar retardation*, which together form the Breit interaction (see Appendix F.2.2). Each term in the expansion – which are all time independent in the Schrödinger picture – will together with the Coulomb interaction ($V_{\rm C}=e^2/4\pi r_{12}$) form the (time-independent) perturbation

$$V_{\rm F} = V_{\rm C} + V_{\rm G}^l(\kappa r) + V_{\rm sr}^l(\kappa r).$$
 (10.10)

10.2 Single-Photon Potential in Coulomb Gauge: No Virtual Pairs

We consider first the case where no virtual pairs are present. Inserting the perturbation (10.10) into the Bloch equation (10.5) yields

$$[\Omega, H_0]P = (V_C + V^l)\Omega P - \Omega V_{\text{eff}}, \qquad (10.11)$$

where we use V^l as a short-hand notation for the Gaunt and scalar-retardation parts in (10.10). We consider first a number of instantaneous Coulomb interaction, forming a standard pair function (2.97), including also the zeroth order,

$$\Omega_{\rm I} P_{\mathcal{E}} = \left[1 + \Gamma_O(\mathcal{E}) I^{\rm Pair} \right] P_{\mathcal{E}}. \tag{10.12}$$

This includes also the folds and is represented by the first diagram in Fig. 10.1. Then we can perturb this by one of the V^I terms, representing part of the transverse Breit interaction, leading to the equation

$$[\Omega^l, H_0] P_{\mathcal{E}} = V^l \Omega_1 P_{\mathcal{E}} - \Omega^l P_{\mathcal{E}'} I^{\text{Pair}} P_{\mathcal{E}}$$
 (10.13)

or

$$\left(\mathcal{E} - h_0(1) - h_0(2) - c\kappa\right) |\Omega_{ab}^l\rangle = V^l |\Omega_{Iab}\rangle - |\Omega_{cd}^l\rangle \langle cd| I^{\text{Pair}} |ab\rangle \,, \qquad (10.14)$$

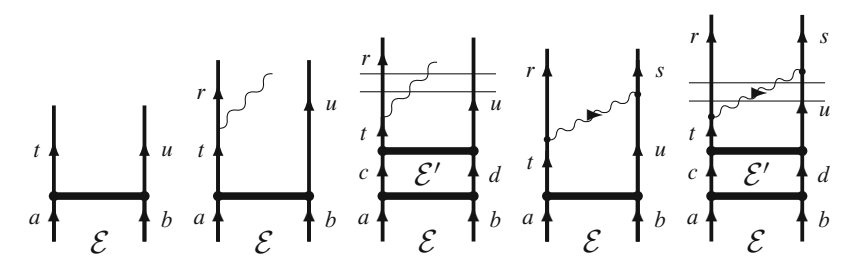


Fig. 10.1 Expansion of the Bloch equation (10.11) in the Fock space, no virtual pairs, leading to single-photon exchange, including folded diagrams

 $(\mathcal{E},\mathcal{E}')$ are here the energies of the unperturbed states $|ab\rangle$ and $|cd\rangle$, respectively). This equation has the solution

$$\langle ru|\Omega_{ab}^{l}\rangle = \langle ru|\frac{V^{l}}{\mathcal{E} - \varepsilon_{r} - \varepsilon_{u} - c\kappa} |\Omega_{1ab}\rangle$$

$$-\langle ru|\frac{V^{l}}{(\mathcal{E} - \varepsilon_{r} - \varepsilon_{u} - c\kappa)(\mathcal{E}' - \varepsilon_{r} - \varepsilon_{u} - c\kappa)} |\Omega_{1cd}\rangle \langle cd|I^{\text{Pair}}|ab\rangle, \quad (10.15)$$

where Ω_{Ipq} represents a pair function (10.12) starting from the state $|pq\rangle$. Here, the first term is represented by the second diagrams in the Fig. 10.1 and the last term by the third "folded" diagram. The double bar indicates here the double denominator, which yields the first-order derivative (difference ratio) of the potential.

By adding a second perturbation V^l , we can complete the single-photon exchange between the electrons, which corresponds to solving the pair equation

$$(\mathcal{E} - h_0(1) - h_0(2)) \Omega_{\rm sp} P_{\mathcal{E}} = V^l \Omega^l P_{\mathcal{E}} - \Omega_{\rm sp} P_{\mathcal{E}'} I^{\rm Pair} P_{\mathcal{E}}.$$
 (10.16)

This yields

$$\langle rs|\Omega_{\rm sp}|ab\rangle = \frac{\langle rs|V^{l}|ru\rangle \langle ru|V^{l}|\Omega_{\rm I}ab\rangle}{(\mathcal{E} - \varepsilon_{r} - \varepsilon_{s})(\mathcal{E} - \varepsilon_{r} - \varepsilon_{u} - c\kappa)} - \frac{\langle rs|V^{l}|ru\rangle \langle ru|V^{l}|\Omega_{\rm I}cd\rangle}{(\mathcal{E} - \varepsilon_{r} - \varepsilon_{s})(\mathcal{E} - \varepsilon_{r} - \varepsilon_{u} - c\kappa)\mathcal{E}' - \varepsilon_{r} - \varepsilon_{u} - c\kappa)} \times \langle cd|I^{\rm Pair}|ab\rangle - \frac{\langle rs|\Omega_{\rm sp}|cd\rangle \langle cd|I^{\rm Pair}|ab\rangle}{\mathcal{E} - \varepsilon_{r} - \varepsilon_{s}}.$$

$$(10.17)$$

This is illustrated by the last two diagrams of Fig. 10.1 (except for the final folded contribution).

Summing over κ and l, including the Gaunt as well as the scalar-retardation parts and considering photon emission from both electrons, we see that the result is in agreement with the Bloch equation (8.68) to first order

$$\Omega_{\rm sp} P_{\mathcal{E}} = \Gamma_{\mathcal{Q}}(\mathcal{E}) V_{\rm sp} \Omega_{\rm I} P_{\mathcal{E}} + \frac{\delta(\Gamma_{\mathcal{Q}} V_{\rm sp})}{\delta \mathcal{E}} P_{\mathcal{E}'} I^{\rm Pair} P_{\mathcal{E}}
= \Gamma_{\mathcal{Q}}(\mathcal{E}) V_{\rm sp} \Omega_{\rm I} P_{\mathcal{E}} + \Gamma_{\mathcal{Q}}(\mathcal{E}) \frac{\delta V_{\rm sp}}{\delta \mathcal{E}} P_{\mathcal{E}'} I^{\rm Pair} P_{\mathcal{E}}
-\Gamma_{\mathcal{Q}}(\mathcal{E}) \Gamma_{\mathcal{Q}}(\mathcal{E}') V_{\rm sp} P_{\mathcal{E}'} I^{\rm Pair} P_{\mathcal{E}}$$
(10.18)

with (the first part of) the potential (6.16),

$$\langle rs|V_{\rm sp}(E_0)|tu\rangle = \left\langle rs \left| \int_0^\infty c \, \mathrm{d}\kappa \, f_{\rm T}^{\rm C}(\kappa) \right| \right. \\ \left. \times \left[\frac{1}{E_0 - \varepsilon_r - \varepsilon_u - c\kappa} + \frac{1}{E_0 - \varepsilon_t - \varepsilon_s - c\kappa} \right] \right| tu \right\rangle (10.19)$$

(the second part of the potential is generated by emitting a photon from the second electron.)

We see that

• the energy dependence of the potential is generated by an energy denominator and the energy derivative (difference ratio) by a folded contribution (double denominator), when operating in the extended space (10.15).

After the first interaction V_1^l , it is possible to add one or more Coulomb interactions, <u>before</u> closing the photon, corresponding to the first diagram in Fig. 10.2. This can be achieved by another iteration of the pair equation (10.14)

$$(\mathcal{E} - h_0(1) - h_0(2) - c\kappa) \Omega^l P_{\mathcal{E}} = V_{\mathcal{C}} \Omega^l P_{\mathcal{E}} - \Omega^l P_{\mathcal{E}'} I^{\text{Pair}} P_{\mathcal{E}}.$$
 (10.20)

Instead of closing the uncontracted perturbation on the other electron, it can be closed on the *same* electron as the emission occurred from. This leads to a *self-energy interaction*, represented by the first diagram in Fig. 10.3. This is a *radiative effect* (see Sect. 2.6), which is infinite and has to be *renormalized*, as discussed in Chap. 12.

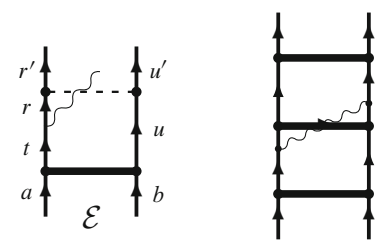


Fig. 10.2 Crossing Coulomb interactions before closing the retarded interaction (*left*). Continuing the process leads to the single transverse-photon exchange combined with high-order electron correlation, including crossing Coulomb interactions (*right*)

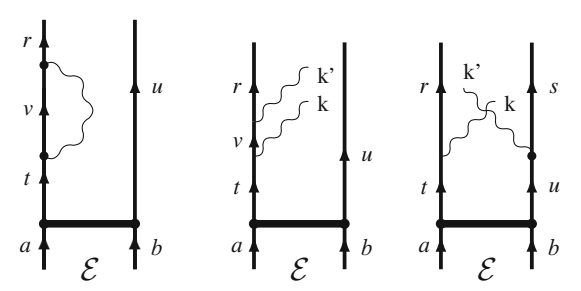


Fig. 10.3 Second-order contribution to the wave operator in the extended Fock space

A second perturbation V^l can also be applied without contracting the first one, leading to diagrams indicated by the second and third diagrams in Fig. 10.3. Closing these photons lead to irreducible two-photon interactions, discussed in Sect. 8.2.

10.3 Single-Photon Exchange: Virtual Pairs

10.3.1 Illustration

The iterative procedure of the previous section works well in the no-pair situation, when the repeated single-photon exchange leads to *reducible* diagrams of ladder type, which means that they can in time-ordered form be separated into legitimate diagrams by horizontal cuts.

In the presence of virtual pairs, we have to use a different procedure. As we have seen above (Sect. 8.3), we have to combine the general potential with Coulomb interactions (8.67) to be able to treat the potential in an iterative process. This will at the same time eliminate the so-called Brown–Ravenhall effect of vanishing energy denominators.

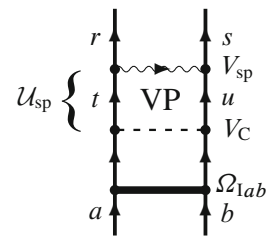
This potential (8.67) can be used directly in the Bloch equation (8.68). In principle, we can use the corresponding full potential with QED effects (8.67), but for simplicity we shall consider only the pure single-photon part.

We use pair functions (10.12) as input, and perturbing this with the potential (8.67) leads in next order to

$$\Omega_{\rm sp}P = \left(\Gamma_{Q}V^{\rm QED}\Omega_{\rm I} + \frac{\delta(\Gamma_{Q}V^{\rm QED})}{\delta\mathcal{E}}\Omega_{\rm I}PI^{\rm Pair}\right)P. \tag{10.21}$$

For the evaluation we use, as before, the expansion (10.8)

$$\langle rs | f_{T}^{C}(\kappa) | tu \rangle = \sum_{l=0}^{\infty} \left[\langle s | V_{G}^{l}(\kappa r_{2}) | u \rangle \cdot \langle r | V_{G}^{l}(\kappa r_{1}) | t \rangle + \langle s | V_{sr}^{l}(\kappa r_{2}) | u \rangle \cdot \langle r | V_{sr}^{l}(\kappa r_{1}) | t \rangle \right].$$
(10.22)



As an illustration we consider the second term in Fig. 8.11 (shown above), when there is a single hole (t) [c.f. (8.13)]. Then (10.21) becomes

$$\Omega_{\rm sp} P = \left(\Gamma_{\mathcal{Q}} \mathcal{U}_{\rm sp} \Omega_{\rm I} + \frac{\delta(\Gamma_{\mathcal{Q}} \mathcal{U}_{\rm sp})}{\delta \mathcal{E}} \Omega_{\rm I} P I^{\rm Pair} \right) P, \tag{10.23}$$

where $U_{\rm sp} = V_{\rm sp} \Gamma_Q V_{\rm C}$ represents the transverse photon $(V_{\rm sp})$ with a Coulomb interaction. Here, only the first and the third terms of the potential $V_{\rm sp}$ (8.11) are relevant, yielding for the first term

$$\frac{|r_{+}s_{+}\rangle}{\mathcal{E} - \varepsilon_{r} - \varepsilon_{s}} \left[-\frac{\langle s_{+}|V^{l}|u_{+}\rangle \langle r_{+}|V^{l}|t_{-}\rangle}{\varepsilon_{t} - \varepsilon_{r} - c\kappa} + \frac{\langle s_{+}|V^{l}|u_{+}\rangle \langle r_{+}|V^{l}|t_{-}\rangle}{\mathcal{E} - \varepsilon_{r} - \varepsilon_{u} - c\kappa} \right] \times \frac{\langle t_{-}u_{+}|V_{C}|\Omega_{Iab}\rangle}{\mathcal{E} - \varepsilon_{t} - \varepsilon_{u}},$$
(10.24)

where again V^l represents the Gaunt and the scalar-retardation potentials for the two electrons.

In order to evaluate the expression above, we first perform an additional iteration of the pair equation (10.12)

$$\left(\mathcal{E} - h_0(1) - h_0(2)\right)|\Omega_{ab}^{\pm}\rangle = V_{\rm C}|\Omega_{1ab}\rangle - \Gamma_Q V_{\rm C}|\Omega_{1cd}\rangle \langle cd|I^{\rm Pair}|ab\rangle \quad (10.25)$$

yielding a new pair function with a single hole output. The solution can be expressed in analogy with (10.15)

$$\langle t_{-}u_{+}|\Omega_{ab}^{\pm}\rangle = \frac{\langle t_{-}u_{+}|V_{C}|\Omega_{Iab}\rangle}{\mathcal{E} - \varepsilon_{t} - \varepsilon_{u}} - \frac{\langle t_{-}u_{+}|V_{C}|\Omega_{Icd}\rangle}{(\mathcal{E} - \varepsilon_{t} - \varepsilon_{u})(\mathcal{E}' - \varepsilon_{t} - \varepsilon_{u})} \langle cd|I^{\text{Pair}}|ab\rangle.$$
(10.26)

The first part of the solution, illustrated in Fig. 10.4 (a), represents the last factor in the expression (10.24). The second folded part will be used later in constructing the complete folded contribution.

In evaluating the first term within the square brackets of (10.24), we first multiply the pair function (10.26) *without* folded contribution by

$$-\frac{\langle r_{+}|V_{1}^{l}|t_{-}\rangle}{\varepsilon_{t}-\varepsilon_{r}-c\kappa}$$

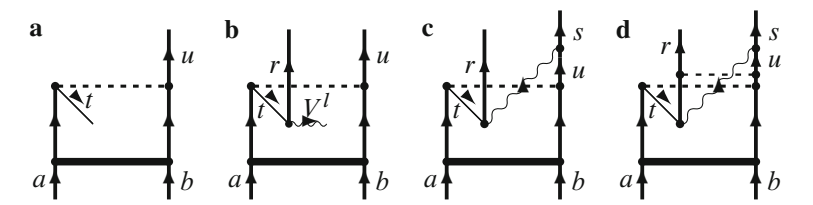


Fig. 10.4 (a-c): Generating a pair function with a hole output (10.25), combined with a single-particle perturbation V_1 , and closed with a perturbation V_2 . The *last diagram* contains a crossing Coulomb interaction, as discussed at the end of the section

yielding

$$\langle r_{+}u_{+}|\Omega_{ab}^{l}\rangle = -\frac{\langle r_{+}|V_{1}^{l}|t_{-}\rangle\langle t_{-}u_{+}|\Omega_{ab}^{\pm}\rangle}{\varepsilon_{t} - \varepsilon_{r} - c\kappa} = -\frac{\langle r_{+}|V_{1}^{l}|t_{-}\rangle}{\varepsilon_{t} - \varepsilon_{r} - c\kappa}\frac{\langle t_{-}u_{+}|V_{C}|\Omega_{1ab}\rangle}{\mathcal{E} - \varepsilon_{t} - \varepsilon_{u}}$$

and represented by the diagram (b) in Fig. 10.4. Then we close the photon by multiplying with $\langle s_+|V_2^I|u_+\rangle$ and including the final denominator, yielding

$$\langle r_{+}s_{+}|\Omega_{\rm sp}|ab\rangle = -\frac{\langle s_{+}|V_{2}^{l}|u_{+}\rangle}{\mathcal{E} - \varepsilon_{r} - \varepsilon_{s}} \frac{\langle r_{+}|V_{1}^{l}|t_{-}\rangle}{\varepsilon_{t} - \varepsilon_{r} - c\kappa} \frac{\langle t_{-}u_{+}|V_{\rm C}|\Omega_{\rm I}ab\rangle}{\mathcal{E} - \varepsilon_{t} - \varepsilon_{u}}, \quad (10.27)$$

which agrees with the corresponding part of (10.24) (Fig. 10.4c).

The second term in the brackets of (10.24) is evaluated in a similar way with a different denominator.

The folded contribution is in lowest order from (10.21)

$$\frac{\delta(\Gamma_{Q}\mathcal{U}_{\mathrm{sp}})}{\delta\mathcal{E}}|\Omega_{\mathrm{I}cd}\rangle\langle cd|I^{\mathrm{Pair}}|ab\rangle = \frac{\delta(\Gamma_{Q}V_{\mathrm{sp}}\Gamma_{Q}V_{\mathrm{C}})}{\delta\mathcal{E}}|\Omega_{\mathrm{I}cd}\rangle\langle cd|I^{\mathrm{Pair}}|ab\rangle. \tag{10.28}$$

Here,

$$\frac{\delta(\Gamma_{Q}V_{\rm sp}\Gamma_{Q}V_{\rm C})}{\delta\mathcal{E}} = \frac{\delta\Gamma_{Q}}{\delta\mathcal{E}}V_{\rm sp}\Gamma_{Q}V_{\rm C} + \Gamma_{Q}\frac{\delta V_{\rm sp}}{\delta\mathcal{E}}\Gamma_{Q}V_{\rm C} + \Gamma_{Q}V_{\rm sp}\frac{\delta(\Gamma_{Q}V_{\rm C})}{\delta\mathcal{E}}. (10.29)$$

The difference ratio $\delta(\Gamma_Q V_{\rm C})/\delta \mathcal{E}$ is obtained from the folded part of (10.26) ($V_{\rm C}$ is energy independent). Similarly, the difference ratio of the relevant part of $V_{\rm sp}$ is obtained by including an extra factor

$$-\frac{1}{\mathcal{E}'-\varepsilon_r-\varepsilon_u-c\kappa}.$$

Finally, the difference ratio of Γ_O is

$$\frac{\delta \Gamma_Q}{\delta \mathcal{E}} = -\frac{1}{(\mathcal{E}' - \varepsilon_r - \varepsilon_s)(\mathcal{E} - \varepsilon_r - \varepsilon_s)}.$$

It should be noted that the last term in (10.29) is combined with the pair function (10.26) <u>with</u> folded contribution, while the other terms are combined with that function <u>without</u> that contribution. This is important to avoid the singularities of Brown–Ravenhall type, mentioned above.

10.3.2 Full Treatment

We shall now generalize the treatment above and consider all 16 combinations of the single-photon exchange (8.11) (see Fig. 8.3) essentially in one single step.

To begin with, we leave out the folded contribution. Then, the expression to evaluate is

$$\frac{\langle r|V^{l}|t\rangle \ \langle s|V^{l}|u\rangle \ \langle tu|V_{\rm C}|\Omega_{\rm I}ab\rangle}{\mathcal{E} - \varepsilon_{r} - \varepsilon_{s}} \times \left[\pm \frac{t_{\pm}r_{\mp}}{\varepsilon_{t} - \varepsilon_{r} \pm c\kappa} \pm \frac{t_{\pm}s_{\pm}}{\mathcal{E} - \varepsilon_{t} - \varepsilon_{s} \mp c\kappa} \pm \frac{u_{\pm}r_{\pm}}{\mathcal{E} - \varepsilon_{r} - \varepsilon_{u} \mp c\kappa} \pm \frac{u_{\pm}s_{\mp}}{\varepsilon_{u} - \varepsilon_{s} \pm c\kappa}\right]. \tag{10.30}$$

If we in this expression make the substitution $tr \leftrightarrow us$, we get an identical result but with a and b interchanged. Therefore, we can replace the expression above by the much simpler expression

$$\frac{\langle r|V^{l}|t\rangle \langle s|V^{l}|u\rangle \langle tu|V_{C}|\Omega_{Iab} + \Omega_{Iba}\rangle}{\mathcal{E} - \varepsilon_{r} - \varepsilon_{s}} \times \left[\pm \frac{t_{\pm}r_{\mp}}{\varepsilon_{t} - \varepsilon_{r} \pm c\kappa} \pm \frac{u_{\pm}r_{\pm}}{\mathcal{E} - \varepsilon_{r} - \varepsilon_{u} \mp c\kappa}\right].$$
(10.31)

The last expression can be evaluated in the following way. We first evaluate the matrix element $\langle tu|V_C|\Omega_{1ab}\rangle$ by iterating the pair equation (10.25) once, allowing negative-energy states as output. We can separate the solutions into four block, depending on the signs of the outgoing orbital energies, as illustrated in the matrix in Fig. 10.5.

Next, we evaluate the matrix elements $\langle r|V_1|t\rangle$ for each value of κ and l, and separate them in a similar way, shown in Fig. 10.6.

We now multiply the matrices in Figs. 10.5 and 10.6 (in that order), leading to the matrix in Fig. 10.7. Here, we include the two denominator terms in the brackets of (10.31) and sum over <u>all</u> t, particle as well as hole states.

Finally, we multiply the result by $\langle s|V_2|u\rangle$ and sum over κ and l, corresponding to closing the photon (c.f. Fig. 10.4c), and apply the final denominator in (10.31).

If the input orbitals a, b are different, the procedure is repeated with $a \leftrightarrow b$.

The folded contribution in (10.21) is evaluated in a similar way [c.f. (10.28)].

Fig. 10.5 Representation of the pair function in (10.25) iterated one extra time and separated into four blocks, depending on the signs of the outgoing orbital energies

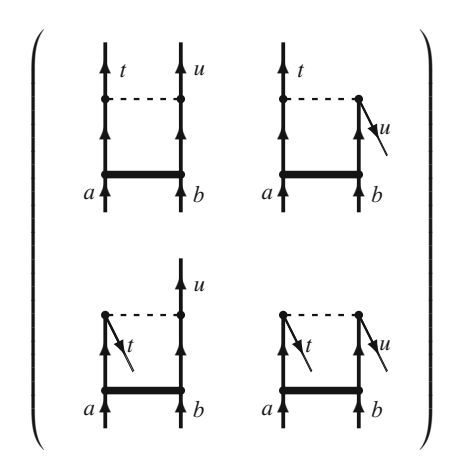


Fig. 10.6 The matrix elements $\langle r|V_1|t\rangle$, separated in analogy with Fig. 10.5

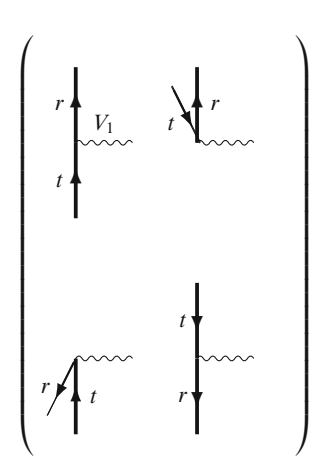
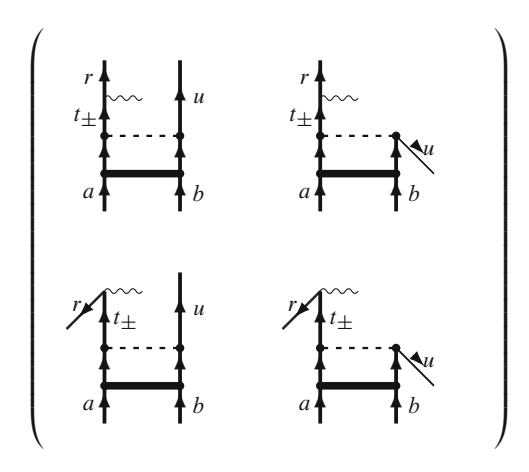


Fig. 10.7 Result of multiplying the matrices in Figs. 10.5 and 10.6. The *t* line represents particle as well as hole states



10.4 Numerical Results 221

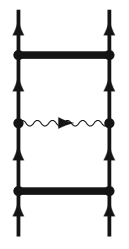


Fig. 10.8 The Feynman diagrams representing a single transverse photon exchange combined with high-order electron correlation (*heavy horizontal line*). The *internal vertical lines* represent electron propagators with particle and holes. The numerical evaluation of this diagram is given below

10.3.3 Higher Orders

In most of the cases treated above, it is possible also to insert Coulomb interaction before the photon interaction is completed, as discussed in the no-pair case. This is the case when the orbitals u, r or t, s are of the same kind (particle or hole), as indicated in Fig. 10.4d. This corresponds to including another part of the potential in (8.66).

After the completion of the single-photon exchange, the iteration process can be continued with further Coulomb interactions, leading to the *complete single-photon* exchange with electron correlation, including all combinations of particles and holes, as illustrated in Fig. 10.8.

10.4 Numerical Results

10.4.1 Two-Photon Exchange

In Chap. 7 (Fig. 7.3), we showed the results of two-photon exchange for the ground-state of helium-like ions, calculated using the S-matrix formulation. In Table 10.1, we compare these results with those obtained by Hedendahl et al. [1,3], in testing the new covariant method described in the present chapter. The agreement, which is found to be very good, is also displayed in Fig. 10.9, where the solid lines represent the old S-matrix results and the squares the new covariant method. As before, the scale is logarithmic and the norm is the nonrelativistic ionization energy.

10.4.2 Beyond Two Photons

Calculations have also been performed of the effect of electron correlation *beyond two-photon exchange* for the ground state of helium-like ions by Hedendahl et al. [1–3]. Some results are shown in Table 10.2 and also displayed in Fig. 10.10.

Table 10.1 Comparisons between two-photon effects for He-like ions ground states, evaluated with the S-matrix and the covariant-evolution-operator methods (in μ Hartree) (see Fig. 7.3)

		CoulBreit	CoulBreit.	CoulBreit
Z	Method	NVPA	retard.	VP uncrossed.
6	S-matrix	-1,054.2	31.4	-10.1
6	CEO	-1,054.9	31.5	-10.0
10	S-matrix	-2,070.4	122.3	-45.9
10	CEO	-2,071.0	122.4	-45.9
14	S-matrix	-5,515	292.8	-121.5
14	CEO	-5,517	292.8	-121.2
18	S-matrix	-8,947	553.1	-247.3
18	CEO	-8,950	553.3	-248.2
30	CEO	-23,632	1,909.9	-1,010

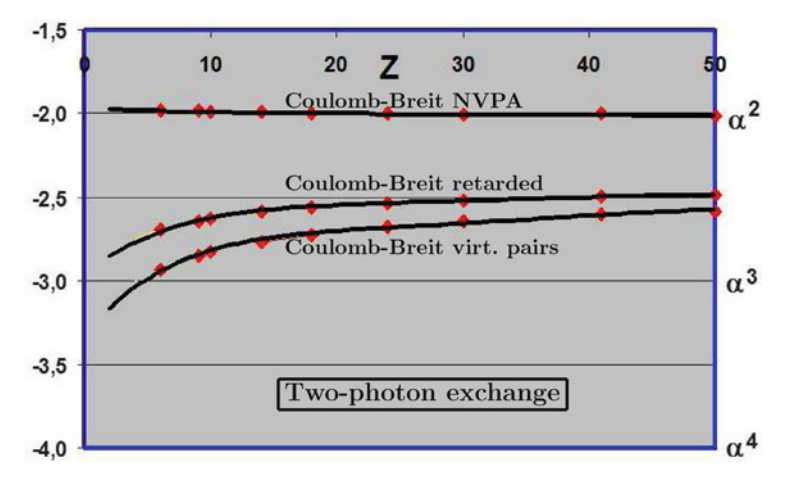


Fig. 10.9 Comparison of some two-photon exchange contributions (Coulomb–Breit NVPA, Coulomb–Breit retardation, and Coulomb–Breit virtual pairs, no correlation) for the ground-state of some helium-like ions obtained by S-matrix calculations (see Fig. 7.3) (*heavy lines*) and by means of the covariant-evolution procedure (*squares*), described in this chapter (see Table 10.1, c.f. Fig. 7.3 in Chap. 7) (from [1,3])

The top line of the figure, representing the Coulomb–Breit interaction with correlation *without* virtual pairs, contains the instantaneous as well as the retarded Breit interaction. The former part lies within the no-virtual-pair approximation (NVPA) and is therefore NOT a QED effect with the definition we have previously made. In order to obtain the pure QED effect, the instantaneous part is subtracted, yielding the *retarded* part, represented by the second line of the figure. The next line represents the same effect with Coulomb crossings, and the bottom line represents the effect of electron correlation on the Coulomb–Breit interaction with virtual pairs and no

10.4 Numerical Results 223

Table 10.2 Contributions due to electron correlation beyond two-photon exchange for the ground state of some helium-like ions. This can be compared with the corresponding two-photon exchange in Table 10.1 (in μH)

	Beyond two-photon CoulBreit				
Z	Unretarded	Retarded	Virt.pairs		
6	137	-17	2.7		
10	223	-4 0	7.3		
14	301	-68	13		
18	372	-100	21		
30	553	-210	46		
42	688	-322	71		

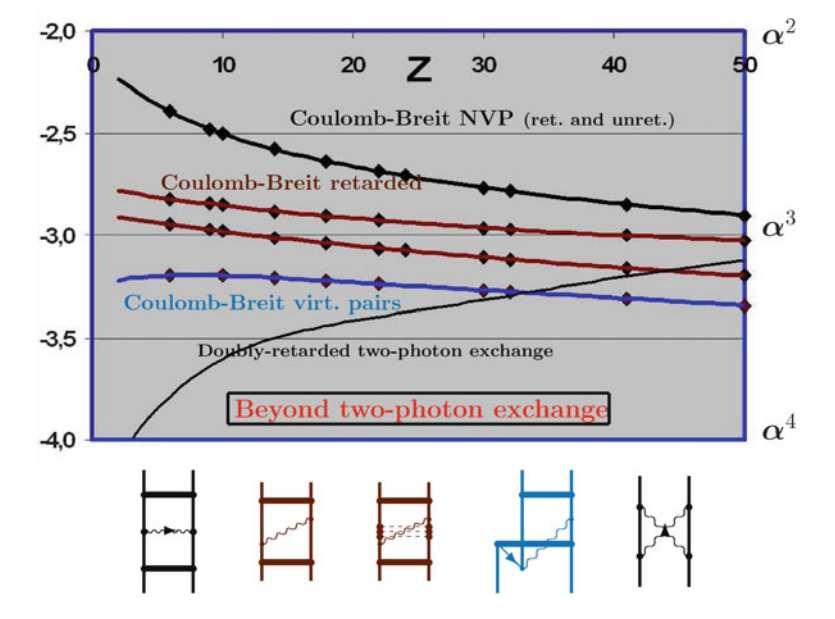


Fig. 10.10 The effect of electron correlation beyond two-photon exchange – Coulomb–Breit NVPA, Coulomb–Breit retardation with and without Coulomb crossings, and Coulomb–Breit virtual pairs, all WITH electron correlation, for the ground-state of helium-like ions (c.f. Fig. 10.9) (from [1, 3]). For comparison, the effect of pure retarded two-photon exchange without additional correlation is also indicated

crossing Coulomb interactions. The corresponding Feynman diagrams are shown at the bottom of the figure. This represents *the first numerical bound-state calculation beyond two-photon exchange*.

In the figure, we have for comparison also indicated the effect due to doubly retarded two-photon interactions (thin black line), estimated from the S-matrix results. This comparison demonstrates the important result that – starting from single-photon exchange – for light and medium-heavy elements the effect of electron correlation is much more important than a second retarded photon interaction.

10.4.3 *Outlook*

The results presented here are incomplete and represent only the *nonradiative* part of the QED effect in combination with electron correlation. The corresponding radiative effects with a single transverse photon are also possible to evaluate. Such calculations are underway by the Gothenburg group. The effect due to double transverse photons is presently beyond reach, but the effect can be estimated by replacing the second transverse photon by an *instantaneous* Breit interaction.

The calculations performed so far with the procedure described here concern the ground states of helium-like ions [3]. By extending the calculations to excited states, it will be possible to make detailed comparison with experimental data. For instance, very accurate data exist for some helium-like ions, as shown in Tables 7.7 and 7.8. In some of these cases, the experimental results are at least two orders of magnitude more accurate than the best theoretical estimates made so far. Furthermore, it seems that standard procedures applied until now cannot be significantly improved in this respect, so – to be able to make significant progress – there might be a need for a new, improved procedure, like the MBPT–QED procedure presented here. Then, it might be possible for the first time to observe the combined effect of QED and electron correlation.

References

- 1. Hedendahl, D.: *Towards a Relativistic Covariant Many-Body Perturbation Theory*. Ph.D. thesis, University of Gothenburg, Gothenburg, Sweden (2010)
- 2. Hedendahl, D., Lindgren, I., Salomonson, S.: Towards numerical implementation of the relativistically covariant many-body perturbation theory. Can. J. Phys. 87, 817–24 (2008)
- 3. Hedendahl, D., Salomonson, S., Lindgren, I.: . Phys. Rev. p. (to be published) (2011)
- 4. Lindgren, I., Morrison, J.: *Atomic Many-Body Theory*. Second edition, Springer-Verlag, Berlin (1986, reprinted 2009)
- 5. Lindgren, I., Salomonson, S., Hedendahl, D.: Many-body procedure for energy-dependent perturbation: Merging many-body perturbation theory with QED. Phys. Rev. A 73, 062,502 (2006)

Chapter 11 Analytical Treatment of the Bethe–Salpeter Equation

11.1 Helium Fine Structure

The leading contributions to the helium fine structure beyond the first-order relativistic contribution (NVPA, see, Sect. 2.6) were first derived in 1957 by Araki [1] and Sucher [6, 7], starting from the Bethe–Salpeter (BS) equation [5] and including the nonrelativistic as well as the relativistic momentum regions. Following the approach of Sucher, Douglas and Kroll [2] have derived all terms of order α^4 H(artree)¹, where no contributions in the relativistic region were found. The same approach was later used by Zhang [8, 12] to derive corrections of order $\alpha^5 \log \alpha$ H and of order α^5 H in the nonrelativistic region and recoil corrections to order $\alpha^4 m/M$ H (see also [10]). Later some additional effects of order α^5 H due to relativistic momenta were found by Zhang and Drake [11]. The radiative parts are treated more rigorously by Zhang in a separate paper [9]. Using a different approach, Pachucki and Sapirstein [4] have derived all contributions of order α^5 H and reported some disagreement with the early results of Zhang [8].

We shall here follow the approach of Sucher in his thesis [7]. This is based directly on the BS equation, which makes it possible to identify the contributions in terms of Feynman diagrams and therefore to compare them with the results obtained in the previous chapters. This approach of Sucher is closely followed by Douglas and Kroll [2] and by Zhang [8], and we shall in our presentation make frequent references to the corresponding equations of Sucher (S), Douglas and Kroll (DK), and Zhang (Z).

 $^{^1}$ H(artree) is the energy unit of the *Hartree atomic unit system* (see Appendix K.1). In the relativistic unit system, the energy unit is $mc^2 = \alpha^{-2}H$.

² This chapter is largely based on the paper [3].

11.2 The Approach of Sucher

The treatment of Sucher starts from the Bethe–Salpeter equation (9.5), which in our notations (9.6) reads, leaving out the inhomogeneous term (S 1.1, DK 2.5),

$$\Psi(x, x') = \iiint d^4x_1 d^4x_2 d^4x'_1 d^4x'_2 \times G'_0(x, x'; x_2, x'_2) (-i) \Sigma^*(x_2, x'_2; x_1, x'_1) \Psi(x_1, x'_1).$$
(11.1)

 G_0' is the zeroth-order two-particle Green's function, dressed with all kinds of single-particle self-energies. Σ^* is identical to the irreducible potential \mathcal{V} (Fig. 6.6). The undressed zeroth-order Green's function is, using the relation (5.38),

$$G_0(x, x'; x_2, x_2') = G_0(x, x_2) G_0(x', x_2') = iS_F(x, x_2) iS_F(x', x_2')$$
 (11.2)

and the corresponding dressed function is then

$$G'_0(x, x'; x_2, x_2') = G(x, x_2) G(x', x_2') = iS'_F(x, x_2) iS'_F(x', x_2'),$$
 (11.3)

where G is the full single-particle Green's function, generated in the field of the nucleus (Furry representation) (see Fig. 5.1), and S'_F the correspondingly dressed electron propagator. The Green's functions satisfy the relation (5.36) (S 1.5)

$$\left(i\frac{\partial}{\partial t} - h_1\right)G(x, x_0) = i\delta^4(x - x_0),\tag{11.4}$$

which leads to (S 1.6, DK 2.19)

$$\left(i\frac{\partial}{\partial t} - h_1\right) \left(i\frac{\partial}{\partial t'} - h_2\right) \Psi(x, x') = i \iiint d^4 x_1 d^4 x_2 d^4 x'_1 d^4 x'_2 \delta^4(x - x_2)
\times \delta^4(x' - x'_2) \Sigma^*(x_2, x'_2; x_1, x'_1) \Psi(x_1, x'_1)
= i \iint d^4 x_1 d^4 x'_1 \Sigma^*(x, x'; x_1, x'_1) \Psi(x_1, x'_1), (11.5)$$

where $h_{1,2}$ are the Dirac single-electron Hamiltonians for electron 1 and 2. We assume that the wave function is of the form

$$\Psi(x, x') = \Psi(T, \tau, \mathbf{x}, \mathbf{x}') = e^{-iET} \Psi(\tau, \mathbf{x}, \mathbf{x}'),$$
 (11.6)

where T = (t + t')/2 is the average time and $\tau = t - t'$ is the *relative time*. Then

$$\begin{split} &\mathrm{i} \frac{\partial}{\partial t} \Psi(x, x') = \left(E/2 + \mathrm{i} \frac{\partial}{\partial \tau} \right) \Psi(x, x'), \\ &\mathrm{i} \frac{\partial}{\partial t'} \Psi(x, x') = \left(E/2 - \mathrm{i} \frac{\partial}{\partial \tau} \right) \Psi(x, x') \end{split}$$

leading to (S 1.9, DK 2.23)

$$\left(E/2 + i\frac{\partial}{\partial \tau} - h_1\right) \left(E/2 - i\frac{\partial}{\partial \tau} - h_2\right) \Psi(\tau, x, x')$$

$$= i \int d\tau_1 \iint d^3x_1 d^3x_1' \, \Sigma^*(\tau, x, x'; \tau_1, x_1, x_1') \, \Psi(\tau_1, x_1, x_1') (11.7)$$

leaving out the average time.

Sucher then transfers to the momentum representation, but we shall here still work in the coordinate representation with a Fourier transform only of the time variables.

We define the Fourier transform with respect to time

$$F(\epsilon) = \int d\tau \ e^{i\epsilon\tau} F(\tau)$$
 (11.8)

and the inverse transformation

$$F(\tau) = \int \frac{\mathrm{d}\epsilon}{2\pi} \,\mathrm{e}^{-\mathrm{i}\epsilon\tau} \,F(\epsilon). \tag{11.9}$$

Fourier transforming (11.7) with respect to τ yields

$$(E/2 + \epsilon - h_1) (E/2 - \epsilon - h_2) \Psi(\epsilon, x_1, x_1')$$

$$= i \int d\tau_1 \iint d^3x_1 d^3x_1' \Sigma^*(\epsilon, x, x'; \tau_1, x_1, x_1') \Psi(\tau_1, x_1, x_1'). (11.10)$$

Performing the Fourier transform of the right-hand side with respect to τ_1 yields

$$\int d\tau_1 \iint \frac{d\epsilon'_1}{2\pi} \frac{d\epsilon_1}{2\pi} e^{-i\epsilon'_1\tau_1} e^{-i\epsilon_1\tau_1} \Sigma^*(\epsilon, \boldsymbol{x}, \boldsymbol{x}'; \epsilon'_1, \boldsymbol{x}_1, \boldsymbol{x}'_1) \Psi(\epsilon_1, \boldsymbol{x}_1, \boldsymbol{x}'_1)$$

$$= \iint \frac{d\epsilon'_1}{2\pi} \frac{d\epsilon_1}{2\pi} 2\pi \delta(\epsilon_1 + \epsilon'_1) \Sigma^*(\epsilon, \boldsymbol{x}, \boldsymbol{x}'; \epsilon'_1, \boldsymbol{x}_1, \boldsymbol{x}'_1) \Psi(\epsilon_1, \boldsymbol{x}_1, \boldsymbol{x}'_1)$$
(11.11)

or (S 1.16)

$$(E/2 + \epsilon - h_1) (E/2 - \epsilon - h_2) \Psi(\epsilon, x_1, x_1')$$

$$= i \int \frac{d\epsilon_1}{2\pi} \iint d^3x_1 d^3x_1' \Sigma^*(\epsilon, x, x_1'; -\epsilon_1, x_1, x_1') \Psi(\epsilon_1, x_1, x_1').$$
(11.12)

Following Sucher, we express the relation (11.10) in operator form

$$\hat{\mathcal{F}}|\Psi\rangle = \hat{g}|\Psi\rangle. \tag{11.13}$$

The operator $\hat{\mathcal{F}}$ has the (diagonal) coordinate representation

$$\langle \epsilon, \mathbf{x}, \mathbf{x}' | \mathcal{F} | \epsilon, \mathbf{x}, \mathbf{x}' \rangle = (E/2 + \epsilon - h_1) (E/2 - \epsilon - h_2)$$
 (11.14)

and the operator \hat{g} has the (nondiagonal) representation

$$\langle \epsilon, x, x' | \hat{g} | \epsilon_1, x_1, x_1' \rangle = \frac{\mathrm{i}}{2\pi} \langle \epsilon, x, x' | \hat{\Sigma}^* | \epsilon_1, x_1, x_1' \rangle. \tag{11.15}$$

We expand the interaction into

$$\hat{g} = \hat{g}_c + \hat{g}_\Delta, \tag{11.16}$$

where \hat{g}_c represents the Columbic part of \hat{g}

$$\hat{g}_c = \frac{\mathrm{i}}{2\pi} \, \hat{I}_c \tag{11.17}$$

and \hat{I}_c is the Coulomb interaction with the (diagonal) coordinate representation

$$\langle \epsilon, \mathbf{x}, \mathbf{x}' | \hat{I}_c | \epsilon, \mathbf{x}, \mathbf{x}' \rangle = \frac{e^2}{4\pi |\mathbf{x} - \mathbf{x}_1|},$$
 (11.18)

 \hat{g}_{Δ} represents the remaining part of \hat{g}

$$\hat{g}_{\Delta} = \hat{g}_T + g_{T \times c} + \hat{g}_{T \times c^2} + \hat{g}_{T \times T} + \dots + \hat{g}^{rad},$$
 (11.19)

where \hat{g}_T represents a single transverse photon, $\hat{g}_{T \times c}$ and $\hat{g}_{T \times c^2}$ a transverse photon with one and two crossing Coulomb interactions, respectively, $\hat{g}_{T \times T}$ with two irreducible transverse photons, and finally \hat{g}^{rad} all radiative corrections. This corresponds to the diagrams are shown in Fig. 11.1.

With the decomposition (11.16), the relation (11.13) becomes (S 1.30, DK 3.6)

$$|\Psi\rangle = \left(\hat{\mathcal{F}} - \hat{g}_{\Delta}\right)^{-1} \hat{g}_{c} |\Psi\rangle$$
 (11.20)

with the coordinate representation

$$\langle \epsilon, x, x' | \Psi \rangle = \langle \epsilon, x, x' | (\hat{\mathcal{F}} - \hat{g}_{\Delta})^{-1} | \epsilon_{2}, x_{2}, x'_{2} \rangle$$

$$\times \langle \epsilon_{2}, x_{2}, x'_{2} | \hat{g}_{c} | \epsilon_{1}, x_{1}, x'_{1} \rangle \langle \epsilon_{1}, x_{1}, x'_{1} | \Psi \rangle \qquad (11.21)$$

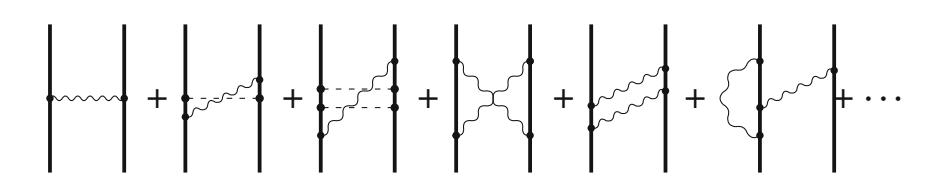


Fig. 11.1 Diagrammatic representation of the approximation in (11.19), used by Sucher

or noting that the representation of \hat{g}_c is diagonal

$$\langle \epsilon, \mathbf{x}, \mathbf{x}' | \Psi \rangle = \langle \epsilon, \mathbf{x}, \mathbf{x}' | (\hat{\mathcal{F}} - \hat{g}_{\Delta})^{-1} | \epsilon_1, \mathbf{x}_1, \mathbf{x}_1' \rangle \, \hat{g}_c \, \langle \epsilon_1, \mathbf{x}_1, \mathbf{x}_1' | \Psi \rangle \,. \tag{11.22}$$

Sucher defines the *equal-time wave function* (S 1.32, DK 3.8)

$$\Phi(\mathbf{x}, \mathbf{x}') = \int d\epsilon \, \Psi(\epsilon, \mathbf{x}, \mathbf{x}') \tag{11.23}$$

or in operator form

$$|\Phi\rangle = |\epsilon\rangle \langle \epsilon | \Psi \rangle,$$
 (11.24)

which gives with (11.22)

$$\langle \epsilon, x, x' | \Psi \rangle = \langle \epsilon, x, x' | (\hat{\mathcal{F}} - \hat{g}_{\Delta})^{-1} | x_1, x_1' \rangle \, \hat{g}_c \, \langle x_1, x_1' | \Phi \rangle \,. \tag{11.25}$$

Summing over ϵ with the replacement (11.17), this can be expressed as (S 1.34)

$$|\Phi\rangle = i \int \frac{d\epsilon}{2\pi} \left(\hat{\mathcal{F}} - \hat{g}_{\Delta}\right)^{-1} \hat{I}_{c} |\Phi\rangle.$$
 (11.26)

Using the identity (S 1.35, DK 3.11)

$$(A - B)^{-1} \equiv A^{-1} + A^{-1}B(A - B)^{-1}, \tag{11.27}$$

the BSE (11.26) becomes (DK 3.12)

$$|\Phi\rangle = i \int \frac{d\epsilon}{2\pi} \left[\hat{\mathcal{F}}^{-1} + \hat{\mathcal{F}}^{-1} \hat{g}_{\Delta} (\hat{\mathcal{F}} - \hat{g}_{\Delta})^{-1} \right] \hat{I}_c |\Phi\rangle. \tag{11.28}$$

The inverse of the operator OF is

$$\hat{\mathcal{F}}^{-1} = \frac{1}{E/2 + \epsilon - \hat{h}_1} \frac{1}{E/2 - \epsilon - \hat{h}_2},\tag{11.29}$$

which is a product of electron propagators in operator form (4.14)

$$\hat{\mathcal{F}}^{-1} = \hat{S}_{F}(E/2 + \epsilon) \, \hat{S}_{F}(E/2 - \epsilon). \tag{11.30}$$

In the coordinate representation (4.12),

$$S_{F}(\omega; \mathbf{x}, \mathbf{x}_{0}) = \frac{\langle \mathbf{x} | j \rangle \langle j | \mathbf{x}_{0} \rangle}{\omega - \varepsilon_{j} + i\eta \operatorname{sgn}(\varepsilon_{j})} = \frac{\langle \mathbf{x} | j \rangle \langle j | \mathbf{x}_{0} \rangle}{\omega - \varepsilon_{j} + i\eta} \Lambda_{+} + \frac{\langle \mathbf{x} | j \rangle \langle j | \mathbf{x}_{0} \rangle}{\omega - \varepsilon_{j} - i\eta} \Lambda_{-}.$$
(11.31)

Integration over ϵ then yields (S 1.44, DK 3.24)

$$\int \frac{d\epsilon}{2\pi} \mathcal{F}^{-1} = -i \frac{\langle x, x' | rs \rangle \langle rs | x_0, x_0' \rangle}{E - \varepsilon_r - \varepsilon_s} (\Lambda_{++} - \Lambda_{--}), \qquad (11.32)$$

which is also the negative of the Fourier transform of the zeroth-order Green's function $-G_0(E; x, x_0; x', x'_0)$, or in operator form

$$\int \frac{d\epsilon}{2\pi} \hat{\mathcal{F}}^{-1} = -G_0(E) = -\frac{i}{E - \hat{h}_1 - \hat{h}_2} (\Lambda_{++} - \Lambda_{--}).$$
 (11.33)

Equation (11.28) then becomes (S 1.47, DK 3.26)³

$$\left[h_1 + h_2 + (\Lambda_{++} - \Lambda_{--}) I_c + D i \int \frac{d\epsilon}{2\pi} \mathcal{F}^{-1} g_{\Delta} (\mathcal{F} - g_{\Delta})^{-1} I_c \right] \Phi = E \Phi,$$
(11.34)

where

$$D = E - h_1 - h_2. (11.35)$$

This is the starting point for the further analysis.

The operator on the left-hand side can be written in the form $H_c + H_{\Delta}$, where

$$H_c = h_1 + h_2 + \Lambda_{++} I_c \Lambda_{++} \tag{11.36}$$

is the Hamiltonian of the no-(virtual-) pair Dirac-Coulomb equation (Z 16)

$$H_c \Psi_c = E_c \Psi_c \tag{11.37}$$

and

$$H_{\Delta} = \Lambda_{++} I_c (1 - \Lambda_{++}) - \Lambda_{--} I_c + D i \int \frac{d\epsilon}{2\pi} \mathcal{F}^{-1} g_{\Delta} (\mathcal{F} - g_{\Delta})^{-1} I_c$$

= $H_{\Delta 1} + H_{\Delta 2}$ (11.38)

is the *remaining "QED part"* (S 2.3, DK 3.29, Z 17). The first part $H_{\Delta 1}$ represents virtual pairs due to the Coulomb interaction and the second part effects of transverse photons (Breit interaction).

In order to include electron self-energy and vacuum polarizations, the electron propagators (5.37) are replaced by propagators with self-energy insertions $\Sigma(\epsilon)$, properly renormalized (DK 2.10),

$$S'(\epsilon) = \frac{|r\rangle \langle r|}{\epsilon - \varepsilon_r + \beta \Sigma(\epsilon) + i\eta_r}.$$
 (11.39)

Also renormalized photon self-energies have to be inserted into the photon lines.

³ In the following, we leave out the hat symbol on the operators.

11.3 Perturbation Expansion of the BS Equation

The effect of the QED Hamiltonian (11.38) can be expanded perturbatively, using the Brillouin–Wigner perturbation theory,

$$\Delta E = E - E_c = \langle \Psi_c | V + V \Gamma V + V \Gamma V \Gamma V + \cdots | \Psi_c \rangle$$

$$= \langle \Psi_c | \frac{V}{1 - \Gamma V} | \Psi_c \rangle, \qquad (11.40)$$

where Γ is the reduced resolvent (2.65)

$$\Gamma = \Gamma_{Q}(E) = \frac{Q}{E - H_{c}} = \frac{1 - |\Psi_{c}\rangle \langle \Psi_{c}|}{E - H_{c}} = \frac{1 - |\Psi_{c}\rangle \langle \Psi_{c}|}{D_{c}}$$
(11.41)

with

$$D_c = E - H_c. ag{11.42}$$

The unperturbed wave function is in our case one solution of the no-pair Dirac–Coulomb equation (11.37), Ψ_c , and we can assume that the perturbation is expanded in other eigenfunctions of H_c . Q is the projection operator that excludes the state Ψ_c (assuming no degeneracy). This leads to the expansion (S 2 19–21, DK 3.43, Z 28)

$$\Delta E^{(1)} = \langle \Psi_c | H_\Delta | \Psi_c \rangle, \qquad (11.43a)$$

$$\Delta E^{(2)} = \langle \Psi_c | H_\Delta \Gamma H_\Delta | \Psi_c \rangle , \qquad (11.43b)$$

$$\Delta E^{(3)} = \langle \Psi_c | H_\Delta \Gamma H_\Delta \Gamma H_\Delta | \Psi_c \rangle, \qquad (11.43c)$$

etc.

Since $\Lambda_{++}|\Psi_c\rangle = |\Psi_c\rangle$ and $\Lambda_{--}|\Psi_c\rangle = 0$, it follows that $\langle \Psi_c|H_{\Delta 1}|\Psi_c\rangle \equiv 0$, and the first-order correction becomes (DK 3.44)

$$\Delta E^{(1)} = \langle \Psi_c | H_{\Delta 2} | \Psi_c \rangle = \langle \Psi_c | D i \int \frac{d\epsilon}{2\pi} \mathcal{F}^{-1} J \mathcal{F}^{-1} I_c | \Psi_c \rangle$$
 (11.44)

and (DK 3.45)

$$J = g_{\Delta} (1 - \mathcal{F}^{-1} g_{\Delta})^{-1}. \tag{11.45}$$

The second-order corrections are $(DK 3.46)^4$

$$\Delta E_a^{(2)} = \langle \Psi_c | H_{\Delta 1} \Gamma H_{\Delta 1} | \Psi_c \rangle = -\langle \Psi_c | I_c \Lambda_{--} \Gamma \Lambda_{--} I_c | \Psi_c \rangle, \quad (11.46a)$$

⁴ Note that the two I_c in (11.46a) are missing from [2, Eq. 3.46]. Equation (11.46b) agrees with [8, Eq.3.30] but not with [2], where the factor $I_c \mathcal{L}_{++}$ should be removed.

$$\Delta E_b^{(2)} = \langle \Psi_c H_{\Delta 1} \Gamma H_{\Delta 2} \rangle \Psi_c = \left\langle \Psi_c I_c \Lambda_{--} D\Gamma i \int \frac{d\epsilon}{2\pi} \mathcal{F}^{-1} J \mathcal{F}^{-1} I_c \Psi_c \right\rangle, \tag{11.46b}$$

$$\Delta E_c^{(2)} = \langle \Psi_c H_{\Delta 2} \Gamma H_{\Delta 1} \rangle \Psi_c = \left\langle \Psi_c D i \int \frac{d\epsilon}{2\pi} \mathcal{F}^{-1} J \mathcal{F}^{-1} I_c \Gamma \Lambda_{--} I_c \Psi_c \right\rangle, \tag{11.46c}$$

$$\Delta E_d^{(2)} = \langle \Psi_c H_{\Delta 2} \Gamma H_{\Delta 2} \rangle \Psi_c$$

$$= \left\langle \Psi_c D i \int \frac{d\epsilon}{2\pi} \mathcal{F}^{-1} J \mathcal{F}^{-1} I_c \Gamma D i \int \frac{d\epsilon}{2\pi} \mathcal{F}^{-1} J \mathcal{F}^{-1} I_c \Psi_c \right\rangle. \quad (11.46d)$$

These formulas can be simplified, noting that

$$\Lambda_{--}\Gamma D = \Lambda_{--} \frac{Q}{E - H_c} (E - h_1 - h_2), \tag{11.47}$$

which, using the relation (11.42), becomes (DK 3.41)

$$\Lambda_{--}\Gamma D = \Lambda_{--} \left(1 + \frac{\Lambda_{++} I_c \Lambda_{++}}{E - H_c} \right) = \Lambda_{--}.$$
(11.48)

According to DK $\Delta E_a^{(2)}$, $\Delta E_c^{(2)}$ and $\Delta E^{(3)}$ do not contribute to the fs in order α^4 (Hartree). This holds also in the next order according to Zhang, but $\Delta E^{(3)}$ will contribute to the singlet energy in that order. In the relativistic momentum region, the second-order part $\Delta E_a^{(2)}$ contributes to the energy already in order α^3 H and to the fine structure in order α^5 H [8, p. 1256].

Using the relation (11.42), we have $E_c - H_c = D_c - \Lambda_{++}D_c\Lambda_{++}$, and the no-pair equation (11.37) can be written (DK 3.51)

$$(D_c - \Lambda_{++} I_c) \Psi_c = 0. (11.49)$$

Then the second-order correction $\Delta E_h^{(2)}$ (11.46b) can be expressed as

$$\Delta E_b^{(2)} = \langle \Psi_c | (I_c - D_c) i \int \frac{d\epsilon}{2\pi} \mathcal{F}^{-1} J \mathcal{F}^{-1} I_c | \Psi_c \rangle.$$
 (11.50)

This can be combined with the first-order correction $\Delta E^{(1)}$ (11.44), yielding

$$\langle \Psi_c | (I_c + \Delta E) i \int \frac{d\epsilon}{2\pi} \mathcal{F}^{-1} J \mathcal{F}^{-1} I_c | \Psi_c \rangle$$
 (11.51)

with

$$\Delta E = E - E_c = D - D_c. \tag{11.52}$$

Here, the ΔE term differs in sign from (DK 3.54) and (Z 37).

The reason for the discrepancy between our result here and those of DK and Z seems to be that the latter make the replacement (DK 3.48)

$$\mathcal{F}^{-1} = S_1 S_2 \equiv (S_1 + S_2) \left(S_1^{-1} + S_2^{-1} \right)^{-1} = \frac{S_1 + S_2}{E - h_1 - h_2} = D^{-1} \left(S_1 + S_2 \right), \tag{11.53}$$

which follows from (11.30), and then approximate D with D_c in the second-order expression.

11.4 Diagrammatic Representation

To continue, we make the expansion (DK 3.45, Z 32)

$$J = g_{\Delta}(1 - \mathcal{F}^{-1}g_{\Delta})^{-1} = g_{\Delta} + g_{\Delta}\mathcal{F}^{-1}g_{\Delta} + \cdots,$$
 (11.54)

where the first term represents *irreducible* terms and the remaining ones are *reducible*. Furthermore, we make the separation (DK 3.53, Z 12)

$$g_{\Delta} = g_T + \Delta g,\tag{11.55}$$

where g_T represents the interaction of a single transverse photon and Δg the irreducible multiphoton exchange of (11.19). The first-order expression (11.44) becomes

$$\Delta E^{(1)} = \langle \Psi_c | D i \int \frac{d\epsilon}{2\pi} \mathcal{F}^{-1} \left[g_T + g_T \mathcal{F}^{-1} g_T + \Delta g + \cdots \right] \mathcal{F}^{-1} I_c | \Psi_c \rangle \quad (11.56)$$

and the leading terms are illustrated in Fig. 11.2. The first term can be expanded in no-pair and virtual-pair terms (a–c)

$$\Delta E^{(1)} = \langle \Psi_c | D i \int \frac{d\epsilon}{2\pi} \mathcal{F}^{-1} g_T \mathcal{F}^{-1} (\Lambda_{++} + \Lambda_{+-} + \Lambda_{-+} + \Lambda_{--}) I_c | \Psi_c \rangle.$$
 (11.57)

The second term in (11.56) represents in lowest order two *reducible* transverse photons (d) and the third term *irreducible* (inclusive radiative) multiphoton part, (e-h).

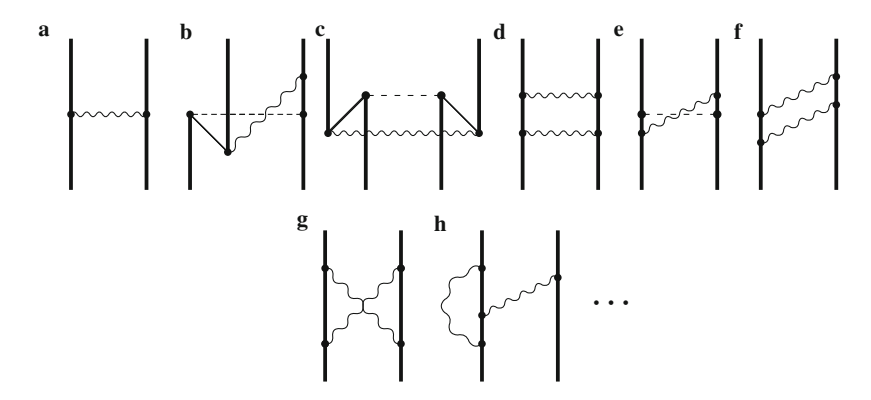


Fig. 11.2 Diagrammatic representation of the first-order expression (11.56)

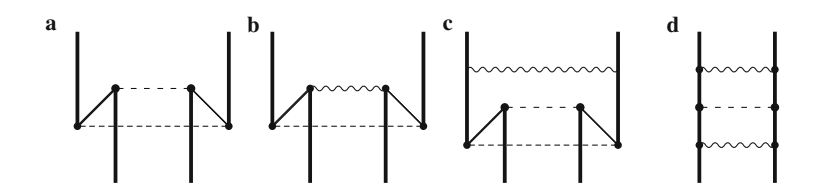


Fig. 11.3 Diagrammatic representation of the second-order expressions (11.58a)–(11.58d)

Similarly, the second-order expressions above become

$$\Delta E_a^{(2)} = -\langle \Psi_c | I_c \Lambda_{--} \Gamma \Lambda_{--} I_c | \Psi_c \rangle, \qquad (11.58a)$$

$$\Delta E_b^{(2)} = \left\langle \Psi_c I_c \Lambda_{--} i \int \frac{d\epsilon}{2\pi} \mathcal{F}^{-1} \left[g_T + g_T \mathcal{F}^{-1} g_T + \Delta g + \cdots \right] \mathcal{F}^{-1} I_c \Psi_c \right\rangle, \tag{11.58b}$$

$$\Delta E_c^{(2)} = \left\langle \Psi_c i \int \frac{d\epsilon}{2\pi} \mathcal{F}^{-1} \left[g_T + g_T \mathcal{F}^{-1} g_T + \Delta g + \cdots \right] \mathcal{F}^{-1} I_c \Lambda_{--} I_c \Psi_c \right\rangle, \tag{11.58c}$$

$$\Delta E_d^{(2)} = \left\langle \Psi_c D i \int \frac{d\epsilon}{2\pi} \mathcal{F}^{-1} \left[g_T + \cdots \right] \mathcal{F}^{-1} I_c \right.$$

$$\times \Gamma D i \int \frac{d\epsilon}{2\pi} \mathcal{F}^{-1} \left[g_T + \cdots \right] \mathcal{F}^{-1} I_c \Psi_c \left. \right\rangle. \tag{11.58d}$$

This is illustrated in Fig. 11.3. The first second-order contribution (11.58a) represents two Coulomb interactions with double pair (Fig. 11.3a) and the next

References 235

contribution (11.58b) in lowest order a transverse photon and a Coulomb interaction with double pair (b). The third contribution represents in lowest order one transverse photon and two Coulomb interactions with a double pair (c). The last term represents two *reducible* transverse photons with at least one Coulomb interaction (d).

11.5 Comparison with the Numerical Approach

In the previous chapter, we have described an approach that is presently being developed by the Gothenburg group of treating the Bethe–Salpeter equation numerically. This is based on the covariant-evolution approach and the Green's-operator technique, described previously, and to a large extent upon the numerical techniques developed by the group and applied to numerous atomic systems (see Sect. 2.7). This new technique has the advantage over the analytical approach that all relativistic effects are automatically included in the procedure. This simplifies the handling appreciably, and it corresponds to the treatment of the entire Sect. 4 of Douglas and Kroll [2] or to Sect. VII in the paper of Zhang [8].

The numerical technique of solving the Bethe–Salpeter equation, described in the previous chapter, is presently only partly developed, but the effect of one transverse photon with arbitrary number of crossing Coulomb interactions can presently be handled as well as virtual pairs. This corresponds to most of the terms $g_T + g_{T \times c} + g_{T \times c^2} + \cdots$ of the expansion in (11.19) and to the numerous formulas of Sect. 5 of Douglas–Kroll and of Sect. IV of Zhang.

Also part of the multiphoton effect can be treated numerically by iterating reducible interactions with a single transverse photon, corresponding to the operator $g_T \mathcal{F} g_T$ in the formulas above with crossing Coulomb interactions. These effects are treated in Sect. 6 of Douglas and Kroll. The irreducible interaction with several transverse photons cannot be teated at present with the numerical technique, but this can be approximated with one retarded and one or several unretarded photons (instantaneous Breit). Also radiative effects can be handled with the same approximation.

References

- Araki, H.: Quantum-Electrodynamical Corrections to Energy-levels of Helium. Prog. Theor. Phys. (Japan) 17, 619–42 (1957)
- Douglas, M.H., Kroll, N.M.: Quantum Electrodynamical Corrections to the Fine Structure of Helium. Ann. Phys. (N.Y.) 82, 89–155 (1974)
- 3. Lindgren, I.: The helium fine-structure controversy. arXiv;quant-ph p. 0810.0823v (2008)
- 4. Pachucki, K., Sapirstein, J.: Contributions to helium fine structure of order $m\alpha^7$. J. Phys. B 33, 5297–5305 (2000)
- Salpeter, E.E., Bethe, H.A.: A Relativistic Equation for Bound-State Problems. Phys. Rev. 84, 1232–42 (1951)

- 6. Sucher, J.: Energy Levels of the Two-Electron Atom to Order α^3 Ry; Ionization Energy of Helium. Phys. Rev. 109, 1010–11 (1957)
- 7. Sucher, J.: Ph.D. thesis, Columbia University (1958). Univ. Microfilm Internat., Ann Arbor, Michigan
- 8. Zhang, T.: Corrections to $O(\alpha^7(\ln \alpha)mc^2)$ fine-structure splittings and $O(\alpha^6(\ln \alpha)mc^2)$ energy levels in helium. Phys. Rev. A **54**, 1252–1312 (1996)
- 9. Zhang, T.: QED corrections to $O(\alpha^7 mc^2)$ fine-structure splitting in helium. Phys. Rev. A 53, 3896–3914 (1996)
- 10. Zhang, T.: Three-body corrections to $O(\alpha^6)$ fine-structure in helium. Phys. Rev. A **56**, 270–77 (1997)
- 11. Zhang, T., Drake, G.W.F.: Corrections to $O(\alpha^7 mc^2)$ fine-structure splitting in helium. Phys. Rev. A **54**, 4882–4922 (1996)
- 12. Zhang, T., Yan, Z.C., Drake, G.W.F.: QED Corrections of O(mc²α⁷ ln α) to the Fine Structure Splitting of Helium and He-like Ions. Phys. Rev. Lett. 77, 1715–18 (1996)

Chapter 12

Regularization and Renormalization

(See, for instance, Mandl and Shaw [17, Chap. 9] and Peskin and Schroeder [23, Chap. 7].)

In previous chapters, we have evaluated some radiative effects in the S-matrix (Chap. 4) and covariant-evolution operator formulations (Chap. 8). In this chapter, we discuss the important processes of renormalization and regularization in some detail.

Many integrals appearing in QED are divergent, and these divergences can be removed by replacing the bare electron mass and charge by the corresponding *physical* quantities. Since infinities are involved, this process of *renormalization* is a delicate matter. In order to do this properly, the integrals first have to be *regularized*, which implies that the integrals are modified so that they become finite. This has to be done so that the process is gauge-independent. After renormalization, the regularization modification is removed. Several regularization schemes have been developed, and we shall consider some of them in this chapter. If the procedure is performed properly, the way of regularization should have no effect on the final result.

12.1 The Free-Electron QED

12.1.1 The Free-Electron Propagator

The wave functions for free electrons are given by (D.29) in Appendix D

$$\begin{cases} \phi_{p_{+}}(x) = (2\pi)^{-3/2} u_{+}(\mathbf{p}) e^{i\mathbf{p} \cdot x} e^{-iE_{p}t} \\ \phi_{p_{-}}(x) = (2\pi)^{-3/2} u_{-}(\mathbf{p}) e^{i\mathbf{p} \cdot x} e^{iE_{p}t} \end{cases},$$
(12.1)

where **p** is the momentum vector and p_+ represents positive-energy states (r=1,2) and p_- negative-energy states (r=3,4). $E_p=cp_0=\sqrt{c^2\mathbf{p}^2+m^2c^4}$. The coordinate representation of the free-electron propagator (4.10) then becomes

$$\langle x_1 | \hat{S}_{F}^{\text{free}} | x_2 \rangle = \int \frac{d\omega}{2\pi} \sum_{\mathbf{p},r} \frac{\phi_{\mathbf{p},r}(x_1) \, \phi_{\mathbf{p},r}^{\dagger}(x_2)}{\omega - \varepsilon_p^{\text{free}} \, (1 - \mathrm{i} \eta)} \, \mathrm{e}^{-\mathrm{i}\omega(t_1 - t_2)}, \tag{12.2}$$

where $\varepsilon_p^{\text{free}}$ is the energy eigenvalue of the free-electron function $(E_p = |\varepsilon_p^{\text{free}}|)$. The Fourier transform with respect to time then becomes

$$\langle x_{1} | \hat{S}_{F}^{\text{free}} | x_{2} \rangle = \sum_{\mathbf{p},r} \frac{\phi_{\mathbf{p},r}(x_{1}) \phi_{\mathbf{p},r}^{\dagger}(x_{2})}{\omega - \varepsilon_{p}^{\text{free}} (1 - \mathrm{i}\eta)} \Rightarrow$$

$$= \int \frac{\mathrm{d}^{3}\mathbf{p}}{(2\pi)^{3}} \sum_{r} u_{r}(\mathbf{p}) u_{r}^{\dagger}(\mathbf{p}) \frac{\mathrm{e}^{\mathrm{i}\mathbf{p}\cdot(x_{1} - x_{2})}}{\omega - \varepsilon_{p}^{\text{free}} (1 - \mathrm{i}\eta)}$$

$$= \int \frac{\mathrm{d}^{3}\mathbf{p}}{(2\pi)^{3}} \left[u_{+}(\mathbf{p}) u_{+}^{\dagger}(\mathbf{p}) \frac{1}{\omega - E_{\mathbf{p}} (1 - \mathrm{i}\eta)} + u_{-}(\mathbf{p}) u_{-}^{\dagger}(\mathbf{p}) \frac{1}{\omega + E_{\mathbf{p}} (1 - \mathrm{i}\eta)} \right] \mathrm{e}^{\mathrm{i}\mathbf{p}(x_{1} - x_{2})}.$$

The square bracket above is the Fourier transform of the propagator, and using the relations (D.35, D.36), this becomes¹

$$S_{F}^{free}(\omega, \mathbf{p}) = \frac{1}{2} \left[\frac{1}{\omega - E_{\mathbf{p}} (1 - i\eta)} + \frac{1}{\omega + E_{\mathbf{p}} (1 - i\eta)} \right]$$

$$+ \frac{c \boldsymbol{\alpha} \cdot \mathbf{p} + \beta mc^{2}}{2p_{0}} \left[\frac{1}{\omega - E_{\mathbf{p}} (1 - i\eta)} - \frac{1}{\omega + E_{\mathbf{p}} (1 - i\eta)} \right]$$

$$= \frac{\omega + c \boldsymbol{\alpha} \cdot \mathbf{p} + \beta mc^{2}}{\omega^{2} - E_{p}^{2} + i\eta} = \frac{\omega + c \boldsymbol{\alpha} \cdot \mathbf{p} + \beta mc^{2}}{\omega^{2} - (c^{2}\mathbf{p}^{2} - m^{2}c^{4}) (1 - i\eta)}$$

$$= \frac{1}{\omega - (c \boldsymbol{\alpha} \cdot \mathbf{p} + \beta mc^{2}) (1 - i\eta)}$$

$$(12.3)$$

with $E_p^2 = c^2 p_0^2 = c^2 \mathbf{p}^2 + m^2 c^4$ and $\alpha \beta = -\beta \alpha$. This can also be expressed

$$S_{\rm F}^{\rm free}(\omega, \mathbf{p}) = \frac{1}{\omega - h_{\rm D}^{\rm free}(\mathbf{p}) (1 - i\eta)},\tag{12.4}$$

where $h_{\rm D}^{\rm free}({\bf p})$ is the momentum representation of the free-electron Dirac Hamiltonian operator (D.21), $\hat{h}_{\rm D}^{\rm free}(\hat{\boldsymbol p})$.

Formally, we can write (12.3) in covariant four-component form with $\omega = cp_0$ with cp_0 disconnected from $E_p = \sqrt{c^2\mathbf{p}^2 + m^2c^4}$ – known as off the mass-shell. Then we have²

$$S_{\rm F}^{\rm free}(p) = c S_{\rm F}^{\rm free}(\omega, \mathbf{p}) = \beta \frac{1}{\not p - mc + \mathrm{i}\eta}$$
 (12.5)

¹ In the following, we shall for simplicity denote the electron physical mass by m instead of m_e .

² The factor of β appears here because we define the electron propagator (4.9) by means of $\hat{\psi}^{\dagger}$ instead of the more conventionally used $\bar{\hat{\psi}} = \hat{\psi}^{\dagger}\beta$.

with $p = \gamma_{\sigma} p^{\sigma} = \beta \alpha_{\sigma} p^{\sigma} = \beta (p_0 - \alpha \cdot \mathbf{p}) = (p_0 + \alpha \cdot \mathbf{p}) \beta$ (see Appendix D). Note that the two transforms differ by a factor of c (c.f. Sect. 4.3, see also Appendix K).

12.1.2 The Free-Electron Self-Energy

The S-matrix for the first-order free-electron self-energy (Fig. 12.1) is obtained from (4.84) and (4.44) with the momentum functions (12.1) after time integrations

$$S^{(2)}(\omega; \mathbf{p}', r', \mathbf{p}, r) = e^{2}c^{2} \int \frac{\mathrm{d}z}{2\pi} \iint \mathrm{d}^{3}x \, \mathrm{d}^{3}x' \, u_{r'}^{\dagger}(\mathbf{p}') \, \mathrm{e}^{-\mathrm{i}\mathbf{p}'\cdot\mathbf{x}'}$$

$$\times \alpha^{\nu} \mathrm{i}S_{F}^{\text{free}}(\omega - z; \mathbf{x}', \mathbf{x}) \, \alpha^{\mu}u_{r}(\mathbf{p}) \, \mathrm{e}^{\mathrm{i}\mathbf{p}\cdot\mathbf{x}} \, \mathrm{i}D_{F\mu\nu}(z, \mathbf{x}' - \mathbf{x}). \tag{12.6}$$

The relation between the momentum and coordinate representations is

$$S_{F}^{\text{free}}(\omega; \mathbf{x}', \mathbf{x}) = \int \frac{d^{3}\mathbf{q}}{(2\pi)^{3}} S_{F}^{\text{free}}(\omega, \mathbf{q}) e^{i\mathbf{q}\cdot(\mathbf{x}'-\mathbf{x})}, \qquad (12.7)$$

$$D_{F\nu\mu}(z; x', x) = \int \frac{d^3k}{(2\pi)^3} D_{F\nu\mu}^{free}(z, k) e^{ik \cdot (x'-x)}.$$
 (12.8)

Integration over the space coordinates then yields

$$S^{(2)}(\omega; \mathbf{p}', r', \mathbf{p}, r) = e^{2}c^{2} \int \frac{\mathrm{d}^{3}\mathbf{q}}{(2\pi)^{3}} \int \frac{\mathrm{d}^{3}\mathbf{k}}{(2\pi)^{3}} \, \delta^{3}(\mathbf{p} - \mathbf{q} - \mathbf{k}) \, \delta^{3}(\mathbf{p}' - \mathbf{q} - \mathbf{k})$$

$$\times u_{r'}^{\dagger}(\mathbf{p}') \int \frac{\mathrm{d}z}{2\pi} \alpha^{\nu} S_{F}^{\text{free}}(\omega - z, \mathbf{k}) \, \alpha^{\mu} D_{F\nu\mu}^{\text{free}}(z, \mathbf{k}) \, u_{r}(\mathbf{p})$$
(12.9)

and integration over q

$$S^{(2)}(\omega; \mathbf{p}', r', \mathbf{p}, r) = \delta^{3}(\mathbf{p}' - \mathbf{p}) u_{r'}^{\dagger}(\mathbf{p}') (-i) \Sigma^{\text{free}}(\omega, \mathbf{p}) u_{r}(\mathbf{p}), \qquad (12.10)$$

where

$$\Sigma^{\text{free}}(\omega, \mathbf{p}) = ie^2 c^2 \int \frac{\mathrm{d}z}{2\pi} \int \frac{\mathrm{d}^3k}{(2\pi)^3} \, \alpha^{\nu} S_{\text{F}}^{\text{free}}(\omega - z, \mathbf{k}) \, \alpha^{\mu} D_{\text{F}\nu\mu}(z, \mathbf{k}).$$

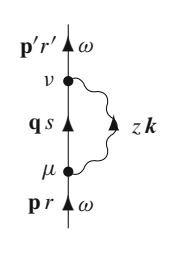


Fig. 12.1 Diagram representing the first-order free-electron self-energy

In covariant notation we have, using $z = ck_0$,

$$\Sigma^{\text{free}}(p) = ie^2 c^2 \int \frac{d^4 k}{(2\pi)^4} \, \alpha^{\nu} S_F^{\text{free}}(p-k) \, \alpha^{\mu} D_{F\nu\mu}(k), \tag{12.11}$$

which is the *free-electron self-energy function*. With the expression (12.5) for the free-electron propagator, this becomes expressed in terms of gamma matrices

$$\beta \Sigma^{\text{free}}(p) = ie^2 c^2 \int \frac{d^4k}{(2\pi)^4} \gamma^{\nu} \frac{\not p - \not k + mc}{(p-k)^2 - m^2 c^2 + i\eta} \gamma^{\mu} D_{\text{F}\nu\mu}(k)$$
(12.12)

or

$$\beta \Sigma^{\text{free}}(p) = ie^2 c^2 \int \frac{d^4 k}{(2\pi)^4} \gamma^{\nu} \frac{1}{\not p - \not k - mc + i\eta} \gamma^{\mu} D_{F\nu\mu}(k).$$
 (12.13)

With the commutation rules in Appendix (D.58), this becomes

$$\beta \Sigma^{\text{free}}(p) = -2ie^2c^2 \int \frac{d^4k}{(2\pi)^4} \frac{\not p - \not k - 2mc}{(p-k)^2 - m^2c^2 + i\eta} \gamma^{\nu} \gamma^{\mu} D_{\text{F}\nu\mu}(k)$$
(12.14)

and with the photon propagator (4.28) we have in the Feynman gauge

$$\beta \Sigma^{\text{free}}(p) = \frac{2ie^2c}{\epsilon_0} \int \frac{d^4k}{(2\pi)^4} \frac{\not p - \not k - 2mc}{(p-k)^2 - m^2c^2 + i\eta} \frac{1}{k^2 + i\eta}.$$
 (12.15)

{As mentioned above, the factor of β is due to our definition of the electron propagator [c.f. (12.5)]}.

12.1.3 The Free-Electron Vertex Correction

We consider first the single interaction with an external energy potential (Appendix D.41) $-e\alpha_{\sigma}A^{\sigma}$ (Fig. 12.2 left). The S-matrix is given by

$$S^{(1)}(\omega', \omega; \mathbf{p}'r', \mathbf{p}r, \mathbf{q}) = iec \int d^3x \, u_{r'}^{\dagger}(\mathbf{p}') \, e^{-i\mathbf{p}' \cdot \mathbf{x}} \, \alpha_{\sigma} A^{\sigma}(\mathbf{x}) \, u_r(\mathbf{p}) \, e^{i\mathbf{p} \cdot \mathbf{x}}$$
(12.16)

or

$$S^{(1)}(\omega', \omega; \mathbf{p}'r', \mathbf{p}r, \mathbf{q}) = iec \,\delta^3(\mathbf{p} - \mathbf{p}') \,u_{r'}^{\dagger}(\mathbf{p}') \,\alpha_{\sigma} A^{\sigma}(\mathbf{p} - \mathbf{p}') \,u_r(\mathbf{p}), \quad (12.17)$$

where $A^{\sigma}(\mathbf{q})$ is the Fourier transform of $A^{\sigma}(x)$.

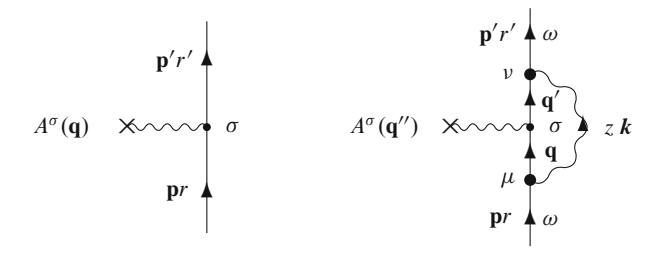


Fig. 12.2 Diagram representing the first-order free-electron vertex correction

The vertex-modified free-electron self-energy diagram in Fig. 12.2 (right) becomes similarly

$$S^{(3)}(\omega', \omega; \mathbf{p}'r', \mathbf{p}r) = (ie)^{3}c^{2} \int \frac{\mathrm{d}z}{2\pi} \iiint d^{3}x_{1} d^{3}x_{2} d^{3}x_{3} u_{r'}^{\dagger}(\mathbf{p}') e^{-i\mathbf{p}' \cdot \mathbf{x}'}$$

$$\times \alpha^{\nu} i S_{F}^{\text{free}}(\omega' - z, \mathbf{x}', \mathbf{x}'') \alpha_{\sigma} A^{\sigma}(\mathbf{x}'') \alpha^{\mu}$$

$$\times i S_{F}^{\text{free}}(\omega - z, \mathbf{x}'', \mathbf{x}) u_{r}(\mathbf{p}) e^{i\mathbf{p}\cdot\mathbf{x}} i D_{F\mu\nu}(z, \mathbf{x}' - \mathbf{x}).$$

$$(12.18)$$

In analogy with (12.9), this becomes

$$S^{(3)}(\omega', \omega; \mathbf{p}'r', \mathbf{p}r) = -e^{3}c^{2} \int \frac{d^{3}\mathbf{q}}{(2\pi)^{3}} \int \frac{d^{3}\mathbf{q}'}{(2\pi)^{3}} \int \frac{d^{3}\mathbf{q}''}{(2\pi)^{3}} \int \frac{d^{3}\mathbf{k}}{(2\pi)^{3}} u_{r'}^{\dagger}(\mathbf{p}')$$

$$\times \delta^{3}(\mathbf{p} - \mathbf{q} - \mathbf{k}) \delta^{3}(\mathbf{p}' - \mathbf{q}' - \mathbf{k}) \delta^{3}(\mathbf{q} - \mathbf{q}' + \mathbf{q}'')$$

$$\times \int \frac{dz}{2\pi} \alpha^{\nu} S_{F}^{\text{free}}(\omega' - z, \mathbf{q}')$$

$$\times \alpha_{\sigma} A^{\sigma}(\mathbf{q}'') \alpha^{\mu} S_{F}^{\text{free}}(\omega - z, \mathbf{q}) u_{r}(\mathbf{p}) D_{F\mu\nu}(z, \mathbf{k})$$

$$(12.19)$$

and after integrations over \mathbf{q} , \mathbf{q}' , and \mathbf{q}''

$$S^{(3)}(\omega', \omega; \mathbf{p}'r', \mathbf{p}r) = ie \,\delta^{3}(\mathbf{p} - \mathbf{p}') \,u_{r'}^{\dagger}(\mathbf{p}') \,\Lambda_{\sigma}(\omega', \omega; \mathbf{p}', \mathbf{p}) \,A^{\sigma}(\mathbf{p} - \mathbf{p}') \,u_{r}(\mathbf{p}),$$
(12.20)

where

$$\Lambda_{\sigma}(\omega', \omega; \mathbf{p}', \mathbf{p}) = ie^{2}c^{2} \int \frac{\mathrm{d}z}{2\pi} \int \frac{\mathrm{d}^{3}\mathbf{k}}{(2\pi)^{3}} \alpha^{\nu} S_{F}^{\text{free}}(\omega' - z, \mathbf{p}' - \mathbf{k})$$
$$\times \alpha_{\sigma} S_{F}^{\text{free}}(\omega - z, \mathbf{p} - \mathbf{k}) \alpha^{\mu} D_{F\nu\mu}(z, \mathbf{k})$$
(12.21)

is the *vertex correction function*. In covariant notations, this becomes in analogy with (12.10)

$$\Lambda_{\sigma}(p',p) = ie^{2}c \int \frac{d^{4}k}{(2\pi)^{4}} \alpha^{\nu} S_{F}^{free}(p'-k) \alpha_{\sigma} S_{F}^{free}(p-k) \alpha^{\mu} D_{F\nu\mu}(k) \quad (12.22)$$

In the Feynman gauge, this becomes

$$\Lambda_{\sigma}(p',p) = -\frac{\mathrm{i}e^{2}}{\epsilon_{0}} \int \frac{\mathrm{d}^{4}k}{(2\pi)^{4}} \gamma_{\mu} \frac{1}{\not p' - \not k - mc + \mathrm{i}\eta} \gamma_{\sigma}$$

$$\times \frac{1}{\not p - \not k - mc + \mathrm{i}\eta} \gamma^{\mu} \frac{1}{k^{2} + \mathrm{i}\eta}. \tag{12.23}$$

Comparing with the self-energy function (12.15), we find the *Ward identity* (4.100) [17, Eq. 9.60]

$$\frac{\partial}{\partial c p^{\sigma}} \Sigma(p) = \Lambda_{\sigma}(p, p).$$
 (12.24)

Obviously, this relation holds independently of the gauge.

12.2 Renormalization Process

We shall here derive expressions for the mass and charge renormalization in terms of counterterms that can be applied in evaluating the QED effects on bound states. The process of regularization will be treated in the next section.

12.2.1 Mass Renormalization

We consider now a *bare* electron with the mass m_0 . The corresponding free-electron propagator (12.5) is then

$$S_{\rm F}^{\rm bare}(\omega, \mathbf{p}) = \beta \frac{1}{\not p c - m_0 c^2 + i\eta}$$
 (12.25)

with $\omega = c p_0$.

We now "dress" the bare-electron propagator with all kinds of self-energy insertions in the same way as for the bound-electron propagator in Fig. 5.7. This corresponds to the S-matrix in operator form³

$$iS_{F}(\omega, \mathbf{p}) + iS_{F}(\omega, \mathbf{p})(-i)\Sigma(\omega, \mathbf{p}) iS_{F}(\omega, \mathbf{p}) + \dots = \frac{iS_{F}(\omega, \mathbf{p})}{1 - \Sigma(\omega, \mathbf{p}) S_{F}(\omega, \mathbf{p})},$$
(12.26)

³ Note that $\Sigma(\omega, \mathbf{p})$ has the dimension of energy and that the product $\Sigma(\omega, \mathbf{p})$ $S_F(\omega, \mathbf{p})$ is dimensionless (see Appendix K).

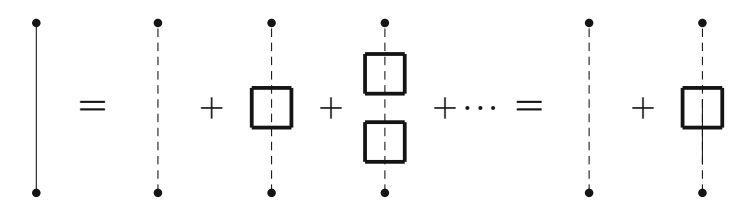


Fig. 12.3 Dyson equation for the dressed bare-mass electron propagator

$$\Sigma^{\mathrm{free}}(p)$$
= $+\cdots$

Fig. 12.4 Expansion of the proper self-energy operator for a bare electron

which leads to

$$S_{\rm F}^{\rm bare, dressed}(\omega, \mathbf{p}) = \beta \frac{1}{\not p c - m_0 c^2 - \beta \Sigma_{\rm bare}^*(\omega, \mathbf{p}) + i\eta}$$
(12.27)

illustrated in Fig. 12.3. Here, the box represents the *irreducible* or *proper* self-energy insertions, $\Sigma_{\text{bare}}^*(\omega, \mathbf{p})$, illustrated in Fig. 12.4. We shall in the following refer to this as the *free-electron self-energy*, $\Sigma^{\text{free}}(\omega, \mathbf{p})$,

$$\Sigma_{\text{bare}}^*(\omega, \mathbf{p}) = \Sigma^{\text{free}}(\omega, \mathbf{p}).$$
 (12.28)

To lowest order, the free-electron self-energy is in analogy with (4.85)

$$\Sigma^{\text{free}}(\omega, \mathbf{p}) = i \int \frac{d\omega}{2\pi} S_{\text{F}}^{\text{bare}}(\omega, \mathbf{p}) I^{\text{bare}}(\omega; \mathbf{p}), \qquad (12.29)$$

where I^{bare} is the interaction (4.44) in the momentum representation with the electronic charge replaced by the bare charge, e_0 .

The bare-electron propagator itself is also associated with a bare-electron charge (e_0) at each vertex. The dressing of the electron propagator leads to a modification of the electron mass as well as of the electron charge. One part of the free-electron self-energy is indistinguishable from the mass term in the electron propagator, and another part is indistinguishable from the electronic charge, and these parts give rise to the *mass renormalization* and the *charge renormalization*, respectively. The modification of the electron charge is here compensated by a corresponding modification of the vertex (to be discussed below), so that there is no net effect on the electron charge in connection with the electron self-energy. On the other hand, there is a real modification of the electron charge in connection with the modification of the *photon* propagator, as we shall discuss later.

Instead of working with the bare-electron mass and charge with self-energy insertions, we can use the <u>physical</u> mass and charge and introduce corresponding *counterterms* (see, for instance, [13, p. 332]). The free-electron propagator with the *physical* electron mass, m, is

$$S_{\rm F}^{\rm free}(\omega, \mathbf{p}) = \beta \frac{1}{\not p \ c - mc^2 + i\eta}$$
 (12.30)

and it has its poles "<u>on the mass shell</u>," p = mc [see Appendix (D.19)]. The dressed propagator (12.27) should have the same pole positions, which leads with

$$m = m_0 + \delta m \tag{12.31}$$

to

$$\delta mc^2 = \beta \Sigma^{\text{free}}(\omega, \mathbf{p})|_{p'=mc}.$$
 (12.32)

This is the <u>mass-counterterm</u>. We can now in the dressed operator (12.27) replace m_0c^2 by

$$mc^2 - \beta \Sigma^{\text{free}}(\omega, \mathbf{p})|_{\mathbf{p}'=mc}$$

which leads to

$$S_{\rm F}^{\rm free,ren}(\omega, \mathbf{p}) = \beta \frac{1}{\not p \, c - mc^2 - \beta \Sigma_{\rm ren}^{\rm free}(\omega, \mathbf{p}) + i\eta},$$
 (12.33)

where

$$\Sigma_{\text{ren}}^{\text{free}}(\omega, \mathbf{p}) = \Sigma^{\text{free}}(\omega, \mathbf{p}) - \Sigma^{\text{free}}(\omega, \mathbf{p})|_{p'=mc}.$$
 (12.34)

This represents the *mass-renormalization*. Both the free-electron self-energy and the mass counterterms are divergent, while *the renormalized self-energy is finite*.

12.2.2 Charge Renormalization

12.2.2.1 Electron Self-Energy

The *pole values* (residues) of the dressed bare electron propagator should also be the same as for the physical propagator, including the associated electronic charges. The physical propagator (12.30) with the electronic charge

$$e^2 S_{\rm F}^{\rm free}(\omega, \mathbf{p}) = \beta \frac{e^2}{\cancel{p} c - mc^2 + i\eta}$$

has the pole value $\beta e^2/c$. The dressed propagator (12.27) with the bare electron charge is

$$\beta \frac{e_0^2}{\not p c - m_0 c^2 - \beta \Sigma^{\text{free}}(\omega, \mathbf{p}) + i\eta} = \beta \frac{e_0^2}{\not p c - mc^2 - \beta \Sigma^{\text{free}}_{\text{ren}}(\omega, \mathbf{p}) + i\eta}$$

and its pole value at the pole p = mc is

$$\lim_{p \to mc} \frac{\beta}{c} \frac{e_0^2(p - mc)}{p \cdot c - mc^2 - \beta \Sigma_{\text{ren}}^{\text{free}}(\omega, \mathbf{p}) + i\eta} = \frac{\beta}{c} \frac{e_0^2}{1 - \beta \frac{\partial}{\partial \sigma'} \Sigma_{\text{ren}}^{\text{free}}(\omega, \mathbf{p})|_{p' = mc} + i\eta}$$

using l'Hospital's rule. This gives us the relation

$$e^{2} = \frac{e_{0}^{2}}{1 - \beta \frac{\partial}{\partial c p'} \Sigma_{\text{ren}}^{\text{free}}(\omega, \mathbf{p})|_{p'=mc}}$$
(12.35)

or

$$e^{2} = e_{0}^{2} \left(1 + \beta \frac{\partial}{\partial c \not p} \Sigma_{\text{ren}}^{\text{free}}(\omega, \mathbf{p}) \Big|_{\mathbf{p}' = mc} - \cdots \right).$$
 (12.36)

Here, the second term, which is divergent, represents the first-order *charge renor-malization*.

It is convenient to express the free-electron self-energy as

$$\Sigma^{\text{free}}(\omega, \mathbf{p}) = A + B(\not p c - mc^2) + C(\not p c - mc^2)^2.$$
 (12.37)

It then follows that the constant A is associated with the mass renormalization,

$$A = \Sigma^{\text{free}}(\omega, \mathbf{p})|_{\mathbf{p}' = mc} = \beta \delta mc^2$$
 (12.38)

and B with the charge renormalization,

$$B = \frac{\partial}{\partial c \not p} \Sigma^{\text{free}}(\omega, \mathbf{p})|_{\mathbf{p}'=mc}.$$
 (12.39)

From (12.36), it follows that for the charge renormalization due to the dressing of the electron propagator becomes

$$e = e_0(1 + B/2 + \cdots).$$
 (12.40)

The constant C represents the renormalized free-electron self-energy that is finite.

12.2.2.2 Vertex Correction

The modification of the vertex function shown in Fig. 12.2 can be represented by

$$ie_0 \Gamma_{\sigma}(p, p') = ie_0 \alpha_{\sigma} - ie_0 \beta \Lambda_{\sigma}(p, p'),$$
 (12.41)

where e_0 is the "bare" electron charge. The vertex correction is divergent and can be separated into a divergent part and a renormalized, finite part

$$\Lambda_{\sigma}(p, p') = L\alpha_{\sigma} + \Lambda_{\sigma}^{\text{ren}}(p, p'). \tag{12.42}$$

The divergent vertex part corresponds to a charge renormalization, in first order being

$$e = e_0(1 - \beta L). \tag{12.43}$$

But this should be combined with the charge renormalization due to the dressing of the electron propagators (12.40), which yields

$$e = e_0(1 - \beta L + \beta B),$$
 (12.44)

since there are two propagators associated with each vertex. Due to the *Ward identity* (12.24), it then follows that *the charge renormalization due to the electron self-energy and the vertex correction exactly cancel*. This holds also in higher orders.

12.2.2.3 Photon Self-Energy

We first transform the first-order photon self-energy (4.108) to the momentum representation, using

$$D_{F\nu\mu}(x_1, x_3) = \int \frac{d^4k}{(2\pi)^4} e^{-ik(x_1 - x_3)} D_{F\nu\mu}(k),$$

$$D_{F\nu\mu}(x_4, x_2) = \int \frac{d^4k}{(2\pi)^4} e^{-ik'(x_4 - x_2)} D_{F\nu\mu}(k'),$$

$$S_F(x_3, x_4) = \int \frac{d^4q}{(2\pi)^4} e^{-iq(x_3 - x_4)} S_F(q),$$

$$S_F(x_4, x_3) = \int \frac{d^4q}{(2\pi)^4} e^{-iq'(x_4 - x_3)} S_F(q').$$
(12.45)

The space integrations over x_3 and x_3 give rise to the delta functions $\delta^4(k-q+q')$ and $\delta^4(k'-q+q')$, yielding with the bare electron charge e_0^2 ,

$$\int \frac{\mathrm{d}^4 k}{(2\pi)^4} \, \mathrm{i} e_0^2 \alpha_1^{\mu} D_{F\nu\mu}(k) \, \mathrm{i} \Pi_{3,4}^{\sigma\tau}(k) \, \mathrm{i} e_0^2 \alpha_2^{\nu} D_{F\nu\mu}(k)$$

$$\mathrm{i} \Pi_{3,4}^{\sigma\tau}(k) = \int \frac{\mathrm{d}^4 q}{(2\pi)^4} \, \mathrm{Tr} \left[\mathrm{i} \alpha_3^{\sigma} S_F(q) \, \mathrm{i} \, \alpha_4^{\tau} S_F(q-k) \right]. \tag{12.46}$$

$$1\mu$$
 2ν + 1μ 2σ 3τ 2ν + \cdots

Fig. 12.5 Diagram representing the first-order vacuum polarization of the single photon (first-order photon self-energy)

The photon self-energy represents a modification of the single-photon exchange, illustrated in Fig. 12.5,

$$ie_0^2 D_{F\nu\mu}(k) \Rightarrow ie_0^2 D_{F\nu\mu}(k) + ie_0^2 D_{F\mu\sigma}(k) i\Pi^{\sigma\tau}(k) ie_0^2 D_{F\tau\nu}(k) + \cdots$$
 (12.47)

With the form (4.28) of the photon propagator in the Feynman gauge, this becomes

$$\frac{-\mathrm{i}e_0^2}{c\epsilon_0} \frac{g_{\mu\nu}}{k^2 + \mathrm{i}\eta} \Rightarrow \frac{-\mathrm{i}e_0^2}{c\epsilon_0} \frac{g_{\mu\nu}}{k^2 + \mathrm{i}\eta} + \frac{-\mathrm{i}e_0^2}{c\epsilon_0} \frac{g_{\mu\sigma}}{k^2 + \mathrm{i}\eta} \,\mathrm{i}\Pi^{\sigma\tau}(k) \,\frac{-\mathrm{i}e_0^2}{c\epsilon_0} \frac{g_{\tau\nu}}{k^2 + \mathrm{i}\eta}.$$
(12.48)

From the Lorentz covariance, it follows that the polarization tensor must have the form

$$\Pi^{\sigma\tau}(k) = -g^{\sigma\tau}A(k^2) + k^{\sigma}k^{\tau}B(k^2)$$
(12.49)

and it can be shown that in this case only the second term can contribute [4, p. 155], [17, p. 184]. This reduces the expression above to

$$\frac{-ie_0^2}{c\epsilon_0} \frac{g_{\mu\nu}}{k^2 + i\eta} \Rightarrow \frac{-ie_0^2}{c\epsilon_0} \frac{g_{\mu\nu}}{k^2 + i\eta} \left[1 - \frac{e_0^2}{c\epsilon_0} \frac{A(k^2)}{k^2 + i\eta} \right]$$

$$\equiv \frac{-ie_0^2}{c\epsilon_0} \frac{g_{\mu\nu}}{k^2 + \left(\frac{e_0^2}{c\epsilon_0}\right) A(k^2) + i\eta}.$$
(12.50)

The expression above represents the modification of the photon propagator due to the photon self-energy. It is infinite and can be interpreted as a change of the electronic charge – or *charge renormalization* – in analogy with the mass renormalization treated above.

The photon propagator has a pole at $k^2 = 0$, corresponding to the zero photon mass [c.f. the free-electron propagator in (12.5)], and the pole value is proportional to the electron charge squared, e_02 . If

$$A(k^2 = 0) = 0, (12.51)$$

then also the modified propagator has a pole at the same place with a pole value proportional to

 $\frac{e_0^2}{1 + \frac{e_0^2}{c\epsilon_0} \frac{dA(k^2)}{dk^2} \Big|_{k^2 = 0}}.$ (12.52)

This cannot be distinguished from the bare charge and represents the physical electron charge,

$$e^{2} = \frac{e_{0}^{2}}{1 + \frac{e_{0}^{2}}{c\epsilon_{0}} \frac{dA(k^{2})}{dk^{2}} \Big|_{k^{2} = 0}} \approx e_{0}^{2} \left[1 - \frac{e_{0}^{2}}{c\epsilon_{0}} \frac{dA(k^{2})}{dk^{2}} \Big|_{k^{2} = 0} \right], \tag{12.53}$$

which is the charge renormalization.

The polarization tensor may have a finite part that vanishes at $k^2 = 0$, Π_{ren} , which is the *renormalized photon self-energy*. This is *physically observable*.

12.2.2.4 Higher-Order Renormalization

The procedure described above for the first-order renormalization can be extended to higher orders. A second-order procedure has been described by Labzowsky and Mitrushenkov [14] and by Lindgren et al. [15], but we shall not be concerned with that further here.

12.3 Bound-State Renormalization: Cutoff Procedures

Before applying the renormalization procedure, the divergent integrals have to modified so that they become finite, which is the *regularization procedure*. Details of this process depend strongly on the gauge used. Essentially, all QED calculations performed so far have been carried out in the so-called covariant gauges (see Appendix G), preferably the Feynman gauge. In the remaining sections of this chapter, we shall review some of the procedures used in that gauge, and also consider the question of regularization in the Coulomb gauge.

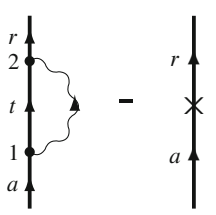
Several regularization procedures have been developed, and the conceptually simplest ones are the cutoff procedures. The most well known of these procedure is that of *Pauli–Willars* and another is the so-called *partial-wave regularization*. A more general and more sophisticated procedure is the *dimensional regularization*, which has definite advantages and is frequently used today. We shall consider some of these processes in the following sections.

12.3.1 Mass Renormalization

When we express the Dirac Hamiltonian (2.108) with the physical mass

$$\hbar_{\rm D} = c\boldsymbol{\alpha} \cdot \hat{\mathbf{p}} + \beta mc^2 + v_{\rm ext}, \tag{12.54}$$

Fig. 12.6 Diagram representing the renormalization of the first-order self-energy of a bound electron



we have to include the mass counterterm (12.32) in the perturbation density (6.35)

$$\mathcal{H}(x) = -ec\hat{\psi}^{\dagger}(x)\alpha^{\mu}A_{\mu}(x)\hat{\psi}(x) - \delta mc^{2}\hat{\psi}^{\dagger}(x)\beta\hat{\psi}(x). \tag{12.55}$$

The bound-electron self-energy operator is given by (8.47)

$$\langle r|\Sigma^{\text{bou}}(\varepsilon_a)|a\rangle = \left\langle rt\left|\int \frac{\mathrm{d}z}{2\pi} \mathrm{i}S_{\mathrm{F}}^{\text{bou}}(\varepsilon_a - z; \boldsymbol{x}_2, \boldsymbol{x}_1) I(z; \boldsymbol{x}_2, \boldsymbol{x}_1)\right| ta\right\rangle$$
 (12.56)

and subtracting the corresponding mass-counterterm yields the *renormalized self-energy operator*

$$\langle r | \Sigma_{\text{ren}}^{\text{bou}}(\varepsilon_a) | a \rangle = \langle r | \Sigma^{\text{bou}}(\varepsilon_a) - \beta \delta m c^2 | a \rangle$$
 (12.57)

illustrated in Fig. 12.6. Here, both terms contain singularities, which have to be eliminated, which is the regularization process.

In the regularization process due to Pauli and Villars [21], [17, Eq. 9.21], the following replacement is made in the photon propagator

$$\frac{1}{k^2 + i\eta} \Rightarrow \frac{1}{k^2 - \lambda^2 + i\eta} - \frac{1}{k^2 - \Lambda^2 + i\eta},$$
 (12.58)

which cuts off the ultraviolet and possible infrared divergence.

12.3.2 Evaluation of the Mass Term

(See Mandl and Shaw [17, Sect. 10.2].)

On the mass shell, p = mc, the free-electron self-energy (12.15) becomes [17, Eq. 10.16]

$$\delta m c^2 = \frac{\beta}{c} \Sigma^{\text{free}}(p) \mid_{p = mc} = -i \frac{2e^2}{\epsilon_0} \int \frac{d^4k}{(2\pi)^4} \frac{k + mc}{k^2 - 2pk + i\eta} \frac{1}{k^2 + i\eta}. \quad (12.59)$$

In order to evaluate this integral, we apply the Pauli-Villars regularization scheme, which we can express as

$$\frac{1}{k^2 + i\eta} \Rightarrow \frac{1}{k^2 - \lambda^2 + i\eta} - \frac{1}{k^2 - \Lambda^2 + i\eta} = -\int_{\lambda^2}^{\Lambda^2} \frac{dt}{(k^2 - t + i\eta)^2}.$$
 (12.60)

By means of the identity (J.4) in Appendix J with $a=k^2-t$ and $b=k^2-2pk$ we can express the mass term

$$\delta m c^2 = \frac{4ie^2}{\epsilon_0} \int \frac{d^4k}{(2\pi)^4} \int_{\lambda^2}^{\Lambda^2} dt \int_0^1 dx \, \frac{(\cancel{k} + mc)x}{[k^2 - 2pk(1 - x) - tx]^3}.$$
 (12.61)

With the substitutions q = -p(1-x) and s = -tx, the k integral becomes, using the integral (J.8) and (J.9) and p = mc,

$$\int \frac{\mathrm{d}^4 k}{(2\pi)^4} \frac{(\cancel{k} + mc)x}{[k^2 + 2qp + s]^3} = \frac{\mathrm{i}}{32\pi^2} \frac{mc \, x(2 - x)}{m^2 c^2 (1 - x)^2 + tx}$$
(12.62)

yielding

$$\delta mc^2 = \frac{e^2 mc}{8\pi^2 \epsilon_0} \int_0^1 dx \, (2 - x) \ln \frac{\Lambda^2 x + m^2 c^2 (1 - x)^2}{\lambda^2 x + m^2 c^2 (1 - x)^2}.$$
 (12.63)

This is logarithmically divergent as $\Lambda \to \infty$ with the leading term being

$$\delta mc^2 = \frac{e^2 mc}{8\pi^2 \epsilon_0} \int_0^1 dx \, (2 - x) \left[\ln \frac{\Lambda^2}{m^2} + \ln \frac{x}{(1 - x)^2} \right]. \tag{12.64}$$

To evaluate the second part of the integral, we need the following formulas

$$\int dx \ln x = x \ln x - x \qquad \int dx \, x \ln x = \frac{x^2 \ln x}{2} - \frac{x^2}{4}, \tag{12.65}$$

which leads to

$$I = \int_0^1 dx (2 - x) \ln \frac{x}{(1 - x)^2} = \frac{3}{4}.$$
 (12.66)

In all unit systems with $\hbar=1$, the factor $e^2/4\pi\epsilon_0=c\,\alpha$, where α is the fine-structure constant (see Appendix K), and the mass term (12.59) becomes

$$\delta m(\Lambda) c^2 = \frac{3\alpha mc^2}{2\pi} \left(\ln \left(\frac{\Lambda}{mc} \right) + \frac{1}{4} \right).$$
 (12.67)

12.3.3 Bethe's Nonrelativistic Treatment

Bethe's original nonrelativistic treatment of the Lamb shift [3] is of great historical interest, and it also gives some valuable insight into the physical process. Therefore, we shall briefly summarize it here.

From the relation (4.90), we have the bound-state self-energy, using the Feynman gauge (4.55),

$$\langle \mathbf{x}_{2} | \Sigma^{\text{bou}}(\varepsilon_{a}) | \mathbf{x}_{1} \rangle = -\frac{e^{2}c}{4\pi\epsilon_{0} r_{12}} \langle \mathbf{x}_{2} | \alpha_{\mu} | t \rangle \int_{0}^{\infty} \frac{d\kappa \sin \kappa r_{12}}{\varepsilon_{a} - \varepsilon_{t} - c\kappa \operatorname{sgn}\varepsilon_{t}} \langle t | \alpha^{\mu} | \mathbf{x}_{1} \rangle, \tag{12.68}$$

where $r_{12} = |x_1 - x_2|$. For small k values and positive intermediate states, this reduces to

$$\Sigma^{\text{bou}}(\varepsilon_a) = -\frac{e^2 c}{4\pi^2 \epsilon_0} \alpha_\mu |t\rangle \int_0^\infty \frac{\kappa \, d\kappa}{\varepsilon_a - \varepsilon_t - c\kappa} \, \langle t | \alpha^\mu. \tag{12.69}$$

The scalar part of $\alpha_{\mu}\alpha^{\mu}$ cancels in the renormalization, leaving only the vector part to be considered,

$$\Sigma^{\text{bou}}(\varepsilon_a) = \frac{e^2 c}{4\pi^2 \varepsilon_0} \alpha |t\rangle \cdot \int_0^\infty \frac{\kappa \, d\kappa}{\varepsilon_a - \varepsilon_t - c\kappa} \, \langle t | \alpha.$$
 (12.70)

The corresponding operator for a *free electron* in the state \mathbf{p}_{+} is

$$\Sigma^{\text{free}}(\mathbf{p}_{+}) = \frac{e^{2}c}{4\pi^{2}\epsilon_{0}}\alpha|\mathbf{q}_{+}\rangle \cdot \int_{0}^{\infty} \frac{\kappa \,\mathrm{d}\kappa}{\varepsilon_{\mathbf{p}_{+}} - \varepsilon_{\mathbf{q}_{+}} - c\kappa} \,\left\langle \mathbf{q}_{+} \middle| \alpha \right\rangle$$
(12.71)

restricting the intermediate states to *positive* energies. In the momentum representation, this becomes

$$\langle \mathbf{p}'_{+} \big| \Sigma^{\text{free}}(\mathbf{p}_{+}) \big| \mathbf{p}_{+} \rangle = \frac{e^{2}c}{4\pi^{2}\epsilon_{0}} \langle \mathbf{p}'_{+} | \boldsymbol{\alpha} | \mathbf{q}_{+} \rangle \cdot \int_{0}^{\infty} \frac{\kappa \, d\kappa}{\varepsilon_{\mathbf{p}_{+}} - \varepsilon_{\mathbf{q}_{+}} - c\kappa} \, \langle \mathbf{q}_{+} | \boldsymbol{\alpha} | \mathbf{p}_{+} \rangle.$$
(12.72)

But since α is diagonal with respect to the momentum, we must have $\mathbf{q}=\mathbf{p}=\mathbf{p}'.$ Thus,

$$\langle \mathbf{p}'_{+} \big| \Sigma^{\text{free}}(\mathbf{p}_{+}) \big| \mathbf{p}_{+} \rangle = -\delta_{\mathbf{p}',\mathbf{p}}^{3} \frac{e^{2}}{4\pi^{2}\epsilon_{0}} \left| \langle \mathbf{p}_{+} | \boldsymbol{\alpha} | \mathbf{p}_{+} \rangle \right|^{2} \int_{0}^{\infty} d\kappa.$$
 (12.73)

Obviously, this quantity is infinite. Inserting a set of complete states, this becomes

$$\langle \mathbf{p}'_{+} \big| \Sigma^{\text{free}}(\mathbf{p}_{+}) \big| \mathbf{p}_{+} \rangle = -\delta_{\mathbf{p}',\mathbf{p}}^{3} \frac{e^{2}}{4\pi^{2}\epsilon_{0}} \langle \mathbf{p}_{+} | \boldsymbol{\alpha} | t \rangle \cdot \langle t | \boldsymbol{\alpha} | \mathbf{p}_{+} \rangle \int_{0}^{\infty} d\kappa. \tag{12.74}$$

The free-electron self-energy operator can then be expressed as

$$\Sigma^{\text{free}}(\mathbf{p}_{+}) = -\delta_{\mathbf{p}',\mathbf{p}}^{3} \frac{e^{2}}{4\pi^{2}\epsilon_{0}} \alpha |t\rangle \cdot \int_{0}^{\infty} d\kappa \langle t | \alpha, \qquad (12.75)$$

which should be subtracted from the bound-electron self-energy operator (12.70). We can assume the intermediate states $\{t\}$ to be identical to those in the bound case. This gives the **renormalized self-energy operator**

$$\Sigma_{\text{ren}}^{\text{bou}}(\varepsilon_a) = \frac{e^2}{4\pi^2 \epsilon_0} \alpha |t\rangle \cdot \int_0^\infty d\kappa \, \frac{\varepsilon_a - \varepsilon_t}{\varepsilon_a - \varepsilon_t - c\kappa} \, \langle t | \alpha \,. \tag{12.76}$$

The expectation value of this operator in a bound state $|a\rangle$ yields the renormalized bound-electron self-energy in this approximation, i.e., the corresponding contribution to the physical **Lamb shift**,

$$\langle a | \ \Sigma_{\rm ren}^{\rm bou}(\varepsilon_a) \ | a \rangle = \frac{e^2}{4\pi^2 \epsilon_0 \ r_{12}} \left\langle a | \pmb{\alpha} | t \right\rangle \cdot \left\langle t | \pmb{\alpha} | a \right\rangle \ \int_0^\infty {\rm d}\kappa \ \frac{\varepsilon_a - \varepsilon_t}{\varepsilon_a - \varepsilon_t - c\kappa} \ . \tag{12.77}$$

This result is derived in a covariant Feynman gauge, where the quantized radiation has transverse as well as longitudinal components. In the Coulomb gauge, only the former are quantized. Since all three vector components above yield the same contribution, we will get the result in the Coulomb gauge by multiplying by 2/3. Furthermore, in the nonrelativistic limit, we have $\alpha \to \mathbf{p}/c$, which leads to

$$\langle a | \Sigma_{\text{ren}}^{\text{bou}}(\varepsilon_a) | a \rangle = \frac{e^2}{6\pi^2 c^2 \epsilon_0 r_{12}} \langle a | \mathbf{p} | t \rangle \cdot \langle t | \mathbf{p} | a \rangle \int_0^\infty d\kappa \, \frac{\varepsilon_a - \varepsilon_t}{\varepsilon_a - \varepsilon_t - c\kappa} \,, \quad (12.78)$$

which is essentially the result of Bethe.

Numerically, Bethe obtained the value 1,040 MHz for the shift in the first excited state of the hydrogen atom, which is very close to the value 1,000 MHz obtained experimentally by Lamb and Retherford. Later, the experimental shift has been determined to be about 1,057 MHz. Bethe's results was, of course, partly fortuitous, considering the approximations made. However, it was the first success performance of a renormalization procedure and represented a breakthrough in the theory of QED.

We can note that the nonrelativistic treatment leads to a *linear* divergence of the self-energy, while the relativistic treatment above gives only a *logarithmic* divergence.

12.3.4 Brown-Langer-Schaefer Regularization

The bound-state electron propagator can be expanded into a zero-potential term, a one-potential term, and a many-potential term

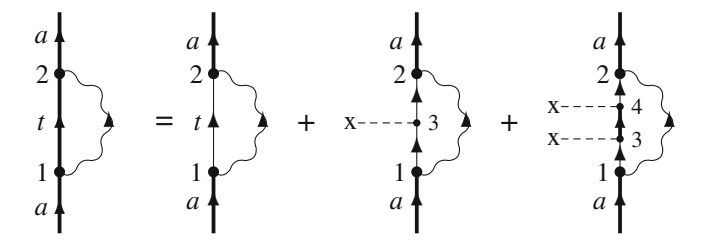


Fig. 12.7 Expanding the bound-state self-energy in free-electron states according to (4.107)

$$S_{F}^{\text{bou}}(\omega, x_{2}, x_{1}) = S_{F}^{\text{free}}(\omega, x_{2}, x_{1})$$

$$+ \int d^{3}x_{3} S_{F}^{\text{free}}(\omega, x_{2}, x_{3}) v(x_{3}) S_{F}^{\text{free}}(\omega, x_{3}, x_{1})$$

$$+ \int d^{3}x_{3} d^{3}x_{4} S_{F}^{\text{free}}(\omega, x_{2}, x_{4}) v(x_{4})$$

$$\times S_{F}^{\text{bou}}(\omega, x_{4}, x_{3}) v(x_{3}) S_{F}^{\text{free}}(\omega, x_{3}, x_{1}),$$
(12.79)

which leads to the expansion of the bound-electron self-energy, as illustrated in Fig. 12.7,

$$\langle a|\Sigma^{\text{bou}}(\varepsilon_{a})|a\rangle = \left\langle at \left| \int \frac{\mathrm{d}z}{2\pi} S_{\text{F}}^{\text{free}}(\varepsilon_{a} - z; \boldsymbol{x}_{2}, \boldsymbol{x}_{1}) I(z; \boldsymbol{x}_{2}, \boldsymbol{x}_{1}) \right| ta \right\rangle$$

$$+ \left\langle at \left| \int d^{3}\boldsymbol{x}_{3} \int \frac{\mathrm{d}z}{2\pi} S_{\text{F}}^{\text{free}}(\varepsilon_{a} - z; \boldsymbol{x}_{2}, \boldsymbol{x}_{3}) v(\boldsymbol{x}_{3}) \right.$$

$$+ S_{\text{F}}^{\text{free}}(\varepsilon_{a} - z; \boldsymbol{x}_{3}, \boldsymbol{x}_{1}) I(z; \boldsymbol{x}_{2}, \boldsymbol{x}_{1}) \left| ta \right\rangle \left\langle at \right| \int d^{3}\boldsymbol{x}_{3} d^{3}\boldsymbol{x}_{4}$$

$$\times \int \frac{\mathrm{d}z}{2\pi} \int d^{3}\boldsymbol{x}_{3} d^{3}\boldsymbol{x}_{4} S_{\text{F}}^{\text{free}}(\omega, \boldsymbol{x}_{2}, \boldsymbol{x}_{4}) v(\boldsymbol{x}_{4})$$

$$\times S_{\text{F}}^{\text{bou}}(\omega, \boldsymbol{x}_{4}, \boldsymbol{x}_{3}) v(\boldsymbol{x}_{3}) S_{\text{F}}^{\text{free}}(\omega, \boldsymbol{x}_{3}, \boldsymbol{x}_{1}) I(z; \boldsymbol{x}_{2}, \boldsymbol{x}_{1}) \left| ta \right\rangle,$$

$$(12.80)$$

where $I(z; x_2, x_1)$ represents the single-photon interaction (4.45). We can then express this as

$$\langle a|\Sigma^{\text{bou}}(\varepsilon_a)|a\rangle = \langle a|\Sigma^{\text{free}}(\varepsilon_a)|a\rangle - \langle a|ecA^{\sigma}\Lambda_{\sigma}^{\text{free}}(\varepsilon_a)|a\rangle + \langle a|\Sigma_{\text{mp}}|a\rangle.$$
(12.81)

Here, the first term on the right-hand side is the average of the free-electron self-energy in the bound state $|a\rangle$, the second term a vertex correction (4.98) with $v(x) = -e\alpha_{\sigma}A^{\sigma}$, and the last term the "many-potential" term.

We can now use the expansion (12.37) of the free-electron self-energy in (12.81), where the first term (A) will be eliminated by the mass-counterterm in (12.57). We are then left with the average of the mass-renormalized free-electron self-energy (12.34), which is still charge divergent. If we separate the vertex operator in a divergent and a renormalized part according to (12.42), it follows from (12.44) that the charge-divergent parts cancel, and we are left with three finite contributions, the mass-renormalized free-electron self-energy (12.34), the many-potential term (12.79), and the finite part of the vertex correction (12.42)

$$\langle r | \Sigma_{\text{ren}}^{\text{bou}}(\varepsilon_a) | a \rangle = \langle r | \Sigma_{\text{ren}}^{\text{free}}(\varepsilon_a) | a \rangle - \langle r | e A^{\sigma} \Lambda_{\sigma}^{\text{free,ren}}(\varepsilon_a) | a \rangle + \langle r | \Sigma_{\text{mp}} | a \rangle.$$
(12.82)

This is the method of Brown et al. [6], introduced already in 1959. It was first applied by Brown and Mayers [7] and later by Desidero and Johnson [10], Cheng et al. [8,9], and others. The problem in applying this expression lies in the many-potential term, but Blundell and Snyderman [5] have devised a method of evaluating this terms numerically with high accuracy (and the remaining terms analytically).

We can also express the renormalized, bound self-energy (12.57) as

$$\langle r | \Sigma_{\text{ren}}^{\text{bou}}(\varepsilon_a) | a \rangle = \left(\langle r | \Sigma^{\text{bou}}(\varepsilon_a) | a \rangle - \langle r | \Sigma^{\text{free}}(\varepsilon_a) | a \rangle \right) + \left(\langle r | \Sigma^{\text{free}}(\varepsilon_a) | a \rangle - \langle r | \beta \delta m c^2 | a \rangle \right), \tag{12.83}$$

where the second term is the renormalized free-electron self-energy (12.34), evaluated between bound states. This is illustrated in Fig. 12.8. The mass term can be evaluated by expanding the bound states in momentum representation

$$\langle r|\beta\delta mc^2|a\rangle = \langle r|\mathbf{p}',r'\rangle\langle \mathbf{p}',r'|\Sigma^{\text{free}}(\varepsilon_p)|\mathbf{p},r\rangle\langle \mathbf{p},r|a\rangle$$
 (12.84)

as illustrated in Fig. 12.9. The relation (12.83) can then be written as

$$\langle r | \Sigma_{\text{ren}}^{\text{bou}}(\varepsilon_{a}) | a \rangle = \langle r | \Sigma^{\text{bou}}(\varepsilon_{a}) - \Sigma^{\text{free}}(\varepsilon_{a}) | a \rangle + \langle r | \mathbf{p}', r' \rangle \langle \mathbf{p}', r' | \Sigma^{\text{free}}(\varepsilon_{a}) - \Sigma^{\text{free}}(\varepsilon_{p}) | \mathbf{p}, r \rangle \langle \mathbf{p}, r | a \rangle,$$
(12.85)

where we note that in the last term the energy parameter of the self-energy operator is equal to the energy of the free particle.

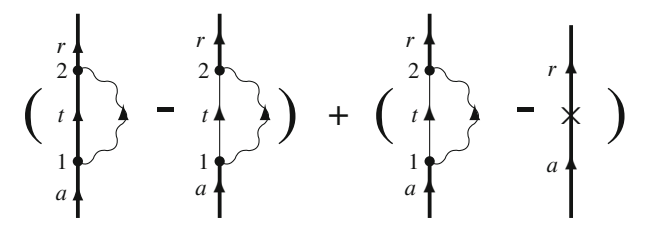


Fig. 12.8 Illustration of the method of Brown et al.

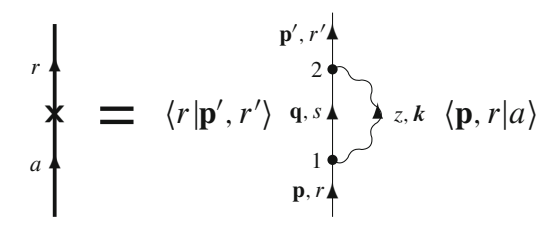


Fig. 12.9 Expansion of the mass term in momentum space

In this way, the leading mass-divergence term is eliminated, while the parts are still charge-divergent, but this divergence is cancelled between the parts. The elimination of the mass-renormalization improves the numerical accuracy.

Mohr has developed the method further and included also the one-potential part of the expansion in the two parts, thereby eliminating also the charge divergence. In this way, very accurate self-energies have been evaluated for hydrogenic systems [18–20].

12.3.5 Partial-Wave Regularization

An alternative scheme for regularizing the electron self-energy is known as the *partial-wave regularization* (PWR), introduced independently by the Gothenburg and Oxford groups [16, 24].

12.3.5.1 Feynman Gauge

Using the expansion (10.7)

$$\frac{\sin \kappa r_{12}}{\kappa r_{12}} = \sum_{l=0}^{\infty} (2l+1) j_l(\kappa r_1) j_l(\kappa r_2) C^l(1) \cdot C^l(2), \qquad (12.86)$$

the expression (4.90) for the bound-state self-energy in the Feynman gauge can be expressed as

$$\Sigma^{\text{bou}}(\varepsilon_a) = -\frac{e^2}{4\pi^2 \epsilon_0} \sum_{l=0}^{\infty} (2l+1) \int_0^{\infty} c\kappa \, d\kappa \, \frac{\alpha_{\mu} j_l(\kappa r) C^l |t\rangle \cdot \langle t | \alpha^{\mu} j_l(\kappa r) C^l}{\varepsilon_a - \varepsilon_t - c\kappa \, \text{sgn}(\varepsilon_t)}$$
(12.87)

with a summation over the intermediate bound state $|t\rangle$. Similarly, for the free electron

$$\Sigma^{\text{free}}(\omega) = -\frac{e^2}{4\pi^2 \epsilon_0} \sum_{l=0}^{\infty} (2l+1) \int_0^{\infty} c\kappa \, d\kappa \, \frac{\alpha_{\mu} j_l(\kappa r) C^l |\mathbf{q}, s\rangle \cdot \langle \mathbf{q}, s | \alpha^{\mu} j_l(\kappa r) C^l}{\omega - \varepsilon_q - c\kappa \, \text{sgn}(\varepsilon_q)}$$
(12.88)

summed over free-electron states $|\mathbf{q}, r\rangle$. Here, ω is the free-running energy parameter and ε_q represents the energy of the free-electron state $|\mathbf{q}, s\rangle$. On the mass shell, $\omega = \varepsilon_p = \sqrt{c^2 \mathbf{p}^2 + m^2 c^4}$, this becomes

$$\Sigma^{\text{free}}(\varepsilon_p) = -\frac{e^2}{4\pi^2 \epsilon_0} \sum_{l=0}^{\infty} (2l+1) \int_0^{\infty} c\kappa \, d\kappa \, \frac{\alpha_{\mu} j_l(\kappa r) C |\mathbf{q}, s\rangle \cdot \langle \mathbf{q}, s | \mu^{\mu} j_l(\kappa r) C^l}{\varepsilon_p - \varepsilon_q - c\kappa \, \text{sgn}(\varepsilon_q)}.$$
(12.89)

The PWR can be combined with the Brown–Langer–Schaefer method discussed above by expanding the remaining terms in (12.83) in a similar way.

The free-electron self-energy is diagonal with respect to the momentum \mathbf{p} , when all partial waves are included, but this is NOT the case for a truncated sum. Furthermore, it has nondiagonal elements with respect to the spinor index r.

12.3.5.2 Coulomb Gauge

The partial-wave regularization has not yet been applied in the Coulomb gauge, but to be able to include the self-energy in a many-body calculation this will be necessary.

In analogy with the Feynman-gauge result (12.87), the *transverse* part of the self-energy in Coulomb gauge becomes

$$\Sigma^{\text{bou,trans}}(\varepsilon_{a}) = -\frac{e^{2}}{4\pi^{2}\epsilon_{0}} \sum_{l=0}^{\infty} (2l+1) \int_{0}^{\infty} c\kappa \, d\kappa$$

$$\times \frac{\alpha j_{l}(\kappa r) C^{l} |t\rangle \cdot \langle t | \alpha j_{l}(\kappa r) C^{l} - (\alpha \cdot \nabla) j_{l}(\kappa r) C^{l} |t\rangle \langle t | (\alpha \cdot \nabla) j_{l}(\kappa r) C^{l} / \kappa^{2}}{\varepsilon_{a} - \varepsilon_{t} - c\kappa \, \text{sgn}(\varepsilon_{t})}$$
(12.90)

using the expression (4.92). The corresponding mass term becomes in analogy with (12.89)

$$\begin{split} & \boldsymbol{\Sigma}^{\text{free,trans}}(\varepsilon_{p}) = -\frac{e^{2}}{4\pi^{2}\epsilon_{0}} \sum_{l=0}^{\infty} (2l+1) \int_{0}^{\infty} c\kappa \, \mathrm{d}\kappa \\ & \times \frac{\boldsymbol{\alpha} j_{l}(\kappa r) \boldsymbol{C}^{l} |\mathbf{q},s\rangle \cdot \langle \mathbf{q},s | \boldsymbol{\alpha} j_{l}(\kappa r) \boldsymbol{C}^{l} - (\boldsymbol{\alpha} \cdot \boldsymbol{\nabla}) j_{l}(\kappa r) \boldsymbol{C}^{l} |\mathbf{q},s\rangle \langle \mathbf{q},s | (\boldsymbol{\alpha} \cdot \boldsymbol{\nabla}) j_{l}(\kappa r) \boldsymbol{C}^{l} / \kappa^{2}}{\varepsilon_{p} - \varepsilon_{\mathbf{q},s} - c\kappa \, \mathrm{sgn}(\varepsilon_{q})}. \end{split}$$

The Coulomb part in Coulomb gauge is obtained similarly from (4.93)

$$\Sigma(\varepsilon_a)^{\text{bou,Coul}} = \frac{e^2}{8\pi^2 \epsilon_0 r_{12}} \operatorname{sgn}(\varepsilon_t) \sum_{l=0}^{\infty} (2l+1)$$

$$\times \int_0^{\infty} 2\kappa \, d\kappa \, j_l(\kappa r) \, C^l |t\rangle \cdot \langle t | j_l(\kappa r) C^l \qquad (12.92)$$

using the value $-i \operatorname{sgn}(\varepsilon_t)/2$ for the integral, and the corresponding mass term

$$\Sigma(\varepsilon_a)^{\text{free,Coul}} = \frac{e^2}{8\pi^2 \epsilon_0 r_{12}} \operatorname{sgn}(\varepsilon_l) \sum_{l=0}^{\infty} (2l+1)$$

$$\times \int_0^{\infty} 2\kappa \, d\kappa \, j_l(\kappa r) \, \boldsymbol{C}^l |\mathbf{q}, s\rangle \cdot \langle \mathbf{q}, s | j_l(\kappa r) \boldsymbol{C}^l. \quad (12.93)$$

The main advantage of the PWR is that the bound- and free-electron self-energies are calculated in exactly the same way, which improves the numerical accuracy, compared to the standard procedure, where the mass term is evaluated analytically (12.67). Since all terms are here finite, no further regularization is needed. The maximum L value, $L_{\rm max}$, is increased until sufficient convergence is achieved. This scheme has been successfully applied in a number of cases [16, 24].

It has been shown by Persson et al. [22] that the method of PWR gives the correct result in lowest order with an arbitrary number of Coulomb interactions, while a correction term is needed when there is more than one magnetic interaction. This is due to the double summation over partial waves and photon momenta, which is not unique due to the infinities involved. This problem might be remedied by combining this method with dimensional regularization, as will be briefly discussed at the end of the chapter.

12.4 Dimensional Regularization in Feynman Gauge*

The most versatile regularization procedure developed so far is the *dimensional regularization*, which is nowadays frequently used in various branches of field theory. In treating the number of dimensions (D) as a continuous variable, it can be shown that the integrals of the radiative effects are singular only when D is an integer. Then by choosing the dimensionality to be $4-\epsilon$, where ϵ is a small, positive quantity, the integrals involved will be well defined and finite. After renormalization, one lets the parameter $\epsilon \to 0$. This method has been found to preserve the gauge invariance and the validity of the Ward identity to all orders. The method was developed mainly by t'Hooft and Veltman in the 1970s [27] (see, for instance, Mandl and Shaw [17, Chap. 10], Peskin and Schroeder [23, Chap. 7] and Snyderman [25]).

Most applications are made in so-called covariant gauges, where the procedure is now well developed. For our purpose, however, it is necessary to apply the Coulomb gauge, and here the procedure is less developed. Important contributions have been made more recently, though, by Adkins [1,2], Heckarthon [11], and others.

Here, we shall first illustrate the method by evaluating the renormalized freeelectron self-energy, using the Feynman gauge. The problem with the Coulomb gauge will be discussed in the next section.

12.4.1 Evaluation of the Renormalized Free-Electron Self-Energy in Feynman Gauge

We start now from the form (12.12) of the free-electron self-energy in the *Feynman gauge* and the photon propagator in momentum space (4.28)

$$\beta \Sigma^{\text{free}}(p) = ie^2 c^2 \int \frac{\mathrm{d}^4 k}{(2\pi)^4} \, \gamma^{\nu} \frac{\not p - \not k + mc}{(p-k)^2 - m^2 c^2 + i\eta} \, \gamma^{\mu} D_{\text{F}\nu\mu}(k)$$

$$= -\frac{ie^2 c}{\epsilon_0} \int \frac{\mathrm{d}^4 k}{(2\pi)^4} \, \gamma_{\mu} \frac{\not p - \not k + mc}{(p-k)^2 - m^2 c^2 + i\eta} \, \gamma^{\mu} \frac{1}{k^2 + i\eta}.$$
(12.94)

Using the Feynman integral (J.2) (second version) with $a = k^2$ and $b = (p - k)^2 - m^2c^2$, this can be expressed as

$$\beta \Sigma^{\text{free}}(p) = -\frac{\mathrm{i}e^2c}{\epsilon_0} \int_0^1 \mathrm{d}x \int \frac{\mathrm{d}^4k}{(2\pi)^4} \frac{\gamma_\mu \left(p - k + mc\right) \gamma^\mu}{\left[k^2 + \left(p^2 - 2pk - m^2c^2\right)x\right]^2}.$$
 (12.95)

We shall now evaluate this integral using nonintegral dimension $D = 4 - \epsilon$,

$$\beta \Sigma^{\text{free}}(p) = -\frac{ie^2c}{\epsilon_0} \int_0^1 dx \int \frac{d^Dk}{(2\pi)^D} \frac{\gamma_\mu \left(\not p - \not k + mc\right) \gamma^\mu}{\left[k^2 + \left(p^2 - 2pk - m^2c^2\right)x\right]^2}$$

$$= \frac{2ie^2c}{\epsilon_0} \int_0^1 dx \int \frac{d^Dk}{(2\pi)^D} \frac{(1 - \epsilon/2)(\not p - \not k) - (2 - \epsilon/2) mc}{\left[k^2 + \left(p^2 - 2pk - m^2c^2\right)x\right]^2},$$
(12.96)

after applying the anticommutation rules for the gamma matrices in Appendix D.59. With the substitutions q = -px and $s = (p^2 - m^2c^2)x$, this becomes

$$\beta \Sigma^{\text{free}}(p) = \frac{2ie^2c}{\epsilon_0} \int_0^1 dx \int \frac{d^Dk}{(2\pi)^D} \frac{(1 - \epsilon/2)(\not p - \not k) - (2 - \epsilon/2) \, mc}{[k^2 + 2kq + s]^2},$$
(12.97)

which is of the form of (G.23) and (G.24). This leads to

$$\beta \Sigma^{\text{free}}(p) = -\frac{2e^2 c (mc)^{-\epsilon}}{\epsilon_0 (4\pi)^{D/2}} \int_0^1 dx \, \frac{\Gamma(\epsilon/2)}{\Gamma(2)} \times \left[(1 - \epsilon/2) (\not p - \not p \, x) - (2 - \epsilon/2) \, mc \right] \left(\frac{m^2 c^2}{w} \right)^{\epsilon/2}$$
(12.98)

with $w = q^2 - s = [m^2c^2 - p^2(1-x)]x$. The Gamma function can be expanded as (see Appendix G.3)

$$\Gamma(\epsilon/2) = \frac{2}{\epsilon} - \gamma_{\rm E} + \cdots$$

with $\gamma_E = 0.5722...$ being Euler's constant, and furthermore

$$\frac{1}{(4\pi)^{D/2}} = \frac{1}{(4\pi)^2} \left(1 + \frac{\epsilon}{2} \ln 4\pi + \cdots \right),$$
$$\left(\frac{m^2 c^2}{w} \right)^{\epsilon/2} = 1 - \frac{\epsilon}{2} \ln \left(\frac{w}{m^2 c^2} \right) + \cdots.$$

This yields

$$\frac{\Gamma(\epsilon/2)}{(4\pi)^{D/2}} \left(\frac{m^2 c^2}{w}\right)^{\epsilon/2} = \frac{1}{(4\pi)^2} \left(2/\epsilon - \gamma_{\rm E} + \cdots\right) \times \left(1 + \frac{\epsilon}{2} \ln 4\pi + \cdots\right) \left(1 - \frac{\epsilon}{2} \ln \left(w/m^2 c^2\right) + \cdots\right) \\
= \frac{1}{(4\pi)^2} \left[\Delta - \ln\left(\frac{w}{m^2 c^2} + \cdots\right)\right], \tag{12.99}$$

where

$$\Delta = \frac{2}{\epsilon} - \gamma_{\rm E} + \ln 4\pi + \cdots$$
 (12.100)

This leads to

$$\beta \Sigma^{\text{free}}(p) = -2K \left[\int_0^1 dx \, \left(\not p - \not p \, x - 2mc \right) \left[\Delta - \ln \left(\frac{w}{m^2 c^2} + \cdots \right) \right] - \int_0^1 dx \, \left(\not p - \not p \, x + mc \right) \right]$$
(12.101)

with

$$K = \frac{e^2c}{\epsilon_0(4\pi)^2} = \frac{c^2\alpha}{4\pi}.$$

We write the denominator in (12.98) as

$$w = m^2 c^2 x X$$
; $X = 1 - \frac{p^2}{m^2 c^2} (1 - x) = -[\rho + (1 - \rho)x]$

with

$$\rho = \frac{p^2 - m^2 c^2}{m^2 c^2}. (12.102)$$

We then express the integral (12.101) as 2K(A + B + C) with

$$A = -\int_0^1 dx \ (\not p - \not p \, x - 2mc) \ \Delta + \int_0^1 dx \ (\not p - \not p \, x - mc) \,,$$

$$B = \int_0^1 dx \ (\not p - \not p \, x - 2mc) \ln x \,,$$

$$C = \int_0^1 dx \ (\not p - \not p \, x - 2mc) \ln \left[\rho + (1 - \rho)x \right] \,.$$

To evaluate this integral, we can use the formulas (12.65), yielding

$$\int_0^1 dx \ln(1-x) = -1 \qquad \int_0^1 dx \, x \ln(1-x) = -3/4,$$

$$\int_0^1 dx \, \ln\left[\rho + (1-\rho)x\right] = -1 - \frac{\rho \ln \rho}{1-\rho},$$

$$\int_0^1 dx \, x \ln\left[\rho + (1-\rho)x\right] = \frac{\rho}{(1-\rho)} \left(1 + \frac{\rho \ln \rho}{1-\rho}\right) - \frac{1}{4(1-\rho)^2} \left(1 + 2\rho^2 \ln \rho - \rho^2\right),$$

which gives

$$A = -(p/2 - 2mc) \Delta + (p/2 - mc)$$
$$B = -3 p/4 + 2mc$$

$$C = -\frac{\not p \ \rho}{(1-\rho)} \left(1 + \frac{\rho \ln \rho}{1-\rho} \right) + \frac{\not p}{4(1-\rho)^2} \left(1 + 2\rho^2 \ln \rho - \rho^2 \right)$$

$$- (\not p - 2m) \left(1 + \frac{\rho \ln \rho}{1-\rho} \right)$$

$$= \not p \left[-\frac{1}{(1-\rho)} \left(1 + \frac{\rho \ln \rho}{1-\rho} \right) + \frac{\rho^2 \ln \rho}{2(1-\rho)^2} + \frac{1+\rho}{4(1-\rho)} \right]$$

$$+ 2mc \left(1 + \frac{\rho \ln \rho}{1-\rho} \right).$$

Subtracting the on-the-mass-shell value (p = m, $\rho = 0$) yields for the A and B terms

$$(A+B)^{\rm ren} = -\frac{\not p - mc}{2} \left(\Delta + \frac{1}{2} \right).$$

For the C term, the on-shell value is 5mc/4, yielding

$$C^{\text{ren}} = -\not p \left\{ \frac{\rho(2-\rho)\ln\rho}{2(1-\rho)^2} + \frac{\rho}{(1-\rho)} + \frac{3}{4} \right\} + mc \left\{ \frac{2\rho\ln\rho}{1-\rho} + \frac{3}{4} \right\}.$$

The total on-shell value (mass-counter term) becomes

$$\delta mc^2 = \frac{mc^2 \alpha}{4\pi} (3\Delta + 4 + \cdots).$$
 (12.103)

Collecting all parts, we obtain the following expression for the mass-renormalized free-electron self-energy

$$\beta \Sigma^{\text{free}}(p) = -\frac{c^2 \alpha}{4\pi} \left[(\not p - mc) \left(\Delta + 2 + \frac{\rho}{1 - \rho} + \frac{\rho(2 - \rho) \ln \rho}{(1 - \rho)^2} \right) + \frac{\rho mc}{1 - \rho} \left(1 - \frac{2 - 3\rho}{1 - \rho} \ln \rho \right) \right]$$

$$(12.104)$$

with $\rho = (p^2 - m^2c^2)/m^2c^2$. This agrees with the result of Snyderman [25, 26].

12.4.2 Free-Electron Vertex Correction in Feynman Gauge

Next, we consider the free-electron vertex correction (12.23)

$$\Lambda_{\sigma}(p',p) = \frac{ie^{2}}{\epsilon_{0}} \int \frac{d^{4}k}{(2\pi)^{4}} \gamma_{\mu} \frac{p' - \not k + mc}{(p' - k)^{2} - m^{2}c^{2} + i\eta} \gamma_{\sigma} \times \frac{p - \not k + mc}{(p - k)^{2} - m^{2}c^{2} + i\eta} \gamma^{\mu} \frac{1}{k^{2} + i\eta}.$$
(12.105)

The Feynman parametrization (J.4), similar to the self-energy case, $a=k^2$, $b=(k-p)^2-m^2c^2$, and $c=(k-p')^2-m^2c^2$, yields

$$\begin{split} \Lambda_{\sigma}(p',p) &= \frac{2\mathrm{i}e^2}{\epsilon_0} \int_0^1 \mathrm{d}x \int_0^{1-x} \mathrm{d}y \int \frac{\mathrm{d}^4k}{(2\pi)^4} \\ &\times \frac{\gamma_{\mu}(p'-\not k+mc)\gamma_{\sigma}(p-\not k+mc)\gamma^{\mu}}{\left[k^2+(p^2-2pk-m^2c^2)x+(p'^2-2p'k-m^2c^2)y\right]^3}. \end{split}$$

With q = -(px + p'y) and $s = p^2x + p'^2y - m^2c^2(x + y)$, the denominator is of the form $k^2 + 2kq + s$

$$\begin{split} \Lambda_{\sigma}(p',p) &= \frac{2\mathrm{i}e^2}{\epsilon_0} \int_0^1 \mathrm{d}x \int_0^{1-x} \mathrm{d}y \int \frac{\mathrm{d}^D k}{(2\pi)^D} \frac{\gamma_{\mu}(p' - k + mc)\gamma_{\sigma}(p - k + mc)\gamma^{\mu}}{(k^2 + 2kq + s)^3} \\ &= \frac{2\mathrm{i}e^2}{c\epsilon_0} \int_0^1 \mathrm{d}x \int_0^{1-x} \mathrm{d}y \left[C_0 + C_1 + C_2 \right], \end{split}$$

where the index indicates the power of k involved,

$$C_{0} = \int \frac{\mathrm{d}^{D}k}{(2\pi)^{D}} \frac{\gamma_{\mu}(p' + mc)\gamma_{\sigma}(p' + mc)\gamma^{\mu}}{(k^{2} + 2kq + s)^{3}},$$

$$C_{1} = \int \frac{\mathrm{d}^{D}k}{(2\pi)^{D}} \frac{\gamma_{\mu}(-\cancel{k})\gamma_{\sigma}(p' + mc)\gamma^{\mu} + \gamma_{\mu}(p' + mc)\gamma_{\sigma}(-\cancel{k})\gamma^{\mu}}{(k^{2} + 2kq + s)^{3}},$$

$$C_{2} = \int \frac{\mathrm{d}^{D}k}{(2\pi)^{D}} \frac{\gamma_{\mu} \cancel{k}\gamma_{\sigma} \cancel{k}\gamma^{\mu}}{(k^{2} + 2kq + s)^{3}}.$$

The coefficients C_0 and C_1 are convergent and we can let $\epsilon \to 0$. With the formula (G.23) (n = 3) and the contraction formulas (D.59), we then have

$$C_0 = \frac{\mathrm{i}}{(4\pi)^2} \frac{(\not p + mc)\gamma_\sigma(\not p' + mc)}{w}$$

with

$$w = s - q^2 = s - (px + p'y)^2$$
.

Similarly, we have for the numerator in C_1

$$\gamma_{\mu}(-\not k)\gamma_{\sigma}(\not p+mc)\gamma^{\mu}+\gamma_{\mu}(\not p'+mc)\gamma_{\sigma}(-\not k)\gamma^{\mu}=2(\not p\gamma_{\sigma}\not k+\not k\gamma_{\sigma}\not p')-8mck_{\sigma}$$
 and with (G.24)

$$C_1 = \frac{\mathrm{i}}{(4\pi)^2} \frac{p \gamma_\sigma \not q + \not q \gamma_\sigma \not p' - 4mcq_\sigma}{w}.$$

The C_2 coefficient is divergent and has to be evaluated with more care. Then the situation is analogous to that of the self-energy (12.98). The numerator becomes

$$\gamma_{\mu} \not k \gamma_{\sigma} \not k \gamma^{\mu} = -(2 - \epsilon) \not k \gamma_{\sigma} \not k - \widetilde{\jmath} \widetilde{\jmath} \widetilde{\jmath} \widetilde{\jmath} \widetilde{\jmath}$$

and

$$C_2 = -\int \frac{\mathrm{d}^D k}{(2\pi)^D} \frac{(2-\epsilon) \cancel{k} \gamma_\sigma \cancel{k} + \cancel{\widetilde{k}} \widetilde{\gamma}_\sigma \cancel{\widetilde{k}}}{(k^2 + 2kq + s)^3},$$

which can be evaluated with (G.25).

The evaluation of the integrals above is straightforward but rather tedious. The complete result is found in [25].

12.5 Dimensional Regularization in Coulomb Gauge*

12.5.1 Free-Electron Self-Energy in the Coulomb Gauge

For our main purpose of combining MBPT and QED, it is necessary to apply the Coulomb gauge to take advantage of the developments in standard MBPT.

We shall first follow Adkins [1] in regularizing the free-electron self-energy in the Coulomb gauge by expressing the bound states in terms of free-electron states. We then start from the expression (12.12)

$$\beta \Sigma^{\text{free}}(p) = ie^2 c^2 \int \frac{d^4 k}{(2\pi)^4} \gamma^{\nu} \frac{\not p - \not k + mc}{(p-k)^2 - m^2 c^2 + i\eta} \gamma^{\mu} D_{\text{F}\nu\mu}(k). \quad (12.106)$$

For the photon propagator, we use the expressions (4.32) and (4.36)

$$D_{\mathrm{F}\mu\nu}^{\mathrm{C}}(k;\boldsymbol{k}) = \frac{1}{c\epsilon_0} \left[\frac{\delta_{\mu,0}\delta_{\nu,0}}{\boldsymbol{k}^2} - \delta_{\mu,i}\delta_{\nu,j} \left(g_{ij} + \frac{k_i k_j}{\boldsymbol{k}^2} \right) \frac{1}{k^2 + \mathrm{i}\eta} \right]. \quad (12.107)$$

The three terms in the propagator correspond to the *Coulomb*, *Gaunt*, *and scalar-retardation* parts, respectively, of the interaction (4.59).

The Coulomb part of the self-energy becomes

$$\frac{\mathrm{i}e^2c}{\epsilon_0} \int \frac{\mathrm{d}^4k}{(2\pi)^4} \frac{\gamma^0(\not p - \not k + mc)\gamma^0}{(\not p - k)^2 - m^2c^2 + \mathrm{i}\eta} \frac{1}{k^2 + \mathrm{i}\eta},\tag{12.108}$$

$$= \frac{ie^2c}{\epsilon_0} \int \frac{d^4k}{(2\pi)^4} \frac{\widetilde{p} - \widetilde{k} + mc}{(p-k)^2 - m^2c^2 + i\eta} \frac{1}{k^2 + i\eta}$$
(12.109)

using the commutation rules in Appendix (D.58). With q=-p and $s=p^2-m^2c^2$, the denominator is of the form $k^2+2kq+s$ and we can apply the formulas (G.26) and (G.27) without any further substitution (n=1). This gives with $k^0 \to q^0 = -p^0$, $k_i \to q_i y = -p_i y$, $\mathbf{\gamma} \cdot \mathbf{k} = -\gamma^i k_i \to -\mathbf{\gamma} \cdot \mathbf{p} y$, and $w=p^2y^2+(1-y)yp_0^2-(p^2-m^2c^2)y$

$$\frac{\mathrm{i}e^{2}c\ (mc)^{\epsilon}}{\epsilon_{0}} \int \frac{\mathrm{d}^{D}k}{(2\pi)^{D}} \frac{\widetilde{p} - \widetilde{k} + mc}{k^{2} + 2kq + s + \mathrm{i}\eta} \frac{1}{k^{2} + \mathrm{i}\eta}$$

$$= \frac{e^{2}c}{\epsilon_{0}\ (4\pi)^{D/2}} \int_{0}^{1} \frac{\mathrm{d}y}{\sqrt{y}} \left[\boldsymbol{y} \cdot \mathbf{p}(1 - y) + mc \right] \frac{\Gamma(\epsilon/2)}{(w/m^{2}c^{2})^{\epsilon/2}}.$$

Using (12.99), this yields the Coulomb contribution

$$K \int_0^1 \frac{\mathrm{d}y}{\sqrt{y}} \left(\boldsymbol{\gamma} \cdot \mathbf{p} \left(1 - y \right) + mc \right) \left(\Delta - \ln(yX) \right)$$

with $K = e^2 c / (\epsilon_0 (4\pi)^2)$ and $w = m^2 c^2 y X$, $X = 1 + (\mathbf{p}^2 / m^2 c^2)(1 - y)$. This leads to

$$K \int_0^1 \frac{\mathrm{d}y}{\sqrt{y}} \left((\mathbf{y} \cdot \mathbf{p} (1 - y) + mc) \left(\Delta - \ln y - \ln X \right) \right)$$

and the Coulomb part becomes (times K)

$$\left[\left(\frac{4}{3} \boldsymbol{\gamma} \cdot \mathbf{p} + 2mc \right) \Delta + \left(\frac{32}{9} \boldsymbol{\gamma} \cdot \mathbf{p} + 4mc \right) - \int_0^1 \frac{\mathrm{d}y}{\sqrt{y}} \left((\boldsymbol{\gamma} \cdot \mathbf{p} (1 - y) + mc) \ln X \right) \right]$$
(12.110)

The *Gaunt term* becomes, using (12.106) and the second term of (12.107),

$$-\frac{ie^2c}{\epsilon_0} \int \frac{d^4k}{(2\pi)^4} \frac{\gamma_i (\not p - \not k + mc) \gamma^i}{(p - k)^2 - m^2 c^2 + i\eta} \frac{1}{k^2 + i\eta}.$$
 (12.111)

The denominator is here the same as in the treatment of the self-energy in the Feynman gauge, and we can use much of the results obtained there.⁴

In analogy with (12.95), we then have

$$-\frac{ie^{2}c}{\epsilon_{0}} \int_{0}^{1} dx \int \frac{d^{4}k}{(2\pi)^{4}} \frac{\gamma_{i} (\not p - \not k + mc) \gamma^{i}}{\left[k^{2} + (p^{2} - 2pk - m^{2}c^{2})x\right]^{2}}$$

$$= -\frac{ie^{2}c}{\epsilon_{0}} \int_{0}^{1} dx \int \frac{d^{4}k}{(2\pi)^{4}} \frac{(3 - \epsilon)mc - (2 - \epsilon)(\not p - \not k) - \widetilde{p} + \widetilde{k}}{\left[k^{2} + (p^{2} - 2pk - m^{2}c^{2})x\right]^{2}}, \quad (12.112)$$

after inserting the Feynman integral (J.2) and applying the commutation rules in Appendix (D.59).

With the substitutions $k \to -q = px$ and $s = (p^2 - m^2c^2)x$, the equation above leads after applying (G.23) and (G.24) in analogy with (12.98) to

$$\begin{split} -\frac{\mathrm{i}e^2c}{\epsilon_0} \int_0^1 \mathrm{d}x \, \int \frac{\mathrm{d}^D k}{(2\pi)^D} \, \frac{(3-\epsilon)mc - (2-\epsilon)(\not p - \not k) - \widetilde{p} + \widetilde{k}}{[k^2 + 2kq + s)]^2} \\ &= \frac{e^2c}{\epsilon_0 (4\pi)^{D/2}} \int_0^1 \mathrm{d}x \left[(3-\epsilon)mc - (2-\epsilon) \not p (1-x) - \widetilde{p} (1-x) \right] \frac{\Gamma(\epsilon/2)}{(w/\epsilon)^{\epsilon/2}} \\ &= \frac{e^2c}{\epsilon_0 (4\pi)^{D/2}} \int_0^1 \mathrm{d}x \left[-(1-x) \left(3\gamma^0 p_0 - \boldsymbol{\gamma} \cdot \mathbf{p} \right) + 3mc \right. \\ &+ \epsilon \left((1-x) \not p - mc \right) \right] \frac{\Gamma(\epsilon/2)}{(w/\epsilon)^{\epsilon/2}}, \end{split}$$

⁴ We use the convention that μ , ν , ... represent all four components (0,1,2,3), while i, j, ... represent the vector part (1,2,3).

where $w = q^2 - s = p^2 x^2 - (p^2 - m^2 c^2)x = m^2 c^2 x Y$. This yields (times K)

$$-\int_0^1 dx \left\{ \left[(1-x) \left(3\gamma^0 p_0 - \boldsymbol{\gamma} \cdot \mathbf{p} \right) - 3mc \right] \left[\Delta - \ln(xY) \right] \right.$$
$$\left. -2 \left((1-x) \not p - mc \right) \right\}$$

using the relation (12.99) and the fact that $\epsilon \Delta \to 2$ as $\epsilon \to 0$. Then the *Gaunt* part becomes

$$\left[-\frac{1}{2} \left(3\gamma^{0} p_{0} - \boldsymbol{\gamma} \cdot \mathbf{p} \right) - 3mc \right] \Delta - \frac{5}{4} \gamma^{0} p_{0} - \frac{1}{4} \boldsymbol{\gamma} \cdot \mathbf{p} + mc + \int_{0}^{1} dx \left[(1 - x) \left(3\gamma^{0} p_{0} - \boldsymbol{\gamma} \cdot \mathbf{p} \right) - 3mc \right] \ln Y.$$
 (12.113)

Finally, the *scalar-retardation part* becomes similarly, using the third term of (12.107) and the commutation rules (D.57),

$$\begin{split} &-\frac{\mathrm{i}e^{2}c}{\epsilon_{0}}\int\frac{\mathrm{d}^{4}k}{(2\pi)^{4}}\,\frac{\gamma^{i}k_{i}\,(\not p-\not k+mc)\,\gamma^{j}k_{j}}{(p-k)^{2}-m^{2}c^{2}+\mathrm{i}\eta}\,\frac{1}{\pmb{k}^{2}}\,\frac{1}{k^{2}+\mathrm{i}\eta}\\ &=\frac{\mathrm{i}e^{2}c}{\epsilon_{0}}\int\frac{\mathrm{d}^{4}k}{(2\pi)^{4}}\,\frac{\gamma^{i}k_{i}\gamma^{j}k_{j}(\not p-\not k-mc)-2\gamma^{i}k_{i}(k^{j}\,p_{j}-k^{j}k_{j})}{(p-k)^{2}-m^{2}c^{2}+\mathrm{i}\eta}\,\frac{1}{\pmb{k}^{2}}\,\frac{1}{k^{2}+\mathrm{i}\eta}\\ &=-\frac{\mathrm{i}e^{2}c}{\epsilon_{0}}\int\frac{\mathrm{d}^{4}k}{(2\pi)^{4}}\,\frac{\not p-\widetilde{k}-mc+2\gamma^{i}k_{i}\,k^{j}\,p_{j}/\pmb{k}^{2}}{(p-k)^{2}-m^{2}c^{2}+\mathrm{i}\eta}\,\frac{1}{k^{2}+\mathrm{i}\eta} \end{split}$$

with $\gamma^i k_i \gamma^j k_j = -k^2 = -k_i k_i$. With the same substitutions as in the Gaunt case, this becomes

$$-\frac{ie^2c}{\epsilon_0} \int_0^1 dx \int \frac{d^Dk}{(2\pi)^D} \frac{\not p - \widetilde{k} - mc + 2\gamma^i k_i \, k^j \, p_j / k^2}{\left[k^2 - 2pkx + (p^2 - m^2c^2)x\right]^2}.$$
 (12.114)

With the substitutions $k \to -q = px$ and $s = (p^2 - m^2)x$ the first part is of the form (G.23) and (G.24) and becomes

$$\frac{e^2c}{\epsilon_0(4\pi)^{D/2}} \int_0^1 \mathrm{d}x \left[\not p - \widetilde{p} x - mc \right] \frac{\Gamma(\epsilon/2)}{w^{\epsilon/2}} \tag{12.115}$$

and with (12.99)

$$K \int_0^1 \mathrm{d}x \left[\not p - \widetilde{p} x - mc \right] \left(\Delta - \ln(xY) \right) \tag{12.116}$$

with $K = e^2c/(\epsilon_0 (4\pi)^2)$ and w being the same as in the Gaunt case, $w = q^2 - s = p^2x^2 - p^2x + m^2c^2x = m^2c^2xY$.

The second part of (12.114) is of the form (G.28) and becomes $(k_i k^j \rightarrow q_i q^j y^2 = p_i p^j x^2 y^2$ in first term, $\rightarrow -\frac{1}{2} g^i_j = -\frac{1}{2} \delta_{ij}$ in second)

$$K \int_{0}^{1} dx \int_{0}^{1} dy \sqrt{y} \left\{ 2\gamma^{i} p_{i} p^{i} p_{j} p^{j} \frac{\Gamma(1+\epsilon/2)}{w^{1+\epsilon/2}} - \gamma^{j} p_{j} \frac{\Gamma(\epsilon/2)}{w^{\epsilon/2}} \right\},$$

$$K \int_{0}^{1} dx \int_{0}^{1} dy \sqrt{y} \left\{ \frac{2\gamma^{i} p_{i} p^{j} p_{j}}{m^{2} c^{2}} \frac{xy}{Z} - \gamma^{j} p_{j} (\Delta - \ln(xyZ)) \right\},$$

$$= K \int_{0}^{1} dx \int_{0}^{1} dy \sqrt{y} \left\{ \frac{2\mathbf{y} \cdot \mathbf{p} \mathbf{p}^{2}}{m^{2} c^{2}} \frac{xy}{Z} + \mathbf{y} \cdot \mathbf{p} (\Delta - \ln(xyZ)) \right\}$$

with $w = xy \left[-\mathbf{p}^2 xy + p_0^2 x - p^2 + m^2 c^2 \right] = xy \left[\mathbf{p}^2 (1 - xy) - p_0^2 (1 - x) + m^2 c^2 \right] = m^2 c^2 Zxy$.

Integration by parts of the first term yields (times K), noting that $dZ/dy = -\mathbf{p}^2x$,

$$-\int_0^1 \mathrm{d}x \left[\sqrt{y} y \, 2\boldsymbol{\gamma} \cdot \mathbf{p} \ln Z\right]_0^1 + 3 \int_0^1 \mathrm{d}x \int_0^1 \mathrm{d}y \, \sqrt{y} \, \boldsymbol{\gamma} \cdot \mathbf{p} \ln Z.$$

The total scalar-retardation part then becomes (with Z(y = 1) = Y)

$$\int_{0}^{1} dx \left[\not p - \widetilde{p} x - mc \right] \left(\Delta - \ln(xY) \right) - \int_{0}^{1} dx \, 2 \not y \cdot \mathbf{p} \ln Y$$

$$+ 3 \int_{0}^{1} dx \int_{0}^{1} dy \, \sqrt{y} \, \not y \cdot \mathbf{p} \ln Z + \int_{0}^{1} dx \int_{0}^{1} dy \, \sqrt{y} \, \not y \cdot \mathbf{p} \left(\Delta - \ln(xyZ) \right)$$

or

$$\int_{0}^{1} dx \left(\gamma^{0} p_{0}(1-x) - \boldsymbol{\gamma} \cdot \mathbf{p}(1+x) - mc \right) \left(\Delta - \ln x \right) + \int_{0}^{1} dy \sqrt{y} \, \boldsymbol{\gamma} \cdot \mathbf{p} \, \Delta$$

$$- \int_{0}^{1} dx \left(\gamma^{0} p_{0}(1-x) - \boldsymbol{\gamma} \cdot \mathbf{p}(1-x) - mc \right) \ln Y$$

$$- \int_{0}^{1} dx \int_{0}^{1} dy \sqrt{y} \, \boldsymbol{\gamma} \cdot \mathbf{p} \ln(xy) + 2 \int_{0}^{1} dx \int_{0}^{1} dy \sqrt{y} \, \boldsymbol{\gamma} \cdot \mathbf{p} \ln(xy)$$

$$- 3 \int_{0}^{1} dx \int_{0}^{1} dy \sqrt{y} \, \boldsymbol{\gamma} \cdot \mathbf{p} \ln Z,$$

which gives⁵

$$\left(\frac{1}{2}\gamma^{0}p_{0} - \frac{5}{6}\boldsymbol{\gamma}\cdot\mathbf{p} - mc\right)\Delta + \frac{3}{4}\gamma^{0}p_{0} - \frac{5}{36}\boldsymbol{\gamma}\cdot\mathbf{p} - mc$$

$$-\int_{0}^{1} dx \left(\gamma^{0}p_{0}(1-x) - \boldsymbol{\gamma}\cdot\mathbf{p}(1-x) - mc\right) \ln Y$$

$$-3\int_{0}^{1} dx \int_{0}^{1} dy \sqrt{y} \boldsymbol{\gamma}\cdot\mathbf{p} \ln Z.$$

Summarizing all contributions yields the mass-renormalized free-electron self-energy in Coulomb gauge

$$\frac{e^2c}{\epsilon_0 (4\pi)^2} \left[-(\not p - mc) \Delta - \frac{1}{2} \gamma^0 p_0 + \frac{19}{6} \gamma \cdot \mathbf{p} - \int_0^1 \frac{\mathrm{d}y}{\sqrt{y}} (\gamma \cdot \mathbf{p} (1 - y) + mc) \ln X + 2 \int_0^1 \mathrm{d}x \left[(1 - x) \not p - mc \right] \ln Y + \int_0^1 \mathrm{d}x \int_0^1 \mathrm{d}y \sqrt{y} 2\gamma \cdot \mathbf{p} \ln Z \right],$$

(12.117)

where we have subtracted the on-shell (p = mc) value, $mc(3\Delta + 4)$. (The expressions for X, Y, Z are given in the text.) This is in agreement with the result of Adkins [1].

The treatment of the vertex correction is more complex and will not be reproduced here. Interested readers are referred to the papers by Adkins.⁶

12.6 Direct Numerical Regularization of the Bound-State Self-Energy

As an alternative to the regularization procedure discussed above, we shall consider a new more direct procedure, where the regularization is performed directly in the bound state, without any transformation to free-electron states. This is presently being tested by the Gothenburg group [12].

$$\int_0^1 dx \int_0^1 dy \sqrt{y} \ln(xy) = -\frac{10}{9}; \quad \int_0^1 dx \, x \int_0^1 dy \sqrt{y} \ln(xy) = -\frac{1}{18};$$
$$\int_0^1 dx \, x \int_0^1 dy \, y \sqrt{y} \ln(xy) = -\frac{9}{50}.$$

⁶ A complete treatment of the vertex correction is being published separately in arXiv:quant-ph.

12.6.1 Feynman Gauge

The bound-state self-energy in the Feynman gauge is from (8.48)

$$\langle r|\Sigma(\varepsilon_a)|a\rangle = \left\langle rt \left| \int \frac{c \, \mathrm{d}\kappa \, f^{\mathrm{F}}(\kappa)}{\varepsilon_a - \varepsilon_t - (c\kappa - \mathrm{i}\eta)_t} \right| ta \right\rangle,$$
 (12.118)

where $\kappa = |\mathbf{k}|$ and the function f^{F} is given by (4.55). The integral over κ is convergent, while the summation over t is (logarithmically) divergent.

With $3 - \epsilon$ dimensions of the k-vector space, we make the substitution

$$\int \frac{\mathrm{d}^3 k}{(2\pi)^3} \Rightarrow \int \mathrm{d}\Omega \int \frac{\kappa^{2-\epsilon} \,\mathrm{d}\kappa}{(2\pi)^{3-\epsilon}}$$

and the self-energy becomes

$$\langle a|\Sigma_{\epsilon}(\varepsilon_{a})|a\rangle = -\frac{e^{2}(2\pi)^{\epsilon}}{4\pi^{2}\epsilon_{0}} \left\langle at \left| \frac{\alpha_{1}^{\mu}\alpha_{2\mu}}{r_{12}} \int \frac{c \, d\kappa \, \kappa^{-\epsilon} \sin \kappa r_{12}}{\varepsilon_{a} - \varepsilon_{t} - (c\kappa - i\eta)_{t}} \right| ta, \right\rangle \quad (12.119)$$

which would make the expression convergent for $\epsilon \neq 0$. In a similar way, the the free-electron self-energy can be expressed. In analogy with the expression (12.85), this leads to the renormalized bound-state self-energy

$$\langle r | \Sigma_{\text{ren}}^{\text{bou}}(\varepsilon_{a}) | a \rangle = \lim_{\epsilon \to 0} \left(\langle r | \Sigma_{\epsilon}^{\text{bou}}(\varepsilon_{a}) - \Sigma_{\epsilon}^{\text{free}}(\varepsilon_{a}) | a \rangle + \langle r | \mathbf{p}', r' \rangle \langle \mathbf{p}', r' | \Sigma_{\epsilon}^{\text{free}}(\varepsilon_{a}) - \Sigma_{\epsilon}^{\text{free}}(\varepsilon_{p}) | \mathbf{p}, r \rangle \langle \mathbf{p}, r | a \rangle \right).$$
(12.120)

12.6.2 Coulomb Gauge

The transverse part of the self-energy expression in Coulomb gauge is in analogy with the Feynman expression (12.118)

$$\langle r | \Sigma(\varepsilon_a) | a \rangle_{\text{Trans}} = \left\langle rt \left| \int \frac{c \, d\kappa \, f_{\text{T}}^{\,\text{C}}(\kappa)}{\varepsilon_a - \varepsilon_t - (c\kappa - i\eta)_t} \right| t a \right\rangle,$$
 (12.121)

where $f_{\rm T}^{\rm C}$ is given by (4.60). The Coulomb part is given by (8.49)

$$\langle b|\Sigma(\varepsilon_a)|a\rangle_{\text{Coul}} = \frac{1}{2}\operatorname{sgn}(\varepsilon_t)\left\langle bt\left|\frac{e^2}{4\pi^2\epsilon_0 r_{12}}\int\frac{2\kappa\,\mathrm{d}\kappa\,\sin\kappa r_{12}}{\kappa^2}\right|ta\right\rangle$$
 (12.122)

and the renormalization can be performed as in the Feynman gauge.

The procedure of direct numerical regularization outlined here is presently being tested by the Gothenburg group.

References 269

References

 Adkins, G.: One-loop renormalization of Coulomb-gauge QED. Phys. Rev. D 27, 1814–20 (1983)

- Adkins, G.: One-loop vertex function in Coulomb-gauge QED. Phys. Rev. D 34, 2489–92 (1986)
- 3. Bethe, H.A.: The Electromagnetic Shift of Energy Levels. Phys. Rev. 72, 339–41 (1947)
- 4. Bjorken, J.D., Drell, S.D.: Relativistic Quantum Mechanics. Mc-Graw-Hill Pbl. Co, N.Y. (1964)
- 5. Blundell, S., Snyderman, N.J.: Basis-set approach to calculating the radiative self-energy in highly ionized atoms. Phys. Rev. A 44, R1427–30 (1991)
- 6. Brown, G.E., Langer, J.S., Schaeffer, G.W.: Lamb shift of a tightly bound electron. I. Method. Proc. R. Soc. London, Ser. A 251, 92–104 (1959)
- 7. Brown, G.E., Mayers, D.F.: Lamb shift of a tightly bound electron. II. Calculation for the K-electron in Hg. Proc. R. Soc. London, Ser. A 251, 105–109 (1959)
- 8. Cheng, K.T., Johnson, W.R.: Self-energy corrections to the K-electron binding energy in heavy and superheavy atoms. Phys. Rev. A 1, 1943–48 (1976)
- 9. Cheng, T.K., Johnson, W.R., Sapirstein, J.: Screend Lamb-shift calculations for Lithiumlike Uranium, Sodiumlike Platimun, and Copperlike Gold. Phys. Rev. Lett. 23, 2960–63 (1991)
- 10. Desiderio, A.M., Johnson, W.R.: Lamb Shift and Binding Energies of K Electrons in Heavy Atoms. Phys. Rev. A 3, 1267–75 (1971)
- 11. Heckarthon, D.: Dimensional regularization and renormalization of Coulomb gauge quantum electrodynamics. Nucl. Phys. B **156**, 328–46 (1978)
- 12. Hedendahl, D.: p. (private communication)
- 13. Itzykson, C., Zuber, J.B.: Quantum Field Theory. McGraw-Hill (1980)
- Labzowsky, L.N., Mitrushenkov, A.O.: Renormalization of the second-order electron selfenergy for a tightly bound atomic electron. Phys. Lett. A 198, 333–40 (1995)
- Lindgren, I., Persson, H., Salomonson, S., Sunnergren, P.: Analysis of the electron self-energy for tightly bound electrons. Phys. Rev. A 58, 1001–15 (1998)
- Lindgren, I., Persson, H., Salomonson, S., Ynnerman, A.: Bound-state self-energy calculation using partial-wave renormalization. Phys. Rev. A 47, R4555–58 (1993)
- 17. Mandl, F., Shaw, G.: Quantum Field Theory. John Wiley and Sons, New York (1986)
- 18. Mohr, P.J.: Numerical Evaluation of the $1s_{1/2}$ -State Radiative Level Shift. Ann. Phys. (N.Y.) **88**, 52–87 (1974)
- 19. Mohr, P.J.: Self-Energy Radiative Corrections. Ann. Phys. (N.Y.) 88, 26–51 (1974)
- 20. Mohr, P.J.: Self-energy of the n=2 states in a strong Coulomb field. Phys. Rev. A 26, 2338–54 (1982)
- Pauli, W., Willars, F.: On the Invariant Regularization in Relativistic Quantum Theory. Rev. Mod. Phys. 21, 434–44 (1949)
- Persson, H., Salomonson, S., Sunnergren, P.: Regularization Corrections to the Partial-Wave Renormalization Procedure. Presented at the conference Modern Trends in Atomic Physics, Hindås, Sweden, May, 1996. Adv. Quantum Chem. 30, 379–92 (1998)
- 23. Peskin, M.E., Schroeder, D.V.: *An introduction to Quantun Field Theory*. Addison-Wesley Publ. Co., Reading, Mass. (1995)
- 24. Quiney, H.M., Grant, I.P.: Atomic self-energy calculations using partial-wave mass renormalization. J. Phys. B 49, L299–304 (1994)
- 25. Snyderman, N.J.: *Electron Radiative Self-Energy of Highly Stripped Heavy-Atoms*. Ann. Phys. (N.Y.) **211**, 43–86 (1991)
- Sunnergren, P.: Complete One-Loop QED CAlculations for Few-Electron Ions. Ph.D. thesis, Department of Physics, Chalmers University of Technology and University of Gothenburg, Gothenburg, Sweden (1998)
- t'Hooft, G., Veltman, M.: Regularization and renormalization of gauge fields. Nucl. Phys. B 44, 189–213 (1972)

Chapter 13 Summary and Conclusions

The all-order forms of many-body perturbation theory (MBPT), like the coupled-cluster approach (CCA), have been extremely successful in calculations on atomic and in particular on molecular systems. Here, the dominating parts of the electron correlation can be evaluated to essentially all orders of perturbation theory.

A shortcoming, however, of the standard MBPT/CCA procedures is that quantum-electrodynamics (QED) can only be included in a very limited fashion (first-order energy). Particularly for highly charged systems, QED effects can be quite important. Certain experimental data on such systems are now several orders of magnitude more accurate than the best available theoretical calculation. It is believed that this shortcoming is due to the omitted <u>combination</u> of many-body and QED effects in presently available theoretical procedures.

The procedure presented in this book, which is based on quantum-field theory, describes – for the first time – a road toward a rigorous unification of QED and MBPT. The procedure is based on the *covariant evolution operator*, which describes the time evolution of the relativistic wave function or state vector. The procedure is for two-electron systems fully compatible with the relativistically covariant Bethe–Salpeter equation, but it is more versatile.

The procedure is – in contrast to the standard Bethe–Salpeter equation – applicable to a general multi-reference (quasi-degenerate) model space. It can also be combined with the coupled-cluster approach and is, in principle, applicable to systems with more than two electrons.

The covariant evolution operator contains generally singularities that can be eliminated. The regular part is referred to as the *Green's operator*, which is a generalization of the Green's-function concept.

In principle, the Green's operator – as well as the Bethe–Salpeter equation – has individual times for the particles involved. Most applications, though, use the *equal-time approximation*, where the times are equalized, to make the procedure consistent with the quantum-mechanical picture.

The Green's operator for time t=0 corresponds to the *wave operator* used in standard MBPT, and the time derivative at t=0, operating within the model space, to the many-body *effective interaction*. This connects the field-theoretical procedure with the standard MBPT.

The formalism presented here has been partially tested numerically by the Gothenburg atomic theory group, and in cases where comparison can be made with the more restricted S-matrix formulation, very good agreement is reported.

A big challenge is the renormalization of the radiative effects, which generally has to be performed using the Coulomb gauge, to take advantage of the developments in MBPT/CCA. Schemes have been developed for this process but so far not been implemented in a QED-MBPT procedure.

When the procedure is more developed, critical tests can be performed to find out to what extent the new effects will improve the agreement between theory and accurate experimental data.

Appendix A

Notations and Definitions

A.1 Four-Component Vector Notations

A four-dimensional *contravariant vector* is defined as ¹

$$x = x^{\mu} = (x^{0}, x^{1}, x^{2}, x^{3}) = (x^{0}, x) = (ct, x),$$
 (A.1)

where μ =0, 1, 2, 3 and x is the three-dimensional coordinate vector x=(x^1 , x^2 , x^3) $\equiv (x, y, z)$. The four-dimensional differential is

$$d^4x = cdt - d^3x$$
 and $d^3x = dx dy dz$.

A corresponding covariant vector is defined as

$$x_{\mu} = (x_0, x_1, x_2, x_3) = g_{\mu\nu} x^{\nu} = (x_0, -x) = (ct, -x),$$
 (A.2)

which implies that

$$x^0 = x_0$$
 $x^i = -x_i$ $(i = 1, 2, 3),$ (A.3)

 $g_{\mu\nu}$ is a *metric tensor*, which can raise the so-called *Lorentz indices* of the vector. Similarly, an analogous tensor can lower the indices

$$x^{\mu} = g^{\mu\nu} x_{\nu}. \tag{A.4}$$

These relations hold generally for four-dimensional vectors.

There are various possible choices of the metric tensors, but we shall use the following

$$g_{\mu\nu} = g^{\mu\nu} = \begin{pmatrix} 1 & 0 & 0 & 0 \\ 0 & -1 & 0 & 0 \\ 0 & 0 & -1 & 0 \\ 0 & 0 & 0 & -1 \end{pmatrix}. \tag{A.5}$$

¹ In all appendices, we display complete formulas with all fundamental constants. As before, we use the Einstein summation rule with summation over repeated indices.

I. Lindgren, *Relativistic Many-Body Theory: A New Field-Theoretical Approach*, Springer Series on Atomic, Optical, and Plasma Physics 63, DOI 10.1007/978-1-4419-8309-1, © Springer Science+Business Media, LLC 2011

The four-dimensional *scalar product* is defined as the product of a contravariant and a covariant vector:

$$ab = a^{\mu}b_{\mu} = a^{0}b_{0} - \boldsymbol{a} \cdot \boldsymbol{b}, \tag{A.6}$$

where $a \cdot b$ is the three-dimensional scalar product

$$\mathbf{a} \cdot \mathbf{b} = a_x b_x + a_y b_y + a_z b_z.$$

The *covariant* gradient operator is defined as the gradient with respect to a *contravariant* coordinate vector:

$$\partial_{\mu} = \frac{\partial}{\partial x^{\mu}} = \left(\frac{1}{c}\frac{\partial}{\partial t}, \nabla\right)$$
 (A.7)

and the contravariant gradient operator analogously

$$\partial^{\mu} = \frac{\partial}{\partial x_{\mu}} = \left(\frac{1}{c}\frac{\partial}{\partial t}, -\nabla\right),$$
 (A.8)

 ∇ is the three-dimensional gradient operator

$$\nabla = \frac{\partial}{\partial x}\,\hat{\boldsymbol{e}}_x + \frac{\partial}{\partial y}\,\hat{\boldsymbol{e}}_y + \frac{\partial}{\partial z}\,\hat{\boldsymbol{e}}_z,$$

where $(\hat{e}_x, \hat{e}_y, \hat{e}_z)$ are unit vectors in the coordinate directions.

The four-dimensional divergence is defined as

$$\partial_{\mu}A^{\mu} = \frac{1}{c} \frac{\partial A^{0}}{\partial t} + \nabla \cdot A = \nabla A, \tag{A.9}$$

where $\nabla \cdot A$ is the three-dimensional divergence

$$\nabla \cdot A = \frac{\partial A_x}{\partial x} + \frac{\partial A_y}{\partial y} + \frac{\partial A_z}{\partial z}.$$

The d'Alembertian operator is defined as

$$\Box = \partial^{\mu} \partial_{\mu} = \frac{1}{c^2} \frac{\partial^2}{\partial t^2} - \nabla^2 = \nabla^2, \tag{A.10}$$

where

$$\nabla^2 = \Delta = \frac{\partial^2}{\partial x^2} + \frac{\partial^2}{\partial y^2} + \frac{\partial^2}{\partial z^2}$$

is the Laplacian operator.

A.2 Vector Spaces 275

A.2 Vector Spaces

A.2.1 Notations

 X, Y, \ldots are sets with elements x, y, \ldots

 $x \in X$ means that x is an element in the set X.

N is the set of nonnegative integers. R is the set of real numbers. C is the set of complex numbers.

 \mathbb{R}^n is the set of real *n*-dimensional vectors. \mathbb{C}^n is the set of complex *n*-dimensional vectors.

 $A \subset X$ means that A is a subset of X.

 $A \cup B$ is the *union* of A and B. $A \cap B$ is the intersection of A and B.

 $A = \{x \in X : P\}$ means that A is the set of all elements x in X that satisfy the condition P.

 $f: X \to Y$ represents a function or operator, which means that f maps uniquely the elements of X onto elements of Y.

A *functional* is a unique mapping $f: X \to R$ (C) of a function space on the space of real (complex) numbers.

The set of arguments $x \in A$ for which the function $f : A \to B$ is defined is the *domain*, and the set of results $y \in B$ which can be produced is the *range*.

(a,b) is the open interval $\{x \in \mathbf{R} : a < x < b\}$. [a,b] is the closed interval $\{x \in \mathbf{R} : a \le x \le b\}$.

sup represents the *supremum*, the least upper bound of a set *inf* represents the *infimum*, the largest lower bound of a set.

A.2.2 Basic Definitions

A real (complex) *vector space* or function space X is an infinite set of elements, x, referred to as *points* or *vectors*, which is *closed* under addition, $x + y = z \in X$, and under multiplication by a real (complex) number c, $cx = y \in X$. The continuous functions f(x) on the interval $x \in [a, b]$ form a vector space, also with some boundary conditions, like f(a) = f(b) = 0.

A subset of X is a *subspace* of X if it fulfills the criteria for a vector space. A *norm* of a vector space X is a function $p: X \to [0, \infty]$ with the properties

- (1) $p(\lambda x) = |\lambda| p(x)$
- (2) $p(x + y) \le p(x) + p(y)$ for all real λ ($\lambda \in \mathbf{R}$) and all $x, y \in X$
- (3) that p(x) = 0 always implies x = 0

The norm is written as p(x) = ||x||. We then have $||\lambda x|| = |\lambda| ||x||$, $||x + y|| \le ||x|| + ||y||$, and $||x|| = 0 \Rightarrow x = 0$. If the last condition is not fulfilled, it is a *seminorm*.

A vector space with a norm for all its elements is a *normed space*, denoted by $(X, ||\cdot||)$. The continuous functions, f(x), on the interval [a, b] form a normed space by defining a norm, for instance, $||f|| = [\int_a^b dt |f(t)|^2]^{1/2}$. By means of the Cauchy–Schwartz inequality, it can be shown that this satisfies the criteria for a norm [4, p. 93].

If f is a function $f:A\to Y$ and $A\subset X$, then f is defined in the *neighborhood* of $x_0\in X$, if there is an $\epsilon>0$ such that the entire sphere $\{x\in X: ||x-x_0||<\epsilon\}$ belongs to A [4, p. 309].

A function/operator $f: X \to Y$ is bounded, if there exists a number C such that

$$\sup_{0 \neq x \in X} \left\lceil \frac{||fx||}{||x||} \right\rceil = C < \infty.$$

Then C = ||f|| is the *norm* of f. Thus, $||fx|| \le ||f|| ||x||$.

A function f is *continuous* at the point $x_0 \in X$, if for every $\delta > 0$ there exists an $\epsilon > 0$ such that for every member of the set $x : ||x - x_0|| < \epsilon$ we have $||fx - fx_0|| \le \delta$ [4, p. 139]. This can also be expressed so that f is continuous at the point x_0 , if and only if $fx \to fx_0$ whenever $x_n \to x_0$, $\{x_n\}$ being a sequence in X, meaning that fx_n converges to fx_0 , if fx_n converges to fx_n converges to fx_n .

A linear function/operator is continuous if and only if it is bounded [4, p. 197, 213], [2, p. 22].

A functional $f: X \to \mathbf{R}$ is *convex* if

$$f(tx + (t-1)y) < tf(x) + (t-1)f(y),$$

for all $x, y \in X$ and $t \in (0, 1)$.

A subset $A \subset X$ is *open*, if for every $x \in A$ there exists an $\epsilon > 0$ such that the entire ball $B_r(x) = \{y \in X | ||y - x|| < \epsilon\}$ belongs to A, i.e., $B_r(x) \subset A$ [1, p. 363], [4, p. 98], [5, p. 57].

A sequence $\{x_n\}$, where n is an integer $(n \in \mathbb{N})$, is an infinite numbered list of elements in a set or a space. A subsequence is a sequence, which is a part of a sequence.

A sequence $\{x_n \in A\}$ is (strongly) *convergent* toward $x \in A$, if and only if for every $\epsilon > 0$ there exists an N such that $||x_n - x|| < \epsilon$ for all n > N [4, p. 95, 348].

A sequence is called a *Cauchy sequence* if and only if for every $\epsilon > 0$ there exists an N such that $||x_n - x_m|| < \epsilon$ for all m, n > N. If a sequence $\{x_n\}$ is convergent, then it follows that for n, m > N

$$||x_m - x_n|| = ||(x_n - x) + (x - x_m)|| \le ||x_n - x|| + ||x_m - x|| < 2\epsilon$$

which means that a convergent sequence is always a Cauchy sequence. The opposite is not necessarily true, since the point of convergence need not be an element of X [3, p. 44].

A subset A of a normed space is termed *compact*, if every infinite sequence of elements in A has a subsequence, which converges to an element in A. The closed interval [0,1] is an example of a compact set, while the open interval (0,1) is noncompact, since the sequence 1, 1/2, 1/3... and all of its subsequences converge to 0, which lies outside the set [5, p. 149]. This sequence satisfies the Cauchy convergence criteria but not the (strong) convergence criteria.

A *dual space* or *adjoint space* of a vector space X, denoted as X^* , is the space of all functions on X.

An *inner or scalar product* in a vector space X is a function $\langle \cdot, \cdot \rangle : X \times X \to \mathbf{R}$ with the properties (1)

$$\langle x, \lambda_1 y_1 + \lambda_2 y_2 \rangle = \lambda_1 \langle x, y_1 \rangle + \lambda_2 \langle x, y_2 \rangle, \quad \langle x, y \rangle = \langle y, x \rangle,$$

for all $x, y, y_1, y_2 \in X$ and all $\lambda_j \in \mathbf{R}$, and (2) $\langle x, x \rangle = 0$ only if x = 0.

A.2.3 Special Spaces

A.2.3.1 Banach Space

A *Banach space* is a normed space in which every Cauchy sequence converges to a point in the space.

A.2.3.2 Hilbert Space

A Banach space with the norm $||x|| = +\sqrt{\langle x, x \rangle}$ is called a *Hilbert space* [1, p. 364].

A.2.3.3 Fock Space

A Fock space is a *Hilbert space*, where the number of particles is variable or unknown.

A.3 Special Functions

A.3.1 Dirac Delta Function

We consider the integral

$$\int_{-L/2}^{L/2} \mathrm{d}x \,\mathrm{e}^{\mathrm{i}kx}.\tag{A.11}$$

Assuming *periodic boundary conditions*, $e^{-iLx/2} = e^{iLx/2}$, limits the possible k values to $k = k_n = 2\pi n/L$. Then

$$\frac{1}{L} \int_{-L/2}^{L/2} dx \, e^{ik_n x} = \delta_{k_n,0} = \delta(k_n,0), \tag{A.12}$$

where $\delta_{n,m}$ is the Kronecker delta factor

$$\delta_{n,m} = \begin{cases} 1 & \text{if } m = n \\ 0 & \text{if } m \neq n \end{cases}$$
 (A.13)

If we let $L \to \infty$, then we have to add a "damping factor" $e^{-\gamma |x|}$, where γ is a small positive number, to make the integral meaningful,

$$\int_{-\infty}^{\infty} dx \, e^{ikx} \, e^{-\gamma |x|} = \frac{2\gamma}{k^2 + \gamma^2} = 2\pi \, \Delta_{\gamma}(k). \tag{A.14}$$

In the limit $\gamma \to 0$, we have

$$\lim_{\gamma \to 0} \Delta_{\gamma}(k) = \frac{1}{2\pi} \lim_{\gamma \to 0} \int_{-\infty}^{\infty} dx \, e^{ikx} \, e^{-\gamma|x|} = \delta(k), \tag{A.15}$$

which can be regarded as a definition of the *Dirac delta function*, $\delta(k)$. Formally, we write this relation as

$$\int_{-\infty}^{\infty} \frac{\mathrm{d}x}{2\pi} \,\mathrm{e}^{\mathrm{i}kx} = \delta(k). \tag{A.16}$$

The Δ function also has the following properties

$$\lim_{\gamma \to 0} \pi \gamma \, \Delta_{\gamma}(x) = \delta_{x,0},$$

$$\int_{-\infty}^{\infty} dx \, \Delta_{\gamma}(x - a) \Delta_{\eta}(x - b) = \Delta_{\gamma + \eta}(a - b). \tag{A.17}$$

In three dimensions, (A.12) goes over into

$$\frac{1}{V} \int_{V} d^{3}x \, e^{ik_{n} \cdot x} = \delta^{3}(k_{n}, 0) = \delta(k_{nx}, 0) \, \delta(k_{ny}, 0) \, \delta(k_{nz}, 0). \tag{A.18}$$

In the limit where the integration is extended over the entire three-dimensional space, we have in analogy with (A.16)

$$\int \frac{\mathrm{d}^3 x}{(2\pi)^3} \,\mathrm{e}^{\mathrm{i}k \cdot x} = \delta^3(k). \tag{A.19}$$

A.3 Special Functions 279

A.3.2 Integrals over Δ Functions

We consider the integral

$$\int_{-\infty}^{\infty} dx \, \delta(x-a) \, f(x) = \lim_{\gamma \to 0} \int_{-\infty}^{\infty} dx \, \Delta_{\gamma}(x-a) \, f(x)$$
$$= \frac{1}{2\pi} \lim_{\gamma \to 0} \int_{-\infty}^{\infty} dx \, \frac{2\gamma}{(x-a)^2 + \gamma^2} \, f(x). \quad (A.20)$$

The integral can be evaluated using residue calculus and leads to

$$\int_{-\infty}^{\infty} dx \, \delta(x - a) \, f(x) = f(a)$$
(A.21a)

provided the function f(x) has no poles. In three dimensions, we have similarly

$$\int d^3x \, \delta(x - x_0) \, f(x) = f(x_0) \tag{A.21b}$$

integrated over all space.

The relations above are often taken as the definition of the Dirac delta function, but the procedure applied here is more rigorous.

Next, we consider the integral over $two \Delta$ functions

$$\int dx \, \Delta_{\gamma}(x-a) \, \Delta_{\eta}(x-b) = \frac{1}{(2\pi)^2} \int dx \, \frac{2\gamma}{(x-a)^2 + \gamma^2} \, \frac{2\eta}{(x-b)^2 + \eta^2}$$

$$= \frac{1}{4\pi^2 i} \int dx \left[\frac{1}{x-a-i\gamma} - \frac{1}{x-a+i\gamma} \right]$$

$$\times \frac{2\eta}{(x-b+i\eta)(x-b-i\eta)}$$

$$= \frac{1}{2\pi i} \left[\frac{1}{b-a-i(\gamma+\eta)} - \frac{1}{b-a+i(\gamma+\eta)} \right]$$

$$= \frac{1}{2\pi} \frac{2(\gamma+\eta)}{(a-b)^2 + (\gamma+\eta)^2}$$
(A.22)

after integrating the first term over the negative and the second term over the positive half plane. Thus,

$$\int dx \, \Delta_{\gamma}(x-a) \, \Delta_{\eta}(x-b) = \Delta_{\gamma+\eta}(a-b)$$
(A.23)

and we see that here the widths of the Δ functions are added.

Now, we consider some integrals with the Δ functions in combination with electron and photon propagators that are frequently used in the main text.

First, we consider the integral with one Δ function and an *electron* propagator (4.10)

$$\int d\omega \frac{1}{\omega - \varepsilon_j + i\eta} \Delta_{\gamma}(\varepsilon_a - \omega) = \int \frac{d\omega}{2\pi} \frac{1}{\omega - \varepsilon_j + i\eta} \frac{2\gamma}{(\varepsilon_a - \omega)^2 + \gamma^2}$$
$$= \int \frac{d\omega}{2\pi} \frac{1}{\omega - \varepsilon_j + i\eta} \frac{2\gamma}{(\varepsilon_a - \omega + i\gamma)(\varepsilon_a - \omega - i\gamma)}.$$

The pole of the propagator yields the contribution $\Delta_{\gamma}(\varepsilon_a - \varepsilon_j)$, which vanishes in the limit $\gamma \to 0$, if $\varepsilon_a \neq \varepsilon_j$. Nevertheless, we shall see that this pole has a significant effect on the result.

Integrating above over the *positive* half plane, with the single pole $\varepsilon_a + i\gamma$, yields

$$\frac{1}{\varepsilon_a - \varepsilon_j + i\gamma + i\eta}$$

and integrating over the *negative* half plane, with the two poles $\varepsilon_j - i\eta$, $\varepsilon_a - i\gamma$, yields

$$-\frac{2i\gamma}{(\varepsilon_a - \varepsilon_j + i\gamma + i\eta)(\varepsilon_a - \varepsilon_j - i\gamma + i\eta)} + \frac{1}{\varepsilon_a - \varepsilon_j - i\gamma + i\eta}$$

$$= \frac{1}{\varepsilon_a - \varepsilon_j + i\gamma + i\eta},$$

which is identical to the previous result. We observe here that the pole of the propagator, which has a vanishing contribution in the limit $\gamma \to 0$, has the effect of reversing the sign of the iy term.

The γ parameter originates from the adiabatic damping and is small but finite, while the η parameter is infinitely small and only determines the position of the pole of the propagator. Therefore, if they appear together, the γ term dominates, and the η term can be omitted. This yields

$$\int d\omega \, \frac{1}{\omega - \varepsilon_j + i\eta} \, \Delta_{\gamma}(\varepsilon_a - \omega) = \frac{1}{\varepsilon_a - \varepsilon_j + i\gamma}$$
 (A.24)

noting that the η parameter of the propagator is replaced by the damping parameter γ .

Second, we consider the integral with the *photon* propagator (4.31)

$$\int d\omega \frac{1}{\omega^2 - \kappa^2 + i\eta} \Delta_{\gamma}(\varepsilon_a - \omega) = \frac{1}{2\kappa} \int \frac{d\omega}{2\pi} \left[\frac{1}{\omega - \kappa + i\eta} - \frac{1}{\omega + \kappa - i\eta} \right] \times \frac{2\gamma}{(\varepsilon_a - \omega + i\gamma)(\varepsilon_a - \omega - i\gamma)}$$

$$= \frac{1}{2\kappa} \left[\frac{1}{\varepsilon_a + i\gamma - \kappa + i\eta} - \frac{1}{\varepsilon_a - i\gamma + \kappa - i\eta} \right]$$
$$= \frac{1}{\varepsilon_a^2 - (\kappa - i\gamma - i\eta)^2}$$
(A.25)

or, neglecting the η term,

$$\int d\omega \, \frac{1}{\omega^2 - \kappa^2 + i\eta} \, \Delta_{\gamma}(\varepsilon_a - \omega) = \frac{1}{\varepsilon_a^2 - \kappa^2 + i\gamma}$$
 (A.26)

noting that $\kappa \geq 0$.

Finally, we consider the integrals of $two \Delta$ functions and the propagators. With the electron propagator, we have

$$\int d\omega \, \frac{1}{\omega - \varepsilon_j + i\eta} \, \Delta_{\gamma}(\varepsilon_a - \omega) \, \Delta_{\gamma}(\varepsilon_b - \omega)$$

$$= \frac{1}{(2\pi i)^2} \int d\omega \, \frac{1}{\omega - \varepsilon_j + i\eta} \left[\frac{1}{\varepsilon_a - \omega - i\gamma} - \frac{1}{\varepsilon_a - \omega + i\gamma} \right]$$

$$\times \left[\frac{1}{\varepsilon_b - \omega - i\gamma} - \frac{1}{\varepsilon_b - \omega + i\gamma} \right].$$

Here, three of the combinations with poles on both sides of the real axis contribute, which yields

$$\frac{1}{2\pi i} \left[\frac{1}{(\varepsilon_b - \varepsilon_j + i\gamma)(\varepsilon_a - \varepsilon_b - 2i\gamma)} + \frac{1}{(\varepsilon_a - \varepsilon_j + i\gamma)(\varepsilon_b - \varepsilon_a - 2i\gamma)} - \frac{1}{(\varepsilon_a - \varepsilon_j + i\gamma)(\varepsilon_b - \varepsilon_j + i\gamma)} \right].$$

The last two terms become

$$\frac{1}{\varepsilon_{a} - \varepsilon_{j} + i\gamma} \left[\frac{1}{\varepsilon_{b} - \varepsilon_{a} - 2i\gamma} - \frac{1}{\varepsilon_{b} - \varepsilon_{j} + i\gamma} \right] \approx \frac{1}{(\varepsilon_{b} - \varepsilon_{a} - 2i\gamma)(\varepsilon_{b} - \varepsilon_{j} + i\gamma)}$$

neglecting an imaginary term in the numerator. This leads to

$$\int d\omega \, \frac{1}{\omega - \varepsilon_j + i\eta} \, \Delta_{\gamma}(\varepsilon_a - \omega) \, \Delta_{\gamma}(\varepsilon_b - \omega) \approx \frac{1}{\varepsilon_a - \varepsilon_j + i\gamma} \, \Delta_{2\gamma}(\varepsilon_a - \varepsilon_b).$$
(A.27)

Similarly, we find for the photon propagator

$$\boxed{\int d\omega \, \frac{1}{\omega^2 - \kappa^2 + i\eta} \, \Delta_{\gamma}(\varepsilon_a - \omega) \, \Delta_{\gamma}(\varepsilon_b - \omega) \approx \frac{1}{\varepsilon_a - \kappa^2 + i\gamma} \, \Delta_{2\gamma}(\varepsilon_a - \varepsilon_b).}$$
(A.28)

Formally, we can obtain the integral with propagators by replacing the Δ function by the corresponding Dirac delta function, noting that we then have to replace the imaginary parameter η in the denominator by the damping factor γ .

A.3.3 The Heaviside Step Function

The Heaviside step function is defined as

$$\Theta(t) = 1 \quad t' > t$$

$$= 0 \quad t' < t. \tag{A.29}$$

The step function can also be given the integral representation

$$\Theta(t) = \lim_{\epsilon \to 0} i \int_{-\infty}^{\infty} \frac{d\omega}{2\pi} \frac{e^{-i\omega t}}{\omega + i\epsilon}$$
(A.30)

from which we obtain the derivative of the step function

$$\frac{d\Theta(t)}{dt} = \lim_{\epsilon \to 0} \int_{-\infty}^{\infty} \frac{d\omega}{2\pi} \frac{\omega}{\omega + i\epsilon} e^{-i\omega t} = \delta(t)$$
 (A.31)

where $\delta(t)$ is the Dirac delta function.

References

- 1. Blanchard, P., Brüning, E.: *Variational Methods in Mathematical Physics. A Unified Approach*. Springer-Verlag, Berlin (1992)
- Debnath, L., Mikusiński, P.: Introduction to Hilbert Spaces with Applications., second edn. Academic Press, New York (1999)
- 3. Delves, L.M., Welsh, J.: *Numerical Solution of Integral Equations*. Clarendon Press, Oxford (1974)
- 4. Griffel, D.H.: Applied Functional Analysis. Wiley, N.Y. (1981)
- 5. Taylor, A.E.: Introduction to Functional Analysis. Wiley and Sons (1957)

Appendix B Second Quantization

B.1 Definitions

(See, for instance [2, Chap. 5], [1, Chap. 11].) In second quantization – also known as the number representation – a state is represented by a vector (see Appendix C.1) $|n_1, n_2, \dots\rangle$, where the numbers represent the number of particles in the particular basis state (which for fermions can be equal only to one or zero).

Second quantization is based on *annihilation/creation operators* c_j/c_j^{\dagger} , which annihilate and create, respectively, a single particle. If we denote by $|0\rangle$ the vacuum state with no particle, then

$$c_{j}^{\dagger}|0\rangle = |j\rangle$$
 (B.1)

represents a single-particle state. In the coordinate representation (C.19), this corresponds to the wave function

$$\phi_j(\mathbf{x}) = \langle \mathbf{x}|j\rangle \tag{B.2}$$

satisfying the single-electron Schrödinger or Dirac equation. Obviously, we have

$$c_j|0\rangle = 0. (B.3)$$

For fermions, the operators satisfy the anticommutation relations

$$\begin{aligned} &\{c_i^{\dagger}, c_j^{\dagger}\} = c_i^{\dagger} c_j^{\dagger} + c_j^{\dagger} c_i^{\dagger} = 0, \\ &\{c_i, c_j\} = c_i c_j + c_j c_i = 0, \\ &\{c_i^{\dagger}, c_j\} = c_i^{\dagger} c_j + c_j c_i^{\dagger} = \delta_{ij}, \end{aligned}$$
(B.4)

where δ_{ij} is the Kronecker delta factor (A.13). It then follows that

$$c_i^{\dagger} c_j^{\dagger} |0\rangle = -c_j^{\dagger} c_i^{\dagger} |0\rangle , \qquad (B.5)$$

which means that $c_i^{\dagger} c_i^{\dagger} | 0 \rangle$ represents an *antisymmetric* two-particle state, which we denote in the following way¹

$$c_i^{\dagger} c_j^{\dagger} |0\rangle = |\{i, j\}\rangle.$$
 (B.6)

The antisymmetric form is required for fermions by the quantum-mechanical rules. A corresponding bra state is

$$\langle 0|c_l c_k = \langle \{k, l\}| \tag{B.7}$$

and it then follows that the states are orthonormal.

In the coordinate representation, the state above becomes

$$\langle x_1 x_2 | \{i, j\} \rangle = \frac{1}{\sqrt{2}} \left[\phi_i(x_1) \phi_j(x_2) - \phi_j(x_1) \phi_i(x_2) \right].$$
 (B.8)

Generalizing this to a general many-particle system leads to an antisymmetric product, known as the *Slater determinant*,

$$\langle \mathbf{x}_{1}, \mathbf{x}_{2}, \cdots \mathbf{x}_{N} | c_{a}^{\dagger} c_{b}^{\dagger} \cdots c_{N}^{\dagger} | 0 \rangle = \frac{1}{\sqrt{N!}} \operatorname{Det}\{a, b, \cdots N\}$$

$$= \frac{1}{\sqrt{N!}} \begin{vmatrix} \phi_{1}(\mathbf{x}_{1}) & \phi_{1}(\mathbf{x}_{2}) \cdots \phi_{1}(\mathbf{x}_{N}) \\ \phi_{2}(\mathbf{x}_{1}) & \phi_{2}(\mathbf{x}_{2}) \cdots \phi_{2}(\mathbf{x}_{N}) \\ \cdots & \cdots \\ \phi_{N}(\mathbf{x}_{1}) & \phi_{N}(\mathbf{x}_{2}) \cdots \phi_{N}(\mathbf{x}_{N}) \end{vmatrix} . \quad (B.9)$$

For an N-particle system, we define one- and two-particle operators by

$$F = \sum_{n=1}^{n} f_n, \tag{B.10}$$

$$G = \sum_{m < n=1}^{n} g_{mn}, \tag{B.11}$$

respectively, where the f_n and the g_{mn} operators are identical, differing only in the particles they operate on. In second quantization these operators can be expressed (see, for instance [1, Sect. 11.1])²

¹ We shall follow the convention of letting the notation $|i,j\rangle$ denote a straight product function $|i,j\rangle = \phi_i(x_1)\phi_j(x_2)$, while $|\{i,j\}\rangle$ represents an antisymmetric function.

² Occasionally, we use a "hat" on the operators to emphasize their second-quantized form. We also use the Einstein summation rule with summation over all indices that appear twice. Note the order between the annihilation operators.

B.1 Definitions 285

$$\hat{F} = c_i^{\dagger} \langle i | f | j \rangle c_j,$$

$$\hat{G} = \frac{1}{2} c_i^{\dagger} c_j^{\dagger} \langle i j | g | k l \rangle c_l c_k,$$
(B.12)

etc. (note order between the operators in the two-particle case). Here,

$$\langle i|f|j\rangle = \int d^3x_1 \,\phi_i^*(x_1) \,f \,\phi_j(x_1),$$

$$\langle ij|g|kl\rangle = \iint d^3x_1 \,d^3x_2 \,\phi_i^*(x_1)\phi_j^*(x_2) \,g \,\phi_k(x_1)\phi_l(x_2). \tag{B.13}$$

We can check the formulas above by evaluating

$$\langle \{cd\} | \hat{G} | \{ab\} \rangle = \langle \{cd\} | \frac{1}{2} c_i^{\dagger} c_j^{\dagger} \langle ij | g | kl \rangle c_l c_k | \{ab\} \rangle$$

$$= \frac{1}{2} \langle 0 | c_d c_c c_i^{\dagger} c_j^{\dagger} \langle ij | g | kl \rangle c_l c_k c_a^{\dagger} c_b^{\dagger} | 0 \rangle. \tag{B.14}$$

Normal-ordering the operators yields

$$c_l c_k c_a^{\dagger} c_b^{\dagger} |0\rangle = \delta_{k,a} \delta_{l,b} - \delta_{l,a} \delta_{k,b}$$

and similarly

$$\langle 0|c_d c_c c_i^{\dagger} c_j^{\dagger} = \delta_{i,d} \delta_{j,c} - \delta_{j,c} \delta_{i,d}.$$

Then we have

$$\langle \{cd\} | \hat{G} | \{ab\} \rangle = \langle cd | g | ab \rangle - \langle dc | g | ab \rangle$$

which agrees with the results using determinantal wave functions (see, for instance [1, Eq. 5.19])

$$\langle \{cd\}|\hat{G}|\{ab\}\rangle = \frac{1}{2} \langle cd - dc|\hat{G}|ab - ba\rangle. \tag{B.15}$$

We define the *electron-field operators* in the *Schrödinger representation* (3.1) by

$$\hat{\psi}_{S}(\mathbf{x}) = c_{j} \,\phi_{j}(\mathbf{x}); \quad \hat{\psi}_{S}^{\dagger}(\mathbf{x}) = c_{j}^{\dagger} \,\phi_{j}^{*}(\mathbf{x}). \tag{B.16}$$

Then, the second-quantized one-body operator can be expressed as

$$\hat{F} = \int d^3x \, c_i^{\dagger} \phi_i^*(x) \, f \, c_j \phi_j(x) = \int d^3x \, \hat{\psi}_S^{\dagger}(x) \, f \, \hat{\psi}_S(x)$$
 (B.17)

and similarly

$$\hat{G} = \frac{1}{2} \iint d^3 \mathbf{x}_1 d^3 \mathbf{x}_2 \, \hat{\psi}_S^{\dagger}(x_1)_S^{\dagger}(x_2) \, g \, \hat{\psi}_S(x_2) \hat{\psi}_S(x_1). \tag{B.18}$$

The nonrelativistic Hamiltonian for an N-electron system (2.11) consists of a single-particle and a two-particle operator

$$H_{1} = \sum_{n=1}^{N} \left(-\frac{\hbar^{2}}{2m} \nabla_{n}^{2} + v_{\text{ext}}(\boldsymbol{x}_{n}) \right) = \sum_{n=1}^{N} h_{1}(n),$$

$$H_{2} = \sum_{m < n}^{N} \frac{e^{2}}{4\pi \epsilon_{0} r_{mn}} = \sum_{m < n}^{N} h_{2}(m, n),$$
(B.19)

and in second quantization this can be expressed as

$$\hat{H} = \int d^3 x_1 \, \hat{\psi}_S^{\dagger}(x_1) \, h_1 \, \hat{\psi}_S(x_1)$$

$$+ \frac{1}{2} \iint d^3 x_1 \, d^3 x_2 \, \hat{\psi}_S^{\dagger}(x_1) \, \hat{\psi}_S^{\dagger}(x_2) \, h_2 \, \hat{\psi}_S(x_2) \, \hat{\psi}_S(x_1).$$
 (B.20)

B.2 Heisenberg and Interaction Pictures

In an alternative to the Schrödinger picture, the *Heisenberg picture* (HP), the states are time independent and the time dependence is transferred to the operators,

$$|\Psi_{\rm H}\rangle = |\Psi_{\rm S}(t=0)\rangle = \mathrm{e}^{\mathrm{i}\hat{H}t/\hbar}|\Psi_{\rm S}(t)\rangle \; ; \qquad \hat{O}_{\rm H} = \mathrm{e}^{\mathrm{i}\hat{H}t/\hbar}\hat{O}_{\rm S}\,\mathrm{e}^{-\mathrm{i}\hat{H}t/\hbar}.$$
 (B.21)

In perturbation theory, the Hamiltonian is normally partitioned into a zeroth-order Hamiltonian H_0 and a perturbation V (2.48), which using second-quantized notations becomes

$$\hat{H} = \hat{H}_0 + \hat{V}. \tag{B.22}$$

We can then define an intermediate picture, known as the *interaction picture* (IP), where the operators and state vectors are related to those in the Schrödinger picture by

$$|\Psi_{\rm I}(t)\rangle = {\rm e}^{{\rm i}\hat{H}_0 t/\hbar} |\Psi_{\rm S}(t)\rangle; \qquad \hat{O}_{\rm I}(t) = {\rm e}^{{\rm i}\hat{H}_0 t/\hbar} \,\hat{O}_{\rm S} \, {\rm e}^{-{\rm i}\hat{H}_0 t/\hbar}.$$
 (B.23)

The relation between the Heisenberg and the interaction pictures is³

$$|\Psi_{\rm H}\rangle = \mathrm{e}^{\mathrm{i}\hat{H}t/\hbar}\mathrm{e}^{-\mathrm{i}\hat{H}_0t/\hbar}|\Psi_{\rm I}(t)\rangle; \qquad \hat{O}_{\rm H}(t) = \mathrm{e}^{\mathrm{i}\hat{H}t/\hbar}\mathrm{e}^{-\mathrm{i}\hat{H}_0t/\hbar}\;\hat{O}_{\rm I}\,\mathrm{e}^{\mathrm{i}\hat{H}_0t/\hbar}\mathrm{e}^{-\mathrm{i}\hat{H}t/\hbar}. \tag{B.24}$$

Using the relation (3.9), we then have

$$|\Psi_{\rm H}\rangle = U(0,t)|\Psi_{\rm I}(t)\rangle; \qquad \hat{O}_{\rm H}(t) = U(0,t)\,\hat{O}_{\rm I}\,U(t,0).$$
 (B.25)

³ Note that \hat{H} and \hat{H}_0 generally do not commute, so that in general $e^{i\hat{H}t/\hbar}e^{-i\hat{H}_0t/\hbar} \neq e^{i\hat{V}t/\hbar}$.

References 287

The state vector of time-independent perturbation theory corresponds in all pictures considered here to the time-dependent state vectors with t = 0,

$$|\Psi\rangle = |\Psi_{\rm H}\rangle = |\Psi_{\rm S}(0\rangle) = |\Psi_{\rm I}(0)\rangle.$$
 (B.26)

In the Heisenberg picture (B.21), the electron-field operators (B.16) become

$$\hat{\psi}_{\mathrm{H}}(x) = \mathrm{e}^{\mathrm{i}\hat{H}t/\hbar}\,\hat{\psi}_{\mathrm{S}}(x)\,\mathrm{e}^{-\mathrm{i}\hat{H}t/\hbar}\,;\qquad \hat{\psi}_{\mathrm{H}}^{\dagger}(x) = \mathrm{e}^{\mathrm{i}\hat{H}t/\hbar}\,\hat{\psi}_{\mathrm{S}}^{\dagger}(x)\,\mathrm{e}^{-\mathrm{i}\hat{H}t/\hbar} \tag{B.27}$$

and in the interaction picture (IP) (B.23)

$$\hat{\psi}_{I}(x) = e^{i\hat{H}_{0}t/\hbar}\hat{\psi}_{S}(x) e^{-i\hat{H}_{0}t/\hbar} = e^{i\hat{H}_{0}t/\hbar}c_{j} \phi_{j}(x) e^{-i\hat{H}_{0}t/\hbar}
= c_{j} \phi_{j}(x) e^{-i\varepsilon_{j}t/\hbar} = c_{j} \phi_{j}(x)
\hat{\psi}_{I}^{\dagger}(x) = c_{j}^{\dagger} \phi_{j}^{*}(x) e^{i\varepsilon_{j}t/\hbar} = c_{j}^{\dagger} \phi_{j}^{*}(x),$$
(B.28)

where $\phi_j(x)$ is an eigenfunction of H_0 . We also introduce the *time-dependent* creation/annihilations operators in the IP by

$$c_j(t) = c_j e^{-i\varepsilon_j t/\hbar}; \qquad c_j^{\dagger}(t/\hbar) = c_j^{\dagger} e^{i\varepsilon_j t/\hbar},$$
 (B.29)

which gives

$$\hat{\psi}_{\rm I}(x) = c_j(t) \, \phi_j(x) \,; \qquad \hat{\psi}_{\rm I}^{\dagger}(x) = c_j^{\dagger}(t) \, \phi_j^*(x).$$
 (B.30)

From the definition (B.23), we have

$$\frac{\partial}{\partial t}\,\hat{O}_{\mathrm{I}}(t) = \frac{\partial}{\partial t}\left[\mathrm{e}^{\mathrm{i}\hat{H}_{0}t/\hbar}\,\hat{O}_{\mathrm{S}}\,\mathrm{e}^{-\mathrm{i}\hat{H}_{0}t/\hbar}\right] = \mathrm{i}\left[H_{0},\,\hat{O}_{\mathrm{I}}(t)\right].\tag{B.31}$$

References

- 1. Lindgren, I., Morrison, J.: *Atomic Many-Body Theory*. Second edition, Springer-Verlag, Berlin (1986, reprinted 2009)
- 2. Schweber, S.S.: An Introduction to Relativistic Quantum Field Theory. Harper and Row, N.Y. (1961)

Appendix C

Representations of States and Operators

C.1 Vector Representation of States

A state of a system can be represented by the wave function or Schrödinger function $\Psi(x)$, where x stands for all (space) coordinates. If we have a complete basis set available in the same Hilbert space (see Appendix A.2), $\{\phi_j(x)\}$, then we can expand the function as

$$\Psi(x) = a_j \phi_j(x) \tag{C.1}$$

with summation over *j* according to the Einstein summation rule. If the basis set is *orthonormal*, implying that the *scalar or inner product* satisfies the relation

$$\langle i|j\rangle = \int dx \,\phi_i^* \,\phi_j(x) = \delta_{i,j},$$
 (C.2)

then the expansion coefficients are given by the scalar product

$$a_{j} = \int dx \, \phi_{j}^{*} \Psi(x) = \langle j | \Psi \rangle. \tag{C.3}$$

These numbers form a vector, which is the *vector representation of the state* Ψ or the *state vector*,

$$|\Psi\rangle = \begin{pmatrix} \langle 1|\Psi\rangle \\ \langle 2|\Psi\rangle \\ \cdot \\ \cdot \\ \langle N|\Psi\rangle \end{pmatrix}. \tag{C.4}$$

Note that this is just a set of numbers – no coordinates are involved. N is here the number of basis states, which may be finite or infinite. [The basis set need not be numerable and can form a *continuum* in which case the sum over the states is replaced by an integral.] The basis states are represented by unit vectors $|j\rangle$

$$|1\rangle = \begin{pmatrix} 1\\0\\0\\\cdot\\\cdot\\\cdot \end{pmatrix} \qquad |2\rangle = \begin{pmatrix} 0\\1\\0\\\cdot\\\cdot\\\cdot \end{pmatrix} \quad \text{etc.} \tag{C.5}$$

The basis vectors are time independent, and for time-dependent states the time dependence is contained in the coefficients

$$|\Psi(t)\rangle = a_j(t)|j\rangle,$$
 (C.6)

 $|\Psi\rangle$ is a *ket vector*, and for each ket vector there is a corresponding *bra vector*

$$\langle \Psi | = \left(a_1^*, a_2^*, \cdots \right), \tag{C.7}$$

where the asterisk represents complex conjugate. It follows from (C.1) that

$$a_j^* = \langle \Psi | j \rangle. \tag{C.8}$$

The scalar product of two general vectors with expansion coefficients a_j and b_j , respectively, becomes

$$\langle \Psi | \Phi \rangle = a_j^* \, b_j \tag{C.9}$$

with the basis vectors being orthonormal. This is identical to the scalar product of the corresponding vector representations

$$\langle \Psi | \Phi \rangle = \left(a_1^*, a_2^*, \cdots \right) \begin{pmatrix} b_1 \\ b_2 \\ \vdots \\ \vdots \end{pmatrix}.$$
 (C.10)

The ket vector (C.4) can be expanded as

$$|\Psi\rangle = |j\rangle \langle j|\Psi\rangle.$$
 (C.11)

But this holds for any vector in the Hilbert space, and therefore we have the formal relation in that space

$$|j\rangle\langle j| \equiv I$$
, (C.12)

where I is the *identity operator*. This is known as the *resolution of the identity*. Using the expression for the coefficients, the scalar product (C.9) can also be expressed as

$$\langle \Psi | \Phi \rangle = \langle \Psi | j \rangle \langle j | \Phi \rangle,$$
 (C.13)

which becomes obvious, considering the expression for the identity operator.

C.2 Matrix Representation of Operators

The operators we are dealing with have the property that when acting on a function in our Hilbert space, they generate another (or the same) function in that space,

$$\hat{\mathcal{O}}\Psi(x) = \Phi(x) \tag{C.14}$$

or with vector notations

$$\hat{\mathcal{O}}|\Psi\rangle = |\Phi\rangle. \tag{C.15}$$

Expanding the vectors on the left-hand side according to the above yields

$$|i\rangle\langle i|\hat{\mathcal{O}}|j\rangle\langle j|\Psi\rangle = |\Phi\rangle.$$
 (C.16)

Obviously, we have the identity

$$\hat{\mathcal{O}} \equiv |i\rangle \langle i|\hat{\mathcal{O}}|j\rangle \langle j. \tag{C.17}$$

The numbers $\langle i | \hat{\mathcal{O}} | j \rangle$ are matrix elements

$$\langle i|\hat{\mathcal{O}}|j\rangle = \int dx \,\phi_i^*(x)\,\hat{\mathcal{O}}\,\phi_j(x)$$
 (C.18)

and they form the matrix representation of the operator

$$\hat{\mathcal{O}} \Rightarrow \begin{pmatrix} \langle 1|\hat{\mathcal{O}}|1\rangle & \langle 1|\hat{\mathcal{O}}|2\rangle & \cdots \\ \langle 2|\hat{\mathcal{O}}|1\rangle & \langle 2|\hat{\mathcal{O}}|2\rangle & \cdots \\ \cdots & \cdots & \cdots \end{pmatrix}.$$

Standard matrix multiplication rules are used in operations with vector and matrix representations, for instance,

$$\hat{\mathcal{O}} |\Psi\rangle = |\Phi\rangle \Rightarrow \begin{pmatrix} \langle 1|\hat{\mathcal{O}}|1\rangle \ \langle 1|\hat{\mathcal{O}}|2\rangle \cdots \\ \langle 2|\hat{\mathcal{O}}|1\rangle \ \langle 2|\hat{\mathcal{O}}|2\rangle \cdots \\ \cdots & \cdots \end{pmatrix} \begin{pmatrix} \langle 1|\Psi\rangle \\ \langle 2|\Psi\rangle \\ \vdots \\ \langle N|\Psi\rangle \end{pmatrix} = \begin{pmatrix} \langle 1|\Phi\rangle \\ \langle 2|\Phi\rangle \\ \vdots \\ \langle N|\Phi\rangle \end{pmatrix},$$

where

$$\langle k|\Phi\rangle = \langle k|\hat{\mathcal{O}}|j\rangle\,\langle j|\Phi\rangle$$

summed over the index j.

C.3 Coordinate Representations

C.3.1 Representation of Vectors

The *coordinate representation* of the ket vector $|\Psi\rangle$ (C.4) is denoted as $\langle x|\Psi\rangle$, and this is identical to the corresponding state or (Schrödinger) wave function

$$\langle x|\Psi\rangle \equiv \Psi(x); \qquad \langle \Psi|x\rangle \equiv \Psi^*(x).$$
 (C.19)

This can be regarded as a generalization of the expansion for the expansion coefficients (C.1), where the space coordinates correspond to a continuous set of basis functions.

The basis functions $\phi_j(x)$ have the coordinate representation $\langle x|j\rangle$, and the coordinate representation (C.1) becomes

$$\langle x|\Psi\rangle = a_j \,\phi_j(x) = a_j \,\langle x|j\rangle$$
. (C.20)

The scalar product between the functions $\Psi(x)$ and $\Phi(x)$ is

$$\langle \Psi | \Phi \rangle = \int dx \, \Psi^*(x) \, \Phi(x),$$
 (C.21)

which we can express as

$$\langle \Psi | \Phi \rangle = \int dx \ \langle \Psi | x \rangle \langle x | \Phi \rangle.$$
 (C.22)

We shall assume that an *integration is always understood*, when Dirac notations of the kind above are used, i.e.,

$$\langle \Psi | \Phi \rangle = \langle \Psi | x \rangle \langle x | \Phi \rangle$$
 (C.23)

in analogy with the summation rule for discrete basis sets. This leads to the formal identity

$$|x\rangle\langle x| \equiv I,$$
 (C.24)

which is consistent with the corresponding relation (C.12) with a numerable basis set.

C.3.2 Closure Property

From the expansion (C.1), we have

$$\Psi(x) = \int dx' \,\phi_j^*(x') \,\Psi(x') \,\phi_j(x). \tag{C.25}$$

This can be compared with the integration over the Dirac delta function

$$\Psi(x) = \int dx' \, \delta(x - x') \, \Psi(x'), \tag{C.26}$$

which leads to the relation known as the closure property

$$\phi_j^*(x')\phi_j(x) = \delta(x - x')$$
 (C.27)

(with summation over j). In Dirac notations, this becomes

$$\langle x|j\rangle \langle j|x'\rangle = \delta(x-x')$$

or

which implies that the delta function is the coordinate representation of the identity operator (C.12). Note that there is no integration over the space coordinates here.

C.3.3 Representation of Operators

The coordinate representation of an operator is expressed in analogy with that of a state vector

$$\hat{\mathcal{O}} \Rightarrow \langle x | \hat{\mathcal{O}} | x' \rangle = \hat{\mathcal{O}}(x, x').$$
 (C.29)

which is a function of x and x'. An operator $\hat{\mathcal{O}}$ acting on a state vector $|\Psi\rangle$ is represented by

$$\langle x\hat{\mathcal{O}}|\Psi\rangle \Rightarrow \langle x|\hat{\mathcal{O}}|x'\rangle\langle x'|\Psi\rangle = \int dx'\,\hat{\mathcal{O}}(x,x')\,\Psi(x'),$$
 (C.30)

which is a function of x.

Appendix D

Dirac Equation and the Momentum Representation

D.1 Dirac Equation

D.1.1 Free Particles

The standard quantum-mechanical operator representation

$$E \to \hat{E} = i\hbar \frac{\partial}{\partial t}; \quad \mathbf{p} \to \hat{\mathbf{p}} = -i\hbar \nabla; \quad \mathbf{x} \to \hat{\mathbf{x}} = \mathbf{x},$$
 (D.1)

where E, \mathbf{p} , \mathbf{x} represent the energy, momentum, and coordinate vectors, and \hat{E} , $\hat{\mathbf{p}}$, $\hat{\mathbf{x}}$ the corresponding quantum-mechanical operators, was previously used to obtain the nonrelativistic Schrödinger equation (2.9). If we apply the same procedure to the *relativistic* energy relation

$$E^2 = c^2 \mathbf{p}^2 + m_{\rm e}^2 c^4, \tag{D.2}$$

where c is the velocity of light in vacuum and $m_{\rm e}$ the mass of the electron, this would lead to

$$-\hbar^2 \frac{\partial^2 \psi(x)}{\partial t^2} = \left(c^2 \hat{\boldsymbol{p}}^2 + m_{\rm e}^2 c^4\right) \psi(x),\tag{D.3}$$

which is the *Schrödinger relativistic wave equation*. It is also known as the *Klein–Gordon equation*. In covariant notations (see Appendix, Sect. A.1), it can be expressed as

 $(\hbar^2 \Box + m_e^2 c^2) \psi(x) = 0.$ (D.4)

In contrast to the nonrelativistic Schrödinger equation (2.9), the Klein–Gordon equation is *nonlinear*, and therefore the superposition principle of the solutions cannot be applied. In order to obtain a *linear* equation that is consistent with the energy relation (D.2) and the quantum-mechanical substitutions (D.1), Dirac proposed the form for a free electron

$$i\hbar \frac{\partial \psi(x)}{\partial t} = \left(c\alpha \cdot \hat{p} + \beta m_{\rm e}c^2\right) \psi(x), \tag{D.5}$$

where α and β are constants (but not necessarily pure numbers). This equation is the famous *Dirac equation for a relativistic particle in free space*.

The equivalence with the equation (D.3) requires

$$(c\boldsymbol{\alpha}\cdot\hat{\boldsymbol{p}}+\beta m_{\rm e}c^2)(c\boldsymbol{\alpha}\cdot\hat{\boldsymbol{p}}+\beta m_{\rm e}c^2)\equiv c^2\hat{\boldsymbol{p}}^2+m_{\rm e}^2c^4,$$

which leads to

$$\alpha_x^2 = \alpha_y^2 = \alpha_z^2 = \beta^2 = 1,$$

$$\alpha_x \alpha_y + \alpha_y \alpha_x = 0 \quad \text{(cyclic)},$$

$$\alpha \beta + \beta \alpha = 0,$$
(D.6)

where "cyclic" implies that the relation holds for $x \to y \to z \to x$.

The solution proposed by Dirac is the so-called *Dirac matrices*

$$\alpha = \begin{pmatrix} 0 & \sigma \\ \sigma & 0 \end{pmatrix}; \quad \beta = \begin{pmatrix} 1 & 0 \\ 0 & -1 \end{pmatrix}, \tag{D.7}$$

where $\sigma = (\sigma_x, \sigma_y, \sigma_z)$ are the *Pauli spin matrices*

$$\sigma_x = \begin{pmatrix} 0 & 1 \\ 1 & 0 \end{pmatrix}; \quad \sigma_y = \begin{pmatrix} 0 & -i \\ i & 0 \end{pmatrix}; \quad \sigma_z = \begin{pmatrix} 1 & 0 \\ 0 & -1 \end{pmatrix}.$$
 (D.8)

The Dirac matrices anticommute

$$\alpha \beta + \beta \alpha = 0. \tag{D.9}$$

With the covariant four-dimensional momentum vector (A.2) $p_{\mu} = (p_0, -\mathbf{p})$, and the corresponding vector operator

$$\hat{p}_{\mu} = (\hat{p}_{0}, -\hat{p}) = \left(\frac{i\hbar}{c} \frac{\partial}{\partial t}, i\hbar \nabla\right),$$
 (D.10)

the Dirac equation (D.5) becomes

$$\left(c\,\hat{p}_0 - c\boldsymbol{\alpha}\cdot\hat{\boldsymbol{p}} - \beta m_e c^2\right)\,\psi(x) = 0\tag{D.11}$$

or with

$$\alpha^{\mu} = (1, \boldsymbol{\alpha}) \tag{D.12}$$

and $\alpha^{\mu} \hat{p}_{\mu} = \hat{p}_0 - \alpha \cdot \hat{p}$ we obtain the *covariant form of the Dirac Hamiltonian* for a free particle

$$H_{\rm D} = -c\alpha^{\mu}\,\hat{p}_{\mu} + \beta m_{\rm e}c^2$$
 (D.13)

D.1 Dirac Equation 297

and the corresponding Dirac equation

$$\left[\left(c\alpha^{\mu}\,\hat{p}_{\mu}-\beta m_{\rm e}c^2\right)\,\psi(x)=0.\right] \tag{D.14}$$

With the Dirac gamma matrices

$$\gamma^{\mu} = \beta \alpha^{\mu}, \tag{D.15}$$

this can also be expressed as $(\beta^2 = 1)$

$$(D.16)$$

$$(\psi^{\mu}\hat{p}_{\mu} - m_{e}c) \psi(x) = (\hat{p} - m_{e}c) \psi(x) = 0,$$

where \hat{p} is the "p-slash" operator

$$\hat{p} = \gamma^{\mu} \hat{p}_{\mu} = \beta \alpha^{\mu} \hat{p}_{\mu} = \beta \left(\hat{p}_{0} - \boldsymbol{\alpha} \cdot \hat{\boldsymbol{p}} \right). \tag{D.17}$$

It should be observed that in the covariant notation \hat{p}_0 is normally disconnected from the energy, i.e.,

$$\hat{p}_0 \neq \sqrt{\hat{p}^2 + m_e^2 c^2}.$$
 (D.18)

This is known as *off the mass shell*. When the equality above holds, it is referred to as *on the mass shell*, which can also be expressed as

$$\hat{p}^2 = \hat{p}_0^2 - \hat{p}^2 = m_e^2 c^2$$
 or $\hat{p} = m_e c$. (D.19)

In separating the wave function into space and time parts,

$$\psi(x) = \phi_p(x) e^{-i\varepsilon_p t/\hbar}, \qquad (D.20)$$

the time-independent part of the Dirac equation (D.5) becomes

$$\hat{h}_{D}^{\text{free}}(\hat{\mathbf{p}})\,\phi_{D}(\mathbf{x}) = \varepsilon_{D}\,\phi_{D}(\mathbf{x}),\tag{D.21}$$

where

$$\hat{h}_{\rm D}^{\rm free} = c \boldsymbol{\alpha} \cdot \hat{\mathbf{p}} + \beta m_{\rm e} c^2 \tag{D.22}$$

is the *free-electron Dirac Hamiltonian*. The Dirac equation can also be expressed as

$$\left(\beta \frac{\varepsilon_p}{c} - \beta \boldsymbol{\alpha} \cdot \hat{\mathbf{p}} - m_e c\right) \phi_p(\mathbf{x}) = 0. \tag{D.23}$$

Here, $\phi_p(x)$ is a four-component wave function, which can be represented by

$$\phi_p(\mathbf{x}) = \frac{1}{\sqrt{V}} u_r(\mathbf{p}) e^{i\mathbf{p} \cdot \mathbf{x}}; \qquad \hat{\mathbf{p}} \phi_p(\mathbf{x}) = \mathbf{p} \phi_p(\mathbf{x}). \tag{D.24}$$

(Note the difference between the momentum *vector* \mathbf{p} and the momentum *operator* $\hat{\mathbf{p}}$). $e^{i\mathbf{p}\cdot x}$ represents a *plane wave*, and $u_r(\mathbf{p})$ is a four-component vector function of the momentum \mathbf{p} . For each \mathbf{p} , there are four independent solutions (r = 1, 2, 3, 4). The parameter p in our notations ϕ_p and ε_p represents \mathbf{p} and r or, more explicitly,

$$\phi_p(x) = \phi_{\mathbf{p},r}(x); \qquad \varepsilon_p = \varepsilon_{\mathbf{p},r}.$$

With the wave function (12.1), the Dirac equation (D.23) leads to the following equation for the $u_r(\mathbf{p})$ functions

$$\left(\beta \frac{\varepsilon_p}{c} - \beta \boldsymbol{\alpha} \cdot \hat{\boldsymbol{p}} - m_e c\right) u_r(\mathbf{p}) = 0$$

or

$$\begin{pmatrix} \varepsilon_p/c - m_e c & -\boldsymbol{\sigma} \cdot \hat{\boldsymbol{p}} \\ \boldsymbol{\sigma} \cdot \hat{\boldsymbol{p}} & -\varepsilon_p/c - m_e c \end{pmatrix} u_r(\mathbf{p}) = 0,$$
 (D.25)

where each element is a 2×2 matrix. This equation has *two* solutions for each momentum vector **p**:

$$u_{+}(\mathbf{p}) = N_{+} \begin{pmatrix} \varepsilon_{p}/c + m_{e}c \\ \mathbf{\sigma} \cdot \mathbf{p} \end{pmatrix}; \qquad u_{-}(\mathbf{p}) = N_{-} \begin{pmatrix} -\mathbf{\sigma} \cdot \mathbf{p} \\ -\varepsilon_{p}/c + m_{e}c \end{pmatrix}$$
 (D.26)

corresponding to positive (r=1,2) and negative (r=3,4) eigenvalues, respectively. Defining the momentum component p_0 – to be distinguished from the corresponding *operator* component \hat{p}_0 (D.10) – by

$$|\varepsilon_p| = E_p = cp_0; p_0 = \sqrt{\mathbf{p}^2 + m_e^2 c^2}$$
 (D.27)

gives

$$u_{+}(\mathbf{p}) = N_{+} \begin{pmatrix} p_{0} + m_{e}c \\ \mathbf{\sigma} \cdot \mathbf{p} \end{pmatrix}; \qquad u_{-}(\mathbf{p}) = N_{-} \begin{pmatrix} -\mathbf{\sigma} \cdot \mathbf{p} \\ p_{0} + m_{e}c \end{pmatrix}.$$
 (D.28)

The corresponding eigenfunctions (12.1) are

$$\phi_{p_{+}}(x) = \frac{1}{\sqrt{V}} u_{+}(\mathbf{p}) e^{i\mathbf{p}\cdot x} e^{-iE_{p}t/\hbar} \quad \phi_{p_{-}}(x) = \frac{1}{\sqrt{V}} u_{-}(\mathbf{p}) e^{i\mathbf{p}\cdot x} e^{iE_{p}t/\hbar}$$
(D.29)

including the time dependence according to (D.20) and (D.27).

The vectors

$$u(\mathbf{p}) = u_{+}(\mathbf{p})$$
 and $v(\mathbf{p}) = u_{-}(-\mathbf{p}) = N_{-} \begin{pmatrix} \sigma \cdot \mathbf{p} \\ p_{0} + m_{e}c \end{pmatrix}$ (D.30)

D.1 Dirac Equation 299

satisfy the equations

$$(\not p - m_e c) u(\mathbf{p}) = 0$$
 and $(\not p + m_e c) v(\mathbf{p}) = 0$, (D.31)

where p_0 is given by (D.27). Note that the negative energy solution corresponds here to the momentum $-\mathbf{p}$ for the electron (or $+\mathbf{p}$ for the hole/positron).

Normalization

Several different schemes for the normalization of the *u* matrices have been used (see, for instance, Mandl and Shaw [1, Chap. 4]). Here, we shall use

$$u_{r'}^{\dagger}(\mathbf{p}) u_r(\mathbf{p}) = \delta_{r',r}, \tag{D.32}$$

which leads to

$$u_{+}(\mathbf{p}) = |N_{+}|^{2} (p_{0} + m_{e}c, \boldsymbol{\sigma} \cdot \mathbf{p}) \begin{pmatrix} p_{0} + m_{e}c \\ \boldsymbol{\sigma} \cdot \mathbf{p} \end{pmatrix}$$
$$= |N_{+}|^{2} (p_{0} + m_{e}c)^{2} + (\boldsymbol{\sigma} \cdot \mathbf{p})^{2} = |N_{+}|^{2} 2 p_{0} (p_{0} + m_{e}c) \quad (D.33)$$

using $(\boldsymbol{\sigma} \cdot \mathbf{p})^2 = \mathbf{p}^2 = p_0^2 - m_e^2 c^2$. This gives

$$N_{+} = \frac{1}{\sqrt{2p_{0}(p_{0} + m_{e}c)}}$$
 (D.34)

and the same for N_{-} .

With the normalization above, we have

$$u_{+}(\mathbf{p}) u_{+}^{\dagger}(\mathbf{p}) = |N_{+}|^{2} \begin{pmatrix} p_{0} + m_{e}c \\ \boldsymbol{\sigma} \cdot \mathbf{p} \end{pmatrix} (p_{0} + m_{e}c, \boldsymbol{\sigma} \cdot \mathbf{p})$$

$$= \frac{1}{2p_{0}} \begin{pmatrix} p_{0} + m_{e}c & \boldsymbol{\sigma} \cdot \mathbf{p} \\ \boldsymbol{\sigma} \cdot \mathbf{p} & p_{0} - m_{e}c \end{pmatrix} = \frac{p_{0} + \boldsymbol{\alpha} \cdot \mathbf{p} + \beta m_{e}c}{2p_{0}}$$
(D.35)

and similarly

$$u_{-}(\mathbf{p}) u_{-}^{\dagger}(\mathbf{p}) = \frac{p_0 - (\boldsymbol{\alpha} \cdot \mathbf{p} + \beta m_e c)}{2 p_0},$$
(D.36)

which gives

$$u_{+}(\mathbf{p}) u_{+}^{\dagger}(\mathbf{p}) + u_{-}(\mathbf{p}) u_{-}^{\dagger}(\mathbf{p}) = I.$$
 (D.37)

D.1.2 Dirac Equation in an Electromagnetic Field

Classically, the interaction of an electron with electromagnetic fields is given by the "minimal substitution" (E.15), which in covariant notations can be expressed as ¹

$$p_{\mu} \to \hat{p}_{\mu} + eA_{\mu} \tag{D.38}$$

with the four-dimensional potential being

$$A_{\mu}(x) = \left(\frac{\phi(x)}{c}, -A(x)\right). \tag{D.39}$$

This implies that the Dirac Hamiltonian (D.13) becomes

$$H_{\rm D} = -c\alpha^{\mu}(\hat{p}_{\mu} + eA_{\mu}) + \beta m_{\rm e}c^2$$
 (D.40)

and that the interaction with the fields is given by the term

$$H_{\rm int} = -ec\alpha^{\mu}A_{\mu}. \tag{D.41}$$

D.2 Momentum Representation

D.2.1 Representation of States

Above in Sect. C.3 we have considered the coordinate representation of a state vector, $\phi_a(x) = \langle x | a \rangle$. An alternative is the *momentum representation*, where the state vector is expanded in momentum eigenfunctions. A state $|a\rangle$ is then represented by $\phi_a(\mathbf{p}r) = \langle \mathbf{p}r | a \rangle$, which are the expansion coefficients of the state in momentum eigenfunctions

$$\langle x|a\rangle = \langle x|\mathbf{p}r\rangle \langle \mathbf{p}r|a\rangle$$
 (D.42)

with summations over \mathbf{p} and r. The expansion coefficients become

$$\langle \mathbf{p}r|a\rangle = \int d^3x \ \langle \mathbf{p}r|x\rangle \langle x|a\rangle = \sqrt{\frac{1}{V}} \int d^3x \ e^{-i\mathbf{p}\cdot\mathbf{x}} \ u_r^{\dagger}(\mathbf{p}) \ \phi_a(x).$$
 (D.43)

In the limit of continuous momenta, the sum over **p** is replaced by an integral and V replaced by $(2\pi)^3$.

¹ In many text books, the minimal substitution is expressed as $p_{\mu} \rightarrow \hat{p}_{\mu} + \frac{e}{c}A_{\mu}$, because a mixed unit system, like the cgs system, is used. In the SI system – or any other consistent unit system – the substitution has the form given in the text. The correctness of this expression can be checked by means of dimensional analysis (see Appendix K).

Note that the *momentum representation is distinct from the Fourier transform*. The latter is defined as

$$\langle \mathbf{p}|a\rangle = u_r(\mathbf{p}) \langle \mathbf{p}r|a\rangle = \sqrt{\frac{1}{V}} \int d^3x \, e^{-i\mathbf{p}\cdot\mathbf{x}} \, \phi_a(\mathbf{x})$$

$$\rightarrow (2\pi)^{-3/2} \int d^3x \, e^{-i\mathbf{p}\cdot\mathbf{x}} \, \phi_a(\mathbf{x})$$
(D.44)

using the identity (D.37).

In analogy with (C.23), we have

$$\langle a|b\rangle = \langle a|\mathbf{p},r\rangle \langle \mathbf{p},r|b\rangle,$$
 (D.45)

which yields

$$|\mathbf{p}, r\rangle \langle \mathbf{p}, r| \equiv I$$
 (D.46)

with implicit summation/integration over \mathbf{p} and summation over r.

D.2.2 Representation of Operators

Coordinate representation of an operator $\hat{\mathcal{O}}$: $O(x_2, x_1) = \langle x_2 | \hat{\mathcal{O}} | x_1 \rangle$. Momentum representation of an operator $\hat{\mathcal{O}}$: $O(\mathbf{p}_2 r_2, \mathbf{p}_1 r_1) = \langle \mathbf{p}_2 r_2 | \hat{\mathcal{O}} | \mathbf{p}_1 r_1 \rangle$. Transformation between the representations

$$\langle \mathbf{p}_2 r_2 | \hat{\mathcal{O}} | \mathbf{p}_1 r_1 \rangle = \iint d^3 x_2 d^3 x_1 \langle \mathbf{p}_2 r_2 | x_2 \rangle \langle x_2 | \hat{\mathcal{O}} | x_1 \rangle \langle x_1 | \mathbf{p}_1 r_1 \rangle. \tag{D.47}$$

The corresponding Fourier transform is according to (D.44)

$$u_{r_2}(\mathbf{p}_2) \langle \mathbf{p}_2 r_2 | \hat{\mathcal{O}} | \mathbf{p}_1 r_1 \rangle u_{r_1}^{\dagger}(\mathbf{p}_1).$$
 (D.48)

Any operator with a complete set of eigenstates can be expanded as

$$\hat{\mathcal{O}} = |j\rangle \ \varepsilon_i \ \langle j| \quad \text{where} \quad \hat{\mathcal{O}}|j\rangle = \varepsilon_i |j\rangle.$$
 (D.49)

This gives the coordinate and momentum representations

$$\langle x_2 | \hat{\mathcal{O}} | x_1 \rangle = \langle x_2 | j \rangle \, \varepsilon_j \, \langle j | x_1 \rangle,$$
 (D.50a)

$$\langle \mathbf{p}_{2} r_{2} | \hat{\mathcal{O}} | \mathbf{p}_{1} r_{1} \rangle = \langle \mathbf{p}_{2}, r_{2} | j \rangle \, \varepsilon_{j} \, \langle j | \mathbf{p}_{1} r_{1} \rangle. \tag{D.50b}$$

D.2.3 Closure Property for Momentum Functions

In three dimensions, we have the closure property (C.27)

$$\phi_i^*(x)\phi_i(x') = \delta^3(x - x')$$
 (D.51)

and for a continuous set of momentum eigenfunctions this becomes

$$\int d^{3}\mathbf{p} \,\phi_{\mathbf{p}r}^{*}(x) \,\phi_{\mathbf{p}r}(x') = \delta^{3}(x - x')$$
 (D.52)

with summation over r. This can also be expressed as

$$\langle x | \mathbf{p}r \rangle \langle \mathbf{p}r | x \rangle = \delta^3(x - x')$$
 (D.53)

also with integration over \mathbf{p} . From the closure property (D.51), we have

$$\phi_j^*(\mathbf{p}, r)\phi_j(\mathbf{p}', r') = \delta_{r,r'}\delta^3(\mathbf{p} - \mathbf{p}'), \tag{D.54}$$

which leads to

$$\langle \mathbf{p}, r | j \rangle \langle j | \mathbf{p}', r' \rangle = \delta_{r,r'} \delta^3(\mathbf{p} - \mathbf{p}').$$
 (D.55)

D.3 Relations for the Alpha and Gamma Matrices

From the definition of the alpha matrices and the definitions in Appendix A, we find the following useful relations:

$$\alpha^{\mu}\alpha_{\mu} = 1 - \alpha^{2} = -2,$$

$$\alpha^{\mu}\alpha_{\mu} = \alpha\alpha^{\mu}\alpha_{\mu} = -2\alpha,$$

$$\alpha^{\mu}\beta\alpha_{\mu} = \beta - \alpha\beta\alpha = 4\beta,$$

$$\alpha^{\mu}\beta\alpha^{\mu} = \beta + \alpha\beta\alpha = -2\beta,$$

$$\alpha^{\mu}\beta\alpha_{\mu} = \alpha^{\mu}\beta\alpha_{\sigma}A^{\sigma}\alpha_{\mu} = 4\beta,$$
(D.56)

where A is defined in (D.17). The gamma matrices satisfy the following anticommutation rule:

$$\gamma^{\nu}\gamma^{\mu} + \gamma^{\mu}\gamma^{\nu} = 2g^{\mu\nu},$$
 $A B + B A = 2AB.$ (D.57)

This leads to

$$\gamma^{\mu}\gamma^{\nu}\gamma_{\mu} = -2\gamma_{\mu},$$
$$\gamma^{\mu} \mathcal{A}\gamma_{\mu} = -2 \mathcal{A},$$

Reference 303

$$\gamma^{\mu}\gamma_{\mu} = 4,$$

$$\gamma^{\mu}\gamma^{\nu}\gamma_{\mu} = -2\gamma_{\mu},$$

$$\gamma^{\mu}\mathcal{A}\gamma_{\mu} = -2\mathcal{A},$$

$$\gamma^{0}\gamma_{0} = \gamma^{0}\gamma^{0} = 1,$$

$$\gamma^{\sigma}\gamma^{0} = \gamma^{0}\widetilde{\gamma}^{\sigma},$$

$$\mathcal{A}\gamma^{0} = \gamma^{0}\widetilde{A},$$

$$\gamma^{0}\gamma^{\sigma}\gamma^{0} = \widetilde{\gamma}^{\sigma},$$

$$\gamma^{0}\mathcal{A}\gamma^{0} = \widetilde{A},$$

$$\gamma^{0}\gamma^{\sigma}\gamma^{\tau}\gamma^{0} = \widetilde{\gamma}^{\sigma}\widetilde{\gamma}^{\tau},$$

$$\gamma^{0}\mathcal{A}\mathcal{B}\gamma^{0} = \widetilde{A}B,$$

$$\gamma^{0}\gamma^{\beta}\gamma^{\sigma}\gamma^{\tau}\gamma^{0} = \widetilde{\gamma}^{\beta}\widetilde{\gamma}^{\sigma}\widetilde{\gamma}^{\tau},$$

$$\gamma^{0}\mathcal{A}\mathcal{B}\mathcal{C}\gamma^{0} = \widetilde{A}\widetilde{B}\widetilde{C},$$
(D.58)

where $\widetilde{A} = \gamma^0 A_0 - \gamma^i A_i = \gamma^0 A_0 + \gamma \cdot A$

With the number of dimensions being equal to $4 - \epsilon$, to be used in dimensional regularization (see Chap. 12), the relations become

$$\gamma^{\mu}\gamma_{\mu} = 4 - \epsilon,$$

$$\gamma^{\mu}\gamma^{\sigma}\gamma_{\mu} = -(2 - \epsilon)\gamma^{\sigma},$$

$$\gamma^{\mu} \mathcal{A}\gamma_{\mu} = -(2 - \epsilon)\mathcal{A},$$

$$\gamma^{\mu}\gamma^{\sigma}\gamma^{\tau}\gamma_{\mu} = 4g^{\sigma\tau} - \epsilon\gamma^{\sigma}\gamma^{\tau},$$

$$\gamma^{\mu} \mathcal{A} \mathcal{B}\gamma_{\mu} = 4AB - \epsilon \mathcal{A} \mathcal{B},$$

$$\gamma^{\mu}\gamma^{\beta}\gamma^{\sigma}\gamma^{\tau}\gamma_{\mu} = -2\gamma^{\tau}\gamma^{\sigma}\gamma^{\beta} + \epsilon\gamma^{\beta}\gamma^{\sigma}\gamma^{\tau},$$

$$\gamma_{i}\gamma^{i} = 3 - \epsilon,$$

$$\gamma_{i}\gamma^{\sigma}\gamma^{i} = -(2 - \epsilon)\gamma^{\sigma} - \widetilde{\gamma}^{\sigma},$$

$$\gamma_{i} \mathcal{A}\gamma^{i} = -(2 - \epsilon)\mathcal{A} - \widetilde{A},$$

$$\gamma_{i}\gamma^{\sigma}\gamma^{\tau}\gamma^{i} = 4g^{\sigma\tau} - \widetilde{\gamma}^{\sigma}\widetilde{\gamma}^{\tau} - \epsilon\gamma^{\sigma}\gamma^{\tau},$$

$$\gamma_{i} \mathcal{A} \mathcal{B} \gamma^{i} = 4AB - \widetilde{A}\widetilde{B} - \epsilon \mathcal{A} \mathcal{B},$$

$$\gamma_{i}\gamma^{\beta}\gamma^{\sigma}\gamma^{\tau}\gamma^{i} = -2\gamma^{\tau}\gamma^{\sigma}\gamma^{\beta} - \widetilde{\gamma}^{\beta}\widetilde{\gamma}^{\sigma}\widetilde{\gamma}^{\tau} + \epsilon\gamma^{\beta}\gamma^{\sigma}\gamma^{\tau},$$

$$\gamma_{i} \mathcal{A} \mathcal{B} \mathcal{C} \gamma^{i} = -2\mathcal{C} \mathcal{B} \mathcal{A} - \widetilde{A}\widetilde{B}\widetilde{C} + \epsilon \mathcal{A} \mathcal{B} \mathcal{C}.$$
(D.59)

Reference

1. Mandl, F., Shaw, G.: Quantum Field Theory. John Wiley and Sons, New York (1986)

Appendix E

Lagrangian Field Theory

Concerning notations, see Appendix A.

E.1 Classical Mechanics

In classical mechanics, the Lagrangian function for a system is defined as

$$L = T - V, (E.1)$$

where T is the kinetic energy and V the potential energy of the system. Generally, this depends on the coordinates q_i , the corresponding velocities $\dot{q}_i = \frac{\partial q_i}{\partial t}$, and possible explicitly on time (see, for instance [2, Sect. 23])

$$L(t; q_1, q_2 \cdots; \dot{q_1}, \dot{q_2} \cdots).$$
 (E.2)

The action is defined as

$$I = \int dt L(t; q_1, q_2 \cdots; \dot{q_1}, \dot{q_2} \cdots).$$
 (E.3)

The principle of least action implies that

$$\delta I(q_1, q_2 \cdots ; \dot{q_1}, \dot{q_2} \cdots) = 0,$$
 (E.4)

which leads to the Lagrange equations

$$\frac{\mathrm{d}}{\mathrm{d}t} \left(\frac{\partial L}{\partial \dot{q}_i} \right) - \frac{\partial L}{\partial q_i} = 0.$$
 (E.5)

The Hamilton function can be defined as

$$H = p_i \dot{q}_i - L, \tag{E.6}$$

where p_i is the canonically conjugate momentum to the coordinate q_i

$$p_i = \frac{\partial L}{\partial \dot{q_i}}. (E.7)$$

It then follows that

$$\frac{\partial H}{\partial p_i} = \dot{q}_i = \frac{\partial q_i}{\partial t}.$$
 (E.8a)

Furthermore, from the definitions above and the Lagrange equations, we have

$$\boxed{\frac{\partial H}{\partial q_i} = -\dot{p}_i.} \tag{E.8b}$$

These are *Hamilton's canonical equations of motion*.

We consider a general function of time and the coordinates and canonical momenta $f(t; p_i, q_i)$. Then the *total* derivative with respect to time becomes

$$\frac{\mathrm{d}f}{\mathrm{d}t} = \frac{\partial f}{\partial t} + \frac{\partial f}{\partial q_i} \frac{\partial q_i}{\partial t} + \frac{\partial f}{\partial p_i} \frac{\partial p_i}{\partial t} = \frac{\partial f}{\partial t} + \frac{\partial f}{\partial q_i} \frac{\partial H}{\partial p_i} - \frac{\partial f}{\partial p_i} \frac{\partial H}{\partial q_i}.$$
 (E.9)

With the *Poisson bracket* of two functions A and B, defined by

$$A, B = \frac{\partial A}{\partial q_i} \frac{\partial B}{\partial p_i} - \frac{\partial B}{\partial q_i} \frac{\partial A}{\partial p_i}, \qquad (E.10)$$

the derivative can be expressed as

$$\frac{\mathrm{d}f}{\mathrm{d}t} = \frac{\partial f}{\partial t} + \{f, H\}. \tag{E.11}$$

For a single-particle system in one dimension (x), the kinetic energy is $T = p^2/2m$, where m is the mass of the particle, which yields

$$L = \frac{p^2}{2m} - V = \frac{mv^2}{2} - V,$$

where $v = \dot{x}$ is the velocity of the particle. Furthermore, $p_i \dot{q}_i = p \dot{x} = p^2/m = mv^2$, yielding with (E.6)

$$H = \frac{p^2}{2m} + V = \frac{mv^2}{2} + V,$$

E.1 Classical Mechanics 307

which is the classical energy expression. The canonically conjugate momentum (E.7) is then

$$p = \frac{\partial L}{\partial \dot{x}} = \frac{\partial L}{\partial v} = mv,$$

which is the classical momentum.

E.1.1 Electron in External Field

The Lagrangian for an electron (charge -e) in an external field, $A_{\mu} = (\phi(x)/c, -A)$, is [1, p. 25]

$$L(x, \dot{x}) = \frac{1}{2}m\dot{x}^2 - eA \cdot \dot{x} + e\phi(x),$$
 (E.12)

where the last two terms represent (the negative of) a velocity-dependent potential. The conjugate momentum corresponding to the variable x is then according to (E.7)

$$p_i \to \mathbf{p} = m\dot{\mathbf{x}} - eA. \tag{E.13}$$

Using the relation (E.6), we get the corresponding Hamilton function

$$H = \mathbf{p} \cdot \dot{\mathbf{x}} - L = \frac{1}{2}m\dot{\mathbf{x}}^2 - e\phi(\mathbf{x}) = \frac{1}{2m}(\mathbf{p} + eA)^2 - e\phi(\mathbf{x}).$$
 (E.14)

We see that the interaction with the fields (ϕ, A) is obtained by means of the substitutions

$$H \to H - e\phi(x)$$
 $\mathbf{p} \to \mathbf{p} + eA$ (E.15)

known as the minimal substitutions.

The corresponding equations of motion can be obtained from either the Lagrange's or Hamilton's equation of motion. We then have

$$\frac{\mathrm{d}}{\mathrm{d}t} \left(\frac{\partial L}{\partial \dot{q}_i} \right) \to \frac{\mathrm{d}}{\mathrm{d}t} \left(m \dot{x} - e A \right)$$

and

$$\frac{\partial L}{\partial q_i} \rightarrow -e\nabla(A \cdot \dot{x}) + e\nabla\phi(x).$$

The same equations are obtained from the Hamilton's equations of motion (E.8b). The *total* time derivative can in analogy with (E.9) be expressed as

$$\frac{\mathrm{d}}{\mathrm{d}t} = \frac{\partial}{\partial t} + \frac{\mathrm{d}x}{\mathrm{d}t} \frac{\partial}{\partial x} + \dots = \frac{\partial}{\partial t} + \dot{x} \cdot \nabla$$

giving

$$\frac{\mathrm{d}}{\mathrm{d}t} (m\dot{x} - eA) = m\ddot{x} - e\frac{\partial A}{\partial t} - e(\dot{x} \cdot \nabla)A.$$

From the identity

$$\dot{x} \times (\nabla \times A) = \nabla (A \cdot \dot{x}) - (\dot{x} \cdot \nabla) A,$$

we then obtain the equations of the motion

$$m\ddot{\mathbf{x}} = e\nabla\phi(\mathbf{x}) + e\frac{\partial \mathbf{A}}{\partial t} - e\dot{\mathbf{x}} \times (\nabla \times \mathbf{A}) = -e\left(\mathbf{E} + \mathbf{v} \times \mathbf{B}\right)$$
(E.16)

with $v = \dot{x}$ being the velocity of the electron. This is the classical equations of motion for an electron of charge -e in an electromagnetic field. The right-hand side is the so-called *Lorentz force* on an electron in a combined electric and magnetic field. This verifies the Lagrangian (E.12).

E.2 Classical Field Theory

In classical field theory, we consider a Lagrangian density of the type

$$\mathcal{L} = \mathcal{L}(\phi_r, \partial_u \phi_r), \tag{E.17}$$

where $\phi_r = \phi_r(x)$ represents different fields and

$$\partial_{\mu}\phi_{r} = \frac{\partial\phi_{r}}{\partial x^{\mu}}.\tag{E.18}$$

The requirement that the action integral

$$I = \int d^4x \, \mathcal{L}(\phi_r, \partial_\mu \phi_r) \tag{E.19}$$

be stationary over a certain volume leads to the Euler-Lagrange equations

$$\left| \frac{\partial \mathcal{L}}{\partial \phi_r} - \partial_\mu \frac{\partial \mathcal{L}}{\partial (\partial_\mu \phi_r)} = 0. \right|$$
 (E.20)

The field conjugate to $\phi_r(x)$ is

$$\pi_r(x) = \frac{\partial \mathcal{L}}{\partial \dot{\phi}_r},\tag{E.21}$$

where the "dot" represents the time derivative. The Lagrangian function is defined as

$$L(t) = \int d^3x \, \mathcal{L}(\phi_r, \partial_\mu \phi_r). \tag{E.22}$$

The Hamiltonian density is defined as

$$\mathcal{H}(x) = \pi_r(x)\dot{\phi}_r(x) - \mathcal{L}(\phi_r, \partial_\mu \phi_r). \tag{E.23}$$

In quantized Lagrangian field theory, the fields are replaced by *operators*, satisfying the *Heisenberg commutation rules* at equal times [1, Eq. 2.31]

$$\left[\hat{\phi}_{\mu}(x), \hat{\pi}^{\nu}(x')\right] = i\hbar \,\delta_{\mu,\nu} \,\delta^{3}(x - x') \tag{E.24}$$

with the remaining commutations vanishing. In our applications, the quantized field will normally be the electron field in the interaction picture (B.28) or the electromagnetic field (G.2).

E.3 Dirac Equation in Lagrangian Formalism

From the Dirac equation for a free electron (D.14), we can deduce the corresponding Lagrangian density

$$\mathcal{L}(x) = \hat{\psi}^{\dagger}(x) \left(i\hbar c \,\alpha^{\mu} \partial_{\mu} - \beta m_{e} c^{2} \right) \hat{\psi}(x). \tag{E.25}$$

Using the relation (B.17), the space integral over this density yields the corresponding operator

$$L = \int d^3x \, \mathcal{L}(x) = i\hbar c \, \alpha^{\mu} \partial_{\mu} - \beta m_e c^2 = c \, \alpha^{\mu} p_{\mu} - \beta m_e c^2 \qquad (E.26)$$

(with $\hat{p}_{\mu}=\mathrm{i}\hbar\,\partial_{\mu}$) and the corresponding Hamilton operator (E.6)

$$H = -L = -c \alpha^{\mu} p_{\mu} + \beta m_{\rm e} c^2,$$
 (E.27)

since the fields are time independent. This leads to the Dirac equation for a free electron (D.14).

We can also apply the Euler–Lagrange equations (E.20) on the Lagrangian (E.25), which leads to

$$\partial_{\mu} \frac{\partial \mathcal{L}}{\partial(\partial_{\mu} \hat{\psi})} = \partial_{\mu} \left(\hat{\psi}^{\dagger}(x) i \hbar c \alpha^{\mu} \right),$$
$$\frac{\partial \mathcal{L}}{\partial \hat{\psi}} = -\hat{\psi}^{\dagger}(x) \beta m_{e} c^{2},$$

and

$$\partial_{\mu} i\hbar \, c \, \alpha^{\mu} \hat{\psi}^{\dagger}(x) + \beta m_{\rm e} c^2 \hat{\psi}^{\dagger}(x) = 0$$

with the hermitian adjoint

$$\left(-i\hbar c \alpha^{\mu} \partial_{\mu} + \beta m_{e} c^{2}\right) \hat{\psi}(x) = 0, \tag{E.28}$$

which is consistent with the Dirac equation for the free electron.

In the presence of an electromagnetic field, we make the *minimal substitution* (D.38)

$$p_{\mu} \to p_{\mu} + eA_{\mu}(x)$$
 or $\partial_{\mu} \to \partial_{\mu} - \frac{ie}{\hbar} A_{\mu}(x)$, (E.29)

which leads to the Lagrangian density in the presence of an electromagnetic field

$$\mathcal{L}(x) = \hat{\psi}^{\dagger}(x) \left(c \alpha^{\mu} p_{\mu} - \beta m_{e} c^{2} + e c \alpha^{\mu} A_{\mu}(x) \right) \hat{\psi}(x). \tag{E.30}$$

This gives the the corresponding Hamiltonian density

$$\mathcal{H}(x) = \hat{\psi}^{\dagger}(x) \left(-c \alpha^{\mu} p_{\mu} + \beta m_{e} c^{2} - e c \alpha^{\mu} A_{\mu}(x) \right) \hat{\psi}(x), \tag{E.31}$$

where the last term represents the interaction density

$$\mathcal{H}_{int}(x) = -\hat{\psi}^{\dagger}(x) e c \alpha^{\mu} A_{\mu}(x) \hat{\psi}(x).$$
 (E.32)

The corresponding Hamilton operator can then be expressed as

$$\hat{H} = \int d^3 x_1 \, \hat{\psi}^{\dagger}(x_1) \left(-c \, \alpha^{\mu} p_{\mu} + \beta m_{e} c^2 - e c \alpha^{\mu} A_{\mu}(x) \right) \hat{\psi}(x_1). \quad (E.33)$$

References

- 1. Mandl, F., Shaw, G.: Quantum Field Theory. John Wiley and Sons, New York (1986)
- 2. Schiff, L.I.: Quantum Mechanics. McGraw-Hill Book Co, N.Y. (1955)

Appendix F

Semiclassical Theory of Radiation

F.1 Classical Electrodynamics

F.1.1 Maxwell's Equations in Covariant Form

The Maxwell equations in vector form are¹

$$\nabla \cdot E = \rho/\epsilon_0, \tag{F.1a}$$

$$\nabla \times \mathbf{B} = \frac{1}{c^2} \frac{\partial \mathbf{E}}{\partial t} + \mu_0 \, \mathbf{j} \,, \tag{F.1b}$$

$$\nabla \cdot \mathbf{B} = 0, \tag{F.1c}$$

$$\nabla \times \mathbf{E} + \frac{\partial \mathbf{B}}{\partial t} = 0, \tag{F.1d}$$

where ρ is the electric charge density and j the electric current density. Equation (F.1c) gives

$$\boldsymbol{B} = \nabla \times \boldsymbol{A},\tag{F.2}$$

where A is the *vector potential*. From (F.1d), it follows that the electric field is of the form

$$E = -\frac{\partial A}{\partial t} - \nabla \phi, \tag{F.3}$$

where ϕ is the *scalar potential*. The (F.1a) and (F.1b) give together with (F.3) and (F.2)

$$-\nabla^{2}\phi - \frac{\partial}{\partial t}\nabla \cdot \mathbf{A} = \rho/\epsilon_{0} = c\,\mu_{0}\,j^{0}$$

$$\left(\nabla^{2}\mathbf{A} - \frac{1}{c^{2}}\frac{\partial^{2}\mathbf{A}}{\partial^{2}t}\right) - \nabla\left(\nabla \cdot \mathbf{A} + \frac{1}{c^{2}}\frac{\partial\phi}{\partial t}\right) = -\mu_{0}\,\mathbf{j} \tag{F.4}$$

¹ As in the previous Appendices, the formulas are here given in a complete form and valid in any consistent unit system, like the SI system (see Appendix K).

using the vector identity $\nabla \times (\nabla \times A) = \nabla (\nabla \cdot A) - \nabla^2 A$. Here, $j^0 = c\rho$ (with $\epsilon_0 \mu_0 = c^{-2}$) is the *scalar or "time-like"* part of the four-dimensional current density

$$j = j^{\mu} = (c\rho, \boldsymbol{j}), \tag{F.5}$$

where the vector part is the three-dimensional current density j. Similarly, the four-dimensional vector potential

$$A^{\mu} = (\phi/c, A)$$
 $A_{\mu} = (\phi/c, -A)$ (F.6)

has the scalar part ϕ/c and the vector part A. With the d'Alambertian operator (A.10), these equations can be expressed as²

$$\Box \phi - \frac{\partial}{\partial t} (\nabla A) = c \mu_0 j^0, \tag{F.7}$$

$$\Box A + \nabla (\nabla A) = \mu_0 \, \boldsymbol{j} \,, \tag{F.8}$$

which leads to Maxwell's equations in covariant form

$$\Box A - \nabla(\nabla A) = \mu_0 j$$
 (F.9)

or

$$\partial_{\nu}\partial^{\nu}A^{\mu} - \partial^{\mu}(\partial_{\nu}A^{\nu}) = \mu_0 j^{\mu}. \tag{F.10}$$

F.1.1.1 Electromagnetic-Field Lagrangian

We introduce the field tensor [2, Eq. 5.5]

$$F^{\mu\nu} = \partial^{\nu} A^{\mu} - \partial^{\mu} A^{\nu}. \tag{F.11}$$

Then we find for instance

$$F^{01} = \partial^1 A^0 - \partial^0 A^1 = \frac{\partial \phi/c}{\partial x} - \frac{\partial A_x}{\partial ct} = E_x,$$

$$F^{12} = \partial^2 A^1 - \partial^1 A^2 = \frac{\partial A_x}{\partial y} - \frac{\partial A_y}{\partial x} = B_z,$$

etc., leading to the matrix

$$F^{\mu\nu} = \begin{pmatrix} 0 & E_x/c & E_y/c & E_y/c \\ -E_x/c & 0 & B_x & -B_z \\ E_y/c & -B_z & 0 & B_x \\ -E_z & B_x & -B_x & 0 \end{pmatrix}.$$
 (F.12)

² Concerning covariant notations, see Appendix A.1.

The Maxwell equations (F.10) can now be expressed as [2, Eq. 5.2]

$$\partial_{\nu}F^{\mu\nu} = \mu_0 j^{\mu} \tag{F.13}$$

using the identity

$$\partial_{\nu}\partial^{\mu}A^{\mu} \equiv \partial^{\mu}\partial_{\nu}A^{\mu}.$$

With $\phi_r = A_\mu$, the Euler-Lagrange equations (E.20) become

$$\frac{\partial \mathcal{L}}{\partial A_{\mu}} - \partial_{\nu} \frac{\partial \mathcal{L}}{\partial (\partial_{\nu} A_{\mu})} = 0.$$
 (F.14)

Using the field tensor (F.11) and the form of the metric tensor (A.5), we have

$$F_{\mu\nu}F^{\mu\nu} = (\partial_{\nu}A_{\mu} - \partial_{\mu}A_{\nu})(\partial^{\nu}A^{\mu} - \partial^{\mu}A^{\nu})$$

= $(\partial_{\nu}A_{\mu} - \partial_{\mu}A_{\nu})(g^{\nu\sigma}\partial_{\sigma}g^{\mu\pi}A_{\pi} - g^{\mu\sigma}\partial_{\sigma}g^{\nu\pi}A_{\pi}).$ (F.15)

Here, μ and ν are running indices that are summed over, and we can replace them with μ' and ν' , respectively. The derivative with respect to fixed μ and ν then gives

$$\frac{\partial}{\partial(\partial_{\nu}A_{\mu})}F_{\mu'\nu'}F^{\mu'\nu'} = F^{\mu\nu} - F^{\nu\mu} + F_{\mu'\nu'}g^{\nu'\nu}g^{\mu'\mu} - F_{\nu'\mu'}g^{\mu'\nu}g^{\nu'\mu} = 4F^{\mu\nu}.$$
(F.16)

We then find that with the Lagrangian

$$\mathcal{L} = -\frac{1}{4\mu_0} F_{\mu\nu} F^{\mu\nu} - j^{\mu} A_{\mu}, \tag{F.17}$$

the Euler–Lagrange equations (F.14) lead to the Maxwell equations (F.13). With the same Lagrangian, the conjugate fields (E.21) are

$$\pi^{\mu}(x) = \frac{\partial \mathcal{L}}{\partial \dot{A}_{\mu}} = \frac{1}{c} \frac{\partial \mathcal{L}}{\partial (\partial^{0} A_{\mu})}, \tag{F.18}$$

where the dot represents the time derivative and $\partial^0 = \frac{\partial}{\partial x_0} = \frac{1}{c} \frac{\partial}{\partial t} = \partial_0$. Using the relation (F.16), this yields

$$\pi^{\mu}(x) = -\frac{1}{\mu_0 c} F^{\mu 0}(x). \tag{F.19}$$

The Hamiltonian is given in terms of the Lagrangian by [2, 5.31]

$$H = \int d^3x \, sN\{\pi^{\mu}(x)\dot{A}_{\mu}(x) - \mathcal{L}\},\tag{F.20}$$

where $N\{\}$ represents normal order [1, Chap. 11] (see Sect. 2.2).

F.1.1.2 Lorenz Condition

The Lorenz condition is³

$$\nabla A = \partial_{\mu} A^{\mu} = \nabla \cdot A + \frac{1}{c^2} \frac{\partial \phi}{\partial t} = 0$$
 (F.21)

and with this condition the Maxwell equations get the simple form

$$\Box A = \mu_0 j.$$
 (F.22)

Then also the electromagnetic fields have particularly simple form, given in (G.2).

F.1.1.3 Continuity Equation

Operating on Maxwell's equations (F.9) with ∇ yields:

$$\nabla (\Box A) - \nabla \nabla (\nabla A) = \mu_0 \nabla j.$$

Since $\Box = \nabla^2$ and ∇ commute, this leads to the *continuity equation*

$$\nabla j = \partial_{\mu} j^{\mu} = 0.$$
 (F.23)

F.1.1.4 Gauge Invariance

A general gauge transformation is represented by

$$A \Rightarrow A + \nabla \Lambda,$$
 (F.24)

where Λ is an arbitrary scalar.

Inserted into the Maxwell equations (F.9), this yields:

$$\Box (\nabla \Lambda) - \nabla (\nabla \nabla \Lambda) = \Box (\nabla \Lambda) - \nabla (\Box \Lambda) = 0.$$

which shows that the Maxwell equations are gauge invariant.

³ This condition is named after the Danish physicist Ludvig Lorenz, not to be confused with the more well-known Dutch physicist Hendrik Lorentz.

F.1.2 Coulomb Gauge

F.1.2.1 Transverse and Longitudinal Field Components

The vector part of the electromagnetic field can be separated into *transverse* (divergence-free) and *longitudinal* (rotation-free) components

$$A = A_{\perp} + A_{\parallel}; \qquad \nabla \cdot A_{\perp} = 0; \qquad \nabla \times A_{\parallel} = 0.$$
 (F.25)

The electric field can be similarly separated

$$\mathbf{E} = \mathbf{E}_{\perp} + \mathbf{E}_{\parallel}; \qquad \mathbf{E}_{\perp} = -\frac{\partial \mathbf{A}_{\perp}}{\partial t}; \qquad \mathbf{E}_{\parallel} = -\frac{\partial \mathbf{A}_{\parallel}}{\partial t} - \nabla \phi,$$

while the magnetic field has only transverse components due to the relation (F.2). The separated field equations (F.4) then become

$$\nabla^2 \phi + \frac{\partial}{\partial t} \nabla \cdot A_{\parallel} = -\rho/\epsilon_0, \tag{F.26a}$$

$$\left(\nabla^{2} A_{\parallel} - \frac{1}{c^{2}} \frac{\partial^{2} A_{\parallel}}{\partial^{2} t}\right) - \nabla \left(\nabla \cdot A_{\parallel} + \frac{1}{c^{2}} \frac{\partial \phi}{\partial t}\right) = -\mu_{0} j_{\parallel}, \tag{F.26b}$$

$$\left(\nabla^2 - \frac{1}{c^2} \frac{\partial^2}{\partial^2 t}\right) \boldsymbol{A}_{\perp} = -\mu_0 \boldsymbol{j}_{\mathrm{T}}.$$
 (F.26c)

The longitudinal and the scalar or "time-like" components (A_{\parallel}, ϕ) represent the *instantaneous Coulomb interaction* and the transverse components (A_{\perp}) represent retardation of this interaction and all magnetic interactions, as well as the *electromagnetic radiation field* (see Sect. F.2.4).

The energy of the electromagnetic field is given by

$$E_{\text{rad}} = \frac{1}{2} \int d^3 x \left[\frac{1}{\mu_0} |\mathbf{B}|^2 + \epsilon_0 |\mathbf{E}|^2 \right]$$
$$= \frac{1}{2} \int d^3 x \left[\frac{1}{\mu_0} |\mathbf{B}|^2 + \epsilon_0 |\mathbf{E}_{\perp}|^2 \right] + \frac{1}{2} \int d^3 x \, \epsilon_0 |\mathbf{E}_{\parallel}|^2. \quad (F.27)$$

The last term represents the energy of the instantaneous Coulomb field, which is normally already included in the hamiltonian of the system. The first term represents the radiation energy.

Semiclassically, only the transverse part of the field is quantized, while the longitudinal part is treated classically [3, Chaps. 2 and 3]. It should be noted that the separation into transverse and longitudinal components is not Lorentz covariant and therefore, strictly speaking, not physically justified, when relativity is taken into account. It can be argued, though, that the separation (as made in the Coulomb gauge) should ultimately lead to the same result as a covariant gauge, when treated properly.

In a fully covariant treatment also the longitudinal component is quantized. The field is then represented by *virtual photons with four directions of polarizations*. A *real photon* can only have *transverse polarizations*.

The *Coulomb gauge* is defined by the condition

$$\nabla \cdot A(x) = 0. \tag{F.28}$$

Using the Fourier transform

$$A(x) = \int d^4k A(k) e^{-ikx}, \qquad (F.29)$$

this condition leads to

$$\frac{\partial A^i}{\partial x^i} = \int d^4k \ A^i(k)(-i)k_i \ e^{-ikx} = 0$$

or

$$\mathbf{A}(k) \cdot \mathbf{k} = 0. \tag{F.30}$$

This is also known as the *transversally condition* and implies that there is *no longitudinal component of A*. Maxwell's equations then reduce to

$$\nabla^2 \phi = -\rho/\epsilon_0. \tag{F.31}$$

This has the solution

$$\phi(x) = \frac{1}{4\pi\epsilon_0} \int d^3x' \frac{\rho(x')}{|x - x'|},$$
 (F.32)

which is the instantaneous Coulomb interaction.

In free space, the scalar potential ϕ can be eliminated by a gauge transformation. Then the Lorenz condition (F.21) is automatically fulfilled in the Coulomb gauge. The field equation (F.4) then becomes

$$\nabla^2 A - \frac{1}{c^2} \frac{\partial^2 A}{\partial^2 t} = 0. \tag{F.33}$$

The relativistic interaction with an atomic electron (D.41) is then in the Coulomb gauge given by

$$H_{\rm int} = ec \,\alpha \cdot A \, \, (\text{F.34})$$

and in second quantization (see Appendix B)

$$\hat{H}_{\text{int}} = \sum_{ij} c_j^{\dagger} \langle i | ec \, \alpha \cdot A_{\perp} | j \rangle \, c_j, \tag{F.35}$$

where c^{\dagger} , c represent creation/annihilation operators for electrons. In the *interaction picture*, this becomes

$$\hat{H}_{\text{int,I}}(t) = \sum_{ij} c_i^{\dagger} \langle i | ec \, \alpha \cdot A_{\perp} | j \rangle \, c_j \, e^{i(\varepsilon_i - \varepsilon_j)t/\hbar}. \tag{F.36}$$

F.2 Quantized Radiation Field

F.2.1 Transverse Radiation Field

Classically the transverse components of the radiation field can be represented by the vector potential [3, Eq. 2.14]

$$A(x,t) = \sum_{k} \sum_{p=1}^{2} \left[c_{kp} \, \boldsymbol{\varepsilon}_{p} \, e^{i(k \cdot x - \omega t)} + c_{kp}^{*} \, \boldsymbol{\varepsilon}_{p} \, e^{-i(k \cdot x - \omega t)} \right], \tag{F.37}$$

where k is the wave vector, $\omega = c|k|$ the frequency, and c_{kp}/c_{kp}^* represents the amplitude of the wave with a certain k vector and a certain polarization ε_p . The energy of this radiation can be shown to be equal to [3, p.22]

$$E_{\text{rad}} = 2\epsilon_0 \sum_{kp} \omega^2 c_{kp}^* c_{kp} = \epsilon_0 \sum_{kp} \omega^2 \left(c_{kp}^* c_{kp} + c_{kr} c_{kp}^* \right).$$
 (F.38)

By making the substitution

$$c_{kp} \to \sqrt{\frac{\hbar}{2\epsilon_0 \, \omega V}} \, a_{kp} \quad \text{and} \quad c_{kp}^* \to \sqrt{\frac{\hbar}{2\epsilon_0 \, \omega V}} \, a_{kp}^{\dagger},$$

where a_{kp}^{\dagger} , $/a_{kp}$ are photon creation/annihilation operators, the radiation energy goes over into the hamiltonian of a collection of harmonic oscillators

$$H_{\text{harm.osc}} = \frac{1}{2} \sum_{kp} \hbar \omega \left(a_{kp} \, a_{kp}^{\dagger} + a_{kp}^{\dagger} \, a_{kp} \right).$$

Therefore, we can motivate that the quantized *transverse* radiation field can be represented by the operator [3, Eq. 2.60]

$$A_{\perp}(\mathbf{x},t) = \sum_{k} \sqrt{\frac{\hbar}{2\epsilon_0 \omega V}} \sum_{p=1}^{2} \left[a_{kp} \, \boldsymbol{\varepsilon}_p \, \mathrm{e}^{i(k \cdot \mathbf{x} - \omega t)} + a_{kp}^{\dagger} \, \boldsymbol{\varepsilon}_p \, \mathrm{e}^{-i(k \cdot \mathbf{x} - \omega t)} \right]. \quad (\text{F.39})$$

F.2.2 Breit Interaction

The exchange of a single transverse photon between two electrons is illustrated by the time-ordered diagram (left) in Fig. F.1, where one photon is *emitted* at the time t_1 and *absorbed* at a later time t_2 . The second-order *evolution operator* for this process, using the interaction picture, is given by (see Sect. 3.1)

$$U_{\gamma}^{(2)}(0, -\infty) = \left(\frac{-\mathrm{i}}{\hbar}\right)^2 \int_{-\infty}^0 \mathrm{d}t_2 \, \hat{H}_{\text{int,I}}(t_2) \int_{-\infty}^0 \mathrm{d}t_1 \, \hat{H}_{\text{int,I}}(t_1) \, \mathrm{e}^{\gamma(t_1 + t_2)}, \quad (F.40)$$

where γ is the parameter for the *adiabatic damping* of the perturbation. The interaction Hamiltonians are in the Coulomb gauge given by (F.36) with the vector potential (F.39)

$$\hat{H}_{\text{int,I}}(t_{1}) = \sum_{k_{1}} \sqrt{\frac{\hbar}{2\epsilon_{0}\omega_{1}V}} \sum_{p_{1}=1}^{2} c_{r}^{\dagger} \left\langle r \left| \left(a_{kp}^{\dagger} e c \, \boldsymbol{\alpha} \cdot \boldsymbol{\varepsilon}_{kp} \, e^{-ik \cdot x} \right)_{1} \right| a \right\rangle \right. \\
\left. \times c_{a} \, e^{-it_{1}(\varepsilon_{a} - \varepsilon_{p} - \hbar\omega_{1})/\hbar}, \right. \\
\hat{H}_{\text{int,I}}(t_{2}) = \sum_{k_{2}} \sqrt{\frac{\hbar}{2\epsilon_{0}\omega_{2}V}} \sum_{p_{2}=1}^{2} c_{s}^{\dagger} \left\langle r \left| \left(a_{kp} \, e c \, \boldsymbol{\alpha} \cdot \boldsymbol{\varepsilon}_{kp} \, e^{ik \cdot x} \right)_{2} \right| a \right\rangle \\
\left. \times c_{b} \, e^{-it_{2}(\varepsilon_{b} - \varepsilon_{s} + \hbar\omega_{2})/\hbar}, \right. \tag{F.41}$$

which leads to the evolution operator

$$U_{\gamma}^{(2)}(0, -\infty) = -c_{r}^{\dagger} c_{a} c_{s}^{\dagger} c_{b} \sum_{k} \frac{e^{2} c^{2}}{2 \hbar \epsilon_{0} V \sqrt{\omega_{1} \omega_{2}}} \times \sum_{p_{1} p_{2}} \langle rs | (a_{kp} \alpha \cdot \varepsilon_{p} e^{ik \cdot x})_{2} (a_{kp}^{\dagger} \alpha \cdot \varepsilon_{p} e^{-ik \cdot x})_{1} | ab \rangle \times I,$$
(F.42)

where I is the time integral. The *contraction* between the creation and annihilation operators (G.10) yields ($\omega = \omega_1 = \omega_2$)

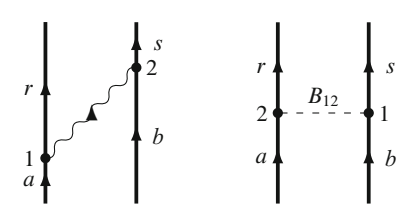


Fig. F.1 Diagrammatic representation of the exchange of a single, transverse photon between two electrons (*left*). This is equivalent to a potential (Breit) interaction (*right*)

$$\sum_{p_1 p_2} \langle rs | (a_{kp} \boldsymbol{\alpha} \cdot \boldsymbol{\varepsilon}_p e^{ik \cdot x})_2 (a_{kp}^{\dagger} \boldsymbol{\alpha} \cdot \boldsymbol{\varepsilon}_p e^{-ik \cdot x})_1 | ab \rangle$$

$$= \sum_{p=1}^2 \langle rs | (\boldsymbol{\alpha} \cdot \boldsymbol{\varepsilon}_p)_2 (\boldsymbol{\alpha} \cdot \boldsymbol{\varepsilon}_p)_1 e^{-ik \cdot r_{12}} \qquad (r_{12} = x_1 - x_2). \quad (F.43)$$

The time integral in (F.42) is

$$I = \int_{-\infty}^{0} dt_2 e^{-it_2(\varepsilon_b - \varepsilon_s + \hbar\omega + i\gamma)/\hbar} \int_{-\infty}^{t_2} dt_1 e^{-it_1(\varepsilon_a - \varepsilon_r - \hbar\omega + i\gamma)/\hbar}$$

$$= -\frac{1}{(cq + cq' + 2i\gamma)(cq - \omega + i\gamma)}$$
(F.44)

with $cq = (\varepsilon_a - \varepsilon_r)/\hbar$ and $cq' = (\varepsilon_b - \varepsilon_s)/\hbar$.

The result of the opposite time ordering $t_1 > t_2$ is obtained by the exchange $1 \leftrightarrow 2$ ($r_{12} \leftrightarrow -r_{12}$), $a \leftrightarrow b$, and $r \leftrightarrow s$, and the total evolution operator, including both time-orderings, can be expressed as

$$U_{\gamma}^{(2)}(0, -\infty) = c_r^{\dagger} c_a c_s^{\dagger} c_b \frac{e^2 c^2}{2\hbar \epsilon_0 \omega V} \sum_{k} \sum_{p=1}^{2} \langle rs | (\boldsymbol{\alpha} \cdot \boldsymbol{\varepsilon}_p)_1 (\boldsymbol{\alpha} \cdot \boldsymbol{\varepsilon}_p)_2 \mathcal{M} | ab \rangle$$
(F.45)

with

$$\mathcal{M} = \frac{e^{-i\boldsymbol{k}\cdot\boldsymbol{r}_{12}}}{(cq + cq' + 2i\gamma)(cq - \omega + i\gamma)} + \frac{e^{i\boldsymbol{k}\cdot\boldsymbol{r}_{12}}}{(cq + cq' + 2i\gamma)(cq' - \omega + i\gamma)}.$$
(F.46)

This can be compared with the evolution operator corresponding to a *potential interaction* B_{12} between the electrons, as illustrated in the right diagram of Fig. F.1,

$$U_{\eta}^{(2)}(0, -\infty) = c_r^{\dagger} c_a c_s^{\dagger} c_b \langle rs|B_{12}|ab\rangle \left(\frac{-\mathrm{i}}{\hbar}\right) \int_{-\infty}^{0} \mathrm{d}t \, \mathrm{e}^{-\mathrm{i}t(\varepsilon_a + \varepsilon_b - \varepsilon_r - \varepsilon_s + \mathrm{i}\eta)/\hbar}$$

$$= \frac{c_r^{\dagger} c_a c_s^{\dagger} c_b}{\hbar} \frac{\langle rs|B_{12}|ab\rangle}{c_q + c_{q'} + \mathrm{i}\eta}. \tag{F.47}$$

Identification then leads to

$$B_{12} = \frac{e^2 c^2}{2\epsilon_0 \omega V} \sum_{kp} (\boldsymbol{\alpha} \cdot \boldsymbol{\varepsilon}_p)_1 (\boldsymbol{\alpha} \cdot \boldsymbol{\varepsilon}_p)_2 \left[\frac{e^{-i\boldsymbol{k} \cdot \boldsymbol{r}_{12}}}{cq - \omega + i\gamma} + \frac{e^{i\boldsymbol{k} \cdot \boldsymbol{r}_{12}}}{cq' - \omega + i\gamma} \right]. \quad (F.48)$$

We assume now that *energy is conserved* by the interaction, i.e.,

$$\varepsilon_a - \varepsilon_r = \varepsilon_s - \varepsilon_b$$
 or $q + q' = 0$. (F.49)

It is found that the sign of the imaginary part of the exponent is immaterial (see Appendix J.2), and the equivalent interaction then becomes

$$B_{12} = \frac{e^2}{\epsilon_0 V} \sum_{kp} (\boldsymbol{\alpha} \cdot \boldsymbol{\varepsilon}_p)_1 (\boldsymbol{\alpha} \cdot \boldsymbol{\varepsilon}_p)_2 \frac{e^{\mathrm{i} \boldsymbol{k} \cdot \boldsymbol{r}_{12}}}{q^2 - k^2 + \mathrm{i} \gamma}$$
 (F.50)

with $\omega = ck$.

The ε_p vectors are orthogonal unit vectors, which leads to [3, Eq. 4.312]

$$\sum_{p=1}^{3} (\boldsymbol{\alpha} \cdot \boldsymbol{\varepsilon}_{p})_{1} (\boldsymbol{\alpha} \cdot \boldsymbol{\varepsilon}_{p})_{2} = \boldsymbol{\alpha}_{1} \cdot \boldsymbol{\alpha}_{2}. \tag{F.51}$$

This gives

$$\sum_{p=1}^{2} (\boldsymbol{\alpha} \cdot \boldsymbol{\varepsilon}_{p})_{1} (\boldsymbol{\alpha} \cdot \boldsymbol{\varepsilon}_{p})_{2} = \boldsymbol{\alpha}_{1} \cdot \boldsymbol{\alpha}_{2} - (\boldsymbol{\alpha}_{1} \cdot \hat{\boldsymbol{k}}) (\boldsymbol{\alpha}_{2} \cdot \hat{\boldsymbol{k}})$$
 (F.52)

assuming $\epsilon_3 = \hat{k}$ to be the unit vector in the k direction. The interaction (F.50) then becomes in the limit of continuous momenta (Appendix D)

$$B_{12} = \frac{e^2}{\epsilon_0} \int \frac{\mathrm{d}^3 \mathbf{k}}{(2\pi)^3} \left[\boldsymbol{\alpha}_1 \cdot \boldsymbol{\alpha}_2 - (\boldsymbol{\alpha}_1 \cdot \hat{\mathbf{k}})(\boldsymbol{\alpha}_2 \cdot \hat{\mathbf{k}}) \right] \frac{\mathrm{e}^{\mathrm{i} \mathbf{k} \cdot \mathbf{r}_{12}}}{q^2 - k^2 + \mathrm{i} \gamma}. \tag{F.53}$$

With the Fourier transforms in Appendix J, this yields the **retarded Breit interaction**

$$B_{12}^{\text{Ret}} = -\frac{e^2}{4\pi\epsilon_0} \left[\alpha_1 \cdot \alpha_2 \frac{e^{i|q|r_{12}}}{r_{12}} - (\alpha_1 \cdot \nabla_1)(\alpha_2 \cdot \nabla_2) \frac{e^{i|q|r_{12}} - 1}{q^2 r_{12}} \right].$$
 (F.54)

Setting q = 0, we obtain the instantaneous Breit interaction (real part)

$$B_{12}^{\text{Inst}} = -\frac{e^2}{4\pi\epsilon_0} \left[\frac{\alpha_1 \cdot \alpha_2}{r_{12}} + \frac{1}{2} (\alpha_1 \cdot \nabla_1) (\alpha_2 \cdot \nabla_2) r_{12} \right]$$

or using

$$(\boldsymbol{\alpha}_1 \cdot \nabla_1)(\boldsymbol{\alpha}_2 \cdot \nabla_2) \, r_{12} = -\frac{\boldsymbol{\alpha}_1 \cdot \boldsymbol{\alpha}_2}{r_{12}} + \frac{(\boldsymbol{\alpha}_1 \cdot \boldsymbol{r}_{12})(\boldsymbol{\alpha}_1 \cdot \boldsymbol{r}_{12})}{r_{12}^2},$$

we arrive at

$$B_{12}^{\text{Inst}} = -\frac{e^2}{4\pi\epsilon_0 r_{12}} \left[\frac{1}{2} \alpha_1 \cdot \alpha_2 + \frac{(\alpha_1 \cdot r_{12})(\alpha_1 \cdot r_{12})}{2r_{12}} \right], \quad (F.55)$$

which is the standard form of the **instantaneous Breit interaction**.

F.2.3 Transverse Photon Propagator

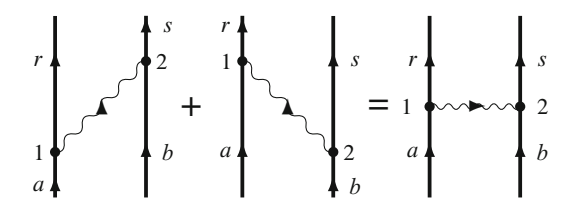


Fig. F.2 The two time-orderings of a single-photon exchange can be represented by a single Feynman diagram

We shall now consider both time-orderings of the interaction represented in Fig. F.2 simultaneously. The evolution operator can then be expressed as

$$U_{\gamma}^{(2)}(0, -\infty) = \left(\frac{-\mathrm{i}}{\hbar}\right)^2 \int_{-\infty}^0 \mathrm{d}t_2 \int_{-\infty}^0 \mathrm{d}t_1 \, T\left[\hat{H}_{\mathrm{int,I}}(t_2) \, \hat{H}_{\mathrm{int,I}}(t_1)\right] \, \mathrm{e}^{-\gamma(|t_1|+|t_2|)},\tag{F.56}$$

where

$$T\left[\hat{H}_{\text{int,I}}(t_2)\,\hat{H}_{\text{int,I}}(t_1)\right] = \begin{cases} \hat{H}_{\text{int,I}}(t_2)\,\hat{H}_{\text{int,I}}(t_1) & t_2 > t_1\\ & . \end{cases}$$

$$\hat{H}_{\text{int,I}}(t_1)\,\hat{H}_{\text{int,I}}(t_2) & t_1 > t_2$$
(F.57)

In the Coulomb gauge, the interaction is given by (F.36) and the vector potential is given by (F.39). The evolution operator for the combined interactions will then be

$$U_{\gamma}^{(2)}(0,-\infty) = -c_r^{\dagger} c_a c_s^{\dagger} c_b \frac{e^2 c^2}{\hbar^2} \int_{-\infty}^{0} dt_2 \int_{-\infty}^{0} dt_1 T \left[(\boldsymbol{\alpha} \cdot \boldsymbol{A}_{\perp})_1 (\boldsymbol{\alpha} \cdot \boldsymbol{A}_{\perp})_2 \right] \times e^{-it_1(\varepsilon_a - \varepsilon_r + i\gamma)/\hbar} e^{-it_2(\varepsilon_b - \varepsilon_s + i\gamma)/\hbar}. \tag{F.58}$$

Here

$$\begin{split} T\left[(\boldsymbol{\alpha} \cdot \boldsymbol{A}_{\perp})_{1} \left(\boldsymbol{\alpha} \cdot \boldsymbol{A}_{\perp} \right)_{2} \right] &= \sum_{kp} \frac{\hbar}{2\omega\epsilon_{0}V} \left(\boldsymbol{\alpha} \cdot \boldsymbol{\varepsilon}_{p} \right)_{1} (\boldsymbol{\alpha} \cdot \boldsymbol{\varepsilon}_{p})_{2} \\ &\times \begin{cases} \mathrm{e}^{-\mathrm{i}(k_{1} \cdot x_{1} - \omega t_{1})} \, \mathrm{e}^{\mathrm{i}(k_{2} \cdot x_{2} - \omega t_{2})} \, t_{2} > t_{1} \\ \mathrm{e}^{-\mathrm{i}(k_{2} \cdot x_{2} - \omega t_{2})} \, \mathrm{e}^{\mathrm{i}(k_{1} \cdot x_{1} - \omega t_{1})} \, t_{1} > t_{2} \end{split}$$

or with $r_{12} = x_1 - x_2$ and $t_{12} = t_1 - t_2$

$$T\left[(\boldsymbol{\alpha} \cdot \boldsymbol{A}_{\perp})_{1} (\boldsymbol{\alpha} \cdot \boldsymbol{A}_{\perp})_{2} \right] = \frac{\hbar}{\epsilon_{0}} \sum_{p=1}^{2} (\boldsymbol{\alpha} \cdot \boldsymbol{\varepsilon}_{p})_{1} (\boldsymbol{\alpha} \cdot \boldsymbol{\varepsilon}_{p})_{2} \frac{1}{V} \sum_{k} \frac{e^{\mp i(\boldsymbol{k} \cdot \boldsymbol{r}_{12} - \omega t_{12})}}{2\omega}, \tag{F.59}$$

where the upper sign is valid for $t_2 > t_1$. This yields

$$U_{\gamma}^{(2)}(0, -\infty) = -c_{r}^{\dagger} c_{a} c_{s}^{\dagger} c_{b} \frac{e^{2} c^{2}}{\epsilon_{0} \hbar^{2}} \int_{-\infty}^{0} dt_{2} \int_{-\infty}^{0} dt_{1} \sum_{p=1}^{2} (\boldsymbol{\alpha} \cdot \boldsymbol{\varepsilon}_{p})_{1} (\boldsymbol{\alpha} \cdot \boldsymbol{\varepsilon}_{p})_{2}$$

$$\times \left[\frac{1}{V} \sum_{k} \frac{e^{\mp i(k \cdot r_{12} - \omega t_{12})}}{2\omega} \right] e^{-icq t_{12}} e^{\gamma(t_{1} + t_{2})}$$
(F.60)

using the energy conservation (F.49).

The boxed part of the equation above is essentially the **photon propagator** (4.23)

$$D_{\rm F}(1,2) = \frac{1}{V} \sum_{k} \frac{e^{\mp i(k \cdot r_{12} - \omega t_{12})}}{2\omega} \implies \int \frac{d^3k}{(2\pi)^3} \frac{e^{\mp i(k \cdot r_{12} - \omega t_{12})}}{2\omega}.$$
 (F.61)

This can be represented by a complex integral

$$D_{\rm F}(1,2) = i \int \frac{\mathrm{d}^3 \mathbf{k}}{(2\pi)^3} \int \frac{\mathrm{d}z}{2\pi} \, \frac{\mathrm{e}^{\mathrm{i}zt_{12}}}{z^2 - \omega^2 + \mathrm{i}\eta} \, \mathrm{e}^{\mathrm{i}\mathbf{k} \cdot \mathbf{r}_{12}}, \tag{F.62}$$

where η is a small, positive quantity. As before, the sign of the exponent $i\mathbf{k} \cdot \mathbf{r}_{12}$ is immaterial. The integrand has poles at $z = \pm (\omega - i\eta)$, assuming ω to be positive. For $t_2 > t_1$, integration over the *negative* half plane yields $\frac{1}{2\omega} e^{i\omega t_{12}} e^{i\mathbf{k}\cdot\mathbf{r}_{12}}$ and for $t_1 > t_2$ integration over the *positive* half plane yields $\frac{1}{2\omega} e^{-i\omega t_{12}} e^{i\mathbf{k}\cdot\mathbf{r}_{12}}$, which is identical to (F.61). The evolution operator (F.60) can then be expressed as

$$U_{\gamma}^{(2)}(0,-\infty) = -c_r^{\dagger} c_a c_s^{\dagger} c_b \frac{e^2 c^2}{\epsilon_0 \hbar} \int_{-\infty}^{0} dt_2 \int_{-\infty}^{0} dt_1$$

$$\times \sum_{p=1}^{2} (\boldsymbol{\alpha} \cdot \boldsymbol{\varepsilon}_p)_1 (\boldsymbol{\alpha} \cdot \boldsymbol{\varepsilon}_p)_2 D_{F}(1,2) e^{-icq t_{12}/\hbar} e^{\gamma (t_1 + t_2)\hbar}.$$
(F.63)

F.2.4 Comparison with the Covariant Treatment

It is illuminating to compare the quantization of the transverse photons with the fully covariant treatment, to be discussed in the next chapter. Then we simply have to replace the sum in (F.42) by the corresponding covariant expression

$$\sum_{p_1 p_2=1}^{2} (a_{kp} \boldsymbol{\alpha} \cdot \boldsymbol{\varepsilon}_p)_1 (a_{kp}^{\dagger} \boldsymbol{\alpha} \cdot \boldsymbol{\varepsilon}_p)_2 \Rightarrow \sum_{p_1 p_2=0}^{3} (a_{kp} \alpha^{\mu} \varepsilon_{\mu p})_1 (a_{kp}^{\dagger} \alpha^{\nu} \varepsilon_{\nu p})_2.$$
(F.64)

The commutation relation (G.10) yields

$$\sum_{p_1 p_2 = 0}^{3} (a_{kp} \, \alpha^{\mu} \varepsilon_{\mu p})_1 \, (a_{kp}^{\dagger} \, \alpha^{\nu} \varepsilon_{\nu p})_2 = \alpha_1 \cdot \alpha_2 - 1.$$
 (F.65)

We then find that the equivalent potential interaction (F.50) under energy conservation is replaced by

$$V_{12} = -\frac{e^2}{\epsilon_0} \int \frac{\mathrm{d}^3 \mathbf{k}}{(2\pi)^3} (1 - \alpha_1 \cdot \alpha_2) \frac{\mathrm{e}^{\mathrm{i} \mathbf{k} \cdot \mathbf{r}_{12}}}{q^2 - k^2 + \mathrm{i}\gamma}$$
 (F.66)

and with the Fourier transform given in Appendix J.2

$$V_{12} = \frac{e^2}{4\pi\epsilon_0 r_{12}} (1 - \alpha_1 \cdot \alpha_2) e^{i|q|r_{12}}.$$
 (F.67)

We shall now compare this with the exchange of *transverse* photons, treated above. We then make the decomposition

$$1 - \alpha_1 \cdot \alpha_2 = \begin{cases} 1 - (\alpha_1 \cdot \hat{k})(\alpha_2 \cdot \hat{k}) \\ -\alpha_1 \cdot \alpha_2 + (\alpha_1 \cdot \hat{k})(\alpha_2 \cdot \hat{k}) \end{cases}$$
 (F.68)

The last part, which represents the exchange of *transverse* photons, is identical to (F.52), which led to the Breit interaction. The first part, which represents the exchange of *longitudinal and scalar* photons, corresponds to the interaction

$$V_{\rm C} = -\frac{e^2}{\epsilon_0} \int \frac{\mathrm{d}^3 \mathbf{k}}{(2\pi)^3} \left[1 - (\alpha_1 \cdot \hat{\mathbf{k}})(\alpha_2 \cdot \hat{\mathbf{k}}) \right] \frac{\mathrm{e}^{\mathrm{i} \mathbf{k} \cdot \mathbf{r}_{12}}}{q^2 - k^2 + \mathrm{i}\gamma}. \tag{F.69}$$

This Fourier transform is evaluated in Appendix J.3 and yields

$$V_{\rm C} = -\frac{e^2}{\epsilon_0} \int \frac{\mathrm{d}^3 \mathbf{k}}{(2\pi)^3} \left(1 - \frac{q^2}{k^2} \right) \frac{\mathrm{e}^{\mathrm{i} \mathbf{k} \cdot \mathbf{r}_{12}}}{q^2 - k^2 + \mathrm{i} \gamma} = \frac{e^2}{\epsilon_0} \int \frac{\mathrm{d}^3 \mathbf{k}}{(2\pi)^3} \frac{\mathrm{e}^{\mathrm{i} \mathbf{k} \cdot \mathbf{r}_{12}}}{k^2 - \mathrm{i} \gamma}$$
(F.70)

provided that the orbitals are generated in a **local potential**. Using the transform in Appendix J.2, this becomes

$$V_{\text{Coul}} = \frac{e^2}{4\pi\epsilon_0 \, r_{12}}.\tag{F.71}$$

Thus, we see that the exchange of longitudinal and scalar photons corresponds to the instantaneous Coulomb interaction, while the exchange of the transverse photons corresponds to the Breit interaction. Note that this is true only if the orbitals are generated in a local potential.

If instead of the separation (F.68), we would separate the photons into the scalar part (p = 0) and the vector part (p = 1, 2, 3),

$$1 - \boldsymbol{\alpha}_1 \cdot \boldsymbol{\alpha}_2 = \begin{cases} 1 \\ -\boldsymbol{\alpha}_1 \cdot \boldsymbol{\alpha}_2 \end{cases}$$
 (F.72)

then the result would be

$$\begin{split} V_{\text{Coul}}^{\text{Ret}} &= \frac{e^2}{4 \text{i} \epsilon_0 \, r_{12}} \, \text{e}^{\text{i} |q| r_{12}}, \\ V_{\text{Gaunt}}^{\text{Ret}} &= -\frac{e^2}{4 \pi \epsilon_0 \, r_{12}} \, \boldsymbol{\alpha}_1 \cdot \boldsymbol{\alpha}_2 \, \text{e}^{\text{i} |q| r_{12}}, \end{split} \tag{F.73}$$

which represents the *retarded Coulomb and the retarded magnetic (Gaunt) interaction*. This implies that *the longitudinal photon represents the retardation of the Coulomb interaction*, which is included in the Breit interaction (F.54).

If we would set q=0, then we would from (F.73) retrieve the *instantaneous* Coulomb interaction (F.71) and

$$-\frac{e^2}{4\pi\epsilon_0}\,\alpha_1\cdot\alpha_2,\tag{F.74}$$

which is known as the *Gaunt interaction*. The Breit interaction will then turn into the instantaneous interaction (F.55). This will still have some effect of the retardation of the Coulomb interaction, although it is instantaneous.

We shall see later that the interactions (F.73) correspond to the interactions in the Feynman gauge (4.56), while the instantaneous Coulomb and Breit incinerations correspond to the Coulomb gauge.

References

- 1. Lindgren, I., Morrison, J.: *Atomic Many-Body Theory*. Second edition, Springer-Verlag, Berlin (1986, reprinted 2009)
- 2. Mandl, F., Shaw, G.: Quantum Field Theory. John Wiley and Sons, New York (1986)
- 3. Sakurai, J.J.: Advanced Quantum Mechanics. Addison-Wesley Publ. Co., Reading, Mass. (1967)

Appendix G

Covariant Theory of Quantum ElectroDynamics

G.1 Covariant Quantization: Gupta-Bleuler Formalism

With the Lorenz condition (F.21) $\partial_{\mu}A^{\mu}=0$, the Maxwell equations have a particularly simple form (F.22)

$$\Box A = \mu_0 j. \tag{G.1}$$

In this case, the covariant electromagnetic radiation field can be expressed in analogy with the semiclassical expression (F.39) and represented by the four-component vector potential [4, Eq. 5.16]

$$A_{\mu}(x) = A_{\mu}^{+}(x) + A_{\mu}^{-}(x) = \sqrt{\frac{\hbar}{2\omega\epsilon_{0}V}} \sum_{kr} \varepsilon_{\mu r} \left[a_{kr} e^{-ikx} + a_{kr}^{\dagger} e^{ikx} \right].$$
(G.2)

However, different equivalent choices can be made, as further discussed in Sect. G.2. Here, we use the covariant notations

$$k = k^{\mu} = (k_0, \mathbf{k});$$
 $k_0 = \omega/c = |\mathbf{k}|;$ $kx = \omega t - \mathbf{k} \cdot \mathbf{x}$

defined in Appendix A.1, and r = (0, 1, 2, 3) represents the four polarization states. Normally, the polarization vector for r = 3 is defined to be along the k vector – longitudinal component – and for r = 1, 2 to be perpendicular – transverse components. The component r = 0 is referred to as the time-like or scalar component (see Sect. F.1.2).

The electromagnetic fields components are Heisenberg operators and should satisfy the canonical commutation (quantization) rules (E.24) at equal times

$$\left[A_{\mu}(t, \mathbf{x}), \pi^{\nu}(t, \mathbf{x}')\right] = i\hbar \delta_{\mu, \nu} \,\delta^{3}(\mathbf{x} - \mathbf{x}'),\tag{G.3}$$

where $\pi^{\nu}(x)$ is the conjugate field (E.21). With the Lagrangian (F.17) the field π^{0} vanishes according to the relation (F.19), which is inconsistent with the quantization

rule (G.3). In order to remedy the situation, we add a term $-\frac{\lambda}{2\mu_0} (\partial_{\nu} A^{\nu})^2$ to the Lagrangian (F.17), where λ is an arbitrary constant [3, Eq. 1-49, Eq. 3-98]

$$\mathcal{L} = -\frac{1}{4\mu_0} F_{\mu\nu} F^{\mu\nu} - \frac{\lambda}{2\mu_0} (\partial_{\nu} A^{\nu})^2 - j^{\mu} A_{\mu}. \tag{G.4}$$

We can rewrite the extra term as

$$-\frac{\lambda}{2\mu_0} \left(\partial_{\nu} g^{\nu\sigma} A_{\sigma}\right) \left(\partial_{\nu} A^{\nu}\right).$$

Then the conjugate field (F.19) becomes [3, Eq. 3-100]

$$\pi^{\mu}(x) = \frac{\partial \mathcal{L}}{\partial (\partial^0 A_{\mu})} = -\frac{1}{c\mu_0} F^{\mu 0} - \frac{\lambda}{\mu_0} g^{0\mu} \partial_{\nu} A^{\nu} \tag{G.5}$$

and $\pi^0 \neq 0$ for $\lambda \neq 0$.

The extra term in the Euler-Lagrange equations (F.14) leads to

$$\frac{\lambda}{2\mu_0} \partial_{\nu} \frac{\partial}{\partial(\partial_{\nu} A_{\mu})} (\partial_{\nu} g^{\nu\sigma} A_{\sigma}) (\partial_{\nu} A^{\nu}) = \frac{\lambda}{\mu_0} \partial_{\nu} g^{\nu\mu} (\partial_{\sigma} A^{\sigma})
= \frac{\lambda}{\mu_0} \partial_{\mu} g^{\mu\mu} (\partial_{\sigma} A^{\sigma}) = \lambda \partial^{\mu} (\partial_{\sigma} A^{\sigma}).$$

The Maxwell equations (F.10) then take the modified form [3, Eq. 3-99]

$$\partial_{\nu}\partial^{\nu}A^{\mu} - (1 - \lambda)\,\partial^{\mu}(\partial_{\nu}A^{\nu}) = \mu_0 j^{\mu}.\tag{G.6}$$

Setting $\lambda = 1$, we retrieve the same simple form of Maxwell's equations as with the Lorenz condition (G.1) – without introducing this condition explicitly. This is usually referred to as the Feynman gauge.

The Lagrangian (G.4) is incompatible with the Lorenz condition, and to resolve the dilemma this condition is replaced by its expectation value

$$\langle \Psi | \partial_{\mu} A^{\mu} | \Psi \rangle = 0,$$
 (G.7)

which is known as the **Gupta–Bleuler proposal** [4, 5.35].

In the Feynman gauge, the commutation relations (G.3) become [4, 5.23]

$$[A_{\mu}(t, \mathbf{x}), \dot{A}^{\nu}(t, \mathbf{x}')] = ic^{2} \mu_{0} \hbar g_{\mu\nu} \, \delta_{\mu,\nu} \, \delta^{3}(\mathbf{x} - \mathbf{x}'). \tag{G.8}$$

To satisfy this relation, we can assume that the polarization vectors fulfill the orthogonality/completeness relations [4, Eq. 5.18,19]

$$\varepsilon_{\mu r} \varepsilon_{\mu r'} = g_{rr'},$$

$$\sum_{r} g_{rr} \varepsilon_{\mu r} \varepsilon_{\nu r} = g_{\mu \nu},$$
(G.9)

and the photon creation and absorption operators the commutation relation [4, Eq. 5.28]

$$\left[a_{kr}, a_{k'r'}^{\dagger}\right] = -\delta_{k,k'} g_{rr'}. \tag{G.10}$$

Considering that the g-matric (A.5) used is diagonal, this leads to

$$\sum_{rr'} \left[\varepsilon_{\mu r} a_{kr}, \varepsilon_{\nu r'} a_{k'r'}^{\dagger} \right] = \sum_{rr'} \varepsilon_{\mu r} \varepsilon_{\nu r'} \left[a_{kr}, a_{k'r'}^{\dagger} \right] = -g_{\mu,\nu} \delta_{k,k'} \quad (G.11)$$

and then it follows that the field operators (G.2) satisfy the commutation relation (G.8).

With the Lagrangian (G.4) and the conjugate fields (G.5), the Hamiltonian of the free field (F.20) becomes in the Feynman gauge ($\lambda = 1$) [4, Eq. 5.32]

$$H_{\text{Rad}} = -\sum_{k,r} \hbar \omega \, g_{rr} \, a_{kr}^{\dagger} a_{kr}. \tag{G.12}$$

G.2 Gauge Transformation

G.2.1 General

The previous treatment is valid in the Feynman gauge, where the Maxwell equations have the form (G.1), and we shall here investigate how the results will appear in other gauges.

The interaction between an electron and the electromagnetic field is given by the Hamiltonian interaction density (D.41)

$$\mathcal{H}_{\rm int} = j_{\mu} A^{\mu},\tag{G.13}$$

where j_{μ} is the current density. The Maxwell equations are invariant for a gauge transformation (F.24) $A \Rightarrow A + \nabla A$, which transforms this interaction to

$$H_{\rm int} = j_{\mu}A^{\mu} \Rightarrow \left(A^{\mu} + \frac{\partial \Lambda}{\partial x_{\mu}}\right)j_{\mu}.$$

Integration over space leads after partial integration to

$$\int \mathrm{d}^3 x \, \frac{\partial \Lambda}{\partial x_\mu} \, j_\mu = - \int \mathrm{d}^3 x \, \frac{\partial j_\mu}{\partial x_\mu} \, \Lambda = 0.$$

Since Λ is arbitrary, it follows that

$$\frac{\partial j_{\mu}}{\partial x_{\mu}} = \delta^{\mu} j_{\mu} = \nabla j = 0,$$

which is the *continuity equation* (F.23). In analogy with (F.30), the corresponding relation in the k space is

$$j_{\mu}(k) k^{\mu} = 0. {(G.14)}$$

The single-photon exchange is represented by the interaction (4.44)

$$I(x_2, x_1) = e^2 c^2 \alpha_1^{\mu} \alpha_2^{\nu} D_{F\nu\mu}(x_2, x_1), \tag{G.15}$$

which corresponds to the interaction density $j^{\mu}D_{F\nu\mu}j^{\nu}$. In view of the relation (G.14), it follows that the transformation

$$D_{\mathrm{F}\nu\mu}(k) \Rightarrow D_{\mathrm{F}\nu\mu}(k) + k_{\mu} f_{\nu}(k) + k_{\nu} f_{\mu}(k),$$

where $f_{\mu}(k)$ and $f_{\nu}(k)$ are arbitrary functions of k, will leave the interaction unchanged.

G.2.2 Covariant Gauges

In a *covariant gauge*, the components of the electro-magnetic field are expressed in a covariant way. We shall consider three gauges of this kind.

G.2.2.1 Feynman Gauge

The photon propagator in the Feynman gauge is given by the expression (4.28)

$$D_{\mathrm{F}\nu\mu}(k) = -\frac{g_{\mu\nu}}{c\epsilon_0} \frac{1}{k^2 + \mathrm{i}\eta}.\tag{G.16}$$

G.2.2.2 Landau Gauge

With

$$f_{\mu}(k) = \frac{1}{c\epsilon_0} \frac{k_{\mu}}{(k^2 + i\eta)^2},$$

the propagator (G.16) becomes

$$D_{F\mu\nu}(k) = -\frac{1}{c\epsilon_0} \frac{1}{k^2 + i\eta} \left(g_{\mu\nu} - \frac{k_{\mu}k_{\nu}}{k^2 + i\eta} \right). \tag{G.17}$$

This leads to $k^{\mu}D_{F\mu\nu}=0$, which is consistent with the Lorenz condition (F.21)

$$\nabla A = \partial^{\mu} A_{\mu} = 0.$$

G.2.2.3 Fried-Yennie Gauge

With

$$f_{\mu}(k) = \frac{1}{2c\epsilon_0} (1 - \lambda) \frac{k_{\mu}}{(k^2 + i\eta)^2},$$

the propagator (G.16) becomes

$$D_{F\mu\nu}(k) = -\frac{1}{c\epsilon_0} \frac{1}{k^2 + i\eta} \left(g_{\mu\nu} - (1 - \lambda) \frac{k_{\mu}k_{\nu}}{k^2 + i\eta} \right).$$
 (G.18)

With $\lambda=1$, this yields the Feynman gauge, and with $\lambda=0$ we retrieve the Landau gauge. The value $\lambda=3$ yields the Fried-Yennie gauge [2], which has some improved properties, compared to the Feynman gauge, in the infrared region.

G.2.3 Noncovariant Gauge

We consider only one example of a *noncovariant gauge*, the Coulomb gauge, which is of vital importance in treating the combined QED-correlation problem. Here, the Coulomb interaction is treated differently from the transverse part.

G.2.3.1 Coulomb Gauge

With

$$f_0 = \frac{1}{2c\epsilon_0} \frac{1}{k^2 + i\eta} \frac{k_0}{k^2}; \quad f_i = -\frac{1}{2c\epsilon_0} \frac{1}{k^2 + i\eta} \frac{k_i}{k^2} \quad (i = 1, 2, 3),$$

the propagator (G.16) can be expressed as

$$D_{\text{F00}}(k) = \frac{1}{c\epsilon_0} \begin{pmatrix} \frac{1}{k^2} & 0\\ 0 & \frac{1}{k^2 + i\eta} \left(\delta_{i,j} - \frac{k_i k_j}{k^2}\right) \end{pmatrix}, \tag{G.19}$$

where the first row/column corresponds to the component $\mu=0$ and the second row/column to $\mu=1,2,3$.

This leads to $k^i D_{\mathrm{F}ij} = 0$, which is consistent with the Coulomb condition (F.30)

$$\nabla \cdot A = \partial^i A_i = 0 \qquad (i = 1, 2, 3).$$

The formulas above can be generalized to be used in dimensional regularization (see Sect. 12.4), where the number of dimensions is noninteger (mainly from Adikins [1], see also t'Hooft and Veltman [6]).

Following the book by Peskin and Schroeder [5], we can by means of *Wick rotation* evaluate the integral

$$\int \frac{\mathrm{d}^D l}{(2\pi)^D} \frac{1}{(l^2 - \Delta)^m} = \mathrm{i}(-1)^m \int \frac{\mathrm{d}^D l}{(2\pi)^D} \frac{1}{(l_E^2 + \Delta)^m}$$
$$= \mathrm{i}(-1)^m \int \frac{\mathrm{d}\Omega_D}{(2\pi)^4} \int_0^\infty \mathrm{d}l_E^0 \frac{l_E^{D-1}}{(l_E^2 + \Delta)^m}.$$

We have here made the replacements $l^0 = \mathrm{i} l_E^0$ and $l = l_E$ and rotated the integration contour of l_E 90°, which with the positions of the poles should give the same result. The integration over $\mathrm{d}^D l_E$ is separated into an integration over the D-dimensional sphere Ω_D and the linear integration over the component l_E^0 . This corresponds in three dimensions to the integration over the two-dimensional angular coordinates and the radial coordinate (see below).

$$\int \frac{\mathrm{d}^D k}{(2\pi)^D} \frac{1}{(k^2 + s + \mathrm{i}\eta)^n} = \frac{\mathrm{i}(-1)^n}{(4\pi)^{D/2}} \frac{\Gamma(n - D/2)}{\Gamma(n)} \frac{1}{s^{n - D/2}},\tag{G.20}$$

$$\int d^4k \, \frac{k^{\mu}}{(k^2 + s + i\eta)^n} = 0, \tag{G.21}$$

$$\int \frac{\mathrm{d}^D k}{(2\pi)^D} \frac{k^\mu k^\nu}{(k^2 + s + \mathrm{i}\eta)^n} = \frac{\mathrm{i}(-1)^n}{(4\pi)^{D/2}} \frac{\Gamma(n - D/2 - 1)}{\Gamma(n)} \frac{1}{s^{n - D/2 - 1}}.$$
 (G.22)

G.2.3.2 Covariant Gauge

Compared to Adkins [1] (A1a), (A3), and (A5a):

$$p \to -q; \ M^2 \to -s; \ \omega \to D/2; \ \alpha \to n; \ \xi \to n; \ Q = p \to -q; \ A_{\mu\nu} \to g_{\mu\nu};$$

$$\Delta \to w = q^2 - s,$$

$$\int \frac{\mathrm{d}^D k}{(2\pi)^D} \frac{1}{(k^2 + 2kq + s + i\eta)^n} = \frac{\mathrm{i}(-1)^n}{(4\pi)^{D/2}} \frac{1}{\Gamma(n)} \frac{\Gamma(n - D/2)}{w^{n - D/2}}, \quad (G.23)$$

$$\int \frac{\mathrm{d}^D k}{(2\pi)^D} \frac{k^{\mu}}{(k^2 + 2kq + s + \mathrm{i}\eta)^n} = -\frac{\mathrm{i}(-1)^n}{(4\pi)^{D/2}} \frac{1}{\Gamma(n)} q^{\mu} \frac{\Gamma(n - D/2)}{w^{n - D/2}}, \quad (G.24)$$

$$\int \frac{\mathrm{d}^{D}k}{(2\pi)^{D}} \frac{k^{\mu}k^{\nu}}{(k^{2} + 2kq + s + i\eta)^{n}}$$

$$= \frac{\mathrm{i}(-1)^{n}}{(4\pi)^{D/2}} \frac{1}{\Gamma(n)} \left[q^{\mu}q^{\nu} \frac{\Gamma(n - D/2)}{w^{n - D/2}} - \frac{g^{\mu\nu}}{2} \frac{\Gamma(n - 1 - D/2)}{w^{n - 1 - D/2}} \right]. \quad (G.25)$$

G.2.3.3 Noncovariant Gauge

Compared to Adkins [1] (A1b), (A4), and (A5b):

$$p \to -q; M^{2} \to -s; \omega \to D/2; \alpha \to n; \beta \to 1; \xi \to n+1; \mathbf{k}^{2} \to -\mathbf{k}^{2};$$

$$Q = py \to -qy;$$

$$A_{\mu\nu} \to g_{\mu\nu} + \delta_{\mu,0}\delta_{\nu,0}\frac{1-y}{y}; (AQ)_{\mu} \to -q^{\mu}y - \delta_{\mu 0}(1-y)q_{0},$$

$$\Delta \to w = q^{2}y^{2} + (1-y)yq_{0}^{2} - sy + \lambda^{2}(1-y)$$

$$= -\mathbf{q}^{2}y^{2} + yq_{0}^{2} - sy + \lambda^{2}(1-y),$$

$$\int \frac{d^{D}k}{(2\pi)^{D}} \frac{1}{(k^{2} + 2kq + s + i\eta)^{n}} \frac{1}{\mathbf{k}^{2} - \lambda^{2}}$$

$$= \frac{i(-1)^{n}}{(4\pi)^{D/2}} \frac{1}{\Gamma(n+1)} \int_{0}^{1} dy \, y^{n-1-1/2} \frac{\Gamma(n+1-D/2)}{w^{n+1-D/2}}, \quad (G.26)$$

$$\int \frac{d^{D}k}{(2\pi)^{D}} \frac{k^{\mu}}{(k^{2} + 2kq + s + i\eta)^{n}} \frac{1}{\mathbf{k}^{2} - \lambda^{2}}$$

$$= -\frac{i(-1)^{n}}{(4\pi)^{D/2}} \frac{1}{\Gamma(n)} \int_{0}^{1} dy \, y^{n-1-1/2} \left[q^{\mu}y + \delta_{\mu,0} \, q_{0}(1-y)\right] \frac{\Gamma(n+1-D/2)}{w^{n+1-D/2}}, \quad (G.27)$$

$$\not\!k \to -\not\!q y - \gamma^0 q_0 (1 - y) = \gamma \cdot \mathbf{q} y - \gamma^0 q_0,$$

$$\int \frac{d^{D}k}{(2\pi)^{D}} \frac{k^{\mu}k^{\nu}}{(k^{2} + 2kq + s + i\eta)^{n}} \frac{1}{k^{2} - \lambda^{2}}$$

$$= \frac{i(-1)^{n}}{(4\pi)^{D/2}} \frac{1}{\Gamma(n)} \int_{0}^{1} dy \, y^{n-1-1/2} \left[\left\{ \left[q^{\mu}y + \delta_{\mu,0} \, q_{0}(1-y) \right] \right\} \right] \times \left[q^{\nu}y + \delta_{\nu,0} \, q_{0}(1-y) \right] \left\{ \frac{\Gamma(n+1-D/2)}{w^{n+1-D/2}} \right]$$

$$- \frac{1}{2} \left\{ \left[g^{\mu\nu} + \delta_{\mu,0} \delta_{\nu,0} (1-y)/y \right] \right\} \frac{\Gamma(n-D/2)}{w^{n-D/2}} \right]$$
(G.28)

 $\not\!\! k \to \gamma \cdot \mathbf{q} \ y - \gamma^0 q_0 \ \text{in first part and} \not\!\! k \not\!\! k \to -\frac{1}{2} \left[\gamma^\mu \gamma_\mu + (1-y)/y \right] \ \text{in second}.$

$$\int \frac{\mathrm{d}^{D}k}{(2\pi)^{D}} \frac{k^{i}k^{\mu}k^{j}}{(k^{2} + 2kq + s + i\eta)^{n}} \frac{1}{k^{2} - \lambda^{2}}$$

$$= -\frac{\mathrm{i}(-1)^{n}}{(4\pi)^{D/2}} \frac{1}{\Gamma(n)} \int_{0}^{1} \mathrm{d}y \, y^{n-1-1/2} \left[\left\{ q^{i}q^{\mu}q^{j}y^{3} + q^{i}q^{\mu}q^{j}\delta_{\mu 0}(1 - y)y^{2} \right\} \right] \times \frac{\Gamma(n+1-D/2)}{w^{n+1-D/2}} + \frac{1}{2} \left\{ y \left(g^{i\mu}q^{j} + g^{\mu j}q^{i} + g^{ji}q^{\mu} \right) \right\} - \delta_{\mu 0} g^{ij} q_{0}(1 - y) \right\} \frac{\Gamma(n-D/2)}{w^{n-D/2}}$$
(G.29)

G.3 Gamma Function

The Gamma function can be defined by means of Euler's integral

$$\Gamma(z) = \int_{-\infty}^{\infty} dt \, t^{z-1} e^{-t}. \tag{G.30}$$

For integral values, we have the relation

$$\Gamma(n) = (n-1)! \tag{G.31}$$

and generally

$$\Gamma(z) = (z-1)\Gamma(z-1). \tag{G.32}$$

The Gamma function can also be expressed by means of

$$\frac{1}{\Gamma(z)} = z e^{\gamma_{\rm E} z} \prod_{n=1}^{\infty} \left(1 + \frac{z}{n} \right) e^{-z/n},\tag{G.33}$$

where γ_E is Euler's constant, $\gamma_E = 0.5772...$

The Gamma function is singular, when z is zero or equal to a negative integer. Close to zero, the function is equal to

$$\Gamma(\epsilon) = \frac{1}{\epsilon} - \gamma_{\rm E} + \mathcal{O}(\epsilon),$$
 (G.34)

which follows directly from the expansion above. We shall now derive the corresponding expression close to negative integers.

G.3 Gamma Function 333

G.3.1 $z = -1 - \epsilon$

$$\frac{1}{\Gamma(-1-\epsilon)} = -(1+\epsilon) e^{-\gamma_{\rm E}(1+\epsilon)} \prod_{n=1}^{\infty} \left(1 - \frac{1+\epsilon}{n}\right) e^{(1+\epsilon)/n} \tag{G.35}$$

The first few factors of the product \prod are (to orders linear in ϵ)

$$-\epsilon e^{1+\epsilon} = -\epsilon e^{1}(1+\epsilon),$$

$$\left(1 - \frac{1+\epsilon}{2}\right) e^{(1+\epsilon)/2} = \frac{1}{2} (1-\epsilon) e^{1/2} (1+\epsilon/2),$$

$$\left(1 - \frac{1+\epsilon}{3}\right) e^{(1+\epsilon)/3} = \frac{2}{3} (1-\epsilon/2) e^{1/3} (1+\epsilon/3),$$

$$\left(1 - \frac{1+\epsilon}{4}\right) e^{(1+\epsilon)/4} = \frac{3}{4} (1-\epsilon/3) e^{1/4} (1+\epsilon/4),$$

which in the limit becomes

$$-e^{\gamma_E} \left(1 + \epsilon \left[1 - 1/2 - 1/(2 \cdot 3) - 1/(3 \cdot 4) - \cdots \right] \right) \approx -e^{\gamma_E}$$

using the expansion

$$1 + 1/2 + 1/3 + 1/4 + \dots + 1/M \Rightarrow \ln M + \gamma_{E}.$$
 (G.36)

This gives

$$\Gamma(-1 - \epsilon) = \frac{1}{\epsilon} + \gamma_{E} - 1 + \mathcal{O}(\epsilon). \tag{G.37}$$

This can also be obtained from (G.32).

$G.3.2 \quad z = -2 - \epsilon$

$$\frac{1}{\Gamma(-2-\epsilon)} = -(2+\epsilon) e^{-\gamma_{\rm E}(2+\epsilon)} \prod_{n=1}^{\infty} \left(1 - \frac{2+\epsilon}{n}\right) e^{(2+\epsilon)/n}.$$
 (G.38)

The first few factors of the product \prod are (to orders linear in ϵ)

$$-(1 + \epsilon) e^{2+\epsilon} = -(1 + \epsilon) e^{2} (1 + \epsilon),$$

$$-\epsilon/2 e^{(2+\epsilon)/2} = -\epsilon/2 e^{1} (1 + \epsilon/2),$$

$$\left(1 - \frac{2 + \epsilon}{3}\right) e^{(2 + \epsilon)/3} = \frac{1}{3} (1 - \epsilon) e^{2/3} (1 + \epsilon/3),$$

$$\left(1 - \frac{2 + \epsilon}{4}\right) e^{(2 + \epsilon)/4} = \frac{2}{4} (1 - \epsilon/2) e^{2/4} (1 + \epsilon/4),$$

$$\left(1 - \frac{2 + \epsilon}{5}\right) e^{(2 + \epsilon)/5} = \frac{3}{5} (1 - \epsilon/3) e^{2/5} (1 + \epsilon/5),$$

which in the limit becomes

$$e^{2\gamma_E} (1 + \epsilon [5/2 - 2/(1 \cdot 3) - 2/(2 \cdot 4) - 2/(3 \cdot 5) - \cdots]) \approx e^{2\gamma_E} (1 + \epsilon).$$

This gives

$$\Gamma(-2 - \epsilon) = -\frac{1}{2} \left[\frac{1}{\epsilon} + \gamma_{\rm E} - 1 - 1/2 + \mathcal{O}(\epsilon) \right]. \tag{G.39}$$

This is consistent with the formula

$$\Gamma(2z) = (2\pi)^{-1/2} 2^{2z-1/2} \Gamma(z) \Gamma(z+1/2).$$
 (G.40)

The step-down formula (G.32) yields

$$\Gamma(-3 - \epsilon) = \frac{1}{2 \cdot 3} \left[\frac{1}{\epsilon} + \gamma_{\rm E} - 1 - 1/2 - 1/3 \right],\tag{G.41}$$

which can be generalized to

$$\Gamma(-N-\epsilon) = \frac{(-1)^{N-1}}{N!} \left[\frac{1}{\epsilon} + \gamma_{\rm E} - \sum_{n=1}^{N} \frac{1}{n} \right].$$
 (G.42)

References

- Adkins, G.: One-loop renormalization of Coulomb-gauge QED. Phys. Rev. D 27, 1814–20 (1983)
- Fried, H.M., Yennie, D.M.: New techniques in the Lamb shift calculation. Phys. Rev. 112, 1391–1404 (1958)
- 3. Itzykson, C., Zuber, J.B.: Quantum Field Theory. McGraw-Hill (1980)
- 4. Mandl, F., Shaw, G.: Quantum Field Theory. John Wiley and Sons, New York (1986)
- Peskin, M.E., Schroeder, D.V.: An introduction to Quantum Field Theory. Addison-Wesley Publ. Co., Reading, Mass. (1995)
- t'Hooft, G., Veltman, M.: Regularization and renormalization of gauge fields. Nucl. Phys. B 44, 189–213 (1972)

Appendix H

Feynman Diagrams and Feynman Amplitude

In this appendix, we shall summarize the rules for evaluating Feynman diagrams of the different schemes, discussed in this book. These rules are based on the rules formulated by Feynman for the so-called *Feynman amplitude*, a concept we shall also use here.

H.1 Feynman Diagrams

H.1.1 S-Matrix

The Feynman diagrams for the S-matrix have an *outgoing* orbital line for each electron-field *creation* operator

$$\hat{\psi}^{\dagger}(x)$$

and an incoming orbital line for each electron-field absorption operator



and a vertex diagram

$$\mu \longrightarrow A_{\mu}$$
 $iec \alpha^{\mu} A_{\mu}$

for each interaction point.

This leads to an *electron propagator* for each contracted pair of electron-field operators:

$$\hat{\psi}(x_1)\hat{\psi}^{\dagger}(x_2) = i S_F(x_2, x_1) = i \int \frac{d\omega}{2\pi} S_F(\omega; \boldsymbol{x}_2, \boldsymbol{x}_1)$$

and a *photon propagator* for each contracted pair of photon-field operators:

$$1, \mu \bullet \sim \nu, 2 \qquad A_{\mu}(x_1) A_{\nu}(x_2) = i D_{F\nu\mu}(x_2, x_1) = i \int \frac{dz}{2\pi} D_{F\nu\mu}(z; x_2, x_1).$$

Thus, there is a photon interaction (4.45), including the vertices,

$$\mu$$
, 1 ν , 2 $\int \frac{dz}{2\pi} (-i) I(z; x_2, x_1) = \int dz (-i) e^2 c^2 \alpha_1^{\mu} \alpha_2^{\nu} D_{F\nu\mu}(z; x_2, x_1)$

for each photon exchange, and a corresponding diagram

$$1 - -iV_{\rm C} = -i\frac{e^2}{4\pi\epsilon_0 r_{12}}$$

for each Coulomb interaction, $V_{\rm C}$, between the electrons, and a potential diagram

for each energy potential, V (Fig. 4.6).

H.1.2 Green's Function

The Feynman diagrams of the Green's function are identical to those of the S-matrix with the exception that all outgoing and incoming lines represent electron orbitals.

H.1.3 Covariant Evolution Operator

The Feynman diagrams of the Covariant evolution operator are identical to those of the Green's function with the exception that there are creation/absorption operator lines attached to all outgoing/incoming orbital lines.

H.2 Feynman Amplitude

The Feynman amplitude, \mathcal{M} , contains

• An electron propagator (4.10)

$$\int \frac{\mathrm{d}\omega}{2\pi} \,\mathrm{i}\, S_{\mathrm{F}}(\omega; \boldsymbol{x}_{2}, \boldsymbol{x}_{1})$$

for each internal orbital line.

• A photon interaction

$$\int \frac{\mathrm{d}z}{2\pi} (-\mathrm{i}) I(z; \mathbf{x}_2, \mathbf{x}_1) = \int \frac{\mathrm{d}z}{2\pi} (-\mathrm{i}) e^2 c^2 \alpha_1^{\mu} \alpha_2^{\nu} D_{F\nu\mu}(z; \mathbf{x}_2, \mathbf{x}_1)$$

for each photon exchange, including the vertices.

- At each vertex space integrations and a time integral $2\pi\Delta_{\gamma}(arg)$, where the argument is equal to incoming minus outgoing energy parameters.
- A factor of -1 and a *trace symbol* for each closed orbital loop.
- The integration over the energy parameters leads to a factor of -i for each "non-trivial." (The integral is considered to be "trivial," when it contains a Δ function from the time integration.)

The **S-matrix** is related to the Feynman amplitude by (4.110)

$$S = 2\pi \,\delta(E_{\rm in} - E_{\rm out}) \,\mathcal{M},\tag{H.1}$$

which gives the energy contribution (4.111)

$$\Delta E = \delta_{E_{\text{in}}, E_{\text{out}}} \langle |i\mathcal{M}| \rangle. \tag{H.2}$$

The *Green's function* is in the equal-time approximation related to the Feynman amplitude, \mathcal{M} , by (5.25)

$$G(x, x'; x_0, x_0') = e^{-it(E_0 - H_0)} \mathcal{M}(x, x'; x_0, x_0') e^{it_0(E_0 - H_0)}$$
(H.3)

and analogously for the *covariant-evolution operator* (6.10)

$$U(t, -\infty)|ab\rangle = e^{-it(E_0 - H_0)} |rs\rangle \langle rs|i\mathcal{M}|ab\rangle e^{it_0(E_0 - H_0)}.$$
 (H.4)

In this formalism, the contribution to the *effective interaction* is

$$\langle |V_{\text{eff}}| \rangle = \langle |\mathcal{M}| \rangle.$$
 (H.5)

Illustrations

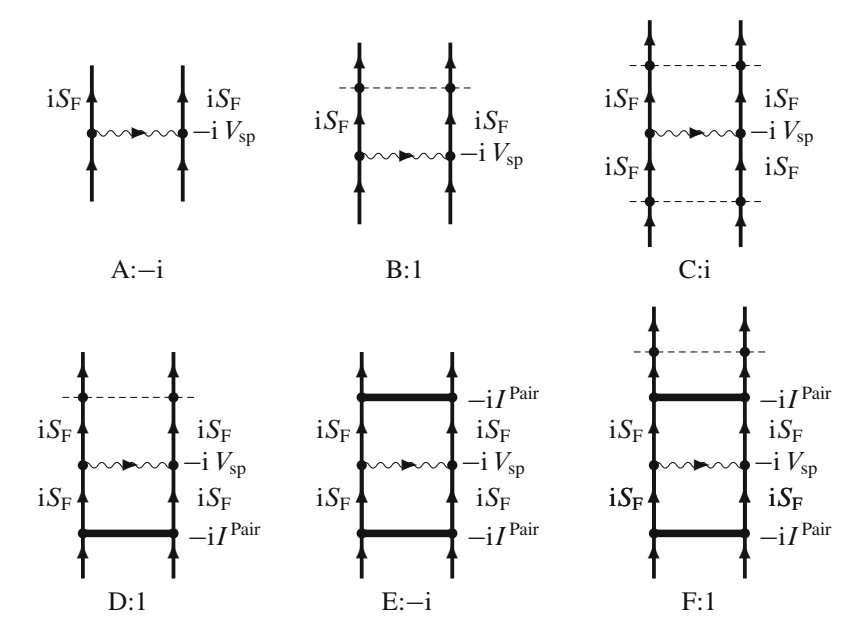


Diagram A is a first-order S-matrix (Sect. 4.4), and the Feynman amplitude is

$$\mathcal{M} = -iV_{sp}(E_0).$$

Diagram B is a first-order covariant evolution-operator diagram with the unperturbed state as input and with outgoing electron propagators (Sect. 6.2). Here, there are three energy parameters and two subsidiary conditions. This leaves one nontrivial integration, giving a factor of -i. This gives a factor of $i^2(-i)^2 = 1$ and

$$\mathcal{M} = \Gamma(E_0) V_{\rm sp}(E_0).$$

Diagram C is a first-order covariant evolution-operator diagram with incoming and outgoing electron propagators (Sect. 8.1). Here, there are five parameters and three conditions, leaving two nontrivial integrations. This gives the factor $i^4(-i)^3 = i$ and (8.9)

$$\mathcal{M} = \Gamma(E_0) i V_{\rm sp}(E_0) \Gamma(E_0).$$

Diagram D is a first-order covariant evolution-operator diagram with incoming pair function (Sect. 6.2.1). This gives $i^4(-i)^4 = 1$

$$\mathcal{M} = I^{\text{Pair}} \Gamma(E_0) V_{\text{sp}}(E_0) \Gamma(E_0) I^{\text{Pair}}.$$

Diagram E is an S-matrix diagram with incoming and outgoing pair functions (Sect. 6.2.1). This gives $i^4(-i)^5 = -i$ and

$$\mathcal{M} = -\mathrm{i} I^{\mathrm{Pair}} \Gamma(E_0) \, V_{\mathrm{sp}}(E_0) \Gamma(E_0) \, I^{\mathrm{Pair}}.$$

Diagram F is a first-order covariant evolution-operator diagram with incoming and outgoing pair functions (Sect. 6.2.1). Here, there are seven parameters and four subsidiary conditions, yielding $i^6(-i)^6 = 1$ and

$$\mathcal{M} = \Gamma(E_0) I^{\text{Pair}} \Gamma(E_0) V_{\text{sp}}(E_0) \Gamma(E_0) I^{\text{Pair}}.$$

Appendix I

Evaluation Rules for Time-Ordered Diagrams

In nonrelativistic (MBPT) formalism, all interaction times are restricted to the interval $(t, -\infty)$, and the Goldstone diagrams are used for the graphical representation. In the relativistic (QED) formalism, on the other hand, times are allowed in the entire interval $(\infty, -\infty)$, and then Feynman diagrams, which contain all possible time orderings, are the relevant ones to use.

For computational as well as illustrative purpose, it is sometimes useful also in the relativistic case to work with *time-ordered diagrams*. It should be observed, though, that time-ordered Feynman diagrams are distinct from Goldstone diagrams, as we shall demonstrate here.¹

When only *particles states* (above the Fermi level) are involved, time runs in the *positive* direction, and the time-evolution operator can be expressed as (3.12)

$$U(t, -\infty) = 1 - i \int_{-\infty}^{t} dt_1 \ V(t_1) + (-i)^2 \int_{-\infty}^{t} dt_1 \ V(t_1) \int_{-\infty}^{t_1} dt_2 \ V(t_2) + \cdots,$$
(I.1)

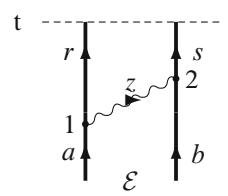
where V(t) is the perturbation in the interaction picture (3.16)

$$V(t) = -\int d^3 \mathbf{x} \, \hat{\psi}^{\dagger}(x) e c \alpha^{\mu} A_{\mu}(x) \, \hat{\psi}(x). \tag{I.2}$$

Core states and negative energy states are regarded as *hole states* below the Fermi level with time running in the negative direction. Then, the corresponding *time integration should be performed in the negative direction*.

¹ The treatment here is partly based on that in [2, Appdices C and D].

I.1 Single-Photon Exchange



We consider first the time-ordered diagram for single-photon exchange with only particle states involved. The time restrictions are here

$$t > t_2 > t_1 > -\infty$$

which corresponds to the evolution operator (I.1)

$$(-i)^2 \int_{-\infty}^t dt_2 \, V(t_2) \, e^{-it_2 d_2} \int_{-\infty}^{t_2} dt_1 \, V(t_1) \, e^{-it_1 d_1}. \tag{I.3}$$

The contraction of the radiation-field operators gives rise to a photon propagator (4.18)

$$A_{\nu}(x_2)A_{\mu}(x_1) = i D_{F\nu\mu}(x_2, x_1)$$

and this leads to the interaction (4.46)

$$I(x_2,x_1) = e^2 c^2 \alpha_1^\mu \alpha_2^\nu D_{\mathrm{F}\nu\mu}(x_2,x_1) = \int \frac{\mathrm{d}z}{2\pi} \; \mathrm{e}^{-\mathrm{i}z(t_2-t_1)} \int \frac{2c^2k \; \mathrm{d}k \; f(k;\boldsymbol{x}_1,\boldsymbol{x}_2)}{z^2-c^2k^2+\mathrm{i}\eta}.$$

The time dependence at vertex 1 then becomes $e^{-it_1d_1}$, where

$$d_1 = \varepsilon_a - \varepsilon_r - z + i\gamma$$
.

This parameter is referred to as the *vertex value* and given by *the incoming minus* the outgoing orbital energies/energy parameters at the vertex. Similarly, we define

$$d_2 = \varepsilon_b - \varepsilon_s + z + i\gamma$$

$$d_{12} = d_1 + d_2 = \mathcal{E} - \varepsilon_r - \varepsilon_s$$
 (I.4)

with $\mathcal{E} = \varepsilon_a + \varepsilon_b$. This leads to the time integrals

$$(-i)^2 \int_{-\infty}^t dt_2 e^{-it_2 d_2} \int_{-\infty}^{t_2} dt_1 e^{-it_1 d_1} = \frac{e^{-it d_{12}}}{d_{12}} \frac{1}{d_1}.$$
 (I.5)

Together with the opposite time ordering, $t > t_1 > t_2 > -\infty$, the denominators become

$$\frac{1}{d_{12}} \left(\frac{1}{d_1} + \frac{1}{d_2} \right) = \frac{1}{\mathcal{E} - \varepsilon_r - \varepsilon_s} \left(\frac{1}{\varepsilon_a - \varepsilon_r - z + i\gamma} + \frac{1}{\varepsilon_b - \varepsilon_s + z + i\gamma} \right). \quad (I.6)$$

This leads to the Feynman amplitude (6.11)

$$\mathcal{M}_{sp} = i \int \frac{dz}{2\pi} \frac{1}{\mathcal{E} - \varepsilon_r - \varepsilon_s} \left(\frac{1}{\varepsilon_a - \varepsilon_r - z + i\gamma} + \frac{1}{\varepsilon_b - \varepsilon_s + z + i\gamma} \right) \times \int \frac{2c^2k \, dk \, f(k)}{z^2 - c^2k^2 + i\eta}$$
(I.7)

or

$$\langle rs|\mathcal{M}_{\rm sp}|ab\rangle = \frac{1}{E - \varepsilon_r - \varepsilon_s} \langle rs|V_{\rm sp}(\mathcal{E})|ab\rangle$$
 (I.8)

with

$$V_{\rm sp}(\mathcal{E}) = \int c \, \mathrm{d}k \, f(k) \, \left(\frac{1}{\varepsilon_a - \varepsilon_r - ck + \mathrm{i}\gamma} + \frac{1}{\varepsilon_b - \varepsilon_s - ck + \mathrm{i}\gamma} \right). \tag{I.9}$$

If the interaction is instantaneous, then the time integral becomes

$$-i\int_{-\infty}^{t} dt_{12} e^{-it_{12}d_{12}} = \frac{e^{-it d_{12}}}{d_{12}} = \frac{e^{-it (\mathcal{E} - \varepsilon_r - \varepsilon_s)}}{\mathcal{E} - \varepsilon_r - \varepsilon_s},$$
 (I.10)

which for t = 0 is the standard MBPT result.

I.2 Two-Photon Exchange

Next, we consider the diagrams in Fig. I.1.

We extend the definitions of the *vertex values*:

$$\begin{split} d_1 &= \varepsilon_a - \varepsilon_t - z; \quad d_2 = \varepsilon_b - \varepsilon_u + z; \quad d_3 = \varepsilon_t - \varepsilon_r - z' \quad d_4 = \varepsilon_u - \varepsilon_s + z', \\ d_{12} &= d_1 + d_2 = \mathcal{E} - \varepsilon_t - \varepsilon_u; \quad d_{13} = \varepsilon_a - \varepsilon_r - z - z'; \quad d_{24} = \varepsilon_b - \varepsilon_s + z + z', \\ d_{123} &= \mathcal{E} - \varepsilon_r - \varepsilon_u - z'; \quad d_{124} = \mathcal{E} - \varepsilon_t - \varepsilon_s + z'; \quad d_{1234} = \mathcal{E} - \varepsilon_r - \varepsilon_s, \end{split}$$

i.e., given by the *incoming minus the outgoing energies* of the vertex. There is a damping term $\pm i\gamma$ for integration going to $\mp \infty$.

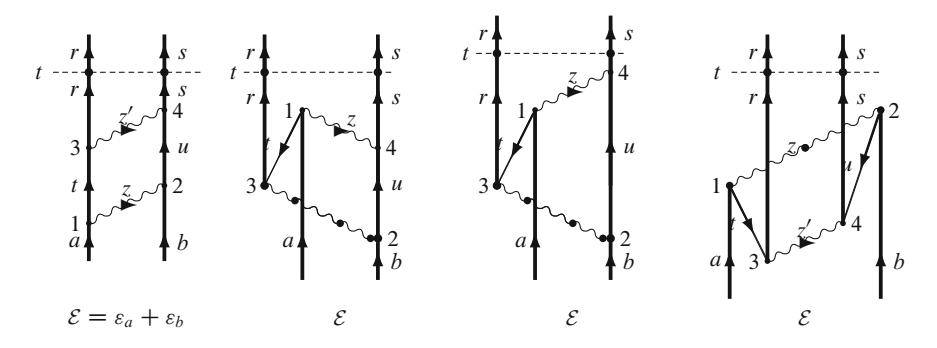


Fig. I.1 Time-ordered Feynman diagrams for the two-photon ladder with only particle states (*left*) and with one and two intermediate hole states (*right*)

I.2.1 No Virtual Pair

We consider now the first diagram above, where only particle states are involved. We assume that it is *reducible*, implying that the two photons do not overlap in time. Then the time ordering is

$$t > t_4 > t_3 > t_2 > t_1 > -\infty$$
.

This leads to the time integrations

$$(-i)^{4} \int_{-\infty}^{t} dt_{4} e^{-it_{4}d_{4}} \int_{-\infty}^{t_{4}} dt_{3} e^{-it_{3}d_{3}} \int_{-\infty}^{t_{3}} dt_{2} e^{-it_{2}d_{2}} \int_{-\infty}^{t_{2}} dt_{1} e^{-it_{1}d_{1}}$$

$$= \frac{e^{-it d_{1234}}}{d_{1234} d_{123} d_{12} d_{1}}.$$
(I.11)

Changing the order between t_1 and t_2 and between t_3 and t_4 leads to the denominators

$$\frac{1}{d_{1234}} \left(\frac{1}{d_{123}} + \frac{1}{d_{124}} \right) \frac{1}{d_{12}} \left(\frac{1}{d_1} + \frac{1}{d_2} \right). \tag{I.12}$$

Here, all integrations are being performed upward, which implies that all denominators are evaluated from below.

If the interaction 1–2 is *instantaneous*, then the integrations become

$$(-i)^{3} \int_{-\infty}^{t} dt_{4} e^{-it_{4}d_{4}} \int_{-\infty}^{t_{4}} dt_{3} e^{-it_{3}d_{3}} \int_{-\infty}^{t_{3}} dt_{12} e^{-it_{12}d_{12}} = \frac{e^{-it d_{1234}}}{d_{1234} d_{123} d_{12}}$$
(I.13)

and together with the other time ordering

$$\frac{e^{-it} d_{1234}}{d_{1234}} \left(\frac{1}{d_{123}} + \frac{1}{d_{124}} \right) \frac{1}{d_{12}}.$$
 (I.14)

If both interactions are instantaneous, we have

$$(-i)^{2} \int_{-\infty}^{t} dt_{34} e^{-it_{34}d_{34}} \int_{-\infty}^{t_{34}} dt_{12} e^{-it_{12}d_{12}} = \frac{e^{-it d_{1234}}}{d_{1234} d_{12}}$$
(I.15)

consistent with the MBPT result [1, Sect. 12.2].

I.2.2 Single Hole

Next, we consider the two-photon exchange with a single hole, represented by the second diagram above. We still assume that the diagram is reducible, implying that the two photons do not overlap in time. The time ordering is now

$$t > t_4 > t_3 > t_2 > -\infty$$
 and $\infty > t_1 > t_4$,

but the order between t_1 and t is not given.

If this is considered as a *Goldstone diagram*, all times (including t_1) are restricted to $t_n < t$, which leads to

$$\int_{t}^{-\infty} dt_{1} e^{-it_{1}d_{1}} \int_{-\infty}^{t_{1}} dt_{4} e^{-it_{4}d_{4}} \int_{-\infty}^{t_{4}} dt_{3} e^{-it_{3}d_{3}} \int_{-\infty}^{t_{3}} dt_{2} e^{-it_{2}d_{2}}$$

$$= -\frac{e^{-it d_{1234}}}{d_{1234} d_{234} d_{23} d_{2}}.$$
(I.16)

Note that the last integration is being performed in the negative direction, due to the core hole. This is illustrated in Fig. I.2 (left).

Considered as a Feynman diagram, the time t_1 can run to $+\infty$, which leads to

$$\int_{\infty}^{t_4} dt_1 e^{-it_1 d_1} \int_{-\infty}^{t} dt_4 e^{-it_4 d_4} \int_{-\infty}^{t_4} dt_3 e^{-it_3 d_3} \int_{-\infty}^{t_3} dt_2 e^{-it_2 d_2}$$

$$= \frac{e^{-it d_{1234}}}{d_{1234} d_1 d_{23} d_2}.$$
(I.17)

Here, the last integration is still performed in the negative direction, this time from $+\infty$ to t_4 , and this leads to a result different from the previous one. In the Goldstone case all denominators are evaluated from below, while in the Feynman case one of them is evaluated from above (see Fig. I.2, right). For *diagrams diagonal in energy* we have $d_{1234} = 0$, and hence $d_1 = -d_{234}$, which implies that in this case the two results are identical.

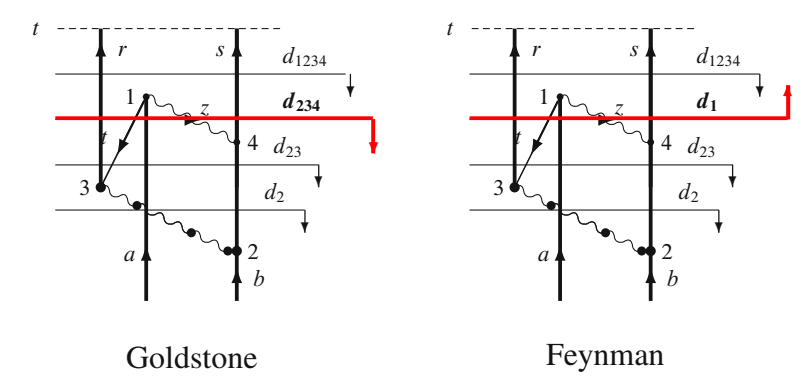


Fig. I.2 Time-ordered Goldstone and Feynman diagrams, respectively, for two-photon exchange with one virtual pair. In the latter case, one denominator (at vertex 1) is evaluated *from above*

Let us next consider the third diagram in Fig. I.1, where the time ordering is

$$t > t_4 > t_1 > t_3 > t_2 > -\infty$$
.

Here, all times are limited from above in the Goldstone as well as the Feynman interpretation, and this leads in both cases to

$$\int_{-\infty}^{t} dt_4 e^{-it_4 d_4} \int_{t_4}^{-\infty} dt_1 e^{-it_1 d_1} \int_{-\infty}^{t_1} dt_3 e^{-it_3 d_3} \int_{-\infty}^{t_3} dt_2 e^{-it_2 d_2}$$

$$= -\frac{e^{-it d_{1234}}}{d_{1234} d_{123} d_{23} d_2}.$$
(I.18)

I.2.3 Double Holes

The last diagram in Fig. I.1, also reproduced in Fig. I.3, represents double virtual pair. Considered as a Goldstone diagram, the time ordering is

$$t > t_2 > t_1 > t_4 > t_3 > -\infty$$

which yields

$$\int_{-\infty}^{t} dt_2 e^{-it_2 d_2} \int_{-\infty}^{t_2} dt_1 e^{-it_1 d_1} \int_{-\infty}^{t_1} dt_4 e^{-it_4 d_4} \int_{-\infty}^{t_4} dt_3 e^{-it_3 d_3}$$

$$= \frac{e^{-it d_{1234}}}{d_{1234} d_{134} d_{34} d_3}.$$
(I.19)

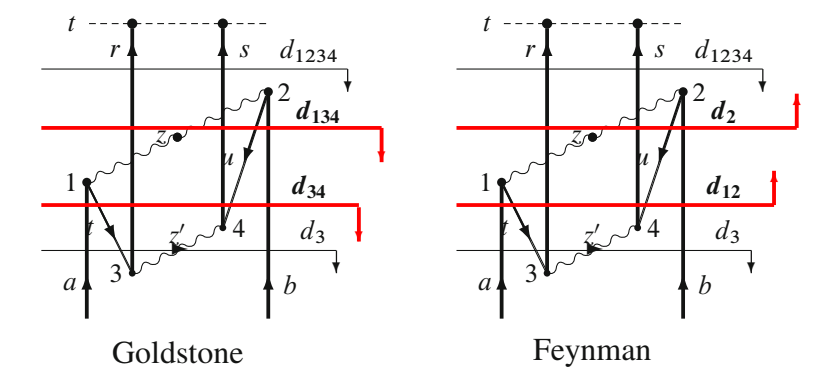


Fig. I.3 Time-ordered Goldstone and Feynman diagrams, respectively, for two-photon exchange with two virtual pairs. In the latter case, two denominators (at vertices 1 and 2) are evaluated *from above*

This is illustrated in Fig. I.3 (left).

Considered as a Feynman diagram, we have instead $\infty > t_2 > t_1$, which leads to

$$\int_{-\infty}^{t} dt_4 e^{-it_4 d_4} \int_{-\infty}^{t_4} dt_3 e^{-it_3 d_3} \int_{\infty}^{t_4} dt_1 e^{-it_1 d_1} \int_{\infty}^{t_1} dt_2 e^{-it_2 d_2}$$

$$= \frac{e^{-it d_{1234}}}{d_{1234} d_3 d_{12} d_2},$$
(I.20)

where two integrations are performed in the negative direction.

I.3 General Evaluation Rules

We can now formulate evaluation rules for the two types of diagrams considered here. For (nonrelativistic) Goldstone diagrams, the rules are equivalent to the standard *Goldstone rules* [1, Sect. 12.2]

- There is a matrix element for each interaction.
- For each vertex, there is a denominator equal to the *vertex sum* (sum of vertex values): incoming minus outgoing orbital energies and $z+i\gamma$ for crossing photon line (leading to -ck after integration) *below* a line immediately above the vertex.
- For particle/hole lines, the integration is performed in the positive/negative direction.

For the relativistic *Feynman diagrams*, the same rules hold, with the exception that

• For a vertex where time can run to $+\infty$, the denominator should be *evaluated* from above with the denominator equal to the vertex sum above a line immediately below the vertex (with $z - i\gamma$ for crossing photon line, leading to +ck).

References

- 1. Lindgren, I., Morrison, J.: *Atomic Many-Body Theory*. Second edition, Springer-Verlag, Berlin (1986, reprinted 2009)
- Lindgren, I., Salomonson, S., Åsén, B.: The covariant-evolution-operator method in boundstate QED. Physics Reports 389, 161–261 (2004)

Appendix J Some Integrals

J.1 Feynman Integrals

In this section, we shall derive some integrals, which simplify many QED calculations considerably (see the books of Mandl and Shaw [1, Chap. 10] and Sakurai [2, Appendix D]), and we shall start by deriving some formulas due to Feynman.

We start with the identity

$$\frac{1}{ab} = \frac{1}{b-a} \int_a^b \frac{\mathrm{d}t}{t^2}.\tag{J.1}$$

With the substitution t = b + (a - b)x, this becomes

$$\frac{1}{ab} = \int_0^1 \frac{\mathrm{d}x}{[b + (a - b)x]^2} = \int_0^1 \frac{\mathrm{d}x}{[a + (b - a)x]^2}.$$
 (J.2)

Differentiation with respect to a yields

$$\frac{1}{a^2b} = 2\int_0^1 \frac{x dx}{[b + (a - b)x]^3}.$$
 (J.3)

Similarly, we have

$$\frac{1}{abc} = 2 \int_0^1 dx \int_0^x dy \frac{1}{[a + (b - a)x + (c - b)y]^3}$$

$$= 2 \int_0^d x \int_0^{1-x} dy \frac{1}{[a + (b - a)x + (c - a)y]^3}.$$
(J.4)

Next we consider the integral

$$\int d^4k \, \frac{1}{(k^2 + s + i\eta)^3} = 4\pi \int |\mathbf{k}|^2 d|\mathbf{k}| \int_{-\infty}^{\infty} \frac{dk_0}{(k^2 + s + i\eta)^3}.$$

350 J Some Integrals

The second integral can be evaluated by starting with

$$\int_{-\infty}^{\infty} \frac{\mathrm{d}k_0}{k_0^2 - |\mathbf{k}|^2 + s + \mathrm{i}\eta} = \frac{\mathrm{i}\pi}{\sqrt{|\mathbf{k}|^2 - s}}$$

evaluated by residue calculus, and differentiating twice with respect to s. The integral then becomes

$$\int d^4k \, \frac{1}{(k^2 + s + i\eta)^3} = \frac{3i\pi^2}{2} \int \frac{|\boldsymbol{k}|^2 d|\boldsymbol{k}|}{(|\boldsymbol{k}|^2 + s)^{5/2}} = \frac{i\pi^2}{2s}.$$
 (J.5)

The second integral can be evaluated from the identity

$$\frac{x^2}{(x^2+s)^{5/2}} = \frac{1}{(x^2+s)^{3/2}} - \frac{s}{(x^2+s)^{5/2}}$$

and differentiating the integral

$$\int \frac{\mathrm{d}x}{\sqrt{x^2 + s}} = \ln\left(x + \sqrt{x^2 + s}\right)$$

yielding

$$\int \frac{x^2}{(x^2+s)^{5/2}} = \frac{1}{3s}.$$

For symmetry reason, we find

$$\int d^4k \, \frac{k^{\mu}}{(k^2 + s + i\eta)^3} = 0. \tag{J.6}$$

Differentiating this relation with respect to k_{ν} leads to

$$\int d^4k \, \frac{k^{\mu}k^{\nu}}{(k^2 + s + i\eta)^4} = \frac{g^{\mu\nu}}{3} \int d^4k \, \frac{1}{(k^2 + s + i\eta)^3} = \frac{i\pi^2 g^{\mu\nu}}{6s} \tag{J.7}$$

using the relation (A.4).

By making the replacements

$$k \Rightarrow k + q$$
 and $s \Rightarrow s - q^2$,

the integrals (J.5) and (J.6) lead to

$$\int d^4k \, \frac{1}{(k^2 + 2kq + s + i\eta)^3} = \frac{i\pi^2}{2(s - q^2)},\tag{J.8}$$

$$\int d^4k \, \frac{k^{\mu}}{(k^2 + 2kq + s + i\eta)^3} = -\int d^4k \, \frac{q^{\mu}}{(k^2 + 2kq + s + i\eta)^3} = -\frac{i\pi^2 q^{\mu}}{2(s - q^2)}.$$
(J.9)

351

Differentiating the last relation with respect to q_{ν} leads to

$$\int d^4k \, \frac{k^\mu k^\nu}{(k^2 + 2kq + s + i\eta)^4} = \frac{i\pi^2}{12} \left[\frac{g^{\mu\nu}}{s - q^2} + \frac{2q^\mu q^\nu}{(s - q^2)^2} \right] \quad ??. \tag{J.10}$$

Differentiating the relation (J.8) with respect to s yields

$$\int d^4k \, \frac{1}{(k^2 + 2kq + s + i\eta)^4} = \frac{i\pi^2}{6(s - q^2)^2},\tag{J.11}$$

which can be generalized to arbitrary integer powers ≥ 3

$$\int d^4k \, \frac{1}{(k^2 + 2kq + s + i\eta)^n} = i\pi^2 \frac{(n-3)!}{(n-1)!} \frac{1}{(s-q^2)^{n-2}}.$$
 (J.12)

This can also be extended to nonintegral powers

$$\int d^4k \, \frac{1}{(k^2 + 2kq + s + i\eta)^n} = i\pi^2 \frac{\Gamma(n-2)}{\Gamma(n)} \frac{1}{(s-q^2)^{n-2}} \tag{J.13}$$

and similarly

$$\int d^4k \, \frac{k^{\mu}}{(k^2 + 2kq + s + i\eta)^n} = -i\pi^2 \frac{\Gamma(n-2)}{\Gamma(n)} \frac{q^{\mu}}{(s-q^2)^{n-2}},\tag{J.14}$$

$$\int d^4k \, \frac{k^{\mu}k^{\nu}}{(k^2 + 2kq + s + i\eta)^n} = i\pi^2 \frac{\Gamma(n-3)}{2\Gamma(n)} \left[\frac{(2n-3) \, q^{\mu}q^{\nu}}{(s-q^2)^{n-2}} + \frac{g^{\mu\nu}}{(s-q^2)^{n-3}} \right],\tag{J.15}$$

J.2 Evaluation of the Integral $\int \frac{d^3k}{(2\pi)^3} \frac{e^{ik \cdot r_{12}}}{q^2 - k^2 + i\eta}$

Using spherical coordinates $k=(\eta,\theta,\phi)$, $(\eta=|k|)$, we have with $\mathrm{d}^3k=\eta^2\mathrm{d}\eta\sin\Theta\,\mathrm{d}\Theta\,\mathrm{d}\Phi$ and $r_{12}=|x_1-x_2|$

$$\int \frac{d^{3} \mathbf{k}}{(2\pi)^{3}} \frac{e^{i\mathbf{k}\cdot(\mathbf{k}_{1}-\mathbf{k}_{2})}}{q^{2}-\mathbf{k}^{2}+i\eta} = (2\pi)^{-2} \int_{0}^{\infty} \frac{\eta^{2} d\eta}{q^{2}-\kappa^{2}+i\eta} \int_{0}^{\pi} d\Theta \sin\Theta e^{i\kappa r_{12}\cos\Theta}$$

$$= -\frac{i}{4\pi^{2} r_{12}} \int_{0}^{\infty} \frac{\kappa d\kappa \left(e^{i\kappa r_{12}}-e^{-i\kappa r_{12}}\right)}{q^{2}-\kappa^{2}+i\eta}$$

$$= -\frac{i}{8\pi^{2} r_{12}} \int_{-\infty}^{\infty} \frac{\kappa d\kappa \left(e^{i\kappa r_{12}}-e^{-i\kappa r_{12}}\right)}{q^{2}-\kappa^{2}+i\eta}, \quad (J.16)$$

352 J Some Integrals

where we have in the last step used the fact that the integrand is an *even* function of κ . The poles appear at $\kappa = \pm q(1+\mathrm{i}\eta/2q)$. $\mathrm{e}^{\mathrm{i}\kappa r_{12}}$ is integrated over the *positive* and $\mathrm{e}^{-\mathrm{i}\kappa r_{12}}$ over the *negative* half-plane, which yields $-\mathrm{e}^{\pm\mathrm{i}qr_{12}}/(4\pi\,r_{12})$ with the upper sign for q>0. The same result is obtained if we change the sign of the exponent in the numerator of the original integrand. Thus, we have the result

$$\int \frac{\mathrm{d}^3 \mathbf{k}}{(2\pi)^3} \frac{\mathrm{e}^{\pm \mathrm{i}\mathbf{k} \cdot (\mathbf{x}_1 - \mathbf{x}_2)}}{q^2 - \mathbf{k}^2 + \mathrm{i}\eta} = \frac{1}{4\pi^2 r_{12}} \int_0^\infty \frac{2\kappa \, \mathrm{d}\kappa \, \sin(\kappa r_{12})}{q^2 - \kappa^2 + \mathrm{i}\eta} = -\frac{\mathrm{e}^{\mathrm{i}|q|r_{12}}}{4\pi \, r_{12}}.$$
 (J.17)

The imaginary part of the integrand, which is an *odd* function, does not contribute to the integral.

J.3 Evaluation of the Integral

$$\int \frac{d^3k}{(2\pi)^3} \left(\alpha_1 \cdot \hat{k}\right) \left(\alpha_2 \cdot \hat{k}\right) \frac{e^{ik \cdot r_{12}}}{q^2 - k^2 + i\eta}$$

The integral appearing in the derivation of the Breit interaction (F.53) is

$$I_{2} = \int \frac{d^{3}k}{(2\pi)^{3}} (\alpha_{1} \cdot k) (\alpha_{2} \cdot k) \frac{e^{ik \cdot r_{12}}}{q^{2} - k^{2} + i\eta}$$

$$= -(\alpha_{1} \cdot \nabla_{1}) (\alpha_{2} \cdot \nabla_{2}) \int \frac{d^{3}k}{(2\pi)^{3}} \frac{e^{ik \cdot r_{12}}}{k^{2} (q^{2} - k^{2} + i\eta)}.$$
(J.18)

Using (J.16), we then have

$$I_{2} = -\frac{\mathrm{i}}{8 \pi^{2} r_{12}} (\boldsymbol{\alpha}_{1} \cdot \nabla_{1}) (\boldsymbol{\alpha}_{2} \cdot \nabla_{2}) \int_{-\infty}^{\infty} \frac{\mathrm{d}\kappa \left(\mathrm{e}^{\mathrm{i}\kappa r_{12}} - \mathrm{e}^{-\mathrm{i}\kappa r_{12}} \right)}{(q^{2} - \kappa^{2} + \mathrm{i}\eta)}$$

$$= \frac{1}{4 \pi^{2} r_{12}} (\boldsymbol{\alpha}_{1} \cdot \nabla_{1}) (\boldsymbol{\alpha}_{2} \cdot \nabla_{2}) \int_{0}^{\infty} \frac{2\kappa \, \mathrm{d}\kappa \, \sin(k r_{12})}{\kappa^{2} (q^{2} - \kappa^{2} + \mathrm{i}\eta)}. \tag{J.19}$$

The poles appear at $\kappa=0$ and $\kappa=\pm(q+\mathrm{i}\eta/2q)$. The pole at $\kappa=0$ can be treated with half the pole value in each half plane. For q>0, the result becomes

$$-\frac{1}{4\pi \, r_{12}} \frac{\mathrm{e}^{\mathrm{i}q r_{12} - 1}}{q^2}$$

and for q>0 the same result with -q in the exponent. The final result then becomes

J.3 Evaluation of the Integral
$$\int \frac{d^3k}{(2\pi)^3} \left(\alpha_1 \cdot \hat{k}\right) \left(\alpha_2 \cdot \hat{k}\right) \frac{e^{ik \cdot r_{12}}}{q^2 - k^2 + i\eta}$$
 353

$$\int \frac{\mathrm{d}^{3} \boldsymbol{k}}{(2\pi)^{3}} (\boldsymbol{\alpha}_{1} \cdot \boldsymbol{k}) (\boldsymbol{\alpha}_{2} \cdot \boldsymbol{k}) \frac{\mathrm{e}^{\mathrm{i}\boldsymbol{k} \cdot \boldsymbol{r}_{12}}}{q^{2} - \boldsymbol{k}^{2} + \mathrm{i}\eta} = -\frac{1}{4\pi r_{12}} (\boldsymbol{\alpha}_{1} \cdot \nabla_{1}) (\boldsymbol{\alpha}_{2} \cdot \nabla_{2}) \frac{\mathrm{e}^{\mathrm{i}|\boldsymbol{q}|\boldsymbol{r}_{12} - 1}}{q^{2}}$$

$$= \frac{1}{4\pi^{2} r_{12}} (\boldsymbol{\alpha}_{1} \cdot \nabla_{1}) (\boldsymbol{\alpha}_{2} \cdot \nabla_{2})$$

$$\times \int_{0}^{\infty} \frac{2\kappa \, \mathrm{d}\kappa \, \sin(\kappa r_{12})}{\kappa^{2} (q^{2} - \kappa^{2} + \mathrm{i}\eta)}. \tag{J.20}$$

Assuming that our basis functions are eigenfunctions of the Dirac hamiltonian \hat{h}_D , we can process this integral further. Then the commutator with an arbitrary function of the space coordinates is

$$\left[\hat{h}_D, f(\mathbf{x})\right] = c \,\alpha \cdot \hat{\mathbf{p}} \,f(\mathbf{x}) + \left[U, f(\mathbf{x})\right]. \tag{J.21}$$

The last term vanishes if the potential U is a local function, yielding

$$\left[\hat{h}_{D}, f(\mathbf{x})\right] = c \,\alpha \cdot \hat{\mathbf{p}} f(\mathbf{x}) = -\mathrm{i} c \,\alpha \cdot \nabla f(\mathbf{x}). \tag{J.22}$$

In particular

$$\left[\hat{h}_D, e^{ik \cdot x}\right] = -ic \,\alpha \cdot \nabla e^{ik \cdot x} = c \,\alpha \cdot \hat{k} e^{ik \cdot x}. \tag{J.23}$$

We then find that

$$(\boldsymbol{\alpha} \cdot \boldsymbol{\nabla})_1 (\boldsymbol{\alpha} \cdot \boldsymbol{\nabla})_2 e^{i\boldsymbol{k} \cdot \boldsymbol{x}} = \frac{1}{c^2} \left[h_D, e^{i\boldsymbol{k} \cdot \boldsymbol{x}} \right]_1 \left[h_D, e^{i\boldsymbol{k} \cdot \boldsymbol{x}} \right]_2$$
 (J.24)

with the matrix element

$$\langle rs | (\boldsymbol{\alpha} \cdot \nabla)_1 (\boldsymbol{\alpha} \cdot \nabla)_2 e^{i \boldsymbol{k} \cdot \boldsymbol{x}} | ab \rangle = q^2 e^{i \boldsymbol{k} \cdot \boldsymbol{x}}$$
 (J.25)

using the notation in (F.49). The integral (J.18) then becomes

$$I_{2} = \int \frac{d^{3}\mathbf{k}}{(2\pi)^{3}} (\boldsymbol{\alpha}_{1} \cdot \hat{\mathbf{k}}) (\boldsymbol{\alpha}_{2} \cdot \hat{\mathbf{k}}) \frac{e^{i\mathbf{k} \cdot \mathbf{r}_{12}}}{q^{2} - \mathbf{k}^{2} + i\eta} = \int \frac{d^{3}\mathbf{k}}{(2\pi)^{3}} \frac{q^{2}}{\mathbf{k}^{2}} \frac{e^{i\mathbf{k} \cdot \mathbf{r}_{12}}}{q^{2} - \mathbf{k}^{2} + i\eta}$$
(J.26)

provided that the orbitals are generated by a hamiltonian with a *local* potential.

354 J Some Integrals

References

- 1. Mandl, F., Shaw, G.: Quantum Field Theory. John Wiley and Sons, New York (1986)
- 2. Sakurai, J.J.: Advanced Quantum Mechanics. Addison-Wesley Publ. Co., Reading, Mass. (1967)

Appendix K Unit Systems and Dimensional Analysis

K.1 Unit Systems

K.1.1 SI System

The standard unit system internationally agreed upon is the SI system or *System Internationale*. The basis units in this system are given in the following table:

Quantity	SI unit	Symbol
Length	Meter	m
Mass	Kilogram	kg
Time	Second	S
Electric current	Ampere	A
Thermodynamic temperature	Kelvin	K
Amount of substance	Mole	mol
Luminous intensity	Candela	cd

For the definition of these units, the reader is referred to the NIST WEB page (see footnote). From the basis units – particularly the first four – the units for most other physical quantities can be derived.

K.1.2 Relativistic or "Natural" Unit System

In scientific literature, some simplified unit system is frequently used for convenience. In relativistic field theory the *relativistic unit system* is mostly used, where the first four units of the SI system are replaced by

¹ For further details, see *The NIST Reference on Constants, Units, and Uncertainty* (http://physics.nist.gov/cuu/Units/index.html).

Quantity	Relativistic unit	Symbol	Dimension
Mass	Rest mass of the electron	m	kg
Velocity	Light velocity in vacuum	c	ms^{-1}
Action	Planck's constant divided by 2π	\hbar	$kg m^2 s^{-1}$
Dielectricity	Dielectricity constant of vacuum	ϵ_0	$A^2s^4kg^{-1}m^{-3}$

In the table, the dimension of the relativistic units in SI units are also shown. From these four units, all units that depend only on the four SI units kg, s, m, A can be derived. For instance, *energy* that has the dimension kg m⁻²m⁻² has the relativistic unit $m_e c^2$, which is the rest energy of the electron ($\approx 511 \, \text{keV}$). The unit for *length* is

$$\frac{\hbar}{m_e c} = \lambda/2\pi \approx 0,386 \times 10^{-12} \,\mathrm{m},$$

where λ is *Compton wavelength* and the unit for *time* is $2\pi c/\lambda \approx 7,77 \times 10^{-4}$ s).

K.1.3 Hartree Atomic Unit System

In atomic physics, the *Hartree atomic unit system* is frequently used, based on the following four units

Quantity	Atomic unit	Symbol	Dimension
Mass	Rest mass of the electron	m	kg
Electric charge	Absolute charge of the electron	e	As
Action	Planck's constant divided by 2π	\hbar	$kg m^2 s^{-1}$
Dielectricity	Dielectricity constant of vacuum times	$4\pi\epsilon_0$	$A^2 s^4 kg^{-1} m^{-3}$
	4π		

Here, the unit for energy becomes

$$1H = \frac{me^4}{(4\pi\epsilon_0)^2\hbar^3},$$

which is known as the *Hartree unit* and equals twice the ionization energy of the hydrogen atom in its ground state (\approx 27.2 eV). The atomic unit for *length* is

$$a_0 = \frac{4\pi\epsilon_0\hbar^2}{me^2}$$

known as the *Bohr radius* or the radius of the first electron orbit of the Bohr hydrogen model (\approx 0.529 \times 10⁻¹⁰ m). The atomic unit of *velocity* is αc , where

$$\alpha = \frac{e^2}{4\pi\epsilon_0 c\hbar} \tag{K.1}$$

is the dimensionless *fine-structure constant* ($\approx 1/137,036$). Many units in these two systems are related by the fine-structure constant. For instance, the relativistic length unit is αa_0 .

K.1.4 cgs Unit Systems

In older scientific literature, a unit system, known as the cgs system, was frequently used. This is based on the following *three* units:

Quantity	cgs Unit	Symbol
Length	Centimeter	cm
Mass	Gram	g
Time	Second	S

In addition to the three units, it is necessary to define a fourth unit to be able to derive most of the physical units. Here, two conventions are used. In the *electrostatic version* (ecgs), the proportionality constant of Coulombs law, $4\pi\epsilon_0$, is set equal to unity, and in the *magnetic version* (mcgs) the corresponding magnetic constant, $\mu_0/4\pi$, equals unity. Since these constants have dimension, the systems cannot be used for dimensional analysis (see below).

The most frequently used unit system of cgs type is the so-called *Gaussian unit system*, where electric units are measured in ecgs and magnetic ones in mcgs. This implies that certain formulas will look differently in this system, compared to a system with consistent units. For instance, the *Bohr magneton*, which in any consistent unit system will have the expression

$$\mu_B = \frac{e\hbar}{2m}$$

will in the mixed Gaussian system have the expression

$$\mu_B = \frac{e\hbar}{2mc}$$

which does not have the correct dimension. Obviously, such a unit system can easily lead to misunderstandings and should be avoided.

K.2 Dimensional Analysis

It is often useful to check physical formulas by means of dimensional analysis, which, of course, requires that a consistent unit system, like the SI system, is being

used. Below we list a number of physical quantities and their dimension, expressed in SI units, which could be helpful in performing such an analysis.

In most parts of the book, we have set $\hbar=1$, which simplifies the formulas. This also simplifies the dimensional analysis, and in the last column below we have (after the sign \Rightarrow) listed the dimensions in that case.

$$[\text{force}] = N = \frac{\text{kg m}}{\text{s}^2} \Rightarrow \frac{1}{\text{ms}},$$

$$[\text{energy}] = J = Nm = \frac{\text{kg m}^2}{\text{s}^2} \Rightarrow \frac{1}{\text{s}},$$

$$[\text{action, } \hbar] = J\text{s} = \frac{\text{kg m}^2}{\text{s}} \Rightarrow 1,$$

$$[\text{electric potential}] = V = \frac{J}{A\text{s}} = \frac{\text{kg m}^2}{A\text{s}^3} \Rightarrow \frac{1}{A\text{s}^2},$$

$$[\text{electric field, } \mathbf{E}] = V/m = \frac{\text{kg m}}{A\text{s}^3} \Rightarrow \frac{1}{A\text{ms}^2},$$

$$[\text{magnetic field, } \mathbf{B}] = V\text{s}/m^2 = \frac{\text{kg m}}{A\text{s}^2} \Rightarrow \frac{1}{A\text{m}^2\text{s}},$$

$$[\text{vector potential, } A] = V\text{s}/m = \frac{\text{kg m}}{A\text{s}^2} \Rightarrow \frac{1}{A\text{ms}},$$

$$[\text{momentum, } p] = \frac{\text{kg m}}{\text{s}} \Rightarrow \frac{1}{\text{m}},$$

$$[\text{charge density, } \rho] = \frac{A\text{s}}{m^3},$$

$$[\text{current density, } \rho] = \frac{A\text{s}}{m^2},$$

$$[\mu_0] = N/A^2 = \frac{\text{kg m}}{A^2\text{s}^2} \Rightarrow \frac{1}{A^2\text{ms}},$$

$$[\epsilon_0] = [1/\mu_0 c^2] = \frac{A^2\text{s}^4}{\text{kg m}^3} \Rightarrow \frac{A^2\text{s}^3}{\text{m}}.$$

Fourier transforms

$$D_{F\nu\mu}(x_1, x_2) = \int \frac{dz}{2\pi} D_{F\nu\mu}(z; \mathbf{x}_1, \mathbf{x}_2) e^{-iz(t_2 - t_1)},$$

$$[A(\omega, \mathbf{x})] = s[A(x)],$$

$$[A(\omega, \mathbf{k})] = sm^3 [A(x)],$$

$$[A(k)] = m^4 [A(x)].$$

Photon propagator

$$\begin{split} [D_{\mathrm{F}\nu\mu}(x,x)] &= \frac{1}{\mathrm{A}^2\mathrm{m}^2\mathrm{s}^2}, \\ [\epsilon_0 D_{\mathrm{F}\nu\mu}(x,x)] &= \frac{\mathrm{s}}{\mathrm{m}^3}, \\ [\epsilon_0 D_{\mathrm{F}\nu\mu}(k)] &= \mathrm{sm}, \\ [\epsilon_0 D_{\mathrm{F}\nu\mu}(k_0,x)] &= \frac{\mathrm{s}}{\mathrm{m}^2}, \\ [\epsilon_0 D_{\mathrm{F}\nu\mu}(t,x)] &= \frac{1}{\mathrm{m}^2}, \\ [\epsilon_0 D_{\mathrm{F}\nu\mu}(z,x)] &= \frac{\mathrm{s}^2}{\mathrm{m}^3} \quad z = ck_0, \\ [\epsilon_0 D_{\mathrm{F}\nu\mu}(z,k)] &= \mathrm{s}^2, \\ [\epsilon_0 D_{\mathrm{F}\nu\mu}(z,k)] &= \mathrm{s}^2, \\ [\epsilon_0 D_{\mathrm{F}\nu\mu}(z,x)] &= \frac{1}{\mathrm{s}}, \\ [\epsilon_0 D_{\mathrm{F}\nu\mu}(z,x)] &= \frac{1}{\mathrm{s}}, \end{split}$$

Electron propagator

$$\begin{split} \hat{S}_{F}(x,x) &\Rightarrow s, \\ S_{F}(x,x) &\Rightarrow \frac{1}{m^{3}}, \\ S_{F}(z,x) &\Rightarrow \frac{s}{m^{3}}, \\ S_{F}(z,k) &\Rightarrow s, \\ S_{F}(k) &\Rightarrow m. \end{split}$$

S-matrix

$$\hat{S}(x, x) \Rightarrow 1,$$

 $S(z, x) \Rightarrow s,$
 $S(z, k) \Rightarrow m^4.$

Self energy

$$\hat{\Sigma}(z) \Rightarrow \frac{1}{s},$$

$$\Sigma(z, \mathbf{x}) \Rightarrow \frac{1}{s \text{ m}^3},$$

$$\Sigma(z, \mathbf{k}) \Rightarrow \frac{1}{s},$$

$$\Sigma(k) \Rightarrow \frac{m}{s^2}.$$

Vertex

$$\Lambda(z, \mathbf{k}) \Rightarrow 1,$$

$$\Lambda(p,p') \Rightarrow \frac{\mathrm{m}}{\mathrm{s}}.$$

Abbreviations

CCA Coupled-cluster approach

CEO Covariant evolution operator

GML Gell-Mann-Low relation

HP Heisenberg picture

IP Interaction picture

LDE Linked-diagram expansion

MBPT Many-body perturbation theory

MSC Model-space contribution

NVPA No-virtual-pair approximation

PWR Partial-wave regularization

QED Quantum electrodynamics

SCF Self-consistent field

SI International unit system

SP Schrödinger picture

Index

A Adiabatic damping, 51 all-order method, 30 annihilation operator, 283 antisymmetry, 22	covariant evolution operator, 3, 119 covariant vector, 273 creation operator, 283 cut-off procedure, 248
B Banach space, 277 Bethe–Salpeter equation, 3, 119, 193, 199, 225 effective potential form, 205 Bethe–Salpeter–Bloch equation, 6, 156, 173, 193, 199, 206 Bloch equation for Green's operator, 146 generalized, 20, 23 bra vector, 290 Breit interaction, 38, 73, 318 Brillouin–Wigner expansion, 153 Brown–Ravenhall effect, 2, 38, 178, 194, 216, 219	d'Alembertian operator, 274 de Broglie's relations, 13 density operator, 120 difference ratio, 139 dimensional analysis, 355 dimensional regularization, 163 Dirac delta function, 277 Dirac equation, 1, 295 Dirac matrices, 296 Dirac sea, 38 Dirac-Coulomb Hamiltonian, 37 discretization technique, 42 dot product, 135 Dyson equation, 108, 201, 243
C Cauchy sequence, 276 closure property, 292 complex rotation, 37 configuration, 22 conjugate momentum, 15, 306 connectivity, 37 continuity equation, 314 contraction, 18 contravariant vector, 273 coordinate representation, 63, 292 counterterms, 138 coupled-cluster approach, 30 normal-ordered, 34 coupled-cluster-QED expansion, 196 covariance, 1	E effective Hamiltonian, 5, 20 intermediate, 37 effective interaction, 23, 31 Einstein summation rule, 289 electron field operators, 285 electron propagator, 61, 98 equal-time approximation, 96, 120, 124, 173, 205, 208 Euler-Lagrange equations, 308 evolution operator, 47 exponential Ansatz, 33 normal-ordered, 34 external-potential approach, 4, 208

364 Index

F	intermediate normalization, 21
Feynman amplitude, 88, 96, 124, 174, 335	intruder state, 23, 36
Feynman diagram, 28, 60, 87, 125, 335	irreducible diagram, 40, 127
fine structure, 165	-
first quantization, 13	
Fock space, 133, 277	K
photonic, 6, 51, 132, 211	ket vector, 290
fold, 126	Klein-Gordon equation, 295
folded diagram, 23	Kronecker delta factor, 278
Fourier transform, 63	Troncolor delta factor, 270
functional, 275	
Furry picture, 21, 27	L
Furry's theorem, 86	
Turry's theorem, 60	Lagrange equations, 305
	Lagrangian function, 309
C	Lamb shift, 2, 79, 84, 157
G	Laplacian operator, 274
g-factor, 164	Lehmann representation, 97
gamma function, 332	linked diagram, 28, 107
gauge	Lippmann–Schwinger equation, 205
Coulomb, 59, 68, 76, 81, 315, 324, 329	Lorentz covariance, 1, 39, 60, 94, 119
covariant, 59, 65, 122, 125, 328	Lorentz force, 308
Feynman, 59, 65, 66, 81, 324, 326, 328	Lorentz transformation, 1
Fried-Yennie, 329	Lorenz condition, 314
Landau, 328	
non-covariant, 329	
gauge invariance, 314	M
gauge transformation, 327	many-body Dirac Hamiltonian, 133
Gaunt interaction, 213, 217	matrix elements, 291
Gell-Mann-Low theorem, 51	matrix representation, 291
relativistic, 131	Maxwell's equations, 311, 312
Goldstone diagram, 25	metric tensor, 273
Goldstone rules, 24, 28, 125	minimal substitutions, 307
Green's function, 3, 91	model space, 20
projected, 113	complete, 22
Green's operator, 119, 134	extended, 23
Grotsch term, 164	model state, 20
Gupta-Bleuler formalism, 325	model-space contribution, 29, 56, 126, 138,
, , , , ,	142
	momentum representation, 300
H	MSC, 56, 126
Hamiltonian density, 309	multi-photon exchange, 127
Hartree–Fock model, 26	mani prieteri esteriange, 127
Heaviside step function, 282	
Heisenberg picture, 202, 286	N
Heisenberg representation, 92	no-virtual-pair approximation, 2, 37
helium fine structure, 225	non-radiative effects, 39
Hilbert space, 277	norm, 275
hole state, 119	
	normal order, 18
Hylleraas function, 5, 163	
	n.
T	P
I instantant and a second second second	pair correlation, 30
instantaneous approximation, 4	parent state, 52, 131
interaction picture, 47	partitioning, 21

Index 365

Pauli spin matrices, 296	photon, 87, 246
perturbation	proper, 108
Brillouin-Wigner, 111	sequence, 276
Rayleigh-Schrödinger, 1, 24	set, 275
photon propagator, 65	size consistency, 30
Poisson bracket, 15, 306	size extensive, 207
polarization tensor, 87	size extensivity, 30, 207
principal-value integration, 64	Slater determinant, 22, 284
	spin-orbital, 22
	spline, 41
Q	state-specific approach, 37
QED effects, 39, 59, 79	state-universality, 36
QED potential, 181	subset, 275
quantization condition, 15	Sucher energy formula, 61
quasi-degeneracy, 23, 56	
quasi-potential approximation, 4	
quasi-singularity, 56	T
	target states, 20
	time-ordering, 49
R	Wick, 18
radiative effects, 39	trace, 85
reducible diagram, 40, 127	transverse-photon, 77
reference-state contribution, 78, 142	two-times Green's function, 3, 111
regularization, 79, 237	
Brown-Langer-Schaefer, 252	TT
dimensional, 257	U
partial-wave, 255	Uehling potential, 86, 128
Pauli–Willars, 248	union, 275
renormalization, 79, 237	unit system, 355
charge, 244	cgs, 357 Hartree, 356
mass, 242	mixed, 300
resolution of the identity, 290	natural, 355
resolvent, 24	relativistic, 59, 355
reduced, 24	SI, 355
	unlinked diagram, 28
	diffined diagram, 20
S	
S-matrix, 3, 60, 157	V
scalar potential, 311	vacuum polarization, 2, 39, 84, 87
scalar product, 274	valence universality, 21, 36
scalar retardation, 213, 217	vector potential, 311
scattering matrix, 60	vector space, 275
Schrödinger equation, 15	vertex correction, 39, 82, 186, 240, 246
Schrödinger picture, 47	
Schwinger correction, 164	
second quantization, 16, 283	W
self energy	Ward identity, 83, 242
electron, 39	wave operator, 20
self energy, 108	Wick's theorem, 19
electron, 79, 157, 186, 239, 244	Wickmann-Kroll potential, 86